Universidade de São Paulo
Faculdade de Medicina de Ribeirão Preto

Maria Clara Zanon Zotin

A largura do pico da difusividade média esqueletizada como biomarcador de declínio cognitivo vascular no contexto de angiopatia amiloide cerebral

Peak width of skeletonized mean diffusivity (PSMD) as neuroimaging biomarker for vascular cognitive impairment in the context of cerebral amyloid angiopathy

Ribeirão Preto
2022

Maria Clara Zanon Zotin

A largura do pico da difusividade média esqueletizada como biomarcador de declínio cognitivo vascular no contexto de angiopatia amiloide cerebral

Peak width of skeletonized mean diffusivity (PSMD) as neuroimaging biomarker for vascular cognitive impairment in the context of cerebral amyloid angiopathy

Versão Original

Tese apresentada à Faculdade de Medicina de Ribeirão Preto da Universidade de São Paulo, para a obtenção do título de Doutor em Ciências.

Área de Concentração: Neurologia

Orientador: Prof. Dr. Antônio Carlos dos Santos
Co-orientador: Prof. Dr. Octávio Marques Pontes-Neto

Universidade de São Paulo – USP
Faculdade de Medicina de Ribeirão Preto – FMRP
Programa de Pós-Graduação em Neurologia e Neurociências

Ribeirão Preto
2022

FICHA CATALOGRÁFICA

Maria Clara Zanon Zotin

A largura do pico da difusividade média esqueletizada como biomarcador de declínio cognitivo vascular no contexto de angiopatia amiloide cerebral

Peak width of skeletonized mean diffusivity (PSMD) as neuroimaging biomarker for vascular cognitive impairment in the context of cerebral amyloid angiopathy

Tese apresentada à Faculdade de Medicina de Ribeirão preto da Universidade de São Paulo para a obtenção do título de Doutor em Ciências.

Área de Concentração: Neurologia

Aprovado em:___/___/2022

Banca Examinadora

Prof. Dr. _____
Instituição: _____Assinatura:_____

Prof. Dr. _____
Instituição: _____Assinatura:_____

Prof. Dr. _____
Instituição: _____Assinatura:_____

Prof. Dr. _____
Instituição: _____Assinatura:_____

Prof. Dr. _____
Instituição: _____Assinatura:_____

Ribeirão Preto
2022

Aos amigos e colaboradores do estudo TRIDENT no Brasil, em especial a Ana Cláudia de Souza, agradeço pela confiança e apoio.

Agradeço aos professores, colegas, funcionários e residentes do CCIFM, da Neurologia, da Pediatria, da CEDIRP e da querida Unidade de Emergência, pelo companheirismo, apoio e carinho, tão importantes para mim.

Aos meus queridos amigos Bacurenses e da casa da Dona Silvia, agradeço pelos momentos mágicos que vivemos juntos, por aquecerem o frio de Boston com o calor Brasileiro, e, por, em meio a pior pandemia do século, termos podido sonhar juntos por um Brasil que valorize a Ciência.

Dedicatórias

Dedico este trabalho a todos os pacientes que sofrem os efeitos das doenças cerebrais de pequenos vasos. Que esse estudo possa contribuir de alguma forma no esforço universal por um melhor entendimento e mensuração da doença, e *hopefully* de uma melhor prognóstico.

"Even If I can't cure, I can still care."
Sally P. Karioth RN, PhD

"De tudo, ficaram três coisas: a certeza de que ele estava sempre começando, a certeza de que era preciso continuar e a certeza de que seria interrompido antes de terminar. Fazer da interrupção um caminho novo. Fazer da queda um passo de dança, do medo uma escada, do sono uma ponte, da procura um encontro."
Fernando Sabino

RESUMO

Zanon Zotin, M. C. **A largura do pico da difusividade média esqueletizada como biomarcador de declínio cognitivo vascular no contexto de angiopatia amiloide cerebral.** 385 f. Tese (Doutorado). Faculdade de Medicina de Ribeirão Preto, Universidade de São Paulo, Ribeirão Preto, 2022.

Introdução: No contexto das doenças cerebrais de pequenos vasos (DCPVs), permanece necessário o desenvolvimento de ferramentas que permitam quantificar de forma prática o dano difuso à substância branca que causa o declínio cognitivo vascular. Os marcadores de RM convencional têm papel fundamental no diagnóstico das DCPVs, porém são menos sensíveis às alterações sutis que acometem a substância branca aparentemente normal, e geralmente demonstram associações cognitivas fracas e inconsistentes. A procura pelo marcador de neuroimagem ideal, ou seja, adequado para aplicação em grandes ensaios clínicos, tornou-se prioridade, e o desenvolvimento de terapias modificadoras de doença depende disso. Um marcador de difusão recentemente desenvolvido, chamado a largura do pico da difusividade média esqueletizada (PDME) oferece vantagens alinhadas às necessidades e prioridades atuais de pesquisa. Ele foi desenvolvido especificamente para quantificar a carga de lesão relacionada a DCPV e refletir o declínio cognitivo vascular de forma rápida e automatizada. Entretanto, o conhecimento a respeito do PDME ainda é restrito na comunidade científica e dados sobre sua utilidade no contexto de angiopatia amiloide cerebral (AAC), a segunda forma mais comum de DCPV esporádica, são insuficientes. **Objetivos:** Avaliar de forma crítica o papel do PDME como biomarcador de neuroimagem para declínio cognitivo vascular e investigar suas possíveis aplicações no contexto de AAC. **Métodos:** Com esse fim, conduzimos três projetos de pesquisa. Primeiramente realizamos uma revisão sistemática para identificar e organizar as evidências disponíveis a respeito da utilidade do PDME como biomarcador em DCPV e outras doenças da substância branca. Em seguida, conduzimos um estudo transversal investigando as associações cognitivas e de neuroimagem do PDME em pacientes com AAC e declínio cognitivo leve. Finalmente, investigamos variações regionais de PDME na AAC, além de comparar suas associações cognitivas e de neuroimagem com outros marcadores convencionais de difusão. Baseados nesses três artigos, discutimos de forma crítica o quanto os nossos resultados podem ser generalizados a outras populações, abordamos os desafios relacionados à aplicação do PDME em amostras brasileiras, e enumeramos medidas que podem ser tomadas para avançar potenciais aplicações clínicas. **Resultados:** O PDME está progredindo rapidamente no processo de validação como um desfecho substitutivo para declínio cognitivo vascular, porém sua

validação completa ainda depende de mais estudos técnicos e longitudinais. Na AAC, o PDME demonstra associações cognitivas fortes e consistentes, superiores a outros marcadores de RM convencional e de difusão. Comparado com difusividade média e anisotropia fracionada, o PDME apresenta associações cognitivas mais fortes e um padrão diferente de associação com marcadores de RM convencional, sugerindo uma maior sensibilidade à lesão microestrutural clinicamente relevante. Observamos ainda que os valores de PDME reduzem-se de forma mais acentuada de posterior para anterior em pacientes com AAC-provável em comparação com pacientes sem a doença, indicando dano microestrutural mais acentuado em regiões posteriores, em concordância com estudos histopatológicos e de neuroimagem prévios. **Conclusões:** Nossos resultados sugerem que o PDME é um biomarcador promissor de injúria global ou regional à substância branca e de declínio cognitivo no contexto de AAC e outras doenças de substância branca.

Palavras-chave: Declínio cognitivo vascular, angiopatia amiloide cerebral, imagem por tensor de difusão, ressonância magnética, biomarcador.

ABSTRACT

Zanon Zotin, M. C. **Peak width of skeletonized mean diffusivity (PSMD) as neuroimaging biomarker for vascular cognitive impairment in the context of cerebral amyloid angiopathy.** 385 f. Tese (Doutorado). Faculdade de Medicina de Ribeirão Preto, Universidade de São Paulo, Ribeirão Preto, 2022.

Introduction – An unmet need in the field of cerebral small vessel diseases (cSVDs) is how to measure the widespread white matter (WM) injury that underlies vascular cognitive impairment in a feasible and clinically meaningful way. Though conventional MRI markers play a pivotal role in diagnosing cSVD, they are less sensitive to subtle changes in the normal-appearing white matter and yield generally weak and inconsistent cognitive associations. The quest for the ideal MRI marker to fit the critical role of a reliable outcome measure in large clinical trials has become a research priority in the field, and the future development of disease-modifying therapies depends on it. A recently developed diffusion-based metric, called peak width of skeletonized mean diffusivity (PSMD), aligns with current scientific needs and priorities. It was specifically designed to quantify the burden of cSVD and reflect related cognitive impairment in a fast and automated way. Nonetheless, knowledge about PSMD is still limited in the scientific community, and data on its utility in the context of CAA, the second most common form of sporadic cSVD, is scarce. **Objectives:** We set out to critically evaluate PSMD's role as neuroimaging biomarker for vascular cognitive impairment and investigate its potential applications in CAA. **Methods:** To this end, we conducted three research projects. First, we performed a systematic review to gather and synthesize the evidence supporting PSMD's role as a biomarker in the context of cSVD and other WM disorders. Then, we conducted a cross-sectionally investigation on PSMD's neuroimaging and cognitive associations in patients with CAA and mild cognitive impairment. Finally, we expanded on previous research by investigating PSMD's regional variations in CAA, while comparing its neuroimaging and cognitive associations with other conventional diffusion-based MRI markers. Based on these three articles, we critically discuss the generalizability of our results, the challenges related to applying PSMD in Brazilian samples, and the measures that can be taken to advance clinical translation. **Results:** Several key findings emerge from our investigations. PSMD is on a fast track towards validation as a surrogate for cognitive endpoints in VCI, but full validation depends on further technical and longitudinal studies. In CAA, PSMD shows strong and consistent neuropsychological associations, outperforming other conventional and diffusion-based MRI markers. Compared to mean diffusivity and fractional anisotropy, PSMD presents

specific neuroimaging correlates and stronger cognitive associations, underscoring an increased sensitivity to clinically relevant microstructural disruption. Furthermore, we found that the degree to which PSMD values decrease from posterior to anterior regions is higher among probable-CAA compared to non-CAA subjects, indicating more severe WM microstructural damage in the posterior areas of the brain, which is consistent with several histopathologic and neuroimaging studies. **Conclusions:** Our results support PSMD's promising role as a marker of global/regional WM injury and related cognitive decline in the context of CAA and other WM diseases.

LIST OF FIGURES

LIST OF TABLES

ABREVIATIONS

ACE-R	Addenbrooke's Cognitive Examination-Revised
AD	Alzheimer's Disease
ADNI	Alzheimer's Disease Neuroimaging Initiative
ARIA	Amyloid-related Imaging Abnormalities
ASC	Arteriolosclerosis
ASL	Arterial Spin Labelling
ASPSF	Austrian Stroke Prevention Study Family
BBB	Blood Brain Barrier
BG-PVS	Perivascular Spaces in the Basal Ganglia
BIL&GIN	Brain Imaging of Lateralization study at Groupe D'Imagerie Neurofonctionnelle
BRB	Rao Brief Repeatable Battery
CAA	Cerebral Amyloid Angiopathy
CADASIL	Cerebral Autosomal-dominant Arteriopathy with Subcortical Infarcts and Leukoencephalopathy
CBF	Cerebral Blood Flow
CMB	Cerebral microbleeds
CMI	Cerebral microinfarcts
CSF	Cerebrospinal Fluid
CSO-PVS	Perivascular Spaces in the Centrum Semiovale
cSS	Cortical superficial siderosis
cSVD	Cerebral Small Vessel Disease
CU-RISK	Chinese University of Hong-Kong-Risk Index for Subclinical brain lesions in Hong Kong
CVR	Cerebrovascular Reactivity
DIAN	Dominantly Inherited Alzheimer Network
DTI	Diffusion tensor imaging
DWI	Diffusion weighted imaging
DCE-MRI	Dynamic Contrast-enhanced MRI
DSC-MRI	Dynamic-susceptibility Contrast MRI
EDSS	Expanded Disability Status Scale
FA	Fractional Anisotropy
FAVR	Functional Assessment of Vascular Reactivity Study

FLAIR	Fluid Attenuation Inversion Recovery
FOV	Field-of-view
GM	Gray Matter
GMV	Gray matter volume
GRE	Gradient-recalled Echo
HC	Healthy controls
HCA	Histologic Chorioamnionitis
HCHS	Hamburg City Health Study
D-CAA	Dutch-type hereditary cerebral amyloid angiopathy
ICH	Intracerebral Hemorrhage
IQR	Interquartile range
LBC1936	Lothian Birth Cohort 1936
LLD	Late-life depression
MAS	Memory and Ageing Study
MCI	Mild cognitive Impairment
MD	Mean diffusivity
MGH	Massachusetts General Hospital
MMSE	Mini-Mental State Exam
MoCA	Montreal Cognitive Assessment
MRi-Share	Magnetic Resonance imaging Subcohort of internet-based Students HeAlth Research Enterprise
mRS	Modified Rankin Scale
MS	Multiple sclerosis
NAWM	Normal-appearing white matter
NDI	Neurite Dispersion Index
NIMROD	NeuroInflammation in Memory and Related Other Disorders
NODDI	Neurite orientation dispersion and density imaging
NVU	Neurovascular units
OATS	Older Australian Twin Study
ODI	Orientation Dispersion Index
PIB-PET	Pittsburgh compound ß-positron emission tomography
PET	Positron Emission Tomography
PRISMA	Preferred Reporting Items for Systematic Reviews and Meta-Analyses
PSAD	Peak width of Skeletonized Axial Diffusivity

PSFA	Peak width of Skeletonized Fractional Anisotropy
PSMD	Peak width of Skeletonized Mean Diffusivity
PSNDI	Peak width of Skeletonized Neurite Dispersion Index
PSODI	Peak width of Skeletonized Orientation Dispersion Index
PSRD	Peak width of skeletonized radial diffusivity
PVS	Perivascular spaces
ROI	Region-of-interest
Rs-fMRI	Resting State Functional MRI
RUN	DMC Radboud University Nijmegen Diffusion Tensor and Magnetic resonance Imaging Cohort
SAH	Subarachnoid Hemorrhage
SD	Standard deviation
SDMT	Symbol Digit Modalities Test
SWI	Susceptibility Weighted Imaging
SYS	Saguenay Youth Study
TBSS	Tract-Based Spatial Statistics
TE	Echo time
TFNE	Transient Focal Neurological Episodes
TMTA	Trail Making Test part A
TMTB	Trail Making Test part B
TR	Repetition time
VaD	Vascular dementia
VASCAMY	Vascular and Amyloid Predictors of Neurodegeneration and Cognitive Decline in Nondemented Subjects
VBM	Voxel-Based Morphometry
VCI	Vascular cognitive impairment
VCID	Vascular cognitive impairment and dementia
WM	White matter
WML	White matter lesions
WMV	White matter volume
WMH	White matter hyperintensities
WMHV	White matter hyperintensity volume

TABLE OF CONTENTS

Presentation

Vascular pathologies are currently the second most common cause of dementia worldwide, contributing at some level to the majority of cases. Among all vascular causes, cerebral small vessel disease (cSVD) represents arguably the most prevalent contributor to cognitive decline and dementia in the elderly. In underdeveloped countries, where treatment and control of vascular risk factors are largely insufficient, cSVDs may play an even larger role in explaining age-related cognitive impairment. Importantly, treatment for these pathologies is still largely unavailable, restricted to measures intended to control and prevent vascular risk factors. Future therapeutic developments in the field are hindered by a still limited understanding of the pathophysiology of cSVDs, and by the absence of validated biomarkers to be used as outcome measures in future interventional trials. In the last decade, much effort has been put into developing and validating neuroimaging markers for such a role, but the quest for the ideal marker remains.

This doctoral thesis was organized to provide an integrated discussion on the scientific projects conducted by the author and colleagues in the last years, centered on the investigation and validation of a specific neuroimaging biomarker, called Peak Width of Skeletonized Mean Diffusivity (PSMD), in the context of vascular cognitive impairment caused by the second most prevalent type of cSVD, named cerebral amyloid angiopathy. This thesis is also part of the work conducted by the author as a research fellow at the Neurology Department of the Massachusetts General Hospital – Harvard Medical School, between July 2019 and December 2021.

The text will include an introductory chapter, in which an overview of the epidemiology, pathophysiology and diagnosis of cSVDs and related vascular cognitive impairment is provided, alongside a focused literature review on the neuroimaging biomarkers employed in the context of CAA. Lastly, we will provide a detailed overview of PSMD's technical details. In the following chapter, the general and specific research objectives will be presented, alongside the specific scientific projects designed to address each one, which will be organized throughout Chapter 3. The fourth chapter will include a broad discussion on the generalizability of the aforementioned findings. The challenges involved in applying and generalizing such findings in developing countries, such as our own, will also be discussed. We will also point out future directions to further advance clinical translation. The final chapter will provide our conclusions. In the appendix, we provide other co-authored articles published, in collaboration, in the field of cSVDs.

1. General Introduction

This introductory chapter is based on a narrative review called "Cerebral Small Vessel Disease and Vascular Cognitive Impairment: from Diagnosis to Management", published by the author (co-first author) and collaborators (Lukas Sveikata [co-first author], Anand Viswanathan, and Pinar Yilmaz) in April 2021 in the journal Current Opinion in Neurology.[1] The final peer-reviewed manuscript is available in Appendix 1.1. License for the reproduction of the final manuscript was not needed (see Appendix 1.2). License for the reuse of figures 1 and 2, without modifications, was acquired and is available in Appendix 1.3.

Cerebral white matter (WM) regions harbor organized structural and functional networks essential for neurobehavioral operations.[2] Congenital and acquired diseases, including vascular, autoimmune, infectious, neurodegenerative, and toxic-metabolic pathologies,[3] affect the WM and disrupt its intricate connectivity, contributing to multiple neuropsychological, motor, and autonomic symptoms.

Within the WM disorders, cerebral small vessel diseases (cSVDs) have grown in relevance due to their high prevalence in aging societies.

1.1.   Cerebral Small Vessel Diseases

cSVDs are extremely prevalent pathologies characterized by changes in the structure and function of penetrating arterioles, capillaries, and small veins of the brain, eventually leading to tissue damage and neurological symptoms.[4,5] Overall, cSVDs cause approximately 25% of ischemic, essentially all primary hemorrhagic strokes and contribute to up to 50% of dementia cases.[4] Furthermore, cSVDs are known to confer worse post-stroke prognosis, compromising recovery.[6,7]

Rather than a homogeneous disorder, cSVD is a term that encompasses several sporadic and inherited pathologies, resulting from a complex interaction of genetic and vascular risk factors.[5] cSVD can present sporadically or be inherited. Among the many vascular risk factors linked to cSVD (i.e. age, hypertension, diabetes, smoking, dyslipidemia, and hyperhomocysteinemia), aging and hypertension are considered the most important. Recent studies have demonstrated that genetic variants contribute to both monogenic and sporadic forms of cSVDs.[8–10] For instance the heritability of white matter hyperintensity (WMH), a hallmark of cSVD, has been reported as > 60%.[10]

The two most common types of age-related sporadic cSVD are hypertensive arteriolosclerosis (ASC),[11] also called deep perforating arteriopathy, and cerebral amyloid angiopathy (CAA).

ASC is found in aged individuals and is originally linked to arterial hypertension and type II diabetes.[11] According to autopsy studies, ASC is characterized by arteriolar thickening, predominantly in the basal ganglia, thalamus, and deep white matter, identified in more than 80% of individuals over 80 years of age,.[11] ASC is considered the most prevalent form of cSVD, also referred to as type 1 cSVD, followed by CAA, also named type 2 cSVD.

1.2. Cerebral Amyloid Angiopathy

1.2.1. Definition and epidemiology

CAA is defined by the deposition of amyloid-beta (Aβ) in the walls of cortical and leptomeningeal vessels.[12] Several mutations in the Aβ precursor protein gene have been associated with inherited forms of CAA,[13,14] but the sporadic presentation is much more prevalent.[14]

The cerebrovascular deposition of amyloid was first recognized in 1909 by Gustav Oppenheim.[14] Afterwards, in 1954, Stefanos Pantelakis described CAA's pathological hallmarks: 1) preferential involvement of cortical and leptomeningeal vessels; 2) posterior predominance; 3) sparing of white matter vessels; and 4) association with advanced age and dementia, but not with hypertension, arteriolosclerosis, or systemic amyloidosis.[12,14,15]

CAA is considered ubiquitous in the elderly brain, and age is its strongest known risk factor.[12,16] The only genetic variants consistently associated with sporadic CAA are ApoE ε4 and ε2 alleles.[14] Some degree of vascular amyloid deposition can be found in almost 85% of older community-dwelling persons with and without dementia.[17] In a systematic review of population-based neuropathological studies, CAA was observed in 26-38% of non-demented individuals and 55-59% of demented cases.[18] Severe CAA was present in 7-24%, and 37-43% of those, respectively.[18] In a recent meta-analysis, comprising over 73000 individuals, the prevalence of moderate-to-severe CAA on pathology was estimated in 23% in the general population, and 6.4% in cognitively normal elderly.[19] CAA often co-occurs with Alzheimer's disease (AD),[17] affecting, at some level, nearly all brains with AD.[20,21] Despite the common overlap and shared molecular underpinnings, CAA and AD remain distinct entities.[12,13] Moderate-to-severe CAA in pathology can be found in almost 60% of AD patients,[19] but less than 50% of CAA patients fulfil pathological criteria for AD.[16,21]

1.2.2. Pathophysiology

Environmental risk factors, genetic variants[9,10] and ageing appear to contribute to cSVD pathogenesis, including CAA, from the early stages of the disease (Figure 1.1.A), through the disturbance of interdependent functional units formed by specialized cellular and structural elements encircling the lumens of arterioles and capillaries, named neurovascular units (NVU).[4,22] These units are pivotal to the regulation of blood flow, vascular permeability, immune trafficking and waste clearance.[4,23,24] Once these interdependent units become dysfunctional, several synergistic deleterious effects arise, such as deficient cerebrovascular reactivity (CVR) and blood-brain barrier (BBB) leakage (Figure 1.1.B).[4]

The precise mechanisms linking brain injury with vascular Aβ deposition remain unclear but are centered around vascular dysfunction.[13] Aβ accumulation in the vessel wall may lead to loss of smooth muscle cells, loss of aquaporin 4 channels, and altered configuration of astrocyte's endfeet, thus contributing to impair CVR and the BBB (Figure 1.1.B).[13,25]

Evidence suggests that Aβ vascular accumulation derives not from overproduction but from defective clearance of the peptide, leading to pathologically imbalanced production and excretion.[12,13] The smaller and more soluble nature of $A\beta_{40}$ peptides could underlie its preferential perivascular deposition, while the less soluble $A\beta_{42}$ are more likely to be retained in parenchymal neuritic plaques.[13] Mutations in specific regions of the APP gene can also influence Aβ deposition sites.[13]

Recent discoveries have led to an improved understanding of the brain's clearance pathways, which appear to be centered on perivascular routes. Though the precise anatomical paths, driving forces and the directionality of perivascular flow are still under debate,[26] the prevailing model suggests that vasomotion[23] drives clearance in the opposite direction to blood flow.[26,27] Sleep-induced hemodynamic changes can also act as an important modulator of perivascular clearance.[28] Defective smooth muscle cell function caused by Aβ vascular accumulation could impair vasomotion and compromise perivascular clearance, leading to a self-reinforcing cycle that contributes to amyloid build-up (both vascular and parenchymal) and dysfunctional solute clearance.[12,13,26] This may represent an interactive pathological pathway linking vascular and neurodegenerative diseases which may help explain the common co-occurrence of these diseases, especially CAA and AD (Figure 1.1.B).[13] In this setting, CAA has been associated with a common side-effect of anti-Aβ immunotherapy, named amyloid-related imaging abnormalities (ARIA).[29] ARIA can take the form of edema (ARIA-E), perceived on fluid attenuation inversion recovery (FLAIR) images as hyperintense areas, or hemorrhages (ARIA-

H), characterized by lobar cerebral microbleeds (CMBs) and/or cortical superficial siderosis (cSS).[13,30] Studies investigating the pathophysiology of ARIA have shed some light on CAA's own pathogenesis. An ongoing hypothesis is that anti-Aβ immunotherapy could lead to the solubilization and mobilization of Aβ from parenchymal neuritic plaques into the perivascular space, overwhelming this clearance route and leading to vascular amyloid accumulation, thus characterizing rapidly progressing CAA.[13] The observation that CAA-related inflammation (CAAri) closely resembles ARIA is also in line with this hypothesis.[13] In the era post-FDA approval of aducanumab (an anti-Aβ therapy currently in use in the United States), identifying patients with significant CAA pathology, and thus at increased risk of ARIA, has become a priority.[29]

Knowledge on how mechanisms of cSVD pathology lead to specific brain lesions remains incomplete but has evolved due to recent studies converging *in vivo* and *ex vivo* MRI with histopathology.[31] In summary, vessel frailty and blood-brain-barrier dysfunction could lead to hemorrhagic complications, while the loss of vascular recruitment and reactivity in response to increased metabolic demand could contribute to ischemic lesions.

1.2.3. Diagnosis

Up until the 1980s, the diagnosis of CAA was dependent on histopathological assessment, either through autopsy (*post mortem* diagnosis) or biopsy (i.e. in the setting of surgical evacuation of intracerebral hemorrhage). Developed in the 1990s, the Boston criteria (v1.0) are a set of clinical-radiological features that allow for the diagnosis of CAA during life, making use of blood-sensitive MRI sequences.[32,33] The presence of multiple hemorrhages restricted to lobar regions of the brain in older individuals, not attributable to any other causes, is considered indicative of underlying CAA pathology. These criteria made CAA diagnosis no longer dependent on invasive brain biopsies or full post-mortem examination, and soon became the basis for clinical decision-making (Table 1.1).

In 2010, a modified version of the Boston criteria (v1.5) was released, further incorporating cSS, an emerging hemorrhagic MRI marker of CAA that is associated with a high risk of developing first-ever or recurrent ICH.[34] Applied in a hospital-based cohort, these criteria showed improved sensitivity, without compromising specificity.[34] Since then, extensive neuroimaging research led to the detection of new MRI findings associated with CAA. These advances prompted a multicenter effort to update, improve and validate, soon-to-be-released, new Boston criteria (v2.0), taking advantage of recently identified non-hemorrhagic MRI markers of CAA (Table 1.1).[35]

Importantly, the diagnostic yield of the Boston criteria varies strongly depending on the prevalence of hemorrhagic markers in the studied population. For instance, while sensitivity and specificity among hospital-based cohorts range around 42.4%-76.9% and 87.5%-100% respectively,[36] in a population-based cohort diagnostic yield was much lower (4.5% and 88%, respectively).[37] Another limitation of the aforementioned criteria is its dependence on MRI, which is an expensive and still not widely available imaging method. Performing MRI in acutely unstable patients, which is often the case with those presenting with symptomatic hemorrhagic stroke, may prove challenging. Furthermore, approximately 75% of the deaths due to hemorrhagic strokes in the world and the majority of dementia cases are found in low to middle-income countries, where access to MRI is even more restricted.[38–41] In this context, by making use of computed tomography (CT) findings, the Edinburgh criteria offer several advantages and may be more suited for the acute diagnosis of CAA-related ICH in specific settings.[38] Though the full Edinburgh criteria require the availability of APOE genotype (Table 1.1), its simplified version (CT-only) still offers good diagnostic accuracy, with subarachnoid hemorrhage (SAH) alone offering high sensitivity (89%), and SAH plus finger-like projections offering high specificity (100%).[38]

1.2.4. Clinical presentation

Since its description in the early twentieth century, CAA has evolved from a neuropathological observation to a clinical syndrome linked to well-established neuroimaging features. In specific, several clinical manifestations may occur in the context of CAA, many of which have been associated with specific MRI findings.

The clinical hallmark and most feared complications of CAA are lobar intracerebral hemorrhages (ICHs), thought to derive from the rupture of frail, amyloid-laden cortical and leptomeningeal vessels. In a meta-analysis of 24 studies including a total of 15,828 spontaneous ICH patients, 12% of the episodes were related to CAA.[42] In another meta-analysis of 46 studies comprising 7,159 CAA patients, the pooled prevalence of ICH was estimated at 44%.[43] Importantly, CAA etiology is associated not only with a specific ICH location (lobar) but also with increased volume,[42] and recurrence rates. In a study involving ICH survivors, the annual risk of ICH recurrence was estimated at 10.4% among probable CAA patients, which was a much higher rate than the 1.6% observed among patients with hypertensive bleedings.[44]

Figure 1.1. Potential mechanisms linking cSVD and cognitive impairment.
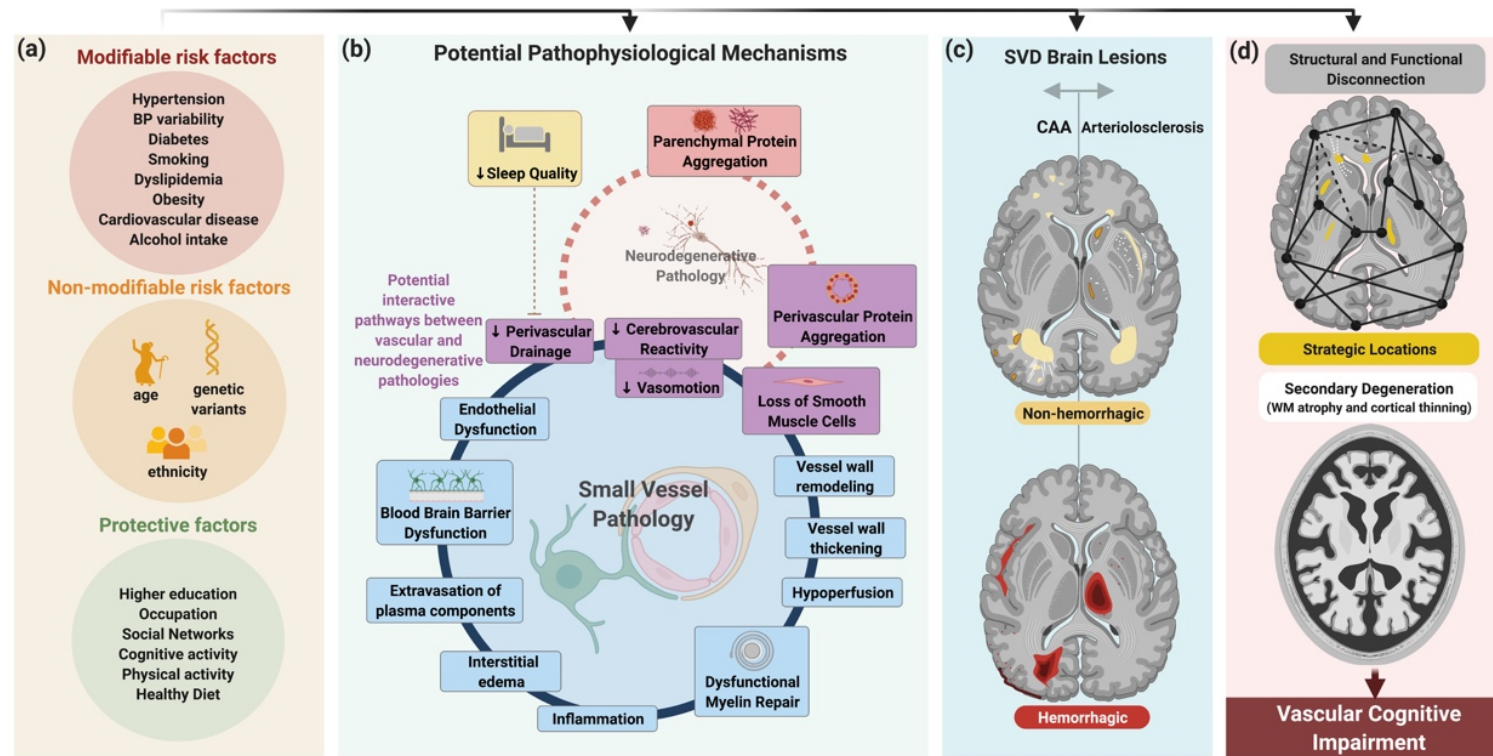
Source: Zanon Zotin MC & Sveikata L, et al. 2021.

(A) Risk factors associated with SVD and related cognitive decline. Aging and hypertension are considered the most important. **(B) Potential Pathophysiological mechanisms of SVD.** Vascular risk factors may cause endothelial dysfunction, contributing to the uncoupling of trophic neurovascular mechanisms. Impaired perivascular drainage may contribute to protein accumulation, including Aβ, and may represent an interactive pathway linking neurodegenerative and vascular pathologies. **(C) Typical brain lesions associated with SVD.** Hemorrhagic lesions (bottom figure) include: CMBs, cSS, SAH, and ICH. Non-hemorrhagic lesions (upper figure) include: WMH, lacunes, PVS, small acute subcortical infarcts, and cortical CMI. The pattern of distribution helps in discriminating between different etiological subtypes of SVD. CAA (left) often presents with cortical CMBs, cortical CMIs, lobar lacunes, CSO-PVS, cSS, convexity SAH, lobar ICH, and multiple WMH subcortical spots. ASC (right) usually presents with deep CMBs, deep lacunes, BG-PVS, deep ICH and peri-basal ganglia WMH. **(D) Mechanisms involved in SVD-related cognitive impairment.** Impairment of structural and functional connectivity, damage to highly connected deep regions in strategic locations, and secondary degeneration culminating in brain atrophy are some of the mechanisms thought to underlie SVD's contribution to cognitive impairment. Adapted from[12,45–47]. Created with Biorender.

In a study that investigated 728 patients with supratentorial hemorrhage, lobar location was associated with larger volumes, increased rates of hematoma expansion, early neurological deterioration and worse outcomes compared to deep ICH.[48]

Acute convexity SAH and transient focal neurological episodes (TFNEs), also named "amyloid spells", are other well-established clinical presentations of CAA.[49] TFNEs are observed in 14.5%-48% of CAA patients,[43,50] and are characterized by positive and/or negative self-limited, often stereotyped, neurologic symptoms, usually lasting less than 30 minutes, and recurring over days or weeks.[49] The observation of concomitant acute convexity SAH or cSS in brain locations matching the reported symptoms support the diagnosis of CAA-related TFNEs.[49] Importantly, patients with CAA-related TFNEs are at increased risk of lobar ICH.[49,50] In a study that followed 25 CAA patients with TFNEs over approximately 14 months, 50% developed symptomatic ICH.[50] The risk of ICH at 8 weeks after a CAA-related TFNE is estimated at 24.5%.[50]

Though CAA was first recognized for its hemorrhagic complications, cognitive impairment is also a currently well-established clinical feature of CAA. Common overlap between CAA, AD and ASC makes it challenging to disentangle CAA's specific role in age-related cognitive impairment.[12] In an autopsy study of older community-dwelling individuals with and without dementia, CAA pathology was associated with memory and perceptual speed even after controlling for concomitant AD pathology, suggesting an independent and separate role of CAA in age-related cognitive impairment.[17] In a case-control study, non-demented patients with CAA performed worse than controls in all the cognitive domains investigated, even though the majority of patients did not have spontaneous cognitive complaints. [51] In another case-control study, CAA patients had impaired performance in memory, executive function and processing speed, and 79% of them had mild cognitive impairment (MCI).[52] Interestingly, they performed similar to AD patients in tests of executive function but had preserved memory.[52] A longitudinal study involving 158 non-demented CAA patients, detected a 73% cumulative incidence of dementia at 5 years of follow-up, and both medial temporal atrophy and a composite score of cSVD MRI markers were independent predictors of dementia.[53] Overall, these findings support a high prevalence of cognitive impairment in CAA and may indicate a neuropsychological profile more similar to vascular than neurodegenerative causes.[12]

1.2.5. Neuroimaging features in CAA and other cSVDs

As is the case with other cSVDs, detection of CAA-related microvascular pathology relies strongly on neuroimaging, from which important diagnostic and prognostic information can be

extracted. Importantly, the small vessels of the brain remain inaccessible to non-invasive imaging methods. Not even intra-arterial arteriography is capable of depicting in detail the microvascular bed, visible only on histopathology. Therefore, we are left with detecting only the consequences of small vessel dysfunction, either in the form of parenchymal injury or disturbed hemodynamics.

MRI is a "gold-standard" requirement for the clinical diagnosis of CAA and other cSVDs. MRI is preferable for many reasons. First, many CAA neuroimaging features, like chronic CMBs, perivascular spaces (PVS), recent small subcortical infarcts and cortical cerebral microinfarcts (CMI) are visible and detectable almost exclusively through MRI.[54] Second, through advanced techniques, MRI can detect several early mechanisms of microvascular dysfunction, such as reduced CVR, BBB leakage, and hypoperfusion. In comparison, CT captures mostly severe diseases, and offers mainly qualitative instead of quantitative markers, besides causing radiation exposure.[55] Nonetheless, in specific acute settings, CT may also offer valuable diagnostic information.[38] A central aspect of neuroimaging in cSVD is the potential to discriminate between different subtypes of microvascular diseases. As will be discussed in more detail in the following sections, the likelihood of underlying ASC or CAA can be inferred from the distribution pattern of several MRI-visible lesions (Figures 1.1.C and 1.2).

1.2.5.1. Conventional MRI markers

1.2.5.1.1. Lobar ICH

ICH is the second most common form of stroke.[56] It is perceived on CT as spontaneously hyperdense expansive lesions located outside the basal ganglia, thalamus and brainstem, in the cortical or cortico-subcortical regions. On MRI, the signal intensity varies depending on the evolution time. Several neuroimaging and clinical findings may help distinguishing secondary from primary ICH and have been routinely incorporated into clinical practice.[57] Essentially all primary ICH are secondary to cSVDs. The location of the ICH, either lobar or deep, helps in distinguish the underlying microvascular pathology (Figure 1.1.C and 1.2).

Several neuroimaging features related to the morphology and attenuation of the acute hematoma predict early expansion rates, offering relevant prognostic information.[58] MRI markers of cSVD can predict ICH recurrence rates, and strong evidence point to cSS being the single most important neuroimaging predictor of recurrence.

Table 1.1. Criteria for *in vivo* diagnosis of Probable CAA
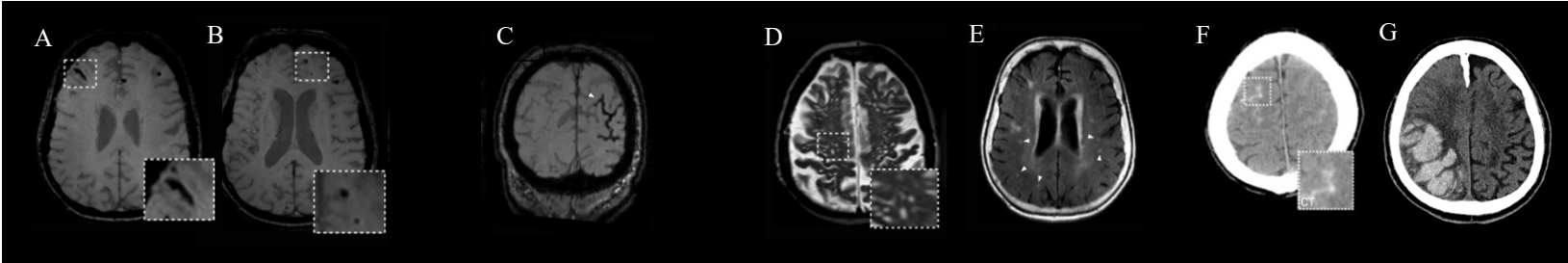
	Boston Criteria v1.0[32]	Boston criteria v1.5[34]	Boston criteria v2.0[35]	Edinburgh criteria[38]
Year	1995	2010	Soon-to-be-released	2018
Neuroimaging techniques required	MRI	MRI	MRI	CT
Clinical/Neuroimaging criteria for Probable CAA	Age ≥ 55 years Absence of other cause of hemorrhage Multiple hemorrhages (CMB/ICH) restricted to lobar, cortical and cortico-subcortical regions	Age ≥ 55 years Absence of other cause of hemorrhage or cSS Multiple hemorrhages (CMB/ICH) restricted to lobar, cortical, or cortico-subcortical regions OR Single lobar, cortical, or cortico-subcortical hemorrhage AND cSS (focal or disseminated)	Soon-to-be-released	Lobar ICH + at least 2 of the following: Subarachnoid hemorrhage APOE ε4 possession Finger-lilke projections
Neuroimaging features				

(A) Lobar intracerebral hemorrhage; (B) lobar cerebral microbleeds; (C) cortical superficial siderosis; (D) enlarged perivascular spaces in the centrum semiovale*[59]; (E) subcortical multi-spot white matter hyperintensities pattern*[60]; (F) subarachnoid hemorrhage[38]; and (G) finger-like projections[38].
* Markers potentially eligible for incorporation in the soon-to-be-released Boston criteria v2.0.

Figure 1.2. Conventional neuroimaging findings associated with cSVD
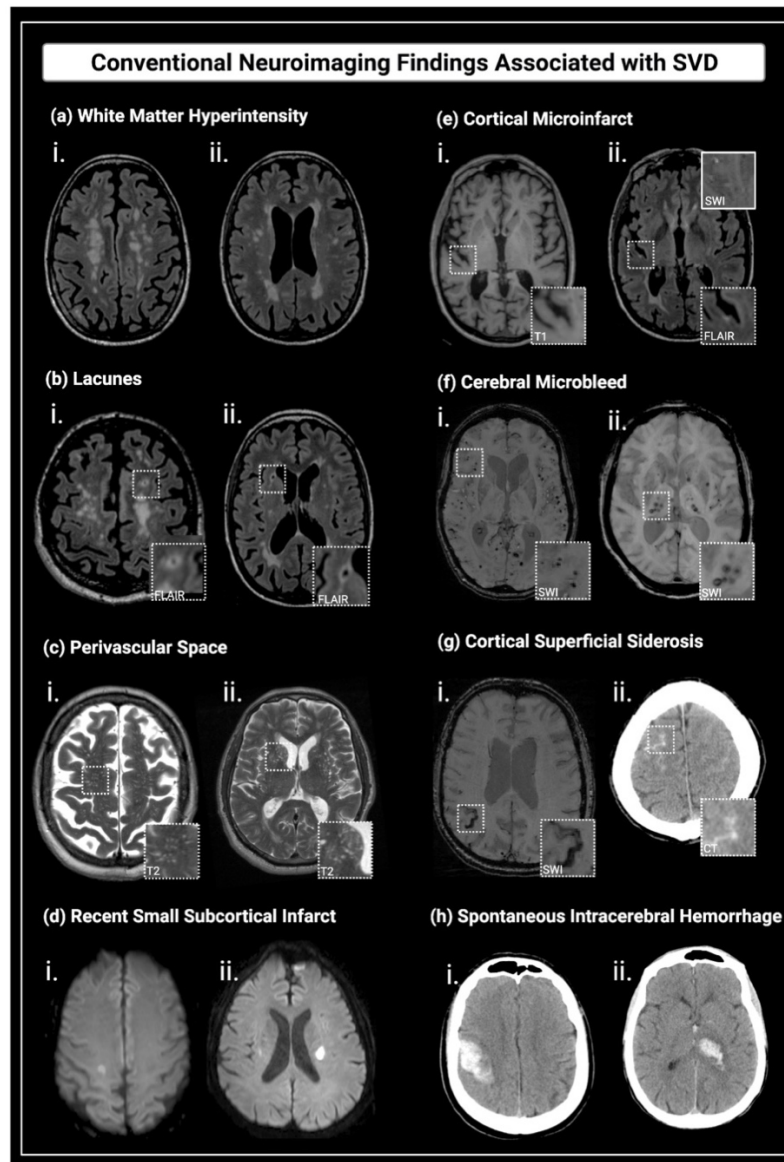
(A) WMH of presumed vascular origin are hyperintense on FLAIR (i. and ii.), and hypointense on T1-weighted images. **(B)** Lacunes of presumed vascular origin are fluid-filled subcortical cavities isointense to CSF, measuring 3-15mm, frequently with a hyperintense rim on FLAIR. (i.) Lobar lacune, more common in CAA. (ii.) deep lacune, typical of ASC. **(C)** PVS are small fluid-filled spaces isointense to CSF, that follow the course of a vessel. (i.) Visible PVS predominating in the centrum semiovale, characteristic of CAA (ii.) Visible deep PVS, in the basal ganglia, commonly seen in ASC. **(D)** Recent small subcortical infarcts typically show restricted diffusion (i. and ii.). **(E)** Cortical CMIs are lesions <5mm perpendicular to the pial surface, hypointense on T1 (i.) and hyperintense/isointense on FLAIR and T2-weighted images (ii.). **(F)** CMBs millimetric hypointense foci on SWI or T2 GRE images. In CAA, they are strictly lobar (i.), but occur in deep regions when related to ASC (ii.).**(G)** cSS are linear hypointense gyriform foci visible on SWI or T2 GRE images (i.). cSAH are visible as linear hyperdense foci on CT (ii.) or hyperintense foci on FLAIR. **(H)** ICH are perceived as focal hyperdense areas on CT (i. and ii.), with diverse signal on T1 and T2-weighted images, depending on temporal stages.

Lobar ICH is a key feature of the Boston and Edinburgh criteria, playing a central role in the *in vivo* diagnosis of CAA.[35,38] In addition, post-ICH cognitive impairment, either early or delayed,[61] is a common finding[62] and represents a major source of morbidity in surviving patients. Larger volumes and lobar location[63] have been associated with early post-ICH cognitive impairment, while the severity of WM disease was linked to delayed cognitive impairment.[61] Accordingly, in a study following 612 ICH-survivors, the presence of several neuroimaging markers of cSVD was also associated with post-ICH cognitive performance and predicted new-onset dementia.[64]

1.2.5.1.2. Lobar CMB

CMBs are defined as small foci of chronic blood metabolites visible within the brain parenchyma.[65,66] CMBs appear in MRI sequences sensitive to susceptibility effects as foci of hypointense signal typically measuring few millimeters in diameter.[31,65] Importantly, due to the *blooming* effect and larger coverage area, CMBs are more easily detected through MRI than histopathology.

Cortical CMBs have heterogeneous pathological substrates, that range from small focal hemorrhages in different stages of evolution, to vasculopathies and chronic ischemic injury, without significant tissue damage.[67] Nonetheless, the vast majority represent "frank" hemorrhages.[68] They are associated with extensive vessel wall remodeling and focal loss of $A\beta$, and likely occur at a late stage in the progression of CAA.[69] Importantly, it appears that CMB's impact on tissue integrity is small, which supports the modest cognitive associations thus far reported.[31]

Several technical parameters influence CMB detection on MRI, including: pulse sequences (gradient-recalled echo [GRE] is considered the optimal pulse sequence for CMB visualization), echo time (longer TEs enlarge the susceptibility effect), spatial resolution (thinner slices increase sensitivity), magnetic field strength (higher field strengths add sensitivity), and post-processing techniques (susceptibility-weighted imaging [SWI] outperforms regular GRE sequences).[66]

The location of CMBs contributes to determining the underlying microvascular pathology. While CAA causes CMBs restricted to cortical, cortico-subcortical and lobar areas, ASC manifests with CMBs in deep regions, such as the basal ganglia, thalamus, and brainstem. Individuals with CMBs located in both deep and lobar regions may be affected by severe ASC or concomitant CAA and ASC.[65] The pooled prevalence of CMBs in a meta-analysis involving 7159 CAA patients was 52%.[43] In population-based studies, the prevalence of CMBs in elderly

groups ranged between 5 and 35%, with 48-79% lobar and 32-52% deep.[65] In samples with ischemic stroke and spontaneous ICH, the prevalence of CMBs at estimated in 33% and 60%, respectively.[65]

Lobar CMBs have significant diagnostic value for CAA, as a pivotal marker employed in the well-established Boston criteria.[35] They increase the risk of first-ever and recurrent ICH and may be associated with an increased risk of ischemic stroke.[65,70] Their association with cognitive outcomes is less clear, usually small and inconsistent.[71] For instance, in a systematic review involving 8736, CMBs were not associated with either increased risk of dementia or AD.[72] However, some population-based studies report cognitive associations.[65,70,73] Specifically for lobar CMBs, a recent systematic review including 6 studies reported significant associations with reduced executive function and visuospatial ability, but not with language or memory.[74]

1.2.5.1.3. cSS/SAH

cSS is yet another bleeding manifestation of CAA, defined as curvilinear foci of hypointense signal visible on blood-sensitive MRI sequences along convexity gyri. It represents the chronic phase of acute convexity SAH, in the form of iron-positive deposits located in the subarachnoid space and superficial cortical layers.[75] It is associated with recruitment of reactive astrocytes and the presence of cortical microinfarcts, suggesting that it may potentially trigger ischemic injury in the underlying cortical tissue.[75] Interestingly, cSS seems to be more strongly linked to CAA in the leptomeningeal than cortical vessels, and its severity is not associated with CMBs.[75] The pooled prevalence of cSS in CAA patients, according to a recent meta-analysis, is estimated at 49%.[43] Considered one of the most clinically meaningful markers of CAA, cSS increases the sensitivity of MRI in detecting CAA pathology,[34] and is considered the most likely cause of transient focal neurological episodes (TFNEs).[50] Besides its diagnostic value, cSS represents the strongest neuroimaging predictor of first-ever and recurrent lobar ICH, with poor functional outcome.[76,77] In a multicenter cohort of 302 possible and probable CAA patients followed over 12 months, ICH recurrence rates were 17% for the subgroup with cSS and 4% for those without it.[77] In a recent meta-analysis, cSS was the only CAA marker that predicted recurrent ICH.[43] Not just the presence, but the severity[78] and progression of cSS predict the occurrence of symptomatic ICH.[76] The acute form of leptomeningeal bleeding, namely CT- and MRI-visible SAH, also predict recurrent ICH and were associated with concomitant dementia.[79,80] cSS' cognitive impacts are less evident, but studies suggest an association with post-ICH cognitive impairment.[62]

1.2.5.1.4. WMH

WMH of presumed vascular origin represent areas of increased signal in T2-weighted images.[81] It is the most common and often earliest marker of cSVD and has been frequently related to chronic hypoperfusion, impaired CVR and BBB leakage, despite the limited evidence supporting a definitive causal relationship.[31,82] In CAA, WMHs appear to be ischemic in nature and correlate with the burden of vascular Aβ and cortical Pittsburg compound B (PiB, a nuclear medicine marker of amyloid) uptake.[71,83,84] Other potential mechanisms such as dysfunction of the glymphatic pathway, venous collagenosis, impairment of oligodendrocyte precursor cells, and Wallerian degeneration have also been more recently suggested in cSVD-related WMH.[31,47,82,85,86] In terms of histopathological substrates, WMHs are heterogeneous and may present different degrees of gliosis, demyelination, dilated perivascular spaces, loss of oligodendrocytes and axons.[31,47,87] Fibrohialinosis and arteriolosclerosis appear to be the main vessel alterations underlying WMH,[87] and the precise mechanisms and neuropathological correlates in the context of CAA remain to be determined.[31]

More than half of CAA patients present moderate-to-severe WMH Fazekas score.[43] Similar to CMBs,[88] WMHs in CAA have been found to have a posterior predominance,[89–91] in accordance with the posterior predilection of CAA pathology. However, more recent investigations point to another pattern of WMH distribution as more strongly linked to CAA.[60] Charidimou *et al.* studied 456 ICH patients and observed that multiple WMH subcortical spots were more prevalent among CAA- than ASC-related ICH subjects, and were associated with lobar CMBs and enlarged PVS in the centrum semiovale.[60] This pattern of distribution has thus been considered a promising feature for the soon-to-be-released Boston criteria v2.0.[35] The pattern of peri-basal ganglia WMH distribution was more strongly associated with ASC-related ICH.[60] Strong scientific evidence supports a link between greater WMHV and worse cognitive performance, though with relatively small effect sizes.[92] Progression of WMH burden correlates with cognitive decline, incident dementia, stroke and death.[92] Data specific for CAA is scarce,[71] but pre-ICH cognitive impairment has been associated with advanced WMH in CAA individuals.[89] Also, WMHV was associated with processing speed in another CAA sample.[52] More recent studies, however, have failed to detect a significant association between WMHV and cognitive impairment in CAA.[53,93]

1.2.5.1.5. Lobar lacunes

Lacunes of presumed vascular origin represent cavities filled with fluid in the white matter or deep gray matter, that substitute tissue destroyed by ischemic or hemorrhagic injury, and are

surrounded by reactive astrocytes, myelin and axonal loss, with significant perilesional tissue disruption.[31,47,87] They are perceived on MRI as 3-15 mm cavities with CSF-like signal, often surrounded by a halum of increased signal on FLAIR.[81] The acute phase of lacunar infarcts shows restricted diffusion and is called "recent small subcortical infarcts".[81] Lacunes in the centrum semiovale have been more often found in CAA-related than ASC-related ICH patients.[94] The prevalence of lacunar infarcts in CAA patients is estimated to be 30%.[43]

In elderly populations and samples with cSVD, incident lacunes have been associated with worse cognitive performance, incident dementia, stroke, heart failure, and death.[95] In patients with ICH, lacunes were associated with worse functional outcomes and increased recurrence.[96] Specific prognostic data on CAA patients is scarce.

1.2.5.1.6. Cortical CMI

Cortical CMI are the most widespread form of brain infarct, commonly found in subjects with dementia and/or cerebrovascular diseases, and more frequently detected in CAA than non-CAA individuals.[71,97] CMIs can be visualized in diffusion-weighted imaging (DWI) during acute phases and in high-resolution structural MRI in chronic phases, and have well-established visual detection criteria.[97] Contrary to CMBs, the vast majority of CMIs are undetectable during life, due to their small sizes. Only CMIs measuring 1-2mm in diameter can be detected on MRI, with increased sensitivity in higher field strengths.[97]

In CAA, cortical microinfarcts are thought to result from increased vascular deposition of Aβ in penetrating cortical arterioles, with loss of smooth muscle cells and presumed local vessel stiffening.[31,69] The prevalence of cortical CMIs in a sample of 102 CAA patients was estimated at 39%.[98] Acute DWI positive microinfarcts are particularly common in patients with CAA-related ICH, even after the event.[71,99] Despite the small numbers detected through MRI, cortical CMIs show strong cognitive associations. This indicates that the burden of CMI is probably much higher in pathology and causes a disruptive effect on surrounding tissues severe enough to compromise connectivity. In CAA, CMIs have been associated with performance in executive function and processing speed.[98] Also, CAA patients with CMIs have higher cumulative dementia rates than those without them.[98]

1.2.5.1.7. Enlarged perivascular spaces in the centrum semiovale

PVS, also called Virchow-Robin spaces, represent fluid-filled cavities that surround blood vessels (mainly arterioles) and act as a route to drain fluid and waste metabolites from the interstitium.[26,100] Widened PVS are likely secondary to the obstruction of perivascular pathways

by waste products, such as Aβ, and cell debris.[26,101] Impaired vascular function (i.e. vasomotion), may also contribute to dysfunctional perivascular flow, thus promoting dilation of PVS.[23] On MRI, they appear as elongated or round foci of CSF-like signal intensity, measuring, in general, less than 3 mm, and often without hyperintense margins.[81] Visual rating scores and automated techniques have been proposed to assess PVS.[59,100] They become more visible with increased age,[100] and their distribution pattern is indicative of the underlying microvascular pathology. Individuals with CAA-related ICH have visible PVS located predominantly in the centrum semiovale (CSO-PVS), while subjects with hypertensive ICH have more PVS visible in the basal ganglia (BG-PVS).[102] In a recent meta-analysis, the pooled prevalence of high-grade CSO-PVS and BG-PVS in CAA patients were estimated at 56% and 21%, respectively.[43] This specific spatial pattern led CSO-PVS to be considered as a potential new marker in the updated, soon-to-be-released, Boston criteria v2.0.[35]

PVS is considered a marker of brain health.[31] However, other than its potential diagnostic utility, evidence on PVS's prognostic value is still scarce, especially in CAA, and its clinical value remains undefined. A recent meta-analysis found that PVS were not associated with post-ICH prognosis,[96] but previous studies indicate an association between high burden of CSO-PVS and risk of recurrent ICH.[103,104] Recent investigations in CAA do not report a significant association between PVS and cognitive performance,[53,105] but in population-based studies, higher burden of PVS has been associated with worse cognition and increased risk of dementia.[106]

1.2.5.1.8. Atrophy

It is well-established that brain volume is lower in individuals with cSVD compared to controls and progresses over time.[107–109] Specific cSVD-related brain lesions have been linked to brain atrophy, such as WMH and lacunes, thought to cause Wallerian degeneration, with consequent loss of brain and gray matter (GM) volume.[4,109,110] Optimal assessment of the degree of brain atrophy is currently achieved through automated quantitative softwares, using 3D T1-weighted images. Technical recommendations to assess brain volume in the context of cSVDs have been recently published.[109] To avoid bias introduced by different head sizes in cross-sectional analyses, measures of brain volume should be controlled for total intracranial volume. Longitudinal pipelines that perform co-registration of images across different time points may also reduce variability.[107]

Importantly, atrophy is the common endpoint of most pathologies affecting the central nervous system, which may explain its strong clinical associations. In patients with ICH, brain atrophy

has been associated with worse functional outcomes and mortality.[96] In cSVD patients, atrophy correlates with cognitive performance,[108,109] and often outperforms other neuroimaging markers.[109] However, disentangling which component of the atrophy is attributed to neurodegenerative or vascular pathologies remains challenging. For instance, in a recent systematic review, none of the studies investigating brain atrophy in cSVD samples controlled for AD (either through cerebrospinal fluid [CSF] biomarkers or amyloid-positron emission tomography [PET]).[109] This distinction may rely on spatial patterns. In amyloid-negative cSVD patients, GM loss predominated in the frontal lobes,[110] while AD-related volume loss is typically more pronounced in parietal and temporal regions.

Patients with Dutch-type CAA (D-CAA) and sporadic CAA have thinner cortices than healthy controls.[111] In D-CAA, the association with cortical thickness was mediated by vascular dysfunction, in the form of CVR measured through blood-oxygen-level-dependent time-to-peak (BOLD-TTP).[111] Patients with sporadic CAA also present greater WM loss in comparison to controls and AD subjects, with more pronounced differences in the posterior occipital regions.[112] In the same study, WM volume (WMV) was independently associated with executive function.[112] A recent case-control study observed that, alongside CVR and a DWI-based marker, atrophy mediated the effect of CAA on cognition.[93] In a study comprising 158 non-demented probable CAA patients, medial temporal atrophy independently predicted conversion to dementia, indicating that there is likely a contributing role of AD pathology.[53] In a case-control study with 58 non-demented CAA patients and 138 cognitively normal controls, TBV was the only neuroimaging marker associated with executive function and processing speed.[51]

1.2.5.2. Burden scores

In an attempt to better capture the cumulative effect of multiple cSVD-induced brain lesions and assess their total impact in a more pragmatic way, different burden scores have been developed merging several imaging markers. As mentioned before, individual markers of cSVD yield limited clinical associations. By employing burden scores, authors aimed to increase the power to detect such associations.

One of the earliest scores was proposed in 2013, called the "Total SVD score", ranging from 0 to 4.[113,114] This score includes the following MRI features: ≥1 lacunes; ≥1 CMB; moderate to severe BG-PVS; and periventricular WMH Fazekas 3 and/or deep WMH Fazekas 2-3.[115] It has been extensively applied in research, yielding relevant clinical associations. For example, it predicted mortality in population-based studies;[116] risk of ICH after venous thrombolytic

therapy,[117] and in patients with atrial fibrillation on anticoagulants;[118] poor functional outcomes post-ICH and ischemic stroke;[119,120] and mild cognitive impairment,[121] among others.

An adapted version of the total SVD score was developed and validated specifically for CAA in 2016, including the MRI markers most relevant for the disease.[122] This score incorporated lobar CMBs, cSS, CSO-PVS, and WMH, ranging from 0 to 6 points.[122] Upon development, it correlated with CAA histopathologic changes (i.e. fibrinoid necrosis and vessel-wall splitting) and symptomatic ICH.[122] In the Rotterdam cohort, a population-based study, the same CAA score was associated with cognitive impairment and increased risk of stroke, dementia and death.[123]

1.2.5.3. Advanced MRI techniques

Although conventional MRI markers are readily available through visual ratings, their prognostic value, especially cognitive associations, are inconsistent and yield small effect sizes in general. These markers are limited in their ability to detect microstructural damage and fail to capture the perilesional and remote abnormalities that greatly contribute to cognitive symptoms. Conversely, advanced techniques have much to offer: their quantitative nature allows for increased statistical power; they are sensitive to a large spectrum of tissue abnormalities that cover more than only MRI-visible changes; and they reflect hallmark pathological features.

Exploring in detail state-of-the-art MRI techniques in cSVD is beyond the scope of this chapter, for which the reader is referred to recent reviews on the subject.[124,125]

As previously discussed, NVU dysfunction is considered an early and pivotal step in the pathogenesis of SVD[126] associated with BBB leakage, impairment of cerebrovascular reactivity and hypoperfusion. Therefore, MRI techniques capable of detecting these early pathological changes are considered promising for mechanistic studies and application as secondary endpoints in future clinical trials.

The technique of choice to quantify BBB dysfunction in cSVD is dynamic contrast-enhanced MRI (DCE-MRI), through which slow rates of gadolinium-based contrast agent tissue extravasation can be detected and quantified via T1-shortening effect on tissue water.[127] Several studies suggest that BBB leakage is increased in patients with cSVD.[128,129] It is associated with WMH burden,[130] total cSVD scores,[131] worse cognitive performance,[130] and may predict worse functional outcome.[132] However, results are still significantly inconsistent across studies,[107,127,133] and evidence of repeatability and reproducibility of the method are missing.[107,127] Furthermore, specific data on CAA is scarce. Recommendations for obtaining

BBB leakage measurements have been recently proposed, in an attempt to standardize the technique and reduce heterogeneity in future studies.[127]

Impaired cerebral blood flow (CBF) is another important feature of cSVD pathophysiology, that has been investigated through neuroimaging. Whole-brain or tissue-resting CBF represents a snapshot of the perfusion status in a specific time and brain region but ignores the expected minute-by-minute and regional variations.[134] Several imaging techniques can be applied to measure whole-brain CBF, accounting for large methodological variability in the literature: phase-contrast MRI, arterial spin labelling (ASL)-MRI, dynamic-susceptibility contrast (DSC)-MRI, PET, single-photon emission computerized tomography, Xenon-CT, CT perfusion, and transcranial Doppler ultrasound.[134] While evidence suggests that CBF and cSVD severity are negatively associated,[134] there are discordant results[135–137] and the temporality of the association is under debate.[134,138] It remains unclear whether reduced CBF is secondary to cSVD severity, contributes to it, or has a bidirectional association.[139] Nonetheless, whole-brain CBF has been found to accelerate cognitive decline and increase the risk of dementia in the population-based Rotterdam Study.[140]

The adequacy of tissue-level blood supply can be better assessed by investigating cerebrovascular reactivity (CVR), that is, whether the arterioles vasodilate efficiently in response to increased blood supply demand (i.e. increased neuronal activity, or metabolic/vasodilatory challenges or maneuvers).[4,107,141] There are multiple imaging techniques available to assess CVR, but blood oxygen level-dependent (BOLD)[141] and ASL[142] are considered the most promising ones, evaluated in response to a stimulus, such as breathing CO_2.[143] Though literature about CVR in cSVD is still scarce and inconsistent, evidence suggests that reduced white matter CVR is associated with increased WMH volume,[144] with subtle microstructural disruption in NAWM[145] and may precede progression to WMH.[146] Recent evidence suggests that lower CVR is associated with cognitive impairment, and this relationship was mediated by periventricular WMH.[147] In CAA, CVR in response to visual stimulation, measured through BOLD-fMRI in the occipital lobes, showed reduced amplitude and prolonged time to peak compared to controls, and correlated with WMHV.[148] The amplitude of the occipital BOLD signal in response to visual stimulation was found to decrease significantly in CAA patients, compared to controls, but did not correlate with longitudinal changes in CMBs or WMHV.[149] BOLD fMRI slope was even used as a surrogate marker for an early-phase clinical trial investigating the safety and preliminary efficacy of immunotherapy with ponezumab in 24 CAA patients.[150]

Besides offering an in-vivo evaluation of cerebral hemodynamics, advanced MRI also provides relevant insights into microstructural integrity and connectivity. Growing evidence suggests that cSVD lesions affect cognition via network disruption. Therefore, methods that directly assess the integrity of network connections may converge the information of several markers with increased power to reflect clinical endpoints. The two MRI methods currently applied to investigate connectivity are: resting-state functional MRI (rs-fMRI) and diffusion imaging. The latter will be discussed in more detail in section 1.3.2.

Rs-fMRI is a technique capable of estimating the disruption of brain networks.[47] By assessing the temporal correlations of hemodynamic changes in different regions of the brain in a resting state, this technique can estimate functional connectivity.[151,152] While studies applying rs-fMRI in cSVD are still in early development, initial results suggest that the main dysfunctional regions in these patients are related to the default mode network, comprising the medial prefrontal cortex, posterior cingulate cortex, precuneus, anterior cingulate cortex, and parietal cortex.[47] With the standardization of processing techniques and image acquisition, it is likely that functional imaging markers will become more useful in the field in the future.

Despite their proven usefulness in the research field, experts' consensus advocate that none of these techniques is yet ready to be applied for diagnosis or to be used in clinical practice.[153]

1.3.   Vascular contributors to cognitive impairment and dementia

Dementia is defined as a progressive and irreversible decline in cognitive functions that compromise activities of daily life.[46] It is a public health priority worldwide, responsible for significant economic and social costs,[154] and expected to increase due to improving life expectancy and aging of the population.[155]

Vascular cognitive impairment (VCI) represents conditions in which neurovascular pathologies contribute to mental disability.[156] After AD, vasculopathies are the most prevalent independent contributors to cognitive deficits and are responsible for at least 20% of dementia cases.[156] However, it has become clear that age-related cognitive decline is typically driven by co-occurring vascular and neurodegenerative diseases, observed in the majority of demented patients.[157] cSVDs are considered the most prevalent vascular contributors to age-related cognitive impairment.[45,158]

Though there have been several attempts to determine which single or combination of neuroimaging markers can define with reasonable certainty an underlying vascular pathology in the context of cognitive decline, no feature can be considered pathognomonic.[54] For instance, typical cSVD conventional MRI features such as WMH, CMBs and PVS can also be seen in non-vascular pathologies, such as demyelination/leukodystrophies, traumatic brain injury/sepsis and inflammatory processes, respectively.[65] Moreover, advanced techniques such as diffusion imaging or fMRI are also not specific to vascular pathology. Therefore, clinical context is paramount when interpreting neuroimaging findings.

Though this remains a controversial issue, some studies and consensus advocate that cSVD-related VCID may occur in the presence of: (1) a single strategically placed lacunar infarct or hemorrhage (thalamus or basal ganglia), (2) multiple (>2) non-brainstem lacunes, (3) multiple (>2) intracerebral hemorrhages, or (4) extensive and confluent white matter lesions.[54,159,160] Since these criteria were suggested, important advances have been made in the neuroimaging field, aiming for the standardization of definitions,[81] harmonization of imaging protocols,[81,107,161] and proposal of a framework for neuroimaging biomarker development,[107] with significant impact on research and, to some extent, in daily practice.

1.3.1. Potential mechanisms of SVD-related cognitive impairment

To understand the mechanisms underlying cSVD-related cognitive impairment, we must remember that cognition depends on the constant exchange of information between brain regions that are anatomically and functionally linked.[2] As previously discussed, cSVD-related brain lesions arise from hemorrhagic or non-hemorrhagic (presumably ischemic) mechanisms, with the latter showing stronger associations with overall cognitive dysfunction. Several studies support the notion that cSVD lesions affect cognition by impairing complex networks, resulting in a disconnection syndrome.[47] By causing micro and macrostructural tissue abnormalities, cSVD lesions disrupt cortical-subcortical and cortical-cortical connections and affect synaptic transmissions (Figure 1.1.D). Damage to white matter tracts can further impair functional connectivity within networks related to attention and executive functions.[47]

The anatomical location of vascular lesions also plays an important role in the development of VCID and helps explain its heterogeneous neuropsychological manifestations.[4] Several studies point to strategic locations associated with global post-stroke cognitive deficits, such as: thalamus, internal capsule, basal ganglia, corpus callosum,[162] cingulate cortex, angular gyrus, frontal subcortical areas and specific white matter tracts of the left hemisphere.[163] Interestingly,

cSVD lesions often affect centrally located and richly interconnected regions, which are responsible for the integration of information.[47]

In addition to causing focal disturbances, subcortical lesions trigger secondary degeneration of long and short white matter tracts, leading to adjacent and remote abnormalities, that culminate in white matter atrophy, cortical thinning, and loss of function.[4] This observation further emphasizes that cSVD affects cognition not only through focal disturbances but also through its whole-brain effects (Figure 1.1.D).[47]

1.3.2. The quest for the ideal neuroimaging biomarker in the context of VCI.

Despite the enormous clinical relevance and economical costs associated with VCI, there are still no specific disease-modifying therapies available. Management of these patients relies mainly on prevention and treatment of vascular risk factors (see details in Appendix 1). While this can be attributed to our limited (though ongoing) understanding of the pathophysiology of cSVDs, the lack of fully validated neuroimaging markers fit for large clinical trials represents a major obstacle to future therapeutic development.

An unmet need in the imaging field is how to measure the widespread brain injury that underlies cSVDs in a feasible and clinically meaningful way. As previously discussed, though conventional MRI markers (i.e., WMH, lacunes, and hemorrhages) play a pivotal role in diagnosing cSVD and other WM disorders, they are less sensitive to subtle changes in the NAWM and usually yield weak and inconsistent cognitive associations. The quest for the ideal MRI marker to fit the critical role of a reliable outcome measure in clinical trials has become a research priority in the field, and the future development of disease-modifying therapies depends on it. When used as surrogate markers for clinical endpoints, neuroimaging features can greatly reduce sample sizes, time of follow-up and, hence, the costs of clinical trials, improving the feasibility of studies.[107]

This scientific gap has prompted experts in the field to organize national and international consortiums aiming for the standardization and harmonization of neuroimaging techniques for the study of VCI. A first step came in 2013, with the publication of a consensus on neuroimaging standards for research on cSVD and related cognitive impairment (STRIVE), which constituted a guideline on the definitions, terminology, reporting standards, and acquisition protocols.[81] However, there was still no consensus in the scientific community concerning which MRI markers were already fit for specific purposes, and which were the most promising ones. To help with this choice and to foment directed research, an international group of experts published in 2019 a framework for developing and validating MRI biomarkers in

VCID.[107] According to this framework, validation of a neuroimaging marker as a surrogate for clinical endpoints requires the fulfillment of 8 steps, namely: proof of concept (the marker must measure a specific abnormality attributed to cSVDs), proof of principle (the measured marker must differ significantly in patients with cSVDs compared to those without cSVDs), repeatability (measurements in the same subject using the same scanner in different moments must be similar), reproducibility (measurements in the same subject using different scanners must be similar), proof of effectiveness (proof of principle demonstrated in large multicenter studies), longitudinal (the marker must have well-established and documented changes over time), monitoring (longitudinal changes in the marker must reflect progression of cSVDs), and, finally, surrogate (longitudinal changes in the marker must reflect clinical outcomes related to cSVDs).[107]

In light of the aforementioned framework, the same group of experts reviewed the literature to address which steps had already been fulfilled for each cSVD MRI marker (i.e. lacunes, WMH, CMB, PVS, atrophy, DTI, perfusion, CVR, and BB integrity).[107] None of them fulfilled the last surrogate step.[107] The two biomarkers in the most advanced stage of validation were atrophy and DTI.[107] As discussed previously, while atrophy represents a promising feature, its nonspecific nature and great influence from neurodegenerative diseases make it a less promising marker. Most studies that reported atrophy's clinical associations in cSVD did not control for AD pathology.[109] On the other hand, DWI has several features that align with current scientific needs and priorities. First, diffusion properties of the water molecules inside brain tissues reflect microstructural integrity and correlate with significant histopathological changes, such as tissue rarefaction, axonal and myelin density.[164] Second, evidence suggests that diffusion abnormalities are more sensitive and predominantly driven by cSVD compared to AD pathology.[165,166] Third, these markers are sensitive to early and diffuse abnormalities not detectable through conventional MRI,[47] and outperform MRI-visible lesions[167,168] by explaining more variance in cognition.[47,169] Fourth, diffusion measures show good reproducibility and repeatability.[107] Finally, longitudinal changes in these markers appear to reflect disease progression.[107]

Despite all these advantages, the widespread use of diffusion markers is hampered by the broad range of post-processing options, which can be labor-intensive and time-consuming. The simplest and most commonly used model to characterize diffusion processes is the diffusion tensor model (DTI). This model quantifies several commonly used diffusion scalar measures, such as fractional anisotropy (FA) and mean diffusivity (MD). The typically observed cSVD pattern of brain injury is characterized by an increase in the amount of water diffusion

(increased MD) and a reduction in its directionality (reduced FA).[170] Studies using the more complex, and probably more realistic, free water diffusion model have shown that cSVD-related diffusion abnormalities are mainly driven by increased extracellular water, and less by alterations in the tissue compartment.[170]

Several other post-processing techniques can be used to obtain more refined measures. For instance, the combination of tractography and graph theory led to the development of valuable connectivity metrics. Network efficiency and other graph-based measures can predict cognitive performance,[166,168,171,172] faster cognitive decline,[168] conversion to dementia,[171,173] and even all-cause mortality in cSVD populations.[174] Furthermore, a higher burden of cSVD MRI lesions is associated with lower network efficiency,[172,175] which mediates the relationship between cSVD and cognition.[176,177] These findings support the pivotal role of network disconnection in the genesis of VCID.

Several DWI post-processing techniques have been used in the context of CAA. In 2006, Salat *et al.* used voxel-based and region-of-interest (ROI) analyses to evaluate the spatial distribution of WM damage in 11 CAA patients, compared to 13 controls.[178] They observed a reduction in FA values in the temporal WM and in the splenium of the corpus callosum.[178] MD changes were not significant. In 2008, Viswanathan *et al.* observed that an increase in the apparent diffusion coefficients (ADC) in the unaffected hemisphere independently predicted ICH-related cognitive impairment.[179] Reijmer *et al.* observed lower network efficiency measures in CAA compared to control patients, with abnormalities more pronounced in posterior regions. Worse network efficiency was associated with increased cortical amyloid levels (PIBPET), WMHV, and CMB numbers.[172] It also correlated with worse processing speed and worse performance in executive function, as well as lower gait speed.[172] Global network efficiency in CAA patients were found to decline over time from posterior to frontal connections.[180] Progressive decline in posterior connectivity correlated with greater progression of occipital cortical thickness.[181]

More recently, automated global DTI-based markers have been developed.[167,169,182] Among them, peak width of skeletonized mean diffusivity (PSMD) is considered a highly promising metric, that aligns with current scientific needs. It is fast and fully automated and demonstrates consistent cognitive associations. It runs in relatively simple DTI data, that is, it does not require highly complex acquisitions. However, knowledge about PSMD is still limited in the scientific community, and data on its utility in the context of CAA, the second most common form of cSVD, is scarce.[183] Thus, we set out to critically evaluate PSMD's role as neuroimaging biomarker of VCID and investigate its potential applications in CAA. To this end, in the next section, we will review, in detail, the technical aspects of this novel biomarker.

1.4. Peak Width of Skeletonized Mean Diffusivity

Peak width of skeletonized mean diffusivity is a DTI-based marker developed in 2016 by Baykara et al.[169] It was envisioned as a robust marker that could quantify cSVD burden, be applied to large samples, and be eventually incorporated into the clinical routine.[169] It relies on the skeletonization of the white matter tracts and histogram analysis, using a freely available pipeline.[154] This marker can be rapidly computed,[154] offers high interscanner reproducibility[154,168,169] and small sample size estimates,[154] showing consistent cognitive associations across different SVD and aging populations.[154,168,170–173]

1.4.1. Technical overview of PSMD

A shell script for calculating of PSMD was developed and made publicly available (www.psmd-marker.com) by Baykara *et al.* in 2016.[169] The fully automated PSMD pipeline runs in approximately 7-15 minutes on a standard desktop computer.[169,184] It combines three main elements: the skeletonization of white matter tracts, application of a custom mask, and histogram analysis.[169] Each step is described in detail in the following sections, discussing aspects relevant for the generalizability and interpretation of the marker.

1.4.1.1. Prerequisites

The pipeline is regularly updated and is currently in its fourth release (v1·8·2; https://github.com/miac-research/psmd/releases). It requires the installation of FMRIB Software Library (FSL, http://www.fmrib.ox.ac.uk/fsl) or the use of the provided Singularity container. It is validated for commonly used single-shell DWI acquisitions, that is, data acquired using only one b-value, other than zero. Ideally, the DWI protocol should include a minimum of 20 diffusion-encoding gradients, b-value between 700 and 1200 s/mm^2, and isotropic resolution of around 2 mm (http://www.psmd-marker.com/usage/).

1.4.1.2. Preprocessing

DWI images are frequently impacted by multiple artifacts, such as motion, eddy-currents, and susceptibility-induced off-resonance fields,[185] which, if not adequately corrected or controlled for, affect DTI indices and may compromise group comparisons and correlations.[185–187] While some measures can be taken during the acquisition process to reduce these artifacts,[188,189] post-

acquisition techniques are more widely used since they can be retrospectively applied and do not require longer scan times.[190]

The completely automated PSMD pipeline applies commonly used methods to correct for motion and off-resonance effects in DWI (eddy currents and motion correction, *eddy_correct*;[191] https://fsl.fmrib.ox.ac.uk/fsl/fslwiki/eddy), followed by brain extraction (*BET*;[192] https://fsl.fmrib.ox.ac.uk/fsl/fslwiki/BET/UserGuide), and tensor fitting (*DTIfit* [weighted linear least squares approach];[193,194] https://fsl.fmrib.ox.ac.uk/fsl/fslwiki/FDT/UserGuide#DTIFIT) (Figure 1.3.A). While the standard pipeline is suited for a broad range of acquisition protocols, researchers can also use more elaborate and effective imaging correction methods[190] (e.g., outlier replacement,[195] slice-to-volume corrections,[196] and susceptibility-by-movement interactions correction[197]) better fitted for specific DWI protocols. The preprocessed images can then be fed into the PSMD pipeline, which is versatile and allows for inputting unprocessed raw DWI data, DWI data corrected for artifacts (preprocessed), or already tensor-fitted FA and MD maps.

1.4.1.3. Skeletonization

A key characteristic of PSMD is that it is computed from a WM skeleton rather than from the whole brain or the entire WM like other global DTI measures. This choice was made as an attempt to reduce contamination from cerebrospinal fluid (CSF),[169] recognized as a major source of bias in diffusion studies.[198–200] WM and gray matter volumes decrease significantly with age, introducing atrophy-based CSF partial volume effects on DTI measures.[200] Mean MD is expected to increase, and mean FA decreases if voxels containing CSF are included (even partially) in DTI analyses.[200] Naturally, the morphology of MD histograms is also impacted if voxels with high MD values are included in the region-of-interest (ROI).

Specifically, periventricular and superficial brain areas are more susceptible to contamination by nature of their proximity to the CSF. Therefore, restricting the analysis only to voxels within a WM skeleton efficiently excludes areas more prone to CSF contamination[169] while increasing statistical power.[201]

Skeletonization of the main WM tracts in the PSMD pipeline is obtained through tract-based spatial statistics (TBSS), as implemented in FSL.[169] Smith *et al.* developed this technique in 2006 as an attempt to address challenges related to applying voxel-based morphometry (VBM) on diffusion data.[202] By combining tractography principles with VBM techniques, TBSS was designed to overcome alignment and smoothing issues.[202]

Figure 1.3. Overview of the PSMD pipeline
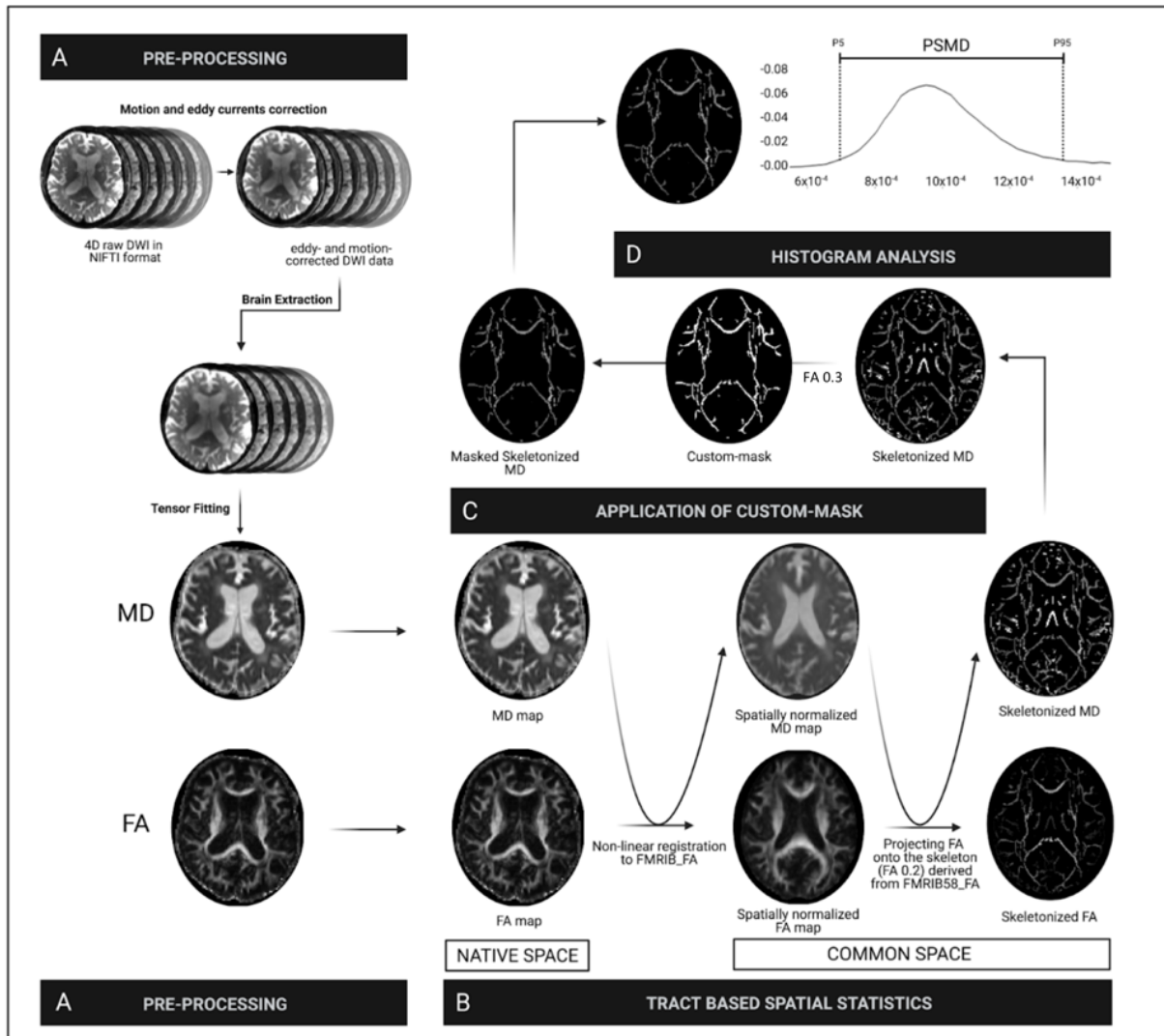
Source: Zanon Zotin MC & Yilmaz P et al. 2022, under review.

A. The preprocessing steps included in PSMD's pipeline perform motion and eddy-currents correction, brain extraction and tensor fitting. The computation of PSMD further relies on three cornerstones: skeletonization, application of a custom-mask and histogram analysis. B. The skeletonization procedure is performed through tract-based spatial statistics, by registering the FA map to common space (FMRIB 1 mm FA template) and projecting it onto the skeleton (derived from the same FA template, thresholded at 0.2). The same transformation matrices are used for MD data, to obtain a skeletonized MD map. C. This map is further masked using the template thresholded at FA 0.3, and a custom-made mask. D. Finally, the width of the histogram derived from the MD values of all the voxels included in the skeleton, that is, the difference between percentiles 95 and 5, represents the peak width of skeletonized mean diffusivity. Created with Biorender.

In summary, TBSS's skeletonization process involves aligning the FA images from all subjects to the same target and averaging them into a mean FA image used to generate a tract skeleton, in which voxels with higher FA are thought to represent the center of WM tracts.[202] Each patient's FA map is then projected onto this skeleton, creating skeletonized FA images that can finally be used for voxelwise statistics.[202]

The PSMD pipeline takes advantage of this skeletonization procedure but is intended to provide a single value representative of the microstructural integrity of the main WM tracts of the brain rather than data for voxelwise analysis. Therefore, instead of performing a group analysis of FA maps from all subjects, the pipeline applies TBSS individually to each subject, always using the same tract skeleton template derived from the FMRIB58 mean FA image thresholded at 0.2 (Figure 1.3.B). The FA-derived transformation parameters are applied on the MD maps to obtain MD skeletons, further masked with the same template thresholded at 0.3 to again decrease the likelihood of CSF partial volume contamination. Using the same fixed target and skeleton template helps to remove the influence that different cohorts may have on individual PSMD results and contributes to the consistent values observed across different populations. Beaudet *et al.* showed yet another benefit of the skeletonization process. They observed that calculating the peak width from the WM MD skeleton, compared to the global WM MD mask, led to a significant decrease in between-subjects variability.[203] Such decrease was much more pronounced in MD than in other mean DTI metrics.[203]

1.4.1.4.   Application of a custom mask

The skeletonized MD maps derived from TBSS are further masked using the custom mask from PSMD's package. This final masking procedure is intended to further mitigate CSF contamination and to exclude non-cerebral areas from the analysis (Figure 1.3.C; Figure 1.4).

1.4.1.5.   Histogram analysis

While ROI analysis is well-suited to investigate specific areas of the brain, histograms are particularly useful to study subtle disorders that affect large portions of the brain, with the advantage of minimizing observer-dependent bias.[169,204,205] Diseases like cSVD and MS were originally thought to affect only areas with visible lesions and thus were extensively studied with ROI analyses.[205] However, abnormalities found in the NAWM of these patients make whole-brain measures at least as sensitive as those extracted from ROIs.[205] Like PSMD, other DWI histogram metrics, such as WM MD peak height, mean, median, peak value, skew, and kurtosis, have been successfully applied in WM diseases.[206,207]

Figure 1.4. PSMD's custom mask
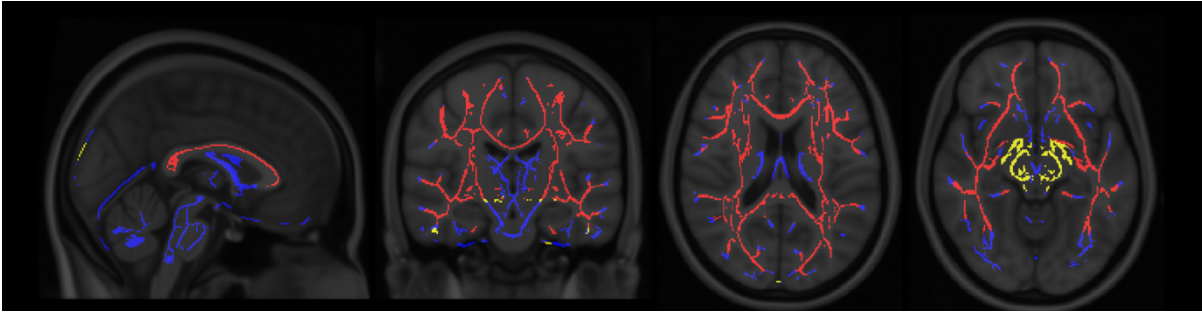
In total, 212,081 skeletonized voxels are obtained through TBSS. The PSMD custom mask released in 2016 keeps only 86,406 of those, and is represented by voxels in red and yellow. In 2019, a new version of the custom mask was released (red), excluding 1,210 more voxels, which were located mainly in the midbrain and in superficial regions (yellow), yielding a final count of 85,186 voxels. This image highlights the importance of harmonizing the pipeline version and hence the custom masks applied, to ensure homogeneity in the number of voxels and to allow for comparability of histogram metrics.

PSMD uses the distance between percentiles 5 and 95 of the MD histogram curve, reflecting the heterogeneity in voxel-based MD values within the WM skeleton. Since the same skeletonization procedure and the same custom mask are applied to all individuals, the obtained histograms are already normalized; that is, they are based on the same number of voxels and have similar bin widths. This allows for direct comparison of PSMD values between subjects with different brain volumes,[205] and helps explain the consistency of PSMD values across different populations.[169]

1.4.1.6.   Known sources of bias

The use of different versions of scanner acquisition software (especially in the case of Philips systems), FSL or operating systems are known to affect PSMD values (http://www.psmd-marker.com/faq/) and should ideally remain stable across patients and cohorts. It is known that different preprocessing methods result in significant variations in FA and MD, but their specific impact on PSMD remains to be investigated.[208] To ensure consistency of environment and stable results, researchers may use the recently developed PSMD Singularity container (https://github.com/miac-research/psmd/tree/main/singularity).

While preprocessing steps reduce inter-individual variability and improve the tensor model estimation,[208] they may not eradicate artifacts.[186] Quality control measures are still needed to identify inadequate scans that may impact results.[186,190] Importantly, visual inspection is a non-quantitative approach, prone to examiner bias and virtually impractical for large datasets. [185] Therefore, automated procedures (i.e., https://fsl.fmrib.ox.ac.uk/fsl/fslwiki/eddyqc; https://surfer.nmr.mgh.harvard.edu/fswiki/FsTutorial/TraculaOutputs) are more suited to detect

and quantify imaging artifacts, with the advantage of providing continuous variables that can be employed as nuisance regressors in statistical analyses.[185–187] The deleterious effects of such artifacts on conventional DTI metrics have been established,[186,187] but their impact on PSMD needs further investigation.[209]

Differences in DWI's field-of-view is also a source of bias since it will change the number of included voxels, compromising normalization and comparability of histogram metrics. A quick check of input images is recommended, and only acquisitions completely covering both cerebral hemispheres should be included. Similarly, the use of different versions of the PSMD's skeleton custom mask may be a source of similar bias since they differ in the number of voxels included (Figure 1.4). To ensure comparability and harmonization of PSMD values, studies should consistently report the version of the PSMD pipeline, and the skeleton-mask applied to their datasets.

Brain lesions such as infarcts or intracerebral hemorrhage are also sources of bias when dealing with PSMD. Ischemic strokes can be accounted for by excluding DWI hyperintense lesions from raw DWI images using a built-in argument (http://www.psmd-marker.com/usage/). Other options to deal with brain lesions include masking out the affected voxels or using only the non-affected contralateral hemisphere to compute PSMD, both available as built-in arguments in recent versions (http://www.psmd-marker.com/faq/).

2. Objectives

2.1. Primary Objective

Our primary objective was to investigate PSMD's performance as neuroimaging biomarker for cognitive impairment in the context of CAA.

2.2. Specific Objectives

- Gather and synthesize the evidence supporting PSMD's role as a promising biomarker in the context of cSVD and other WM disorders. For that, we conducted a systematic review of all studies employing PSMD available in the literature until Feb 01 2021. This systematic review is presented in chapter 3.1.
- Cross-sectionally investigate PSMD's neuroimaging and cognitive associations in patients with CAA. For that, we conducted a case-control study, presented in chapter 3.2.
- Expand on previous research by investigating PSMD's association with other conventional and DWI-based MRI markers. Investigate PSMD's regional variations in CAA. Compare PSMD's cognitive associations against other conventional DWI markers.

3. Results

3.1. Systematic Review on PSMD

This chapter is based on a systematic review written by the author (co-first author) and collaborators (Pinar Yilmaz [co-first author], Lukas Sveikata, Dorothee Schoemaker, Susanne van Veluw, Andreas Charidimou, Marco Duering, Mark Etherton, Steve Greenberg, and Anand Viswanathan), currently under review.

3.1.1. Introduction

Major advances in the field of neuroimaging have enabled *in vivo* appraisal of WM structural integrity. The assessment of brain lesions visible on conventional MRI, such as WMH, lacunes, and hemorrhages, plays a pivotal role in defining cSVD and other WM disorders and has been incorporated into clinical practice.[36] However, these lesions tend to explain only a small portion of the variance in cognitive impairment and clinical disability related to highly prevalent WM disorders,[71] and are susceptible to subjective visual assessments or error-prone automated segmentation approaches.[210] Additionally, significant abnormalities in the NAWM, known to impact clinical outcomes,[211] are not detectable on conventional MRI sequences and call for advanced techniques capable of better capturing the whole spectrum of WM injury, including early-stage alterations.[212]

DWI is one of the best-suited MRI techniques for assessing the extent and nature of global WM damage.[213] The anisotropic diffusion of water molecules inside brain tissues provides quantitative parameters that inform on the microstructural integrity and directionality of WM tracts. The most commonly used model to characterize diffusion processes in the brain is the DTI, generating scalar measures like FA and MD, successfully applied for the diagnosis, categorization, and follow-up of several WM diseases, as well as for assessing normal development and aging.[213] Despite the multiple pipelines currently available, the optimal method through which to analyze diffusion MRI data remains undefined, hindered by labor-intensive and time-consuming options. The development and validation of fast and automated techniques to be applied in large clinical trials is considered crucial for future therapeutic progress in the field of WM disorders.[107]

In this context, a recently developed DTI marker offers several advantages that align with current scientific needs and priorities. PSMD is a fully automated and rapidly computed marker originally designed to quantify the severity of cSVD pathology and related cognitive impairment. In addition, PSMD shows strong neuropsychological associations, outperforming other MRI markers by independently predicting cognitive outcomes.[169] Though PSMD has

been increasingly applied in the research setting, knowledge about this marker is still limited, and the scientific literature lacks a comprehensive review of the evidence supporting its use in multiple neurological conditions.

In this systematic review, we focus on PSMD's clinical-radiological correlations reported in different studies. We also address PSMD's current status of validation as a biomarker, potential challenges, and future directions. Other methods for analyzing diffusion data are beyond the scope of this review, for which the reader is encouraged to refer to other detailed reviews.[125,213]

3.1.2.   Materials and methods

We performed our systematic review following the Preferred Reporting Items for Systematic Reviews and Meta-Analyses (PRISMA) statement (http://www.prisma-statement.org/).

3.1.2.1. Literature search

The literature search was performed in PubMed, EMBASE, Medline, Cochrane Central, Web of Science, and Google Scholar in Feb 1, 2021. Our search terms included 'peak width', 'skeletonized', 'histogram', 'diffusion tensor imaging', 'diffusion weighted imaging' amongst others (further details on search query are provided in Appendix 3.1.A and Table A.3.1.A). Additionally, we manually identified other manuscripts derived from the reference lists of relevant publications and from the authors' personal records.

3.1.2.2. Eligibility criteria

Only original articles applying the PSMD algorithm developed by Baykara *et al*. in 2016 were deemed eligible for analysis.[169] We excluded theses and manuscripts for which no full text was available (conference abstracts), and no original data was reported (editorial and review articles) (Figure 3.1.1).

3.1.2.3. Screening and study selection

Search results were imported to EndNote X9 and duplicates were removed. Two independent reviewers (MCZZ and PY) screened the studies for eligibility. There were no disagreements in the process of screening the articles.

3.1.2.4. Data extraction

The same reviewers systematically extracted data from the included articles, separately. In case of disagreement, a third reviewer (LS) served to reach a consensus. From each article, the

following variables were extracted: study design, number of cohorts and participants, country of origin, neurological disorder(s) investigated, imaging and non-imaging biomarkers, cognitive tests, and main findings. With respect to each investigated cohort, we collected technical details (scanner manufacturer, field strength, TR/TE, voxel size, number of diffusion gradient directions, b-value, as well as the software and procedures used in the preprocessing step), number of participants, their age range, the reported PSMD values, and normalized WMH volume. The majority of studies reported PSMD values in mean ± standard deviation. To allow for the comparison of values across the different samples, we used the BoxCox method[214] to calculate mean and SD from studies originally reporting only median and IQR values.[105,169,184,215,216] This method has been shown to perform better with non-parametric data.[214] Specifically for the cohorts investigated by Beaudet *et al.*, since PSMD values were available only per stratum of age,[203] we identified the most prevalent age range per cohort and displayed PSMD values in respect to that specific stratum. Whenever there was known or suspected overlap between the study cohorts (Appendix 3.1.B., Table A.3.1.B),[169,188,189,203,215–219] only data from the largest reported sample was included in the pooled presentation. Results were plotted using the R package ggplot2.[220]

3.1.2.5. Critical appraisal and risk of bias assessment

Since there are no standardized protocols for quality assessment of neuroimaging studies, we evaluated the risk of bias using the Newcastle Ottawa scale for case-control studies and its adapted version for cross-sectional and cohort studies.[221] To account for variability in the handling of neuroimaging data, we further included key technical parameters in the scales, assessing clarity and availability of information on the DWI acquisition protocols and preprocessing steps.[221] Further details on the assessment, quality indicators, and scoring system are available in Appendix 3.1.C. Studies were examined separately by PY and MCZZ, and rated as very good, good, satisfactory, and unsatisfactory, based on previously defined thresholds,[221,222] and disagreements were resolved by a third rater (LS).

3.1.2.6. Objectives

Our main objectives were to provide a synthesis of PSMD's technical details and to discuss the evidence around PSMD's: (1) reliability, related to inter-scanner reproducibility and test-retest repeatability; (2) clinical and neuroimaging predictors; (3) value as a potential surrogate for clinical endpoints in different neurological conditions, and (4) current status of validation as neuroimaging biomarker for cSVD.

3.1.3. Results

3.1.3.1. Results of the search strategy

We identified 1,084 unique records, of which 638 articles remained after the removal of duplicates. During the screening process, we further excluded 588 articles based on title and abstract. In total, 50 full-text articles were assessed for inclusion, of which 19 met eligibility criteria and were included in the review (Figure 3.1.1).

After selecting only the largest samples from overlapping cohorts,[169,188,189,203,215–219] we calculated that the PSMD pipeline was applied in a total of 23,737 individuals, over 27 cohorts and 43 subsamples. The prevalence of female participants ranged from 29.2 to 76.7% across cohorts and was overall estimated at 53.5%. No studies mentioned the race distribution of the participants. The ethnicity of participants was mentioned in only one study, which included patients of Chinese ethnicity exclusively.[184]

The majority of cohorts came from high-income countries: United States (4), Germany (5), United Kingdom (4), the Netherlands (3), France (3), Canada (3), Australia (2), China (2) Austria (1), Italy (1), and multinational (1). No studies to date have investigated PSMD's performance in cohorts from Latin America, Africa, or among other underrepresented communities.

Figure 3.1.1 PRISMA Flowchart of included studies
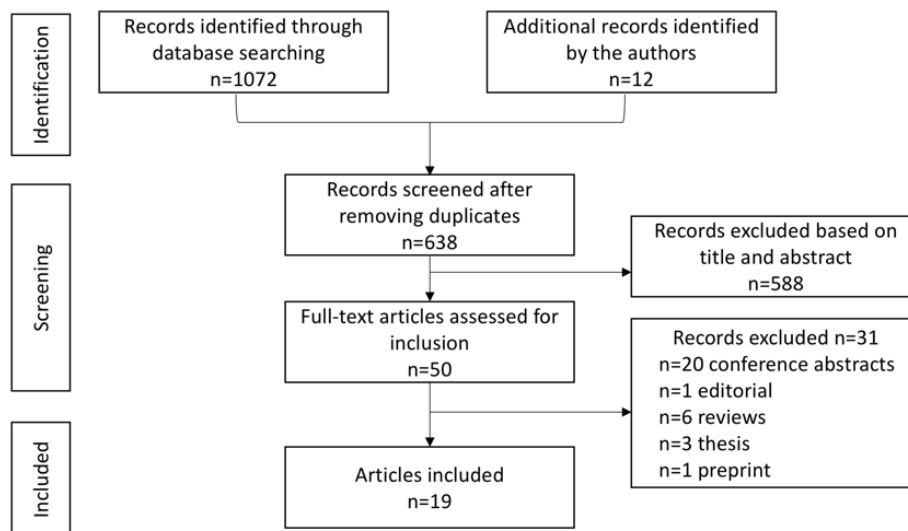
Source: Zanon Zotin MC & Yilmaz P et al. 2022, under review.

3.1.3.2. Study Characteristics

The main characteristics of the included articles are summarized in Table 3.1.1. Studies were all analytical observational.[223] Thirteen studies were performed with data from a single-center, whereas six were multicenter.[166,169,203,217,218,224] The majority of studies employed healthy controls or other comparator groups.[105,166,169,183,188,189,217–219,225–227] Only 3 studies had longitudinal data available.[169,183,184]

Twelve studies tested PSMD's associations with specific clinical outcomes, such as cognitive function,[105,169,183,184,209,216,218,219,225,227,228] physical disability,[219] dysexecutive behavior,[225] functional status,[219] and gestational age at birth in neonates.[189] Other aims included: assessing whether PSMD can detect WM abnormalities related to or preceding rare neurological diseases;[166,226] defining the clinical[184,189,203] and neuroimaging predictors of PSMD,[105,183,209,215,216,219,225,228] establishing the time course and variation in PSMD values throughout adulthood[203] and over a short time interval;[169,183] examining how PSMD correlates with topological patterns of WM injury in cSVD[215,216] and Alzheimer's disease (AD);[166] and, finally, investigating how it relates to specific fluid biomarkers (i.e., derived from CSF and serum samples).[166,188,217]

3.1.3.3. Technical Aspects:

3.1.3.3.1. MRI acquisition protocols

There was significant variability in the DWI acquisition protocols, including the scanner's field strength, manufacturer, b-values, number of excitations, and diffusion-encoding gradients (Table 3.1.2). Though most studies employed a minimum of 20 diffusion-encoding gradients, investigators also applied the pipeline on data acquired with as few as 6 to 15 directions.[183,203] B-values from all protocols were within the recommended range of 700-1200 s/mm^2.

Three studies (n=27) specifically investigated the precision of replicate PSMD measurements using different scanners (i.e., inter-scanner reproducibility).[169,183,224] Baykara *et al.* consecutively scanned a subset of 7 CADASIL patients on 3T and 1.5T scanners[169] In this sample, PSMD offered a higher intraclass correlation coefficient (ICC=0.948), in comparison to whole-brain MD peak height, average of skeletonized MD, and median of skeletonized MD.[169] McCreary *et al.* also scanned a subset of 4 patients using two different protocols, with either 11- or 25-diffusion gradient directions.[183] No significant difference in PSMD values was observed, pointing to PSMD being robust against varying number of gradient directions.[183,229] Maillard *et al*. specifically investigated PSMD's interscanner reproducibility among patients

Table 3.1.1. Overview of the studies

Author	Design	Cohorts	Country	Neurological Conditions/Groups	N	Main findings
Baykara et al. 2016[169]	Case-control; longitudinal	CADASIL exploratory	Germany France	CADASIL	113	PSMD was higher in cSVD than non-cSVD groups. Subsamples with higher WMH load had higher PSMD values. PSMD was associated with speed scores in patients with CADASIL, sporadic cSVD and memory-clinic patients with high burden of WMH, but not in the non-cSVD samples. PSMD outperformed other conventional MRI markers and DTI metrics by explaining more cognitive variance. In the longitudinal sample, PSMD offered the lowest sample size estimation. PSMD offered better inter-scanner reproducibility when compared to other DTI metrics.
		VASCAMY	Germany	CADASIL	57	
				MCI	21	
				HC	48	
		RUN DMC	Netherlands	Sporadic non-amyloid cSVD	444	
		Utrecht	Netherlands	Memory clinic patients with cSVD	105	
		ADNI	US, Canada	ADD	37	
				MCI	68	
				HC	61	
		ASPFS	Austria	Community-dwelling healthy older individuals	132	
Caballero et al., 2018[166]	Case-control	DIAN	Multinational	Autosomal Dominant AD (PSEN1, PSEN2 and APP)	64	PSMD increases faster with estimated years from symptom onset for mutation carriers compared to controls. Higher PSMD was associated with lower CSF amyloid-ß1-42, increased PIBPET binding potential, higher levels of CSF total tau, P-tau, and higher TREM2.
				HC (non-carriers)	45	
Schouten, et al., 2018[226]	Case-control	Leiden University Medical Center	Netherlands	Symptomatic D-CAA Carriers	15	FA decreased and MD/PSMD increased over age for mutation carriers in comparison to controls. Voxel-wise, independent component-wise FA and MD, and structural connectomes differed between D-CAA patients and controls, mainly in periventricular frontal and occipital regions, and occipital lobe. No significant differences were found in any DWI-based marker between presymptomatic carriers and controls.
				Pre-symptomatic D-CAA Carriers	11	
				HC	30	
Wei et al., 2019[227]	Case-control	Beijing Tiantan Hospital	China	Cognitively normal with WML	35	Patients with WML had higher PSMD values and worse cognition than controls. In patients with WML, higher PSMD correlated with worse cognitive impairment. PSMD was markedly associated with global cognition in VCI patients and with executive functions in cognitively normal-WML and VCI patients.
				Vascular cognitive impairment	78	
				HC	48	
Deary et al., 2019[228]	Cross-sectional	LBC 1936	UK	Mostly healthy community-dwelling older individuals (population-based cohort)	672	PSMD was more strongly correlated with WMHV, FA and MD, in comparison to atrophy, perivascular spaces, GMV and WMV. PSMD correlated with processing speed, visuospatial ability, memory and general cognition, and independently predicted visuospatial ability and general cognitive ability
Lam et al., 2019[184]	Cohort	CU-RISK	China	Community-dwelling older individuals (population-based cohort)	801(BL) 515 (FU)	PSMD was associated with speed scores at baseline and at 3-year follow-up, and with memory at 3-year follow-up. PSMD and other DTI metrics mediated the association between vascular risk factors and age-related cognitive impairment.
Low et al., 2020[209]	Cross-sectional	NIMROD	UK	Older individuals with cognitive complaints (memory-clinic patients): MCI, AD, dementia with Lewy bodies, late-life depression, FTD and cognitively normal individuals	145	Head motion significantly impacted PSMD values. WMHV, CMBs and lobar lacunes were independent predictors of PSMD, and WMHV was the strongest. PSMD was more strongly associated with WMHV than with GMV and WMV. PSMD was associated with global cognition, outperforming other cSVD markers. PSMD successfully discriminated patients with and without cognitive impairment, outperforming MD and cSVD markers.
Beaudet et al., 2020[203]	Cross-sectional	MRi-Share	France	Community-dwelling individuals (population-based cohort)	1824	RD, MD, and axial diffusivity exhibited the same J-shape pattern of variation with regards to age. FA showed a reverse profile. PSMD constantly increased, first slowly until the 60s, then more sharply. PSMD values are higher in men in comparison to women, but the effect of sex on PSMD was of small size.
		BIL&GIN	France		410	
		SYS	Canada		512	
		UKBiobank	UK		12397	
		1000Brains	Germany		1209	

		ASPFS	Austria		277	
		LBC1936	UK		672	
		MAS	Australia		412	
		OATS	Australia		386	
		LIFE	Germany		1906	
McCreary et al., 2020[183]	Case-control and longitudinal	FAVR study	Canada	Sporadic CAA	34	PSMD was higher in CAA compared to HC and MCI groups, adjusting for age and sex. Across the whole cohort, PSMD associated with memory and processing speed. In CAA patients, increased PSMD associated with worse processing speed. In CAA, PSMD correlated with higher WMHV and CAA cSVD score, but not with MMSE, executive function, memory, CMB count, or cortical thickness. PSMD increased in similar rates over 1.1-year period in all groups. Changes in PSMD were not associated with changes in cognition or WMHV.
				MCI	21	
				AD	15	
				HC	22	
Petersen et al., 2020[215]	Cross-sectional	HCHS	Germany	Community-dwelling older individuals (population-based cohort)	930	PSMD, representing cSVD, was associated with widespread decrease in connectivity, more strongly in subcortical, and frontal edges. Higher PSMD correlated with decreased connectivity in interhemispheric, long intrahemispheric and short intrahemispheric edges.
Liu et al,. 2020[217]	Cross-sectional	Bankstown-Lidcombe Hospital	Australia	Vascular dementia	48*	Compared to controls, patients with vascular dementia had lower Ceramides, cholesterol esters and phospholipids, and higher glycerides. Levels of ceramides, cholesterol esters achieved the best accuracy in discriminating vascular dementia from controls.
				HC	49*	
		OATS	Australia	Community-dwelling older individuals	161	Patients grouped in the "vascular" group according to lipid profile showed greater cognitive impairment and lower PSMD values, but did not differ in WMHV and other DTI measures.
Frey et al., 2020[216]	Cross-sectional	HCHS	Germany	Community-dwelling older individuals (population-based cohort)	930	cSVD burden, measured through PSMD, was associated with decreased integration and increased segregation of structural brain networks. PSMD was associated with lower global efficiency and small-world propensity, and with higher clustering coefficient and modularity Q. PSMD was associated with performance in MMSE, TMTA and TMTB.
Oberlin et al., 2021[225]	Case control	Cornell Medical College	US	Late-life Depression	44	Presence of LLD modulated PSMD's associations with cognition. PSMD predicted broader and more pronounced cognitive impairment in LLD patients (processing speed, delayed memory and executive function) in comparison to controls (processing speed). PSMD outperformed conventional cSVD and DTI markers in predicting executive function and dysexecutive behaviors in participants with LLD.
				HC	65	
Raposo et al., 2021[105]	Case-control	Massachusetts General Hospital	US	Sporadic CAA with MCI	24	PSMD is higher in MCI patients with CAA than in MCI patients without CAA. In CAA-MCI patients, PSMD is associated with performance in processing speed. With regards to other neuroimaging markers, PSMD was independently associated with WMHV.
				MCI non-CAA	62	
Vinciguerra et al., 2019[219]	Case-control	University of Siena	Italy	Multiple Sclerosis	47	After correction for WMHV, PSMD values in MS surpassed those in CADASIL, and in both patient groups were higher than in HC. PSMD values correlated with WMHV. In MS, PSMD correlated with disease duration and with all Rao Brief Repeatable Battery tests, but not with Expanded Disability Status Scale. In CADASIL, PSMD did not significantly correlate with the modified Rankin Scale.
				CADASIL	25	
				HC	28	
Vinciguerra et al., 2020[218]	Case-control	University of Siena and Florence	Italy	Multiple Sclerosis	60	All MRI measures significantly differed between MS and HC; PSMD correlated with verbal memory, visuospatial memory, verbal fluency and SDMT. The only significant independent predictors of SDMT were PSMD and skeletonized MD.
				HC	15	
Blesa et al., 2020[189]	Case-control	Royal Infirmary of Edinburgh	UK	Pre-term newborns	76	Significant group differences were identified with regards to PSMD, PSAD, PSRD, PSODI and PSNDI. PSMD was higher in preterm than in term infants. All metrics, except PSFA, were highly accurate in distinguishing preterm and term patients.
				Term-newborns	59	

						PSNDI was more strongly associated with gestational age, followed by PSMD.
Sullivan, *et al.*, 2020[188]	Cross-sectional	Royal Infirmary of Edinburgh	UK	Subset serum inflammatory markers x HCA	HCA	24*	Among several inflammatory proteins, umbilical cord blood IL-8 was the strongest predictor of HCA. Only elevated IL-8 in the first week of life correlated with WM microstructural abnormalities at term-equivalent age, in the form of PSNDI. PSMD was not associated with any inflammatory marker.
					No HCA	31*	
				Subset MRI		71	
Maillard, et al, 2021[224]	Technical	MarkVCID	US	Test-retest Repeatability		41	ICC between test and retest PSMD values was excellent (ICC= 0.986, *p*<.001). PSMD's interscanner reproducibility was also excellent, with ICC ranging between 0.919 and 0.956 (*p*<.001).
				Interscanner Reproducibility		16	

* Samples in which PSMD was not calculated. Glossary: AD (Alzheimer's Disease), ADNI (Alzheimer's Disease Neuroimaging Initiative), ASPSF (Austrian Stroke Prevention Study Family), BIL&GIN (Brain Imaging of Lateralization study at Groupe D'Imagerie Neurofonctionnelle), CAA (cerebral amyloid angiopathy), CADASIL (Cerebral Autosomal-dominant Arteriopathy with Subcortical Infarcts and Leukoencephalopathy), CMB (cerebral microbleeds), CSF (cerebrospinal fluid), cSVD (cerebral small vessel disease), CU-RISK (Chinese University of Hong-Kong-Risk Index for Subclinical brain lesions in Hong Kong), D-CAA (Dutch-type hereditary cerebral amyloid angiopathy), DIAN (Dominantly Inherited Alzheimer Network), DTI (Diffusion Tensor Imaging), FA (fractional anisotropy), FAVR (Functional Assessment of Vascular Reactivity Study), FTD (frontotemporal dementia), GM (gray matter volume), HC (Healthy controls), HCA (histologic chorioamnionitis), HCHS (Hamburg City Health Study), LBC1936 (Lothian Birth Cohort 1936), LLD (late-life depression), MAS (Memory and Ageing Study), MCI (mild cognitive impairment), MD (Mean diffusivity), MGH (Massachusetts General Hospital), MMSE (mini-mental status examination), MRi-Share (Magnetic Resonance imaging Subcohort of internet-based Students HeAlth Research Enterprise), MS (multiple sclerosis), NIMROD (NeuroInflammation in Memory and Related Other Disorders), OATS (Older Australian Twin Study), PIB (Pittsburgh compound B), PSAD (peak width of skeletonized axial diffusivity), PSFA (peak width of skeletonized fractional anisotropy), PSMD (peak width of skeletonized mean diffusivity), PSNDI (peak width of skeletonized neurite dispersion index), PSODI (peak width of skeletonized orientation dispersion index), PSRD (peak width of skeletonized radial diffusivity), P-tau (phosphorylated tau), RD (radial diffusivity), RUN DMC (Radboud University Nijmegen Diffusion Tensor and Magnetic resonance Imaging Cohort), SDMT (symbol digit modalities test), SYS (Saguenay Youth Study), TMT A and B (trail-making parts A and B), VASCAMY (Vascular and Amyloid Predictors of Neurodegeneration and Cognitive Decline in Nondemented Subjects), VCI (Vascular cognitive impairment), WMV (white matter volume), WMHV (white matter hyperintensity volume), WML (white matter lesions).

with cSVD (target population) and observed excellent ICC among 16 individuals scanned in 4 different scanners (3T Philips, 3T Siemens [2x], and 3T GE) using harmonized DWI protocols.[224] The same single study investigated PSMD's variability measured in the same individual, scanner, and protocol within a short period of time (i.e., test-retest repeatability) in 41 participants and found high ICC between test and retest PSMD values (Table 3.1.3.).[224] Importantly, no studies to date have specifically investigated the impact that different preprocessing steps may have on PSMD values.

3.1.3.3.2. Preprocessing and processing methods

The three preprocessing steps most commonly performed were: correction for head motion and eddy-currents, brain extraction, and tensor fitting. More complex protocols included correction for susceptibility artifacts,[166,203,215,216] outlier replacement,[188,189,203,209] denoising,[188,189,203,215,216] removal of Gibbs ringing artifacts,[215,216] and bias field correction.[188,189,215,216] In general, FSL was employed in at least part, if not all, of these steps. Other softwares used for preprocessing were: ExploreDTI,[166] MATLAB,[226] dypi tools,[203] Diffusion Toolkit from TrackVis,[203] Lipsia,[203] MRTrix3[215,216] and ANTS.[215,216] Detailed information on these steps was missing or unclear in part of the included articles (Table 3.1.2).[183,184,217,225] The version of FSL used to calculate PSMD was mentioned in 8 studies, ranging from v3.3 to v6.0.1.[105,169,184,209,215,216,225,226] It is known that different preprocessing methods result in significant variations in FA and MD, but their specific impact on PSMD remains to be investigated.[208]

As previously mentioned, brain lesions represent another relevant source of bias when dealing with PSMD. McCreary *et al.* observed a consistent reduction in PSMD values when masking out ICH-voxels in CAA patients.[183] It remains unexplored whether the use of different masks could impact PSMD's comparability, since differences in the number of voxels are expected to impact the width of histograms. Alternatively, PSMD could be computed exclusively from the non-affected hemispheres to keep the histograms normalized, but caution should be taken when comparing with results obtained from both hemispheres. Other than the original publication,[169] only one study[105] reported which version of the PSMD pipeline was employed, which precluded further assessment of the potential impact of different versions/masks on PSMD.

3.1.3.3.3. Quality assessment of DWI

While preprocessing steps reduce inter-individual variability and improve the tensor model estimation,[208] they may not eradicate artifacts.[186] Quality control measures are still needed to identify inadequate scans that may impact results.[186,190] Of the 27 cohorts investigated, quality

assessment of DWI images was reported in 18, performed mainly through visual inspection of gross motion or susceptibility-induced artifacts (Table 3.1.2).[105,169,183,188,189,203,209,224,227] For neonatal data, which are particularly prone to motion artifacts, Blesa *et al*. chose to re-acquire images that were deprecated by motion.[189]

Importantly, visual inspection is a non-quantitative approach, prone to examiner bias and virtually impractical for large datasets.[185] Therefore, automated procedures (i.e., https://fsl.fmrib.ox.ac.uk/fsl/fslwiki/eddyqc;https://surfer.nmr.mgh.harvard.edu/fswiki/FsTutorial/TraculaOutputs) are more suited to detect and quantify imaging artifacts, with the advantage of providing continuous variables that can be employed as nuisance regressors in statistical analyses.[185–187]The deleterious effect of such artifacts on conventional DTI metrics has been established,[186,187] but their impact on PSMD needs further investigation.[209] Three studies employed automated softwares[185,187] to quantify DWI artifacts,[209,215,216] but only one examined their effect on PSMD.[209] Low *et al.* observed that an automated measure of the degree of head motion during DWI acquisition was significantly and positively associated with PSMD ($r = 0.265$, $p = .001$), representing a confounding factor that should be controlled for when examining cognitive associations.[209] Though their findings warrant confirmation in larger samples, they are in line with previous reports using other DTI indices,[186] and highlight the importance of assessing and controlling for artifacts in PSMD studies.[209]

3.1.3.4. Neurological conditions investigated with PSMD

Table 3.1.4 summarizes the main demographic and imaging variables extracted from all the investigated cohorts and subgroups. Data from healthy individuals used as control groups in multiple studies were also included (n=347). The neurological conditions investigated with PSMD, and were stratified into 3 phenotypic categories: age-related cognitive impairment (n=23,154), demyelinating diseases (n=60), and pediatrics (n=135). Age-related cognitive impairment was investigated either in the form of normal aging, in community-dwelling individuals (n=21,736),[169,184,203,215,216,228] or in patients diagnosed with a disorder that predispose to cognitive deterioration in elderly populations, such as: cSVD (n=941; arteriolosclerosis n=662, CAA n=58, and monogenic cSVDs n=221),[105,169,183,226,227] AD (n=116),[166,169,183,209] mild cognitive impairment (MCI, n=317),[105,169,183,209] and late-life depression (n=44).[225] Within neuroinflammatory disorders, two studies investigated relapsing-remitting multiple sclerosis (MS; n=60).[218,219] Finally, an adapted version of the PSMD pipeline was used to investigate brain abnormalities related to preterm birth (n=135), known to cause WM injury and childhood cognitive impairment.[188,189]

Table 3.1.2 Technical Details per Cohort

n	Cohort	Publication	Scanner/Field Strength	TR/TE	Voxel size (mm)	Number Directions	b-value	DTI Quality Assessment	Preprocessing software	Preprocessing steps
1	CADASIL exploratory	Baykara et al., 2016 [169]	GE Signa 1.5T	8300/96	0.9 x 0.9 x 5	41	1000	VI	FSL	MECC, BE, TF
2	VASCAMY	Baykara et al., 2016 [169]	Siemens Magnetom Verio 3T	12700/81	2 x 2 x 2	30	1000	VI	FSL	MECC, BE, TF
3	RUN DMC	Baykara et al., 2016 [169]	Siemens Magnetom Sonata 1.5T	10100/93	2.5 x 2.5 x 2.5	30	900	VI	U	PATCH, BE, TF
4	Memory-clinic Utrecht	Baykara et al., 2016 [169]	Philips Intera 3T	6638/73	1.7 x 1.7 x 2.5	45	1200	VI	FSL	MECC, BE, TF
5	ADNI	Baykara et al., 2016 [169]	GE Signa HDxt/Discovery MR750 3T	13000/68	1.4 x 1.4 x 2.7	41	1000	VI	FSL	MECC, BE, TF
6	ASPFS	Baykara et al., 2016 [169]; Beaudet et al., 2020 [203]	Siemens Magnetom Tim Trio 3T	6700/95	1.9 x 1.9 x 2.5	4x12	1000	VI	FSL	MECC, BE, TF
7	Leiden University Medical Center	Schouten et al., 2018 [226]	Philips Achieva 3T	9033/56	2 x 2 x 2	32	1000	U	FSL/MATLAB	MECC, BE, TF
8	DIAN	Caballero et al., 2018 [166]	Siemens 3T	11000/87	2.5 x 2.5 x 2.5	64	1000	VI	ExploreDTI	MECC,susceptibility correction.,TF
9	Beijing Tiantan Hospital	Wei et al., 2019 [227]	Siemens Magnetom Tim Trio 3T	4900/93	2.5 x 2.5 x 2.5	30	1000	VI	FSL	MECC, BE, TF
10	Lothian Birth Cohort 1936,	Deary et al., 2019 [228]; Beaudet et al., 2020 [203]	GE Signa Horizon HDxt 1.5T	16500/98	2 x 2 x 2	64	1000	U	FSL	MECC, BE, TF
11	CU-RISK,	Lam et al., 2019 [184]	Philips Achieva 3T	8944 and 8647.64/60	1 x 1 x 1	32	1000	VI	FSL	MECC, BE, TF

12	NIMROD	Low *et al.*, 2020 [209]	Siemens Tim Trio or Verio 3T	11700/106	2 x 2 x 2	63	1000	A and VI	FSL	MECC (outlier replacement),BE, TF
13	MRi-Share	Beaudet *et al.*, 2020 [203]	Siemens Prisma 3T	3540 (multiband x 3)/75	1.7 x 1.7 x 1.8	32	1000	U	FSL/*dypi* tools	MECC (outlier replacement), denoising, TF
14	BIL&GIN	Beaudet *et al.*, 2020 [203]	Philips Achieva 3T	8500/81	2 x 2 x 2	2 x 21	1000	U	FSL, TrackVis, dypi tools	FLIRT (for motion/geometrical deformation); averaged DWI with polarity inversion; TF
15	SYS	Beaudet *et al.*, 2020 [203]	Siemens 1.5T	8000/102	2.3 x 2.3 x 3	64	1000	VI	FSL	MECC (outlier removal; +/- 3SD), BE, TF
16	LIFE	Beaudet *et al.*, 2020 [203]	Siemens Verio 3T	13800/100	1.7 x 1.7 x 1.7	60	1000	VI	FSL/Lipsia	MECC (outlier replacement), BE, TF
17	1000 BRAINS	Beaudet *et al.*, 2020 [203]	Siemens Tim Trio 3T	7800/83	2 x 2 x 2	30	1000	VI	FSL, CAT12	MECC, registr. to MNI space, BE, TF
18	UKBiobank	Beaudet *et al.*, 2020 [203]	Siemens Skyra 3T	3600 (multiband x 3)/92	2 x 2 x 2	50	1000	U	FSL,FreeSurfer, HCPG	Gradient correction distortion, MECC, TF
19	OATS	Beaudet *et al.*, 2020 [203], Liu *et al.*, 2020 [217]	Philips (x2), Siemens (x2), 1.5T & 3T	7800 or 8600/68 or 96	2.5 x 2.5 x 2.5	32	1000	U	FSL	MECC, BE, TF
20	MAS	Beaudet *et al.*, 2020 [203]	Philips Achieva Quasar Dual 3T	7800/68	2.5 x 2.5 x 2.5	6 or 32	700 or 1000	U	FSL	MECC, BE, TF
21	FAVR study	McCreary *et al.*, 2020 [183]	GE Signa VH/I or MR750 3T	11000/~88	3.5 slice thickness	11 or 25	850	VI	U	U
22	HCHS	Petersen *et al.*, 2020 [215]; Frey *et al.*, 2020 [216]	Siemens Skyra 3T	8500/75	2 x 2 x 2	64	1000	A	MRTrix3, ANTS, FSL	Denoising, removal of Gibbs artifacts, MEEC, bias field/susceptibility correction
23	Cornell Medical College	Oberlin *et al.*, 2021 [225]	Siemens Tim Trio 3T	9000/91	2 x 2 x 2	30	1000	U	U	U

#	Cohort	Reference	Scanner	TR/TE	Voxel size	Directions	b-value	QC	Software	Preprocessing
24	Memory-clinic MGH	Raposo et al., 2021 [105]	Siemens Tim Trio 3T	8040/84	2 x 2 x 2	60	700	VI	FSL	MECC, BE, TF
25	University of Siena	Vinciguerra et al., 2019 [219]	Philips 1.5T	8500/100	2.5 x 2.5 x 2.5	32	1000	U	FSL	MECC, BE, TF
	Universities of Siena and Florence	Vinciguerra et al., 2020 [218]	3T	NA	NA	32	900	U	FSL	MECC, BE, TF
26	Royal Infirmary of Edinburgh	Blesa et al., 2020 [189]; Sullivan et al., 2020 [188]	Siemens Magnetom Prisma 3T	3400/78	2 x 2 x 2	64	750	Images affected by motion were reacquired as many times as required	Marchenko-Pastur-PCA based algorithm, FSL, N4ITK (from Insight Toolkit - NIH)	Denoising; MECC (outlier replacement and slice-to-volume registration); bias field inhomogeneity correction; TF
27	MarkVCID	Maillard et al, 2022 [224]	Siemens Tim Trio 3T	9800/84	2 x 2 x 2	45	1000	VI	FSL	MECC, BE, TF
			Siemens Prisma 3T	8600/68		45				
			Philips Achieva 3T	9245/76		41				
			GE 750W 3T	8600/68 or 9800/68		40				

Glossary: A (Automated), ADNI (Alzheimer's Disease Neuroimaging Initiative), ASPSF (Austrian Stroke Prevention Study Family), BE (brain extraction), BIL&GIN (Brain Imaging of Lateralization study at Groupe D'Imagerie Neurofonctionnelle), CADASIL (Cerebral Autosomal-dominant Arteriopathy with Subcortical Infarcts and Leukoencephalopathy), CU-RISK (Chinese University of Hong-Kong-Risk Index for Subclinical brain lesions in Hong Kong), DIAN (Dominantly Inherited Alzheimer Network), FAVR (Functional Assessment of Vascular Reactivity Study), HCHS (Hamburg City Health Study), LBC1936 (Lothian Birth Cohort 1936), MAS (Memory and Ageing Study), MGH (Massachusetts General Hospital), MECC (Motion and eddy currents correction), MRi-Share (Magnetic Resonance imaging Subcohort of internet-based Students HeAlth Research Enterprise), NA (not available), NIMROD (NeuroInflammation in Memory and Related Other Disorders), OATS (Older Australian Twin Study), RUN DMC (Radboud University Nijmegen Diffusion Tensor and Magnetic resonance Imaging Cohort), SYS (Saguenay Youth Study), TF (tensor fitting), U (Unspecified), VASCAMY (Vascular and Amyloid Predictors of Neurodegeneration and Cognitive Decline in Nondemented Subjects), VI (Visual Inspection).

Table 3.1.3. Available evidence on PSMD's instrumental properties (repeatability and reproducibility).

Publication	N	Pathology	MRI Scanner (s)	DTI Protocol	Details	Findings
a.	*Test-retest repeatability (differences obtained for the same individual on the same MRI scanner/protocol re-scanned after a certain number of days)*					
Maillard 2022	41 subjects (6 sites x 6 subjects + 1 site x 5 subjects)	Individuals aged 53–78 years, without major illnesses	3T Siemens TIM Trio	TR/TE 9800/84; 2x2x2 mm; b1000, 45 directions	Patients returned for a second MRI on the same scanner and protocol, within 1-14 days after initial exam.	Intra-class correlation coefficient (ICC) between test and retest PSMD values was excellent ICC= 0.986, $p<.001$ (CI: [0.974; 0.993]).
			3T Siemens Prisma	TR/TE 8600/68; 2x2x2 mm; b1000, 45 directions		
			3T Philips Achieva	TR/TE 9245/76; 2x2x2 mm; b1000, 41 directions		
b.	*Inter-scanner reproducibility (differences across different MRI scanners/protocols in the same group of individuals)*					
Baykara 2016	7 subjects (2 scanners x 7 subjects)	CADASIL	3T Siemens Magnetom Verio	TR/TE 12700/81; 2x2x2 mm; b1000, 30 directions	Patients were scanned back to back on both scanners using very similar protocols	ICC was highest for PSMD (ICC=0.948), in comparison to whole brain MD peak height (ICC=0.752), average skeletonized MD (ICC=0.730) and median skeletonized MD (ICC=0.691).
			1.5T Siemens Magnetom Aera	TR/TE 10700/105; 2x2x2 mm; b1000, 30 directions		
McCreary 2020	4 subjects (2 protocols x 4 subjects)	Not specified	3T GE Signa VH/I or MR750	TR/TE 11000/88; 2x2x2 mm; b850, 11 directions	Same scanner but with different protocols (11 and 25 directions protocol, within a single imaging session)	No significant difference was detected between PSMD values obtained from DTI protocols with 11 or 25 directions (p=.25).
			3T GE Signa VH/I or MR750	TR/TE 11000/88; 2x2x2 mm; b850, 25 directions		
Maillard 2022	16 subjects (4 scanners x 16 subjects)	Individuals aged 53–78 years, without major illnesses. 10 with no-to-low WMHV. 10 with moderate-to-high WMHV	3T Siemens TIM Trio	TR/TE 9800/84; 2x2x2 mm; b1000, 45 directions	Patients were scanned in the 4 scanners. The maximum time between the first and last scan was 15 weeks.	Overall ICC between PSMD obtained from the three first scanners was excellent (ICC=0.954, $p<.001$ (CI: [0.899; 0.982]). Pairwise ICC ranged between 0.942 and 0.968 ($p<.001$). Pairwise ICC for PSMD values obtained from GE scanner in comparison to other three scanners ranged between 0.919 and 0.956 ($p<.001$).
			3T Siemens Prisma	TR/TE 8600/68; 2x2x2 mm; b1000, 45 directions		
			3T Philips Achieva	TR/TE 9245/76; 2x2x2 mm; b1000, 41 directions		
			3T GE 750W	TR/TE 8600/68 or 9800/68; 2x2x2 mm; b1000, 40 directions		

Glossary: N (number of participant), MRI (magnetic resonance imaging), DTI (diffusion tensor imaging), ICC (intraclass correlation coefficient), TR (Repetition time), TE (Echo time), WMHV (white matter hyperintensity volume).

Overall, mean PSMD values obtained from all the subgroups ranged from 1.54 ± 0.14 to $6.06 \pm 0.75 \times 10^{-4}$ mm^2/s, (mean $\pm$ SD). For the most part, samples with similar diagnoses presented comparable PSMD values (Figure 3.1.2.B). There was, however, significant overlap in these values across cohorts and pathologies (Figure 3.1.2.A). Low values were observed among community-dwelling individuals and healthy controls (1.54 ± 0.14 to $4.29 \pm 0.77 \times 10^{-4}$ mm^2/s), whereas groups with more widespread WM injury, such as Cerebral Autosomal-dominant Arteriopathy with Subcortical Infarcts and Leukoencephalopathy (CADASIL, 4.5 ± 1.3 to $5.63 \pm 1.56 \times 10^{-4}$ mm^2/s), CAA (4.38 ± 1.08 to $4.97 \pm 1.69 \times 10^{-4}$ mm^2/s) and MS ($4.2 \pm 1.3 \times 10^{-4}$ mm^2/s) presented higher PSMD (Figure 3.1.2.B). When stratifying the PSMD values into three strata, population-based and healthy control groups were represented mainly in the low tertile, whereas the middle tertile comprised primarily memory-clinic cohorts and less advanced sporadic cSVD. Cohorts known to present more severe forms of WM injury (e.g., CADASIL, CAA, advanced sporadic cSVD, and preterm birth) appeared mainly in the highest tertile of PSMD values (Figure 3.1.2.A).

3.1.3.5. Clinical predictors of PSMD

Three cross-sectional studies reported a positive association between PSMD and age. Beaudet *et al.* observed a significant effect of age on PSMD among community-dwelling individuals.[203] Schouten *et al.* detected a greater increase in PSMD values over age among Dutch-type hereditary CAA (D-CAA, previously referred to in the literature as hereditary cerebral hemorrhage with amyloidosis-Dutch type or HCHWA-D) mutation carriers in comparison to controls.[226] In autosomal dominant AD mutation carriers, Caballero *et al* observed a faster progression of PSMD values over the estimated years of symptom onset, in comparison to non-carriers.[166] To better depict this relationship, we plotted PSMD values obtained from all the samples with regards to their reported age (Figure 3.1.3). Beaudet *et al.* also reported higher PSMD among men than women, though with small effect sizes.[203]

Concerning cardiovascular risk factors, PSMD was found to mediate the associations between cognition and smoking, hypertension, and diabetes in a population-based cohort.[184]

3.1.3.6. Neuroimaging predictors of PSMD

Two studies reported higher values of PSMD in groups with increased burden of WMH ($p<.01$).[169,227] Six other studies specifically addressed the relationship between PSMD and conventional markers of cSVD,[105,183,209,219,225,228] observing associations with WMHV (β=0.49-

Table 3.1.4. Overview of the cohorts

Phenotypic Categories	N	Age	Female (%)	nWMHV	PSMD (mm^2/s·10^{-4})
Healthy controls					
1. VASCAMY [169]	48	71·5 ± 6·3	30 (62·5%)	NA	3·05 (0·47)
2. ADNI [169]	61	72·9 ± 5·7	37 (60·7%)	NA	3·02 (0·72)
3. Non-carriers DIAN [166]	45	38·8 ± 10·6	21 (47%)	NA	NA
4. University of Siena [219]	28	45·2 ± 12·3	13 (46%)	NA	2·80 ± 0·30
5. Leiden University Medical Center [226]	30	44·7 ± 13·7	19 (63·3%)	NA	NA
6. Beijing Tiantan Hospital [227]	48	56·8 ± 4·7	24 (50%)	NA	2·40 ± 0·23
7. FAVR [183]	22	67·8 ± 9·6	12 (54·6%)	0·0015 (0·0021)[‡]	3·25 ± 0·49
8. Cornell Medical College [225]	65	72·4 ± 6·3	39 (60%)	0·0015 ± (0·0023)[‡]	3·40 ± 0·55
Age-related cognitive impairment					
a. Population-based cohorts					
1. ASPFS [169,203]	132	66·9 ± 11·4	81 (61·4%)	NA	3·05 (0·72)
2. LBC 1936 [203,228]	672	72·7 ± 0·7	316 (47%)	0·0055 ± 0·0054[‖]	3·17 ± 0·50
3. CU-RISK [184]	801	71·8 ± 5·1	495 (61·8%)	0·0018 (0·0029)[‖]	2·72 (0·42)
4. MRi-Share [203]	1,778*	18 to 28	(72%)[†]	NA	1·54 ± 0·14
5. BIL&GIN [203]	285*	18 to 28	(51%)[†]	NA	2·13 ± 0·17
6. SYS [203]	311*	48 to 58	(54%)[†]	NA	2·82 ± 0·34
7. UKBiobank [203]	5,375*	58 to 68	(53%)[†]	NA	2·27 ± 0·31
8. 1000 BRAINS [203]	431*	58 to 68	(44%)[†]	NA	2·94 ± 0·38
9. LIFE [203]	656*	68 to 78	(51%)[†]	NA	2·78 ± 0·47
10. OATS [203,217]	195*	68 to 78	(64%)[†]	NA	3·10 ± 0·64
11. MAS [203]	258*	78 to 98	(53%)[†]	NA	4·29 ± 0·77
12. HCHS [215,216]	930	64 (14)	424 (45·6%)	0·00044 (0·0009)[¶]	2·18 (0·50)
b. Sporadic cSVD					
i. Sporadic non-amyloid cSVD					
1. RUN DMC [169]	444	65·3 ± 8·9	201 (45·3%)	0·0059 (0·0123)[§]	3·28 (0·87)
2. Memory clinic patients with SVD (Utrecht) [169]	105	74·9 ± 8·3	51 (48·6%)	0·0112 (0·0258)[§]	4·24 (1·05)
3. Cognitively normal WML from Beijing Tiantan Hospital [227]	35	61·9 ± 8·5	17 (48·6%)	NA	2·68 ± 0·30
4. VCI patients from Beijing Tiantan Hospital [227]	78	63·0 ± 9·4	36 (46·2%)	NA	4·51 ± 0·39
ii. Sporadic CAA					
1. CAA FAVR study [183]	34	74·4 ± 7·4	13 (38·2%)	0·0183 (0·0296)[‡]	4·97 ± 1·69
2. CAA MGH [105]	24	74·7 ± 6·0	7 (29·2%)	0·0042 (0·0146)[‡]	4·48 (1·28)
c. Monogenic cSVD					
i. D-CAA					
1. Presymptomatic Carriers; Leiden Univ. Medical Center [226]	11	33·2 ± 11·9	8 (72·7%)	NA	NA
2. Symptomatic Carriers; Leiden University Medical Center [226]	15	55·1 ± 5·2	8 (53·3%)	NA	NA
ii. CADASIL					
1. CADASIL Exploratory [169]	113	49·1 ± 9·5	61 (54%)	0·0981 (0·088)[§]	5·43 (2·92)
2. VASCAMY [169]	57	53·4 ± 10·7	19 (33·3%)	0·0738 (0·0753)[§]	5·47 (2·69)
3. University of Siena [21]	25	46·9 ± 10·5	9 (36%)	0·011 ± 0·0078[‖]	4·50 ± 1·30
d. Mild Cognitive Impairment					
1. MCI ADNI [169]	68	74·7 ± 8·1	24 (35·3%)	NA	3·20 (0·88)

2. MCI VASCAMY [169]	21	76·5 ± 4·4	11 (52·4%)	NA	3·33 (0·62)
3. MCI FAVR study[26]	21	70·6 ± 5·9	8 (38·1%)	0·0041 (0·0057)[‡]	3·62 ± 1·09
4. Non-CAA-MCI MGH[15]	62	73·3 ± 8·3	26 (41·9%)	0·0029 (0·0061)[‡]	3·63 (0·85)
e. Alzheimer's Disease					
i. Typical					
1. AD ADNI [169]	37	74 ± 8·2	12 (32·4%)	NA	3·47 (0·96)
2. AD FAVR [183]	15	68·7 ± 7·2	6 (40%)	0·0056 (0·0039)[‡]	3·89 ± 1·05
ii. Autosomal Dominant Alzheimer's Disease					
1. Autosomal Dominant AD - Carriers DIAN [166]	64	38·0 ± 11·2	36 (56%)	NA	NA
f. Mild Cognitive Impairment and Dementia (multiple causes)					
1. NIMROD [209]	145	70·6 ± 7·8	57 (39·3%)	0·0069 ± 0·0071[‡]	5·51 ± 1·03
g. Late-life Depression					
1. Cornell Medical College [225]	44	71·6 ± 7·0	29 (65·9%)	0·0027 ± 0·0033[‡]	3·64 ± 0·83
Demyelinating diseases					
a. Multiple Sclerosis					
1. Universities of Siena and Florence [218]	60	43·1 ± 9·9	46 (76·7%)	0·0023 ± 0·0021[‖]	4·20 ± 1·30
Pediatrics					
a. Preterm birth					
1. Royal Infirmary of Edinburgh: pre-term infants [188,189]	76	29·5(23·4–32)[**]	33 (43·4%)	NA	6·00 (0·90)
2. Royal Infirmary of Edinburgh: term infants [189]	59	39·5 (36·4–42)[**]	28 (47·5%)	NA	5·00 (0·60)

Glossary: AD (Alzheimer's disease), ADNI (Alzheimer's Disease Neuroimaging Initiative), ASPSF (Austrian Stroke Prevention Study Family), BIL&GIN (Brain Imaging of Lateralization study at Groupe D'Imagerie Neurofonctionnelle), CADASIL (Cerebral Autosomal-dominant Arteriopathy with Subcortical Infarcts and Leukoencephalopathy), CU-RISK (Chinese University of Hong-Kong-Risk Index for Subclinical brain lesions in Hong Kong), D-CAA (Dutch-type hereditary cerebral amyloid angiopathy), DIAN (Dominantly Inherited Alzheimer Network), FAVR (Functional Assessment of Vascular Reactivity Study), HCHS (Hamburg City Health Study), LBC1936 (Lothian Birth Cohort 1936), MAS (Memory and Ageing Study), MCI (mild cognitive impairment), MGH (Massachusetts General Hospital), MRi-Share (Magnetic Resonance imaging Subcohort of internet-based Students HeAlth Research Enterprise), NA (not available), NIMROD (NeuroInflammation in Memory and Related Other Disorders), OATS (Older Australian Twin Study), RUN DMC (Radboud University Nijmegen Diffusion Tensor and Magnetic resonance Imaging Cohort), SYS (Saguenay Youth Study), VASCAMY (Vascular and Amyloid Predictors of Neurodegeneration and Cognitive Decline in Nondemented Subjects).

Continuous variables are reported as mean ± standard deviation or median (interquartile range).

*Specifically for the cohorts investigated by Beaudet *et al.*, since PSMD values were available only per stratum of age, we identified the most prevalent age range per cohort and displayed PSMD values in respect to that specific stratum.

† Due to data availability, gender prevalence is in reference to the total number of participants in each cohort, and not to the specific age-stratum reported.

‡ WMHV originally normalized by total intracranial volume.

§ WMHV originally normalized by total brain volume.

¶ WMHV originally normalized by brain tissue volume (intracranial volume – ventricle volume).

‖ WMHV originally reported in cm^3 and normalized by estimated total intracranial volume extracted from MNI152 template using FreeSurfer v6·0.

** Mean gestational age at birth in weeks (range)

Figure 3.1.2. PSMD values across the cohorts and pathologies
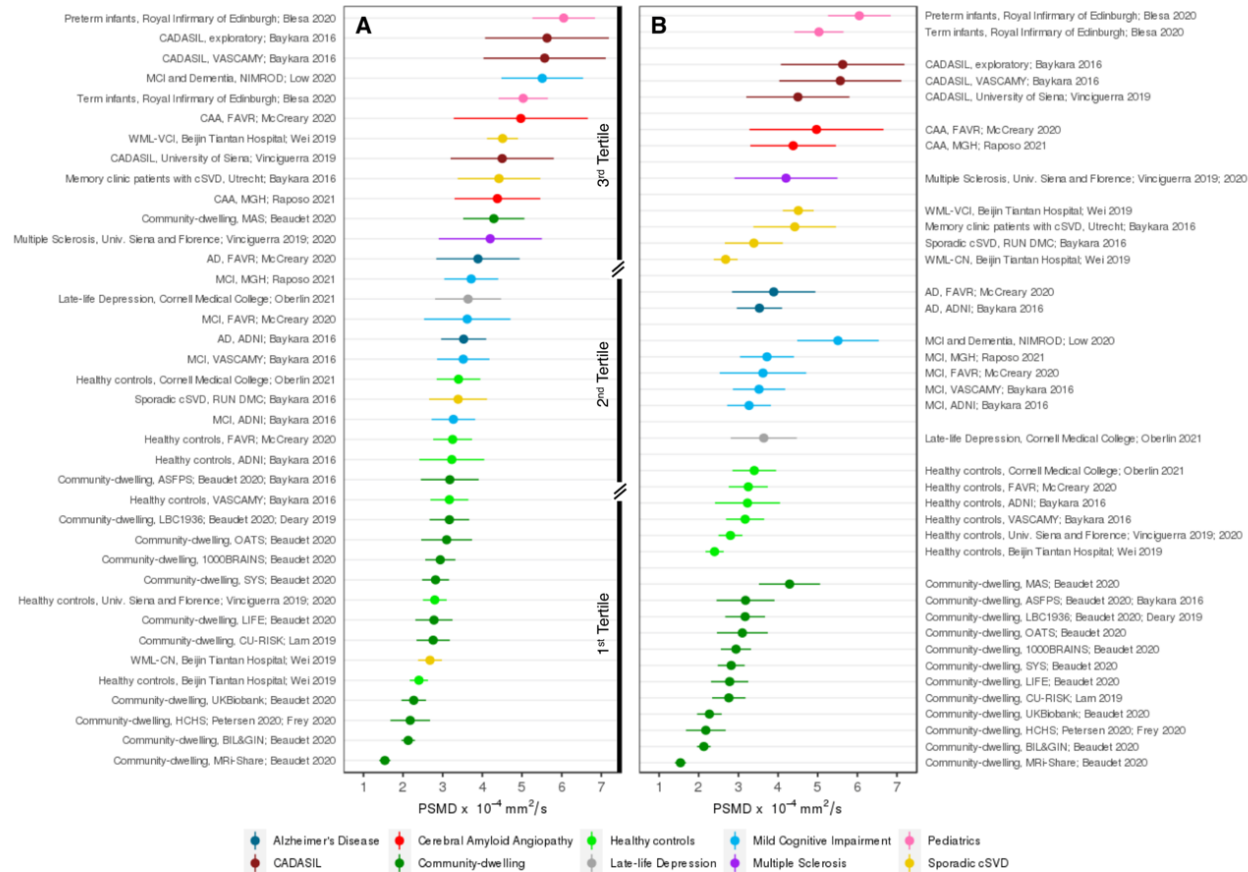
Source: Zanon Zotin MC & Yilmaz P et al. 2022, under review.

A. Cleveland plot displaying the PSMD values obtained from each sample in descending order. The dots represent mean PSMD values, and the bars represent ± standard deviation. The underlying neurological conditions are depicted in different colors, listed below the figure. The samples were further divided into tertiles, demonstrating that population-based and healthy control groups were represented mainly in the low tertile, whereas the middle tertile comprised primarily memory-clinic cohorts and less advanced sporadic cSVD. Cohorts known to present more severe forms of WM injury (e.g., CADASIL, CAA, advanced sporadic cSVD, and preterm birth) appeared mainly in the highest tertile of PSMD values. B. Samples were grouped according to the main underlying condition represented. Despite extensive technical and clinical heterogeneity, there was reasonable homogeneity in the values obtained from equivalent samples. The overlap of values derived from multiple neurologic diseases suggests that PSMD is not specific to any pathology but likely reflects WM injury irrespective of the cause.

Figure 3.1.3 PSMD and age
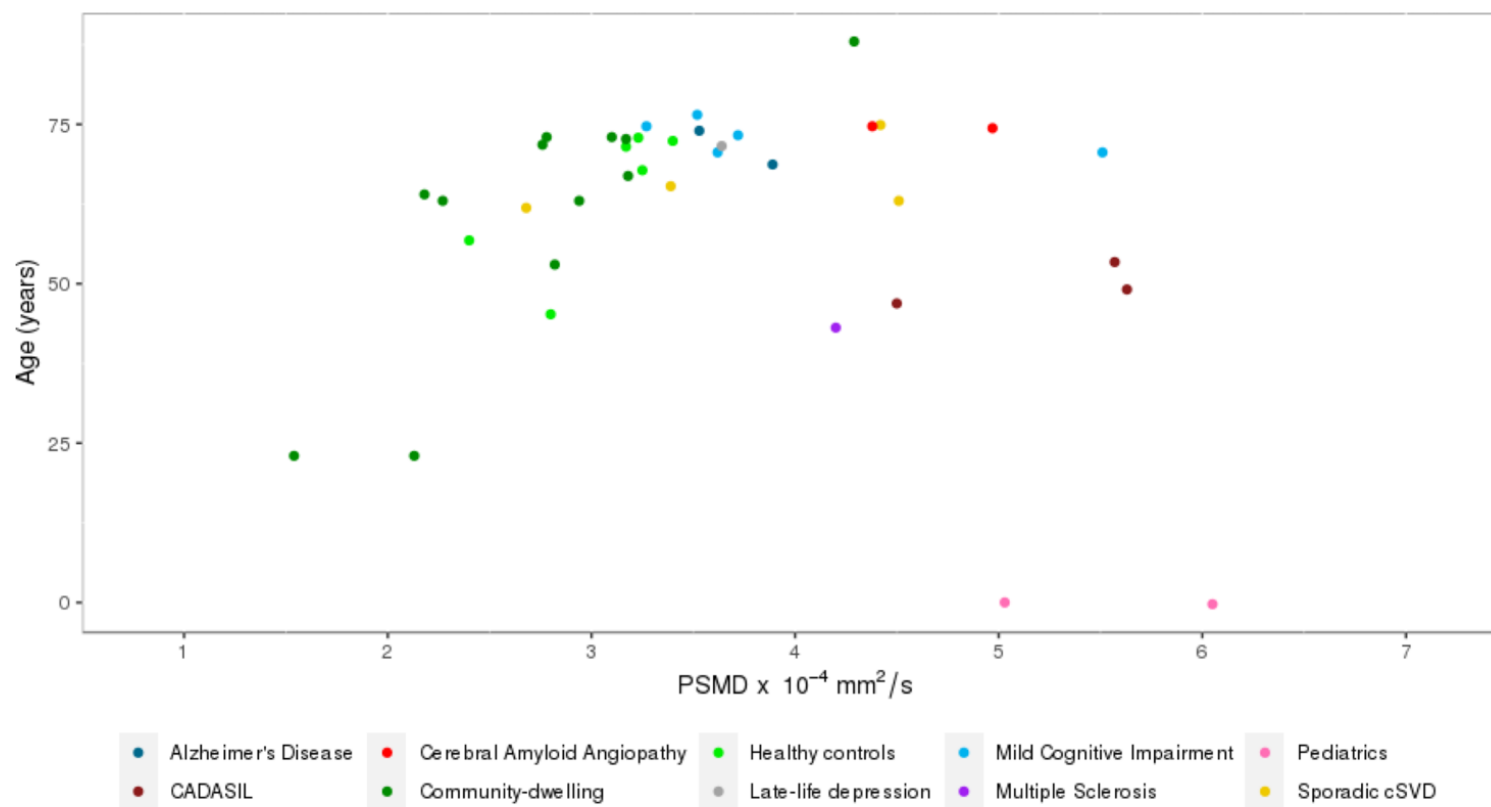
Scatter plot depicting the mean age and mean PSMD values reported in 40 subsamples from the 26 investigated cohorts (for which PSMD values and age were provided). The main pathologies investigated in each subsample are represented in colors, specified below the figure.

$0.75;$[105,183,209] $t=5.08;$[209] $r=0.6$-$0.8,$[219,225] $p<.05$ for all), number of lobar lacunes ($t=3.78$, p<.001),[209] and a composite burden score of cSVD ($\beta=0.68$; $p<.05$).[183] PVS were not significantly correlated with PSMD in adjusted models.[105,209] Associations with CMBs, both in lobar ($t=4.85$, p<.001) and deep locations ($t=4.10$, p<.001), were reported in one memory-clinic study.[209] Conversely, in CAA patients, PSMD was not associated with either CMBs or cSS ($p>.05$).[105,183] Overall, markers of global neurodegeneration, such as atrophy, gray matter volume (GMV), WMV, and cortical thickness were not associated with PSMD ($p>.05$).[105,183,209] Two studies also found PSMD to be correlated with FA and MD measures extracted through tractography.[225,228] PSMD was further associated with global and topological network graph DTI parameters (Table 3.1.5).[215,216]

3.1.3.7. Longitudinal changes in PSMD

In a cohort of 58 CADASIL patients, Baykara *et al.* measured the longitudinal changes in neuroimaging markers (PSMD, whole-brain MD peak height, normalized WMHV, brain parenchymal fraction, normalized lacune volume) and processing speed scores over 18 months. PSMD and WMHV, but not other imaging or clinical variables, showed significant longitudinal change.[169] These changes were used to calculate sample sizes for hypothetical clinical trials, and PSMD offered the smallest estimated sample size requirement among all the investigated variables.[169] McCreary *et al.* also measured changes in clinical and neuroimaging markers over a mean period of 1.1 years in 64 patients, including controls, CAA, MCI, and AD participants. Changes in PSMD were detectable ($0.42 \pm 0.53 \times 10^{-4}$ mm^2/s; p<0.001) and larger than changes in skeletonized mean MD ($0.11 \pm 0.21 \times 10^{-4}$ mm^2/s; p=0.001), but similar across all groups. Significant longitudinal changes were also observed in psychomotor speed scores and normalized median WMHV, but none were associated with baseline PSMD or changes in PSMD.[183]

Table 3.1.5. PSMD's neuroimaging associations

| Study | Conventional MRI markers | | | | | | | | | | | | DWI markers |
| | cSVD makers | | | | | | Global brain measures | | | | FA | MD | Connectivity (graph-based analysis) |
	WMHV	Lobar Lacune	CMB	PVS	cSS	cSVD score	Atrophy/ TBV	GMV	WMV	Cortical Thickness			
Deary, 2019 [228]	r=0.57[†]	NA	NA	r=0.30[†]	NA	NA	r=-0.29[†]	r=-0.10[†]	r=-0.16[†‡]	NA	r=-0.59[†]	r=0.61[†]	NA
Low, 2020 [209]	t=5.08 [§*]	t=3.78 [§*]	t=4.84 [§*]	t=-1.56-1.46[§]	NA	t=0.56[§]	NA	β=-0.15[¶]	β=-0.18[¶]	NA	NA	NA	NA
Vinciguerra, 2019 [219]	r=0.60-0.80[‖*]	NA	NA	NA	NA	NA	NA	NA	NA	NA	NA	NA	NA
McCreary, 2020 [183]	β=0.74 [a*]	NA	β=0.36[a]	NA	NA	β=0.68[a*]	NA	NA	NA	β=-0.20[a]	NA	NA	NA
Petersen, 2020 [215]	NA	NA	NA	NA	NA	NA	NA	NA	NA	NA	NA	NA	R²=0.11/ 0.35[b*]
Frey, 2020 [216]	NA	NA	NA	NA	NA	NA	NA	NA	NA	NA	NA	NA	R=-0.57/-0.66 [c*]; R=0.37/0.46 [c*]
Raposo, 2021 [105]	β=0.66-0.71[d*]	NA	β=0.15 [d]	β=0.10-0.20 [d]	β=0.12[d]	NA	β=-0.14/-0.17[d]	NA	NA	NA	NA	NA	NA
Oberlin, 2021 [225]	*r=0.62* [‖*]	NA	NA	NA	NA	NA	NA	NA	NA	NA	r=-0.6 [‖*]	r=0.76 [‖*]	NA

Glossary: WMHV (white matter hyperintensity volume), CMB (cerebral microbleeds), PVS (perivascular spaces), cSS (cortical superficial siderosis), TBV (total brain volume), GMV (gray matter volume), WMV (white matter volume), FA (fractional anisotropy), MD (mean diffusivity).

[*] p<.05

[†] Pearson's *r* adjusted for age and sex. P-values of the correlations were not reported.

[‡] Value is in reference to the normal-appearing white matter volume.

[§] Linear regression models adjusted for motion, age, sex and diagnosis, in which each neuroimaging marker was entered individually as a predictor of PSMD.

[¶] Multivariable linear regression models, simultaneously including WMHV, Atrophy, GMV and WMV as independent variables.

[‖] Pearson/Spearman correlation.

[a] Linear regression models adjusted for age and sex, in which each neuroimaging marker was entered individually as a predictor of PSMD.

[b] Linear models, adjusted for age, sex and brain volume. Values are in reference to subcortical, frontal, occipital, parietal, inter- and intra-hemispheric connectivity.

[c] Simple linear regression. Positive values are in reference to normalized clustering coefficient and modularity Q. Negative values are in reference to normalized global efficiency and small-world propensity.

[d] Multivariable regression models, adjusted for age, *simultaneously* including WMHV, CSO-PVS, lobar CMBs, cSS and TBV as independent variables.

3.1.3.8 Neurocognitive associations

There was high variability across studies in the choice of neuropsychological tests used to compute the scores for each cognitive domain and in the statistical procedures employed to examine the associations with PSMD and clinical outcomes (Table 3.1.6), precluding more objective comparisons. Processing speed was the cognitive domain most consistently correlated with PSMD,[105,169,183,216,225,228] although with highly variable statistical estimates (β=-0.071 to -1.08). Associations were also found with global cognition/general cognitive ability (β=-0.146 to -0.558),[209,216,227,228] executive function (β=-0.382 to -1.583),[216,225,227] visuospatial ability (β=-0.184),[228] verbal/semantic fluency (r=0.1-0.25, β=-0.525),[218,219,225] cognitive inhibition (β=-0.80),[225] memory (β=-0.075 to -0.62),[184,218,219,225,228] and dysexecutive behavior (β=0.5).[225] In 7 different cohorts, the strength of PSMD's associations with cognition was compared against that of other MRI markers using multivariable models. Across all cohorts, PSMD explained additional variance in at least one domain, including global cognition/general cognitive ability,[209,228] processing speed,[105,169,216,218] executive function,[216] visuospatial ability,[228] semantic fluency,[225] cognitive inhibition,[225] and memory.[225] PSMD also outperformed other markers in predicting dysexecutive behavior,[225] discriminating patients with and without cognitive impairment (AUC=77%; 95%CI=69-85%),[209] and distinguishing between term and preterm neonates (classification accuracy: 0.77 ± 0.09).[189]

3.1.3.9. Risk of Bias

Overall, the quality of the included studies ranged between satisfactory and very good (Appendix 3.1.D, Table A.3.1.D). Data on the frequency of individuals who refused to participate and their characteristics were missing from all cross-sectional and case-control studies, whereas in longitudinal studies, information on whether the outcome of interest was accounted for and if there was loss to follow-up was not available. In the technical domain, though sufficient details on the MRI protocols were provided in almost all studies, information on the quality assessment of the DWI images and preprocessing steps employed were not consistently available. The definition and inclusion criteria of control groups were also not consistently provided. Finally, all studies performed well in providing details on the assessment of outcome (if applicable), presence of an exposure, and statistical tests.

Table 3.1.6 Details on the neuropsychological battery employed across the cohorts and the observed cognitive associations.

Cohort	Population/n	Domain(s)/Functions investigated	Neuropsychological Tests	Domains associated with PSMD	Associations with PSMD	
					Statistics	*p*
CADASIL exploratory [169]	CADASIL/104	2. Processing Speed	1. Trail Making Test (TMT) A and B	1. Processing Speed*§	ß=-0.886‡	2.8 x 10⁻¹³
VASCAMY [169]	CADASIL/57	1. Processing Speed	1. TMT A and B	1. Processing Speed*§	ß=-0.550‡	8.7 x 10⁻⁶
RUN DMC [169]	Sporadic cSVD/436	1. Processing Speed	2. 1-letter subtask of the Paper-Pencil Memory Scanning Test; Letter-Digit Substitution Task	1. Processing Speed*§	ß=-0.299‡	1.8 x 10⁻¹⁰
Memory-clinic Utrecht (High WMH) [169]	Sporadic cSVD/ 47	1. Processing Speed	1. TMT A and B	1. Processing Speed*§	ß=-0.376‡	.005
LBC 1936 [228]	Population-based 656-680	1. Processing Speed	1. Digit symbol and symbol search (WAI-III); simple reaction time; 4-choice reaction time; inspection time	1. Processing Speed*	ß=-0.273†	4.64 x10⁻¹¹
		2. Visuospatial ability	2. Matrix reasoning and block design (WAI-III); spatial span (WMS-III).	2. Visuospatial ability*§	ß=-0.184‡	.024
		3. Verbal Memory	3. Verbal paired associates and Logical memory (WMS-III); Backward digit span (WAI-III)	3. Verbal Memory*	ß=-0.168†	2.37 x 10⁻⁴
		4. Crystallized ability	4. National adult reading test; Wechsler test of adult reading; Phonemic verbal fluency test.	4. Crystallized ability	ß=-0.072†	.07
		5. General cognitive ability	5. Shared variance among the four cognitive domains.	5. General Cognition*§	ß=-0.146‡	.032
Beijing Tiantan Hospital [227]	Memory-clinic/ 113WML patients	1. Global cognitive function	1. MoCA	1. Global cognitive function (WML-VCI)*	ß=-0.558†	<.001
		2. Executive function	2. Stroop color and word test B and C, TMT A and B, symbol digital replacement task, verbal fluency test.	2. Executive function (WML-CN and WML-VCI)*	ß=-1.583/-0.382†	.008/<.001
CU-RISK [184]	Population/ 801 (BL); 515 (FU)	1. Processing Speed	1. Symbol Digit Modalities Test	1. Processing Speed* (baseline and follow-up)	ß=-0.089/-0.071†	.001/.003
		2. Executive function	2. Executive function subscores from MoCA	2. Executive function (baseline and follow-up)	ß=-0.013/-0.010†	.686/.789

Study	Population/ N	Domain	Measure	Outcome	Statistic	p/CI
		3. Memory	3. Memory subscores from MoCA	3. Memory* (baseline and follow-up)	ß =-0.075/-0.107[†]	.031/.009
NIMROD [209]	Memory-clinic/ 145	1. Global Measures of Cognition	1. MMSE	1. MMSE*	t=-2.13[†]	.033
			2. Addenbrooke's Cognitive Examination Revised (ACE-R)	2. ACE-R*[§]	ß =-0.373[‡]	<.001
				3. Cognitive Impairment (ACE-R cut-off of 83)*	AUC=77%	95%CI=69-85%
FAVR study [183]	CAA/32-34	1. Global cognition	1. MMSE	1. Global Cognition	ß=-0.313[†]	.111
		2. Processing Speed	2. Digit Symbol Substitution; TMT A	2. Processing Speed*	ß=-0.627[†]	<.001
		3. Executive function	3. TMT B; Controlled Oral Word Association	3. Executive function	ß=-0.206[†]	.197
		4. Memory	4. California Verbal Learning II delayed recall; Rey Osterrieth Complex Figure	4. Memory	ß=-0.303[†]	.08
Memory-clinic MGH [105]	CAA/24	1. Global cognitive status	1. MMSE	1. Global cognitive status	ß=-0.40[‡]	.31
		2. Processing Speed	2. TMT A; Digit Span Forward; Digit Symbol Coding (WAI-III)	2. Processing Speed*[§]	ß=-1.08[‡]	.004
		3. Executive function	3. TMT B; Digit Span Backward	3. Executive function	ß=-0.64[‡]	.09
		4. Memory	4. Hopkins Verbal Learning Test; Logical memory (WMS) immediate recall and delayed recall	4. Memory	ß=-0.69[‡]	.10
		5. Language	5. Boston naming test and animal naming test	5. Language	ß=-0.47[‡]	.16
HCHS [216]	Population-based/930	1. Global cognitive status	1. MMST	1. Global cognitive status*[¶]	NA[† a]	.017
		2. Processing Speed	2. TMT A	2. Processing Speed*	NA[† a]	.021
		3. Executive function	3. TMT B	3. Executive function*	NA[† a]	<.001
Cornell Medical College [225]	Late-life Depression/ 44	1. Global functioning	1. Dementia Rating Scale	1. Global functioning	NA	NA
		2. Processing Speed	2. TMT A	2. Processing Speed*	estimate=5.34[† b]	<.001
		3. Executive function	3. animal naming (semantic fluency); Stroop Interference (cognitive inhibition); TMT B-A	3. Executive function*[§]	ß=-0.525/-0.80[‡]	<.05/<.001

		4. Immediate verbal memory	4. Immediate verbal memory (Hopkins Verbal Learning Test-Revised)	4. Immediate verbal memory	N/A	N/A
		5. Delayed verbal memory	5. Delayed verbal memory (Hopkins Verbal Learning Test-Revised)	5. Delayed verbal memory*§	ß=-0.62‡	<.05
		6. Dysexecutive behavior	6. Executive function subscale of the Frontal Systems Behavior Scale (FrSBe)	6. Dysexecutive behavior*§	ß=0.5‡	<.05
University of Siena [219]	Multiple Sclerosis/ 47	1. Physical Disability	1. Expanded disability Status Scale (EDSS).	1. Physical Disability	r=0.2†	.2
		2. Processing speed	2. Paced Auditory Serial Addition Test; Symbol Digit Modalities Test	2. Processing speed*	r=0.3/0.6†	.013/<.001
		3. Verbal memory	3. Tests of verbal memory acquisition and delayed recall (Selective Reminding Test)	3. Verbal memory*	r=0.4-0.5†	<.001
		4. Visual memory	4. Visual memory acquisition and delayed recall (Spatial Recall Test)	4. Visual memory*	r=0.4†	.003
		5. Verbal fluency	5. Verbal fluency on semantic stimulus (Word List Generation)	5. Verbal fluency*	r=0.5†	.001
		6. Functional status	6. Modified Rankin Score (in 25 CADASIL patients)	6. Functional status	r=0.4†	.06
Universities of Siena and Florence [218]	Multiple Sclerosis/ 60	1. Processing speed	1. Paced Auditory Serial Addition Test, Symbol Digit Modalities Test	1. Processing speed*§	ß=-0.736‡; r=-0.7†	<.001
		2. Verbal memory	2. Selective Reminding Test, Long-Term Storage, Consistent Long-Term Retrieval and Delayed.	2. Verbal memory*	r=-0.35/-0.37†	.02/.016
		3. Visual memory	3. Spatial recall Test	3. Visual memory*	r=-0.28†	.02
		4. Verbal fluency	4. Word List Generation	4. Verbal fluency*	r=0.25†	.04
Royal Infirmary of Edinburgh [189]	Preterm birth/76	1. Gestational age at birth	1. Gestational age at birth in weeks	1. Gestational age at birth*	r=-0.52	2.72×10^{-10}

Glossary: CADASIL (Cerebral Autosomal-dominant Arteriopathy with Subcortical Infarcts and Leukoencephalopathy), CU-RISK (Chinese University of Hong-Kong-Risk Index for Subclinical brain lesions in Hong Kong), FAVR (Functional Assessment of Vascular Reactivity Study), HCHS (Hamburg City Health Study), WMH (white matter hyperintensity), LBC1936 (Lothian Birth Cohort 1936), MGH (Massachusetts General Hospital), NA (not available), NIMROD (NeuroInflammation in Memory and Related Other Disorders), RUN DMC (Radboud University Nijmegen Diffusion Tensor and Magnetic resonance Imaging Cohort), VASCAMY (Vascular and Amyloid Predictors of Neurodegeneration and Cognitive Decline in Nondemented Subjects), BL (patients with baseline data), FU (patients with follow-up data).

* Statistically significant.
† Models in which PSMD was the only neuroimaging marker entered as an independent variable.
‡ Models including other neuroimaging markers as concomitant independent variables.
§ PSMD explained additional cognitive variance in models including other MRI markers.
¶ Association did not remain significant after correcting for age, sex and years of education.
ª Statistical estimates are not available from the original manuscript, only *p*-values were reported.
ᵇ These values are in reference to the whole cohort (44 individuals with late-life depression and 65 controls); the association between PSMD and worse processing speed was reportedly stronger in the late-life depression group.

3.1.4. Discussion

Several key findings can be drawn from this systematic review involving 19 studies and 23,737 participants. Cohorts with WM injury from multiple causes display increased PSMD values, which are comparable in samples with similar diagnoses recruited from different cohorts, though with significant overlap between pathologies. PSMD appears robust against different scanners and MRI protocols, and there is promising data arguing in favor of high test-retest repeatability. PSMD is associated with age and progressively increases throughout adulthood. WMH is the neuroimaging marker most strongly correlated with PSMD. Cognitive associations are consistent across multiple cohorts and are strongest but not limited to the domain of processing speed. Finally, PSMD outperforms other conventional MRI markers (including WMHV) and primary DTI metrics (i.e., FA and MD) by explaining more variance in cognitive performance.

3.1.4.1. PSMD's instrumental properties

There was significant variability in DWI acquisition protocols and preprocessing steps across studies (Table 3.1.2). Primary DTI parameters (i.e., FA and MD) display good inter-scanner reproducibility in healthy subjects[230] and cSVD patients[231] and have been considered well-suited for multi-center trials without demanding extensive harmonization.[203,232,233] PSMD could be similarly robust, based on its comparable values in samples with similar diagnoses and contrasting DWI acquisition protocols and on formal reproducibility assessments (Table 3.1.3).[169,183,224]

3.1.4.2. PSMD and different WM disorders

The similarly increased PSMD values observed in cohorts with sporadic and inherited cSVD, like hypertensive arteriopathy, CAA and CADASIL, indicate that this metric is not specific to any small vessel pathology (Table 3.1.4; Figure 3.1.2). Furthermore, values obtained from non-cSVD cohorts, such as demyelinating disorders,[218,219] and even premature birth,[188,189] show significant overlap with cSVD samples (Table 3.1.4; Figure 3.1.2), favoring PSMD as a marker of global WM microstructural damage irrespective of cause.

Evidence suggests that PSMD is also sensitive to WM changes in AD[166,169,183] and possibly in other neurodegenerative conditions.[209] Abnormally increased PSMD values were estimated to precede the onset of clinical symptoms by 5 to 10 years in autosomal dominant AD mutation carriers.[166] How much of these WM changes are due to concomitant cSVD or exclusively to primary neurodegeneration is unknown since concomitant pathologies are ubiquitous in the aging brain, with mechanisms known to interact and aggravate each other.[13] Nonetheless, when applied specifically to elderly populations, PSMD is expected to reflect microvascular disease to the detriment of primary neurodegenerative abnormalities since the former more predominantly affects the WM, and its core lesions are better captured by PSMD. As recently shown for other DWI measures (MD, FA, and free water) in analyses across multiple samples, including genetically-defined diseases,[165] PSMD may also be predominantly influenced by cSVD- in comparison to AD-related abnormalities. Though evidence suggests that PSMD can detect WM changes in neurodegenerative disorders,[166,169,183,209] in a sample of AD patients, only the group with increased WMH burden presented increased PSMD.[169] Thus, PSMD has been considered a marker of cSVD-induced WM injury in the elderly and was employed as a surrogate for cSVD in several studies.[215–217,225] In one of these studies, PSMD values were unexpectedly lower in a sample of non-demented community-dwelling individuals classified as having presumed "vascular" cognitive impairment according to their plasma lipid profile,

which was similar to that observed in patients with vascular dementia.[217] Importantly, this "vascular" group displayed similar WMHV and conventional DTI metrics compared to the "control" group, implying that other pathologies than cSVD, mainly neurodegenerative diseases, were likely in place and could help explain this discrepant result.[217] Given the nonspecific nature of the DTI model and the still incompletely understood pathophysiology of WM lesions in AD and other neurodegenerative disorders, further studies are needed to determine if PSMD can disentangle the vascular contributions to disease burden.

3.1.4.3. PSMD and age

During normal maturation and aging, changes in water content, microstructural integrity, and volume of the brain occur and are reflected in several neuroimaging markers, including diffusion parameters such as FA and MD.[234] Previous studies reported non-linear associations between age and DTI metrics, with MD being considered the most age-sensitive measure.[234–236] In a multicenter study with cross-sectional data from 10 different population-based cohorts, divided into subsamples of 10-years age-range (18.1 to 92.6 years), Beaudet *et al.* observed that distinct from other DTI metrics, PSMD displays a specific lifespan profile, characterized by a constant and accelerating increase with age.[203] In contrast, metrics such as axial diffusivity, radial diffusivity, and MD show a J-shaped profile, and FA behaves inversely, initially displaying a small increase followed by a decrease.[203] This particular behavior supports a promising role of PSMD as a marker of brain aging.[184,203]

Nonetheless, it is important to highlight that PSMD values obtained from neonates in Edinburgh were the highest thus far reported, even higher than in CADASIL cohorts.[188,189] These values appear to decrease over the first neonatal weeks, as they were lower in term compared to preterm infants. Therefore, the consistent increase in PSMD values over the years may be specific to adulthood. More studies are required to better understand, from a developmental perspective, how this metric behaves during infancy and adolescence.

3.1.4.4. PSMD and other neuroimaging markers

Multiple studies have tried to identify which brain lesions preponderantly drive changes in PSMD, also as a means to shed some light on its unclear biological correlates. Early observations of higher PSMD values in cohorts with severe burden of WMH pointed to a strong association between PSMD and core cSVD markers.[169,227] This relationship was confirmed and addressed in more detail in several studies, which found PSMD to be associated with WMHV,[105,183,209,219,225,228] and the number of lobar lacunes.[209] For hemorrhagic markers, results

are conflicting. Though PSMD was associated with CMBs in a memory-clinic cohort,[209] studies in CAA patients failed to identify a relevant association with any hemorrhagic marker.[105,183] It is possible the correlation observed in the former study was not independent but driven by a higher overall burden of ischemic cSVD pathology since the adjustment for other cSVD imaging markers was not performed. The absence of association among CAA patients between PSMD and hemorrhagic features may be due to their predominantly cortical and leptomeningeal distribution and small impact on perilesional tissues.[71,183] Regarding the spatial distribution of established cSVD markers, one study found PSMD to be sensitive to different distribution patterns.[209] In this memory-clinic cohort, periventricular WMH, lobar CMBs, CSO-PVS, and lobar lacunes had a stronger influence on PSMD than deep WMH, basal ganglia CMBs, basal ganglia-PVS, and deep lacunes, respectively.[209] It is possible that the presence of cSVD markers in lobar regions could be sorting out the memory-clinic patients more likely to have underlying CAA pathology, and thus increased burden of WM injury and higher PSMD. Overall, global brain measures such as atrophy,[228] total brain volume,[105] GMV,[209,228] WMV,[209,228] and cortical thickness[183] have a small, and usually non-significant, influence on PSMD. In fact, dominance analyses have shown that WMHV contributes significantly more to PSMD than GM and WM volumes,[53] which is in line with the hypothesis that PSMD, like other diffusion metrics,[165] is more sensitive to cSVD than neurodegenerative abnormalities. This strong association with WMH may help explain the higher PSMD values observed in the NIMROD cohort [209] in comparison to other MCI/AD samples (Figure 3.1.B). Though there were no striking differences in age or technical parameters, most patients from the NIMROD cohort were cognitively impaired, and the reported mean WMHV was higher than in other cohorts. FA and MD measures [225,228], global and topological network graph DTI parameters [215,216]were also associated with PSMD.

With regards to other DWI-based markers, PSMD correlated with general MD and FA measures derived from tractography in two different cohorts.[225,228] PSMD was also associated with DTI graph-based network parameters even in patients with low burden of WMH,[215] and outperformed WMHV by explaining a larger variance of global efficiency.[216] Abnormally high PSMD was found in pre-symptomatic autosomal dominant AD mutation carriers, when only subtle MD changes restricted to callosal fibers were detectable, suggesting that PSMD could be sensitive to very early and localized WM injury.[166] In contrast, PSMD, like other diffusion-based markers, failed to detect WM abnormalities in pre-symptomatic D-CAA mutation carriers but was sensitive to changes in the symptomatic phase of the disease.[226]

3.1.4.5. PSMD and cognition

PSMD has been consistently associated with cognitive endpoints, especially in cohorts with severe burden of WM lesions, in which it explained alone between 8.8 and 54% of the variance in cognitive performance.[105,169,183,218] These associations were frequently absent in cohorts with low burden of cSVD,[105,169,227] probably because WM injury is less likely to be the main mechanism leading to cognitive impairment in that context. Nonetheless, strong associations were found in population-based samples, despite the low burden of cSVD, probably driven by abnormalities in the NAWM and detectable due to the increased statistical power of large samples.[184,216,228]

Concerning the cognitive functions associated with PSMD, Baykara *et al.* suggested a particular link with the domain of processing speed, which is further supported by two independent studies in sporadic CAA patients and a control sample of non-depressed individuals, in whom PSMD was exclusively associated with processing speed scores.[105,169,183,225] Indeed, impairment in processing speed and executive function are consistent findings in cohorts with vascular cognitive impairment and dementia (VCID).[169] However, most studies that favored a predilection of PSMD for processing speed scores used a limited number of neuropsychological tests, covering few cognitive domains. To address these issues, Deary *et al.* investigated how PSMD related with five individual tests of processing speed and with other cognitive domains in patients from the Lothian Birth Cohort 1936.[228] They observed that PSMD was inversely correlated not only with all measures of processing speed but also with the domains of memory, visuospatial ability, and general cognitive ability, independently predicting performance in the latter two.[228] Other studies found PSMD to be associated with global cognition,[209,227] executive function,[225,227] semantic fluency,[225] cognitive inhibition,[225] and other clinical outcomes such as physical disability.[219]

Such correlation with a broad range of neurocognitive outcomes could be regarded as an advantageous feature since recent studies on age-related cognitive impairment point to multiple co-occurring pathologies contributing to heterogeneous cognitive profiles.[1] A marker capable of capturing disturbances across a wide range of domains may be particularly suited to investigate cognitive impairment in the elderly, and could potentially be used as a clinical trial endpoint.

Several studies indicate that PSMD is a superior biomarker compared to conventional MRI measures, explaining additional variance in clinical endpoints.[105,169,209,218,225,228] Though this could be simply secondary to the general superiority of DTI, studies have shown that PSMD also outperforms other primary diffusion metrics in predicting cognitive/functional variance,

like mean FA[209,228] and other established MD parameters (mean,[169,209,225,228] median,[169] peak height[169] and full width at half maximum[169]). Importantly, these findings were not consistent across cohorts or cognitive domains. For instance, PSMD explained the greatest extent of variance in processing speed in cohorts with sporadic[105,169,183] and inherited cSVD,[169] and MS,[218] but did not outperform other markers when the same domain was assessed in a population-based cohort[228] or in patients with late-life depression.[225] In population-based and memory-clinic cohorts, PSMD outperformed other markers in predicting visuospatial ability/general cognitive ability[228] and Addenbrooke's Cognitive Examination-Revised (ACE-R) scores,[209] respectively. The vast heterogeneity in cognitive tests and neuroimaging markers used in the studies precludes more detailed comparisons. In addition, differences in cohorts regarding the preponderant brain pathologies at play influence how specific biomarkers contribute to predicting cognitive function.

3.1.4.6. PSMD's biological correlates in the context of cSVD

Unlike other DTI indices, such as mean MD and FA, PSMD represents a dispersion rather than central tendency statistic,[203] that reflects the heterogeneity of MD values across voxels that fall in the main WM tracts. It has been hypothesized that PSMD could capture a variety of heterogeneity sources in diffusion parameters of the skeletonized WM since MD itself is already a weighted average of axial and radial diffusivity.[203] Beaudet *et al.* further suggested that regional heterogeneity and heterochrony in MD values are more likely to impact a dispersion metric like PSMD than a central tendency one like average MD, which could help explain PSMD's high sensitivity to WM injury and stronger cognitive associations.[203] Nonetheless, McCreary *et al.* showed that both PSMD and mean MD values were increased in CAA subjects, which could indicate similar underlying microstructural abnormalities.[183] Though PSMD's histopathological correlates remain unexplored, studies in CAA and MS show that MD values correlate with tissue rarefaction,[164] myelin density,[164,237] axonal count,[237] and WM microinfarcts.[164] PSMD likely reflects similar histopathological abnormalities. Higher tissue rarefaction and lower myelin density could reflect disruption of cortico-subcortical connections and slowing of synaptic transmission, thus affecting cognition. Accordingly, higher PSMD has been associated with a widespread decrease in structural connectivity, especially in inter- and long intra-hemispheric connections, as well as in subcortical and frontal areas.[215] In addition, PSMD correlated with a decrease in the brain's capacity to integrate information in the form of reduced global efficiency, which has been reported to mediate the association between cSVD and cognitive decline.[216] Interestingly, the same network parameter was more

strongly correlated with periventricular than deep WMHV, which could be related to a disproportionate decrease in long-range connectivity.[216] This observation contributes to explaining PSMD's strong cognitive associations since the novel marker also seems to be predominantly driven by WMH located in the periventricular, in comparison to deep regions.[209]

3.1.4.7. Validation of PSMD as a VCID biomarker

As part of a global scientific effort to promote the development and validation of neuroimaging markers for the study of age-related cognitive impairment, a framework was proposed in 2019, containing the steps that must be fulfilled to validate a neuroimaging marker as a surrogate for clinical endpoints.[107] The status of different imaging techniques was assessed, and DTI markers were among the most promising ones.[107] A complete assessment of PSMD's status as biomarker has not yet been performed, and to fill this gap, we organized the available evidence addressing each validating step (Table 3.1.7). Substantial evidence for proof of concept, principle, effectiveness and reproducibility are available in the literature, but data on the monitoring, and surrogate steps are largely absent. Specifically, though there is some evidence on the longitudinal changes of PSMD, only one study assessed whether these were related to the progression of disease or aggravation of clinical endpoints, with negative results.[183] Regarding PSMD's repeatability, results from 1 study in 41 patients are promising, but warrant confirmation by other studies.[224]

PSMD's weaknesses include the loss of anatomical information in favor of a single global metric and the lack of specificity with regard to the underlying pathological abnormality. PSMD is also susceptible to motion artifacts and large ischemic or hemorrhagic brain lesions, but several approaches can be taken to mitigate these biases, as mentioned in the introductory technical overview (section 1.4).

Table 3.1.7 HARNESS[9] framework to validation of neuroimaging biomarkers

Steps towards validation	Definition	Evidence
Proof of Concept [169,184,209,215,216]	Evidence that the marker reflects a specific abnormality	🟢
Proof of Principle [105,169,183,184,209,216,225–228]	Evidence that the marker distinguishes cases from controls or is associated with clinical outcomes	🟢
Repeatability [224]	Precision of repeated measurements under the same conditions and scanner.	🟡
Reproducibility [169,183,224]	Precision of replicate measurements on the same or similar subjects using different scanners.	🟢
Proof of Effectiveness [166,169,203]	Evidence that it is possible to apply the marker across larger groups of patients at multicenter studies.	🟢
Longitudinal [169,183]	The marker's rate of change over time has been define.	🟡
Monitoring [183]	Evidence that changes over time are associated with progression of cerebral small vessel disease	🔴
Surrogate	Evidence that changes are associated with and could substitute a clinical endpoints in cSVD.	🔴

Glossary: cSVD (cerebral small vessel disease).
The green circles represent supporting data from at least two independent research groups. The yellow circles represent steps for which there is either evidence from a single study or conflicting evidence from multiple. The red circles refers to steps for which there is insufficient evidence. Though PSMD's longitudinal changes were investigated by two independent studies, the sample sizes were small and only one of the studies reported the magnitude of the change, warranting future confirmation.

3.1.4.8. Strengths and limitations

Our systematic review is the first to present a detailed overview of this promising marker, covering its relevant technical aspects and research applications. Synthesizing the evidence around PSMD was hindered by the striking heterogeneity across studies, touching multiple fields. As previously reported, PSMD values may have been impacted by differences in the MRI protocols and the choices of software packages and preprocessing methods used. For instance, technical heterogeneity probably played a relevant role in explaining inter-study PSMD variability, particularly among non-pathological cohorts with similar age ranges, such as MRi-Share and BIL&GIL, or 1000BRAINS and HCHS (Figure 3.1.2). Similarly, cognitive and neuroimaging associations were influenced by characteristics intrinsic to each cohort, the neuropsychological battery, and even the statistical models applied. Despite all these heterogeneities, we could identify and report consistent patterns in terms of range, associations with clinical variables and other MRI markers, and prediction of neurocognitive outcomes. By organizing the available evidence around each step required for validating a neuroimaging biomarker, we could provide an up-to-date synthesis of PSMD's place and relevance in the research field.

3.1.4.9. Future Directions

While the intense heterogeneity across studies limited our analyses, it was also an important result per se, indicating the need for standardizing methods to homogenize neuroimaging and clinical data for future multi-center trials and meta-analyses. Despite the growing scientific evidence advocating for PSMD's excellent reproducibility, these discrepancies support the need for standardization of techniques to ensure more reliable comparisons in multi-center studies.

Accordingly, PSMD was recently included as candidate marker in initiatives to disseminate and standardize neuroimaging techniques for the study of VCID (i.e., https://markvcid.partners.org, https://harness-neuroimaging.org).

Several questions must be addressed for PSMD's validation as a surrogate marker. More longitudinal studies are required to examine if changes in PSMD over time reflect changes in the burden of disease or in clinical outcomes. It remains unknown how PSMD correlates with other advanced MRI markers of cSVD, reflecting hypoperfusion and blood-brain barrier dysfunction. In addition, the underlying histopathological substrates are so far unexplored, arguing for a more purposeful biological understanding of the marker. Moreover, PSMD's potential roles in other diseases, including neurodegenerative pathologies (e.g., Parkinson's, amyotrophic lateral sclerosis), traumatic brain injury, optic neuromyelitis, post-stroke recovery, and leukodystrophies, remain largely unexplored.

From a technical perspective, confirmation of repeatability is still needed and determining if changes in PSMD over time reflect changes in the burden of disease or clinical outcomes is a research priority. The best way to compute PSMD in cohorts with frequent ICH, infarct, or other, larger lesions remains unknown, and would help design future clinical trials. Since PSMD is sensitive to head motion, studies should also attempt to control for it in their analyses. In order to increase the comparability and generalizability of future results and to maximize the benefits of larger and longitudinal samples,[203] it is essential to harmonize all technical and analytical steps. Clinical translation would further benefit from future development of standardized protocols for 1.5T scanners and optimized post-acquisition DWI harmonizing techniques. In addition, PSMD's histopathological correlations are unexplored, arguing for a more purposeful biological understanding of the marker in the context of different underlying pathologies. Given the promising results already observed in several vascular and neurodegenerative disorders, PSMD could potentially be useful in other yet to be investigated neurological diseases, such as traumatic brain injury and leukodystrophies.

3.1.5. Conclusion

A growing body of evidence supports PSMD as a robust quantitative imaging marker capable of reflecting widespread WM injury related to multiple pathologies. In aging cohorts, PSMD is particularly sensitive to microvascular disease and has been successfully applied as a marker of cSVD. The superiority of PSMD over other MRI metrics relates to its fast and completely automated calculation, strong and consistent associations with clinical endpoints, and high

sensitivity to microstructural abnormalities not visible on conventional MRI. Future longitudinal studies will further elucidate PSMD's potential role as a surrogate marker for clinical trials, and could lead to its application in interventional studies and eventual incorporation into clinical practice.

3.2.   PSMD's cross-sectional associations in CAA

3.2.1. Introduction

Sporadic CAA is a highly prevalent cSVD in the elderly.[238] CAA is a well-known cause of lobar ICH and is also increasingly recognized as a major contributor to VCID.[239,240] Although underlying mechanisms leading to cognitive impairment in CAA remain uncertain, it has been hypothesized that recurrent vascular lesions cause progressive disruption of the brain's structural connectivity, compromising network efficiency.[241,242] Conventional MR markers of CAA, including lobar CMB,[243] cSS,[244] WMH,[89] and cortical CMI[98] have been linked to cognitive functions. However, these associations are mostly weak and inconsistent across studies, suggesting that these markers may reflect only the tip of the iceberg in the whole spectrum of vascular pathology.[12]

Accumulating evidence suggests that DTI methods detect loss of microstructural integrity and other abnormalities not captured by structural MRI, and tend to show stronger associations with cognition in cSVD subjects.[60,172] Yet, the direct application of DTI in routine clinical practice is hampered by highly variable, complex, and time-consuming processing techniques.

PSMD is a recently developed, fully automated DTI marker, based on the skeletonization of white matter tracts and histogram analysis of the mean diffusivity.[169] PSMD has been shown to be particularly sensitive to vascular-related white matter abnormalities, demonstrating consistent associations with processing speed in cSVD subjects.[169] However, despite the common nature and high prevalence of CAA in ageing populations, potential applications of PSMD in CAA have been scarcely investigated.

In the current study, we tested whether PSMD reflects the burden of underlying cSVD and cognitive dysfunctions in subjects with CAA. Among subjects with mild cognitive impairment recruited specifically from a memory-clinic setting, we explored whether (1) PSMD is increased

in subjects with CAA compared to non-CAA, (2) PSMD is associated with structural MRI markers of CAA, and (3) PSMD is correlated with cognitive functions.

3.2.2. Methods

The data supporting findings of this study is available from the corresponding author upon reasonable request.

3.2.2.1. Participants

We analyzed data from a memory-clinic research cohort from the Massachusetts General Hospital (MGH) between March 2010 and October 2016, and designed a case-control study. Patients underwent clinical examination, neuropsychological evaluation, and research MRI. The Institutional Review Board of the MGH approved this study, and written informed consent was obtained from all participants or their surrogates.

We included subjects ≥ 55 years old meeting Petersen's criteria (2004)[245] for MCI, based on clinical assessment of functional status, neurological evaluation, and extensive neuropsychological assessment. Upon visual examination of research MRIs, MCI patients were categorized as 1) CAA-MCI if they fulfilled the modified Boston criteria[34] for probable CAA (age ≥ 55 years old; and multiple CMB with or without cSS or single CMB and presence of cSS), or 2) non-CAA-MCI. In both groups, exclusion criteria were dementia, history of symptomatic or asymptomatic ICH (defined as hemorrhagic focus > 5 mm in diameter), presence of deep CMB (suggesting arteriolosclerosis as underlying cSVD), contraindication for MRI, and presence of excessive motion artifacts on DTI upon careful qualitative visual inspection.

3.2.2.2. Data collection

We systematically collected demographic information and medical history for each participant. All subjects underwent a standardized neuropsychological test battery, as previously described.[98] Global cognitive status was assessed with the Mini-Mental State Examination (MMSE).[246] Performance on neuropsychological tests was clustered to create composite scores exploring specific cognitive domains[247]: executive function [Trail Making Test B[248] and Digit Span Backward[249]], processing speed/attention [Trail Making Test A,[250] Digit Span Forward and Wechsler Adult Intelligence Scale−Third Edition (WAIS-III) Digit Symbol Coding[249]], memory

[Hopkins Verbal Learning Test–Revised[251] and Wechsler Memory Scale logical memory,[252] immediate recall and delayed recall], and language function [Boston Naming Test[253] and Animal Naming [254]]. Performance on each test was first transformed into sex-, age- and education-adjusted z-scores using published normative data.[246,254–256] Then, z-scores were averaged within each composite domain to obtain domain-specific scores for each subject.

3.2.2.3.   **MRI acquisition**

Neuroimaging was acquired on a 3-Tesla MRI scanner (Siemens Healthcare, Magnetom Prisma-Fit), using a 32-channel head coil. MRI sequences included high resolution diffusion weighted imaging (60 directions; repetition time [TR], 8020 ms; echo time [TE], 83 ms; slice thickness, 2 mm; in-plane 2 x 2 mm; b-value, 700 s/mm^2), 3D T1-weighted multi-echo (TR, 2300; TE, 2.98; slice thickness, 1 mm; in-plane 1 x 1 mm), 3D FLAIR sequence (TR, 6000; TE, 455; slice thickness, 1 mm; in-plane 1 x 1 mm), and a SWI sequence (TR, 30; TE 20; slice thickness, 1.4 mm; in-plane 0.86 x 0.86 mm).

The median delay between neuropsychological evaluation and MRI was 1.85 months [IQR, 0.00-3.06] and was shorter in subjects with CAA-MCI compared to those with non-CAA-MCI (0 [0.0-0.24] vs. 2.1 [1.17-3.30]; $p < 0.001$).

3.2.2.4.   **DTI and PSMD processing**

PSMD was calculated from unprocessed DTI data using a publicly available script (v.1.0) (http://www.psmd-marker.com).[169] This fully automated pipeline relies on Functional Magnetic Resonance Imaging of the Brain (FMRIB) Software Library (FSL v.6.0.1) for the preprocessing of DTI data (eddy current and motion correction [*eddy_correct*], brain extraction [*bet*], and tensor fitting [*dtifit*]), followed by skeletonization of preprocessed DTI data, application of a custom mask, and histogram analysis (Figure 3.2.1.A-E). Precisely, DTI data were skeletonized using the Tract-Based Spatial Statistics procedure (TBSS), part of the FSL, and the FMRIB 1mm fractional anisotropy (FA) template (thresholded at an FA value of 0.2). MD images were projected onto the skeleton, using the FA derived projection parameters. Next, to avoid contamination of the skeleton through CSF partial volume effects, the MD skeleton was further masked with a standard skeleton thresholded at an FA value of 0.3 and a mask provided with the PSMD pipeline in order to exclude regions adjacent to the ventricles, such as the fornix. Finally, PSMD was calculated as the

difference between the 95th and 5th percentiles of the MD values of voxels contained within the skeleton.[169] To ensure that results were not driven by outliers, extreme PSMD were identified (values below 1.5 x IQR from the 1st quartile or above 1.5 x IQR from the 3rd quartile) and excluded from analyses.

Figure 3.2.1. PSMD in MCI patients with and without CAA
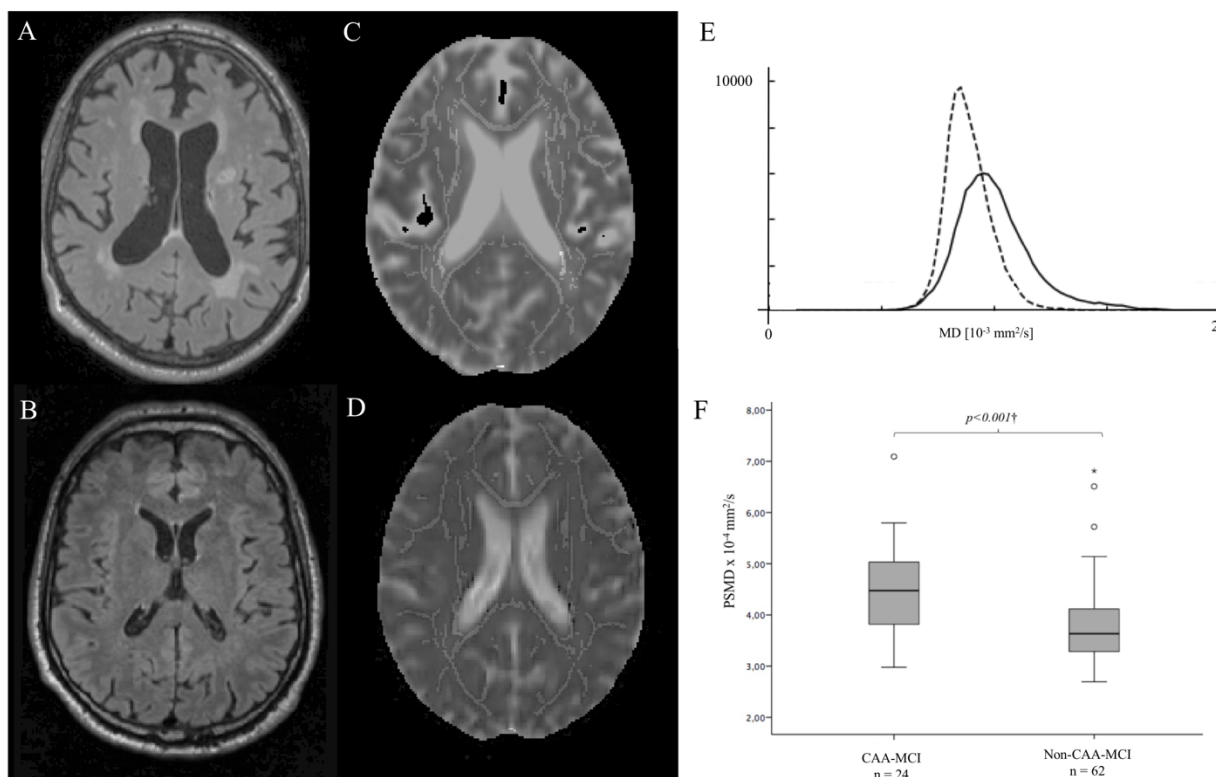
Source: Raposo N & Zanon Zotin MC, et al. 2021.

FLAIR images from a subject with CAA-MCI (A) and one with a non-CAA-MCI (B), demonstrating different burdens of WMH. MD maps display the skeletonized WM tracts from the same subjects with CAA-MCI (C) and non-CAA-MCI (D). E, Histograms depict the MD values of the voxels contained in the WM tract skeleton from the same subjects with CAA-MCI (solid line) and non-CAA-MCI (dashed line). F, The boxplot represents group differences in PSMD between CAA-MCI and non-CAA-MCI. The dagger indicates the results derived from ANCOVA, adjusting for age at MRI (P , .001).

3.2.2.5.   **Neuroimaging markers of cSVD**

MRI markers of cSVD were quantified by investigators blinded to all clinical data and according to the Standards for Reporting Vascular Changes on Neuroimaging (STRIVE) recommendations.[81] The presence, number, and location of CMB were evaluated on the SWI images according to the current consensus criteria.[66,81] They were classified as lobar when located in cortical and cortico-

subcortical areas. cSS was visually assessed according to recently proposed criteria and transformed into a dichotomous variable (absence versus presence).[257] CSO-PVS were rated on axial T1-weighted MRI, according to a previously developed score,[59] and were analyzed both as dichotomous (≤2 versus >2) and as ordinal variables. CMB, cSS, and CSO-PVS were analyzed by two experienced raters (NR & DS) using validated scales, and final ratings were obtained via a consensus.

After visual inspection of MR images quality, WMHV, total brain volume (TBV), and total intracranial volume (ICV) were calculated using FreeSurfer version 5.3, as previously described.[111] Normalized TBV (nTBV) was calculated as the TBV/ICV ratio, and normalized WMHV (nWMHV) calculated as WMHV/ICV * 100.

3.2.2.6.   **Statistical analysis**

We compared the clinical and imaging characteristics between MCI subjects with and without CAA using $\chi2$ or Fisher test for categorical variables and independent t-test or Mann-Whitney U-test for continuous variables, as appropriate. The distribution of continuous variables was tested for normality with the Shapiro-Wilk test.

Log-transformed PSMD values were compared between CAA-MCI and non-CAA-MCI patients using an ANOVA, adjusted for age. We further adjusted for log-transformed nWMHV and cognitive status (MMSE).

Receiver operating characteristic (ROC) curves analyses were used to quantify the performance of PSMD and nWMHV in discriminating CAA from non-CAA subjects.

The association between (1) PSMD and MRI markers of cSVD, and (2) PSMD and cognitive performances were evaluated in CAA-MCI and non-CAA-MCI separately. Linear regression models were used to explore relationships between PSMD and structural MRI markers of cSVD (lobar CMB count, CSO-PVS score, presence of cSS, nWMHV, and nTBV), adjusting for age. The associations between PSMD and cognitive scores in each domain were explored using linear regression models in both groups separately, adjusting for structural MRI markers of cSVD and the time delay between the neuropsychological evaluation and the MRI. Because cognitive scores were already adjusted for age, sex, and education level, these variables were not included in the models.

The statistical significance level was set at 0.05 for all analyses. We used the Statistical Package for the Social Sciences (SPSS) version 24.0 (for Windows; SPSS Inc, Chicago, IL) for statistical analysis.

3.2.3. Results

We identified 134 subjects with cognitive impairment enrolled in this prospective study who underwent a research MRI. Of them, 42 subjects were excluded based on the pre-specified criteria: diagnosis of dementia (n=6), possible CAA category (n=10), presence of deep CMB (n=5), lack of neuropsychological tests (n=19) and presence of excessive motion artifacts on DTI, based on qualitative visual inspection (n=2). Additionally, three outliers with extreme PSMD values (all with high values) were identified in each group and were excluded from the analysis. The final cohort consisted of 86 subjects with MCI (mean age 73.7 ± 7.7; 38.4% female) without a history of ischemic stroke or ICH, including 24 subjects with probable CAA (CAA-MCI; 27.9%) and 62 without CAA (non-CAA-MCI; 72.1%).

3.2.3.1. **Comparison between CAA and non-CAA subjects.**

Subjects with CAA-MCI and non-CAA-MCI were similar in age and vascular risk factors (Table 3.2.1). MMSE scores were lower in subjects with CAA-MCI compared to subjects with non-CAA-MCI ($p = 0.003$). Patients with CAA-MCI had worse performance in memory than subjects with non-CAA-MCI ($p = 0.005$). The two groups had similar scores across all other cognitive domains ($p > 0.05$, for all). Compared to non-CAA-MCI, subjects with CAA-MCI presented a higher burden of MRI markers of cSVD, including a higher prevalence of cSS ($p < 0.001$), higher lobar CMB count ($p < 0.001$), greater nWMHV ($p = 0.016$), higher prevalence of high CSO-PVS scores ($p < 0.001$), and lower nTBV ($p = 0.004$). PSMD values were significantly higher in CAA-MCI in comparison to non-CAA-MCI ($p < 0.001$) (Figure 3.2.1.F), even after adjusting for age ($p < 0.001$). In a post-hoc analyses, we found that PSMD remained significantly higher in subjects with CAA-MCI compared to subjects with non-CAA-MCI when further controlling for nWMHV ($p = 0.007$) or cognitive status [MMSE-z-scores] ($p < 0.001$). In ROC analyses, PSMD (area under the curve [AUC]= 0.755; 95% confidence interval [CI] 0.636-0.873, $p < 0.001$) was able to significantly discriminate CAA subjects from non-CAA subjects, and yielded a greater AUC than nWMHV (AUC= 0.668; 95% CI 0.544-0.792, $p = 0.016$; Figure 3.2.2).

Table 3.2.1. Baseline characteristics of subjects with CAA-MCI and those with non-CAA-MCI

	CAA-MCI (n=24)	non-CAA-MCI (n=62)	*p*-value
Demographics			
Age at NPT, mean (SD)	74.73 (5.99)	73.25 (8.33)	0.36
Female, n (%)	7 (29.2)	26 (41.9)	0.27
Education (years), median (IQR)	16 (16, 18)	16 (14, 18)	0.04*
Vascular risk factors			
Hypertension, n (%)	13 (54.2)	40 (64.5)	0.38
Diabetes, n (%)	1 (4.2)	10 (16.1)	0.17
Atrial Fibrillation, n (%)	4 (16.7)	5 (8.1)	0.26
Dyslipidemia, n (%)	13 (54.2)	44 (71.0)	0.14
Neuropsychological performances			
MMSE, median (IQR)	25.5 (24, 28)	28 (26, 29)	0.006*
MMSE (Z score), median (IQR)	-1.88 (-3.28, -0.16)	0 (-1.48, 1.11)	0.003*
Memory (Z score), median (IQR)	-1.91 (-2.38, -0.75)	-0.47 (-1.60, 0.56)	0.005*
Processing Speed (Z score), median (IQR)	-0.24 (-0.62, 0.15)	-0.11 (-0.46, 0.27)	0.34
Language (Z score), median (IQR)	-0.44 (-0.91, 0.36)	-0.36 (-1.17, 0.19)	0.95
Executive Function (Z score), median (IQR)	-0.59 (-1.89, 0.22)	-0.21 (-0.86, 0.12)	0.20
Imaging			
PSMD (x 10^{-4} mm^2/s), median (IQR)	4.48 (3.81, 5.09)	3.63 (3.28, 4.13)	< 0.001*
Lobar CMB count, median (IQR)	5.5 (3.0-24.50)	0 (0-0)	< 0.001*
cSS (presence), n (%)	9 (37.5)	0 (0.0)	< 0.001*
High CSO-PVS score (>2), n (%)	11 (45.8)	3 (4.8)	< 0.001*
nWMHV, median (IQR)	0.42 (0.28, 1.74)	0.29 (0.14, 0.75)	0.02*
nTBV, mean (SD)	0.61 (0.04)	0.64 (0.05)	0.004*

Abbreviations: NPT = Neuropsychological tests; MMSE = Mini-mental State Examination; PSMD = Peak Width of Skeletonized Mean Diffusivity; CMB = cerebral microbleeds; cSS = cortical superficial siderosis; CSO-PVS = perivascular spaces in the centrum semiovale; nWMHV = normalized white matter hyperintensities volume; nTBV = normalized total brain volume.
* = significant.

Figure 3.2.2. Receiver operating characteristic curve analyses investigating the classification performance of PSMD and nWMHV
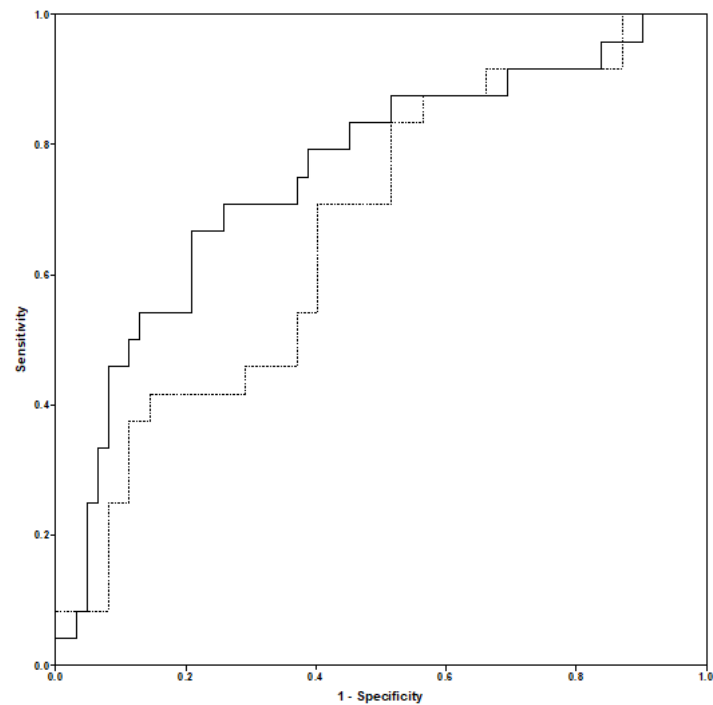
ROC curve illustrating the ability of peak width of skeletonized mean diffusivity (PSMD; solid line) and normalized white matter hyperintensities volume (nWMHV; dotted line) in differentiating between cerebral amyloid angiopathy (CAA) subjects with mild cognitive impairment (CAA-MCI) and subjects with mild cognitive impairment not attributable to CAA (non-CAA-MCI). PSMD (AUC=0.755, p<0.001) and nWMHV (AUC=0.668, p=0.016) significantly distinguished the MCI groups.

3.2.3.2.   Associations between PSMD and markers of cSVD.

In linear regression analyses adjusting for age, increased PSMD was associated with greater nWMHV both in CAA-MCI ($b = 0.75$; p <0.001) and non-CAA-MCI ($b = 0.69$; p <0.001) groups, but not with nTBV, CMB, CSO-PVS or cSS (Table 3.2.2). In multiple regression models including all quantified structural MRI markers of cSVD, only nWMHV remained independently associated with PSMD in subjects with CAA-MCI ($b = 0.66$; p <0.001) and non-CAA-MCI ($b = 0.71$; p <0.001) (Table 3.2.2 and Figure 3.2.3).

Table 3.2.2. Association between PSMD and MRI markers of small vessel disease in CAA-MCI and non-CAA-MCI subjects.

	Model 1‡			Model 2†		
	Std. b	95% CI		p	Std. b	95% CI		p
CAA-MCI (n=24)								
Lobar CMB count	0.15	-0.27	0.58	0.46	0.15	-0.13	0.42	0.28
cSS	0.27	-0.15	0.70	0.20	0.12	-0.16	0.40	0.38
CSO-PVS score	0.31	-0.09	0.71	0.13	0.20	-0.10	0.49	0.18
nWMHV	0.75	0.49	1.02	<0.001*	0.66	0.37	0.95	<0.001*
nTBV	-0.26	-0.79	0.26	0.31	-0.17	-0.54	0.20	0.34
Non-CAA-MCI (n=62)								
CSO-PVS	-0.02	-0.24	0.21	0.87	0.10	-0.07	0.27	0.25
nWMHV	0.69	0.50	0.89	<0.001*	0.71	0.51	0.91	<0.001*
nTBV	-0.23	-0.51	0.06	0.11	-0.14	-0.36	0.08	0.20

Linear regression models with PSMD (x 10^{-4} mm^2/s) as the dependent variable. ‡ Linear regression analyses adjusted for age. † Multiple regression models, including all neuroimaging markers and adjusting for age. In non-CAA-MCI subjects, the presence of cSS and lobar CMB count were automatically excluded from the models due to the absence of variance within the group.

Abbreviations: CMB = cerebral microbleeds; cSS = cortical superficial siderosis; CSO-PVS = perivascular spaces in the centrum semiovale; nWMHV = normalized white matter hyperintensities volume; nTBV = normalized total brain volume *=significant.

Figure 3.2.3. Association between imaging markers and PSMD in CAA-MCI and non-CAA-MCI subjects.
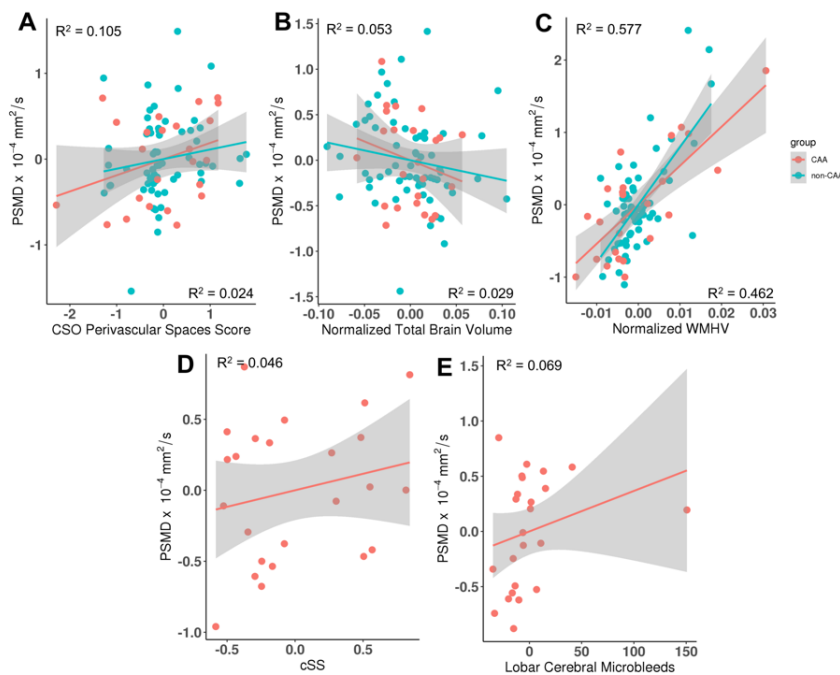
Source: Raposo N & Zanon Zotin MC, et al. 2021.

Partial regression plots illustrate the association between PSMD and multiple neuroimaging markers, adjusted for age at MRI. The plots illustrate a multiple linear regression model in which PSMD is the dependent variable and (A) centrum semiovale perivascular space score (CSO PVS), (B) normalized total brain volume (nTBV), (C) normalized white matter hyperintensities volume (nWMHV), (D) presence of cortical superficial siderosis (cSS), and (E) lobar cerebral microbleed count (CMBs) are included together as independent variables, adjusted for age at MRI. The values from the CAA-MCI group are displayed in red and those from non-CAA-MCI are displayed in blue. The R^2 provided in the left upper corners refer to the CAA-MCI group, whereas the R^2 provided in the bottom right corners refer to the non-CAA-MCI group.

3.2.3.3. Associations between PSMD and cognitive functions.

In the CAA-MCI group, multiple regression models accounting for lobar CMB count, cSS, CSO-PVS score, nWMHV, and nTBV demonstrated that increased PSMD was independently associated with worse performance in processing speed (b = -1.08; p =0.004) (Table 3.2.3 and Figure 3.2.4). In the non-CAA-MCI group, multiple regression analyses did not reveal any significant associations between PSMD and scores reflecting each cognitive domain (Table 3.2.3 and Figure 3.2.4).

Table 3.2.3. Association between PSMD and cognitive performance in CAA-MCI and non-CAA-MCI subjects.

	Adjusted model†		
	Std. b	95% CI		p-value
CAA-MCI (n=24)				
Global Cognitive Status	-0.40	-1.21	0.41	0.31
Memory	-0.69	-1.52	0.15	0.10
Processing Speed / Attention	-1.08	-1.76	-0.40	0.004*
Language	-0.47	-1.16	0.21	0.16
Executive Function	-0.64	-1.37	0.10	0.09
non-CAA-MCI (n=62)				
Global Cognitive Status	0.30	-0.13	0.72	0.17
Memory	0.14	-0.28	0.56	0.50
Processing Speed / Attention	0.16	-0.27	0.59	0.46
Language	0.14	-0.29	0.57	0.52
Executive Function	0.11	-0.30	0.53	0.58

Multiple regression model with cognitive performance as the dependent variable. †Model including nWMHV, nTBV, CSO-PVS score, presence of cSS, lobar CMB count, and adjusting for the time delay between the neuropsychological evaluation and the MRI. In non-CAA-MCI subjects, the presence of cSS and lobar CMB count were automatically excluded from the models due to an absence of variance within the group.
*=significant.

Figure 3.2.4. Association between PSMD and performance in multiple cognitive domains in CAA-MCI subjects and non-CAA-MCI.
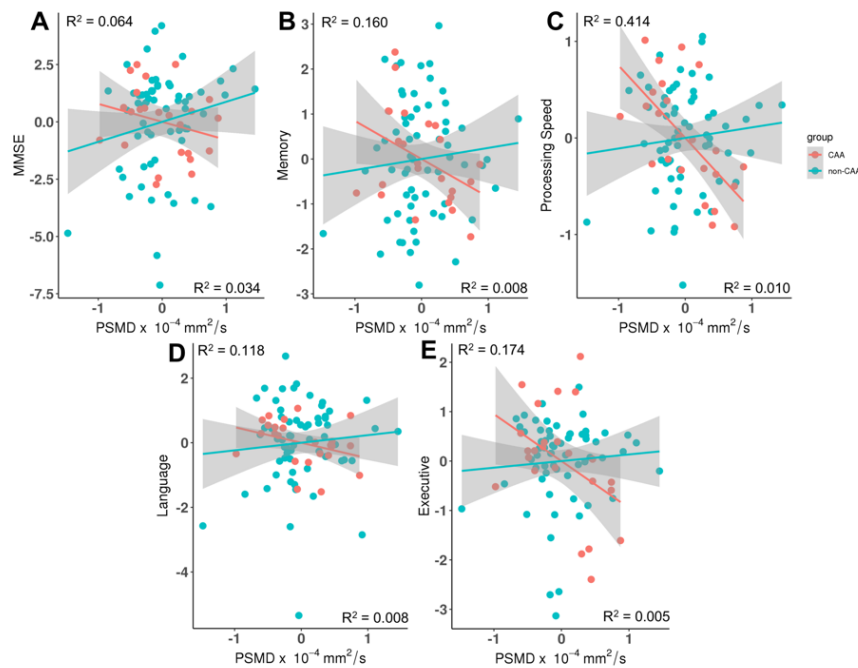
Partial regression plots illustrate the association between PSMD and performance in multiple cognitive domains. The plots illustrate linear regression models in which each cognitive function ([A] MMSE, [B] Memory, [C] Processing Speed/Attention, [D] Language, and [E] Executive) is entered as dependent variable and all neuroimaging markers (lobar cerebral microbleed count, centrum semiovale perivascular space score, presence of cortical superficial siderosis, normalized total hyperintensities volume (nWMHV), normalized total brain volume (nTBV) and PSMD) are included together as independent variables, adjusting for time delay between the neuropsychological evaluation and the MRI. The values from the CAA-MCI group are displayed in red and those from non-CAA-MCI are displayed in blue. The R^2 provided in the left upper corners refer to the CAA-MCI group, whereas the R^2 provided in the bottom right corners refer to the non-CAA-MCI group.

3.2.4. Discussion

Several key findings emerge from this study on PSMD in patients with CAA presenting with MCI in the absence of ICH. First, MCI subjects with CAA showed increased PSMD values compared to MCI subjects without CAA, even after adjusting for baseline differences in age, nWMHV, and cognitive status. Second, we confirmed that PSMD was strongly associated with WMHV in our CAA population, but not with other structural markers of cSVD. Third, we found that PSMD values were associated with worse performance in processing speed among CAA-MCI subjects, after controlling for the presence of other MRI markers of cSVD. In contrast, PSMD was not associated with cognitive function in subjects with non-CAA-MCI.

PSMD studies have so far focused mainly on community-dwelling[169,184,228] and cognitively impaired elderlies,[169,209] as well as inherited,[169,226] and sporadic cSVDs.[169,227] To our knowledge, only one previous study has investigated PSMD's performance in sporadic CAA, including subjects with and without ICH recruited from both stroke prevention and memory-clinics [183]. Since CAA pathology is highly prevalent and significantly contributes to vascular cognitive impairment in the elderly populations,[21] further investigating PSMD's performance in the context of CAA is an important step for the validation of this new neuroimaging biomarker as a surrogate for cognitive dysfunction in cSVDs.[107]

As expected, the PSMD values we obtained in memory-clinic CAA subjects were remarkably similar to those found in other sporadic cSVD cohort,[169,227] including another CAA cohort,[183] which corroborates reproducibility and stability of PSMD across different scanners, sequences, and even clinical samples.[169,203]

The observed increase in PSMD values among CAA-MCI subjects supports the hypothesis that whole-brain microstructural integrity is impaired in this population. Our results are in accordance with previous studies showing microstructural abnormalities in CAA relying on other DTI-based methods.[172,178] Importantly, PSMD offers several advantages in comparison to other DTI methods: it is a fully automated and fast technique; it offers higher interscanner reproducibility; power calculations have shown smaller sample size estimates for PSMD; and it is more strongly associated with performance in processing speed.[169]

Group differences in PSMD remained significant (CAA-MCI vs. non-CAA-MCI) even after adjusting for age, nWMHV, and MMSE. This suggests that PSMD differences are not solely driven by these factors and may indicate that this marker, like other global DTI measures, might capture abnormalities not visible on structural MRI sequences.

In our CAA-MCI sample, PSMD was strongly associated with nWMHV, but not with hemorrhagic markers of CAA (lobar CMBs and cSS), which is in line with findings from a recent study on a different CAA sample,[183] and suggests that white matter tracts disruption in CAA may be more closely linked to cSVD damage from ischemic than hemorrhagic origin.

The encouraging finding that PSMD is independently associated with processing speed in our subjects with CAA-MCI, after adjusting for other conventional MRI markers of cSVD, is in consonance with recently published results from another CAA sample.[183] The lack of association between PSMD and cognition in the non-CAA-MCI sample is consistent with findings from other

studies in cohorts with low burden of cSVD.[169,227] PSMD, like other DTI metrics, appears to be more sensitive to cSVD-related white matter abnormalities than to neurodegenerative pathology.[165,169] The low burden of cSVD pathology observed in our non-CAA sample might explain the absence of association between PSMD and processing speed.

Our results argue in favor of a strong link between PSMD and processing speed in cSVD populations, as advocated in the original PSMD study.[169] However, mechanisms underlying these strong associations with cognition are incompletely understood. McCreary *et al.* reported that a greater variation in white matter MD could be seen in microarchitectural disruption caused by pathological processes.[183] Though the histopathological features specifically associated with increases in PSMD remain unknown, tissue rarefaction and lower myelin density have been related to MD variations in CAA subjects.[164] It is possible that similar microstructural abnormalities underlie changes in PSMD in CAA, reflecting disruption of synaptic transmission that could affect cognition.

Our study has limitations. The small sample size of our cohort may account for the relatively weak cognitive correlations observed. Hence, our findings should be considered preliminary and require external validation in larger CAA cohorts. By including only subjects with MCI (cognitively-normal and demented CAA subjects were excluded), our study was not designed to assess relationships between PSMD and the full spectrum of cognitive impairment, ranging from MCI to dementia. Still, our significant findings in subjects with mild forms of cognitive impairment argue in favor of the robustness of PSMD as a biomarker for cognitive function in CAA. Additionally, our study included participants with a specific presentation of CAA (i.e., mild cognitive symptoms without ICH). We excluded subjects with ICH, as this likely represents a different phenotype of the disease.[258] While we designed our study to examine this specific group of CAA subjects that frequently present in memory clinic settings, our results cannot be generalized to other CAA populations or phenotypes. Another limitation of our study is the absence of comparisons between PSMD and other previously validated DTI-based markers to assess whether this new method constitutes a superior biomarker.

Nonetheless, this study also has several strengths and expands on previous literature by evaluating the relevance of PSMD in a specific phenotype of CAA and investigating its independent cognitive and neuroimaging associations.

3.2.5. Conclusions:

PSMD values are higher among cognitively impaired subjects with CAA in comparison to non-CAA subjects and are associated with nWMHV and performance in processing speed. Our preliminary results support the relevance of PSMD, a completely automated DTI-based method, in capturing microstructural brain changes in subjects with CAA, even in the absence of ICH. PSMD may serve as a biomarker in future clinical trials involving CAA and other cSVDs.

3.3. PSMD's spatial signature in CAA and comparison with conventional DTI markers

This analysis was performed by the author (first author) and collaborators (Dorothee Schoemaker, Nicolas Raposo, Valentina Perosa, Martin Bretzner, Lukas Sveikata, Qi, Li, Susanne van Veluw, Mitchell J. Horn, Mark R. Etherton, Andreas Charidimou, M. Edip Gurol, Steve Greenberg, Marco Duering, Antônio Carlos dos Santos, Octávio Marques Pontes-Neto, and Anand Viswanathan), and is currently under review.
Preliminary results were also the subject of an e-poster presentation in the 2021 Virtual International Stroke Conference (Appendix 3.3).

3.3.1. Introduction

CAA is a form of cSVD related to the deposition of amyloid-beta around cortical and leptomeningeal vessels.[21] CAA is highly prevalent among older individuals and is recognized to impact cognition independently from commonly co-occurring AD.[17] CAA has thus emerged as an important vascular contributor to cognitive impairment and dementia, even in the absence of ICH.[53]

In order to facilitate future development of disease-modifying therapies for VCID, much effort has been put into validating neuroimaging markers able to quantify the widespread parenchymal injury associated with cSVD.[107] Among the many MRI markers available, those based on DTI provide more consistent cognitive associations due to their continuous quantitative nature and higher sensitivity to microstructural abnormalities.[259]

In this setting, a novel and fully automated DTI marker called PSMD has been considered particularly promising.[169] PSMD is a fully automated histogram marker that reflects the heterogeneity of the MD values across the main WM tracts. It was developed to quantify the WM injury related to VCID and has provided consistent cognitive associations in several populations, especially among cohorts with cSVD.[105,169,183,184,209,227,228] According to previous data, PSMD explains a considerable proportion of the variance in processing speed in CAA samples, and could become a relevant marker for CAA-related cognitive impairment.[105,183]

However, several questions concerning the utility of this marker in the field of CAA remain unanswered. In general, PSMD values found in samples with cSVD are higher than in those with predominantly neurodegenerative pathology. However, it remains unknown whether PSMD values vary significantly across different forms of sporadic cSVD. Though it has been suggested that a regional analysis of PSMD values is feasible,[203,209] no studies to date have investigated variances in PSMD values across different brain lobes. Specifically, it is unknown whether PSMD

could capture the posterior predominance of CAA pathology, like other diffusion techniques.[172] Furthermore, only one study in CAA has compared PSMD with other simpler DTI markers in terms of cognitive and neuroimaging associations, but the extent to which this new marker outperforms MD and fractional anisotropy (FA) remains uncertain.

In this context, our aims were: (1) to compare PSMD values in different MRI phenotypes of sporadic cSVDs and in subjects without evidence of cSVD on MRI; (2) to investigate whether the posterior predominance of CAA pathology is reflected on regional variations of PSMD values; (3) to investigate PSMD's cognitive and neuroimaging associations in CAA, in comparison to other conventional and DTI-based MRI markers.

3.3.2. Materials and Methods

3.3.2.1. Standard Protocol Approvals and Patient Consents

This study was approved by the Institutional Review Board of the Massachusetts General Hospital (MGH), and written informed consent was obtained from all subjects or their surrogates.

3.3.2.2. Study Participants

This study is a retrospective analysis of an ongoing single-center prospective memory-clinic research cohort from the MGH. Subjects were recruited between August 2010 and November 2019.

We included non-demented subjects aged 55 years or more with complete clinical evaluation, neuropsychological examination, and 3T MRI. Exclusion criteria were: dementia (defined as MMSE ≤ 24 and/or impairment of independent activities of daily living [IADs]); a history of symptomatic ICH; incomplete neuropsychological examination and/or research MRI; and presence of motion or other artifacts compromising neuroimaging assessment. To avoid diagnostic uncertainty, we also excluded subjects with a single hemorrhagic MRI marker fulfilling the modified Boston criteria[34] for possible-CAA and those with mixed-pattern of hemorrhages.[44] Based on the examination of MR images for conventional neuroimaging markers of cSVD, and according to the modified Boston criteria,[34] we stratified the participants into three groups: probable-CAA (patients fulfilling Boston criteria for probable CAA); cSVD (subjects not fulfilling criteria for either possible or probable CAA and presenting one or more of the other following MRI markers of cSVD: non-lobar CMB, and/or lacunes, and/or high-grade (>2) BG-PVS,[59] and/or

deep Fazekas score[115] ≥2 and/or periventricular Fazekas score[115] = 3); and non-cSVD (subjects without any of the above neuroimaging markers of cSVD). None of the cSVD subjects had any MRI or clinical features suggesting a hereditary/monogenic pathology. Therefore, they are presumably predominantly affected by the most prevalent etiological subtype of sporadic cSVD, related to aging and/or vascular risk factors such as hypertension (ASC/deep perforator arteriopathy).

3.3.2.3. Clinical and Neuropsychological Assessment

Demographic and clinical data were collected from each participant upon enrollment. All memory-clinic subjects underwent a thorough and standardized neuropsychological test battery. Four different cognitive domains were explored through composite scores created by clustering and averaging performance on different neuropsychological tests[247]: Executive function (Trail Making Test B[248] and Digit Span Backward[249]) processing speed/attention (Trail Making Test A,[250] Digit Span Forward,[249] and WAIS-III [Wechsler Adult Intelligence Scale−Third Edition] Digit Symbol Coding[249]), memory (Hopkins Verbal Learning Test-Revised[251] and Wechsler Memory Scale logical memory;[252] immediate recall and delayed recall), and language function (Boston Naming Test[253] and Animal Naming[254]). First, based on published normative data,[246,255,256] we transformed performance on each test into z-scores adjusted for gender, age, and education level. Then, these z-scores were averaged within composite domains to compute the domain-specific scores for each participant.

3.3.2.4. MRI acquisition

All exams were performed on a 3-T MRI scanner (Siemens Healthcare, Magnetom Prisma-Fit or TIM-Trio), using a 32-channel head coil. The scan protocol included: a 3D T1-weighted sequence (TR 2300-2510 ms; TE 1.69-2.98 ms; resolution 1 x 1 x 1 mm), a 3D FLAIR (TR 5000-6000 ms; TE 356-455 ms; resolution 1 x 1 x 1 mm), a SWI sequence (TR 27-30; TE 20; slice thickness, 1.4 mm; in-plane resolution 0.9 x 0.9 mm), and a 3D diffusion weighted imaging sequence (DWI, 60-64 directions; TR 8000-8040 ms; TE 82-84 ms; resolution 2 x 2 x 2 mm; b-value, 700 s/mm^2).

3.3.2.5. PSMD processing

Initially, a careful visual inspection of all DWI images was conducted, and cases with excessive motion artifacts were excluded. To objectively and quantitatively evaluate the magnitude of head motion during the acquisition of DWI images, we further extracted registration- and intensity-based measures to compute the Total Motion Index (TMI) proposed by Yendiki et al. TMI was originally developed to be used as a nuisance regressor to account for motion confounding in neuroimaging studies.[186] Since the intensity-based measures did not show significant variability across our subjects, only the registration-based measures were applied in the TMI formula.

We ran the fully automated PSMD script (version 1.0/2016) (http://www.psmd-marker.com),[169] including all the pre-processing steps, relying on the Functional Magnetic Resonance Imaging of the Brain (FMRIB) Software Library (FSL) version 6.0.1.[193] Briefly, the script runs motion and eddy-currents correction,[260] brain extraction,[192] and tensor fitting as pre-processing steps, obtaining maps of MD and FA. These maps are fed into TBSS, as implemented in FSL,[202] to achieve skeletonization of the main WM tracts. The obtained skeletonized MD maps are further masked with a custom mask to exclude areas prone to CSF contamination. Finally, a histogram analysis is conducted on the final MD maps, and the difference between percentiles 5 and 95 is computed to obtain PSMD values for each individual. Similar procedures were used to compute skeletonized average MD[183] and FA values.

3.3.2.6. Regional distribution of PSMD

To investigate potential differences in the white matter microstructural integrity across the anteroposterior axis and evaluate whether PSMD could capture the posterior predominance of CAA pathology, we used MNI152 atlas to create masks of the frontal and occipital lobes, manually filling missing voxels in the deep and periventricular WM areas (Figure 3.3.1.A).

We applied these two masks separately on all subjects and computed PSMD values restricted to frontal and occipital lobes. To depict PSMD's variation across the anteroposterior axis, we computed occipital-frontal gradients (occipital PSMD – frontal PSMD) for each participant.

3.3.2.7. Conventional neuroimaging markers

Conventional MRI markers of cSVD were rated by a neuroradiologist (M. C. Z. Z.), blinded to all clinical data, following the Standards for Reporting Vascular Changes on Neuroimaging

(STRIVE) recommendations.[81] CMBs were evaluated on SWI for presence, number, and location.[81] Lacunes were evaluated on FLAIR images as lesions measuring 3-15 mm, isointense to CSF, with hyperintense margins.[81] We evaluated SWI for the presence of cSS.[34] Cortical CMIs, defined as lesions ≤ 4 mm, restricted to the cortex, hypointense on T1, and hyperintense on FLAIR, were counted across the whole brain.[97] We rated CSO-PVS and BG-PVS, using T1-weighted images, according to a previously proposed scale: 0 (none); 1 (1-10); 2 (11-20); 3 (21-40); 4 (>40).[59] WMH were qualitatively assessed using a validated visual scale.[115]

Quantitative measures of TBV and total ICV were calculated using the *FreeSurfer* software suite (www.surfer.nmr.mgh.harvard.edu; version 6.0),[261] following a rigorous visual quality inspection. The normalized TBV (nTBV) was calculated controlling for ICV (TBV/ICV) and multiplied by 100, and was expressed in units of percent ICV. WM hyperintense lesions were segmented on FLAIR using the lesion prediction algorithm (LPA)[262] implemented in the toolbox Lesion Segmentation Tool (LST) version 3.0.0 (www.statistical-modelling.de/lst.html) for Statistical Parametric Mapping 12 (SPM12), following visual inspection for segmentation quality. Different lesion probability thresholds were evaluated on 40 randomly selected individuals from our cohort, and the ideal threshold of 0.5 was defined by careful visual inspection against their respective FLAIR images for accuracy. The normalized WMH volume (nWMHV) was calculated as the WMHV/ICV ratio multiplied by 100 and expressed in units of percent ICV.

Figure 3.3.1. Regional differences in PSMD values between probable-CAA and non-CAA subjects
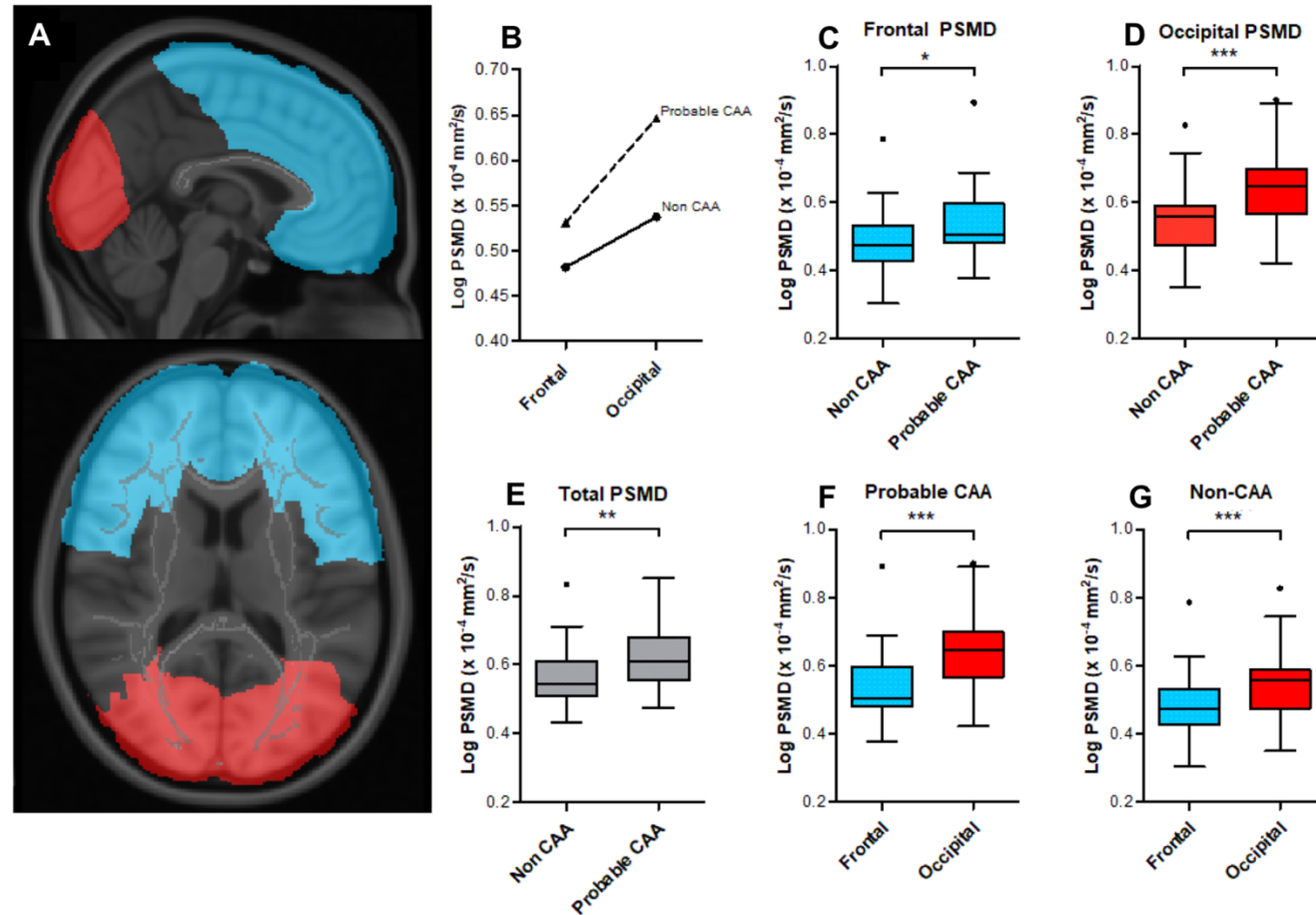
Source: Zanon Zotin MC, et al. under review.

A. Frontal (blue) and occipital (red) masks, used to compute lobe-specific PSMD values. B. The line graph depicts mean log-PSMD values in the frontal and occipital lobes of probable-CAA (solid line) and non-CAA (dashed line) subjects. C-G. Box-plots of PSMD values. The boxes extend from the 25th to 75th percentiles, and the solid line within each box represents the median. The superior and inferior inner fences represent the 75th percentile plus 1.5 times interquartile range and the 25th minus 1.5 times interquartile range, respectively. Outliers are displayed by symbols. C, D, E. Box plots contrasting frontal(C), occipital(D), and total(E) PSMD values between non-CAA and probable-CAA groups. E, F. Box-plots displaying frontal (blue) and occipital (red) PSMD within each study group. General linear models adjusted for age are indicated by the brackets, with p-values (*p < 0.05; ** p <0.01; *** p <0.001).

3.3.2.8. Statistical analysis

The distribution of continuous variables was tested for normality using the Shapiro-Wilk test. Clinical, neuropsychological, and neuroimaging characteristics were compared across the three groups using $\chi2$ or Fisher test and Kruskal-Wallis H test or ANOVA, as appropriate.

We investigated the association between TMI and DTI metrics across all subjects, using simple linear regression, further adjusting for age, gender, and education level to evaluate motion effects. Neuroimaging and cognitive associations were investigated only in the probable CAA group. Linear regression models exploring the associations between DTI metrics and conventional neuroimaging markers were adjusted for age, and those investigating cognitive associations were adjusted for the time interval between the MRI and the neuropsychological tests. Since cognitive scores had already been adjusted for age, gender, and education level, we did not include these variables in the models. We further assessed the relative contribution of each neuroimaging variable by running multiple linear regression models and applying a decomposition method proposed by Lindeman *et al*.[263] and available in the Relaimpo R package (v2.2).[264]

Non-parametric variables were log-transformed for the regional analyses. To investigate regional variances in PSMD, we compared occipital-frontal PSMD gradients between the groups, using ANCOVA, adjusting for age. Furthermore, to evaluate whether CAA diagnosis could influence regional variances of PSMD, we compared probable-CAA subjects against non-CAA subjects (merging non-cSVD and cSVD subjects into a single non-CAA group). We used mixed-factor ANOVA to investigate whether there was an interaction between CAA diagnosis and region on PSMD values. We further investigated the simple main effects of group and region using ANCOVA adjusted for age and repeated-measures ANOVA, respectively. As an exploratory analysis, we ran similar statistical procedures across the three groups (non-cSVD, cSVD, and probable-CAA). All pairwise comparisons were adjusted for false discovery rate (FDR) using the Benjamini-Hochberg procedure.

The statistical significance level was set at 0.05 for all analyses. We used the Statistical Package for the Social Sciences (SPSS) version 20.0 (for IOS; SPSS Inc, Chicago, IL), Prism (v8.4.3), and R (v3.5.3) to run the analyses.

3.3.2.9. Data Availability Statement

The data that support our findings is available from the corresponding author upon reasonable request.

3.3.3. Results

We screened 167 subjects from our memory-clinic cohort who underwent complete research MRI and neuropsychological exam. Of those subjects, 77 were excluded, based on the following pre-specified criteria: dementia (n=46), excessive motion artifacts on visual inspection (n=3); possible-CAA (n=26); and mixed pattern of distribution of hemorrhagic features (n=2). The final cohort was comprised of 90 non-demented memory-clinic subjects (43 probable-CAA, 17 non-CAA-cSVD and 30 non-cSVD). The median delay between MRI and neuropsychological tests was 0 [IQR, 0 - 2.5] months.

In simple linear regression analysis, TMI was not association with any DTI metric (Standardized β coefficient [95% confidence interval]; PSMD β [95% CI] = -0.027 [-0.239, 0.185], p = 0.802; MD β [95% CI] = -0.038 [-0.250, 0.173], p = 0.721; FA β [95% CI] = 0.051 [-0.160, 0.263], p = 0.632), even after adjusting for age, gender and education level. Therefore, TMI was not included as a covariate in the following neuroimaging and cognitive analyses.

3.3.3.1. Between-group comparisons

Demographic, neuropsychological, and neuroimaging data from each group are summarized in Table 3.3.1. Groups differed in age (F(2, 87) = 9.326, p<.001), with both probable-CAA (mean difference±standard error, 4.67±1.52; FDR-adjusted p-value=.004) and cSVD (7.95±1.94; p<.001) being older than non-cSVD subjects. Gender, education level, vascular risk factors, cognitive performance, and head motion (TMI) were evenly distributed across the groups. As expected, the burden of cSVD markers was higher in the probable-CAA and cSVD groups in comparison to the non-cSVD group. nTBV differed across the groups (F(2, 87)=8.905, p<.001), with greater atrophy in probable CAA subjects than in non-cSVD participants (-3.94±0.93; p<.001). PSMD values also differed across the groups, and were lower in the non-cSVD group in comparison to probable-CAA (p<.001), and cSVD (p<.001). PSMD did not differ between probable-CAA and cSVD groups (p=.883). On the other hand, MD values were higher in probable-CAA patients, and FA values were lower in CAA patients, in comparison to both cSVD and non-cSVD groups (p<.001).

Table 3.3.1. Summary of clinical and neuroimaging data

	Total (n=90)	Non-CAA		Probable-CAA[c] (n=43)	p
		non-cSVD[a]	cSVD[b]		
Demographics					
Age (years), mean (SD)	73.5 (7.0)	69.7 (7.4)	77.7 (5.4)	74.4 (5.9)	b>a*** c>a**
Female, n (%)	45 (50)	16 (53.3)	8 (47.1)	21 (48.8)	0.898
Education (years), median [IQR]	16 [14-18]	16 [14-18]	16 [14-17]	17 [16-19]	0.064
Vascular Risk Factors					
Hypertension, n (%)†	55 (65.5)	18 (72.0)	11 (68.8)	26 (60.5)	0.599
Diabetes, n (%)†	11 (13.1)	2 (8.0)	5 (31.2)	4 (9.3)	0.071
Atrial Fibrillation, n (%)†	4 (4.8)	1 (4.0)	1 (6.2)	2 (4.7)	1.000
Dyslipidemia, n (%)†	68 (81.0)	19 (76.0)	13 (81.2)	36 (83.7)	0.761
Cognitive scores (z-scores)					
MMSE, mean (SD)	-0.11(1.43)	-0.18 (1.53)	0.51 (1.29)	-0.30 (1.38)	0.132
Memory, mean (SD)	-0.38 (1.25)	-0.14 (1.29)	-0.04 (1.19)	-0.67 (1.2)	0.092
Processing Speed, mean (SD)	-0.07 (0.53)	-0.04 (0.50)	-0.08 (0.54)	-0.09 (0.55)	0.921
Language, mean (SD)	-0.34 (1.02)	-0.21 (0.81)	-0.27 (1.35)	-0.46 (1.02)	0.570
Executive Function, median [IQR]	-0.26 [-0.8, 0.1]	-0.23 [-0.6,0.2]	-0.07 [-0.6,0.1]	-0.37 [-1.0, 0.1]	0.413
Gap MRIxNPT, months, median [IQR]	0 [-2.3, 0]	-1.05 [-3.4, 0]	-1.33 [-2.8, 0.2]	0 [-1.6, 0]	0.034‡
Conventional MRI markers					
Lobar CMB count, median [IQR]	0 [0, 13.5]	0 [0, 0]	0 [0, 0]	15 [3, 55]	c>a*** c>b***
cSS (presence), n (%)	14 (15.6)	0 (0)	0 (0)	14 (32.6)	c>a*** c>b***
Lacunes count, median [IQR]	0 [0, 1]	0 [0, 0]	1 [0, 1.5]	0 [0, 1]	b>a*** c>a***
Cortical CMI, count, median [IQR]	0 [0, 0]	0 [0, 0]	0 [0, 0]	0 [0, 1]	0.049‡
CSO PVS score, median [IQR]	2 [2, 3]	2 [1, 2]	2 [2, 2]	3 [2, 4]	c>a*** c>b**
BG PVS score, median [IQR]	2 [1, 2]	1 [1, 2]	2 [2, 3]	2 [1, 3]	b>a*** c>a***
nWMHV (% ICV), median [IQR]	0.2 [0.05, 0.8]	0.05 [0.01, 0.1]	0.66 [0.3, 1.2]	0.36 [0.14, 1.8]	b>a*** c>a***
nTBV (% ICV), mean (SD)	64.75 (4.26)	67.06 (4.46)	64.77 (3.26)	63.13 (3.76)	a>c***
DTI markers					
PSMD (x 10^{-4} mm²/s), median [IQR]	3.76 [3.32, 4.37]	3.30 [3.13, 3.6]	4.07 [3.51, 4.62]	4.06 [3.58, 4.79]	b>a*** c>a***
Average MD (x 10^{-4} mm²/s), median [IQR]	8.44[7.86, 9.2]	7.98[7.49, 8.6]	8.06[7.75, 8.3]	9.19[8.45, 9.8]	c>a*** c>b***
Average FA (x 10^{-4} mm²/s), mean (SD)	0.46 (0.04)	0.49 (0.04)	0.48 (0.03)	0.44 (0.04)	a>c*** b>c***
Total Motion Index, median [IQR]	-0.07 [-0.96, 1.26]	0.24[-1.07, 1.3]	0.21 [-0.66, 1.9]	-0.25 [-0.94, 0.6]	0.426
PSMD regional assessment					
Frontal PSMD (x 10^{-4} mm²/s), median [IQR]	3.14 [2.8, 3.5]	2.81 [2.5, 3.2]	3.26 [3.0, 3.9]	3.2 [3.0, 3.9]	b>a*** c>a***

Occipital PSMD (x 10^{-4} mm^2/s), median [IQR]	3.77 [3.2, 4.5]	3.23 [2.8, 3.7]	3.76 [3.5, 4.1]	4.43 [3.7, 5.0]	b>a* c>a***
Occipital-frontal PSMD gradient (x 10^{-4} mm^2/s), mean (SD)	0.76 (1.08)	0.43 (0.54)	0.45 (1.19)	1.11 (1.22)	c>a* c>b*

Kruskal Wallis and ANOVA were used to investigate differences across the three groups, as appropriate. † 6 missing values. We reported the original *p*-values and, when significant differences were found, we ran FDR-adjusted pairwise comparisons: *FDR-adjusted *p*<0.05; **FDR-adjusted *p*<0.01; ***FDR-adjusted *p*<0.001. ‡ No statistical significance in pairwise comparisons, after FDR-correction. Abbreviations: SD = standard deviation; IQR = interquartile range; MMSE = mini mental state examination; CMB = cerebral microbleeds; cSS = cortical superficial siderosis; CMI = cerebral microinfarcts; CSO-PVS = perivascular spaces in the centrum semiovale; BG-PVS = perivascular spaces in the basal ganglia; nWMHV = normalized white matter hyperintensity volume; nTBV = normalized total brain volume; CAA = cerebral amyloid angiopathy; cSVD = cerebral small vessel disease; PSMD = peak width of skeletonized mean diffusivity. Probable-CAA= patients fulfilling the modified Boston criteria for Probable CAA; cSVD = patients with neuroimaging markers of cSVD not attributable to CAA – presumed arteriolosclerosis; non-cSVD = patients without neuroimaging markers of cSVD.

3.3.3.2. Regional Distribution of PSMD

Occipital-frontal PSMD gradients were higher in probable-CAA (mean±standard deviation; 1.11±1.22 x 10^4 mm^2/s) than non-CAA (non-cSVD + cSVD) (0.44±0.82 x 10^{-4} mm^2/s) subjects (mean difference±standard error; 0.668±0.22 x 10^{-4} mm^2/s; $F(1, 88) = 9.445$, *p*=.003), even after adjusting for age (0.634±0.22 x 10^{-4} mm^2/s, $F(1, 87) = 8.392$, *p*=.005).

We identified a statistically significant interaction between CAA diagnosis (non-CAA vs. probable-CAA) and region (frontal vs. occipital) on PSMD values ($F(1, 88) = 7.808$, $p = 0.006$, $\eta^2=0.081$, Figure 3.3.1.B), meaning that regional variances of PSMD were influenced by CAA diagnosis. When investigating the simple main effect of region, adjusting for age, we found that PSMD values in the frontal (mean difference±standard error; 0.041±0.02 x 10^{-4} mm^2/s, $F(1, 87) = 5.153$, $p = 0.026$, $\eta^2=0.056$) and occipital (0.098±0.02 x 10^{-4} mm^2/s, $F(1, 87) = 22.039$, $p < 0.001$, $\eta^2=0.202$) lobes were higher in the probable-CAA group in comparison to non-CAA subjects (Figure 3.3.1.C-D). Moreover, occipital lobes presented higher PSMD values than the frontal lobes in both probable-CAA ($F(1, 42) = 46.059$, $p < 0.001$, $\eta^2=0.523$) and non-CAA groups ($F(1, 46) = 18.046$, $p < 0.001$, $\eta^2=0.282$), but with a larger effect in the former (Figure 3.3.1.F-G).

The exploratory analysis, performed between the three groups (non-cSVD, cSVD and probable-CAA), revealed similar findings: (1) controlling for age, occipital-frontal PSMD gradients were different across the 3 groups ($F(2, 86) = 4.278$, $p = 0.017$, $\eta^2 = 0.090$). Probable-CAA subjects presented higher occipital-frontal PSMD gradients in comparison to both cSVD (0.734±0.30 x 10^{-4} mm^2/s, $p = 0.046$) and non-cSVD (0.567±0.26 x 10^{-4} mm^2/s, $p = 0.046$) groups; (2) there was a significant interaction between region (frontal x occipital) and group (non-cSVD, cSVD, probable-

CAA) on PSMD values ($F(2, 87) = 3.887$, $p = 0.024$, $\eta^2 = 0.082$, Figure 3.3.2.A); (2) Frontal PSMD values, adjusted for age, were lower in the non-cSVD group in comparison to cSVD (mean difference±standard error; FDR-adjusted p-values; $-0.071±0.03$ x 10^{-4} mm^2/s, $p = 0.017$) and probable-CAA ($-0.070±0.02$ x 10^{-4} mm^2/s, $p = 0.004$) groups, but were similar in the latter two ($-0.001±0.02$ x 10^{-4} mm^2/s, $p = 0.955$; Figure 3.3.2.B); (3) PSMD-values from the occipital lobes, adjusted for age, were higher in probable-CAA in comparison to cSVD ($0.069±0.03$ x 10^{-4} mm^2/s, $p = 0.026$) and non-cSVD ($0.117±0.02$ x 10^{-4} mm^2/s, $p < 0.001$; Fig. 3.3.2.C) groups; (4) Occipital PSMD values were higher than frontal values in probable-CAA ($F(1, 42) = 46.059$, $p < 0.001$, $\eta^2 = 0.523$) and non-cSVD ($F(1, 29) = 18.755$, $p < 0.001$, $\eta^2 = 0.393$) groups, but not in the cSVD group ($F(1, 16) = 3.342$, $p = 0.086$, $\eta^2 = 0.173$; Fig. 3.3.2.E-G).

3.3.3.3. Relationship between DTI markers and conventional MRI markers of cSVD in CAA

Among probable-CAA subjects (n=43), regression models with PSMD as the dependent variable, adjusting for age and correcting for multiple comparisons, revealed that higher PSMD was associated with higher number of lacunes (Standardized beta coefficient [95% confidence interval]; FDR-adjusted p-value; β [95% CI] $= 0.38[0.09, 0.67]$; $p = 0.022$), nWMHV (β [95% CI] $= 0.86[0.69, 1.03]$; $p<0.001$), and cortical CMI (β [95% CI] $= 0.40[0.11, 0.69]$; $p=0.022$); and with lower nTBV (β [95% CI] $= -0.48[-0.82, -0.14]$; $p = 0.022$) (Table 3.3.2, Fig. 3.3.3). Among all MRI markers, nWMHV alone explained more than 65% of PSMD's variance in the model (Figure 3.3.4.A). Similar analyses with average skeletonized MD and FA values revealed associations with BG PVS, CSO PVS, lobar cerebral microbleeds, and nWMHV, (Fig. 3.3.4.B,C; Fig 3.3.5; Fig 3.3.6; Table 3.3.2).

Figure 3.3.2. Regional differences in PSMD values between probable-CAA, cSVD and non-cSVD groups.
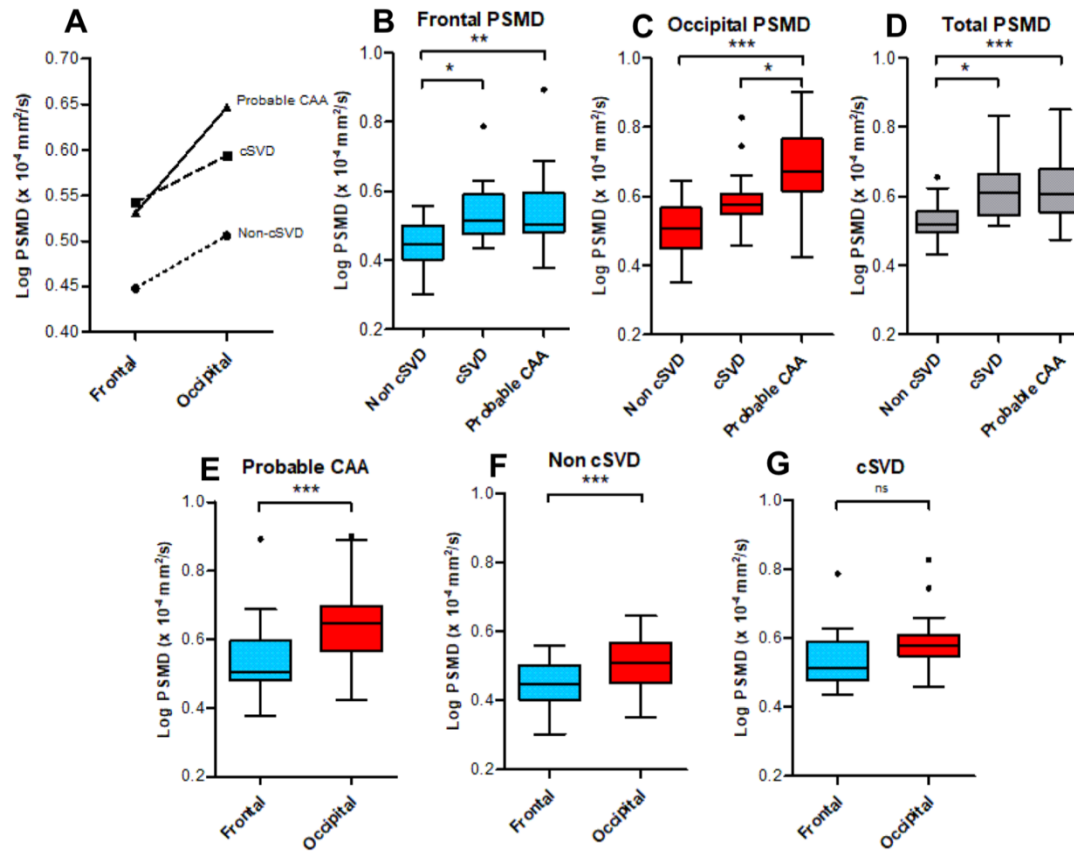
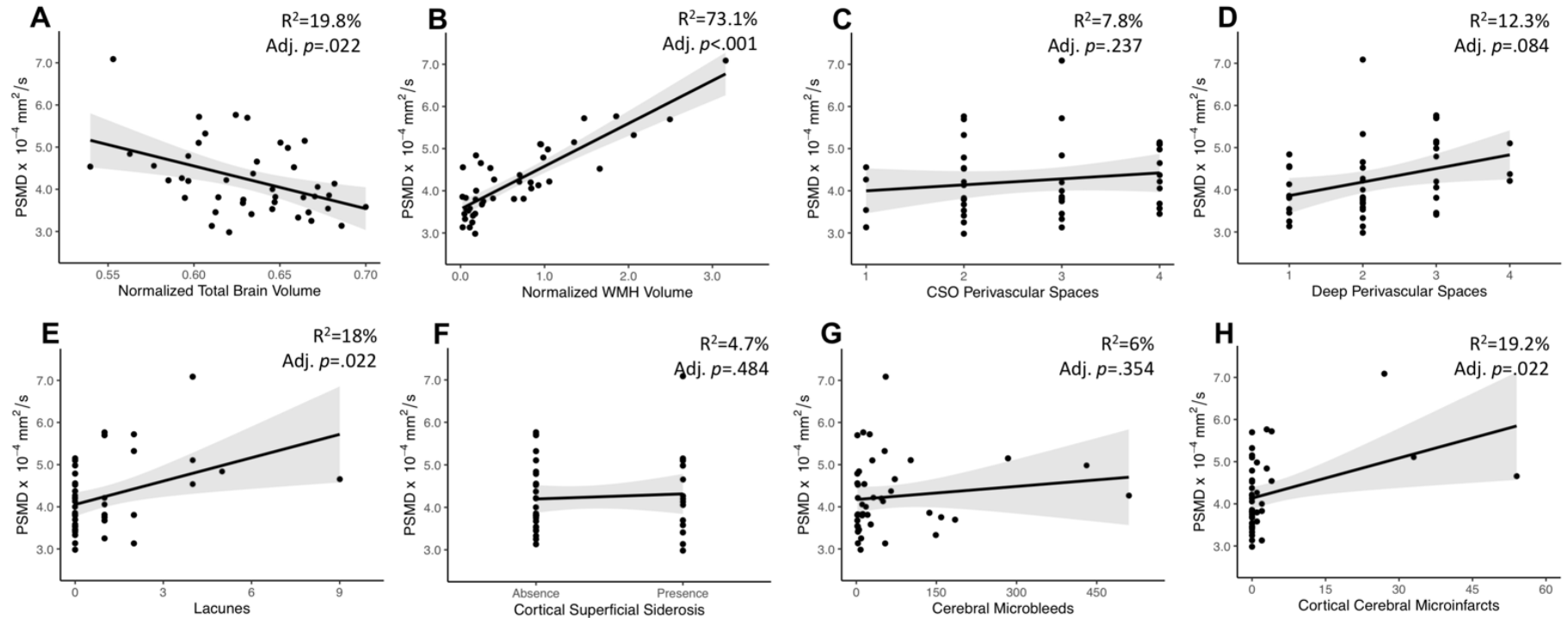Source: Zanon Zotin MC, et al. under review.

The line graph depicts mean log-PSMD values in the frontal and occipital lobes of probable-CAA (solid line), cSVD (dashed line), and non-cSVD (dotted line) subjects. **B-G**. Box-plots of PSMD values. The boxes extend from the 25th to 75th percentiles, and the solid line within each box represents the median. The superior and inferior inner fences represent the 75th percentile plus 1.5 times the interquartile range and the 25th minus 1.5 times the interquartile range, respectively. Outliers are displayed by symbols. **B, C, D.** Box plots contrasting frontal (**B**), occipital (**C**), and total (**D**) PSMD values between non-cSVD, cSVD, and probable-CAA groups. **E, F, G**. Box-plots display frontal (blue) and occipital (red) PSMD within each study group. General linear models adjusted for age are indicated by the brackets, with *p*-values (**p* < 0.05; ** *p* <0.01; *** *p* <0.001).

Table 3.3.2. Associations between DTI metrics and conventional neuroimaging markers of cSVD in probable-CAA subjects.

Probable CAA n=43	PSMD					MD					FA				
	Std.Bet	95% CI		R²	p	Std.Bet	95% CI		R²	p	Std.Beta	95% CI		R²	p
cSVD markers															
Lobar CMB, count	0.159	-0.153	0.472	0.060	.310	0.403	0.111	0.694	0.182	.008*†	-0.285	-0.594	-0024	0.082	.069
cSS, presence	0.112	-0.208	0.432	0.047	.483	0.329	0.023	0.636	0.126	.036*	-0.310	-0.622	0.001	0.094	.051
Lacune, count	0.381	0.091	0.671	0.180	.011*†	0.144	-0.169	0.456	0.043	.359	-0.241	-0.551	0.069	0.060	.124
nWMHV (%ICV)	0.859	0.688	1.030	0.731	<.001*	0.352	0.046	0.657	0.139	.025*	-0.551	-0.829	-0.274	0.289	<.001*†
Cortical CMI, count	0.398	0.109	0.687	0.192	.008*†	0.218	-0.092	0.527	0.069	.163	-0.265	-0.575	0.044	0.072	.091
CSO PVS, score	0.214	-0.101	0.529	0.078	.178	0.584	0.319	0.850	0.346	<.001*	-0.531	-0.812	-0.251	0.270	<.001*†
BG PVS, score	0.308	-0.003	0.619	0.123	.052	0.619	0.357	0.881	0.377	<.001*	-0.619	-0.885	-0.352	0.356	<.001*†
nTBV (%ICV)	-0.477	-0.815	-0.139	0.198	.007*†	-0.345	-0.702	0.012	0.108	.058	0.324	-0.039	0.687	0.077	.079

Linear regression models with PSMD, MD, or FA as the dependent variable, adjusted for age. The provided standardized beta coefficients, confidence intervals, and original *p*-values reflect the obtained independent predictive of the listed MRI marker with regards to PSMD, MD or FA. *Statistically significant in models not corrected for multiple comparisons. †Statistically significant after FDR correction within each model (that is, by column of this table). Abbreviations: Std.Beta = standardized beta coefficient; CI = confidence interval; CMB = cerebral microbleeds; cSS = cortical superficial siderosis; nWMHV = normalized white matter hyperintensities volume; ICV = intracranial volume; CMI = cortical cerebral microinfarcts; CSO-PVS = perivascular spaces in the centrum semiovale; BG-PVS = perivascular spaces in the basal ganglia; nTBV = normalized total brain volume.
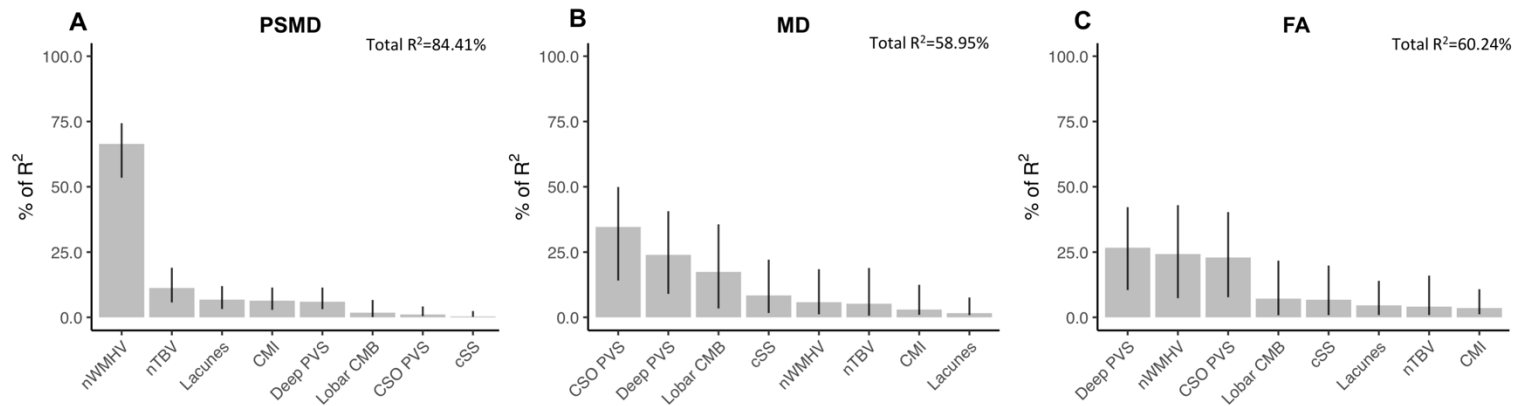
Figure 3.3.3. Associations between PSMD and conventional neuroimaging markers of cSVD in probable-CAA subjects.

Source: Zanon Zotin MC, et al. under review.

Simple linear regression models with PSMD as the dependent variable and (A) nTBV, (B) nWMHV, (C) CSO Perivascular Spaces, (D) Deep Perivascular Spaces, (E) Lacune count, (F) Cortical Superficial Siderosis, (G) Lobar cerebral microbleeds, and (H) CMI count as independent variables. 95% confidence intervals are depicted in gray. The provided R^2 and *p*-values reflect the obtained independent predictive of each MRI marker with regards to PSMD, adjusted for age.
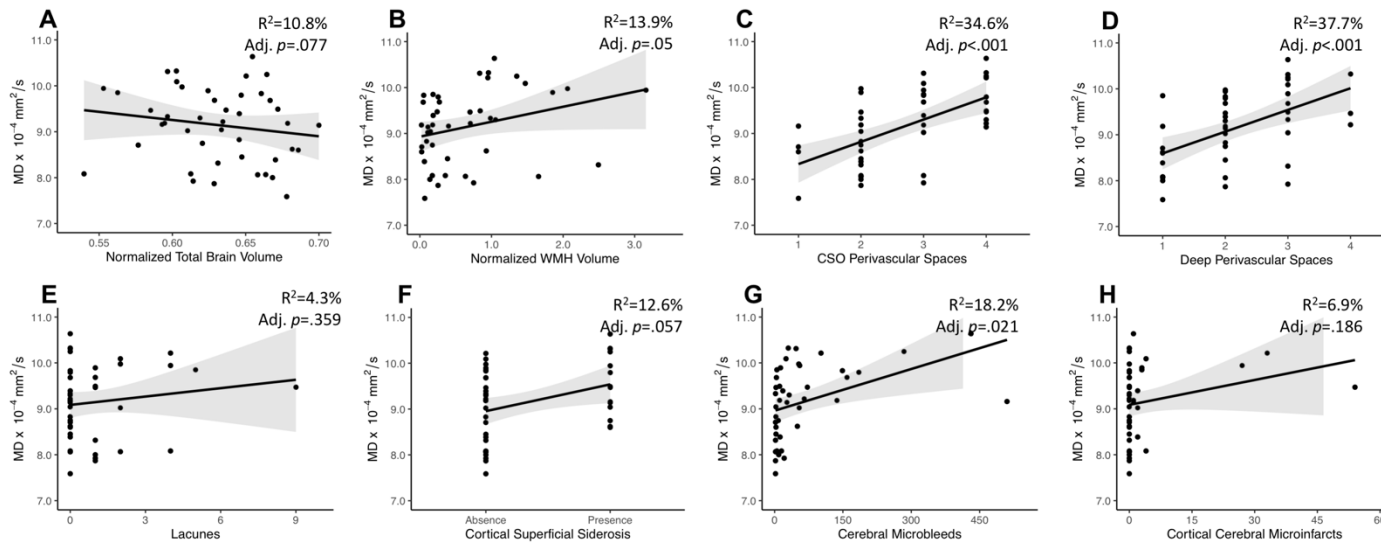
Figure 3.3.4. Associations between DTI metrics and conventional neuroimaging markers of cSVD in probable-CAA subjects.

Source: Zanon Zotin MC, et al. under review.

Bar graphs represent the relative contribution of each neuroimaging marker to explaining the variance in PSMD (A), average skeletonized MD (B), and average skeletonized FA (C) values among probable-CAA subjects. All neuroimaging markers were entered as independent variables in multiple linear regression models, with each DTI metric as the dependent variable. We applied a model decomposition method available in R package "Relaimpo" to compute the LMG metric. Metrics are normalized to sum to 100%. Lines represent 95% confidence intervals after 1000 bootstrapping replications.

Figure 3.3.5. Associations between average skeletonized MD and conventional neuroimaging markers of cSVD in probable-CAA.

Source: Zanon Zotin MC, et al. under review.

Simple linear regression models with average skeletonized MD as the dependent variable and (A) nTBV, (B) nWMHV, (C) CSO Perivascular Spaces, (D) Deep Perivascular Spaces, (E) Lacune count, (F) Cortical Superficial Siderosis, (G) Lobar cerebral microbleeds, and (H) CMI count as independent variables. 95% confidence intervals are depicted in gray. The provided R^2 and p-values reflect the obtained independent predictive of each MRI marker with regards to MD, adjusted for age.

Figure 3.3.6. Associations between average skeletonized FA and conventional neuroimaging markers of cSVD in probable-CAA.
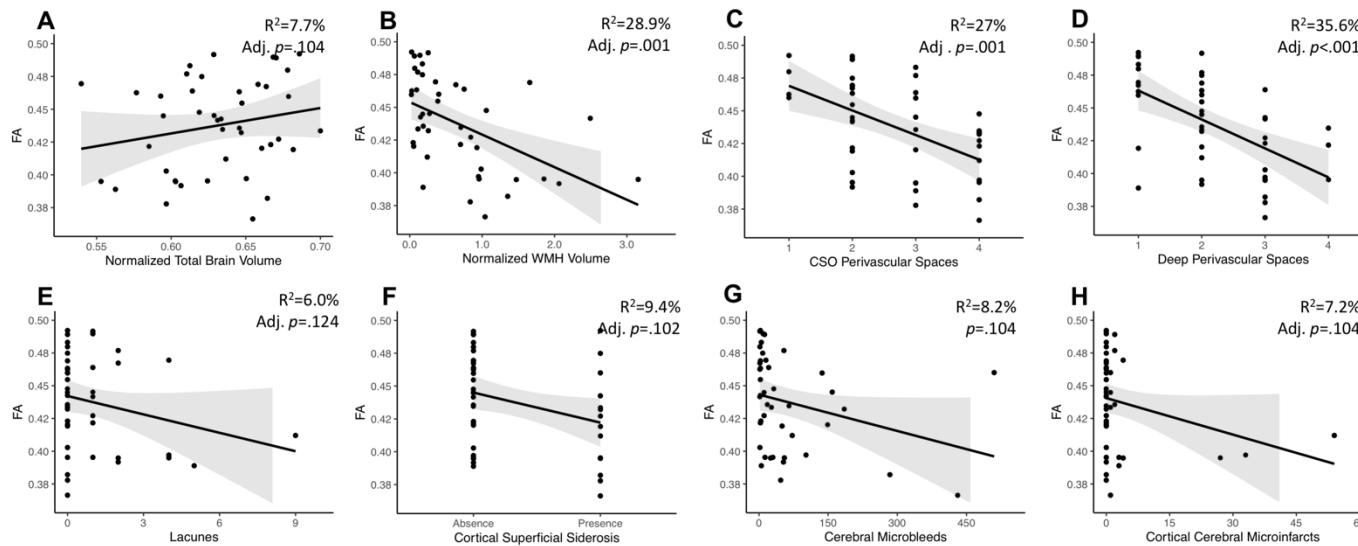
Source: Zanon Zotin MC, et al. under review.

Simple linear regression models with average skeletonized FA as the dependent variable and (A) nTBV, (B) nWMHV, (C) CSO Perivascular Spaces, (D) Deep Perivascular Spaces, (E) Lacune count, (F) Cortical Superficial Siderosis, (G) Lobar cerebral microbleeds, and (H) CMI count as independent variables. 95% confidence intervals are depicted in gray. The provided R^2 and p-values reflect the obtained independent predictive of each MRI marker with regards to FA, adjusted for age.

3.3.3.4. Relationship between DTI markers and cognitive functions in CAA

In the probable-CAA group, linear regression models corrected for time interval between MRI and NPT revealed that higher PSMD values are associated with worse performance in executive function (Standardized beta; FDR-adjusted p-value; β [95% CI] = -0.58[-0.87, -0.30]; p=0.002) and processing speed (β [95% CI] = -0.46[-0.76, -0.17]; p=0.03) (Table 3.3.3). PSMD was not associated with any other cognitive domains (Table 3.3.4). Among all neuroimaging features, other than PSMD, only nWMHV showed an association with cognition, after correction for multiple comparisons (executive function; β [95% CI]=-0.54[-0.84, -0.24; p=.004]). MD and FA were not associated with performance in any of the cognitive domains investigated (Tables 3.3.3, 3.3.4). In multiple regression models applying a model decomposition method, PSMD contributed more than the other conventional MRI markers in explaining cognitive variance in the domains of executive function and processing speed (Fig. 3.3.7).

Table 3.3.3. Associations between neuroimaging markers and performance in executive function and processing speed in subjects with probable-CAA.

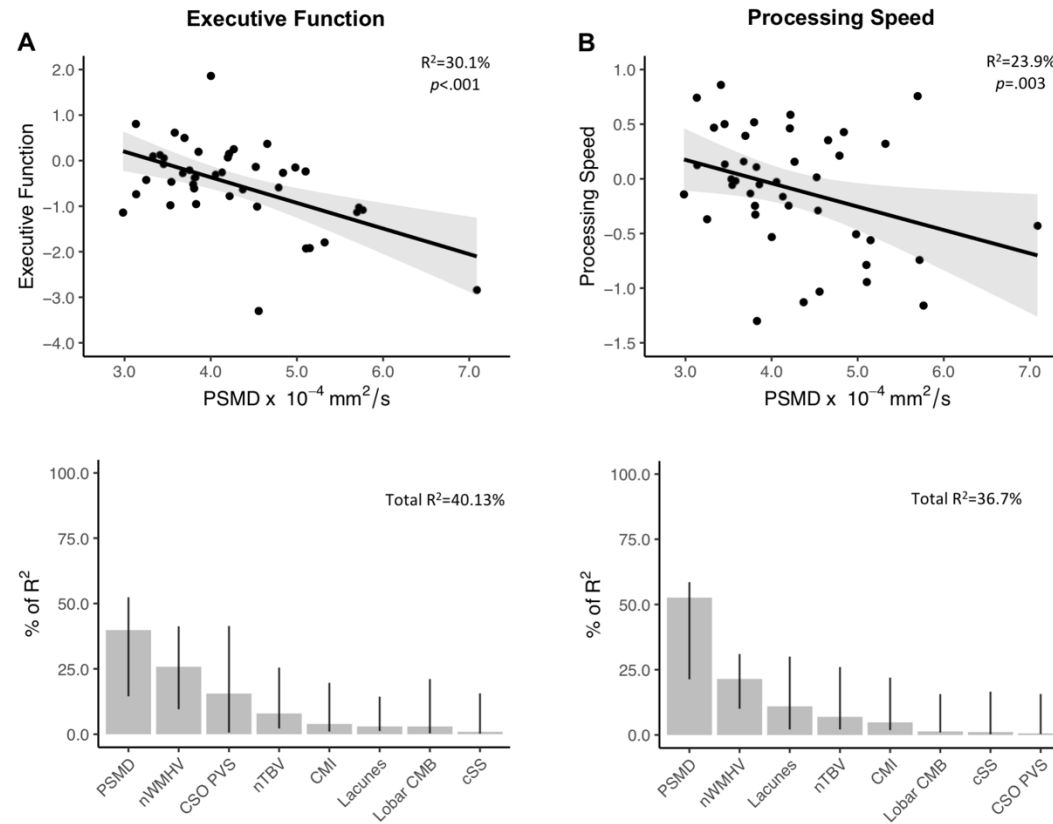| Probable CAA n=43	Processing Speed				Executive Function			
	Std.Beta	95% CI	R^2	*p*	Std.Beta	95% CI	R^2	*p*
PSMD total	-0.463	-0.759 -0.167	0.239	.003*†	-0.581	-0.865 -0.297	0.301	<.001*†
MD	-0.278	-0.616 0.060	0.110	.104	-0.040	-0.398 0.318	0.003	.824
FA	0.247	-0.078 0.572	0.102	.132	0.133	-0.207 0.473	0.017	.433
Lobar CMB, count	-0.093	-0.407 0.221	0.057	.553	0.104	-0.218 0.425	0.012	.519
cSS, presence	0.015	-0.297 0.327	0.049	.925	0.074	-0.245 0.393	0.007	.642
Lacune, count	0.039	-0.273 0.351	0.050	.802	-0.130	-0.447 0.187	0.018	.413
nWMHV (%ICV)	-0.271	-0.597 0.054	0.112	.100	-0.538	-0.838 -0.239	0.249	.001*†
Cortical CMI, count	-0.103	-0.415 0.208	0.059	.505	-0.152	-0.468 0.165	0.024	.340
CSO PVS, score	-0.140	-0.461 0.181	0.067	.383	0.242	-0.081 0.565	0.056	.138
nTBV (%ICV)	-0.007	-0.321 0.308	0.049	.965	0.298	-0.009 0.606	0.089	.057

Simple linear regression models with each cognitive score as the dependent variable and each neuroimaging marker as the independent marker, adjusted for the interval between MRI and NPT. The provided standardized beta coefficients and *p*-values reflect the obtained independent predictive of the listed MRI marker with regards to cognitive scores. Abbreviations: Std.Beta = standardized beta coefficient; PSMD= peak width of skeletonized mean diffusivity ; MD = mean diffusivity ; FA = fractional anisotropy ; CMB = cerebral microbleeds; cSS = cortical superficial siderosis; nWMHV = normalized white matter hyperintensities volume; ICV = intracranial volume; CMI = cortical cerebral microinfarcts; CSO-PVS = perivascular spaces in centrum semiovale; nTBV = normalized total brain volume. * statistically significant in models not corrected for multiple comparisons. † statistically significant after FDR correction within each cognitive domain (that is, by column of this table).

Table 3.3.4. Associations between neuroimaging markers and performance in the domains of language and memory in probable-CAA.

Probable CAA n=43	Language					Memory				
	Std.Beta	95% CI		R^2	*p*	Std.Beta	95% CI		R^2	*p*
PSMD	-0.291	-0.613	.031	0.098	.075	-0.025	-0.362	0.311	0.016	.879
MD	0.048	-0.306	0.402	0.024	.786	0.065	-0.290	0.420	0.018	.714
FA	0.052	-0.287	0.390	0.025	.759	-0.117	-0.456	0.221	0.027	.487
Lobar CMB, count	-0.126	-0.443	0.191	0.038	.427	0.033	-0.288	0.354	0.016	.836
cSS, presence	0.065	-0.251	0.380	0.027	.681	0.010	-0.308	0.327	0.015	.952
Lacune, count	0.026	-0.290	0.342	0.023	.867	0.044	-0.273	0.361	0.017	.781
nWMHV (%ICV)	-0.374	-0.694	-0.054	0.142	.023*	0.039	-0.303	0.382	0.016	.818
Cortical CMI, count	-0.168	-0.480	0.145	0.051	.284	0.022	-0.296	0.340	0.016	.890
CSO PVS, score	-0.069	-0.397	0.259	0.027	.673	0.080	-0.249	0.408	0.021	.628
nTBV (%ICV)	-0.033	-0.352	0.285	0.024	.834	0.040	-0.280	0.360	0.017	.802

Simple linear regression models with each cognitive score as the dependent variable and each neuroimaging marker as the independent marker, adjusted for the interval between MRI and NPT. The provided standardized beta coefficients and *p*-values reflect the obtained independent predictive of the listed MRI marker with regards to cognitive scores. Abbreviations: Std.Beta = standardized beta coefficient; MMSE = mini mental state examination; CMB = cerebral microbleeds; cSS = cortical superficial siderosis; nWMHV = normalized white matter hyperintensities volume ; CMI = cerebral microinfarcts; CSO-PVS = perivascular spaces in centrum semiovale; nTBV = normalized total brain volume. * statistically significant in models not corrected for multiple comparisons. † statistically significant after FDR correction within each cognitive domain (that is, by column of this table).

Figure 3.3.7. Associations between PSMD and performance in executive function and processing speed.

Source: Zanon Zotin MC, et al. under review.

Upper Panel: Results from simple linear regression models between PSMD values and executive function (A. Above) and processing speed (B. Above) in probable-CAA subjects. 95% confidence intervals are depicted in gray. The provided R^2 and p-values reflect the obtained independent predictive of PSMD with regards to cognitive scores adjusted for the interval between MRI and neuropsychological tests. Lower panel: Bar graphs representing the relative contribution of each neuroimaging marker to explaining the variance in executive (A. Below) and processing speed scores (B. Below), using the LMG metric computed with the R package "Relaimpo". Metrics are normalized to sum to 100%. Lines represent 95% confidence intervals after 1000 bootstrapping replications.

3.3.4. Discussion

This study in a well-characterized memory-clinic cohort has several key findings. First, PSMD was higher in individuals with cSVD than in those without evidence of cSVD but similar between different cSVD phenotypes (probable CAA and arteriolosclerosis). Second, taking a regional approach, we observed higher occipital-frontal PSMD gradients in probable-CAA than non-CAA subjects and found a significant interaction between CAA-diagnosis and regional PSMD variation. Third, in probable-CAA, PSMD differed from classical DTI metrics in terms of neuroimaging and cognitive associations. nWMHV was the main predictor of PSMD values, whereas MD and FA were more strongly associated with other markers, particularly with perivascular spaces. PSMD was associated with executive function and processing speed in subjects with probable CAA and explained more variance than conventional neuroimaging markers. MD and FA were not associated with cognitive performance.

Higher PSMD values observed in probable-CAA and cSVD subjects support the idea that PSMD, like other DTI measures, is particularly sensitive to cSVD-related abnormalities.[165,169,209] PSMD values in probable-CAA and cSVD subjects from our study are comparable to those previously reported in other cSVD samples: CADASIL (4.5-5.47 x 10^4 mm^2/s),[169,219] memory-clinic subjects with sporadic cSVD (4.24 x 10^4 mm^2/s),[169] and subjects with WM lesions and VCID (4.51 x 10^4 mm^2/s).[227] McCreary *et al*. reported slightly higher PSMD among 34 CAA subjects (4.97 x 10^4 mm^2/s), which could be explained by the presence of symptomatic ICH in that cohort.[183] As expected, like other DTI-based techniques, global PSMD values are similar across different cSVD phenotypes and do not appear specific to any WM disease.

Though PSMD was originally developed as a global measure of WM integrity, our study suggests that it can be successfully applied in a spatially-oriented way, opening up interesting research possibilities. Expanding on existing research,[203,209] we calculated lobe-specific measures of PSMD, investigating between-group differences. We found that both non-CAA and probable-CAA groups have higher PSMD values in the occipital lobes. However, the degree to which these values increased posteriorly was higher among probable-CAA in comparison to non-CAA subjects, indicating an interaction between the CAA diagnosis and anteroposterior PSMD variations. The higher occipital-frontal PSMD gradients observed in the probable-CAA sample suggest that WM microstructural damage may be more severe in the posterior areas of the brain, which is consistent with several histopathological[69,265] and imaging[88–90,226] studies showing a

posterior predilection of CAA pathology. This finding reflects a pattern of brain injury that is consistent with vascular amyloid deposition and could potentially provide insights into the predominant type of underlying microvascular pathology.

To assess whether PSMD captures similar tissue abnormalities compared to average MD and FA, we investigated the relationship between conventional MRI markers of cSVD and each DTI metric. While PSMD is mainly associated with nWMHV, MD and FA also show strong associations with other markers, especially with PVS. Importantly, average MD and FA are central tendency measures, whereas PSMD is a dispersion metric.[203] This difference could potentially explain the distinct neuroimaging associations observed. The strong associations between PVS and classical DTI metrics align with recent observations that MD and FA changes in cSVD are mainly driven by increased water in the extracellular compartment (free-water).[170] The exclusive and robust relationship we observed between PSMD and non-hemorrhagic markers of cSVD, especially with WMH, has also been reported in previous studies.[183] Ischemic markers are thought to cause structural disruption beyond the core lesions[97] and have been consistently associated with different DTI-measures[172,266] and with cognitive function[267] in other cohorts.

Other DWI-based measures, like FA, apparent diffusion coefficient, and brain network measures, have been linked to loss of microstructural integrity in CAA,[172,178,179] and some were also associated with cognitive performance.[172,179,183] Among these, only brain network analysis has been shown to reflect the anteroposterior gradient of CAA pathology, and, interestingly, it correlated with the same cognitive domains as PSMD (executive function and processing speed).[172] These domains are commonly affected in VCID, which further supports that vascular pathology is the primary mechanism involved in the diffusion abnormalities captured by PSMD. Though it has been advocated that PSMD could be a specific or exclusive marker of processing speed,[259] more recent studies with cSVD[227] and population-based[209,228] cohorts found associations with other cognitive domains. Interestingly, PSMD outperformed other structural and diffusion-based MRI markers of cSVD by explaining more cognitive variance in our CAA cohort, which is consistent with findings from other groups.[169] Most conventional markers did not correlate with cognition in our sample, adding to their previously reported weak and inconsistent associations.[71] Though average MD and FA were not associated with cognition in our CAA sample, McCreary *et al.* found MD values to be associated with processing speed ($p=.004$) in a smaller sample of CAA patients. These conflicting results could potentially be explained by the presence of symptomatic

ICH in the Canadian cohort, which could significantly impact MD values and their cognitive associations.

Importantly, PSMD's histopathological correlates have not yet been investigated. Van Veluw *et al*. found, in an ex-vivo study of CAA patients, that MD values correlate with tissue rarefaction, myelin density, and WM microinfarcts.[164] PSMD and mean MD values are increased in CAA subjects and could reflect somewhat similar histopathological changes.[183] However, the distinct neuroimaging associations observed with PSMD, MD, and FA raise the possibility that these metrics capture slightly different histopathological abnormalities. Therefore, future studies investigating PSMD's histological correlates are warranted and could improve the interpretation and biological understanding of this new and promising marker.

Our study has limitations. First, the cross-sectional design limits causal inference, warranting future longitudinal studies. Second, in this single-center study, we included only non-demented subjects from a memory-clinic setting, which accounts for a very specific CAA-profile and limits generalizability. Nonetheless, we chose to restrict recruitment from stroke-center subjects to avoid combining different phenotypes of CAA[258] in the same sample. By excluding demented patients, we aimed to capture earlier steps in the evolution of CAA and reduce the influence of concomitant AD pathology in our findings. The absence of CSF and PET markers precluded a more detailed etiological characterization of the groups, which was based solely on MRI criteria. Though ours is one of the largest cohorts of CAA subjects investigated with PSMD, our sample size is still small, which could account for the weak associations observed.

3.3.5.   Conclusions

In conclusion, although global PSMD values are similarly increased in different forms of cSVD, regional PSMD analyses may capture disease-specific spatial variations. PSMD outperforms conventional and DTI-based markers as cognitive biomarker in CAA and shows a distinct profile of neuroimaging correlates compared to MD and FA. Future research should focus on investigating PSMD's performance in larger multi-center longitudinal CAA cohorts.

4. General Discussion

Several key findings emerge from our investigations. PSMD is on a fast track towards validation as a surrogate for cognitive endpoints in VCI, but full validation depends on further technical and longitudinal studies. In CAA, PSMD shows strong and consistent neuropsychological associations, outperforming other conventional and DTI-based MRI markers. Compared to MD and FA, PSMD presents specific neuroimaging correlates and stronger cognitive associations, underscoring an increased sensitivity to clinically relevant microstructural disruption. Furthermore, we successfully investigated variations in the pattern of MD heterogeneity at the regional level using PSMD. Our results support PSMD's potential use in ROI analyses and underscore its value as a marker of global and regional WM damage.

We discussed the specific findings from each project in detail in each respective section. We now set out to analyze the generalizability of our results, the challenges related to applying PSMD in Brazilian samples, and the measures that can be taken to advance clinical translation.

4.1. Generalizability

Our analyses were performed in a population of mostly white and highly educated individuals from the northern hemisphere, with broad access to high quality healthcare. Our results are similar to those from other groups, underscoring the consistency of our findings. However, overall, the majority of PSMD studies were performed in high-income countries. We are not aware of any published studies in cohorts from Latin America, Africa, or among other underrepresented communities. This limited diversity raises questions on the generalizability of the reported findings among minorities.

The Boston criteria, used to select patients with probable CAA for our projects, was developed and validated in neuropathological studies from the same center, supporting the accuracy of such criteria in our population. However, these criteria have not yet been validated in underrepresented or minoritized communities. The scarce availability of neuropathological data, especially in low-to-middle income countries, is a major obstacle to widespread validation of clinical-radiological criteria in general. It remains unknown whether genetic differences and variability in the prevalence and severity of cardiovascular risk factors could influence the diagnostic yield of the same criteria in different populations. For instance, a comparative review of CAA autopsy studies

from Asia (Japan and China) and western countries (Canada, UK, US, and Australia) revealed a consistently strong association of vascular amyloid with age and dementia across the studies.[268] However, in eastern countries, CAA's association with ICH was weaker than in western samples, probably influenced by a higher incidence of ASC-related ICH.[268] Furthermore, significant racial disparities in terms of AD-related CSF biomarkers have been found in APOE ε4 positive individuals.[269]

Another aspect that could potentially compromise the generalizability of our results refers to part of our neuropsychological battery being validated mostly in English-speaking samples. Reproducing such studies in non-English speaking communities would require translation and validation of multiple cognitive tests, some of which are currently ongoing.

While inequitable representation and unavailability of measuring tools may hinder the generalizability of our results, they represent challenges faced by medical researchers worldwide. Concepts of inclusion, diversity, and justice have recently become priorities, especially in the field of dementia.[41] Black and Hispanic minorities have higher prevalence of vascular risk factors, greater risk of dementia, and more severe neuroimaging findings documented in several studies.[270–273] Sex-specific differences have also been reported.[274] Neuroimaging population-based cohorts also face recruitment and survival biases.[275] Understanding and accounting for such factors is essential to ensure greater scientific accuracy and generalizability.[41]

4.2.   Challenges for the future application of PSMD in Brazil

Brazil has experienced major demographic changes in the last decades, with ageing of the population. The prevalence of dementia in our population is estimated in 14.3% in a recent meta-analysis.[276] Despite the social and economic impacts of dementia in our country, neuroimaging studies investigating Brazilian samples are still scarce.[40] A recent review identified, over a 10-year period, 74 neuroimaging studies published with Brazilian populations (9 case reports, 55 cross-sectional studies, 8 longitudinal studies, and 2 controlled trials), predominantly from groups in the Southeast of the country.[40] Among those, 18% employed DTI techniques,[40] and the most commonly used processing method was TBSS. Importantly, there was an underrepresentation of vascular dementia compared to AD studies.[40] The authors enumerated several factors that challenge neuroimaging studies in dementia in our country. The Brazilian population is highly miscegenated, with major genetic contributions from Africa, Europe, and native Indigenous

people, showing great geographic variability.[40] On top of that, socioeconomic adversities and low education are an unfortunate reality in our country.[40] Poor control of cardiovascular risk factors further increase the likelihood of vascular brain damage,[277] found to be relatively high in neuropathological studies.[278] Considering the aforementioned evidence that different ethnic groups show different susceptibility to neuropathological changes, and that underprivileged social and economic circumstances increase the risk and impact of dementia, researcher should bear in mind all the multiple factors at play when studying age-related cognitive impairment in Brazil. These must be accounted for when analyzing and comparing our results with other populations. Low education levels also represent a challenge both to the application of neuropsychological batteries and the standardization of the results.[40] Finally, limited funding and the unavailability of national multicenter neuroimaging initiatives further hamper Brazilian MRI investigations in dementia.[40] Leveraging on the challenges cited above, among the multiple pipelines currently available to process DWI data, PSMD has advantages that may be particularly appealing for low-to-middle income countries. Besides its fast and fully automated nature, PSMD requires fairly simple and short acquisition protocols, as well as little computational resources and neuroimaging processing experience. For instance, graph-based network and tractography analyses greatly benefit from high angular resolution diffusion imaging (HARDI), which requires at least 50 gradient directions at a high b-value.[279] On the other hand, PSMD requires only 20 directions (ideally), and comparable results have been recently achieved with as few as 6 directions, in clinical acquisitions.[280] Far from offering a panacea, PSMD may represent a cost-effective way of measuring WM damage that can be particularly appealing in the context of limited funding and need for short MRI protocols.

4.3.   Harmonization and Clinical translation

It has become paramount in neuroimaging to combine MRI data from multiple centers to increase statistical power, generalizability, and ultimately achieve higher levels of evidence. In the table below we enumerate the standardization techniques developed so far to achieve such goals with PSMD and what could to be done to further advance harmonization and clinical translation.

Table 4.1. Standardization of techniques - where we currently are and what could be done to advance clinical translation

Where we are currently	What could be done to advance clinical translation
• PSMD singularity container • Vendor-specific standardized MRI diffusion protocols for multi-site acquisition. • Protocols for phantom quality insurance scans. • Imaging-based biomarker kits, with step-by-step instructions and video tutorials on how to process DWI data and obtain PSMD values. • Validation of PSMD's instrumental properties (including repeatability and reproducibility) for multicenter studies. • Successful application of a technique to retrospectively harmonize raw diffusion signal across centers. • Protocols for harmonizing clinical/cognitive assessment.	• Development of standardized protocols for 1.5T. • Testing retrospective DWI harmonization techniques in more varied samples, including cohorts with distinct MRI field-strengths. • Raise awareness of PSMD, to stimulate further research and enable assessment of standardization procedures over a larger number of centers. • Include sites from underrepresented communities. • Validate clinical/cognitive protocols in underrepresented communities. • Investigate PSMD's associations with other non-imaging biomarkers

The following steps have been taken to achieve harmonization of data for multicenter studies with PSMD:

- PSMD singularity container:

The developers of the PSMD pipeline acknowledge that different environments, that is, different versions of FSL or operating system, have minor impact on PSMD values. Multicenter and longitudinal studies could be more prone to these sources of bias if the computation of PSMD is not centralized. Therefore, to ensure a consistent environment and results, they provided the PSMD Singularity container (https://github.com/miac-research/psmd/tree/main/singularity). Users from different centers may achieve more similar results by using this approach.

- National and International standardizing consortiums:

PSMD has been included as a candidate marker in initiatives to disseminate and standardize neuroimaging techniques to study vascular contributors to cognitive impairment and dementia (i.e., https://markvcid.partners.org, https://harness-neuroimaging.org). These initiatives have developed standard operating procedures to minimize variability in neuroimaging acquisition and processing, such as:

   - Vendor-specific standardized MRI diffusion protocols for multi-site acquisition, adjusted to provide the highest imaging quality within scan times that can be tolerable for patients (i.e., https://markvcid.partners.org/consortium-protocols-resources,https://harness-

neuroimaging.org/mr-protocols). These protocols are freely accessible as exam cards and/or text/PDF files and are meant to be shared and comparable across centers.[161]

- Protocols for phantom quality insurance scans. Modified versions of the DWI protocol (i.e., six-gradient direction DWI sequence with a single b=0) are provided to calculate the apparent diffusion coefficient in the center of the phantom (https://markvcid.partners.org/consortium-protocols-resources). These scans need to be performed and assessed bi-monthly to ensure consistency of imaging quality and comparability of imaging data across centers involved in multi-site studies.[161]

- Imaging-based biomarker kits, including PSMD kits, with step-by-step and video tutorial instructions on how to process DWI and obtain PSMD values (https://markvcid.partners.org/consortium-protocols-resources).

- Validation of PSMD's instrumental properties. The MarkVCID consortium has recently demonstrated PSMD's high repeatability and reproducibility across different sites, significantly accelerating PSMD's validation process.[224]

- The considerable heterogeneity in MRI protocols, preprocessing methods, cognitive tests, and statistical analyses we observed in our systematic review made clear the need for harmonizing not only neuroimaging tools but also clinical and statistical approaches. Consortiums, such as the MarkVCID, are currently standardizing clinical/cognitive data through guidelines and manuals.[281]

- Post-acquisition harmonization of raw diffusion data:

While harmonizing acquisition protocols, using phantom quality insurance scans, and standardizing pre- and post-processing steps facilitates comparison and merging of data in multicenter studies, they do not remove inter-site variability altogether. These differences can still impact results, and joint analysis may benefit from harmonizing raw diffusion data. With regards specifically to PSMD, harmonization techniques focused on the rotation invariant spherical harmonics (RISH) methods have been recently applied to five cohorts of cSVD patients and healthy control individuals in order to assess PSMD's strength of association with WMH and the differences in PSMD values between patients and controls.[282] Interestingly, the RISH technique effectively removed acquisition-related variability while maintaining PSMD's sensitivity to cSVD-related abnormalities.[282] This harmonizing technique is promising and could enable more inclusive and diverse multicenter studies.

We enumerate below some of the challenges that remain to be addressed to further advance PSMD's harmonization and clinical translation.

- Most of the standardized MRI protocols developed are exclusively for 3T MRI scanners and predominantly for Philips and Siemens. Further effort is needed to develop and make available similar protocols for 1.5T scanners and GE scanners.

- Similarly, post-acquisition harmonization techniques could be tested in more varied samples, including cohorts with distinct MRI field strengths. This would allow cohorts imaged in earlier times to be included and would contribute to future multicenter neuroimaging studies.

- Raising awareness about PSMD is paramount to stimulate research and further advance its clinical translation. Given PSMD's promising features, we were surprised to have found relatively few studies applying this marker in the literature. The need for further research to advance understanding, validation, and clinical translation prompted us to write our systematic review on PSMD, aiming to raise awareness while providing a critical overview of the marker.

- Similarly, more effort is needed to validate cognitive tests in more diverse non-English-speaking communities. Importantly, clinical translation of neuroimaging findings also relies on harmonizing clinical/cognitive variables.

- Clinical translation would also benefit from efforts to foment and harmonize neuroimaging studies in low-to-middle income countries and minoritized populations, aiming for more equitable research.

- Investigating PSMD's associations with other, non-imaging, biomarkers of vascular cognitive impairment and AD (i.e. serum/CSF laboratorial markers) would help to advance its biological understanding.

4.4. Next steps

Our next steps will involve the longitudinal analysis of several cSVD neuroimaging biomarkers in memory-clinic individuals, aiming to investigate whether changes in PSMD reflect variability in neuropsychological performance and build-up of cSVD pathology. This is an ongoing project currently carried out in the same population as previous projects, in collaboration with researchers from the department of Neurology at MGH.

In Brazil, we are involved in the neuroimaging core of the MRI and cognitive evaluation substudy of the Triple therapy prevention of Recurrent Intracerebral Disease EveNts Trial (TRIDENT). This

longitudinal multicenter substudy aims to investigate how intensive blood-pressure control influences dementia rates, cognitive performance, and MRI cSVD biomarkers, including PSMD, among Brazilian ASC-related ICH-survivors. Neuroimaging data from multiple Brazilian centers are currently being acquired and processed, alongside cognitive tests.

5. General Conclusions

In this doctoral thesis we aimed to investigate the performance of a novel automated DTI biomarker in quantifying WM damage and reflecting related cognitive impairment in the context of the second most prevalent cSVD worldwide. We first extensively reviewed the literature and assessed PSMD's neurocognitive and neuroimaging associations reported in several WM disorders, discussing limitations, and highlighting scientific questions to be addressed. Our cross-sectional studies in CAA patients were in line with the literature and support PSMD's strong cognitive associations, outperforming conventional MRI and DTI markers. We provided evidence on PSMD's promising role as a measure of both global and regional WM injury, successfully applying it in ROI analyses. Finally, we discussed the gaps that remain to be addressed to fully validate PSMD as a biomarker for VCI and to increase its generalizability and clinical translation. We acknowledged the challenges related to studying dementia in Brazil and discussed PSMD's appeal as a potentially cost-effective metric.

6. Appendix

Appendix 1 Narrative review

Appendix 1.A. cSVD and VCID: from diagnosis to management

Cerebral Small Vessel Disease and Vascular Cognitive Impairment: from diagnosis to management

Maria Clara Zanon Zotin, MD[1,2]*; Lukas Sveikata, MD[1,3]*; Anand Viswanathan, MD, PhD[1];

Pinar Yilmaz, MD[1,4]

[1] J. Philip Kistler Stroke Research Center, Department of Neurology, Massachusetts General Hospital, Harvard Medical School, Boston, MA, United States.

[2] Center for Imaging Sciences and Medical Physics. Department of Medical Imaging, Hematology and Clinical Oncology. Ribeirão Preto Medical School, University of São Paulo, Ribeirão Preto, SP, Brazil.

[3] Division of Neurology, Department of Clinical Neurosciences, Geneva University Hospital, Faculty of Medicine, University of Geneva, Geneva, Switzerland;

[4] Departments of Epidemiology and Radiology and Nuclear Medicine, Erasmus Medical Center, Rotterdam, the Netherlands.

* Both Maria Clara Zanon Zotin and Lukas Sveikata contributed equally to the manuscript.

[a] Corresponding author:

Lukas Sveikata, MD, J. Philip Kistler Stroke Research Center, Department of Neurology, Massachusetts General Hospital; 175 Cambridge St, Suite 300, Boston, MA 02114, USA. Tel: +1 617 643 2713, fax: + 1 617 726 5346, e-mail: lsveikata@mgh.harvard.edu.

ABSTRACT

Purpose of review: We present recent developments in the field of small vessel disease (SVD)-related vascular cognitive decline, including pathological mechanisms, updated diagnostic criteria, cognitive profile, neuroimaging markers, and risk factors. We further address available management and therapeutic strategies.

Recent findings: Vascular and neurodegenerative pathologies often co-occur and share similar risk factors. The updated consensus criteria aim to standardize vascular cognitive impairment (VCI) diagnosis, relying strongly on cognitive profile and MRI findings. Aggressive blood pressure control and multidomain lifestyle interventions are associated with decreased risk of cognitive impairment, but disease-modifying treatments are still lacking. Recent research has led to a better understanding of mechanisms leading to SVD-related cognitive decline, such as blood brain barrier dysfunction, reduced cerebrovascular reactivity, and impaired perivascular clearance.

Summary: SVD is the leading cause of VCI and is associated with substantial morbidity. Tackling cardiovascular risk factors is currently the most effective approach to prevent cognitive decline in the elderly. Advanced imaging techniques provide tools for early diagnosis and may play an important role as surrogate markers for cognitive endpoints in clinical trials. Designing and testing disease-modifying interventions for VCI remains a key priority in healthcare.

KEY POINTS

- VICCCS's recent guideline for diagnosing mild and major vascular cognitive impairment relies on neuropsychological evaluations of core domains, functional assessment (IADLs/ADLs), and MRI.

- Recent discoveries on complex pathological mechanisms underlying SVD, such as blood brain barrier dysfunction, reduced cerebrovascular reactivity, and impaired perivascular clearance of solutes, have provided new potential targets for the development of future therapeutic interventions.

- While conventional neuroimaging markers of SVD are widely available and incorporated into clinical practice, advanced techniques, such as DTI, enable early diagnosis and offer stronger and more consistent associations with cognition.

- Vascular risk factor control and healthy lifestyle interventions are associated with reduced risk of dementia and are key to slowing down SVD progression and cognitive decline.

- Lowering blood pressure control to the standard target (systolic BP <140 mmHg) is the primary modifiable prevention strategy, but a more aggressive blood pressure target (systolic BP <120 mmHg) and reduction of blood pressure variability may be beneficial in selected middle-aged and elderly patients.

INTRODUCTION

Vascular cognitive impairment (VCI) refers to conditions in which cerebrovascular diseases contribute to decline in mental abilities [1,2]. While these diseases can independently lead to cognitive deficits and account for 15-30% of dementia cases, second only to Alzheimer's disease (AD), they rarely occur in isolation [2,3]. Importantly, age-related cognitive impairment is typically driven by co-occurring vascular and neurodegenerative pathologies [4]. For instance, in a recent clinical–pathologic populational study, the majority of participants (~78%) had at least two concomitant neuropathologies at play at the time of death, more commonly neurodegenerative and vascular ones. [3].

Among the multiple mechanisms involved in VCI, cerebral small vessel disease (SVD) is arguably the most prevalent one [5], contributing to cognitive impairment irrespective of stroke [2]. SVDs are characterized by abnormalities that affect the structure and function of small vessels of the brain, with multiple neuroimaging and neurological manifestations, including cognitive decline [6]. Rather than a homogeneous disorder, SVD encompasses different sporadic and inherited pathologies, resulting from a complex mix of genetic and vascular risk factors. The prevalence of SVD increases with age, and the two most common types of sporadic SVD are arteriolosclerosis, also referred to as hypertensive arteriopathy or deep perforator arteriopathy, and cerebral amyloid angiopathy (CAA) [7]; the latter most commonly overlapping with AD [8].

In this narrative review, we focus on the latest advances in the management of sporadic SVD-related VCI, with an update on diagnostic criteria, neuroimaging markers, and cognitive profile. We also address the current state of prevention and therapeutic approaches.

POTENTIAL PATHOLOGICAL MECHANISMS LINKING SVD TO COGNITIVE IMPAIRMENT

Interactions between aging [9], environmental risk factors [10], and genetic variants [11,12] are thought to contribute to the development of sporadic SVDs (Figure 1.A). In the early pathogenic stages, damage to functional units composed of neurons, endothelial cells, astrocytes, and pericytes (neurovascular units) may lead to impaired regulation of blood flow, vascular permeability, immune trafficking, and waste clearance [6,13]. A cascade of events may arise, including blood brain barrier (BBB) leakage, deficient cerebrovascular reactivity (CVR), inflammation, vessel wall thickening and remodeling, as well as luminal narrowing (Figure 1.B) [6,14]. Together, these processes contribute to the broad spectrum of SVD-related brain parenchymal injury, including hemorrhagic and non-hemorrhagic (presumably ischemic) features (Figure 1.C). Through impaired vasomotion and reduced vasoreactivity, SVD might compromise the drainage of solutes along the vessels [8,15,16], potentially facilitating interstitial and perivascular accumulation of proteins, including amyloid-β, that can lead to secondary neuronal degeneration and loss of vascular smooth muscle cells [8]. This potential interactive pathway is thought to play a critical role in comorbid CAA and AD [8] and may lead to a self-reinforcing cycle in which neurodegenerative and vascular pathologies intensify and aggravate each other [8]. Sleep has been found to act as an important modulator of perivascular clearance and may also play a relevant role in age-related cognitive decline [16,17].

Evidence suggests that SVD-related brain lesions affect cognition also by disrupting structural and functional networks, causing a disconnection syndrome [18]. The strategic anatomical location of some lesions plays an important role and helps explain VCI's heterogeneous neuropsychological manifestations [18–20]. In addition, subcortical lesions may further contribute to functional

decline by triggering secondary degeneration of affected white matter (WM) tracts, leading to remote abnormalities such as WM atrophy and cortical thinning (Figure 1.D) [6,18].

CLINICAL CLASSIFICATION

Several classification systems have been proposed over the years to guide clinical diagnosis of VCI, reflecting methodological and diagnostic challenges [5,21–26]. When making use of these classifications, it is important to be aware of the broad overlap between neurodegenerative and vascular diseases in clinical [27] and pathological levels [3], acknowledging the great heterogeneity in the cognitive impact of such pathologies at an individual level [3].

The clinical diagnosis of VCI relies strongly on cognitive profile and neuroimaging findings. According to the most recent diagnostic guidelines, from the Vascular Impairment of Cognition Classification Consensus Study (VICCCS), VCI's definition aligns with the terminology of DSM-V and encompasses a broad clinical spectrum that ranges from mild to major VCI, and incorporates mixed-pathology cases (Table 1) [23,24]. Subcortical ischemic vascular dementia (SIVaD) refers to cases in which SVD is the primary mechanism underlying cognitive decline, and the most common brain lesions are white matter hyperintensities (WMH) and lacunar infarcts [18,28]. Importantly, according to VICCCS guidelines, subjects with neuroimaging signs of SVD may qualify either for SIVaD, post-stroke dementia, or mixed-dementia, depending on temporal associations and comorbidities.

Cognitive profile

Cognitive decline linked to cerebrovascular diseases, including SVD, is thought to typically present in a stepwise and gradual pattern, progressing slowly and affecting processing speed,

complex attention, and frontal-executive functions [5,25]. Disturbances in the frontal-executive domain are considered more likely to be present in mild VCI than in AD-related mild cognitive impairment (MCI), in which decline in episodic memory is the most prominent feature [29].

This observed predilection for frontal-executive functions impairment is thought to result from the disruptive effect of SVD lesions on the brain's structural and functional connectivity [18]. Neuroimaging studies have shown that the degree of structural network disruption is associated with the burden and extent of SVD lesions [30,31] and, at least in part, mediates their association with cognitive endpoints [32,33]. Functional networks associated with attention and executive functions have also been found to be predominantly affected in SVD patients [18].

Traditionally, a history of early onset of memory deficit and worsening of cortical functions (aphasia, apraxia, agnosia), in the absence of corresponding vascular brain imaging lesions, can be suggestive of AD as primary diagnosis [25]. Nonetheless, episodic and semantic memory can also be affected in cognitive impairment of presumably vascular origin [34–36].

Importantly, there is much overlap in cognitive profiles across dementia types [37], possibly related to the multifactorial nature of age-related cognitive decline combined with patient-specific factors related to cognitive reserve and spatial distribution of vascular lesions.

Accordingly, recent findings support a much more heterogeneous spectrum of cognitive impairment related to SVD, suggesting that multiple domains can be affected, owing not only to overlapping pathologies but also to close interdependence of executive function and processing speed to perform fluid cognitive tasks [38]. Interestingly, in severe CAA cases [39], visuospatial dysfunction has also been reported [40], hypothesized to relate to a posterior predominance of amyloid pathology.

Psychiatric, behavioral, and other manifestations

Additional features of VCI, depending on lesion localization and severity, may include a) personality and mood alterations (apathy, depression, emotional incontinence), b) motor and gait disturbances (frequent falls, small-step parkinsonian gait), c) early urinary incontinence, and d) pseudobulbar palsy due to lacunes in basal ganglia or pons [25,26,41–43]. VCI is often associated with psychiatric and behavioral symptoms underlied by lesions in thalamocortical, striatocortical, and prefrontal-basal ganglia pathways [44] and are often amenable to therapy that is reviewed elsewhere [45]. Although depression often manifests with a reversible decline in cognitive function, late-life occurrence can also be an early sign of dementia [46].

A distinct form of SVD is CAA-related inflammation (CAA-ri), characterized by an autoimmune reaction to cerebrovascular amyloid-β deposits [47], and clinical presentation may include subacute cognitive dysfunction [47,48]. Early identification is critical since neurological deficits can be reversible with early immunosuppressive treatment [49].

NEUROIMAGING EVALUATION

In the context of cognitive impairment, detection of underlying microvascular pathology relies strongly on neuroimaging [25], for which MRI is considered the "gold-standard" [23,50]. Many SVD features are visible and detectable almost exclusively through MRI, but none are considered pathognomonic and, hence, must be interpreted in light of clinical findings [25]. Accompanied by clinical information, neuroimaging helps to distinguish etiological subtypes of SVD. The modified Boston criteria [51] and the Edinburgh criteria [52] enable in vivo diagnosis of CAA, with the

former providing high positive predictive values even in the absence of intracerebral hemorrhage (ICH), thus facilitating CAA diagnosis in memory-clinic patients [53]. The likelihood of underlying arteriolosclerosis or CAA can be further inferred based on the distribution pattern of several MRI-visible lesions (Figure 1.C; Figure 2) [54–57]. This distinction is particularly important because CAA frequently overlaps with AD, and confers higher risk of hemorrhagic complications, influencing decision-making on antithrombotic treatment [58]. Importantly, detection of SVD MRI lesions in young individuals without significant risk factors should prompt investigation of monogenic SVDs [59].

Conventional neuroimaging markers in SVD-related cognitive impairment

MRI-visible lesions represent only a small portion of the spectrum of brain injury related to SVD and probably reflect late and irreversible steps in this pathological process [60]. Established SVD markers include WMH, lacunes, perivascular spaces (PVS), recent small subcortical infarcts, cerebral microbleeds (CMB), cortical superficial siderosis (cSS), ICH, and atrophy (Figure 2). More recently, cortical cerebral microinfarcts (CMI) and convexity subarachnoid hemorrhage have been associated with SVD, especially with CAA (Figure 2) [61–63]. Even though these markers are useful for the diagnosis of SVDs, their relevance as predictors of cognitive impairment and dementia is less evident.

CMB's occurrence, number, and topographical distribution reflect the presence, severity, and etiology of the underlying SVD and correlate with higher risk of hemorrhagic and ischemic stroke, and increased mortality [64,65]. However, while there is some evidence linking CMBs to cognitive impairment, studies have yielded conflicting results and small effect sizes [64–66], possibly because CMBs probably do not cause significant disruption of adjacent tissue [66]. Similarly, cSS

contributes to in-vivo CAA diagnosis and is strongly associated with recurrent lobar ICH [67], but there is insufficient data supporting an independent association with cognition [68].

In contrast, non-hemorrhagic markers, in general, are more strongly associated with cognition [66]. WMH is one of the earliest and most established markers of SVD, associated with increased risk of stroke and mortality [64]. Recent meta-analyses support a strong link between WMH and VCI and indicate that extensive baseline burden, progression, and periventricular distribution of WMH are associated with increased risk of dementia [64,69]. Likewise, incident lacunes are associated with dementia, and worse executive function and psychomotor speed [70]. Though the burden of cortical CMI is underestimated in MRI, they are considered the most widespread form of brain infarct, associated with CAA and highly prevalent in cognitively-impaired subjects [61]. In contrast with CMBs, they are strongly associated with cognitive endpoints [71,72], potentially by disrupting adjacent tracts, with secondary perilesional and remote deficits [61]. Though brain atrophy is a well-established consequence of SVD, it reflects the final converging effects of aging and several other pathologies, including neurodegenerative diseases [73,74]. Even though several studies link smaller brain volumes with cognitive impairment, none of them controlled for co-occurring AD, limiting causal inferences [75]. Increased visibility of PVS has also been associated with worse cognitive endpoints [73], but overall results are still conflicting, and its usefulness as a biomarker for cognition remains largely unknown [76].

Finally, to tentatively capture the overall burden of SVD, sum scores have been developed based on visual ratings of several MRI-visible lesions [77,78]. In population-based and patient cohorts, higher scores were associated with cognitive decline and increased risk of dementia [79–82].

Advanced neuroimaging markers in SVD-related cognitive impairment

While conventional MRI markers are appealing for being widely available and easily evaluated, advanced MRI techniques, in general, offer stronger cognitive associations, likely as a result of their sensitivity to microstructural abnormalities and disruption of network connections.

Diffusion tensor imaging (DTI) is considered one of the most promising MRI techniques in the fields of VCI and SVD. Diffusion properties of the water molecules reflect microstructural integrity and correlate with relevant histopathological changes [83]. DTI markers are sensitive to early and widespread abnormalities that go undetected on conventional MRI [18] and outperform MRI-visible lesions [84,85] by explaining more cognitive variance [18,86]. Furthermore, diffusion changes seem to be predominantly driven by SVD in comparison to AD pathology [87]. To overcome challenges imposed by highly complex and time-consuming post-processing techniques, novel automated DTI-based markers, like peak width of skeletonized mean diffusivity (PSMD), have been developed. PSMD reflects the heterogeneity of diffusivity across the main WM tracts [86]. It shows consistent cognitive associations in SVD and aging populations [86,88–92] and is considered a promising biomarker to be applied in future clinical trials in the field of VCI. Furthermore, through the combination of tractography and graph-theory analysis, valuable metrics of structural connectivity can be derived from DTI and have been found to predict cognitive decline [85,93], conversion to dementia [94], and even all-cause mortality [93] in SVD populations.

Other advanced imaging techniques evaluating functional connectivity status [18,95] and pathological changes in perfusion, vascular permeability, and vasoreactivity [96,97] are also under investigation.

Despite their relevance in the research field, the aforementioned emerging modalities require further validation before they can be applied in clinical practice.

MANAGEMENT OF VCI

Currently, management of VCI is centered on preventing and controlling vascular risk factors such as hypertension, obesity, smoking, and diabetes (Figure 1) [45,98,99]. Together, they account for 25-40% of dementia cases [2,45]. Better control of these factors is partly responsible for the decreasing incidence of dementia observed in high-income countries [45,100], mostly driven by lower rates of vascular dementia, considered the most preventable component of age-related cognitive decline [4,98,99]. Known protective factors include markers of increased cognitive reserve, such as higher education, occupation, social networks, cognitive and physical activity [10,101].

Vascular risk factor control

High blood pressure (BP) represents the primary modifiable risk factor involved in SVD progression and VCI [50]. Hypertension affects more than 75% of subjects >65 years-old, of whom nearly 53% are inadequately controlled [102]. While both mid-life and late-life hypertension are associated with WMH progression and disruption of WM microstructure [103,104], mid-life hypertension is more strongly linked to dementia, since BP begins to fall five years before diagnosis [105]. Likewise, blood pressure >130 mmHg at age 50, but not later in life, was associated with increased risk of dementia [106]. Adding to the complexity, decline in BP in late life was associated with cerebral (micro)infarcts, with hypoperfusion as a potential culprit [107]. Interestingly, the effect of elevated BP on cognitive decline appears to be mediated by both vascular pathology and neurofibrillary tangles, suggesting that managing BP can alleviate both vascular and neurodegenerative pathways [107,108]. Beyond elevated mean BP, fluctuations of BP over a period of hours, days, and years have been increasingly found to influence brain health

[109–111]. Emerging evidence suggests a link between BP variability, SVD progression, and dementia risk [110,112]. More insights are needed to define this complex relationship between BP profile in aging and cognitive decline.

Findings from clinical trials support that interventions can lower the risk of VCI progression. In the SPRINT-MIND study, middle-aged individuals (>50 years) and the elderly (mean age 68 years) with increased vascular risk submitted to intensive BP management (systolic BP goal <120 mmHg) showed reduced WMH progression [113] and smaller incidence of cognitive impairment in comparison to the control group (systolic BP goal <140 mmHg) [114]. The ACCORD-MIND substudy and the INFINITY study also supported that intensive BP control might help slow down WMH progression, with varying effects on cognition [115,116]. Of importance, after ICH, inadequate BP control is also associated with increased risk of lobar and non-lobar recurrence [117].

For patients with VCI, expert's consensus advocates that antihypertensive therapy should aim to achieve a standard treatment goal (BP <140/90 mmHg) [50]. In eligible middle-aged and in the elderly with vascular risk factors, targeting systolic BP <120 mmHg with careful side-effect monitoring may prevent development of MCI when compared to standard therapy [50]. Despite limited evidence[118], calcium-channel blockers and angiotensin receptor blockers may be preferred treatments [50,119].

Diabetes is a clear risk factor for future dementia [120] and has been associated with poorer processing speed and executive function, likely by contributing to SVD-related disruption of structural and functional connectivity [103,120]. There is conflicting evidence regarding whether intensive glycemic control in diabetics could reduce micro-/macrovascular complications [121,122], and no evidence insofar has been found for a protective effect on SVD progression or

cognitive decline [115,123,124]. The focus should be on preventing hyperglycemia and repetitive hypoglycemia, since these have been linked to dementia [45,123].

While the effects of hypertension and diabetes on cognition appear to be driven mainly by vascular pathology, evidence suggests that dyslipidemia contributes more to AD-related degeneration [103,125]. For instance, midlife dyslipidemia has been associated with amyloid and tau deposition later in life [125,126]. Though these findings imply a potential benefit of lipid-lowering therapy on cognition, clinical trials have not yet shown encouraging results [127,128]. A large prospective study, including 96,043 participants, suggested that LDL cholesterol <70mg/dL may increase the risk of ICH [129]. Further research should evaluate the benefit/risk ratio of lipid-lowering therapy in patients at higher risk of hemorrhagic complications, such as CAA cases [58].

Mid-life obesity is another emerging risk factor for dementia in later life [130]. Weight-loss of ≥2 kg was associated with improved attention and memory [131]. Not surprisingly, heavy midlife smoking has also been linked to increased risk of cognitive decline [45]. Smoking appears to contribute in a dose-dependent way to increase WMH burden and to disrupt microstructural integrity, effects which may be partly reversible after cessation [132,133].

As expected, stroke itself is a powerful risk factor for dementia, increasing the risk two-fold [134]. The post-event conversion rate to dementia at one year is estimated at 34.4% in patients with severe stroke, 8.2% in minor stroke, and 5.2% in those with TIA [135]. The variability in the incidence and temporality of post-stroke dementia suggests that other factors, such as SVD, may influence post-stroke outcomes [136]. Accordingly, atrial fibrillation is also considered a potent risk factor for cognitive decline [137]. In a large registry study, incident dementia risk was reduced by 48% in patients with atrial fibrillation on oral anticoagulation vs. no anticoagulation [137]. Hemorrhagic

events confer an increased risk of dementia, particularly high in lobar ICH cases, in which CAA pathology plays an important role [58,138].

Symptomatic treatment

Acetylsalicylic acid is considered a reasonable therapy in patients with MCI or dementia presenting covert brain infarcts on imaging, yet confirmatory trials are still missing [50]. On the other hand, aspirin is not recommended for patients presenting with VCI attributable to confluent WMH only, without other evidence-based indications [50]. Of note, the recent ASPREE trial did not show aspirin treatment to be beneficial in terms of cognitive outcomes in the general elderly population (>70 years) [139]. The question still remains if prophylactic antithrombotic treatment can benefit patients with underlying moderate to severe vascular disease.

Cholinesterase inhibitors (donepezil, galantamine, rivastigmine) and N-methyl D-aspartate antagonist memantine may be considered for symptomatic treatment in selected patients with dementia and SVD [22,50]. Only donepezil has shown a modest clinically appreciable effect on cognition in trials that evaluated demented patients with vascular component [140]. Galantamine can be considered for treatment in patients with mixed neurodegenerative and SVD pathology [22]. Because cholinesterase inhibitors and memantine in VCI are considered off-label by FDA, the decision to administer these drugs should be taken with caution and discussed with patients in light of the risk of adverse events. Finally, extracts of *ginkgo biloba* (EGb761) were also reported to have some effect on cognition and ADLs [141].

Protective lifestyle factors

Maintaining cognitive activity in late-life plays a major role in improving and maintaining brain structure and function [101,142]. Evidence suggests that low levels of education contribute to cognitive impairment [38], and physical activity in the elderly decreases the risk of developing dementia [143,144]. Interestingly, the preventive effect of exercise and cultural activities on cognition is enhanced when conducted in company, reinforcing the importance of social networks [145]. Furthermore, Mediterranean diet is generally recommended to reduce the risk of cognitive decline [146,147], and both Mediterranean and vegetarian diets were shown to be associated with stroke risk reduction [148,149].

Combining different interventions is a promising approach. The Finish FINGER trial found improved cognitive performance in at-risk elderly individuals receiving a multidomain lifestyle intervention that included nutritional guidance, exercise, cognitive training, and management of vascular risk factors [150].

Novel insights into sleep and cognition [16,17] suggest that short night sleep (<5 hours), poor quality sleep, and hypnotics use are associated with an increased risk of dementia in healthy adults [151,152]. Accordingly, moderate to severe sleep apnea is linked to WMH and silent brain infarctions [153,154]. Recent findings on the influence of non-REM-sleep in perivascular clearance of metabolites from the brain, with potential impact on neurodegenerative and vascular pathways [17], raise questions as to whether interventions focused on improving sleep quality could prevent or reverse age-related cognitive decline. Further research is required to clarify associations between sleep quality and cognitive decline.

148

CONCLUSION AND FUTURE DIRECTIONS

Recent research has taught us that cognitive decline in the elderly is driven by interacting neurodegenerative and vascular pathways, with significant contribution from SVD. Reports of declining incidence of dementia in high-income countries, together with recent positive trials on multifactorial interventions and blood pressure control, are encouraging and highlight the importance of further investigating the impact of vascular risk-factors on cognition. While there is a challenging path ahead in the quest for disease-modifying interventions, a better understanding of pathological mechanisms underlying SVD could lead to identifying new potential therapeutic targets. Novel neuroimaging markers are promising tools for clinical trials in the field and may act as surrogate markers for cognitive endpoints [73,155]. Since vascular pathology is considered the most preventable component of cognitive decline in the elderly, tackling cardiovascular risk-factors remains the cornerstone therapeutic approach.

ANNOTATIONS

Introduction:

** Wolters et al. Arteriosclerosis Thrombosis Vasc Biology. 2019: This review highlights the multifactorial nature of cognitive decline in the elderly, and suggests that definitions and classifications in the field of dementia should acknowledge the potential contributions from different pathways.

** Iadecola et al. JACC 2019 : This scientific expert panel review provides a comprehensive overview of recent advances in the field of vascular cognitive impairment and dementia.

* Boyle et al. Ann Neurol 2018: A recent clinical–pathologic populational study on the prevalence and co-occurrence of multiple neuropathologies in the elderly, quantifying their contributions to cognitive loss at the individual level.

Classification:

 * Boyle et al. Ann Neurol 2019: The attributable risk of Alzheimer's disease was calculated for nine neuropathologies in two longitudinal clinical-pathological studies.

** Skrobot et al. Alzheimer's & Dementia 2018: Most recent consensus criteria for VCI, including recommendations for neuropsychological examination and imaging.

Pathophysiology:

** Wardlaw et al. Lancet Neurology. 2019:Detailed discussion on the pathophysiology underlying SVD and how its clinical presentation and course are influenced by multiple factors.

** Greenberg et al. Nat Rev Neurol. 2020: Detailed discussion on the similarities and differences in the pathogenesis of CAA and AD, and potential interactive pathways.

** Nedergaard & Goldman. Science 2020 : An updated review on the pathophysiology of the glymphatic system and its relation with sleep and neurodegeneration.

Cognitive profile:

** Williamson et al. 2019: First clinical trial to suggest MCI risk reduction with intensive BP therapy.

* Nasrallah et al. 2019: SPRINT-MIND substudy showing association of intensive BP therapy and reduced WMH and brain atrophy progression.

* Regenhardt et al. 2020: a retrospective analysis of a relatively large cohort of rare CAA-related inflammation cases, evaluating the effectiveness of immunosuppressive therapy on recovery and recurrence.

Neuroimaging evaluation:

** Debette et al. JAMA Neurol. 2019: Systematic review and meta-analysis of imaging markers of covert vascular brain injury, namely white matter hyperintensities, infarcts, cerebral

microbleeds, and perivascular spaces.

*Hilal et al. J Cereb Blood Flow Metabolism. 2019: Study on the association between cerebral microinfarcts and cognitive decline within 2 years of follow-up in memory-clinic subjects.

* Smith et al. Alzheimer's Dementia Diagnosis Assess Dis Monit, 2019: An expert's initiative providing a framework for developing and validating neuroimaging biomarkers in the field of VCI , aimed at harmonizing MRI methods for future studies.

*Boot et al. Neuroimage Clin. 2020: Within the RUN-DMC study, the association of network efficiency measures and cognitive performance have been studied.

*Finsterwalder S et al. Alzheimer's Dementia. 2020: Diffusion abnormalities in memory-clinic patients were found to be more likely driven by SVD than AD components.

Management:

** Livingston et al.Lancet Commission 2020 2020: An extensive recent review on prevention and management of dementia and related neuropsychiatric symptoms.

** Smith et al. Alzheimers Dement 2020: Most recent guidelines form the Canadian Consensus Conference on VCI management.

* Ma et al. Am J Hypertens 2020: A state-of-the-art review on association between blood pressure variability and cognitive decline.

** Ma et al. JACC 2020: Linking blood pressure variability with progression of subclinical small-vessel-disease in the general population.

* Van Sloten et al. Lancet Diabetes Endocrinol 2020: A review on the associations between diabetes, microvascular dysfunction and cognition.

* Ma et al. Neurology 2019: This large community-based study showed an association of intensive LDL-cholesterol lowering targets with increased risk of ICH.

** Kozberg et al. Int J Stroke 2020: A comprehensive review on cerebral amyloid angiopathy management.

** Pendlebury et al. Lancet Neurol 2019: Large population-based study on post-stroke dementia risk.

* Chiu et al. Neurology 2020: A study in two large population cohorts linking vegetarian diet with decreased ischemic and hemorrhagic stroke risk.

* Chokesuwattanaskul et al. 2019: A meta-analysis suggesting an association link between OSA and SVD markers.

REFERENCES

1. Flier WM van der, Skoog I, Schneider JA, Pantoni L, Mok V, Chen CLH, et al. Vascular cognitive impairment. Nat Rev Dis Primers. 2018;4(1):18003.

2. Wolters FJ, Ikram MA. Epidemiology of Vascular Dementia. Arteriosclerosis Thrombosis Vasc Biology. 2019;39(8):1542–9.

3. Boyle PA, Yu L, Wilson RS, Leurgans SE, Schneider JA, Bennett DA. Person-specific contribution of neuropathologies to cognitive loss in old age. Ann Neurol. 2018;83(1):74–83.

4. Viswanathan A, Rocca WA, Tzourio C. Vascular risk factors and dementia. Neurology. 2009;72(4):368–74.

5. Dichgans M, Leys D. Vascular Cognitive Impairment. Circ Res. 2017;120(3):573–91.

6. Wardlaw JM, Smith C, Dichgans M. Small vessel disease: mechanisms and clinical implications. Lancet Neurology. 2019;18(7):684–96.

7. Cannistraro RJ, Badi M, Eidelman BH, Dickson DW, Middlebrooks EH, Meschia JF. CNS small vessel disease: A clinical review. Neurology. 2019;92(24):1146–56.

8. Greenberg SM, Bacskai BJ, Hernandez-Guillamon M, Pruzin J, Sperling R, Veluw SJ van. Cerebral amyloid angiopathy and Alzheimer disease — one peptide, two pathways. Nat Rev Neurol. 2020;16(1):30–42.

9. Li T, Huang Y, Cai W, Chen X, Men X, Lu T, et al. Age-related cerebral small vessel disease and inflammaging. Cell Death Dis. 2020;11(10):932.

10. Iadecola C, Duering M, Hachinski V, Joutel A, Pendlebury ST, Schneider JA, et al. Vascular Cognitive Impairment and Dementia. J Am Coll Cardiol. 2019;73(25):3326–44.

11. Marini S, Anderson CD, Rosand J. Genetics of Cerebral Small Vessel Disease. Stroke. 2019;51(1):12–20.

12. Rutten-Jacobs LCA, Rost NS. Emerging insights from the genetics of cerebral small-vessel disease. Ann Ny Acad Sci. 2020;1471(1):5–17.

13. Iadecola C. The Pathobiology of Vascular Dementia. Neuron. 2013;80(4):844–66.

14. Blevins BL, Vinters HV, Love S, Wilcock DM, Grinberg LT, Schneider JA, et al. Brain arteriolosclerosis. Acta Neuropathol. 2020;1–24.

15. Veluw SJ van, Hou SS, Calvo-Rodriguez M, Arbel-Ornath M, Snyder AC, Frosch MP, et al. Vasomotion as a Driving Force for Paravascular Clearance in the Awake Mouse Brain. Neuron. 2020;105(3):549-561.e5.

16. Nedergaard M, Goldman SA. Glymphatic failure as a final common pathway to dementia. Science. 2020;370(6512):50–6.

17. Fultz NE, Bonmassar G, Setsompop K, Stickgold RA, Rosen BR, Polimeni JR, et al. Coupled electrophysiological, hemodynamic, and cerebrospinal fluid oscillations in human sleep. Science. 2019;366(6465):628–31.

18. Telgte A ter, Leijsen EMC van, Wiegertjes K, Klijn CJM, Tuladhar AM, Leeuw F-E de. Cerebral small vessel disease: from a focal to a global perspective. Nat Rev Neurol. 2018;14(7):387–98.

19. Duering M, Gesierich B, Seiler S, Pirpamer L, Gonik M, Hofer E, et al. Strategic white matter tracts for processing speed deficits in age-related small vessel disease. Neurology. 2014;82(22):1946–50.

20. Zhao L, Biesbroek JM, Shi L, Liu W, Kuijf HJ, Chu WW, et al. Strategic infarct location for post-stroke cognitive impairment: A multivariate lesion-symptom mapping study. J Cereb Blood Flow Metabolism. 2017;38(8):1299–311.

21. Hachinski V, Iadecola C, Petersen RC, Breteler MM, Nyenhuis DL, Black SE, et al. National Institute of Neurological Disorders and Stroke–Canadian Stroke Network Vascular Cognitive Impairment Harmonization Standards. Stroke. 2006;37(9):2220–41.

22. Gorelick PB, Scuteri A, Black SE, Decarli C, Greenberg SM, Iadecola C, et al. Vascular Contributions to Cognitive Impairment and Dementia. Stroke. 2011;42(9):2672–713.

23. Skrobot OA, Black SE, Chen C, DeCarli C, Erkinjuntti T, Ford GA, et al. Progress toward standardized diagnosis of vascular cognitive impairment: Guidelines from the Vascular Impairment of Cognition Classification Consensus Study. Alzheimer's Dementia. 2018;14(3):280–92.

24. Skrobot OA, O'Brien J, Black S, Chen C, DeCarli C, Erkinjuntti T, et al. The Vascular Impairment of Cognition Classification Consensus Study. Alzheimer's Dementia. 2017;13(6):624–33.

25. Sachdev P, Kalaria R, O'Brien J, Skoog I, Alladi S, Black SE, et al. Diagnostic Criteria for Vascular Cognitive Disorders. Alz Dis Assoc Dis. 2014;28(3):206–18.

26. Roman GC, Tatemichi TK, Erkinjuntti T, Cummings JL, Masdeu JC, Garcia JH, et al. Vascular dementia: Diagnostic criteria for research studies: Report of the NINDS-AIREN International Workshop. Neurology. 1993;43(2):250–250.

27. Boyle PA, Yu L, Leurgans SE, Wilson RS, Brookmeyer R, Schneider JA, et al. Attributable risk of Alzheimer's dementia attributed to age-related neuropathologies. Ann Neurol. 2019;85(1):114–24.

28. Veluw SJ van, Scherlek AA, Freeze WM, Telgte A, Kouwe AJ, Bacskai BJ, et al. Different microvascular alterations underlie microbleeds and microinfarcts. Ann Neurol. 2019;86(2):279–92.

29. Albert MS, DeKosky ST, Dickson D, Dubois B, Feldman HH, Fox NC, et al. The diagnosis of mild cognitive impairment due to Alzheimer's disease: Recommendations from the National Institute on Aging-Alzheimer's Association workgroups on diagnostic guidelines for Alzheimer's disease. Alzheimer's Dementia. 2011;7(3):270–9.

30. Frey BM, Petersen M, Schlemm E, Mayer C, Hanning U, Engelke K, et al. White matter integrity and structural brain network topology in cerebral small vessel disease: The Hamburg city health study. Hum Brain Mapp. 2020;

31. Valenti R, Reijmer YD, Charidimou A, Boulouis G, Martinez SR, Xiong L, et al. Total small vessel disease burden and brain network efficiency in cerebral amyloid angiopathy. J Neurol Sci. 2017;382:10–2.

32. Du J, Wang Y, Zhi N, Geng J, Cao W, Yu L, et al. Structural brain network measures are superior to vascular burden scores in predicting early cognitive impairment in post stroke patients with small vessel disease. Neuroimage Clin. 2019;22:101712.

33. Lawrence AJ, Chung AW, Morris RG, Markus HS, Barrick TR. Structural network efficiency is associated with cognitive impairment in small-vessel disease. Neurology. 2014;83(4):304–11.

34. Arvanitakis Z, Leurgans SE, Wang Z, Wilson RS, Bennett DA, Schneider JA. Cerebral amyloid angiopathy pathology and cognitive domains in older persons. Ann Neurol. 2011;69(2):320–7.

35. Boyle PA, Yu L, Nag S, Leurgans S, Wilson RS, Bennett DA, et al. Cerebral amyloid angiopathy and cognitive outcomes in community-based older persons. Neurology. 2015;85(22):1930–6.

36. Xiong L, Davidsdottir S, Reijmer YD, Shoamanesh A, Roongpiboonsopit D, Thanprasertsuk S, et al. Cognitive Profile and its Association with Neuroimaging Markers of Non-Demented Cerebral Amyloid Angiopathy Patients in a Stroke Unit. J Alzheimer's Dis. 2016;52(1):171–8.

37. Smits LL, Harten AC van, Pijnenburg YAL, Koedam ELGE, Bouwman FH, Sistermans N, et al. Trajectories of cognitive decline in different types of dementia. Psychol Med. 2015;45(5):1051–9.

38. Hamilton OKL, Backhouse EV, Janssen E, Jochems ACC, Maher C, Ritakari TE, et al. Cognitive

impairment in sporadic cerebral small vessel disease: A systematic review and meta-analysis. Alzheimer's Dementia. 2020;

39. Thanprasertsuk S, Martinez-Ramirez S, Pontes-Neto OM, Ni J, Ayres A, Reed A, et al. Posterior white matter disease distribution as a predictor of amyloid angiopathy. Neurology. 2014;83(9):794–800.

40. Valenti R, Charidimou A, Xiong L, Boulouis G, Fotiadis P, Ayres A, et al. Visuospatial Functioning in Cerebral Amyloid Angiopathy: A Pilot Study. J Alzheimer's Dis. 2017;Preprint(Preprint):1–5.

41. Reijmer YD, Fotiadis P, Martinez-Ramirez S, Salat DH, Schultz A, Shoamanesh A, et al. Structural network alterations and neurological dysfunction in cerebral amyloid angiopathy. Brain. 2015;138(1):179–88.

42. Jouvent E, Reyes S, Mangin J-F, Roca P, Perrot M, Thyreau B, et al. Apathy is related to cortex morphology in CADASIL. Neurology. 2011;76(17):1472–7.

43. Reyes S, Viswanathan A, Godin O, Dufouil C, Benisty S, Hernandez K, et al. Apathy. Neurology. 2009;72(10):905–10.

44. O'Brien JT, Erkinjuntti T, Reisberg B, Roman G, Sawada T, Pantoni L, et al. Vascular cognitive impairment. Lancet Neurology. 2003;2(2):89–98.

45. Livingston G, Huntley J, Sommerlad A, Ames D, Ballard C, Banerjee S, et al. Dementia prevention, intervention, and care: 2020 report of the Lancet Commission. Lancet. 2020;396(Dement Geriatr Cogn Dis 37 2014):413–46.

46. Li G, Wang LY, Shofer JB, Thompson ML, Peskind ER, McCormick W, et al. Temporal Relationship Between Depression and Dementia: Findings From a Large Community-Based 15-Year Follow-up Study. Arch Gen Psychiat. 2011;68(9):970–7.

47. Auriel E, Charidimou A, Gurol ME, Ni J, Etten ESV, Martinez-Ramirez S, et al. Validation of Clinicoradiological Criteria for the Diagnosis of Cerebral Amyloid Angiopathy–Related Inflammation. Jama Neurol. 2016;73(2):197.

48. Bouthour W, Sveikata L, Vargas MI, Lobrinus JA, Carrera E. Clinical Reasoning: Rapid progression of reversible cognitive impairment in an 80-year-old man. Neurology. 2018 Dec 10;91(24):1109 1113.

49. Regenhardt RW, Thon JM, Das AS, Thon OR, Charidimou A, Viswanathan A, et al. Association Between Immunosuppressive Treatment and Outcomes of Cerebral Amyloid Angiopathy–Related Inflammation. Jama Neurol. 2020;77(10).

50. Smith EE, Barber P, Field TS, Ganesh A, Hachinski V, Hogan DB, et al. Canadian Consensus Conference on Diagnosis and Treatment of Dementia (CCCDTD)5: Guidelines for management of vascular cognitive impairment. Alzheimer's Dementia Transl Res Clin Interventions. 2020;6(1):e12056.

51. Linn J, Halpin A, Demaerel P, Ruhland J, Giese AD, Dichgans M, et al. Prevalence of superficial siderosis in patients with cerebral amyloid angiopathy(CME). Neurology. 2010;74(17):1346–50.

52. Rodrigues MA, Samarasekera N, Lerpiniere C, Humphreys C, McCarron MO, White PM, et al. The Edinburgh CT and genetic diagnostic criteria for lobar intracerebral haemorrhage associated with cerebral amyloid angiopathy: model development and diagnostic test accuracy study. Lancet Neurology. 2018;17(3):232–40.

53. Martinez-Ramirez S, Romero J-R, Shoamanesh A, McKee AC, Etten EV, Pontes-Neto O, et al. Diagnostic value of lobar microbleeds in individuals without intracerebral hemorrhage. Alzheimer's Dementia. 2015;11(12):1480–8.

54. Charidimou A, Boulouis G, Haley K, Auriel E, Etten ES van, Fotiadis P, et al. White matter hyperintensity patterns in cerebral amyloid angiopathy and hypertensive arteriopathy. Neurology. 2016;86(6):505–11.

55. Charidimou A, Hong YT, Jäger HR, Fox Z, Aigbirhio FI, Fryer TD, et al. White Matter Perivascular Spaces on Magnetic Resonance Imaging. Stroke. 2015;46(6):1707–9.

56. Pasi M, Pongpitakmetha T, Charidimou A, Singh SD, Tsai H-H, Xiong L, et al. Cerebellar Microbleed Distribution Patterns and Cerebral Amyloid Angiopathy. Stroke. 2019;50(7):1727–33.

57. Pasi M, Boulouis G, Fotiadis P, Auriel E, Charidimou A, Haley K, et al. Distribution of lacunes in cerebral amyloid angiopathy and hypertensive small vessel disease. Neurology. 2017;88(23):2162–8.

58. Kozberg MG, Perosa V, Gurol ME, Veluw SJ van. A practical approach to the management of cerebral amyloid angiopathy. Int J Stroke. 2020;174749302097446.

59. Mancuso M, Arnold M, Bersano A, Burlina A, Chabriat H, Debette S, et al. Monogenic cerebral small-vessel diseases: diagnosis and therapy. Consensus recommendations of the European Academy of Neurology. Eur J Neurol. 2020;27(6):909–27.

60. Charidimou A, Boulouis G, Gurol ME, Ayata C, Bacskai BJ, Frosch MP, et al. Emerging concepts in sporadic cerebral amyloid angiopathy. Brain. 2017;140(7):1829–50.

61. Veluw SJ van, Shih AY, Smith EE, Chen C, Schneider JA, Wardlaw JM, et al. Detection, risk factors, and functional consequences of cerebral microinfarcts. Lancet Neurology. 2017;16(9):730–40.

62. Raposo N, Charidimou A, Roongpiboonsopit D, Onyekaba M, Gurol ME, Rosand J, et al. Convexity subarachnoid hemorrhage in lobar intracerebral hemorrhage: A prognostic marker. Neurology. 2020;94(9):e968–77.

63. Li Q, Zotin MCZ, Warren AD, Ma Y, Gurol E, Goldstein JN, et al. CT-visible convexity subarachnoid hemorrhage is associated with cortical superficial siderosis and predicts recurrent ICH. Neurology. 2020;10.1212/WNL.0000000000011052.

64. Debette S, Schilling S, Duperron M-G, Larsson SC, Markus HS. Clinical Significance of Magnetic Resonance Imaging Markers of Vascular Brain Injury: A Systematic Review and Meta-analysis. Jama Neurol. 2019;76(1):81.

65. Moulin S, Cordonnier C. Role of Cerebral Microbleeds for Intracerebral Haemorrhage and Dementia. Curr Neurol Neurosci. 2019;19(8):51.

66. Reijmer YD, Veluw SJ van, Greenberg SM. Ischemic brain injury in cerebral amyloid angiopathy. J Cereb Blood Flow Metabolism. 2015;36(1):40–54.

67. Charidimou A, Boulouis G, Roongpiboonsopit D, Xiong L, Pasi M, Schwab KM, et al. Cortical superficial siderosis and recurrent intracerebral hemorrhage risk in cerebral amyloid angiopathy: Large prospective cohort and preliminary meta-analysis. Int J Stroke. 2018;14(7):723–33.

68. Banerjee G, Wilson D, Jäger HR, Werring DJ. Novel imaging techniques in cerebral small vessel diseases and vascular cognitive impairment. Biochimica Et Biophysica Acta Bba - Mol Basis Dis. 2016;1862(5):926–38.

69. Hu H-Y, Ou Y-N, Shen X-N, Qu Y, Ma Y-H, Wang Z-T, et al. White matter hyperintensities and risks of cognitive impairment and dementia: A systematic review and meta-analysis of 36 prospective studies. Neurosci Biobehav Rev. 2020;120:16–27.

70. Ling Y, Chabriat H. Incident cerebral lacunes: A review. J Cereb Blood Flow Metabolism. 2020;40(5):909–21.

71. Cao L, Tan L, Wang H-F, Jiang T, Zhu X-C, Yu J-T. Cerebral Microinfarcts and Dementia: A Systematic Review and Metaanalysis. Curr Alzheimer Res. 2017;14(7).

72. Hilal S, Tan CS, Veluw SJ van, Xu X, Vrooman H, Tan BY, et al. Cortical cerebral microinfarcts predict cognitive decline in memory clinic patients. J Cereb Blood Flow Metabolism. 2019;40(1):44–53.

73. Smith EE, Biessels GJ, Guio FD, Leeuw FE de, Duchesne S, Düring M, et al. Harmonizing brain

magnetic resonance imaging methods for vascular contributions to neurodegeneration. Alzheimer's Dementia Diagnosis Assess Dis Monit. 2019;11(1):191–204.

74. Jouvent E, Viswanathan A, Chabriat H. Cerebral Atrophy in Cerebrovascular Disorders. J Neuroimaging. 2010;20(3):213–8.

75. Guio FD, Duering M, Fazekas F, Leeuw F-ED, Greenberg SM, Pantoni L, et al. Brain atrophy in cerebral small vessel diseases: Extent, consequences, technical limitations and perspectives: The HARNESS initiative. J Cereb Blood Flow Metabolism. 2019;40(2):231–45.

76. Wardlaw JM, Benveniste H, Nedergaard M, Zlokovic BV, Mestre H, Lee H, et al. Perivascular spaces in the brain: anatomy, physiology and pathology. Nat Rev Neurol. 2020;16(3):137–53.

77. Charidimou A, Martinez-Ramirez S, Reijmer YD, Oliveira-Filho J, Lauer A, Roongpiboonsopit D, et al. Total Magnetic Resonance Imaging Burden of Small Vessel Disease in Cerebral Amyloid Angiopathy: An Imaging-Pathologic Study of Concept Validation. Jama Neurol. 2016;73(8):994.

78. Staals J, Booth T, Morris Z, Bastin ME, Gow AJ, Corley J, et al. Total MRI load of cerebral small vessel disease and cognitive ability in older people. Neurobiol Aging. 2015;36(10):2806–11.

79. Olama AAA, Wason JMS, Tuladhar AM, Leijsen EMC van, Koini M, Hofer E, et al. Simple MRI score aids prediction of dementia in cerebral small vessel disease. Neurology. 2020;94(12):10.1212/WNL.0000000000009141.

80. Yilmaz P, Ikram MA, Ikram MK, Niessen WJ, Viswanathan A, Charidimou A, et al. Application of an Imaging-Based Sum Score for Cerebral Amyloid Angiopathy to the General Population: Risk of Major Neurological Diseases and Mortality. Front Neurol. 2019;10:1276.

81. Yilmaz P, Ikram MK, Niessen WJ, Ikram MA, Vernooij MW. Practical Small Vessel Disease Score Relates to Stroke, Dementia, and Death: The Rotterdam Study. Stroke. 2018;49(12):2857–65.

82. Brutto VJD, Ortiz JG, Brutto OHD, Mera RM, Zambrano M, Biller J. Total cerebral small vessel disease score and cognitive performance in community-dwelling older adults. Results from the Atahualpa Project. Int J Geriatr Psych. 2018;33(2):325–31.

83. Veluw SJ van, Reijmer YD, Kouwe AJ van der, Charidimou A, Riley GA, Leemans A, et al. Histopathology of diffusion imaging abnormalities in cerebral amyloid angiopathy. Neurology. 2019;92(9):10.1212/WNL.0000000000007005.

84. Williams OA, Zeestraten EA, Benjamin P, Lambert C, Lawrence AJ, Mackinnon AD, et al. Diffusion tensor image segmentation of the cerebrum provides a single measure of cerebral small vessel disease severity related to cognitive change. Neuroimage Clin. 2017;16:330–42.

85. Boot EM, Leijsen EM van, Bergkamp MI, Kessels RPC, Norris DG, Leeuw F-E de, et al. Structural network efficiency predicts cognitive decline in cerebral small vessel disease. Neuroimage Clin. 2020;27:102325.

86. Baykara E, Gesierich B, Adam R, Tuladhar AM, Biesbroek JM, Koek HL, et al. A Novel Imaging Marker for Small Vessel Disease Based on Skeletonization of White Matter Tracts and Diffusion Histograms. Ann Neurol. 2016;80(4):581–92.

87. Finsterwalder S, Vlegels N, Gesierich B, Caballero MÁA, Weaver NA, Franzmeier N, et al. Small vessel disease more than Alzheimer's disease determines diffusion MRI alterations in memory clinic patients. Alzheimer's Dementia. 2020;16(11):1504–14.

88. Wei N, Deng Y, Yao L, Jia W, Wang J, Shi Q, et al. A Neuroimaging Marker Based on Diffusion Tensor Imaging and Cognitive Impairment Due to Cerebral White Matter Lesions. Front Neurol. 2019;10:81.

89. Deary IJ, Ritchie SJ, Maniega SM, Cox SR, Hernández MCV, Luciano M, et al. Brain Peak Width of

Skeletonized Mean Diffusivity (PSMD) and Cognitive Function in Later Life. Frontiers Psychiatry. 2019;10:524.

90. Low A, Mak E, Stefaniak JD, Malpetti M, Nicastro N, Savulich G, et al. Peak Width of Skeletonized Mean Diffusivity as a Marker of Diffuse Cerebrovascular Damage. Front Neurosci-switz. 2020;14:238.

91. Lam BYK, Leung KT, Yiu B, Zhao L, Biesbroek JM, Au L, et al. Peak width of skeletonized mean diffusivity and its association with age-related cognitive alterations and vascular risk factors. Alzheimer's Dementia Diagnosis Assess Dis Monit. 2019;11(1):721–9.

92. Raposo N, Zotin MCZ, Schoemaker D, Xiong L, Fotiadis P, Charidimou A, et al. Peak Width of Skeletonized Mean Diffusivity as Neuroimaging Biomarker in Cerebral Amyloid Angiopathy. American Journal of Neuroradiology. 2021;

93. Tuladhar AM, Tay J, Leijsen E van, Lawrence AJ, Uden IWM van, Bergkamp M, et al. Structural network changes in cerebral small vessel disease. J Neurology Neurosurg Psychiatry. 2020;91(2):196.

94. Lawrence AJ, Zeestraten EA, Benjamin P, Lambert CP, Morris RG, Barrick TR, et al. Longitudinal decline in structural networks predicts dementia in cerebral small vessel disease. Neurology. 2018;90(21):e1898–910.

95. Wang R, Liu N, Tao Y-Y, Gong X-Q, Zheng J, Yang C, et al. The Application of rs-fMRI in Vascular Cognitive Impairment. Front Neurol. 2020;11:951.

96. Alsop DC, Detre JA, Golay X, Günther M, Hendrikse J, Hernandez-Garcia L, et al. Recommended implementation of arterial spin-labeled perfusion MRI for clinical applications: A consensus of the ISMRM perfusion study group and the European consortium for ASL in dementia. Magnet Reson Med. 2015;73(1):102–16.

97. Thrippleton MJ, Backes WH, Sourbron S, Ingrisch M, Osch MJP van, Dichgans M, et al. Quantifying blood-brain barrier leakage in small vessel disease: Review and consensus recommendations. Alzheimer's Dementia. 2019;15(6):840–58.

98. Satizabal CL, Beiser AS, Chouraki V, Chêne G, Dufouil C, Seshadri S. Incidence of Dementia over Three Decades in the Framingham Heart Study. New Engl J Medicine. 2016;374(6):523–32.

99. Hachinski V, Einhäupl K, Ganten D, Alladi S, Brayne C, Stephan BCM, et al. Preventing dementia by preventing stroke: The Berlin Manifesto. Alzheimer's Dementia. 2019;15(7):961–84.

100. Wu Y-T, Beiser AS, Breteler MMB, Fratiglioni L, Helmer C, Hendrie HC, et al. The changing prevalence and incidence of dementia over time — current evidence. Nat Rev Neurol. 2017;13(6):327–39.

101. Stern Y. Cognitive reserve in ageing and Alzheimer's disease. Lancet Neurology. 2012;11(11):1006–12.

102. Muntner P, Carey RM, Gidding S, Jones DW, Taler SJ, Wright JT, et al. Potential US Population Impact of the 2017 ACC/AHA High Blood Pressure Guideline. Circulation. 2018;137(2):109–18.

103. Power MC, Tingle JV, Reid RI, Huang J, Sharrett AR, Coresh J, et al. Midlife and Late-Life Vascular Risk Factors and White Matter Microstructural Integrity: The Atherosclerosis Risk in Communities Neurocognitive Study. J Am Heart Assoc. 2017;6(5).

104. Amier RP, Marcks N, Hooghiemstra AM, Nijveldt R, Buchem MA van, Roos A de, et al. Hypertensive Exposure Markers by MRI in Relation to Cerebral Small Vessel Disease and Cognitive Impairment. Jacc Cardiovasc Imaging. 2020;

105. Peters R, Peters J, Booth A, Anstey KJ. Trajectory of blood pressure, body mass index, cholesterol and incident dementia: systematic review. Br J Psychiatry. 2020;216(1):16–28.

106. Abell JG, Kivimäki M, Dugravot A, Tabak AG, Fayosse A, Shipley M, et al. Association between

systolic blood pressure and dementia in the Whitehall II cohort study: role of age, duration, and threshold used to define hypertension. Eur Heart J. 2018;39(33):3119–25.

107. Arvanitakis Z, Capuano AW, Lamar M, Shah RC, Barnes LL, Bennett DA, et al. Late-life blood pressure association with cerebrovascular and Alzheimer disease pathology. Neurology. 2018;91(6):e517–25.

108. Petrovitch H, White LR, Izmirilian G, Ross GW, Havlik RJ, Markesbery W, et al. Midlife blood pressure and neuritic plaques, neurofibrillary tangles, and brain weight at death: the HAAS☆. Neurobiol Aging. 2000;21(1):57–62.

109. Rothwell PM. Limitations of the usual blood-pressure hypothesis and importance of variability, instability, and episodic hypertension. Lancet Lond Engl. 2010;375(9718):938–48.

110. Ma Y, Tully PJ, Hofman A, Tzourio C. Blood Pressure Variability and Dementia: A State-of-the-Art Review. Am J Hypertens. 2020;

111. Ma Y, Yilmaz P, Bos D, Blacker D, Viswanathan A, Ikram MA, et al. Blood Pressure Variation and Subclinical Brain Disease. J Am Coll Cardiol. 2020;75(19):2387–99.

112. Ma Y, Wolters FJ, Chibnik LB, Licher S, Ikram MA, Hofman A, et al. Variation in blood pressure and long-term risk of dementia: A population-based cohort study. Plos Med. 2019;16(11):e1002933.

113. Nasrallah IM, Pajewski NM, Chelune G, Cheung AK, Cleveland ML, Auchus AP, et al. Association of Intensive vs Standard Blood Pressure Control With Cerebral White Matter Lesions. Jama. 2019;322(6):524.

114. Williamson JD, Pajewski NM, Auchus AP, Bryan RN, Chelune G, Cheung AK, et al. Effect of Intensive vs Standard Blood Pressure Control on Probable Dementia. Jama. 2019;321(6):553.

115. Havenon A de, Majersik JJ, Tirschwell DL, McNally JS, Stoddard G, Rost NS. Blood pressure, glycemic control, and white matter hyperintensity progression in type 2 diabetics. Neurology. 2019;92(11):e1168–75.

116. White WB, Wakefield DB, Moscufo N, Guttmann CRG, Kaplan RF, Bohannon RW, et al. Effects of Intensive Versus Standard Ambulatory Blood Pressure Control on Cerebrovascular Outcomes in Older People (INFINITY). Circulation. 2019;140(20):1626–35.

117. Biffi A, Anderson CD, Battey TWK, Ayres AM, Greenberg SM, Viswanathan A, et al. Association Between Blood Pressure Control and Risk of Recurrent Intracerebral Hemorrhage. Jama [Internet]. 2015 Aug 21;314(9):904–12. Available from: https://jamanetwork.com/journals/jama/fullarticle/2432164

118. Peters R, Yasar S, Anderson CS, Andrews S, Antikainen R, Arima H, et al. Investigation of antihypertensive class, dementia, and cognitive decline: A meta-analysis. Neurology. 2019;94(3):e267–81.

119. Forette F, Seux M-L, Staessen JA, Thijs L, Babarskiene M-R, Babeanu S, et al. The Prevention of Dementia With Antihypertensive Treatment: New Evidence From the Systolic Hypertension in Europe (Syst-Eur) Study. Arch Intern Med. 2002;162(18):2046–52.

120. Sloten TT van, Sedaghat S, Carnethon MR, Launer LJ, Stehouwer CDA. Cerebral microvascular complications of type 2 diabetes: stroke, cognitive dysfunction, and depression. Lancet Diabetes Endocrinol. 2020;8(4):325–36.

121. Reaven PD, Emanuele NV, Wiitala WL, Bahn GD, Reda DJ, McCarren M, et al. Intensive Glucose Control in Patients with Type 2 Diabetes — 15-Year Follow-up. New Engl J Med. 2019;380(23):2215–24.

122. Group AS, Gerstein HC, Miller ME, Genuth S, Ismail-Beigi F, Buse JB, et al. Long-Term Effects of Intensive Glucose Lowering on Cardiovascular Outcomes. New Engl J Medicine. 2011;364(9):818–28.

123. Biessels GJ, Despa F. Cognitive decline and dementia in diabetes mellitus: mechanisms and clinical implications. Nat Rev Endocrinol. 2018;14(10):591–604.

124. Launer LJ, Miller ME, Williamson JD, Lazar RM, Gerstein HC, Murray AM, et al. Effects of intensive glucose lowering on brain structure and function in people with type 2 diabetes (ACCORD MIND): a randomised open-label substudy. Lancet Neurology. 2011;10(11):969–77.

125. Cheng Y-W, Chiu M-J, Chen Y-F, Cheng T-W, Lai Y-M, Chen T-F. The contribution of vascular risk factors in neurodegenerative disorders: from mild cognitive impairment to Alzheimer's disease. Alzheimer's Res Ther. 2020;12(1):91.

126. Nägga K, Gustavsson A-M, Stomrud E, Lindqvist D, Westen D van, Blennow K, et al. Increased midlife triglycerides predict brain β-amyloid and tau pathology 20 years later. Neurology. 2017;90(1):10.1212/WNL.0000000000004749.

127. Trompet S, Vliet P van, Craen AJM de, Jolles J, Buckley BM, Murphy MB, et al. Pravastatin and cognitive function in the elderly. Results of the PROSPER study. J Neurol. 2009;257(1):85.

128. Biessels GJ, Verhagen C, Janssen J, Berg E van den, Zinman B, Rosenstock J, et al. Effect of Linagliptin on Cognitive Performance in Patients With Type 2 Diabetes and Cardiorenal Comorbidities: The CARMELINA Randomized Trial. Diabetes Care. 2019;42(10):1930–8.

129. Ma C, Gurol ME, Huang Z, Lichtenstein AH, Wang X, Wang Y, et al. Low-density lipoprotein cholesterol and risk of intracerebral hemorrhage: A prospective study. Neurology. 2019;93(5):e445–57.

130. Albanese E, Launer LJ, Egger M, Prince MJ, Giannakopoulos P, Wolters FJ, et al. Body mass index in midlife and dementia: Systematic review and meta-regression analysis of 589,649 men and women followed in longitudinal studies. Alzheimer's Dementia Diagnosis Assess Dis Monit. 2017;8(1):165–78.

131. Veronese N, Facchini S, Stubbs B, Luchini C, Solmi M, Manzato E, et al. Weight loss is associated with improvements in cognitive function among overweight and obese people: A systematic review and meta-analysis. Neurosci Biobehav Rev. 2017;72:87–94.

132. Gons RAR, Norden AGW van, Laat KF de, Oudheusden LJB van, Uden IWM van, Zwiers MP, et al. Cigarette smoking is associated with reduced microstructural integrity of cerebral white matter. Brain. 2011;134(7):2116–24.

133. Power MC, Deal JA, Sharrett AR, Jack CR, Knopman D, Mosley TH, et al. Smoking and white matter hyperintensity progression. Neurology. 2015;84(8):841–8.

134. Kuźma E, Lourida I, Moore SF, Levine DA, Ukoumunne OC, Llewellyn DJ. Stroke and dementia risk: A systematic review and meta-analysis. Alzheimer's Dementia. 2018;14(11):1416–26.

135. Pendlebury ST, Rothwell PM, Study OV. Incidence and prevalence of dementia associated with transient ischaemic attack and stroke: analysis of the population-based Oxford Vascular Study. Lancet Neurology. 2019;18(3):248–58.

136. Mok VCT, Lam BYK, Wong A, Ko H, Markus HS, Wong LKS. Early-onset and delayed-onset poststroke dementia — revisiting the mechanisms. Nat Rev Neurol. 2017;13(3):148–59.

137. Friberg L, Rosenqvist M. Less dementia with oral anticoagulation in atrial fibrillation. Eur Heart J. 2017;39(6):453–60.

138. Biffi A, Bailey D, Anderson CD, Ayres AM, Gurol EM, Greenberg SM, et al. Risk Factors Associated With Early vs Delayed Dementia After Intracerebral Hemorrhage. Jama Neurol. 2016;73(8):969.

139. Ryan J, Storey E, Murray AM, Woods RL, Wolfe R, Reid CM, et al. Randomized placebo-controlled trial of the effects of aspirin on dementia and cognitive decline. Neurology. 2020;95(3):10.1212/WNL.0000000000009277.

140. Kavirajan H, Schneider LS. Efficacy and adverse effects of cholinesterase inhibitors and memantine in vascular dementia: a meta-analysis of randomised controlled trials. Lancet Neurology. 2007;6(9):782–92.

141. Gunten A von, Schlaefke S, Überla K. Efficacy of Ginkgo biloba extract EGh 761® in dementia with behavioural and psychological symptoms: A systematic review. World J Biological Psychiatry. 2015;17(8):1–12.

142. Sajeev G, Weuve J, Jackson JW, VanderWeele TJ, Bennett DA, Grodstein F, et al. Late-life Cognitive Activity and Dementia. Epidemiology. 2016;27(5):732–42.

143. Ravaglia G, Forti P, Lucicesare A, Pisacane N, Rietti E, Bianchin M, et al. Physical activity and dementia risk in the elderly. Neurology. 2008;70(19, Part 2 of 2):1786–94.

144. Buchman AS, Boyle PA, Yu L, Shah RC, Wilson RS, Bennett DA. Total daily physical activity and the risk of AD and cognitive decline in older adults. Neurology. 2012;78(17):1323–9.

145. Monma T, Takeda F, Noguchi H, Takahashi H, Tamiya N. The Impact of Leisure and Social Activities on Activities of Daily Living of Middle-Aged Adults: Evidence from a National Longitudinal Survey in Japan. Plos One. 2016;11(10):e0165106.

146. Scarmeas N, Stern Y, Mayeux R, Manly JJ, Schupf N, Luchsinger JA. Mediterranean Diet and Mild Cognitive Impairment. Arch Neurol-chicago. 2009;66(2):216–25.

147. Keenan TD, Agrón E, Mares JA, Clemons TE, Asten F, Swaroop A, et al. Adherence to a Mediterranean diet and cognitive function in the Age-Related Eye Disease Studies 1 & 2. Alzheimer's Dementia. 2020;16(6):831–42.

148. Estruch R, Ros E, Salas-Salvadó J, Covas M-I, Corella D, Arós F, et al. Primary Prevention of Cardiovascular Disease with a Mediterranean Diet Supplemented with Extra-Virgin Olive Oil or Nuts. New Engl J Med. 2018;378(25):e34.

149. Chiu THT, Chang H-R, Wang L-Y, Chang C-C, Lin M-N, Lin C-L. Vegetarian diet and incidence of total, ischemic, and hemorrhagic stroke in 2 cohorts in Taiwan. Neurology. 2020;94(11):10.1212/WNL.0000000000009093.

150. Ngandu T, Lehtisalo J, Solomon A, Levälahti E, Ahtiluoto S, Antikainen R, et al. A 2 year multidomain intervention of diet, exercise, cognitive training, and vascular risk monitoring versus control to prevent cognitive decline in at-risk elderly people (FINGER): a randomised controlled trial. Lancet. 2015;385(9984):2255–63.

151. Ohara T, Honda T, Hata J, Yoshida D, Mukai N, Hirakawa Y, et al. Association Between Daily Sleep Duration and Risk of Dementia and Mortality in a Japanese Community. J Am Geriatr Soc. 2018;66(10):1911–8.

152. Sindi S, Kåreholt I, Johansson L, Skoog J, Sjöberg L, Wang H, et al. Sleep disturbances and dementia risk: A multicenter study. Alzheimer's Dementia. 2018;14(10):1235–42.

153. Huang Y, Yang C, Yuan R, Liu M, Hao Z. Association of obstructive sleep apnea and cerebral small vessel disease: a systematic review and meta-analysis. Sleep. 2019;43(4).

154. Chokesuwattanaskul A, Lertjitbanjong P, Thongprayoon C, Bathini T, Sharma K, Mao MA, et al. Impact of obstructive sleep apnea on silent cerebral small vessel disease: a systematic review and meta-analysis. Sleep Med. 2020;68:80–8.

155. Leurent C, Goodman JA, Zhang Y, He P, Polimeni JR, Gurol ME, et al. Immunotherapy with ponezumab for probable cerebral amyloid angiopathy. Ann Clin Transl Neur. 2019;6(4):795–806.

TABLES

Table 1. Summary of the Vascular Impairment of Cognition Classification Consensus Study (VICCCS) Criteria

Table 1. Summary of the Vascular Impairment of Cognition Classification Consensus Study (VICCCS) Criteria

Definition:	Vascular cognitive impairment (VCI) is defined as impairment in at least one cognitive domain and in IADL/ADLs independent of the motor/sensory sequelae of the vascular event: ▪ **Mild VCI**: at least one cognitive domain affected and mild to no impairment in IADL/ADLs. ▪ **Major VCI (vascular dementia):** clinically significant deficits of sufficient severity in at least one cognitive domain and severe disruption of IADL/ADLs.
Evaluation:	▪ Cognitive assessment should include five core domains: executive function and processing speed, attention, memory, language, and visuospatial domains. ▪ The full-length protocol takes 60 minutes to complete but can be shortened to 30 or even 5 minutes using Montreal Cognitive Assessment (MoCA) [1].
Imaging:	▪ Magnetic resonance imaging (MRI) is a "gold-standard" for a clinical diagnosis of VCI.
Certainty of evidence:	▪ **Probable VCI**: if (1) only computed tomography (CT) imaging is available or (2) aphasia is present after vascular event, but normal cognition was documented (e.g., annual cognitive evaluations) before the clinical event. ▪ **Possible VCI**: if neither MRI nor CT is available, but VCI is suspected clinically.
Major VCI subtypes:	▪ **Post-stroke dementia (PSD)**: a clear temporal relationship (within 6 months) of irreversible cognitive decline following the vascular event. ▪ **Subcortical ischemic vascular dementia**: small vessel disease with lacunar infarcts and white matter hyperintensities. ▪ **Multi-infarct (cortical) dementia**: large cortical infarcts contributing to dementia. ▪ **Mixed pathology**: VCI-AD, AD-VCI, or VCI-DLB, VCI-# depending on probable contribution.
Exclusion criteria:	▪ Drug/alcohol abuse/dependence within the last 3 months, other causes of sustained impairment, e.g., depression, vitamin D deficiency, other vitamin/hormonal deficiency.

Abbreviations: VCI: vascular cognitive impairment; IADL: instrumental activities of daily living; ADL: activities of daily living; MRI: magnetic resonance imaging; CT: computed tomography; PSD: post-stroke dementia; #: denoting other possible pathology, AD = Alzheimer's disease, DLB = dementia with Lewy bodies, Adapted from Vascular Impairment of Cognition Classification Consensus Study (VICCCS) diagnosis guidelines.[2]

FIGURES

Figure 1. Schematic overview of potential mechanisms leading to vascular cognitive impairment
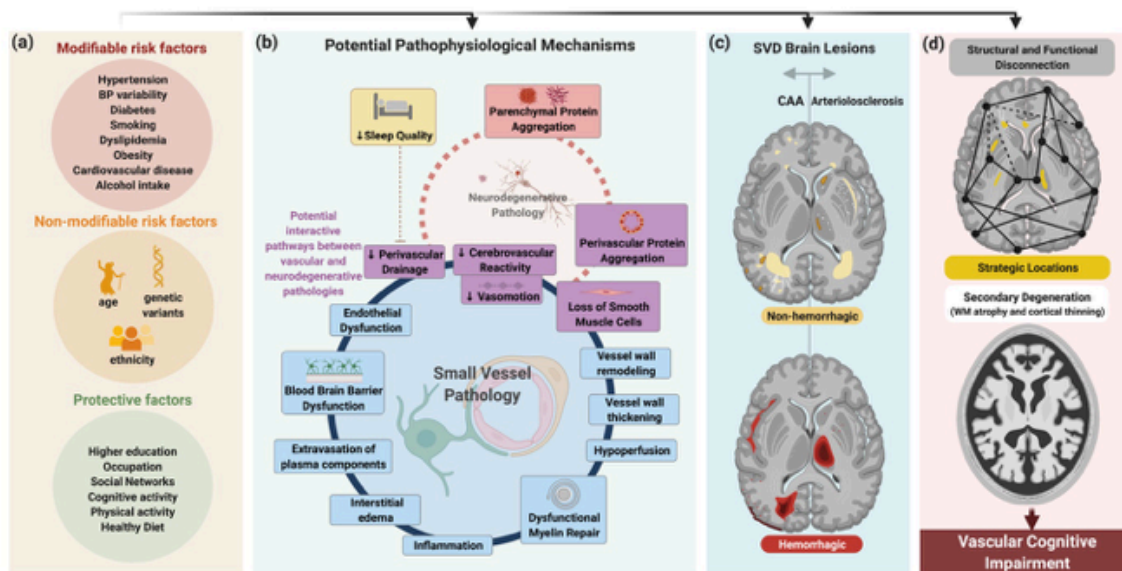
Legend.

(A) Risk factors associated with SVD and related cognitive decline. Several factors are hypothesized to influence small vessel pathology. Among them, aging and hypertension are considered the most important.

(B) Potential Pathophysiological mechanisms of SVD. Schematic representation of the complex mechanisms potentially at play in age-related cognitive impairment. Dysfunctional NVUs have an important role in SVD pathology. Vascular risk factors are hypothesized to cause endothelial dysfunction, contributing to the uncoupling of trophic neurovascular mechanisms [13]. Several other components of the NVU may constitute potential entry points for disease mechanisms [6]. Though the order of the events is not yet established, several effects, described around the blue circle, may occur and, combined, may contribute to exacerbate tissue injury. Impaired perivascular drainage potentially contributes to interstitial and perivascular accumulation of proteins such as

amyloid-β, and may represent an interactive pathway linking neurodegenerative and vascular pathologies, particularly relevant in CAA and AD [8].

(C) Typical brain lesions associated with SVD.

SVD can be diagnosed through the detection of typical MRI-visible lesions. These lesions can be hemorrhagic or non-hemorrhagic in nature. The hemorrhagic lesions (bottom figure) include: CMBs, cSS, SAH (usually in the convexity), and ICH. The non-hemorrhagic lesions (upper figure) include: WMH, lacunes, PVS, small acute subcortical infarcts, and cortical CMI. Depending on the pattern of distribution, different etiological subtypes of SVD can be inferred. CAA (left) more typically presents with cortical CMBs, cortical CMIs, lobar lacunes, PVS visible in the centrum semiovale, cSS, convexity SAH, lobar ICH and multiple WMH subcortical spots. Arteriolosclerosis (right) more commonly presents with deep CMBs, deep lacunes, PVS visible in the basal ganglia, deep ICH and peri-basal ganglia WMH.

(D) Mechanisms involved in SVD-related cognitive impairment.

Impairment of structural and functional connectivity, damage to highly connected deep regions in strategic locations, and secondary degeneration culminating in brain atrophy are some of the mechanisms hypothesized to underlie SVD's contribution to cognitive impairment.

SVD: small vessel disease; NVU: neurovascular unit; CAA: cerebral amyloid angiopathy; AD: Alzheimer's disease; CMB: cerebral microbleed; cSS: cortical superficial siderosis; SAH: subarachnoid hemorrhage; ICH: intracerebral hemorrhage; WMH: white matter hyperintensity; PVS: perivascular spaces; CMI: cerebral microinfarcts.

Figure 2. Conventional neuroimaging findings associated with SVD.
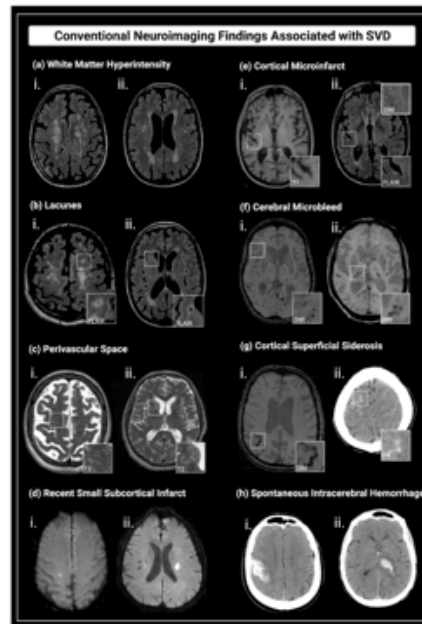
Legend.

(A) WMH of presumed vascular origin, show hyperintense signals on FLAIR (i, and ii.) and T2-weighted images, and hypointense signals on T1-weighted sequences.

(B) Lacunes of presumed vascular origin are fluid-filled subcortical lesions ≥3mm and <15mm with the same signal intensity as CSF on all sequences, presenting a hyperintense rim on FLAIR, when located supratentorially. (i.) Represents a lobar lacune, more commonly seen in CAA, while (ii.) represents a deep lacune, commonly found in arteriolosclerosis.

(C) PVS are linear, ovoid or round-shaped fluid-filled spaces of <3mm that follow the course of a vessel with a similar signal intensity to CSF on all sequences. (i.) Depicts visible PVS predominating in the centrum semiovale, characteristic of CAA, while (ii.) represents deep PVS, affecting the basal ganglia, commonly seen in arteriolosclerosis.

(D) Recent small subcortical infarcts show hyperintense signals in DWI (i. and ii.), FLAIR, and T2-weighted images with a hypointense signal on T1-weighted sequences.

(E) Cortical CMIs are <4mm lesions strictly intra-cortical, perpendicular to the cortical surface, hypointense on T1-weighted images (i.) and hyperintense or isointense on fluid-attenuated inversion recovery and T2-weighted images (ii.).

(F) CMBs are focal areas <5-10mm of very low signal intensity on SWI or T2*-weighted images. When occurring in the context of CAA, they are typically lobar (i.), but tend to affect deep regions such as basal ganglia, thalamus and brainstem, when related to arteriolosclerosis (ii.).

(G) cSS is defined as linear hypointense foci with gyriform patterns over the cerebral cortex on SWI or T2*-weighted images (i.). The acute form of superficial bleeding is the cSAH, seen as linear hyperdense foci on CT (ii.) or with hyperintense signal on FLAIR.

(H) Spontaneous ICH is defined as a non-traumatic hemorrhage without defined secondary cause, depicted as a focal hyperdense lesion on CT (i. and ii.), with varying signal intensities on T1 and T2-weighted images, depending on temporal stages.

SVD: small vessel disease; WMH: white matter hyperintensity; FLAIR: Fluid-attenuated inversion recovery; CSF: cerebrospinal fluid; CAA: cerebral amyloid angiopathy; PVS: perivascular spaces; DWI: diffusion weighted image; CMI: cerebral microinfarcts; CMB: cerebral microbleed; SWI: susceptibility weighted imaging; cSS: cortical superficial siderosis; cSAH: convexity subarachnoid hemorrhage; CT: computed tomography; ICH: intracerebral hemorrhage.

Appendix 1.B. Article reuse license

Copyright/Source: 2021, The Author(s), Published by Wolters Kluwer Health, Inc/Current Opinion in Neurology®

Appendix 1.C. License to reuse figures from a published manuscript[1]

CCC RightsLink®

? Help ∨   Live Chat   Maria Clara Zanon Zotin ∨

Wolters Kluwer

Cerebral small vessel disease and vascular cognitive impairment: from diagnosis to management

Author: Maria Clara Zanon Zotin, Lukas Sveikata, Anand Viswanathan, et al
Publication: Current Opinion in Neurology
Publisher: Wolters Kluwer Health, Inc.
Date: Feb 23, 2021

Copyright © 2021, Copyright © 2021 The Author(s). Published by Wolters Kluwer Health, Inc.

Order Completed

Thank you for your order.

This Agreement between Maria Clara Zanon Zotin ("You") and Wolters Kluwer Health, Inc. ("Wolters Kluwer Health, Inc.") consists of your order details and the terms and conditions provided by Wolters Kluwer Health, Inc. and Copyright Clearance Center.

License number   Reference confirmation email for license number

License date   May, 25 2022

☑ Licensed Content		🗄 Order Details	
Licensed Content Publisher	Wolters Kluwer Health, Inc.	**Type of Use**	Dissertation/Thesis
		Requestor type	University/College
Licensed Content Publication	Current Opinion in Neurology	**Sponsorship**	No Sponsorship
		Format	Electronic
Licensed Content Title	Cerebral small vessel disease and vascular cognitive impairment: from diagnosis to management	**Will this be posted online?**	Yes, on an unrestricted website
		Portion	Figures/tables/illustrations
Licensed Content Author	Maria Clara Zanon Zotin, Lukas Sveikata, Anand Viswanathan, et al	**Number of figures/tables/illustrations**	2
		Author of this Wolters Kluwer article	Yes
Licensed Content Date	Feb 23, 2021		
		Will you be translating?	No
Licensed Content Volume	34	**Intend to modify/change the content**	No
Licensed Content Issue	2		

📄 About Your Work		🗁 Additional Data	
Title	PhD Thesis: Peak Width of Skeletonized Mean Diffusivity (PSMD) as Neuroimaging Biomarker for Vascular Cognitive Impairment in the Context of Cerebral Amyloid Angiopathy	**Order reference number**	001
		Portions	Figure 1 and Figure 2
Institution name	Faculdade de Medicina de Ribeirão Preto - Universidade de São Paulo		
Expected presentation date	Aug 2022		

Rightslink® by Copyright Clearance Center

Requestor Location

Requestor Location

Faculdade de Medicina de
Ribeirão Preto - Universidade
de São Paulo
R. Ten. Catão Roxo, 3900
Monte Alegre

Ribeirão Preto, SP 14015010
Brazil
Attn: Faculdade de Medicina
de Ribeirão Preto -
Universidade de São Paulo

Tax Details

Publisher Tax ID   13-2932696

Billing Information

Billing Type   Invoice

Billing address

Faculdade de Medicina de
Ribeirão Preto - Universidade
de São Paulo
R. Ten. Catão Roxo, 3900
Monte Alegre

Ribeirão Preto, Brazil
14015010
Attn: Faculdade de Medicina
de Ribeirão Preto -
Universidade de São Paulo

Price

Total   0.00 USD

Total: 0.00 USD

CLOSE WINDOW

Appendix 3.1. Systematic Review

Appendix 3.1.A Literature search

We provide below further details on the search query, with the full search terms, that was performed in PubMed, EMBASE, Medline, Cochrane Central, Web of Science and Google Scholar in Feb 1, 2021.

Table A.3.1.A Overview of literature search

Database searched	via	Years of coverage	References	After de-duplication
Embase	Embase.com	1971-Present	437	429
Medline ALL	Ovid	1946- Present	204	12
Web of Science SCI-EXPANDED & SSCI	Web of Knowledge	1975-Present	325	119
Cochrane Central Register of Controlled Trials	Wiley	1992-Present	6	1
Other sources: Google Scholar (100 top-ranked)			100	76
Total (database searching)			**1072**	**637**
Records identified by the authors			12	1
Total (overall)			**1084**	**638**

Embase.com

(Peak NEAR/3 width NEAR/3 skeletoni* NEAR/3 diffus*):ab,ti,kw OR (('diffusion tensor imaging'/de OR 'diffusivity'/exp OR 'diffusion weighted imaging'/de OR (DTI OR DWI OR diffus*):ab,ti,kw) AND ('white matter'/exp OR 'white matter injury'/de OR 'white matter lesion'/de OR 'white matter hyperintensity'/de OR (white-matter* OR arcuate-fasciculus* OR capsula-interna* OR corona-radiata* OR external-capsule* OR extreme-capsule* OR inferior-longitudinal-fasciculus* OR occipitofrontal-fasciculus* OR superior-longitudinal-fasciculus* OR uncinated-fasciculus* OR integrity* OR substantia-alba* OR white-substance*):ab,ti,kw) AND ('skeletonization'/de OR 'skeletonization (imaging)'/de OR 'histogram'/de OR (skeletoni* OR histogram*):ab,ti,kw))

Medline Ovid

(Peak ADJ3 width ADJ3 skeletoni* ADJ3 diffus*).ab,ti,kw. OR ((exp Diffusion Magnetic Resonance Imaging/ OR (DTI OR DWI OR diffus*).ab,ti,kf.) AND (White Matter/ OR (white-matter* OR arcuate-fasciculus* OR capsula-interna* OR corona-radiata* OR external-capsule* OR extreme-capsule* OR inferior-longitudinal-fasciculus* OR occipitofrontal-fasciculus* OR superior-longitudinal-fasciculus* OR uncinated-fasciculus* OR integrity* OR substantia-alba* OR white-substance*).ab,ti,kf.) AND ((skeletoni* OR histogram*).ab,ti,kf.))

Web of Science

TS=((Peak NEAR/2 width NEAR/2 skeletoni* NEAR/2 diffus*) OR (((DTI OR DWI OR diffus*)) AND ((white-matter* OR arcuate-fasciculus* OR capsula-interna* OR corona-radiata* OR external-capsule* OR extreme-capsule* OR inferior-longitudinal-fasciculus* OR occipitofrontal-fasciculus* OR superior-longitudinal-fasciculus* OR uncinated-fasciculus* OR integrity* OR substantia-alba* OR white-substance*)) AND ((skeletoni* OR histogram*))))

Cochrane CENTRAL

(Peak NEAR/3 width NEAR/3 skeletoni* NEAR/3 diffus*):ab,ti,kw OR (((DTI OR DWI OR diffus*):ab,ti,kw) AND ((white-matter* OR arcuate-fasciculus* OR capsula-interna* OR corona-radiata* OR external-capsule* OR extreme-capsule* OR inferior-longitudinal-fasciculus* OR occipitofrontal-fasciculus* OR superior-longitudinal-fasciculus* OR uncinated-fasciculus* OR integrity* OR substantia-alba* OR white-substance*):ab,ti,kw) AND ((skeletoni* OR histogram*):ab,ti,kw))

Google Scholar

Peak width skeletonized|skeletonised diffusion|diffusivity|DTI|DWI

Appendix 3.1.B. Identification of overlapping cohorts

We evaluated potential overlap between cohorts by comparing the cohorts' names, recruitment site(s), the number of participants, the MRI protocol(s), and the reported PSMD values. Depending on how similar the cohorts were based on these variables, we considered them as overlapping. This assessment was made individually by MCZZ and PY. In case of disagreement, a third reviewer (LS) served to reach a consensus.

Table A.3.1.B. Comparison of data from potentially overlapping cohorts.

Cohort's name	Articles	Recruitment site(s)	N	MRI Protocol	Mean/median PSMD
Hamburg City Health Study (HCHS)	Petersen et al. 2020	Hamburg, Germany	930	3T Siemens Skyra. TR/TE 8500/75; 2x2x2 mm; b1000, 64 directions	0.0002 (0.0001) mm^2/s
	Frey et al. 2020	Hamburg, Germany	930	3T Siemens Skyra. TR/TE 8500/75; 2x2x2 mm; b1000, 64 directions	2.18 (0.5) mm^2/s x 10^{-4}
University of Siena/ Universities of Siena and Florence	Vinciguerra et al. 2019	Unclear. All the authors are from the University of Siena.	47 MS/28 healthy controls	1.5T Philips. TR/TE 8500/100; 2.5x2.5x2.5mm; b1000; 32 directions	MS: 4.2 ± 1.2 mm^2/s x 10^{-4} Controls: 2.8 ± 0.3 mm^2/s x 10^{-4}
	Vinciguerra et al. 2020	Universities of Siena and Florence	60 MS/15 healthy controls	3 T brain MRI. TR/TE not informed; resolution not informed; b900; 32 directions	MS: 4.2 ± 1.3 mm^2/s x 10^{-4} Controls: 2.9 ± 0.6 mm^2/s x 10^{-4}
Lothian Birth Cohort 1936 (LBC1936)	Deary et al. 2020	Edinburgh area (Lothian), Scotland	672 individuals with PSMD values available	GE Signa Horizon HDxt 1.5T. TR/TE 16500/98; 2x2x2 mm; b1000, 64 directions	3.17 (0.501) mm^2/s x 10^{-4}
	Beaudet et al. 2020	Edinburgh area (Lothian), Scotland	672	GE Signa Horizon HDxt 1.5T. TR/TE 16500/98; 2x2x2 mm; b1000, 64 directions	3.18 (0.53) mm^2/s x 10^{-4}
Austrian Stroke Prevention Study Family (ASPFS)	Baykara et al. 2016	Graz, Austria	132	3T Siemens TIM Trio. TR/TE 6700/95; 1.95x1.95x2.5 mm; b1000, 4x12 directions.	3.05 (0.72) mm^2/s x 10^{-4}
	Beaudet et al. 2020	Graz, Austria	129 (68 to 78 years)	3T Siemens TIM Trio. TR/TE 4900 or 6700/ 81 or 95; 1.8x1.8x2.5 mm; b1000, 6-12 directions.	68-78years: 3.1(0.6)mm^2/s x10^{-4}
Older Australian Twin Study (OATS)	Beaudet et al. 2020	New South Wales, Victoria and Queensland, Australia	195 (68-78 years)	Philips (x2), Siemens (x2), 1.5T & 3T. TR/TE 7800 or 8600/68 or 96; 2.5 x 2.5 x 2.5 mm; b1000; 32 directions	68-78 years: 3.10 (0.64) mm^2/s x10^{-4}
	Liu et al. 2020	New South Wales, Victoria and Queensland, Australia	161	1.5T Siemens. TR/TE not informed; resolution not informed; b-value not informed; 32 directions	Not available
Royal Infirmary of Edinburgh	Blesa et al. 2020	University of Edinburgh, UK	76 preterm/59 term	Siemens Prisma 3T. TR/TE 3400/78; 2x2x2mm; b750; 64 directions	6.00 (0.90)/ 5.00 (0.60) mm^2/s x 10^{-4}
	Sullivan et al. 2020	University of Edinburgh, UK	71 preterm infants with MRI	Siemens Verio 3T, TR/TE 3500/78; 2x2x2mm; b750; 64 directions	6.01 (0.62) mm^2/s x 10^{-4}

Glossary: TR=repetition time; TE=echo time. Cohorts HCHS, Universities of Siena/Siena and Florence, LBC1936, ASPFS, and OATS were deemed to have been used in more than one article applying PSMD as neuroimaging marker.

Appendix 3.1.C. Details on the quality assessment of the included studies

Quality assessment of included studies using adapted Newcastle Ottawa Quality Assessment Scales and technical parameters

We extended the adapted Newcastle Ottawa Quality Assessment scales with technical parameters.[221] We scored the articles separately, according to the study design, including cross-sectional, case-control, and longitudinal. For each domain: selection, technical parameters, comparability, and outcome/exposure, a maximum of 4 points, 3 points, 2 points, and 2 or 3 points were given, respectively. The criteria for the domain of technical parameters are listed below.

The total score was calculated by adding all the points from each individual quality indicator, thus ranging from 0 (unsatisfactory) to 11 (very good) for the cross-sectional design and 0 (unsatisfactory) to 12 (very good) for the case-control and longitudinal designs.

Technical parameters (maximum 3 points)

1. Details on the technical protocol adequately describing imaging parameters like type of scanner, field strength, TR/TE, voxel size, number of directions and b-value.

a. Complete details of imaging parameters. (score 1 point)

b. Missing 1 or more imaging parameters. (score 0 point)

2. Is quality assessment of technical protocol described?

a. Visual or automated assessment of technical protocol. (score 1 point)

b. None/ not clear. (score 0 point)

3. Pre-processing steps described in imaging protocol?

a. Yes. (score 1 point)

b. No. (score 0 point)

Total scores for longitudinal studies

Very good studies: 11-12 points

Good studies: 9-10 points

Satisfactory studies: 7-8 points

Unsatisfactory studies: 0 to 6 points

Appendix 3.1.D. Quality assessment results

Overall, the quality of the included studies ranged between satisfactory and very good. Data on the frequency of individuals who were not included and their characteristics were missing from all cross-sectional and case-control studies. In longitudinal studies, information on whether the outcome of interest was accounted for and if there were losses to follow-up was not available. In the technical domain, though sufficient details on the MRI protocols were provided in almost all studies, information on the quality assessment of the DWI images and preprocessing steps employed were not consistently available. The definition and inclusion criteria of control groups were also not consistently provided. Finally, all studies performed well in providing details on the assessment of outcome (if applicable), presence of exposure, and statistical tests. See below the details on the risk of bias assessment of the included studies:

Table A.3.1.D Risk bias assessment of included studies

Cross-sectional studies	
Study reference	**Total score**
Deary *et al.*, 2019	9
Lam *et al.*, 2019*	10
Low *et al.*, 2020	10
Beaudet *et al.*, 2020	9
Petersen *et al.*, 2020	8
Frey *et al.*, 2020	9
Sullivan *et al.*, 2020§	9
Case-control studies	
Baykara *et al.*, 2016*	10
Schouten *et al.*, 2018	10
Caballero *et al.*, 2018	11
Wei *et al.*, 2019	9
McCreary *et al.*, 2020*	8
Liu *et al.*, 2020	7
Oberlin *et al.*, 2021	8
Raposo *et al.*, 2021	11
Vinciguerra *et al.*, 2018	9

Vinciguerra *et al.*, 2020	7
Blesa *et al.*, 2020	9
Longitudinal studies	
Baykara *et al.*, 2016*	8
Lam *et al.*, 2019*	10
McCreary *et al.*, 2020*	7
*These studies have two designs. For the longitudinal design, Baykara *et al.* included imaging and cognition as outcomes, Lam *et al.* only cognition, and McCreary *et al.* only imaging features. §This study has a case-control design to identify systemic inflammation in preterm infants with and without histologic chorioamnionitis (n=55). Yet, PSMD was analyzed in 71 infants with blood tests on postnatal day 5 and MRI performed at term-equivalent age in a cross-sectional matter.	

Appendix 3.2. Cross-sectional analysis article

Appendix 3.2.A. Article reuse license

Copyright/Source: American Society of Neuroradiology/ WILLIAMS & WILKINS CO

Maria Clara Zanon Zotin <mczzotin@hcrp.usp.br>

RESPONSE REQUIRED for Your Request to American Society of Neuroradiology

1 mensagem

no-reply@copyright.com <no-reply@copyright.com>   6 de junho de 2022 11:15
Para: mczzotin@hcrp.usp.br

Dear Maria Clara Zanon Zotin,

American Society of Neuroradiology has approved your recent request. Before you can use this content, you must accept the license fee and terms set by the publisher.

Use this link to accept (or decline) the publisher's fee and terms for this order.

Request Summary:
Submit date: 04-Jun-2022
Request ID: 600082841
Publication: American journal of neuroradiology
Title: Peak Width of Skeletonized Mean Diffusivity as Neuroimaging Biomarker in Cerebral Amyloid Angiopathy
Type of Use: Republish in a thesis/dissertation

Please do not reply to this message.

To speak with a Customer Service Representative, call +1-855-239-3415 toll free or +1-978-646-2600 (24 hours a day), or email your questions and comments to support@copyright.com.

Sincerely,

Copyright Clearance Center

Tel: 1-855-239-3415 / +1-978-646-2600
support@copyright.com
Manage Account

Appendix 3.2.B. Oral abstract presented at the International Stroke Conference 2020 – Los Angeles.

Control/Tracking Number: 20-ISC-LB-7388-AHA
Activity: Abstract Late Breaking
Current Date/Time: 11/6/2019 9:59:00 PM

Peak Width Of Skeletonized Mean Diffusivity Is Associated With Cognitive Impairment In Cerebral Amyloid Angiopathy

Letter:
This study was submitted outside the regular submission deadline, as a Late-Breaking Science abstract, because it was only in late September 2019 that we finished recruiting and scanning enough patients to be able to run multivariate regression analysis. Our results argue in favor of a new neuroimaging biomarker associated with cognitive endpoints in the setting of cerebral amyloid angiopathy (an important form of VCID). Therefore, we believe it may impact future clinical trials as it is in line with ongoing NIH-based initiatives to understand small vessel disease and its relationship to cognition (Mark-VCID consortium).

Author Block: Maria Clara Zanon Zotin, Dorothee Schoemaker, Massachusetts General Hosp, Boston, MA; Nicolas Raposo, Univ de Toulouse, Toulouse, France; Mark Etherton, Andreas Charidimou, Li Xiong, M. Edip Gurol, Steven M. Greenberg, Anand Viswanathan, Massachusetts General Hosp, Boston, MA

Abstract:
Introduction: Sporadic cerebral amyloid angiopathy (CAA) is a highly prevalent subtype of cerebral small vessel disease (cSVD) and major contributor to cognitive impairment in the elderly. Peak width of skeletonized mean diffusivity (PSMD) is a fully automated diffusion-based neuroimaging marker that has been consistently associated with cognitive tests in different cohorts. We aimed to assess PSMD's relationship with cognitive function and conventional MRI markers in patients with CAA.
Methods: We recruited 46 subjects with possible and probable CAA from a memory-clinic based longitudinal cohort. Subjects underwent neuropsychological tests and MRI, including diffusion tensor imaging. PSMD was calculated automatically, through a freely available script. Conventional MR markers of CAA (cerebral microbleeds, lacunes and superficial siderosis), normalized total brain volume and white matter lesions volume were obtained. We explored PSMD's relationship with cognitive composite scores (Attention and Processing Speed, Language and Semantics, Executive Function, Memory, and Visuospatial Processing) and other imaging markers through regression and correlation analysis.

Results: In our cohort (mean age 75,8 ± 6.8 years; 34.8% female; PSMD median [IQR] 4.2×10^{-4} [3.6–5.1×10^{-4}] mm^2/s) PSMD was strongly correlated with volume of white matter lesions (r=0.609, p<0.001) and total brain volume (r=-0.465, p=0.001), and remained after adjustment for age (r=0.445, p=0.002; r=-0.390, p=0.008; respectively). There was no significant correlation between PSMD and microbleeds (r=0.135, p=0.371) or lacunes (r=0.191, p=0.205). PSMD was associated with Language (β=-0.406, p=0.005), Memory (β=-0.326; p=0.027) and Processing Speed (β=-0.307, p=0.043). Further, in a multivariate regression analysis with other MRI markers, PSMD was found to be the only significant independent predictor for performance in the Language domain (β=-0.367, p=0.021).
Conclusions: PSMD was associated with selected cognitive endpoints in CAA subjects, outperforming

conventional MR markers. These findings warrant validation in larger cohorts, to further investigate whether PSMD could potentially be used as a surrogate marker in future CAA clinical trials.
:

Category (Complete): Vascular Cognitive Impairment
Additional Information (Complete):
   Yes or No: No
   Segment of Science: Clinical Science
   *Disclosure: There are no unlabeled/unapproved uses of drugs or products.
   *Copyright Transfer Agreement: Yes

Payment (Complete): Your credit card order has been processed on Wednesday 6 November 2019 at 12:57 PM.
 Status: Complete

Appendix 3.2.C. Abstract and poster presented at the European Stroke Conference 2020 – Virtual.

PEAK WIDTH OF SKELETONIZED MEAN DIFFUSIVITY IS ASSOCIATED WITH WHITE MATTER LESIONS AND GLOBAL BURDEN OF CSVD IN CEREBRAL AMYLOID ANGIOPATHY
Type: Abstract Submission
Topic: AS28. SMALL VESSEL DISEASE

Authors: M.C. Zanon Zotin[1], D. Schoemaker[1], M. Etherton[1], N. Raposo[2], S. van Veluw[1], A. Charidimou[1], P. Assis Lopes[1], S. Greenberg[1], A. Viswanathan[1]; [1]United States of America, [2]France

Group Name

Background And Aims

Cerebral amyloid angiopathy (CAA) is associated with multiple MRI markers of cerebral small vessel disease (cSVD). Peak width of skeletonized mean diffusivity (PSMD) is an automated diffusion-based marker, consistently related with cognition. We aimed to investigate associations between individual/combined MRI markers of cSVD and PSMD in CAA subjects.

Methods

We recruited 64 memory-clinic subjects with probable CAA (75.9 years $\pm$ 6.64). Subjects underwent MRI, including high resolution DWI. PSMD was calculated using an automated pipeline. Conventional MRI cSVD markers, including normalized total brain volume (nTBV) and white matter lesions volume (nWML) were obtained. Lobar microbleeds (2-4=1 point; >=5:2 points), perivascular spaces in the centrum semiovale (CSO-PVS) (>20=1point), siderosis (focal=1point; disseminated=2points) and nWML (>p50=1point) were included in a CAA-specific cSVD burden score (cSVDBS). We explored the relationship between cSVDBS, individual MRI markers and PSMD using regression analyses.

Results

cSVDBS was associated with PSMD (R^2=0.205,p=0.001) in univariate regression analysis, adjusted for age/sex. The univariate regression analyses for individual neuroimaging markers, revealed that nWML (R^2=0.741,p<0.001), nTBV (R^2=0.144,p=0.015), cortical thickness (R^2=0.151,p=0.012), lacunes (R^2=0.196,p=0.002), and cortical microinfarcts (R^2=0.149,p=0.015) were significantly associated with PSMD, but hemorrhagic markers and EPVS were not. In a multivariate model (R^2=0.813) including only markers relevant in univariate analysis, nWML (b=0.787, p<0.001) and cortical thickness (b=-0.193,p=0.008) remained independently associated with PSMD.

Conclusions

Global burden of cSVD was associated with PSMD in univariate regression analysis, suggesting an effect on microstructural integrity of the main white matter tracts, which was mostly driven by nWML. Only non-hemorrhagic markers of cSVD were associated with PSMD.

Trial Registration Number

Peak Width of Skeletonized Mean Diffusivity is associated with white matter lesions and global burden of CSVD in Cerebral Amyloid Angiopathy

Maria Clara Zanon Zotin[1,2], Dorothee Schoemaker[1], Mark R. Etherton[1], Nicolas Raposo[1,3,4], Susanne van Veluw[1], Andreas Charidimou[1], Pedro Assis Lopes[1], Steven M. Greenberg[1], Anand Viswanathan[1].

[1] J Philip Kistler Stroke Research Center. Department of Neurology. Massachusetts General Hospital. Harvard Medical School, Boston, MA, USA
[2] Center for Imaging Sciences and Medical Physics. Department of Medical Imaging, Hematology and Clinical Oncology. Ribeirão Preto Medical School, University of São Paulo, Ribeirão Preto, SP, Brazil.
[3] Department of Neurology, Centre Hospitalier Universitaire de Toulouse, Toulouse, France.
[4] Toulouse NeuroImaging Center, Université de Toulouse, Inserm, UPS, France.

Background And Aims

Cerebral amyloid angiopathy (CAA) is associated with multiple MRI markers of cerebral small vessel disease (cSVD). Peak width of skeletonized mean diffusivity (PSMD) is an automated diffusion-based marker consistently related with cognition.[1] We aimed to investigate associations between individual/combined MRI markers of cSVD and PSMD in CAA subjects.

Methods

We recruited 64 memory-clinic subjects with probable CAA (75.9 years ± 6.64). Subjects underwent MRI, including high resolution DWI. PSMD was calculated using an automated pipeline.[1] Conventional MRI cSVD markers, including normalized total brain volume (nTBV) and white matter lesions volume (nWML) were obtained. Lobar microbleeds (2-4=1 point; >=5:2 points), perivascular spaces in the centrum semiovale (CSO-PVS) (>20=1point), superficial siderosis (focal=1point; disseminated=2points) and nWML (>p50=1point) were included in a CAA-specific cSVD burden score (cSVDBS).[2,3] We explored the relationship between cSVDBS, individual MRI markers and PSMD using regression analyses.

Fig 1. Associations between PSMD and MRI markers
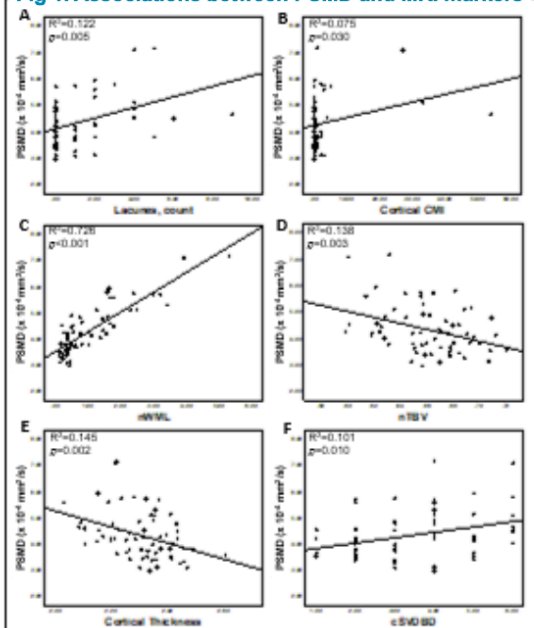
Scatter Plots showing the association between PSMD and (A) lacunes, (B) cortical CMI, (c) nWML, (E) nTBV, (D) cortical Thickness, and (E) cSVDBS. The provided R² and p-values reflect the obtained independent predictive of each neuroimaging marker with regards to PSMD (unadjusted model). PSMD = peak width of skeletonized mean diffusivity; CMI = cerebral microinfarcts; nTBV= normalized total brain volume; nWML = normalized white matter lesions volume; cSVDBS = Total MRI cerebral small vessel disease burden score.

References

[1] Baykara E, Gesierich B, Adam R, et al. A Novel Imaging Marker for Small Vessel Disease Based on Skeletonization of White Matter Tracts and Diffusion Histograms. *Ann Neurol.* 2016;80(4):581-592. doi:10.1002/ana.24758
[2] Charidimou A, Martinez-Ramirez S, Reijmer YD, et al. Total magnetic resonance imaging burden of small vessel disease in cerebral amyloid angiopathy an imaging-pathologic study of concept validation. *JAMA Neurol.* 2016;73(8):994-1001. doi:10.1001/jamaneurol.2016.0832
[3]

Table 1. Demographic, clinical and imaging data

Demographics	
Age, years (mean ± SD)	75.9 ± 6.64
Female, n(%)	24 (37.5)
Vascular Risk Factors	
Hypertension, n(%)	40 (64.5)
Diabetes, n(%)	10 (16.1)
Atrial Fibrillation, n(%)	3 (4.8)
Dyslipidemia, n(%)	47 (75.8)
Neuroimaging Markers	
PSMD (x 10^{-4} mm²/s), median (IQR)	4.20 (3.68-4.79)
Lobar CMB, count, median (IQR)	15.5 (3-58)
cSS (presence) , n(%)	23 (35.9)
CSO-PVS (>20) , n(%)	47 (73.4)
Lacunes, count, median (IQR)	0 (0-2)
Cortical Thickness, mean ± SD	2.3 ± 0.11
Cortical CMI, count, median (IQR)	0 (0-1)
nTBV, mean ± SD	66.07 ± 3.0
nWML, median (IQR)	0.62 (0.34-1.56)
cSVDBS, median (IQR)	3 (2-5)

PSMD = peak width of skeletonized mean diffusivity; CMB = cerebral microbleeds; cSS=cortical superficial siderosis; CSO-PVS=perivascular spaces in the centrum semiovale; CMI = cerebral microinfarcts; nTBV= normalized total brain volume; nWML = normalized white matter lesions volume; cSVDBS = Total MRI cerebral small vessel disease burden score

Results

cSVDBS was associated with PSMD (R^2=0.205,p=0.001) in linear regression analysis, adjusted for age and gender. The regression analyses for other individual neuroimaging markers, adjusted for age and gender, revealed that nWML (R^2=0.741,p<0.001), nTBV (R^2=0.144,p=0.015), cortical thickness (R^2=0.151,p=0.012), lacunes (R^2=0.196,p=0.002), and cortical microinfarcts (R^2=0.149,p=0.015) were significantly associated with PSMD, but hemorrhagic markers and EPVS were not. In a multiple regression model (R^2=0.813), including only markers relevant in the univariate analyses, nWML (β=0.787, p<0.001) and cortical thickness (β=-0.193,p=0.008) remained independently associated with PSMD.

Conclusions

Increased global burden of cSVD markers was associated with higher PSMD values in this CAA sample, implying a possible effect on white matter microstructural integrity. However, this effect was mostly driven by nWML, since only non-hemorrhagic markers of cSVD were associated with PSMD.

ESO-WSO 2020
Jointly Organised by the European Stroke Organisation & the World Stroke Organization

VIRTUAL CONFERENCE 7-9 NOVEMBER

Appendix 3.3. Comparison with other DWI markers

Appendix 3.3.A. Abstract and poster presented at the International Stroke Conference 2021 – Virtual.

Abstract P59: Peak Width of Skeletonized Mean Diffusivity Outperforms Other Diffusion Tensor Imaging Metrics as Biomarker for Cognition in Memory-Clinic Subjects With Cerebral Amyloid Angiopathy

Maria Clara Zanon Zotin, Dorothee Schoemaker, Valentina Perosa, Martin Bretzner, Lukas Sveikata, Susanne Van Veluw, Andreas Charidimou, Mark R Etherton, Edip M Gurol, Steven Greenberg, … See all authors ∨

Abstract

Introduction: Peak width of skeletonized mean diffusivity (PSMD) is a novel fully automated diffusion tensor imaging (DTI) marker that has been consistently associated with cognition in cerebral small vessel disease (SVD) cohorts, including cerebral amyloid angiopathy (CAA). We hypothesized that PSMD would be more strongly associated with cognitive performance compared to other conventional DTI metrics in our CAA sample.

Methods: We recruited non-demented subjects with probable-CAA from a single-center memory-clinic cohort. We analyzed structural MRIs to compute a validated CAA burden score (0-6 points scale, based on the following MRI features: lobar microbleeds, superficial siderosis, perivascular spaces in centrum semiovale, and white matter hyperintensities). PSMD was obtained using a freely available script (www.psmd-marker.com). We used the same skeleton-mask to compute: mean of skeletonized mean diffusivity (mean MD) and mean of skeletonized fractional anisotropy (mean FA). We used linear regression analyses to explore relationships with CAA burden score and cognitive composite scores (processing speed, executive function, memory, and language - z-scores adjusted for age, sex and education level).

Results: We included 43 subjects (mean age 74.4 ± 5.9 years; 48.8% female; PSMD median [IQR]: 4.05 [3.58 - 4.80] x 10^{-4} mm^2/s). In linear regression models adjusting for age, DTI metrics were significantly associated with CAA burden score (mean FA: β = -0.563, Adj. R^2: 0.27; $p < 0.001$; mean MD: β = 0.581; Adj. R^2: 0.32; $p < 0.001$; PSMD: β = 0.364, Adj. R^2: 0.12; $p = 0.018$). PSMD was significantly associated with cognitive performance, specifically in the domains of executive function (β = -0.568; Adj. R^2: 0.25; $p < 0.001$) and processing speed (β = -0.447; Adj. R^2: 0.19; $p = 0.004$). Other DTI metrics were not significantly associated with cognitive scores.

Conclusion: In this CAA sample, all DTI metrics were associated with CAA burden scores, however, only PSMD was significantly associated with cognition, in domains that are commonly affected in vascular cognitive impairment. Our results warrant confirmation in larger samples, but support PSMD as biomarker for cognition in CAA, outperforming other conventional DTI metrics.

Peak Width Of Skeletonized Mean Diffusivity Outperforms Other Diffusion Tensor Imaging Metrics As Biomarker For Cognition In Memory-clinic Subjects With Cerebral Amyloid Angiopathy

Abstract: P59

Maria Clara Zanon Zotin, [1,2] Dorothee Schoemaker, [1] Valentina Perosa, [1] Martin Bretzner, [1] Lukas Sveikata, [1] Susanne Van Veluw, [1] Andreas Charidimou, [1] Mark R Etherton, [1] Edip M Gurol, [1] Steven Greenberg, [1] Marco Duering, [3] Nicolas Raposo, [4] Anand Viswanathan. [1]

[1] J Philip Kistler Stroke Research Center. Department of Neurology. Massachusetts General Hospital. Harvard Medical School, Boston, MA, USA. [2] Center for Imaging Sciences and Medical Physics. Department of Medical Imaging, Hematology and Clinical Oncology. Ribeirão Preto Medical School, University of São Paulo, Ribeirão Preto, SP, Brazil. [3] Medical Image Analysis Center (MIAC) and Quantitative Biomedical Imaging Group; Department of Biomedical Engineering, University of Basel, Base, Switzerland. [4] Department of Neurology, Centre Hospitalier Universitaire de Toulouse and Toulouse Neuroimaging Center, Université de Toulouse, Inserm, UPS, France.

Introduction

Peak width of skeletonized mean diffusivity (PSMD) is a novel fully automated diffusion tensor imaging (DTI) marker that has been consistently associated with cognitive performance in cerebral small vessel disease cohorts, including cerebral amyloid angiopathy (CAA). We hypothesized that PSMD would be more strongly associated with cognitive performance compared to other conventional DTI metrics in our CAA sample.
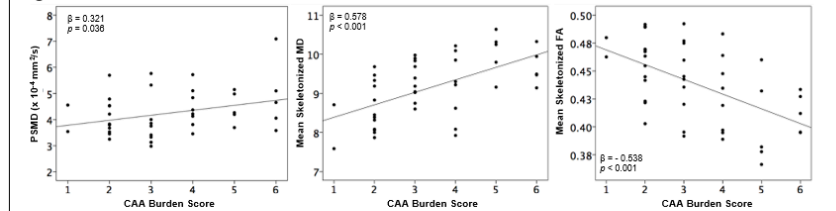
Methods

We recruited non-demented subjects with probable-CAA from a single-center memory-clinic cohort. We analyzed structural MRIs to compute a validated CAA burden score (0-6 points scale, based on the following MRI features: lobar microbleeds (2-4=1 point; ≥5=2 points), superficial siderosis (focal=1point; disseminated=2 points), perivascular spaces in centrum semiovale (moderate or severe [>20]=1 point), and white matter hyperintensities (Deep: Fazekas ≥2 or Periventricular: Fazekas 3 = 1 point). PSMD was obtained using a freely available script (www.psmd-marker.com). We used the same skeleton-mask to compute: mean of skeletonized mean diffusivity (mean MD) and mean of skeletonized fractional anisotropy (mean FA). We used linear regression analyses to explore relationships between different DTI metrics and cognitive performance (processing speed, executive function, memory, and language - z-scores already adjusted for age, sex and education level). We further investigated the association between the DTI metrics and CAA burden scores.

Results

We included 43 subjects (mean age 74.4 ± 5.9 years; 48.8% female; PSMD median [IQR]: 4.06 [3.58 - 4.79] x 10^{-4} mm2/s). In linear regression models adjusting for age, CAA burden scores were significantly associated with DTI metrics (mean FA: β = - 0.550, Adj. R^2: 0.26; $p < 0.001$; mean MD: β = 0.571; Adj. R^2: 0.30; $p < 0.001$; PSMD: β = 0.372, Adj. R^2: 0.13; $p = 0.016$). In models adjusted for the time gap between MRI and neuropsychological evaluation, PSMD was significantly associated with cognitive performance, specifically in the domains of executive function (β = - 0.577; Adj. R^2: 0.26; $p < 0.001$) and processing speed (β = -0.466; Adj. R^2: 0.21; $p = 0.003$). Other DTI metrics were not significantly associated with cognitive scores.

Fig 1. Associations between cognitive scores and DTI metrics
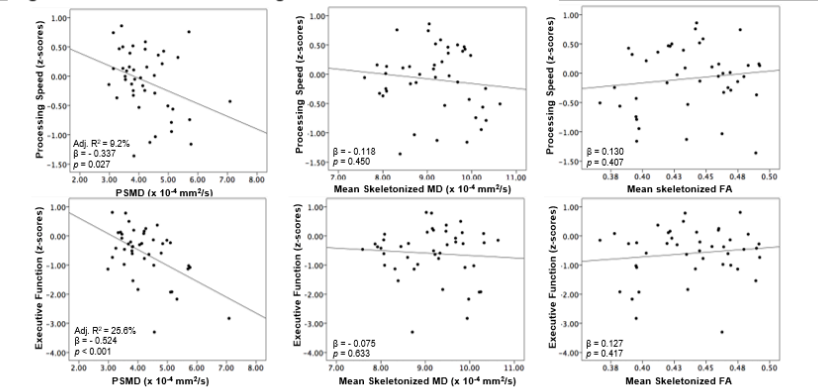
Scatter Plots showing the association between cognitive performance (in the domains of processing speed and executive function) and different DTI metrics: PSMD (A and B), mean skeletonized MD (C and D), and mean skeletonized FA (E and F). The provided R^2 and p-values reflect the obtained independent predictive of each DTI metric with regards to Processing Speed and Executive function (simple linear regression - unadjusted models).

Fig 2. Associations between DTI and CAA burden score

Scatter Plots showing the association between different DTI metrics and CAA burden score. The provided R^2 and p-values reflect the obtained independent predictive CAA burden scores with regards to different DTI metrics (simple linear regression - unadjusted models).

Table 1. Demographic, clinical and imaging data

Demographics	
Age, years (mean ± SD)	74.4 ± 5.9
Female, n(%)	21 (48.8)
Vascular Risk Factors	
Hypertension, n(%)	26 (60.5)
Diabetes, n(%)	4 (9.3)
Atrial Fibrillation, n(%)	2 (4.7)
Dyslipidemia, n(%)	36 (83.7)
Neuroimaging Markers	
PSMD (x 10^{-4} mm²/s), median (IQR)	4.06 (3.58-4.79)
Mean Skeletonized MD, mean ± SD	9.14 ± 0.80
Mean Skeletonized FA, mean ± SD	0.44 ± 0.04
CAA burden score, median (IQR)	3 (2-4)

Conclusions

In this CAA sample, all DTI metrics were associated with CAA burden scores, however, only PSMD was significantly associated with cognition, in domains that are commonly affected in vascular cognitive impairment. Our results warrant confirmation in larger samples, but support PSMD as biomarker for cognition in CAA, outperforming other conventional DTI metrics.

References

[1] Baykara E, Gesierich B, Adam R, et al. A Novel Imaging Marker for Small Vessel Disease Based on Skeletonization of White Matter Tracts and Diffusion Histograms. Ann Neurol. 2016;80(4):581-592. doi:10.1002/ana.24758
[2] Charidimou A, Martinez-Ramirez S, Reijmer YD, et al. Total magnetic resonance imaging burden of small vessel disease in cerebral amyloid angiopathy an imaging-pathologic study of concept validation. JAMA Neurol. 2016;73(8):994-1001. doi:10.1001/jamaneurol.2016.0832

Appendix 4. Other co-authored articles in the field of cSVDs

Appendix 4.1. "Biomarkers Related to Endothelial Dysfunction and Vascular Cognitive Impairment: A Systematic Review"

Reference: Martins-Filho RK, Zotin MC, Rodrigues G, Pontes-Neto O. Biomarkers Related to Endothelial Dysfunction and Vascular Cognitive Impairment: A Systematic Review. Dement Geriatr Cogn. 2020;49(4):365–74.

Copyright/Source: Dementia and Geriatric Cognitive Disorders®/ S. Karger AG, Basel

Article reuse license

6/27/22, 7:40 AM   E-mail de Complexo Hospitalar HCFMRP / FAEPA - Permission: Requested Karger Material

Maria Clara Zanon Zotin <mczzotin@hcrp.usp.br>

Permission: Requested Karger Material
1 mensagem

Rights and Permissions <permission@karger.com>   27 de junho de 2022 05:12
Para: "mczzotin@hcrp.usp.br" <mczzotin@hcrp.usp.br>

Dear Maria Clara Zanon Zotin,

Thank you for your email. As to your request, I am pleased to inform you that permission is granted hereby to reprint your article

Martins-Filho R, K, Zotin M, C, Rodrigues G, Pontes-Neto O: Biomarkers Related to Endothelial Dysfunction and Vascular Cognitive Impairment: A Systematic Review. Dement Geriatr Cogn Disord 2020;49:365-374. doi: 10.1159/000510053

as a chapter in the printed and electronic version of your **thesis/doctoral dissertation**, provided that proper credit will be given to the original source and that S. Karger AG, Basel will be mentioned.

Please note that this is a non-exclusive permission, hence any further use, edition, translation or distribution, either in print or electronically, requires written permission again as this permission is valid for the above mentioned purpose only.

This permission applies only to copyrighted content that S. Karger AG owns, and not to copyrighted content from other sources. If any material in our work appears with credit to another source, you must also obtain permission from the original source cited in our work. All content reproduced from copyrighted material owned by S. Karger AG remains the sole and exclusive property of S. Karger AG. The right to grant permission to a third party is reserved solely by S. Karger AG.

Thank you for your understanding and cooperation.

Hopefully, I have been of assistance to you with the above.

Kind regards

Erika Brunner

ePartner Manager
Rights & Permissions Manager

+41 61 306 12 48
e.brunner@karger.com

Biomarkers related to endothelial dysfunction and vascular cognitive impairment: a systematic review

Rui Kleber Martins-Filho[a], Maria Clara Zotin[b], Guilherme Rodrigues[a]; Octavio Pontes-Neto[a]

[a] Department of Neurosciences and Behavioural Sciences, Hospital das Clínicas – Ribeirão Preto Medical School, University of São Paulo; Ribeirão Preto, SP, Brazil.
[b] Department of Internal Medicine, Radiology Division, Hospital das Clínicas – Ribeirão Preto Medical School, University of São Paulo; Ribeirão Preto, SP, Brazil.

Short title (running head): Endothelial dysfunction and vascular cognitive impairment

Corresponding Author:

Rui Kleber do Vale Martins-Filho

Department of Neurosciences and Behavioural Sciences

Hospital das Clínicas – Ribeirão Preto Medical School, University of São Paulo

Rua Bernardino de Campos 1000, Centro, Ribeirão Preto/SP, CEP 14015-130, Brazil

Telephone/fax number: +55 (16) 996288668

E-mail: ruikleber@usp.br

Number of Tables: 2

Number of Figures: 2

Word count: 3662

Abstract

Introduction: The damage in the endothelium and the neurovascular unit appear to play a key role in the pathogenesis of vascular cognitive impairment (VCI). Although there have been many advances in understanding the physiopathology of this disease, several questions remain unanswered. The association with other degenerative diseases and the heterogeneity of its clinical spectrum establish a diagnostic problem, compromising a better comprehension of the pathology and halting the development of effective treatments. The investigation of biomarkers is an important movement to the development of novel explicative models and treatment targets involved in VCI. Methods: We searched MEDLINE considering the original research based on VCI biomarkers in the past 20 years, following pre-specified selection criteria, data extraction, and qualitative synthesis. Results: We reviewed 42 articles: 16 investigated plasma markers, 17 analyzed neuropathological markers, 4 studied CSF markers, 4 evaluated neuroimaging markers (ultrasound and MRI), and one used peripheral Doppler perfusion imaging. Conclusions: The biomarkers in these studies suggest an intrinsic relationship between endothelial dysfunction and VCI. Nonetheless, there is still a need for identification of a distinctive set of markers that can integrate the clinical approach of VCI, improve diagnostic accuracy, and support the discovery of alternative therapies.

Introduction

Small vessel disease (SVD) is a clinical-radiological syndrome caused by a disorder in perforating cerebral arterioles, capillaries, and venules, resulting in lesions of cerebral white and deep gray matter [1]. It is responsible for about 20% of strokes and 45% cases of dementia in the world [2,3]. Endothelial cells appear to have a pivotal role in the pathogenesis of cerebral SVD and vascular dementia (VaD). Endothelial dysfunction may contribute to SVD pathology through multiple mechanisms, such as blood-brain barrier damage, decrease in whole-brain or

tissue-resting cerebral blood flow, loss of cerebral vasoreactivity, and increase in intracranial pulsatility [4]. Moreover, endothelial dysfunction (ED) may represent a potential link between cerebral SVD and Alzheimer's pathology.

For example, the leakage of fibrinogen through vessel walls contributes to amyloid-beta ($A\beta$) plaques formation [1], and disrupted transport across the blood-brain barrier (BBB) plays a significant role in determining $A\beta$ concentrations in the central nervous system (CNS) [5, 6]. Recently, Alzheimer's Disease-Related Dementia Summit set the study of small vessel VCI biomarkers as a research priority [7]. Considering that a thorough review analyzing markers of endothelial dysfunction in patients with VCI is lacking, we carried out a systematic review on biomarkers of ED in VCI studies undertaken in the last 20 years.

Methods

Search Strategy, Study Selection, and Data acquisition

We searched MEDLINE for studies investigating endothelial dysfunction and VCI with the following free text and Medical Subject Headings (MeSH): "endothelium" or "endothelial" and "cognitive impairment" or "dementia." We limited the search to articles written in English, with human adults as subjects and published in the last twenty years (search period between January 1, 1999, and December 31, 2019).

According to the Preferred Reporting Items for Systematic Reviews and Meta-Analyses (PRISMA) statement [8], two investigators (R.K.M.F. and G.R.) searched MEDLINE independently and compared their results. Differences in the screening phase were resolved by consensus. Three investigators (R.K.M.F., M.C.Z., and G.R.) carried out data extraction independently. They stored the variables in a spreadsheet especially developed for this review, tabulating the following data: number of participants, population studied, study design, biomarker of interest, source of biomarker, and main results.

Results

The combined terms yielded 74 articles: "endothelial" and "vascular cognitive impairment" - 5 articles; "endothelium" and "vascular cognitive impairment" - 3 articles; "endothelial" and "vascular dementia" - 49 articles, and "endothelium" and "vascular dementia" - 17 articles. After excluding studies in duplicates, 58 articles remained. In sequence, R.K.M.F. and G.R. independently reviewed all identified abstracts and excluded articles that met any of the following criteria: a) articles not related to VCI; b) no original research (i.e., reviews, editorials, letters); c) research not focused on endothelial biomarkers. Again, any discrepancies were resolved by consensus.

From 58 articles initially identified, we excluded 16 papers in this second phase (9 reviews; 6 not related to VCI, and one did not study biomarkers) as shown in Figure 1.

From the 42 articles included in the qualitative synthesis, 16 investigated plasma markers, 17 analyzed neuropathological markers, 4 studied CSF markers, 4 evaluated neuroimaging markers (ultrasound and MRI), and one dealt with peripheral Doppler perfusion imaging. The supplementary online Table S1 summarizes the main findings of each study.

Discussion

Summary of evidence

This systematic review aims to describe biomarkers that target pathways linking endothelial dysfunction with cerebral SVD and VCI. We divided such markers in those related to BBB dysfunction, those related to perfusional and hemodynamic changes, and those that assess cerebrovascular and peripheral reactivity. Table 1 summarizes the most important known facts to each category. Some of the main markers are represented in a schematic model illustrated in Figure 2.

1. Blood-brain barrier dysfunction

A functional BBB depends on the adequate interaction between the many components of the neurogliovascular unit to regulate the transit of fluid and nutrients between intravascular and interstitial spaces, maintaining CNS homeostasis [9].

Biochemical markers, found in the CSF and the plasma, are related to BBB dysfunction in patients with VCI:

1.1.1. CSF/plasma albumin ratio:

The ratio between albumin levels in CSF and plasma (Qalb), though not specific, represents a commonly used method to measure the degree of disruption of BBB. Janelidze et al. (2017) found increased Qalb in participants with multiple forms of dementia, though only slightly higher values were demonstrated among subjects with VaD [9]. These findings suggest that BBB dysfunction may be a common feature in different dementia types. Interestingly, Qalb was associated with diabetes (DM), and obesity markers were associated with increased Qalb two decades later [9]. These findings are in line with the expected endothelial damage induced by inflammatory and oxidative effects of chronic DM and support the physiopathological link between vascular risk factors and dementia [9, 10, 11].

1.1.2. Adhesion molecules (ICAM-1, VCAM-1, sICAM-1):

Endothelial cells express intracellular adhesion molecule 1 (ICAM-1) and vascular cell adhesion molecule I (VCAM-1), which participate in trans-endothelial migration and endothelial cell activation. ICAM-1 and VCAM-1 were upregulated in peripheral vascular dysfunction related to DM [9]. In a small subgroup of patients with DM, there is a higher CSF levels of ICAM-1 and VCAM-1, which correlated positively with Qalb levels, suggesting that endothelial damage related DM may be affecting cerebral vessels [9].

The measure of the plasmatic soluble portion of ICAM-1 (sICAM-1) is an independent factor for the onset and severity of white matter disease in patients over 60 years without a history of

neurological disease [9]. In a study with VaD and AD patients, these vascular adhesion molecules had higher levels in plasma compared to the control group [13].

1.1.3. Plasmatic inflammatory markers:

Markers such as platelet factor IV, CD40 ligand, homocysteine, and interleukin-6 are associated with radiological progression of cerebral SVD in patients with lacunar stroke, VaD, and vascular parkinsonism [14]. These findings are in line with the increase in interleukin-6 and tumor necrosis factor-alpha (TNF-α) in patients with VaD compared to late-onset AD [13]. Basolateral interleukin-6 secretion raises in dyslipidemic patients with AD, with or without vascular risk factors [15]. C-reactive protein levels were associated with reduced verbal fluency in non-dementia patients with moderate to high cardiovascular risk [16].

1.1.4. Endothelial function mediators:

Endothelial function regulators and vasodilators, such as endothelin-1 (ET-1) and natriuretic atrial peptide, respectively, are associated with an increased risk of vascular dementia [17]. In a randomized clinical trial investigating the use of medicinal herbs in diabetic patients with vascular dementia, both treatments (the investigational herb and the use of pioglitazone) decreased ET-1 levels after the intervention with a concomitant increase of plasma nitric oxide [15]. The nitric oxide (NO), known as an "endogenous anti-atherosclerotic" agent, is a pivotal mediator of endothelial function, and inhibitors of endothelial NO synthase, such as the asymmetric form of dimethylarginine (ADMA), were investigated in two registries [16, 19]. In the first, ADMA levels are independently associated with silent cerebral infarcts [19]. In the second, ADMA levels were associated with low verbal memory performance in asymptomatic patients with moderate to high cardiovascular risk [16].

In TREX1 mutation carriers, a genetic cause of SVD triggered primarily by endothelial dysfunction, levels of von Willebrand factor (VWF), and angiopoietin-2 were increased. They were also related to disease activity, mainly in individuals over 40 years of age [20, 21].

On the other hand, antibodies against heparan sulfate (HS Abs), a glycosaminoglycan present in endothelial cells, which plays an important role in angiogenesis, the integrity of vessels' barrier and processes of cell adhesion were similar in patients with dementia (VaD and AD) and controls [22].

1.2. Neuropathological findings:

Neuropathologic studies show structural changes in the BBB of patients with VaD with an increment in collagen type I and IV and fibrohyalinosis in brain vessels of VaD subjects [23]. Additionally, there is a higher expression of Kallikrein 6, whose substrates include fibronectin, fibrinogen, collagen types I and VI, and laminin [24, 25].

Tight junctions form an essential structure for the correct functioning of the BBB, and its main components are claudin and occludin proteins. In individuals with VaD, there is a raise in occludin and claudins expression, suggesting a possible compensatory phenomenon [26, 27].

2. Markers related to perfusional and hemodynamic changes

2.1. Angiogenic factors (HIF-1a, VEGF, TNF-α, TGF-β, NGF, and BDNF):

Multiple cytokines have been recently studied for their interconnected role in neuroprotective pathways associated with ischemia and hypoxia-induced brain injury. Many of these cytokines have in common a regulatory effect on the secretion of vascular endothelial growth factor (VEGF). VEGF is a cytokine secreted by astrocytes with significant neurotrophic and neuroprotective effects that binds to endothelial cells to regulate angiogenesis and vascular permeability [26, 27, 28, 31]. Hypoxia-inducible factor (HIF) is a transcriptor factor that mediates neuroprotective effects related to hypoxia-conditioning and ischemia and induces upregulation of VEGF [28]. Nerve growth factor (NGF) and brain-derived neurotrophic growth factor (BDNF) have also demonstrated neuroprotective effects under hypoxia/ischemia-induced brain injury by inducing expression of VEGF, through a pathway dependent on HIF-

1a [28]. TNF-α is a cytokine with proinflammatory effects that upregulates transforming growth factor β (TGF-β) and induces VEGF production [29]. TGF-β has anti-inflammatory effects and also upregulates VEGF [29]. Animal models suggest that TGF-β is also associated with amyloidogenesis [29].

Janelidze et al. (2017) found higher VEGF levels in CSF of patients with different forms of dementia in comparison to controls, with a slightly higher index of bioactive levels of VEGF among patients with VaD, supporting that concomitant vascular factors may participate in the pathogenesis of neurodegenerative diseases [9]. CSF VEGF correlated positively with Qalb, which is in line with the expected increase in BBB permeability induced by VEGF [9]. However, even subgroups without increased Qalb showed higher CSF VEGF levels, which could mean that upregulation of VEGF may precede BBB dysfunction [9]. The GTC haplotype in the VEGF gene is related to VaD, supporting the pathogenic role of this angiogenic factor [33]. There is an increase in CSF VEGF and TGF-β levels in patients with AD and VaD, supporting a potential role in both forms of dementia [29]. Increased levels of intrathecal TNF-α have also been described among patients with stroke, AD, and VaD [29].

In contrast, Chakraborty et al. (2018) found no significant difference in CSF VEGF levels across patients with VaD, AD, and controls [30]. Ke et al. (2013) also did not find significant differences in intrathecal levels of VEGF or BNDF in patients with ischemic cerebrovascular diseases and VCI compared to controls [28]. There were, however, unexpectedly lower levels of HIF-1a and NGF in pathological groups in comparison to controls, which were hypothesized to be secondary to the limited duration of upregulation of those markers in response to ischemia [28].

In another study, patients with VaD showed decreased secretion of VEGF by peripheral lymphocytes, similar to what was found in healthy elderlies [32]. AD patients showed a more substantial decrease in VEGF secretion, hypothesized to be potentially due to an inhibitory

effect of amyloid-β42, which could be compromising angiogenesis and the ability to maintain oxygen and nutrients delivery to the brain in those subjects [32].

Overall, these inconsistent results suggest that angiogenic factors may play a yet incompletely understood role in multiple forms of dementia, including vascular and neurodegenerative pathologies. Studies with VEGF CSF levels in AD populations have also yielded inconsistent results [29, 30, 34].

2.2. Neuropathological findings:

VaD patients have perfusional changes and neovascularization [35]. Burke et al. (2014) found a higher length density of hippocampal microvessels in those cases. The vessels were narrower than those without dementia, suggesting an ineffective neoangiogenesis [36].

The white matter hypoperfusion reduces the relation of myelin-associated glycoprotein (MAG) to proteolipid protein 1 (PLP1) [37]. In subjects with VaD, this ratio is decreased [38]. A reduction in MAG:PLP1 values correspond to an elevation in VEGF levels, which associates with a raise in white matter vascular density [37]. However, this increment in VEGF has not been found in subsequent studies [38, 39]. Angiopoietin like-4 (ANGPTL4) is a protein linked to neovascularization, whose production grows in hypoxia situations [40]. A later study on the brains of VaD patients showed an increase in ANGPTL4 levels in these individuals [41].

Cerebral hypoperfusion triggers compensatory mechanisms to restore blood flow. Endothelin (ET) is a vasoconstrictive peptide produced by endothelial vascular cells and formed by the endothelin-converting enzyme (ECE) [42]. Therefore a decrease in MAG:PLP1 values correlates with a decrease in endothelin 1 (ET-1) levels. However, in VaD patients, this protective mechanism fails, as there is an increase in ET-1 levels, and ECE-1 expression remains normal [37, 43].

Other evidence of hemodynamic changes in brains of patients with VaD is a higher expression of the antithrombotic thrombomodulin in subjects with VaD [44] and raised levels of the

vasodilator dihydroxyeicosatrienoic acid (DHET) [55]. The DHET increment is likewise a compensatory mechanism, since patients with the R287Q polymorphism in the Soluble Epoxide Hydrolase gene, the enzyme that produces DHET, have a higher volume of white matter lesions [55].

3. Vasoreactivity

Vasoreactivity represents the vascular ability to undergo adaptive changes in response to vasodilatory stimuli, such as metabolic changes and increases in neuronal activity [1, 45]. Cerebral vasoreactivity (CVR) is strongly dependent on the normal function of the neurogliovascular unit and may indirectly reflect the efficacy of collateral circulation [46]. Studies suggest that cerebral vasoreactivity may already be impaired when resting cerebral blood flow are still within normal ranges, making vasoreactivity markers particularly promising in patients with SVD [1]. Assessment of cerebral vasoreactivity is possible through multiple techniques, such as single-photon emission tomography (SPECT), PET, and transcranial Doppler ultrasound (TCD) [45].

3.1. Cerebral Vasoreactivity measured through TCD:

Assessment of cerebral vasoreactivity through TCD involves the calculation of the percent increase in the mean flow velocity (MFV) of the middle arterial artery (MCA) in response to different stimuli such as acetazolamide, variation in CO_2 levels (induced by hypo or hyperventilation) and administration of L-arginine.

L-arginine is the precursor of NO, representing a useful tool to assess vasodilation mediated by endothelial cells and executed by vascular smooth muscle cells (VSMC) [47]. On the other hand, direct administration of sublingual nitroglycerin can access vasoreactivity independent of endothelial cells, offering a more direct assessment of VSMC function [48].

Staszewski et al. (2019) showed diminished CVR in response to breath-holding maneuvers in patients with lacunar stroke, vascular dementia, and vascular parkinsonism compared to matched controls [45]. CVR was reduced among participants with severe brain atrophy, enlarged perivascular spaces, and extensive white matter lesions. Both white matter lesions and CSVD burden score on MRI correlated with CVR [45].

In CADASIL patients, there is a higher MCA resting pulsatility index and increased L-arginine induced vasoreactivity when compared to controls. These findings imply that large cerebral arteries of CADASIL subjects may present impaired endothelial function, but inconsistent results and methodological concerns argue against this interpretation [45, 46, 49, 50]. Other findings reinforce that the degeneration of VSMC from small vessels mediates vascular reactivity impairment in CADASIL [47, 48].

4. Peripheral vasoreactivity

4.1. Extracerebral vasoreactivity measured by Doppler US (FMD):

Brachial artery flow-mediated dilatation (FMD) is a useful marker of extracerebral endothelial function in conduit vessels [45, 48]. In this technique, the diameter of the brachial artery is measured serially before and after hyperemia induced by deflating a sphygmomanometer cuff distal to the US site. In order to evaluate endothelium-independent vasodilation capacity, NTG can be administered, followed by consecutive measurements of the diameter of the brachial artery [48].

In patients with severe sporadic SVD or VaD, there is a lower FMD when compared to control subjects, in agreement with concomitant findings of reduced CVR [45, 51]. These findings suggest that, in the setting of CSVD, the vasoreactivity impairment may also be found in systemic vessels and could be more easily accessible through peripheral vessels than in cerebral vessels [45]. A positive, though weak, correlation between CVR and FMD was found in CSVD

patients, suggesting an association between peripheral and cerebral vasoreactivity dysfunction in this population [45]. Moreover, the significant correlation between FMD and MMSE implies that endothelial dysfunction relates to cognitive impairment [51]. Reduced FMD has also been reported among AD subjects, suggesting that endothelial dysfunction may also play a role in neurodegenerative pathologies [51].

In the setting of monogenic SVD pathologies, de Boer et al. (2018) employed FMD in patients with RVCL-S and with CADASIL and found reduced dilation only in the former group [48]. Even though VSMC degeneration is a feature of CADASIL, De Boer and colleagues did not find a significant reduction in FMD after nitroglycerin administration in this population, which corroborates the belief that small vessels, rather than conduit vessels, are primarily affected in this pathology [48].

4.2. Capsaicin induced dermal blood flow variation:

Laser doppler perfusion imaging can access the dermal blood flow (DBF) variation in response to stimuli such as topical administration of capsaicin, with the advantage of providing information about microcirculatory vessels instead of conduit vessels, as is the case with FMD [48].

De Boer et al. (2018) found reduced DBF after capsaicin application in patients with CADASIL, which is hypothesized to be associated with impairment of VSMC relaxation in response to endothelial-independent stimuli [48].

4.3. Forearm resistance vessel function assessment:

This technique involves cannulation of the brachial artery and measures variation of forearm blood flow in response to different vasoactive agents, such as acetylcholine (induces vasodilation dependent on endothelial cells), nitroprusside (NO donor that induces vasodilation independent of endothelial function) and verapamil (directly acts on VSMC independently of endothelial cells or NO) [52].

Moser et al. (2008) found a significant association between VSMC function, measured with the administration of verapamil, and performance on neuropsychological tests for initiation and processing speed in a population with early-stage atherosclerotic vascular disease. Curiously, the same was not found with endothelial function [52].

5. Other markers

In a study of 149 stroke patients with SVD, β-amyloid-40 levels were correlated with diffuse SVD disease rather than isolated lacunar strokes [53]. Such findings may represent a direct and vasoconstrictive toxic effect of this peptide against the endothelium, leading to BBB dysfunction [53].

Quantitative evaluation of endothelial progenitor cells also appears to be associated with VaD and AD. Two markers, CD34 and CD133, are particularly useful in this assessment. CD34 identifies endothelial lineage cells and CD133 allows the quantification of immature lineages, whereas the double staining of these cells allows a measure of reserve capacity and turnover of endothelial cells [54]. Xiao-dong et al. (2011) found a decrease in cell levels with these markers compared to the control group, while patients with AD showed not only a quantitative reduction of progenitor cells but a correlation with a worse performance in the Mini-Mental State Examination (MMSE) [54].

In addition, SVD burden has been associated with the increment of serum neurofilament light chain (NfL), as demonstrated by Duering et al. (2018). In this study, serum NfL was related to processing speed performance, focal neurological symptoms, and disability in patients with CADASIL and sporadic SVD. As a marker of neuroaxonal damage, increased NfL levels in this population suggest that axonal lesion and neuronal loss might be the ultimate consequence of a broader cascade of pathological events involved in SVD [56].

Conclusions

This review suggests an intrinsic relationship between endothelial dysfunction and VCI, establishing the endothelium as a pivotal target involved in the pathogenesis of the disease. The biomarkers studied indicate a dynamic and whole-brain process. The BBB has its integrity affected, as demonstrated by the higher CSF/plasma albumin ratio and the increment of collagen type I, type IV, and fibrohyalinosis. Besides, several inflammatory markers (e.g., interleukin-6, TNF-α, C-reactive protein) are upregulated, also impairing BBB permeability. Hemodynamic biomarkers' dynamic, for its part, suggests a state of hypoperfusion (e.g., decrease in MAG:PLP1 ratio) and abnormal vasoreactivity (e.g., abnormal CO_2 vasodilation). As a consequence, mechanisms of compensation for ineffective neoangiogenesis (increase in ANGPTL4 and ET-1 levels, decrease in CD34+ and CD133+ progenitor endothelial cells) and antithrombogenicity (higher thrombomodulin levels) would eventually culminate in a vicious cycle of lesion progression.

Finally, it is essential to note that the significant heterogeneity of subjects investigated and the multitude of different markers, some with inconsistent results, compromise its application in clinical practice and highlight the importance of establishing this theme as a research priority.

Statement of Ethics

This research did not involve human participants or animals as this was a systematic review of existing publications, and no primary data were collected. Written informed consent was, therefore, not obtained, and ethical approval was not sought.

Funding Sources

Conflicts of Interest

The other authors declare no conflicts of interest.

Author Contributions

R.K.M.F., M.C.Z., and G.R. carried out the literature search and drafted the manuscript.

O.P.N. critically revised the manuscript. All authors read and approved the final version.

References

1   Wardlaw JM, Smith C, Dichgans M. Small vessel disease: mechanisms and clinical implications. Lancet Neurol., vol. 18, no. 7, pp. 684–696, 2019.

2   Pantoni L. Cerebral small vessel disease: from pathogenesis and clinical characteristics to therapeutic challenges. Lancet Neurol., vol. 9, no. 7, pp. 689–701, Jul. 2010.

3   Mok V, Wong A, Tang WK, Lam WWM, Fan YH, Richards PS, et al. Determinants of Prestroke Cognitive Impairment in Stroke Associated with Small Vessel Disease. Dement. Geriatr. Cogn. Disord., vol. 20, no. 4, pp. 225-230, 2005.

4   Huisa BN, Caprihan A, Thompson J, Prestopnik J, Qualls CR, and Rosenberg GA. Long-Term Blood-Brain Barrier Permeability Changes in Binswanger Disease. Stroke, vol. 46, no. 9, pp. 2413–2418, Sep. 2015.

5   Shibata M, Yamada S, Kumar Ram S, Calero M, Bading J, Frangione B, et al. Clearance of Alzheimer's amyloid-ss(1-40) peptide from brain by LDL receptor-related protein-1 at the blood-brain barrier. J. Clin. Invest., vol. 106, no. 12, pp. 1489–99, Dec. 2000.

6   Zlokovic BV, Yamada S, Holtzman D, Ghiso J, Frangione B. Clearance of amyloid beta-peptide from brain: transport or metabolism? Nat. Med., vol. 6, no. 7, pp. 718–9, Jul. 2000.

7   Snyder HM, Corriveau RA, Craft S, Faber JE, Greenberg SM, Knopman D, et al. Vascular contributions to cognitive impairment and dementia including Alzheimer's disease. Alzheimers. Dement., vol. 11, no. 6, pp. 710–7, Jun. 2015.

8   Moher D, Liberati A, Tetzlaff J, Altman DG, PRISMA Group. Preferred reporting items for systematic reviews and meta-analyses: The PRISMA statement. PLoS Medicine, vol. 6, no. 7. Jul-2009.

9   Janelidze S, Hertze J, Nagga K, Nilsson K, Nilsson C, Wennstrom M, et al. Increased blood-brain barrier permeability is associated with dementia and diabetes but not

amyloid pathology or APOE genotype. Neurobiol. Aging, vol. 51, no. 2017, pp. 104–112, 2017.

10 Skoog I. Risk Factors for Vascular Dementia: A Review. Dement. Geriatr. Cogn. Disord., vol. 5, no. 3-4, pp. 137-144, 1994.

11 Carantoni M, Zuliani G, Munari MR, D'Elia K, Palmieri E, Fellin R. Alzheimer Disease and Vascular Dementia: Relationships with Fasting Glucose and Insulin Levels. Dement. Geriatr. Cogn. Disord., vol. 11, no. 3, pp. 176-180, 2000.

12 Hao J, Sing K, Yan Y, Hui J, Ding D, Hong Z. Plasma level of sICAM-1 is associated with the extent of white matter lesion among asymptomatic elderly subjects. Clin Neurol Neurosurg, vol. 111, pp. 847–851, 2009.

13 Zuliani G, Cavalieri M, Galvani M, Passaro A, Munari MR. Markers of endothelial dysfunction in older subjects with late onset Alzheimer's disease or vascular dementia. J Neurol Sci, vol. 272, pp. 164–170, 2008.

14 Staszewski J, Piusińska-Macoch R, Brodacki B, Skrobowska E, Stępień A. IL-6, PF-4, sCD40 L, and homocysteine are associated with the radiological progression of cerebral small-vessel disease: A 2-year follow-up study. Clin. Interv. Aging, vol. 13, pp. 1135–1141, 2018.

15 Dias HKI, Brown CLR, Polidori MC, Lip GYH, Griffiths HR. LDL-lipids from patients with hypercholesterolaemia and Alzheimer ' s disease are inflammatory to microvascular endothelial cells : mitigation by statin intervention. Clin Sci (Lond). 2015 pp. 1195–1206, 2015.

16 Miralbell J, López-Cancio E, López-Oloriz J, Arenillas JF, Barrios M, Soriano-Raya JJ, et al. Cognitive Patterns in Relation to Biomarkers of Cerebrovascular Disease and Vascular Risk Factors. Cerebrovasc Dis. 2013 pp. 98–105, 2013.

17 Holm H, Nagga K, Nilsson ED, Ricci F, Melander O, Hansson O, et al. Biomarkers of

microvascular endothelial dysfunction predict incident dementia : a population-based prospective study. J Intern Med. 2017 no. Cv, pp. 94–101, 2017.

18   Qiang G, Wenzhai C, Huan Z, Yuxia Z, Dongdong Y, Sen Z, et al. Effect of Sancaijiangtang on plasma nitric oxide and endothelin-1 levels in patients with type 2 diabetes mellitus and vascular dementia : a single-blind randomized controlled trial. J Tradit Chin Med. 2015 Aug, vol. 35, no. 4, pp. 375–380, 2015.

19   Pikula A, Boger RH, Beiser AS, Maas R, DeCarli C, Schwedhelm E, et al. Association of plasma ADMA Levels with MRI Markers of Vascular Brain Injury: Framingham Offspring Study. Stroke. 2009 pp. 2959–2964, 2013.

20   Pelzer N, Bijkerk R, Reinders MEJ, Jan van Zonneveld A, Ferrari MD, van den Maagdenberg AMJM, et al. Circulating endothelial markers in retinal vasculopathy with cerebral leukoencephalopathy and systemic manifestations. Stroke, vol. 48, no. 12, pp. 3301–3307, 2017.

21   Stott DJ, Spilg E, Campbell AM, Rumley A, Mansoor MA, Lowe GDO. Haemostasis in ischaemic stroke and vascular dementia. Blood Coagul. Fibrinolysis, vol. 12, no. 8, pp. 651–657, 2001.

22   Briani C, Cagnin A, Gallo L, Toffanin E, Varagnolo M, Zaninotto M, et al. Anti-heparan sulphate antibodies and homocysteine in dementia: Markers of vascular pathology? J Neurol Sci, 2005, vol. 229–230, pp. 215–218.

23   Lin JX, Tomimoto H, Akiguchi I, Matsuo A, Wakita H, Shibasaki H, et al. Vascular cell components of the medullary arteries in Binswanger's disease brains: A morphometric and immunoelectron microscopic study. Stroke, vol. 31, no. 8, pp. 1838–1842, Aug. 2000.

24   Ashby EL, Kehoe PG, Love S. Kallikrein-related peptidase 6 in Alzheimer ' s disease and vascular dementia. Brain Res., vol. 1363, pp. 1–10, 2010.

25   Lemańska-Perek A, Leszek J, Krzyanowska-Gołąb D, Radzik J, Kątnik-Prastowska MI. Molecular status of plasma fibronectin as an additional biomarker for assessment of alzheimer's dementia risk. Dement. Geriatr. Cogn. Disord., vol. 28, no. 4, pp. 338–342, 2009.

26   Romanitan MO, Popescu BO, Spulber S, Bajenaru O, Popescu LM, Winblad B, et al. Altered expression of claudin family proteins in Alzheimer's disease and vascular dementia brains. J Cell Mol Med, vol. 14, no. 5, pp. 1088–1100, 2010.

27   Romanitan MO, Popescu BO, Winblad B, Bajenaru OA, Bogdanovic N. Occludin is overexpressed in Alzheimer ' s disease and vascular dementia. J Cell Mol Med, vol. 11, no. 3, pp. 569–579, 2007.

28   Ke XJ, Zhang JJ. Changes in HIF-1α, VEGF, NGF and BDNF levels in cerebrospinal fluid and their relationship with cognitive impairment in patients with cerebral infarction. J. Huazhong Univ. Sci. Technol. - Med. Sci., vol. 33, no. 3, pp. 433–437, 2013.

29   Tarkowski E, Issa R, Sjogren M, Wallin A, Blennow K, Tarkowski A, et al. Increased intrathecal levels of the angiogenic factors VEGF and TGF-β in Alzheimer's disease and vascular dementia. Neurobiol. Aging, vol. 23, no. 2, pp. 237–243, 2002.

30   Chakraborty A, Chatterjee M, Twaalfhoven H, Milan MDC, Teunissen CE, Scheltens P, et al. Vascular Endothelial Growth Factor remains unchanged in cerebrospinal fluid of patients with Alzheimer's disease and vascular dementia. Alzheimer's Res. Ther., vol. 10, no. 1, pp. 1–7, 2018.

31   Ahmed-Jushuf F, Jiwa NS, Arwani AS, Foot P, Bridges LR, Kalaria RN, et al. Age-dependent expression of VEGFR2 in deep brain arteries in small vessel disease, CADASIL, and healthy brains. Neurobiol. Aging, vol. 42, pp. 110–115, 2016.

32   Solerte SB, Ferrari E, Cuzzoni G, Locatelli E, Giustina A, Zamboni M, et al. Decreased

release of the angiogenic peptide vascular endothelial growth factor in alzheimer's disease: Recovering effect with insulin and DHEA sulfate. Dement. Geriatr. Cogn. Disord., vol. 19, no. 1, pp. 1–10, 2005.

33   Kim Y, Nam YJ, Lee C. Haplotype analysis of single nucleotide polymorphisms in VEGF gene for vascular dementia. American Journal of Medical Genetics, Part B: Neuropsychiatric Genetics, vol. 141, no. 4. pp. 332–335, 2006.

34   Hohman TJ, Bell SP, Jefferson AL. The role of vascular endothelial growth factor in neurodegeneration and cognitive decline: Exploring interactions with biomarkers of Alzheimer disease. JAMA Neurol., vol. 72, no. 5, pp. 520–529, 2015.

35   Baloyannis SJ. Pathological alterations of the climbing fibres of the cerebellum in vascular dementia: A Golgi and electron microscope study. J. Neurol. Sci., vol. 257, no. 1–2, pp. 56–61, 2007.

36   Burke MJC, Nelson L, Slade JY, Oakley AE, Khundakar AA, Kalaria RN. Morphometry of the hippocampal microvasculature in post-stroke and age-related dementias. Neuropathol. Appl. Neurobiol., vol. 40, no. 3, pp. 284–295, 2014.

37   Barker R, Ashby EL, Wellington D, Barrow VM, Palmer JC, Kehoe PG, et al. Pathophysiology of white matter perfusion in Alzheimer's disease and vascular dementia. Brain, vol. 137, no. 5, pp. 1524–1532, 2014.

38   Thomas T, Miners S, Love S. Post-mortem assessment of hypoperfusion of cerebral cortex in Alzheimer's disease and vascular dementia. Brain, vol. 138, no. 4, pp. 1059–1069, 2015.

39   Sinclair LI, Tayler HM, Love S. Synaptic protein levels altered in vascular dementia. Neuropathol. Appl. Neurobiol., vol. 41, no. 4, pp. 533–543, 2015.

40   Babapoor-Farrokhran S, Jee K, Puchner B, Hassan SJ, Xin X, Rodrigues M, et al. Angiopoietin-like 4 is a potent angiogenic factor and a novel therapeutic target for

patients with proliferative diabetic retinopathy. Proc. Natl. Acad. Sci. U. S. A., vol. 112, no. 23, pp. E3030–E3039, 2015.

41   Chakraborty A, Kamermans A, van Het Hof B, Castricum K, Aanhane E, van Horssen J, et al. Angiopoietin like-4 as a novel vascular mediator in capillary cerebral amyloid angiopathy. Brain, vol. 141, no. 12, pp. 3377–3388, 2018.

42   Shimada K, Matsushita Y, Wakabayashi K, Takahashi M, Matsubara A, Iijima Y, et al. Cloning and Functional Expression of Human Endothelin-Converting Enzyme cDNA. Biochem. Biophys. Res. Commun., vol. 207, no. 2, pp. 807–812, Feb. 1995.

43   Palmer JC, Baig S, Kehoe PG, Love S. Endothelin-Converting Enzyme-2 Is Increased in Alzheimer ' s Disease and Up-Regulated by Aß. Am. J. Pathol., vol. 175, no. 1, pp. 262–270, 2009.

44   Giwa MO, Williams J, Elderfield K, Jiwa NS, Bridges LR, Kalaria RN, et al. Neuropathologic evidence of endothelial changes in cerebral small vessel disease. Neurology, vol. 78, no. 3, pp. 167–174, 2012.

45   Staszewski J, Skrobowska E, Piusińska-Macoch R, Brodacki B, Stępień A. Cerebral and Extracerebral Vasoreactivity in Patients With Different Clinical Manifestations of Cerebral Small-Vessel Disease: Data From the Significance of Hemodynamic and Hemostatic Factors in the Course of Different Manifestations of Cerebral Small-Vessel Disease Study. J. Ultrasound Med., vol. 38, no. 4, pp. 975–987, 2019.

46   Migrino RQ, Truran S, Karamanova N, Serrano GE, Madrigal C, Davies HA, et al. Human cerebral collateral arteriole function in subjects with normal cognition, mild cognitive impairment, and dementia. Am. J. Physiol. - Hear. Circ. Physiol., vol. 315, no. 2, pp. H284–H290, 2018.

47   Peters N, Freilinger T, Opherk C, Pfefferkorn T, Dichgans M. Enhanced L-arginine-induced vasoreactivity suggests endothelial dysfunction in CADASIL. J. Neurol., vol.

255, no. 8, pp. 1203–1208, 2008.

48 de Boer I, Stam AH, Buntinx L, Zielman R, van der Steen I, van den Maagdenberg AMJM, et al. RVCL-S and CADASIL display distinct impaired vascular function. Neurology, vol. 91, no. 10, pp. e956–e963, 2018.

49 Brennan-Krohn T, Salloway S, Correia S, Dong M, De La Monte SM. Glial vascular degeneration in CADASIL. J. Alzheimer's Dis., vol. 21, no. 4, pp. 1393–1402, 2010.

50 Craggs LJL, Fenwick R, Oakley AE, Ihara M, Kalaria RN. Immunolocalization of platelet-derived growth factor receptor-β (PDGFR-β) and pericytes in cerebral autosomal dominant arteriopathy with subcortical infarcts and leukoencephalopathy (CADASIL). Neuropathol. Appl. Neurobiol., vol. 41, no. 4, pp. 557–570, 2015.

51 Tachibana H, Washida K, Kowa H, Kanda F, Toda T. Vascular Function in Alzheimer's Disease and Vascular Dementia. Am. J. Alzheimers. Dis. Other Demen., vol. 31, no. 5, pp. 437–442, 2016.

52 Moser DJ, Miller ININ, Hoth KF, Correia M, Arndt S, Haynes WG. Vascular smooth muscle function is associated with initiation and processing speed in patients with atherosclerotic vascular disease. J. Int. Neuropsychol. Soc., vol. 14, no. 4, pp. 535–541, 2008.

53 Gomis M, Sobrino T, Ois A, Millán M, Rodríguez-Campello A, de la Ossa NP, et al. Plasma β-amyloid 1-40 is associated with the diffuse small vessel disease subtype. Stroke, vol. 40, no. 10, pp. 3197–3201, 2009.

54 Kong XD, Zhang Y, Liu L, Sun N, Zhang MY, Zhang JN. Endothelial progenitor cells with Alzheimer's disease. Chin. Med. J. (Engl)., vol. 124, no. 6, pp. 901–906, 2011.

55 Nelson WN, Young JM, Borkar RN, Woltjer RL, Quinn JF, Silbert LC, et al. Role of Soluble Epoxide Hydrolase in Age-Related Vascular Cognitive Decline. Prostaglandins Other Lipid Mediat, vol 113-115, pp. 30-37, 2014.

56   Duering M, Konieczny MJ, Tiedt S, Baykara E, Tuladhar AM, van Leijsen E, et   al. Serum Neurofilament Light Chain Levels Are Related to Small Vessel Disease Burden. J Stroke, vol 20, no. 2, pp. 228-238, 2018.

Table 1 - Main Biomarkers related to endothelial dysfunction in VCI.

Category	Reference
Blood-brain barrier dysfunction markers	
↑ CSF:Plasma Albumin ratio	8
Adhesion molecules: ↑ICAM-1, VCAM-1, sICAM-1	8,9,10
Plasmatic inflammatory markers: ↑Platelet factor IV, CD40 ligand, homocysteine, interleukin-6, TNF-α, C-reactive protein	10,11,12,13
Endothelial function mediators: ↑Endothelin-1, natriuretic atrial peptide, von Willebrand factor, angiopoietin-2 ↓NO synthase	13,14,15,16,17,18
Endothelial assembly: ↑collagen type I and IV, Kallikrein 6, occludin, claudins	20,21,22
Perfusional and hemodynamic markers	
↑Vascular endothelial growth factor, transforming growth factor β	8,26
No change: Vascular endothelial growth factor	25,27
Neoangiogenesis	32,33
↓myelin-associated glycoprotein (MAG):proteolipid protein 1 ratio (hypoperfusion)	35
↑Angiopoietin like-4, Endothelin-1, Thrombomodulin, dihydroxyeicosatrienoic acid	33, 38, 40, 41
Vasoreactivity markers	
↓Cerebral vasoreactivity to CO2	42
↑Peripheral vasoreactivity	42
↓Dermal blood flow after capsaicin	45
Other Markers	
↑β-amyloid 40 (vasoconstrictive effect)	50
↓CD34 and CD 133 (endothelial progenitor cells)	51
↑ Serum NfL (neuroaxonal damage)	56

CSF, cerebral spinal fluid; ICAM-1, brain endothelial intercellular adhesion molecule 1; VCAM-1, vascular cell adhesion molecule 1; sICAM-1, plasma level of soluble intercellular adhesion molecule-1; TNF-α, tumour necrosis factor alpha; NO, nitric oxide; NfL, neurofilament light chain.
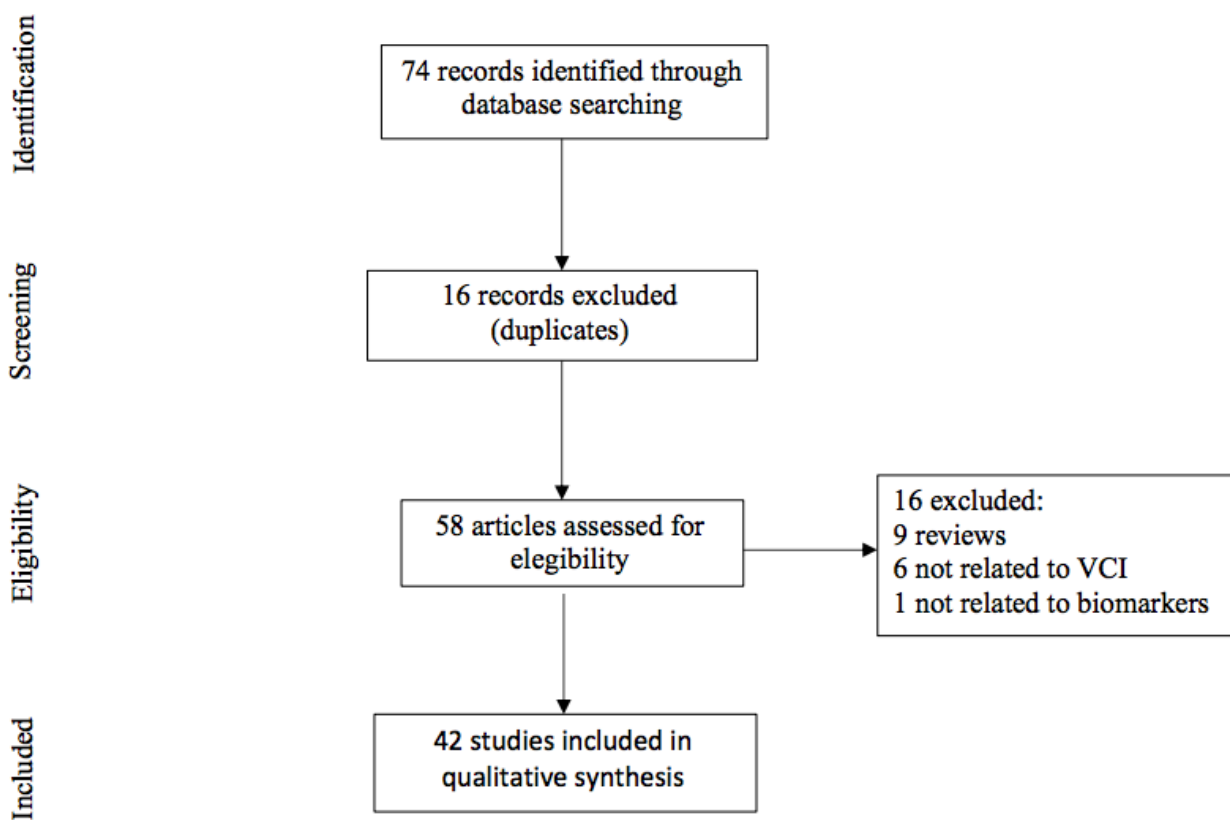
Figure 1. Flow of information through the different phases of this systematic review.
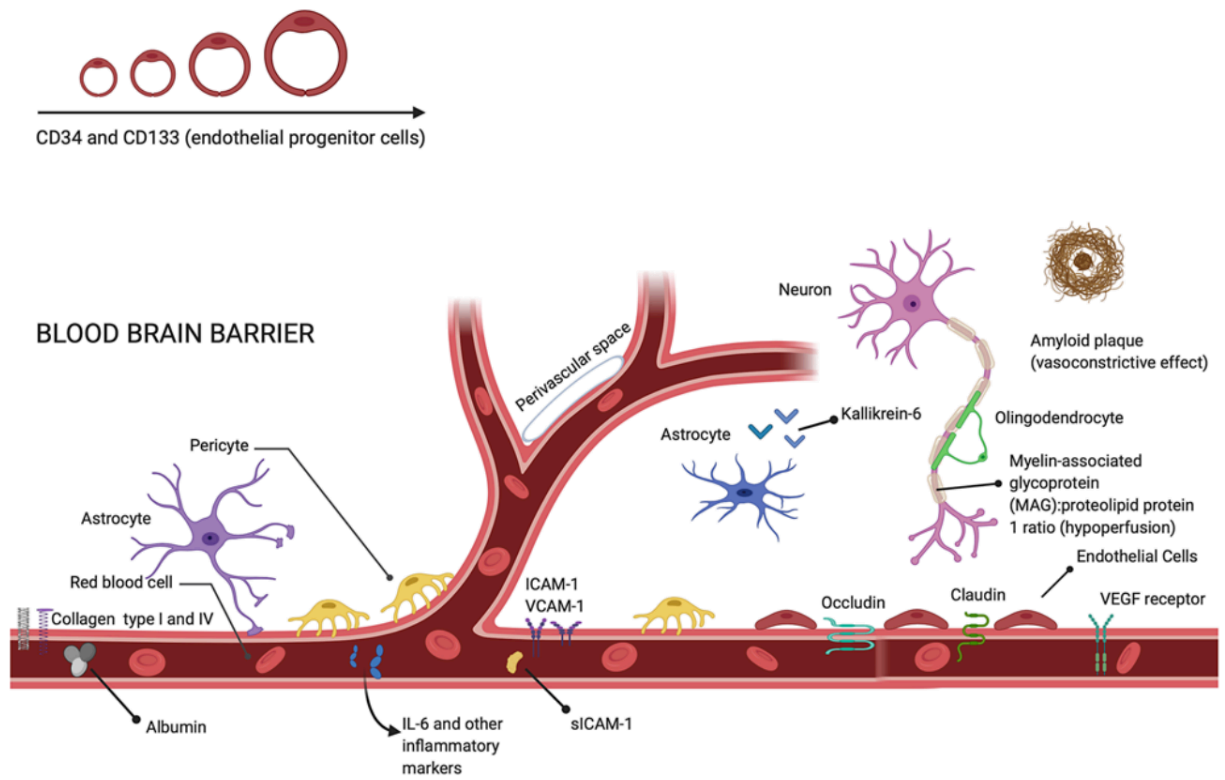VCI: vascular cognitive impairment.

Fig. 2. Schematic model illustrating some of the key markers covered in this review (customized with biorender).

Table S1. Main findings of each study included in the review.

Study, year [Reference]	Population	Number of participants	Design	Marker(s)	Source of marker	Main findings
Peters, 2008 [47]	CADASIL patients	25 cases, 24 controls	Cross-sectional	L-arginine-induced vasoreactivity	TCD	Pulsatility index and L-arginine-induced vasoreactivity was significantly increased in patients versus controls.
Staszewski, 2019 [45]	CSVD patients (lacunar stroke, vascular dementia or vascular parkinsonism)	90 cases, 30 controls	Cross-sectional	VMRr, BHI, and brachial artery FMD	US of brachial artery and TCD	CVR and FMD were reduced in response to breath-holding maneuvers in CSVD patients in comparison to matched controls.
Chakraborty, 2018 [30]	VaD and AD (with and without vascular involvement) patients	50 AD patients, 21 VaD patients and 21 controls	Cross-sectional	VEGF	CSF	VEGF levels in CSF do not reflect cerebral vascular alterations in either VaD or AD patients.
Janelidze, 2017 [9]	Patients with SCD, MCI, and with 5 major dementias types: AD, PDD, DLB, VaD, and FTD	1015 individuals in 2 cohorts	Cross-sectional and prospective	Qalb	Plasma and CSF	BBB permeability is increased in major dementia disorders but does not relate to amyloid pathology or apolipoprotein E genotype.
Ke, 2013 [28]	IS and VCI patients	50 cases, 30 controls	Cross-sectional	HIF-1α, VEGF, NGF, and BDNF	CSF	There were no significant differences in VEGF and BNDF CSF levels between IS/VCI patients and controls. They detected lower levels of HIF-1 and NGF in cases compared to controls.
Tarkowski, 2002 [29]	Patients with VaD and AD	46 patients, 27 controls	Cross-sectional	VEGF and TGF-β	CSF	Patients with AD and VaD demonstrate an intrathecal production of VEGF and TGF-β, supporting the idea that vascular factors might play a role in the pathogenesis of both these conditions.
de Boer, 2018 [48]	RVCL-S and CADASIL patients	41 patients, 26 controls	Cross-sectional	FMD (brachial artery) and dermal blood flow response to capsaicin application	US of brachial artery and laser Doppler perfusion imaging	It identified endothelial dysfunction in RVCL-S and confirmed impaired vascular smooth muscle cell relaxation in CADASIL.
Briani, 2005 [22]	VaD and AD with cerebrovascular disease (mixed dementia)	17 patients, 58 controls	Cross-sectional	HS Abs and homocysteine	Plasma	The present findings suggest that neither elevated HS Abs titres nor increased homocysteinemia may represent a useful biochemical marker for the diagnosis of VaD.
Dias, 2015 [15]	Statin-naive, normo and hyperlipidaemic subjects, AD with vascular dementia (AD-plus) and AD	50 patients (10 from each group)	Prospective	Interleukin 6, Gluthatione, TNF, 8-isoprostane F2α	Plasma	LDL-L from hypercholesterolaemic, AD and AD-plus patients are inflammatory to HMVECs. In vivo intervention with statins reduces the damaging effects of LDL-L on HMVECs.
Gomis, 2009 [53]	Patients with acute ischemic stroke due to SVD	149 patients, 25 controls	Cross-sectional	β-amyloid plasma levels (1-40, 1-42)	Plasma	Plasma β-amyloid 40 levels are independently associated with diffuse-SVD subtype.
Hao, 2009 [12]	Elderly individuals aged ≥ 60 without neurological deficits	175 subjects	Cross-sectional	sICAM-1	Plasma	Increased plasma sICAM-1 suggests inflammatory process may be involved in the pathogenesis of WML.

Holm, 2017 [17]	A population-based cohort of individuals without prevalent dementia	5347 subjects	Prospective	MR-proANP, CT-proET-1, and MR-proADM	Plasma	Elevated plasma concentration of MR-proANP is an independent predictor of all-cause and vascular dementia. Pronounced increase in CT-proET-1 indicates higher risk of vascular dementia.
Kim, 2006 [33]	VaD patients	207 patients, 207 controls	Case-control	Single nucleotide polymorphisms in VEGF gene	Plasma	This study suggests some interaction among -1154G/A, -7C/T, and 13553C/T variants in the determination risk for vascular dementia.
Kong, 2011 [54]	AD and VaD patients	64 patients, 40 controls	Cross-sectional	MCA's flow velocity and EPCs	US and plasma	Patiens with AD and VaD showed a significante decrease in CD34CD133 EPCs and lower MCA's velocity on DTC compared to controls.
Lemanska-Perek, 2009 [25]	AD and VaD patients	53 patients, 22 controls	Cross-sectional	FN	Plasma	The plasma FN molecular status seems to be a molecular additional biomarker for assessment of dementia risk.
Miralbell, 2013 [16]	Subjects older than 50 years with a moderate to high cardiovascular risk	747 subjects	Cross-sectional	CRP, resistin, ADMA, and PAI-1	Plasma	Cognitive functions associated with CRP are typically affected in VCI and overlap those related to VRF. ADMA indicated a dissociation in the cognitive profile involving verbal memory.
Pelzer, 2017 [20]	Three dutch RVCL-S families	31 patients, 64 controls	Cross-sectional	VWF antigen, VWF propeptide, and angiopoietin-2	Plasma	VWF antigen, VWF propeptide, and angiopoietin-2 might serve as early biomarkers of disease activity.
Pikula, 2013 [19]	Stroke-free Framingham offspring	2013 subjects	Prospective	ADMA	Plasma	ADMA may be a potentially useful new biomarker of subclinical vascular brain injury, which is an important correlate of vascular cognitive impairment and risk of stroke.
Qiang, 2015 [18]	Patients with DM and VaD	168 patients	Randomized controlled trial	Nitric oxide and endothelin-1	Plasma	Sancaijiangtang powders could improve the release of nitric oxide and inhibit the secretion of endothelin-1.
Solerte, 2005 [32]	AD and VaD patients	40 patients, 35 controls	Cross-sectional	VEGF	Plasma	VEGF decrease in blood and in circulating and resident cells (i.e., immune and endothelial cells) of AD subjects could impair brain perfusion and angiogenesis.
Staszewski, 2018 [14]	Adult patients with CSVD (lacunar stroke, vascular dementia, and vascular parkinsonism)	123 patients	Prospective	sICAM-1, sP-selectin, sCD40 L, PF-4, and homocysteine; combined high-sensitivity CRP, interleukin-1α and -6 and TNFα	Plasma	Endothelial dysfunction modulates the radiological progression of SVD and WMLs and lacunes are associated with different inflammatory markers .

Stott, 2001 [21]	Acute ischemic stroke (AIS) and vascular dementia patients	116 patients, 40 controls	Case-control	Fibrinogen, fibrin D-dimer, and vWF	Plasma	AIS is associated with transient changes in haemostatic factors; however, most abnormalities persist into the convalescent phase, and are also demonstrable in subjects with VaD.
Zuliani, 2008 [13]	Patients with VaD, Late onset Alzheimer's dementia (LOAD), and stroke but not dementia	180 patients, 30 controls	Cross-sectional	E-selectin and VCAM-1	Plasma	Increased sVCAM-1 levels in LOAD and VaD suggest the existence of an endothelial dysfunction in both these forms of dementia. Severe ischemic lesions were associated with increased E-selectin levels.
Ahmed-Jushuf, 2016 [31]	Older people with and without CSVD, younger patients with CADASIL and healthy subjects	19 patients, 17 controls	Cross-sectional	VEGFR2 in deep gray matter	Brain tissue	VEGFR2 is consistently expressed in small artery myocytes of older people and may mediate effects of VEGF on brain vascular aging.
Ashby, 2010 [24]	AD and VaD patients	30 patients, 15 controls	Cross-sectional	KLK6	Brain tissue	An altered KLK6 expression may contribute to vascular abnormalities in AD and VaD.
Baloyanis, 2007 [35]	VaD patients	9 patients	Observational	Climbing fibres of the cerebellar cortex	Brain tissue	Alterations of the climbing fibres of the cerebellar cortex in cases of vascular dementia might be associated with the frequently noticed difficulty in the performance of fine and skilful movements by the patients.
Barker, 2014 [37]	AD and VaD patients	66 patients, 33 controls	Cross-sectional	Ratio of myelin-associated glycoprotein to proteolipid protein 1	Brain tissue	The downregulation of endothelin 1 and upregulation of vascular endothelial growth factor in the context of reduced ratio of myelin-associated glycoprotein to proteolipid protein 1 are likely to be protective physiological responses to reduced white matter perfusion.
Brennan, 2010 [49]	CADASIL patients	5 patients, 6 controls	Cross-sectional	IGF-1, and IGF-2 receptors, Notch 1, Notch 3, and AAH	Brain tissue	CADASIL is mediated by both glial and vascular degeneration with reduced expression of IGF receptors and AAH, which regulate Notch expression and function.
Burke, 2014 [36]	Post-stroke survivors, AD, and VaD	65 patients, 13 controls	Cross-sectional	Length density (Lv, cumulative vessel length per unit tissue volume) of hippocampal microvessels	Brain tissue	The decreased vessel diameters found in AD and VaD suggests increased vasoconstriction in dementia.

214

Thomas, 2015 [38]	AD and VaD patients	37 patients, 20 controls	Cross-sectional	Amyloid-β40, amyloid-β42, vWF, and endothelin 1	Brain tissue	Abnormal vascular contractility mediated by endothelin-1 is likely to be a more important overall contributor to hypoperfusion of cerebral cortex.
Moser, 2008 [52]	Patients with AVD	80 patients	Cross-sectional	Resistance vessel function by venous occlusion plethysmography	Forearm plethysmography	Decreased vascular smooth muscle function in forearm resistance vessels was significantly associated with relatively poor initiation and processing speed in individuals with AVD.
Tachibana, 2016 [51]	AD and VaD patients	50 patients, 26 controls	Cross-sectional	FMD, (ABI), (CAVI), and (IMT)	US of arms and legs	The FMD was significantly lower in patients with AD or VaD compared to controls. There were no significant differences in ABI, CAVI, or IMT among the 3 groups.

CADASIL, cerebral autosomal dominant arteriopathy with subcortical infarcts and leukoencephalopathy; TCD, transcranial doppler; CSVD, cerebral small vessel disease; VMRr, vasomotor reactivity reserve; BHI, breath-holding index; FMD, flow-mediated dilatation; US, ultrasound; VaD, vascular dementia; AD, Alzheimer's disease; VEGF, vascular endothelial growth factor; CSF, cerebral spinal fluid; SCD, subjective cognitive decline; MCI, mild cognitive impairment; PDD, parkinson's disease dementia; LBD, lewy bodies dementia; FTD, frontotemporal dementia; Qalb, CSF/plasma albumin ratio; IS, ischemic stroke; VCI, vascular cognitive impairment; HIF-1α, hypoxia-inducible factor 1-alpha; NGF, nerve growth factor; BDNF, brain-derived neurotrophic factor; TGF-β, transforming growth factor-beta; RVCL-S, retinal vasculopathy with cerebral leukoencephalopathy and systemic manifestations; HS Abs, anti-heparan sulphate antibodies; TNF, tumour necrosis factor; HMVECs, human microvascular endothelial cells; sICAM-1, plasma level of soluble intercellular adhesion molecule-1; WML, white matter lesions; MR-proANP, pro-atrial natriuretic peptide; CT-proET-1, C-terminal endothelin-1; MR-proADM, midregional proadrenomedullin; MCA, middle cerebral artery; EPCs, endothelial progenitor cells; FN, fibronectin; ADMA, asymmetric dimethylarginine; PAI-1, plasminogen activator inhibitor 1; CRP, c-reactive protein; VRF, vascular risk factors; VWF, von Willebrand factor; DM, diabetes mellitus; sP-selectin, soluble platelet selectin; sCD40 L, CD40 ligand; PF-4, platelet factor-4; TNF-α, tumor necrosis factor-α; VCAM-1, vascular cell adhesion molecule 1; VEGFR2, immunolabeling for vascular endothelial growth factor receptor 2; KLK6, human kallikrein-related peptidase 6; IGF, insulin-like growth factor; AAH, aspartyl-(asparaginyl)-β-hydroxylase; CAA, cerebral amyloid angiopathy; PDGFR-β, immunoreactivities of the platelet-derived growth factor receptor-β; ICAM-1, brain endothelial intercellular adhesion molecule 1; BD, Binswanger's disease; DHET, 14,15-dihydroxyeicosatrienoic acid; sEH; immunoreactivity of soluble epoxide hydrolase; ECE-1 and ECE-2, endothelin-converting enzyme-1 and 2; PSD-95, postsynaptic density protein 95; SNAP-25, synaptosomal-associated protein 25; AVD, atherosclerotic vascular disease; ABI, ankle–brachial index; CAVI, cardioankle vascular index; IMT, intima–media thickness.

Appendix 4.2. "CT-Visible Convexity Subarachnoid Hemorrhage is Associated With Cortical Superficial Siderosis and Predicts Recurrent ICH"

Reference: Li Q, Zotin MCZ, Warren AD, Ma Y, Gurol E, Goldstein JN, et al. CT-visible convexity subarachnoid hemorrhage is associated with cortical superficial siderosis and predicts recurrent ICH. Neurology. 2020;96(7):10.1212/WNL.0000000000011052.

Copyright/Source: 2021, American Academy of Neurology/Wolters Kluwer Heath, Inc./ Neurology®

Article reuse license

CT-Visible Convexity Subarachnoid Hemorrhage is Associated With Cortical Superficial Siderosis and Predicts Recurrent ICH

Qi Li, MD, PhD, Maria Clara Zanon Zotin, MD, Andrew D. Warren, BA, Yuan Ma, MD, PhD, Edip Gurol, MD, Joshua N. Goldstein, MD, PhD, Steven M. Greenberg, MD, PhD, Andreas Charidimou, MD, PhD, Nicolas Raposo, MD, and Anand Viswanathan, MD, PhD

ABSTRACT

Objective: To investigate whether acute convexity subarachnoid hemorrhage (cSAH) detected on CT in lobar intracerebral hemorrhage (ICH) related to cerebral amyloid angiopathy (CAA) is associated recurrent ICH.

Methods: We analyzed data from a prospective cohort of consecutive acute lobar ICH survivors fulfilling the Boston criteria for possible or probable CAA who had both brain CT and MRI at index ICH. Presence of cSAH was assessed on CT blinded to MRI data. Cortical superficial siderosis (cSS), cerebral microbleeds, and white matter hyperintensities were evaluated on MRI. Cox proportional hazard models were used to assess the association between cSAH and the risk of recurrent symptomatic ICH during follow-up.

Results: A total of 244 ICH survivors (76.4 ± 8.7 years; 54.5% female) were included. cSAH was observed on baseline CT in 99 patients (40.5%). Presence of cSAH was independently associated with cSS, hematoma volume, and preexisting dementia. During a median follow-up of 2.66 years, 49 patients (20.0%) had recurrent symptomatic ICH. Presence of cSAH was associated with recurrent ICH (hazard ratio 2.64; 95% confidence interval 1.46–4.79; $p = 0.001$), after adjusting for age, antiplatelet use, warfarin use, and history of previous ICH.

Conclusion: cSAH was detected on CT in 40.5% of patients with acute lobar ICH related to CAA and heralds an increased risk of recurrent ICH. This CT marker may be widely used to stratify the ICH risk in patients with CAA.

Classification of evidence: This study provides Class II evidence that cSAH accurately predicts recurrent stroke in patients with CAA.

INTRODUCTION

Cerebral amyloid angiopathy (CAA) is a small vessel disease that is commonly associated with lobar intracerebral hemorrhage (ICH) in the elderly.[1] It is characterized by progressive deposition of β-amyloid peptide in the small cortical and leptomeningeal vessels and contributes to cognitive impairment.[2,3] The clinical spectrum of CAA varies widely from transient focal neurologic episodes to dementia.[4–6] Symptomatic lobar ICH is the most devastating neurologic manifestation of CAA and is associated with high morbidity and mortality. Despite recent advances in risk factor control, the risk of recurrent ICH events remains high in patients with CAA-related ICH (CAA-ICH).[7–9]

Convexity subarachnoid hemorrhage (cSAH) is a particular form of nontraumatic intracranial hemorrhage that occurs within one or a few cortical sulci at the convexity of the brain.[10] cSAH may be related to a wide spectrum of neurologic disorders ranging from cerebral vein thrombosis to reversible cerebral vasoconstriction syndrome.[3,10,11] It is increasingly recognized as an imaging marker associated with CAA and has distinct pathophysiologic traits from aneurysmal or traumatic subarachnoid hemorrhage.[12,13]

Recently, cortical superficial siderosis (cSS) has emerged as an important imaging marker for CAA according to the revised Boston criteria.[8,14,15] cSAH may be involved in cSS physiopathology and promote development of future cSS. However, they are different imaging markers of hemorrhage and our understanding of the pathophysiologic features of these 2 imaging markers remains limited.[1,7] In addition, the association between cSAH and other imaging markers of small vessel disease remains unclear. cSS is a useful MRI-based imaging marker that is associated with high risk of recurrent ICH.[7] Because cSS is an imaging marker visible only on MRI, developing a novel prognostic marker that can be assessed in the acute setting with noncontrast CT would be desirable, particularly when MRI is not available, not tolerated, or contraindicated.

In this study, we aimed to assess the association between cSAH and small vessel disease markers and to investigate whether cSAH on CT is associated with increased risk of recurrent bleeding in acute lobar ICH with CAA.

METHODS

Standard Protocol Approvals, Registrations, and Patient Consents

This study was approved by the institutional review board of Massachusetts General Hospital. Informed consent was obtained from all participants or their legal representatives.

Patient Selection

We analyzed data from a prospective observational cohort study of consecutive survivors of lobar ICH admitted to the Massachusetts General Hospital between February 1997 and November 2012. Patients were included in the study if they fulfilled the following inclusion criteria: (1) acute symptomatic lobar ICH; (2) diagnosis of definite, probable, or possible CAA based on the modified Boston criteria15; (3) available brain noncontrast CT and MRI including T2*-weighted gradient-recalled echo (T2*GRE) or susceptibility-weighted imaging (SWI) sequences performed within 10 days after symptom onset; (4) still alive at discharge; and (5) availability of follow-up data. Patients were excluded from the study if they had craniotomy before MRI or baseline CT scan. Patients with traumatic ICH were also excluded.

Data collection

The baseline clinical data including demographic, medical history, medication, and vascular risk factors were prospectively collected at the time of event using standardized data collection methods as previously described.[16] APOE genotype was determined in a subgroup of patients who consented to donate blood samples for genetic analysis.[7]

Imaging acquisition and analysis

All CT scans of the indexed event were independently reviewed by 2 readers (Q.L. and M.Z.) who were blinded to the MRI results. The volumes of parenchymal hematoma were calculated with semiautomated planimetric methods (Alice, PAREXEL International Corporation, Waltham, MA; and Analyze 10.0, Mayo Clinic, Rochester, MN). The presence of acute cSAH was visually assessed.17 cSAH was defined as linear hyperintense signal in the subarachnoid space that could be adjacent or remote from the ICH. cSAH was classified as adjacent when the bleeding was strictly confined to sulci within 1 or 2 sulci from acute ICH or as remote when cSAH was observed away from >2 unaffected sulci of acute ICH. The interrater agreement (Q.L. and M.Z.) for the

presence of cSAH was excellent (Cohen κ = 0.772). Discrepancies were settled by consensus reading after independent review of cases. Brain MRI was acquired on a 1.5T scanner and included at least fluid-attenuated inversion recovery (FLAIR) and blood sensitive sequence (T2*-weighted GRE or SWI). All MRIs were assessed by the investigators according to the Standards For Reporting Vascular Changes on Neuroimaging (STRIVE).[17] Severity of cSS was classified as focal (≤3 sulci) or disseminated (≥4 sulci) as previously described.8 Cerebral microbleeds (CMBs) were defined as small areas of signal void on T2*-weighted MRI or SWI.[17,18] White matter hyperintensities (WMH) including periventricular and deep WMH were visually assessed on the axial FLAIR images using the Fazekas rating scale.[19]

Follow-Up

The clinical data including recurrent lobar ICH and death were collected during follow-up from consenting survivors and their caregivers by telephone interview after ICH, as previously described.16 All recurrent ICH events were confirmed by brain imaging studies and medical records.

Statistical analysis

Statistical analyses were performed using SPSS (version 25.0). The baseline demographic, clinical, genetic, and imaging characteristics were compared between patients with and without cSAH, using χ^2 test, Fisher exact test, Student t test, or Mann-Whitney U test, as appropriate. We used multivariable logistic regression analysis to investigate factors associated with cSAH on CT. Multicollinearity was measured by variance inflation factors (VIFs) and tolerance. Predictors with VIF >5 were removed from the model. We determined the presence of cSAH as a predictor of recurrent ICH using Kaplan-Meier plots together with log-rank test. Data were censored after the first recurrent event for patients with multiple recurrent ICH or at the end of follow-up, whichever came first. Multivariable Cox proportional hazards models were used to calculate the hazard ratios (HRs) for recurrent ICH. The proportional hazards assumption of the Cox models were tested by graphical check and Schoenfeld residual tests. We have included prespecified plausible predictors of recurrent ICH as well as factors with p < 0.1 in univariable Cox regression analysis. All p values presented are 2 sided, with a p value of 0.05 or less considered statistically significant.

RESULTS

Of 443 lobar ICH survivors, 100 were evaluated with CT only, 18 with MRI only, and 325 with head CT followed by brain MRI. Among them, 244 patients (mean age 76.4 ± 8.7 years; 54.5% female) were eligible and were included in the final analysis. A flow diagram of patient selection is illustrated in figure 1. Compared to patients with lobar ICH evaluated with CT only, included patients with were younger (76.4 vs 78.8 years, p = 0.017) and had smaller baseline hematoma (24.1 mL vs 32.5 mL, p = 0.001). The median time from symptom onset to baseline CT scan was 1 day (interquartile range 0–2). Our final cohort consisted of 10 (4.0%) patients with pathologically proven CAA, 135 (55.3%) with probable CAA, and 99 (40.5%) with possible CAA.

In the whole cohort, cSAH was observed in 99 patients (40.5%), cSS in 50 patients (20.4%), and lobar CMBs in 135 (55.3%) patients. Of 99 patients with cSAH, 70 had strictly adjacent cSAH and 29 had remote cSAH. Compared to those without cSAH, patients with cSAH had larger baseline ICH volumes (p < 0.001), and were more likely to have prior (before index ICH) symptomatic ICH (p = 0.003), preexisting dementia (p = 0.009), and cSS (p = 0.002) (table 1). In univariable analysis, presence of cSS (odds ratio [OR] 2.72, 95% confidence interval [CI] 1.44–5.14; p = 0.002), previous history of ICH (OR 3.80, 95% CI 1.50–9.62; p = 0.005), APOE ε2 (OR 2.78, 95% CI 1.12–6.91; p = 0.028), baseline hematoma volume (OR 1.03, 95% CI 1.02–1.05; p < 0.0001), and preexisting dementia (OR 2.36, 95% CI 1.22–4.56; p = 0.01) were associated with cSAH on CT. After adjusting for age, history of prior ICH, presence of lobar CMBs, cSS, APOE ε2, and preexisting dementia remained independently associated with cSAH in multivariable logistic regression analysis (table 2).

During a median follow-up of 2.66 years (interquartile range 0.89–5.20 years), 49 of 244 patients (20.0%) had recurrent ICH. Patients who had recurrent ICH were more likely to have prior history of ICH (20.4% vs 6.7%, p = 0.003), significantly higher prevalence of cSS (32.7% vs 17.4%; p = 0.018), and cSAH (63.3% vs 34.9%; p < 0.0001) as compared with those without recurrent ICH during follow-up. The age, vascular risk factors, and presence of lobar CMBs and WMH severity was similar between the 2 patient groups.

In Kaplan-Meier analysis, the presence of cSAH on baseline CT was a predictor of recurrence of ICH (p < 0.001, by the log-rank test) (figure 2). The prespecified univariable predictors of recurrent ICH were illustrated in table 3. In univariable Cox regression analysis, presence of cSAH (HR 2.95, 95% CI 1.65–5.28; p < 0.0001), presence of cSS (HR 2.63, 95% CI 1.44–4.81; p = 0.002),

and history of previous ICH (HR 2.69, 95% CI 1.34–5.41; p = 0.005) were associated with recurrent symptomatic ICH. After adjusting for age, antiplatelet use, warfarin use, history of previous ICH, lobar CMBs, and cSS, presence of cSAH (HR 2.53, 95% CI 1.39–4.62; p = 0.002) remained significant in multivariable Cox regression model. Using a prespecified clinically applicable model controlling for age, antiplatelet use, warfarin use, and previous ICH, cSAH on CT (HR 2.64, 95% CI 1.46–4.79; p = 0.001) was an independent predictor of recurrent ICH (table 3).

In multivariable Cox regression analysis, presence of adjacent cSAH (HR 2.2, 95% CI 1.2–4.0, p = 0.008) was an independent predictor of recurrent ICH, whereas remote cSAH was not significantly associated with recurrent ICH (HR 1.7, 95% CI 0.8–3.6, p = 0.20).

DISCUSSION

Results from our prospective cohort of ICH survivors demonstrated that cSAH is detected by noncontrast CT in up to 40.5% of patients with acute lobar ICH related to CAA. The presence of cSAH is associated with several markers of CAA such as cSS and APOE e2 allele but also appears as an important prognostic marker, heralding an increased risk of recurrent ICH, independently from cSS. Because CT is the most commonly used diagnostic imaging method for patients with ICH, detection and analysis of cSAH on CT may be useful for assessment of future risk of ICH recurrence in patients with CAA, especially in resource-poor areas that have limited access to MRI. In our cohort, we found that CT-based cSAH occurred in 40.6% of patients with CAA-related ICH and was associated with cSS, a key neuroimaging marker of CAA. Our findings are consistent with recent observations showing that cSAH might be an imaging marker of CAA, which can be assessed in the acute setting of ICH.[20,21] Our findings are also in line with results from the Edinburgh CT study, which showed that cSAH detected on CT was associated with pathologically proven CAA in patients with severe ICH who died and had a research autopsy.[22]

cSAH, cSS, and lobar CMBs are all imaging markers associated with CAA.[1,2,23] In our study, we have explored the relationship among these 3 important imaging markers of CAA. We found that cSS, but not CMB, was associated with cSAH. Consistent with previous reports, our findings suggest that cSS and cSAH are likely 2 neuroimaging markers of a single pathophysiologic process and may represent subarachnoid hemorrhage in patients with CAA.[2,24–27] However, lobar CMB may represent a distinct disease subtype from cSS and cSAH.

Although a possible link between cSS and cSAH is proposed, the underlying mechanism is unclear. cSAH may occur as direct extension of lobar hematoma into the adjacent sulci or could be the result of leakage of meningeal vessels into the sulci.[26,27] Previous study suggested that cSAH may present with transient focal neurologic episodes when occurring in eloquent areas.[28] Individuals with CAA who are prone to develop cSAH would therefore likely have higher burden of cSS as many cSAH events in noneloquent areas would not come to clinical attention.

Our findings suggest that cSAH visible on CT is a strong predictor of recurrent ICH, independently from other predictors such as cSS, APOE, and previous symptomatic ICH.[29] In a recent study, we found that cSAH on MRI is a predictor of recurrent ICH after a CAA-ICH.[30] Results from this current study suggested that CT-visible cSAH was an independent prognostic factor of recurrent ICH, and extend MRI findings to patients with ICH evaluated with CT. Because MRI cannot be performed in many ICH cases because MRI is not available, not tolerated, or contraindicated, this CT-based prognostic marker could be widely used in clinical practice to assess the risk of recurrent ICH. Furthermore, we have observed a strong link between cSAH and preexisting dementia that has not been reported before. This may suggest that individuals with preexisting dementia have a higher small vessel disease burden and could be identified with cSAH. Our findings, together with previous reports, suggest that cSAH and cSS are both key hemorrhagic markers of recurrent ICH in patients with CAA. We were interested to observe that adjacent SAH was more strongly associated with recurrent ICH. A possible mechanism might be that adjacent SAH reflects a cascade of rupture of adjacent CAA-laden surface vessels due to pressure and cracking, whereas remote cSAH is less likely to be affected and might occur as a result of redistribution of blood in the subarachnoid space.

Our study has several potential limitations. First, it is a retrospective analysis of a prospectively collected single-center cohort and the sample size is relatively small. Second, we have included patients with both CT and MRI, which may lead to potential selection bias toward less severe ICH cases. Third, we only evaluated cSAH in CAA-related ICH survivors; whether our findings are generalizable to all patients with lobar ICH remains to be investigated in the future. Future studies with larger sample size are needed to validate our findings.

Our study demonstrated that cSAH is associated with cSS but not lobar CMBs. cSAH and cSS might be imaging markers that reflect increased vascular fragility in patients with CAA that makes them prone to develop large hemorrhages. Although MRI is increasingly used for imaging of ICH,

CT is more widely available in almost all institutions worldwide that hospitalize patients with ICH. CT cSAH seems to be a strong imaging marker associated with recurrent ICH in patients with CAA and might be used to stratify the risk of recurrent bleeding in patients with ICH with only CT scans.

References:

1. Viswanathan A, Greenberg SM. Cerebral amyloid angiopathy in the elderly. Ann Neurol 2011;70:871–880.
2. Charidimou A, Gang Q, Werring DJ. Sporadic cerebral amyloid angiopathy revisited: recent insights into pathophysiology and clinical spectrum. J Neurol Neurosurg Psychiatry 2012;83:124–137.
3. Wilson D, Hostettler IC, Ambler G, Banerjee G, Jager HR, Werring DJ. Convexity subarachnoid haemorrhage has a high risk of intracerebral haemorrhage in suspected cerebral amyloid angiopathy. J Neurol 2017;264:674.
4. Moulin S, Labreuche J, Bombois S, et al. Dementia risk after spontaneous intracerebral haemorrhage: a prospective cohort study. Lancet Neurol 2016;15: 820–829.
5. Cordonnier C, Leys D, Dumont F, et al. What are the causes of pre-existing dementia in patients with intracerebral haemorrhages? Brain 2010;133:3281–3289.
6. Charidimou A, Peeters A, Fox Z, et al. Spectrum of transient focal neurological episodes in cerebral amyloid angiopathy multicentre magnetic resonance imaging cohort study and meta-analysis. Stroke 2012;43:2324–2330.
7. Roongpiboonsopit D, Charidimou A, William CM, et al. Cortical superficial siderosis predicts early recurrent lobar hemorrhage. Neurology 2016;87:1863–1870.
8. Charidimou A, Boulouis G, Boulouis G, et al. Cortical superficial siderosis multifocality in cerebral amyloid angiopathy: a prospective study. Neurology 2017;89: 2128–2135.
9. Linn J, Wollenweber FA, Lummel N, et al. Superficial siderosis is a warning sign for future intracranial hemorrhage. J Neurol 2013;260:176–181.

10. Kumar S, Goddeau RP, Selim MH, et al. Atraumatic convexal subarachnoid hemorrhage clinical presentation, imaging patterns, and etiologies. Neurology 2010;74: 893–899.

11. Refai D, Botros JA, Strom RG, Derdeyn CP, Sharma A, Zipfel GJ. Spontaneous isolated convexity subarachnoid hemorrhage: presentation, radiological findings, differential diagnosis, and clinical course clinical article. J Neurosurg 2008;109: 1034–1041.

12. Martinez-Lizana E, Carmona-Iragui M, Alcolea D, et al. Cerebral amyloid angiopathy related atraumatic convexal subarachnoid hemorrhage: an aria before the tsunami. J Cereb Blood Flow Metab 2015;35:710–717.

13. Beitzke M, Enzinger C, Wunsch G, Asslaber M, Gattringer T, Fazekas F. Contribution of convexal subarachnoid hemorrhage to disease progression in cerebral amyloid angiopathy. Stroke 2015;46:1533–1540.

14. Wollenweber FA, Opherk C, Zedde M, et al. Prognostic relevance of cortical superficial siderosis in cerebral amyloid angiopathy. Neurology 2019;92: e792–e801.

15. Linn J, Halpin A, Demaerel P, et al. Prevalence of superficial siderosis in patients with cerebral amyloid angiopathy. Neurology 2010;74:1346–1350.

16. O'Donnell HC, Rosand J, Knudsen KA, et al. Apolipoprotein e genotype and the risk of recurrent lobar intracerebral hemorrhage. N Engl J Med 2000;342:240–245.

17. Wardlaw JM, Smith EE, Biessels GJ, et al. Neuroimaging standards for research into small vessel disease and its contribution to ageing and neurodegeneration. Lancet Neurol 2013;12:822–838.

18. Greenberg SM, Vernooij MW, Cordonnier C, et al. Cerebral microbleeds: a guide to detection and interpretation. Lancet Neurol 2009;8:165–174.

19. Fazekas F, Chawluk JB, Alavi A, Hurtig HI, Zimmerman RA. MR signal abnormalities at 1.5 T in Alzheimer's dementia and normal aging. AJR Am J Roentgenol 1987;149: 351–356.

20. Raposo N, Calviere L, Cazzola V, et al. Cortical superficial siderosis and acute convexity subarachnoid hemorrhage in cerebral amyloid angiopathy. Eur J Neurol 2018; 25:253–259.

21. Viguier A, Raposo N, Patsoura S, et al. Subarachnoid and subdural hemorrhages in lobar intracerebral hemorrhage associated with cerebral amyloid angiopathy. Stroke 2019;50:1567–1569.

22. Rodrigues MA, Samarasekera N, Lerpiniere C, et al. The Edinburgh CT and genetic diagnostic criteria for lobar intracerebral haemorrhage associated with cerebral amyloid angiopathy: model development and diagnostic test accuracy study. Lancet Neurol 2018;17:232–240.

23. Van Veluw SJ, Charidimou A, Van der Kouwe AJ, et al. Microbleed and microinfarct detection in amyloid angiopathy: a high-resolution MRI-histopathology study. Brain 2016;139:3151–3162.

24. Moulin S, Casolla B, Kuchcinski G, et al. Cortical superficial siderosis: a prospective observational cohort study. Neurology 2018;91:e132–e138.

25. Calviere L, Cuvinciuc V, Raposo N, et al. Acute convexity subarachnoid hemorrhage related to cerebral amyloid angiopathy: clinicoradiological features and outcome. J Stroke Cerebrovasc 2016;25:1009–1016.

26. Takeda S, Yamazaki K, Miyakawa T, et al. Subcortical hematoma caused by cerebral amyloid angiopathy: does the first evidence of hemorrhage occur in the subarachnoid space? Neuropathology 2003;23:254–261.

27. Ni J, Auriel E, Jindal J, et al. The characteristics of superficial siderosis and convexity subarachnoid hemorrhage and clinical relevance in suspected cerebral amyloid angiopathy. Cerebrovasc Dis 2015;39:278–286.

28. Charidimou A, Boulouis G, Fotiadis P, et al. Acute convexity subarachnoid haemorrhage and cortical superficial siderosis in probable cerebral amyloid angiopathy without lobar haemorrhage. J Neurol Neurosurg Psychiatry 2018;89:397–403.

29. Charidimou A, Zonneveld HI, Shams S, et al. APOE and cortical superficial siderosis in CAA: meta-analysis and potential mechanisms. Neurology 2019;93:e358–e371.

30. Raposo N, Charidimou A, Roongpiboonsopit D, et al. Convexity subarachnoid hemorrhage in lobar intracerebral hemorrhage. Neurology 2020;94:e968–e977.

Table 1. Baseline demographic, clinical, and imaging characteristics of patients with vs. without convexity subarachnoid hemorrhage.

	Patients with cSAH(N=99)	Patients without cSAH(N=145)	p-value
Demographics			
Age, mean ± SD	77.2 ± 6.3	76.5 ± 9.2	0.595
Female, No. (%)	54(54.5)	75 (51.7)	0.665
Clinical characteristics			
Hypertension, No. (%)	62(62.5)	37(37.4)	0.643
Previous symptomatic ICH, No. (%)	16 (16.2)	7 (4.8)	0.003
Warfarin use, No. (%)	10 (10.1)	18 (12.4)	0.578
Antiplatelet use, No. (%)	37 (37.4)	65 (44.8)	0.246
Dementia diagnosis, n (%)	26 (26.3%)	19(13.1%)	0.009
Imaging characteristics			
ICH volume (mL), median [IQR]	25.2[15.4-42.1]	15.1 [6.4-30.0]	<0.001
Presence of IVH, No. (%)	26 (26.3)	28 (19.3)	0.199
Presence of EDH, No.(%)	20(20.2)	14(9.7)	0.019
Presence of cSS, No. (%)	30 (30.3)	20 (13.8)	0.002
Focal cSS, No. (%)	15(15.2)	11 (7.6)	0.060
Disseminated cSS, No. (%)	15 (15.2)	9 (6.2)	0.021
Presence of lobar CMB, No. (%)	58 (58.6)	77 (53.1)	0.398
Lobar CMB count, median [IQR]	1 [0-3]	1 [0-4]	0.938
Lobar CMB count >5, No. (%)	13(13.1)	30 (20.7)	0.128
Lobar CMB count >10, No. (%)	10(10.1)	18(12.4)	0.578
Fazekas WMH score, median [IQR]	4 [2-5]	4 [3-5]	0.247
APOE ε2 (≥ 1 copy) [a], No. (%)	15(26.3)	9(11.4)	0.024
APOE ε4 (≥ 1 copy) [a], No. (%)	23(40.4)	25(31.6)	0.295

Abbreviations: CMB = cerebral microbleeds; cSAH = subarachnoid hemorrhage; cSS = cortical superficial siderosis; ICH = intracerebral hemorrhage; IQR = interquartile range; IVH = intraventricular hemorrhage; SD = standard deviation; WMH = white matter hyperintensities.
[a] 136 patients consented for APOE genotype testing

Table 2. Univariable and multivariable regression analyses of predictors of cSAH in cerebral amyloid angiopathy-related intracerebral hemorrhage (CAA-ICH).

Variables	OR	95% CI	p-value
Univariable			
cSS presence	2.72	1.44-5.14	0.002
Presence of Lobar CMB	1.25	0.75-2.09	0.398
Previous Symptomatic ICH (other than index ICH)	3.80	1.50-9.62	0.005
Age (per each year increase)	1.00	0.97-1.03	0.847
Antiplatelet use	0.73	0.44-1.24	0.247
Warfarin use	0.78	0.35-1.80	0.578
Preexisting dementia	2.36	1.22-4.56	0.01
APOE ε2 (≥ 1 copy)	2.78	1.12-6.91	0.028
APOE ε4 (≥ 1 copy)	1.46	0.72-2.97	0.295
Prespecified Multivariable Model			
Age	1.00	0.96-1.05	0.947
Previous ICH	1.44	0.35-5.97	0.616
Dementia	8.51	2.58-28.13	<0.001
cSS presence	3.53	1.12-11.15	0.032
Lobar CMB presence	0.93	0.39-2.22	0.870
APOE ε2 (≥ 1 copy)	3.11	1.07-8.99	0.037
Baseline ICH volume	1.04	1.01-1.06	0.002

Abbreviations: CI = confidence interval; CMB = cerebral microbleeds; cSAH = subarachnoid hemorrhage; cSS = cortical superficial siderosis; OR = odds ratio; ICH = intracerebral hemorrhage.

Table 3. Prespecified univariable and multivariable regression analyses of predictors of recurrent ICH in cerebral amyloid angiopathy-related ICH.

Variables	HR	95% CI	p-value
Univariable			
Age (per each year increase)	1.01	0.98-1.05	0.536
Anti platelet use	0.82	0.46-1.46	0.504
Warfarin use	0.51	0.16-1.63	0.253
Presence of cSAH	2.95	1.65-5.28	<0.0001
Presence of cSS	2.63	1.44-4.81	0.002
Presence of Lobar CMB	1.37	0.77-2.46	0.281
Previous Symptomatic ICH	2.69	1.34-5.41	0.005
Prespecified multivariable model I			
Age	1.00	0.97-1.04	0.723
Antiplatelet use	0.82	0.46-1.48	0.514
Warfarin use	0.57	0.17-1.89	0.360
Previous ICH	1.36	0.59-3.15	0.467
cSS presence	2.01	0.99-4.10	0.053
cSAH on CT	2.53	1.39-4.62	0.002
Lobar CMB presence	1.01	0.53-1.95	0.973
Prespecified multivariable model II			
Age	1.01	0.97-1.05	0.640
Antiplatelet use	0.82	0.46-1.47	0.511
Warfarin use	0.57	0.17-1.87	0.354
Previous ICH	1.94	0.93-4.02	0.076
cSAH on CT	2.64	1.46-4.79	0.001

Abbreviations: CI = confidence interval; cSAH = subarachnoid hemorrhage; cSS = cortical superficial siderosis; CMB = cerebral microbleeds; HR = hazard ratio; ICH = intracerebral hemorrhage.
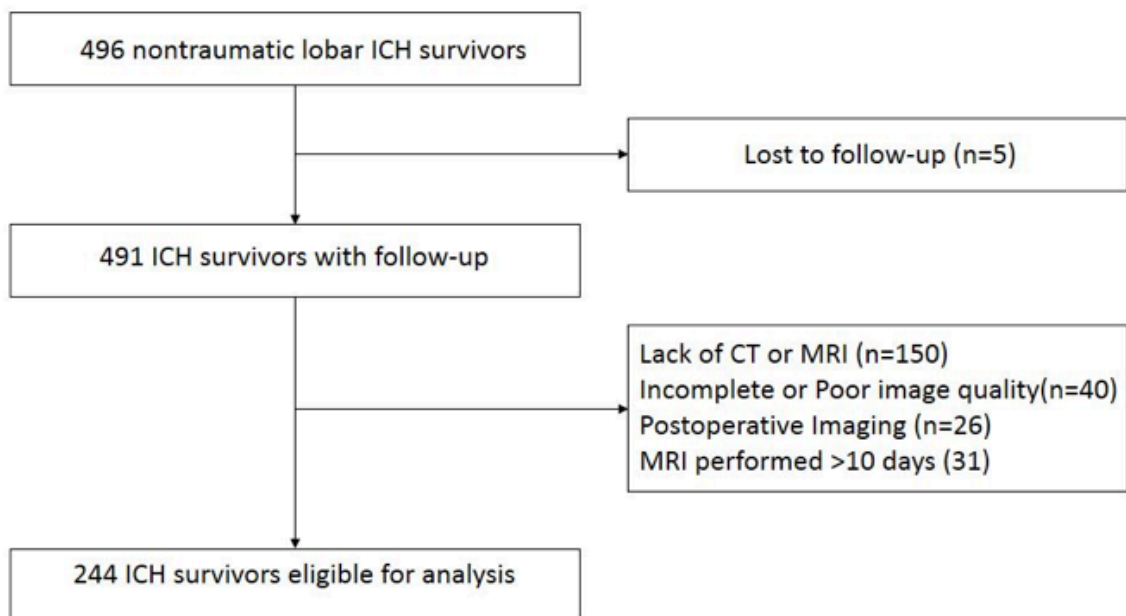
Figure 1 Flow diagram of patient selection


```
┌─────────────────────────────────────────┐
│  496 nontraumatic lobar ICH survivors    │
└─────────────────────────────────────────┘
                    │
                    │────────────►┌────────────────────────┐
                    │             │  Lost to follow-up (n=5)│
                    ▼             └────────────────────────┘
┌─────────────────────────────────────────┐
│   491 ICH survivors with follow-up       │
└─────────────────────────────────────────┘
                    │
                    │────────────►┌──────────────────────────────────┐
                    │             │ Lack of CT or MRI (n=150)        │
                    │             │ Incomplete or Poor image quality │
                    │             │ (n=40)                           │
                    │             │ Postoperative Imaging (n=26)     │
                    ▼             │ MRI performed >10 days (31)      │
┌─────────────────────────────────────────┐└──────────────────────────────────┘
│  244 ICH survivors eligible for analysis │
└─────────────────────────────────────────┘
```

Figure 2   Recurrent Intracerebral Hemorrhage in patients with and without CT convexity subarachnoid Hemorrhage.
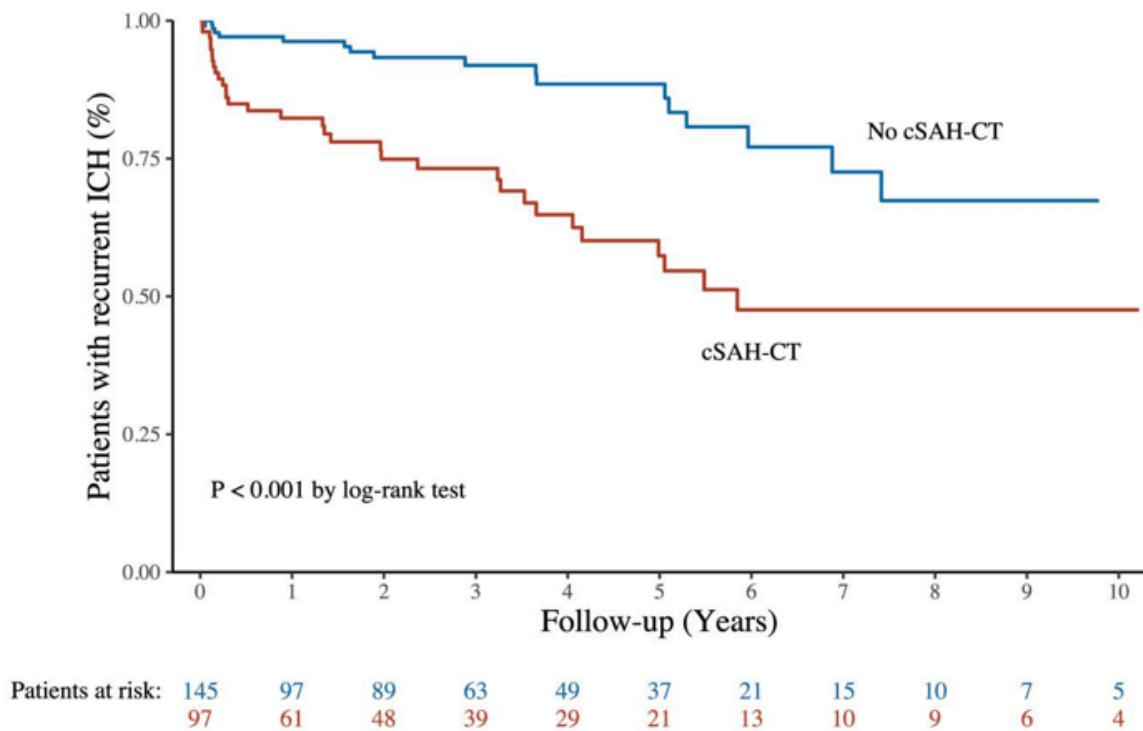
Kaplan-Meier curve estimates time to recurrent symptomatic ICH according to the presence or absence of convexity subarachnoid hemorrhage on baseline CT in all patients with cerebral amyloid angiopathy intracerebral hemorrhage.

Appendix 4.3. "Association of Memory Impairment With Concomitant Tau Pathology in Patients With Cerebral Amyloid Angiopathy"

Reference: Schoemaker D, Charidimou A, Zotin MCZ, Raposo N, Johnson KA, Sanchez JS, et al. Association of Memory Impairment With Concomitant Tau Pathology in Patients With Cerebral Amyloid Angiopathy. Neurology. 2021;96(15):e1975–86.

Copyright/Source: 2021, American Academy of Neurology/ Neurology®/ Wolters Kluwer Health, Inc.

Article reuse license

Association of Memory Impairment With Concomitant Tau Pathology in Patients With Cerebral Amyloid Angiopathy

Dorothee Schoemaker, PhD, Andreas Charidimou, MD, PhD, Maria Clara Zanon Zotin, MD, Nicolas Raposo, MD, PhD, Keith A. Johnson, MD, Justin S. Sanchez, BA, Steven M. Greenberg, MD, PhD, and Anand Viswanathan, MD, PhD

Objective Relying on tau-PET imaging, this cross-sectional study explored whether memory impairment is linked to the presence of concomitant tau pathology in individuals with cerebral amyloid angiopathy (CAA).

Methods Forty-six patients with probable CAA underwent a neuropsychological examination and an MRI for quantification of structural markers of cerebral small vessel disease. A subset of these participants also completed a [11C]-Pittsburgh compound B (n = 39) and [18F]-flortaucipir (n = 40) PET for in vivo estimation of amyloid and tau burden, respectively. Participants were classified as amnestic or nonamnestic on the basis of neuropsychological performance. Statistical analyses were performed to examine differences in cognition, structural markers of cerebral small vessel disease, and amyloid- and tau-PET retention between participants with amnestic and those with nonamnestic CAA.

Results Patients with probable CAA with an amnestic presentation displayed a globally more severe profile of cognitive impairment, smaller hippocampal volume ($p < 0.001$), and increased tauPET binding in regions susceptible to Alzheimer disease neurodegeneration ($p = 0.003$) compared to their nonamnestic counterparts. Amnestic and nonamnestic patients with CAA did not differ on any other MRI markers or on amyloid-PET binding. In a generalized linear model including all evaluated neuroimaging markers, tau-PET retention ($\beta = -0.85$, $p = 0.001$) and hippocampal volume ($\beta = 0.64$ $p = 0.01$) were the only significant predictors of memory performance. The cognitive profile of patients with CAA with an elevated tau-PET retention was distinctly characterized by a significantly lower performance on the memory domain ($p = 0.004$).

Conclusions

These results suggest that the presence of objective memory impairment in patients with probable CAA could serve as a marker for underlying tau pathology.

Introduction

Cerebral amyloid angiopathy (CAA), a condition characterized by the microvascular deposition of amyloid in leptomeningeal and cortical vessels, is a key contributor to vascular cognitive impairment and dementia.[1] While CAA is a common accompanying feature of Alzheimer disease,[2-4] it is an independent neuropathologic condition, with more than half of CAA cases presenting without concomitant Alzheimer disease–related tau pathology.[5] Clinically, differentiating patients with CAA presenting with or without concomitant tau pathology could have important implications for therapeutic approaches and prognosis.

Previous studies in patients with Alzheimer disease have shown that memory performance is closely related to the severity of tau-mediated neuropathologic alterations in the medial temporal lobes and predicts impending cognitive decline.[6-8] Given this evidence, the presence of objective memory deficits in patients with CAA could provide relevant information on underlying neuropathologic processes and hint to an increased severity of concomitant tau pathology.

In the present study, we compare neuroimaging features of patients with probable CAA presenting with or without objective memory impairment. Leveraging recent advances in PET, we further contrast levels of amyloid ([11C]-Pittsburgh compound-B amyloid-PET) and tau ([18F]-flortaucipir tau-PET) aggregation in patients with CAA with and without memory impairment to examine the presumed nature and severity of underlying neuropathologic processes in these 2 groups. We specifically hypothesized that the presence of memory impairment in individuals with CAA is associated with an increased likelihood of concomitant tau pathology and would hence be reflected by increased tau PET binding and medial temporal lobe neurodegeneration.

Methods

The primary research question of this study was to determine whether objective memory impairment was related to neuroimaging markers of tau pathology, including tau-PET retention and medial temporal lobe neurodegeneration, in asymptomatic individuals without dementia with CAA (Class II evidence).

Study Design

This is a cross-sectional study from a single-center prospective memory clinic research cohort

Standard Protocol Approvals, Registrations, and Patient Consents

All research procedures were reviewed and approved by the Institutional Review Board of Massachusetts General Hospital. Written informed consent was obtained from all participants, and research procedures were conducted in accordance with the Declaration of Helsinki.

Participants

Participants were drawn from an ongoing research cohort of patients with CAA at Massachusetts General Hospital. Participants enrolled in this cohort were recruited from a memory clinic affiliated with the Massachusetts Alzheimer's Disease Research Center. Inclusion criteria for cohort enrollment were: suspected diagnosis of CAA based on clinical neuroimaging, age >55 years (no upper limit), ability and willingness to provide written informed consent, no history of symptomatic or asymptomatic intracerebral hemorrhage, no contraindication for MRI (e.g., cranial metallic implant, cardiac pacemaker, severe claustrophobia), and absence of unstable medical illness (e.g., unstable angina, advanced renal or liver failure).

For the present study, we selected participants who (1) were enrolled in the cohort between November 2016 and July 2019; (2) completed a research MRI; (3) completed a neuropsychological evaluation; (4) met criteria for mild cognitive impairment (MCI), as determined from neurologic and neuropsychological examinations confirming the presence of objective cognitive deficits and the absence of functional impairment in daily life activities[9]; and (5) fulfilled the modified Boston criteria for probable CAA,[10,11] as determined from MRI findings confirming the presence of multiple cerebral microbleeds restricted to lobar, cortical, or corticosubcortical regions or a single lobar, cortical, or corticosubcortical microbleed accompanied by evidence of cortical superficial siderosis. A subgroup of included participants completed PET scans for in vivo estimation of amyloid ([11C]-Pittsburgh compound B amyloid-PET, n = 39) and tau ([18F]-flortaucipir tau-PET, n = 40) pathology. A flowchart summarizing the selection process of study participants is presented in figure 1.

Neuropsychological evaluation and characterization of amnestic status

All participants completed a detailed neuropsychological evaluation. Global cognitive status was assessed with the MiniMental State Examination (MMSE).[12] Using standardized neuropsychological tests, we assessed the following cognitive domains: (1) memory (Hopkins Verbal Learning Test, total immediate recall and delayed recall; Free and Cued Selective Reminding Test, free recall and free

and cued recall)[13,14]; (2) attention/processing speed (Wechsler Adult Intelligence Scale–III Digit Symbol-Coding; Trail Making Test A, Digit Span Forward)[15,16]; (3) language/semantics (Boston Naming Test, 15 items, Semantic Fluency, Animals)[17,18]; (4) executive function (Controlled Oral Word Association Test, Trail Making Test B, Digit Span Backward)[15,16,18]; and (5) visuospatial processing (Benton Facial Recognition Test, short form; Benton Judgment of Line Orientation, 30 items).[19] With the use of published normative data, the raw performance on each test was converted to a z score adjusted for age, sex, and education. The z scores were averaged across tests included in a given cognitive domain to create domain-specific composite scores.

Participants with CAA were classified as amnestic or nonamnestic with the use of a previously recommended comprehensive criteria approach.[20] Precisely, participants with at least 2 performances falling below a z score of −1.0 within the memory domain were categorized as amnestic (amnestic CAA), while other participants were classified as nonamnestic (nonamnestic CAA).

MRI acquisition

All participants included in the study completed a 3T research MRI (Siemens Healthcare, Magnetom Prisma-Fit) at the Massachusetts General Hospital with a 32-channel head coil. The MRI procedure was performed within 3 months of the neuropsychological evaluation (median 0.0 days). The MRI protocol included a T1-weighted sagittal multiecho magnetization-prepared rapid acquisition with gradient echo (repetition time 2,510 milliseconds, echo time 1.69 milliseconds, voxel size $1 \times 1 \times 1$ mm), fluid-attenuated inversion recovery (repetition time 5,000 milliseconds, echo time 356 milliseconds, voxel size $0.94 \times 0.94 \times 0.9$ mm), and susceptibility-weighted imaging (repetition time 30 milliseconds, echo time 20 milliseconds, voxel size $0.86 \times 0.86 \times 1.4$ mm).

Quantification of MRI markers of SVD

MRI markers of cerebral small vessel disease were quantified in accordance with published expert guidelines (Standards for Reporting Vascular Changes on Neuroimaging recommendations).[21] In brief, cerebral microbleeds were identified on susceptibility-weighted MRIs and counted across the brain to obtain a total cerebral microbleeds count. Lacunes of presumed vascular origin (i.e., lacunes) were identified on fluidattenuated inversion recovery images as ovaloid areas of signal hypointensity and counted across the brain. The presence of cortical superficial siderosis was assessed on susceptibility weighted MRIs according to newly proposed criteria[22] and transformed into a

dichotomous variable according to its presence or absence. The FreeSurfer volumetric pipeline (version 6.0)[23] was used to automatically segment T1 anatomical MRIs (i.e., magnetization-prepared rapid acquisition with gradient echo) and to obtain the volume of white matter hyperintensity (i.e., white matter hypointensities), the total brain volume (i.e., brain segmentation volume), the left and right hippocampal volumes, and the estimated total intracranial volume. Automated segmentations were visually inspected to ensure validity. To account for variation in brain sizes, the volume of white matter hyperintensity was normalized to the total brain volume: (white matter hyperintensity volume/total brain volume) × 100. To obtain an estimation of global brain atrophy, the brain parenchymal fraction was estimated by computing the ratio of the total brain volume to the total intracranial volume: (total brain volume/estimated total intracranial volume) × 100. Finally, to obtain an estimation of medial temporal lobe atrophy, we computed the ratio of the bilateral hippocampal volume to the total intracranial volume: normalized total hippocampal volume = [(right + left hippocampal volumes)/estimated total intracranial volume] × 1,000.

PET acquisition

PET scans were acquired on a Siemens/CTI (Knoxville, TN) ECAT HR+ (3-dimensional mode, 63 image planes, 15.2-cm axial field of view, 5.6-mm transaxial resolution, 2.4-mm slice interval) at the Massachusetts General Hospital. PET scans were performed within 6 months of the neuropsychological evaluation (median 69.0 days for amyloid-PET and 69.0 days for tau-PET) and MRI scan (median 66.0 days for amyloidPET and 69.2 days for tau-PET). For amyloid-PET imaging, [11C]-Pittsburgh compound B was prepared at the Massachusetts General Hospital, and PET data were acquired according to previously published protocols.[24] Briefly, 8.5 to 15 mCi of [11C]-Pittsburgh compound B was injected as a bolus followed immediately by a 60- to 70-minute dynamic acquisition in 69 frames. For tau-PET imaging, [18F]- flortaucipir was prepared at the Massachusetts General Hospital, and PET data were acquired from 80 to 100 minutes (4 × 5-minute frames) after a 9.0- to 11.0-mCi bolus injection.[25]

Analysis of PET data

PET data were reconstructed, corrected for attenuation, and inspected to verify adequate count statistics and absence of significant head motion. Postacquisition processing was performed with a FreeSurfer-based pipeline (version 6.0). PET images were first aligned to FreeSurfer-processed T1

images, and measurements were made in regions of interest (ROIs) defined by the Desikan-Killiany atlas.[26]

For quantification of amyloid load, [11C]-Pittsburgh compound B amyloid-PET–specific binding was expressed as the distribution volume ratio (DVR) using the Logan graphical method applied to data collected 40 to 60 minutes after injection, with the cerebellar cortex as the reference region.[27,28] DVRs were then extracted in an aggregate ROI consisting of the frontal, lateral temporal/parietal, and retrosplenial cortex (FLR). This ROI was selected on the basis of previous publications demonstrating an increased Pittsburgh compound B-PET retention in these regions in both sporadic Alzheimer disease and CAA.[29,30] Finally, using a previously established cutoff score showing increased sensitivity to the early detection of abnormal β-amyloid levels (i.e., FLR DVR 1.08), participants were classified as either positive or negative amyloid-PET.[31] In the analyses, we used amyloid-PET FLR DVRs not corrected for partial volume effects. However, to ensure that the lack of partial volume correction did not bias our results, we also examined DVRs corrected for partial volume effects using an established approach.[32,33]

For quantification of tau load, [18F]-flortaucipir tau-PET– specific binding was expressed as standardized uptake value ratios (SUVRs) based on data collected 80 to100 minutes after injection, with the cerebellar cortex used as the reference region. Following a previously described method, SUVR measurements were extracted from an aggregate ROI comprising Alzheimer disease cortical signature regions (ADCortSig SUVR), including the entorhinal cortex, fusiform gyrus, inferior, middle, and superior temporal gyri, superior and inferior parietal lobules, posterior cingulate, and precuneus.[34,35] Prior work has demonstrated that these regions are affected at an early stage in Alzheimer disease and are associated with increased levels of tau pathology.[34,35] As a supplementary analysis, tau-PET SUVRs were also extracted from other potential ROIs.[36] Finally, using a previously established cutoff score (i.e., ADCortSig SUVR 1.19), we classified participants as either positive or negative tau-PET.[35] Tau-PET SUVRs presented in the main text were not corrected for partial volume. However, to ensure that this did not bias our results, tau-PET SUVRs corrected for partial volume using an established approach were also examined.[32,33]

Statistical analysis

Statistical analyses were performed with the SPSS version 24.0 (SPSS Inc, Chicago, IL) and R version 3.6.3 (R Foundation for Statistical Computing, Vienna, Austria).

We compared demographic, clinical, and cognitive characteristics between individuals with amnestic and those with nonamnestic CAA using $\chi2$ tests for dichotomous variables and 1-way analyses of variance for continuous variables. Because of their nonparametric distributions, group differences in MRI markers of cerebral small vessel disease were assessed with generalized linear models (GLMs), with age and sex as additional covariates. For count variables (cerebral microbleeds count, lacunes count), we fitted GLMs with a Poisson distribution. For nonparametric continuous variables (normalized white matter hyperintensity volume, brain parenchymal fraction, normalized total hippocampal volume), we fitted GLMs with a gamma distribution and a log link function. Finally, for dichotomous variables (presence of cortical superficial siderosis), we fitted the GLM with a binomial distribution.

In participants with available PET data, group differences in amyloid-PET (FLR DVR) and tau-PET (ADCortSig SUVR) retention were analyzed with GLMs fitted with a gamma distribution and a log link function. To ensure that group differences were not driven by confounds associated with the severity of cerebral small vessel disease or demographic features, we also compared amyloid- and tau-PET retention between amnestic and nonamnestic CAA in similar GLMs adjusting for all quantified MRI markers of cerebral small vessel disease, age, and sex. Finally, group differences in the frequency of participants with positive amyloid- or tau-PET were assessed in GLMs with a binomial distribution.

The association between memory performance and all neuroimaging markers was first assessed in separate univariate GLMs with a gaussian distribution. The statistical significance of each model was adjusted for the total numbers of univariate tests performed, according to the Bonferroni correction (corrected p value = p value $\times$ 8, for the 8 tests performed). The combined influence of PET (amyloid-PET FLR DVR, tau-PET ADCortSig SUVR) and MRI markers on memory performance was also assessed in a multivariate GLM fitted with a gaussian distribution. Because cognitive scores were already adjusted for, age, sex, and education level, these variables were not additionally included in the model. To obtain an estimation of the relative importance of each individual marker with regard to the explained variance in memory performance, we applied a model decomposition method using the relaimpo R package with the glm function (version 1.1-1).[37]

Finally, in separate GLMs, we contrasted scores across cognitive domains between participants with CAA with a positive and negative tau-PET. The statistical significance of each model was adjusted for the total numbers of tests performed according to the Bonferroni correction (corrected p value =

p value × 6, for the 6 tests performed). Because cognitive scores were already corrected for age, sex, and education, these variables were not included in the models.

Classification of Evidence

This study provides Class II evidence that tau-PET retention is related to the presence of objective memory impairment in individuals with CAA.

Data Availability

Anonymized data can be made available to other researchers on request and with adequate justification.

Results

According to our predefined criteria, 25 participants with CAA had an amnestic presentation and 21 were nonamnestic. Between-group differences in demographic, clinical, and cognitive characteristics, as well as in all quantified MRI markers of cerebral small vessel disease, are presented in table 1. Overall, participants with amnestic and nonamnestic CAA did not significantly differ in age, level of education, and vascular risk profile. There was, however, an increased representation of females in the nonamnestic CAA group (χ^2 = 5.39, p = 0.02). In addition to a reduced performance on the memory domain ($F_{1,44}$ = 95.47, p < 0.001), amnestic CAA showed a reduced performance on the MMSE ($F_{1,44}$ = 35.89, p < 0.001), as well as on the language/ semantics domain ($F_{1,44}$ = 13.23, p = 0.001) and executive function ($F_{1,44}$ = 9.87, p = 0.003) domains. After adjustment for age and sex, participants with amnestic CAA had a lower normalized total hippocampal volume (t = 4.06, p < 0 .001) but did not significantly differ from participants with nonamnestic CAA on any other structural MRI markers (p > 0.05 for all).

The results of analysis comparing participants with amnestic and nonamnestic CAA on amyloid- and tau-PET retention are summarized in figure 2. Amyloid-PET was available in 39 participants (18 with nonamnestic and 21 with amnestic CAA), and tau-PET was available in 40 (19 with nonamnestic and 21 with amnestic CAA). While amyloid-PET retention was globally elevated in participants with CAA, there was no difference in FLR DVR values between the amnestic and nonamnestic groups (t = −1.00, p = 0.323). Group differences in amyloid-PET FLR DVR remained nonsignificant after

controlling for the presence of MRI markers of cerebral small vessel disease, age, and sex ($t = -0.71$, $p = 0.485$) or when using FLR DVR values corrected for partial volume effect ($t = -1.14$, $p = 0.261$). Tau-PET retention (ADCortSig SUVR) was increased in participants with amnestic compared to those with nonamnestic CAA ($t = -3.13$, $p = 0.003$). Group differences in tau-PET retention in the ADCortSig region remained significant after controlling for the presence of MRI markers of cerebral small vessel disease, age, and sex ($t = -2.71$, $p = 0.01$). In those with amnestic CAA, a significant increase in tau-PET retention was observed when ADCortSig SUVRs both corrected and not corrected for partial volume effect were used and across multiple other regions affected in Alzheimer disease36 (table 2).

In univariate models, lower memory performance in participants with CAA was associated with greater tau-PET ADCortSig SUVR ($\beta = -0.77$, corrected $p = 0.006$; figure 3A) and lower normalized hippocampal volume ($\beta = 0.73$, corrected $p = 0.005$; figure 3B) but not with any other quantified neuroimaging markers (table 3A). A GLM evaluating the combined influence of all quantified MRI and PET markers on memory performance was significant and explained an estimated 60% ($p < 0.001$) of the variance in scores on the memory composite (table 3B). Tau-PET ADCortSig SUVR ($\beta = -0.85$, $p = 0.001$) and normalized hippocampal volume ($\beta = 0.64$, $p = 0.01$) were the only variables significantly contributing to the model fit, while the influence of global cortical amyloid-PET retention and other quantified MRI markers was not significant. Evaluation of the relative explanatory importance of each regressor in the model (figure 3C) revealed that tau-PET retention accounted for nearly half of the variance in memory performance explained by the model (relative importance 47%), while hippocampal volume accounted for nearly a third of the variance (relative importance 32.7%). A separate multivariate model including only tau-PET retention and normalized hippocampal volume (table 3C) showed that these 2 markers accounted, by themselves, for an estimated 45% ($p < 0.001$) of the variance in memory performance.

To complement our analyses, the effect of tau-PET status on the cognitive profile of individuals with CAA was evaluated (figure 4). Participants with CAA with a positive tau-PET ($n = 21$) had a lower performance on the memory domain ($t = -3.72$, corrected $p = 0.004$) compared to participants with a negative tau-PET ($n = 19$). Performance on other cognitive domains did not differ significantly between groups after correction for multiple comparisons.

Discussion

This comprehensive neuroimaging study explored the correlates of the amnestic presentation in participants fulfilling diagnostic criteria for MCI and probable CAA (CAA-MCI). In this cohort of patients with probable CAA, the amnestic status was associated with increased tau-PET retention, greater medial temporal neurodegeneration, and a globally more severe profile of cognitive impairment. Our results thus suggest that memory impairment in this population could serve as a marker for concomitant tau pathology and disease severity.

The central finding of this study is that patients with amnestic CAA show an increased tau-PET retention in regions susceptible to pathologic tau accumulation in Alzheimer disease (ADCortSig) and a reduced hippocampal volume compared to their nonamnestic counterparts. Patients with amnestic and nonamnestic CAA did not differ on any structural MRI markers of cerebral small vessel disease or on amyloid-PET retention. Tau accumulation and hippocampal atrophy are well-established markers of Alzheimer disease that have not been strongly associated with pure forms of CAA.[38,39] Our findings thus suggest that amnestic patients with CAA present with a mixed neuropathologic profile, consistent with the concomitant presence of both CAA-mediated cerebrovascular alterations and tau pathology.

Participants with CAA in our sample presented elevated levels of amyloid binding on [11C]-Pittsburgh compound B amyloid-PET imaging, with a mean FLR DVR of 1.42 (SD 0.30).[31] Relying on a previously established cutoff sensitive to early amyloid accumulation,[31] we classified the vast majority of individuals with CAA in our sample as amyloid-PET positive. This is consistent with the pathologic nature of CAA, characterized by the cerebrovascular accumulation of amyloid. However, 3 individuals with CAA (2 nonamnestic and 1 amnestic) in our sample were classified as amyloid-PET negative on the basis of this cutoff. Cutoff scores to define amyloid-PET positivity are derived from varied clinical populations and methodologies, with significant discrepancy across laboratories.[40] A previous meta-analysis examining the accuracy of amyloid-PET in the diagnosis of CAA suggests an overall pooled sensitivity of 79% and specificity of 78%.[41] The significance of negative amyloid-PET in patients with CAA remains ambiguous and could reflect the limited sensitivity of these cutoff scores in defining pathologic levels of amyloid accumulation. To ensure that the presence of these amyloidPET negative participants did not influence our results, we performed all analyses without these participants and found that our findings remained highly consistent (data not presented). In addition to elevated amyloid retention on PET imaging, nearly half

of the studied individuals with CAA presented with elevated [18F]-flortaucipir tau-PET retention in regions susceptible to Alzheimer disease neurodegeneration (i.e., ADCortSig). This finding is in accord with the high comorbidity between CAA and Alzheimer pathology.[2-4] Patients with amnestic CAA presented with higher tau-PET retention in ADCortSig than patients with nonamnestic CAA. The mean tau-PET retention in ADCortSig of patients with amnestic CAA (mean [SD] 1.37 [0.25]) was highly consistent with levels previously reported in amyloid-positive patients with Alzheimer disease (mean [SD] 1.3 [0.3]).[35] In contrast, mean SUVR values in nonamnestic CAA (mean [SD] 1.17 [0.15]) were comparable to levels previously reported in amyloid-negative controls (mean [SD] 1.1 [0.1]).[35] Our findings might thus indicate an increased prevalence of comorbid Alzheimer disease neuropathology in amnestic as opposed to nonamnestic patients with CAA.

Our results further demonstrate that greater tau-PET retention is significantly and independently related to lower memory performance in CAA, even after accounting for conventional MRI markers of cerebral small vessel disease and amyloid-PET retention. Tau-PET retention was the most important predictor contributing to the explained variance in memory performance in a GLM including all evaluated neuroimaging markers, with a relative contribution approaching 50%. Hippocampal volume was the only other quantified neuroimaging marker significantly contributing to the variance in memory performance. In contrast, amyloid-PET retention and structural MRI markers of cerebral small vessel disease did not significantly contribute to the variance in memory performance in these individuals with CAA. Our results align with those from a recent postmortem study showing significant associations between episodic memory and Braak stages of neurofibrillary pathology in the presence of CAA.[42] Our findings also intersect with a recent study emphasizing the central role of tau-PET retention with regard to cognitive symptoms in patients with subcortical vascular cognitive impairment[43] and indicate that memory impairment in CAA likely arises in parallel with tau accumulation and neurodegeneration.

In addition to memory impairment, individuals with amnestic CAA exhibited more severe global cognitive impairment (i.e., MMSE score) and more pronounced deficits across multiple cognitive domains, including language/semantics and executive function. The increased severity of cognitive impairments in those with amnestic CAA might be related to the underlying presence of mixed pathology (i.e., vascular and tau), as opposed to a predominantly vascular profile. This interpretation is consistent with findings from recent pathologic studies demonstrating greater cognitive impairment in aging individuals presenting both tau and vascular pathologies.[42,44] Alternatively, the increased

severity of cognitive deficits in persons with amnestic CAA could indicate that memory deficits arise at a more advanced stage of cognitive impairment in CAA.[45] Longitudinal studies to track the progression of cognitive dysfunctions and neuropathologic processes in patients with CAA are needed to shed light on this question.

Finally, to further examine the relationship between memory and tau pathology in CAA, we contrasted the cognitive profile of participants with positive vs negative tau-PET, as determined with the use of a previously established cutoff value.[35] The cognitive profile of patients with CAA with positive tau-PET was distinct from that of individuals with negative tau-PET and predominantly characterized by an increased severity of memory impairment.

While amyloid-PET has previously been used to characterize amyloid burden in patients with CAA,[41] reports using tauPET in this population are sparse. A recent study[46] performed both amyloid and tau-PET in 3 individuals with probable CAA and found higher regional tau-PET retention in regions affected predominantly by cerebral microbleeds and cortical superficial siderosis. However, results presented in this study were limited by the small sample size and the lack of quantitative examination of associations between PET retention and clinical measures. The strength of the current study lies in the combined in vivo quantification of amyloid and tau pathology using PET in a larger sample of individuals with probable CAA, together with a characterization of cognitive correlates. Our initial results suggest that memory performance is related to tau pathology and medial temporal lobe neurodegeneration in patients with CAA. In the advent of tau therapeutic strategies, these findings could potentially inform clinical management and future clinical trials.

Nonetheless, our study has several limitations. First, the diagnosis of CAA in our sample, as well as the evaluation of amyloid and tau pathology, was obtained with neuroimaging and not confirmed via histopathology. This may lead to imprecision in the diagnosis of CAA. However, to favor diagnostic accuracy, we selected only individuals fulfilling the revised Boston Criteria for probable CAA, as opposed to individuals with possible CAA. Previous validation studies have demonstrated that this set of criteria show a high specificity for pathologic CAA.[11,47] The absence of neuropathologic data also limits characterization of the exact nature of amyloid and tau pathology. Although PET scans are informative, they provide an indirect and imprecise measure of both forms of pathologies. For instance, the signal derived from [11C]- Pittsburgh compound B amyloid-PET does not allow parenchymal to be distinguished from vascular amyloid deposition.[41] Regarding tau-PET, tracers for imaging tau pathology have been associated with off-target binding,[48] leading to a lower specificity

in the signal. Furthermore, while we classified participants into positive or negative tau- and amyloid-PET using previously published methods and cutoff values,[31,35] there is currently little consensus in the field on the best approach to define abnormal levels of tau or amyloid pathology based on PET imaging.[40,48] The selection of these cutoff scores remains arbitrary and potentially influenced our results. A second limitation associated with our study is the small sample size. This hindered the investigation of the full clinical spectrum of MCI, including the specific characterization of participants presenting single-domain amnestic or nonamnestic MCI. It also limited the evaluation of other factors potentially influencing the clinical and radiologic presentation of CAA such as the APOE genotype. Finally, the present study comprised patients with CAA from a memory clinic population with no history of intracerebral hemorrhage. It is possible that our results are influenced by our sample selection and would differ in patients with CAA with a history of intracerebral hemorrhage or other overt cerebrovascular diseases.

Our study provides initial and hypothesis-generating evidence for a link between memory impairment and tau pathology in CAA. Future research using different methodologies, including histopathologic data, is needed to replicate these initial results and to provide further evidence for the relevance of memory deficits as an indicator of concomitant tau pathology in patients with CAA. Studies using larger and more diverse samples would allow a deeper understanding of factors influencing the neuroimaging and cognitive presentation of CAA. Longitudinal studies are also necessary to shed light on whether memory impairment in CAA is linked to a distinct disease trajectory. Follow-up research building on the present findings is now warranted to further characterize the diagnostic value of the amnestic presentation, alone or in conjunction with other relevant biomarkers (e.g., CSF tau, plasma tau, APOE genotype), as a clinical marker of tau pathology in patients with CAA.

Our study demonstrates that the presence of memory impairment in patients with CAA is a promising marker of tau pathology and medial temporal lobe integrity. In the absence of advanced neuroimaging technologies, this accessible clinical marker could provide relevant information on the severity and nature of underlying pathologic mechanisms in this heterogeneous population.

the data. They thank the Biostatistical Consulting group of Harvard Catalyst for support with this work.

References

1. Snyder HM, Corriveau RA, Craft S, et al. Vascular contributions to cognitive impairment and dementia including Alzheimer's disease. Alzheimers Demen 2015;11:710–717.
2. De Reuck J. The impact of cerebral amyloid angiopathy in various neurodegenerative dementia syndromes: a neuropathological study. Neurol Res Int 2019;2019:7247325.
3. Boyle PA, Yu L, Wilson RS, Leurgans SE, Schneider JA, Bennett DA. Person-specific contribution of neuropathologies to cognitive loss in old age. Ann Neurol 2018;83:74–83.
4. Thal DR, Griffin WST, de Vos RA, Ghebremedhin E. Cerebral amyloid angiopathy and its relationship to Alzheimer's disease. Acta Neuropathologica 2008;115:599–609.
5. Viswanathan A, Greenberg SM. Cerebral amyloid angiopathy in the elderly. Ann Neurol 2011;70:871–880.
6. Guillozet AL, Weintraub S, Mash DC, Mesulam MM. Neurofibrillary tangles, amyloid, and memory in aging and mild cognitive impairment. Arch Neurol 2003;60: 729–736.
7. Mortimer J, Gosche K, Riley K, Markesbery W, Snowdon D. Delayed recall, hippocampal volume and Alzheimer neuropathology: findings from the Nun Study. Neurology 2004;62:428–432.
8. Lekeu F, Magis D, Marique P, et al. The California Verbal Learning Test and other standard clinical neuropsychological tests to predict conversion from mild memory impairment to dementia. J Clin Exp Neuropsychol 2010;32:164–173.
9. Petersen RC. Mild cognitive impairment as a diagnostic entity. J Intern Med 2004; 256:183–194.
10. Linn J, Halpin A, Demaerel P, et al. Prevalence of superficial siderosis in patients with cerebral amyloid angiopathy. Neurology 2010;74:1346–1350.
11. Greenberg SM, Charidimou A. Diagnosis of cerebral amyloid angiopathy: evolution of the Boston criteria. Stroke 2018;49:491–497.
12. Folstein MF, Folstein SE, McHugh PR. "Mini-Mental State": a practical method for grading the cognitive state of patients for the clinician. J Psychiatr Res 1975;12: 189–198.
13. Brandt J. The Hopkins Verbal Learning Test: development of a new memory test with six equivalent forms. Clin Neuropsychologist 1991;5:125–142.
14. Buschke H. Cued recall in amnesia. J Clin Exp Neuropsychol 1984;6:433–440.
15. Tombaugh TN. Trail Making Test A and B: normative data stratified by age and education. Arch Clin Neuropsychol 2004;19:203–214.
16. Wechsler D. WAIS-III Administration and Scoring Manual. San Antonio: The Psychological Corp; 1997.
17. Fastenau PS, Denburg NL, Mauer BA. Parallel short forms for the Boston Naming Test: psychometric properties and norms for older adults. J Clin Exp Neuropsychol 1998;20:828–834.
18. Tombaugh TN, Kozak J, Rees L. Normative data stratified by age and education for two measures of verbal fluency: FAS and animal naming. Arch Clin Neuropsychol 1999;14:167–177.

19. Benton AL, Abigail B, Sivan AB, Hamsher Kd, Varney NR, Spreen O. Contributions to Neuropsychological Assessment: A Clinical Manual. Oxford: Oxford University Press; 1994.

20. Jak AJ, Bondi MW, Delano-Wood L, et al. Quantification of five neuropsychological approaches to defining mild cognitive impairment. Am J Geriatr Psychiatry 2009;17:368–375.

21. Wardlaw JM, Smith EE, Biessels GJ, et al. Neuroimaging standards for research into small vessel disease and its contribution to ageing and neurodegeneration. Lancet Neurol 2013;12:822–838.

22. Charidimou A, Linn J, Vernooij MW, et al. Cortical superficial siderosis: detection and clinical significance in cerebral amyloid angiopathy and related conditions. Brain 2015;138:2126–2139.

23. Fischl B, Salat DH, Busa E, et al. Whole brain segmentation: automated labeling of neuroanatomical structures in the human brain. Neuron 2002;33:341–355.

24. Becker JA, Hedden T, Carmasin J, et al. Amyloid-β associated cortical thinning in clinically normal elderly. Ann Neurol 2011;69:1032–1042.

25. Johnson KA, Schultz A, Betensky RA, et al. Tau positron emission tomographic imaging in aging and early Alzheimer disease. Ann Neurol 2016;79:110–119.

26. Desikan RS, S´egonne F, Fischl B, et al. An automated labeling system for subdividing the human cerebral cortex on MRI scans into gyral based regions of interest. Neuroimage 2006;31:968–980.

27. Logan J, Fowler JS, Volkow ND, Wang G-J, Ding Y-S, Alexoff DL. Distribution volume ratios without blood sampling from graphical analysis of PET data. J Cereb Blood Flow Metab 1996;16:834–840.

28. Logan J, Fowler JS, Volkow ND, et al. Graphical analysis of reversible radioligand binding from time: activity measurements applied to [N-11C-methyl]-(−)-cocaine PET studies in human subjects. J Cereb Blood Flow Metab 1990;10:740–747.

29. Johnson KA, Gregas M, Becker JA, et al. Imaging of amyloid burden and distribution in cerebral amyloid angiopathy. Ann Neurol Official J Am Neurol Assoc Child Neurol Soc 2007;62:229–234.

30. Mintun M, Larossa G, Sheline Y, et al. [11C] PIB in a nondemented population: potential antecedent marker of Alzheimer disease. Neurology 2006;67:446–452.

31. Villeneuve S, Rabinovici GD, Cohn-Sheehy BI, et al. Existing Pittsburgh compound-B positron emission tomography thresholds are too high: statistical and pathological evaluation. Brain 2015;138:2020–2033.

32. Greve DN, Salat DH, Bowen SL, et al. Different partial volume correction methods lead to different conclusions: an 18F-FDG-PET study of aging. Neuroimage 2016; 132:334–343.

33. Rousset OG, Ma Y, Evans AC. Correction for partial volume effects in PET: principle and validation. J Nucl Med 1998;39:904–911.

34. Wang L, Benzinger TL, Hassenstab J, et al. Spatially distinct atrophy is linked to β-amyloid and tau in preclinical Alzheimer disease. Neurology 2015;84:1254–1260.

35. Wang L, Benzinger TL, Su Y, et al. Evaluation of tau imaging in staging Alzheimer disease and revealing interactions between β-amyloid and tauopathy. JAMA Neurol 2016;73:1070–1077.
36. Cho H, Choi JY, Hwang MS, et al. Tau PET in Alzheimer disease and mild cognitive impairment. Neurology 2016;87:375–383.
37. Gromping U. Relative importance for linear regression in R: the package relaimpo. J Stat Softw 2006;17:1–27.
38. Fotiadis P, van Rooden S, van der Grond J, et al. Cortical atrophy in patients with cerebral amyloid angiopathy: a case-control study. Lancet Neurol 2016;15:811–819.
39. Natt´e R, Maat-Schieman ML, Haan J, Bornebroek M, Roos RA, Van Duinen SG. Dementia in hereditary cerebral hemorrhage with amyloidosis-Dutch type is associated with cerebral amyloid angiopathy but is independent of plaques and neurofibrillary tangles. Ann Neurol 2001;50:765–772.
40. Klunk WE, Koeppe RA, Price JC, et al. The Centiloid Project: standardizing quantitative amyloid plaque estimation by PET. Alzheimers Demen 2015;11:1–15.e14.
41. Charidimou A, Farid K, Baron J-C. Amyloid-PET in sporadic cerebral amyloid angiopathy: a diagnostic accuracy meta-analysis. Neurology 2017;89:1490–1498.
42. Malek-Ahmadi M, Perez SE, Chen K, Mufson EJ. Braak stage, cerebral amyloid angiopathy, and cognitive decline in early Alzheimer's disease. J Alzheimer's Dis 2020;74:189–197.
43. Kim HJ, Park S, Cho H, et al. Assessment of extent and role of tau in subcortical vascular cognitive impairment using 18F-AV1451 positron emission tomography imaging. JAMA Neurol 2018;75:999–1007.
44. Wennberg AM, Whitwell JL, Tosakulwong N, et al. The influence of tau, amyloid, alpha-synuclein, TDP-43, and vascular pathology in clinically normal elderly individuals. Neurobiol Aging 2019;77:26–36.
45. You Y, Perkins A, Cisternas P, et al. Tau as a mediator of neurotoxicity associated to cerebral amyloid angiopathy. Acta Neuropathol Commun 2019;7:26.
46. Kim HJ, Cho H, Werring DJ, et al. 18F-AV-1451 PET imaging in three patients with probable cerebral amyloid angiopathy. J Alzheimers Dis 2017;57:711–716.
47. Martinez-Ramirez S, Romero J-R, Shoamanesh A, et al. Diagnostic value of lobar microbleeds in individuals without intracerebral hemorrhage. Alzheimers Demen 2015;11:1480–1488.
48. Leuzy A, Chiotis K, Lemoine L, et al. Tau PET imaging in neurodegenerative tauopathies: still a challenge. Mol Psychiatry 2019;24:1112–1134.
49. Zhang D. A coefficient of determination for generalized linear models. Am Statistician 2017;71:310–316

Tables

Table 1 - Demographic, Clinical, and Radiologic Characteristics in Participants With Probable CAA-MCI With an Amnestic or Nonamnestic Presentation

	Nonamnestic CAA-MCI (n = 21)	Amnestic CAA-MCI (n = 25)	p Value
Demographics			
Age, mean ± SD, y	74.7 (5.95)	75.0 (7.10)	0.866
Female, n (%)	10 (47.6)	4 (16.0)	0.020[b]
Education, mean ± SD, y	16.3 (2.72)	17.0 (2.37)	0.352
Vascular risk factors, n (%)			
Hypertension	15 (71.4)	18 (72.0)	0.966
Diabetes	3 (14.3)	4 (16.0)	0.872
Hyperlipidemia	17 (80.9)	19 (76.0)	0.685
Atrial fibrillation	2 (9.5)	1 (4.0)	0.450
Neuropsychological performance			
MMSE score, mean ± SD	27.9 ± 1.8	24.8 ± 2.1	<0.001[c]
Executive function composite score, mean ± SD	−0.30 ± 0.57	−1.15 ± 1.13	0.003[c]
Attention/processing speed composite score, mean ± SD	−0.09 ± 0.61	−0.59 ± 1.11	0.070
Language/semantics composite score, mean ± SD	−0.07 ± 0.65	−1.01 ± 1.01	0.001[c]
Visuospatial processing composite score, mean ± SD	0.22 ± 2.75	0.57 ± 1.31	0.576
Memory composite score, mean ± SD	−0.10 ± 0.59	−2.56 ± 1.01	<0.001[c]
Conventional MRI markers of SVD			
Total CMB count, mean ± SD, n	56.7 (66.25)	55.72 (67.53)	0.209
Lacune count, mean ± SD, n	1.24 (2.26)	1.12 (1.72)	0.454
cSS (presence), n (%)	8 (38.1)	10 (40.0)	0.982
nWMH volume, mean ± SD	1.00 (0.88)	1.04 (0.98)	0.832
BPF, mean ± SD	0.66 (0.03)	0.66 (0.03)	0.989
nHC volume, mean ± SD	4.22 (0.60)	3.61 (0.54)	<0.001[c]
PET markers[a]			
Amyloid-PET (FLR DVR), mean ± SD	1.36 (0.29)	1.46 (0.30)	0.323
Positive amyloid-PET status, n (%)	16 (88.9)	20 (95.2)	0.522
Tau-PET (ADCortSig SUVR), mean ± SD	1.17 (0.15)	1.37 (0.25)	0.003[c]
Positive tau-PET status, n (%)	5 (26.31)	16 (76.19)	0.006[c]

Abbreviations: ADCortSig SUVR = non–partial volume–corrected regional [18F]-flortaucipir retention expressed as standardized uptake value ratio in a region of interest regrouping Alzheimer disease cortical signature regions; BPF = brain parenchymal fraction; CMB = cerebral microbleeds; cSS = cortical superficial siderosis; FLR DVR = non–partial volume–corrected global cortical [11C]-

Pittsburgh compound B retention expressed as distribution volume ratio in a region of interest including the frontal, lateral temporal/parietal, and retrosplenial cortex; MCI = mild cognitive impairment; MMSE = Mini-Mental State Examination; nHC = normalized total hippocampal; nWMH = normalized white matter hyperintensities volume; SVD = cerebral small vessel disease. Amyloid PET positive status was determined with a previously described methodology and cutoff score showing higher sensitivity to early amyloid accumulation (Villeneuve et al.[31]). Tau PET positive status was determined with a previously described methodology and cutoff score (Wang et al.[35]). a Amyloid-PET was available in 39 participants (18 nonamnestic CAA-MCI and 21 amnestic CAA-MCI), and tau-PET was available in 40 participants (19 nonamnestic CAA-MCI and 21 amnestic CAA-MCI). b $p < 0.05$. c $p < 0.01$.

Table 2. Regional [18F]-Flortaucipir PET Retention in Individuals With CAA and Comparison of SUVRs Corrected or Not for Partial Volume Effect

Region of Interest	A. SUVRs not Corrected for Partial Volume Effect			B. SUVRs Corrected for Partial Volume Effect		
	Nonamnestic CAA	Amnestic CAA	p Value	Nonamnestic CAA	Amnestic CAA	p Value
Global cortex	1.15 (0.11)	1.29 (0.18)	0.004[b]	1.29 (0.19)	1.55 (0.32)	0.002[b]
Prefrontal	1.12 (0.08)	1.20 (0.14)	0.045[a]	1.32 (0.12)	1.47 (0.25)	0.019[a]
Sensorimotor	0.99 (0.09)	1.03 (0.10)	0.232	1.06 (0.16)	1.11 (0.22)	0.421
Superior parietal	1.04 (0.12)	1.17 (0.29)	0.076	1.18 (0.23)	1.42 (0.58)	0.074
Inferior parietal	1.12 (0.13)	1.34 (0.36)	0.012[a]	1.26 (0.21)	1.67 (0.65)	0.007[b]
Precuneus	1.13 (0.07)	1.36 (0.35)	0.005[b]	1.24 (0.14)	1.69 (0.70)	0.003[b]
Lateral occipital	1.06 (0.12)	1.14 (0.20)	0.119	1.15 (0.19)	1.28 (0.37)	0.156
Fusiform	1.30 (0.22)	1.47 (0.26)	0.032[a]	1.50 (0.38)	1.77 (0.54)	0.072
Superior temporal	1.15 (0.17)	1.29 (0.22)	0.039[a]	1.40 (0.33)	1.65 (0.49)	0.067
Middle temporal	1.23 (0.24)	1.44 (0.31)	0.019[a]	1.44 (0.41)	1.78 (0.59)	0.033[a]
Inferior temporal	1.30 (0.26)	1.56 (0.34)	0.012[a]	1.55 (0.44)	2.01 (0.64)	0.011[a]
Entorhinal	1.17 (0.22)	1.45 (0.22)	<0.001[b]	1.37 (0.62)	1.80 (0.42)	0.019[a]
Hippocampus	1.24 (0.13)	1.39 (0.20)	0.008[b]	1.33 (0.18)	1.54 (0.27)	0.007b
Parahippocampal	1.20 (0.21)	1.41 (0.19)	0.003[b]	1.34 (0.51)	1.74 (0.39)	0.010[a]
Anterior cingulate	1.13 (0.09)	1.21 (0.13)	0.027[a]	1.24 (0.19)	1.40 (0.31)	0.056
Posterior cingulate	1.12 (0.09)	1.28 (0.25)	0.008[b]	1.15 (0.20)	1.48 (0.49)	0.005[b]
Striatum	1.31 (0.12)	1.37 (0.16)	0.219	1.45 (0.20)	1.61 (0.33)	0.057
Thalamus	1.16 (0.08)	1.16 (0.16)	0.937	1.26 (0.11)	1.30 (0.30)	0.567
AD cortical signature	1.17 (0.15)	1.37 (0.25)	0.003[b]	1.34 (0.27)	1.70 (0.46)	0.004[b]

Abbreviations: AD = Alzheimer disease; SUVR = standardized uptake value ratio. Presented values are mean (SD) reflecting regional [18F]-flortaucipir tau-PET SUVRs not corrected (column A) and corrected (column B) for partial volume effect across multiple regions of interest in individuals with probable cerebral amyloid angiopathy with a nonamnestic or amnestic presentation. The p values were obtained with generalized linear models fitted with a gamma distribution and a log link function. a $p < 0.05$. b $p < 0.01$.

Table 3. Summary of Generalized Linear Models Predicting Memory Performance in Individuals With CAA

	A. Univariate Models			B. Multivariate Model [1]			C. Multivariate Model [2]		
	Std β	95% CI	Corr p Value	Std β	95% CI	p Value	Std β	95% CI	p Value
				Model fit: R2 = 0.60, p < 0.001			Model fit: R2 = 0.45, p < 0.001		
Tau-PET	−0.77	−1.18	−0.36	0.006	−0.85	−1.31	−0.39	0.001	−0.71	−1.09	−0.32	<0.001
Amyloid-PET	−0.44	−0.91	0.03	>0.05	−0.06	−0.54	0.41	>0.05				
CMB	0.08	−0.36	0.52	>0.05	0.29	−0.14	0.72	>0.05				
Lacune	0.14	−0.30	0.58	>0.05	−0.04	−0.47	0.40	>0.05				
cSS	−0.36	−1.25	0.53	>0.05	−0.14	−1.11	0.83	>0.05				
nWMH Vol	0.08	−0.36	0.53	>0.05	0.41	−0.06	0.87	>0.05				
nHC Vol	0.73	0.34	1.11	0.005	0.64	0.17	1.11	0.01	0.54	0.16	0.92	0.009
BPF	0.24	−0.19	0.68	>0.05	−0.03	−0.52	0.46	>0.05				

Abbreviations: amyloid-PET = amyloid-PET distribution volume ratio extracted from the frontal, lateral temporal/parietal, and retrosplenial cortex region of interest; BPF = brain parenchymal fraction; CI = confidence interval; CMB = cerebral microbleeds; Corr = corrected for multiple comparisons based on the Bonferroni correction; cSS = cortical superficial siderosis; nHC Vol = normalized total hippocampal volume; nWMH Vol = normalized white matter hyperintensities volume; Std = standardized; tau-PET = tau-PET standardized uptake value ratio extracted from the Alzheimer disease cortical signature region of interest. Results of univariate (A) and multivariate (B and C) generalized linear models with performance on the memory composite as the outcome variable. Because memory composite scores were already adjusted for age, sex, and education, these variables were not entered into the models. Multivariate generalized linear model 1 (B) includes all quantified MRI and PET markers. Multivariate generalized linear model 2 (C) includes only predictors found to be significant in model 1. Model fit and R2 were estimated in R with the rsq package and based on the variance function (Zhang et al.49).

FIGURE LEGENDS

**Figure 1 – Flowchart illustrating the selection of study participants**
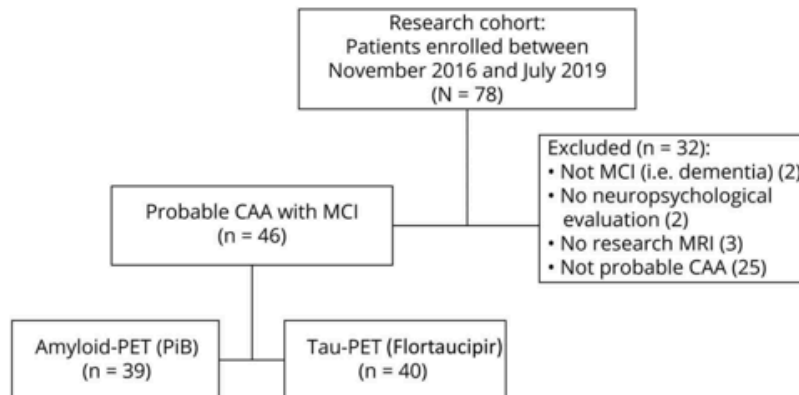
Flowchart illustrating the selection of study participants from a larger study cohort (n = 78). Participants were classified as having probable cerebral amyloid angiopathy (CAA) or not on the basis of the modified Boston criteria.[10,11] Three participants could not be classified due to an absence of research MRI and thus were excluded.
MCI = mild cognitive impairment; PiB = Pittsburgh compound B.

Figure 2 – Differences in Tau- and Amyloid-PET Retention Based on Amnestic Status in Individuals With CAA
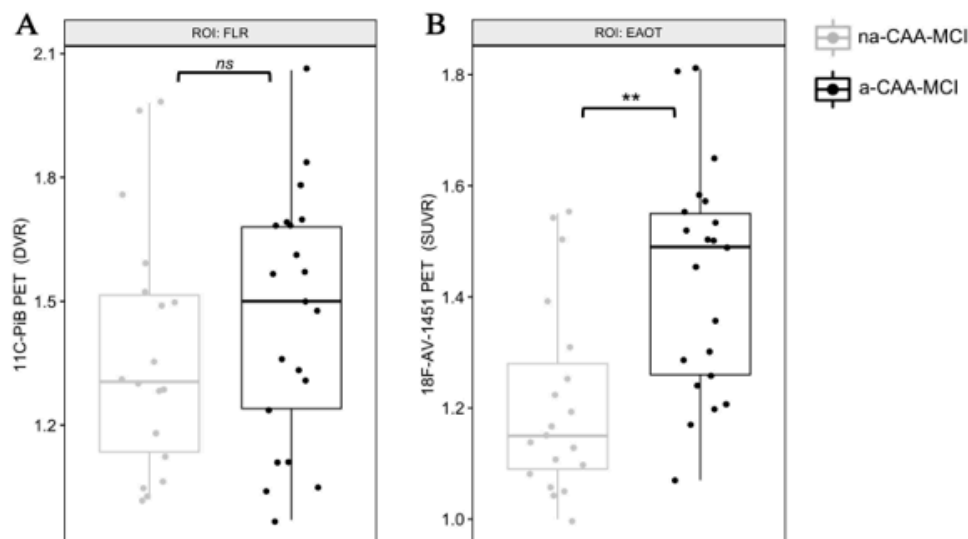

Boxplots representing the dispersion of (A) amyloid-PET retention expressed as distribution volume ratio (DVR) in a region of interest (ROI) including the frontal, lateral temporal/parietal, and retrosplenial cortex (FLR) and (B) tau-PET retention expressed as standardized uptake value ratio (SUVR) in an ROI regrouping Alzheimer disease cortical signature regions (ADCortSig). Participants with probable cerebral amyloid angiopathy (CAA) with a nonamnestic presentation are represented in gray; those with an amnestic presentation are represented in black. ns = not statistically significant, **$p < 0.01$.

Figure 3 – Associations between imaging markers and memory in subjects with probable CAA
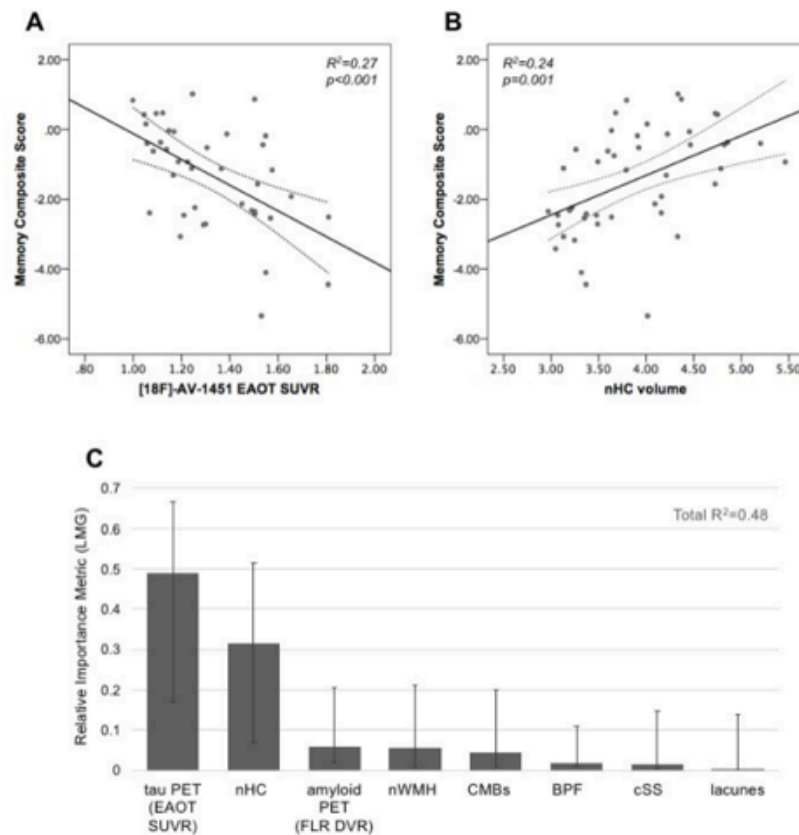
Results of univariate generalized linear models between memory performance and (A) tau-PET retention expressed as standardized uptake value ratio (SUVR) in a region of interest regrouping Alzheimer disease cortical signature regions (ADCortSig) or (B) normalized total hippocampal volume (nHC). Dashed lines represent the 95% confidence intervals. (C) Bar graph representing the relative contribution of each evaluated regressor to the multivariate generalized linear model evaluating the contribution of neuroimaging markers on memory performance, using the LMG metric computed with the R package relaimpo (U. Gromping, 2006). Metrics are normalized to sum to 100%. Lines represent 95% confidence intervals after 1,000 bootstrapping replications. BPF = brain ¨ parenchymal fraction; CAA = cerebral amyloid angiopathy; CMB = cerebral microbleed; cSS = cortical superficial siderosis; DVR = distribution volume ratio; FLR = frontal, lateral temporal/parietal, and retrosplenial cortex; nWMH = normalized white matter hyperintensity volume. *p < 0.05; **p < 0.01.

Figure 4 – Effect of Tau PET Status on the Cognitive Profile of Participants With Probable CA
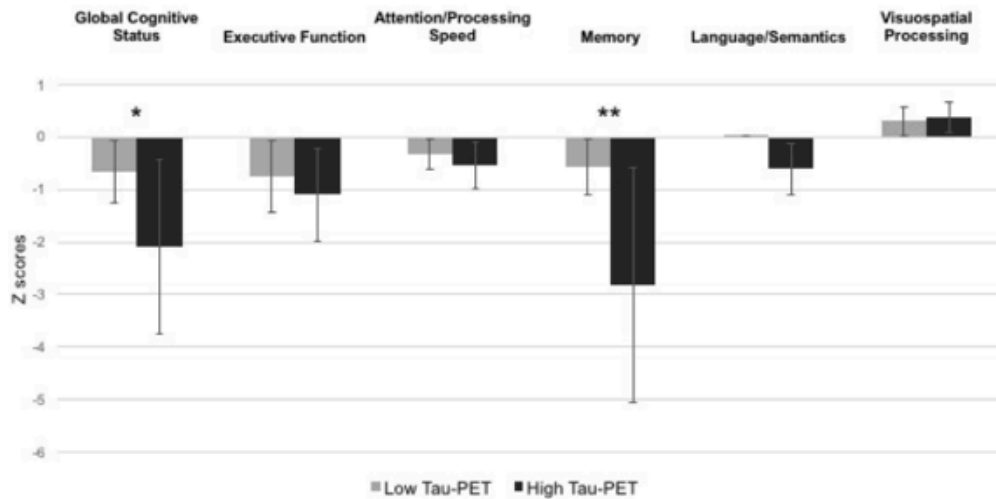
Bar graph contrasting the cognitive profile of participants with cerebral amyloid angiopathy (CAA) presenting with a positive or negative tau-PET. Tau-PET status was determined from the [18F]-flortaucipir standardized uptake value ratio in a region of interest comprising previously described Alzheimer disease cortical signature regions and using a previously established cutoff score.35 The p values were adjusted for multiple comparisons as per the Bonferroni correction. *Corrected $p < 0.05$; **corrected $p < 0.01$.

Appendix 4.4. "Global white matter structural integrity mediates the effect of age on ischemic stroke outcomes"

Reference: Etherton MR, Schirmer MD, Zotin MCZ, Rist PM, Boulouis G, Lauer A, et al. Global white matter structural integrity mediates the effect of age on ischemic stroke outcomes. Int J Stroke. 2021;174749302110559.

Copyright/Source: 2021, SAGE Publications/International Journal of Stroke®

Article reuse license

Global White Matter Structural Integrity Mediates the Effect of Age on Ischemic Stroke Outcomes

Mark R. Etherton MD, PhD;[1] Markus D. Schirmer PhD;[1,2] Maria Clara Zanon Zotin MD; [1,3] Pamela M. Rist ScD;[5] Gregoire Boulouis MD;[1] Arne Lauer MD;[1] Ona Wu PhD;[1,4] Natalia S. Rost MD, MPH[1]

Affiliations:

1. JPK Stroke Research Center, Department of Neurology, Massachusetts General Hospital (MGH) and Harvard Medical School
2. Clinic for Neuroradiology, University Hospital Bonn, Bonn, Germany
3. Center for Imaging Sciences and Medical Physics. Department of Medical Imaging, Hematology and Clinical Oncology. Ribeirão Preto Medical School, University of São Paulo, Ribeirão Preto, SP, Brazil.
4. Athinoula A. Martinos Center for Biomedical Imaging, Department of Radiology, MGH
5. Division of Preventive Medicine, Department of Medicine, Brigham and Women's Hospital and Harvard Medical School

Key words: Ischemic stroke, leukoaraiosis, MRI

Number of tables and figures: 4 tables, 2 figures.

Word count: 4437

Background

The relationship of global white matter microstructural integrity and ischemic stroke outcomes is not well understood.

Aims

To investigate the relationship of global white matter microstructural integrity with clinical variables and functional outcomes after acute ischemic stroke (AIS).

Methods

A retrospective analysis of neuroimaging data from 300 AIS patients with MRI brain obtained within 48 hours of stroke onset and long-term functional outcomes (modified Rankin, mRS) was performed. Peak width of skeletonized mean diffusivity (PSMD), as a measure of global white matter microstructural injury, was calculated in the hemisphere contralateral to the acute infarct. Multivariable linear and logistic regression analyses were performed to identify variables associated with PSMD and excellent functional outcome (mRS < 2) at 90 days, respectively. Mediation analysis was then pursued to characterize how PSMD mediates the effect of age on AIS functional outcomes.

Results

White matter hyperintensity (WMH) volume, age, pre-stroke disability, and normal-appearing white matter mean diffusivity were independently associated with increased PSMD. In logistic regression analysis, increased infarct volume and PSMD were independent predictors of excellent functional outcome. Additionally, the effect of age on functional outcomes was indirectly mediated by PSMD ($P < 0.001$).

Conclusions

As a marker of global white matter microstructural injury, increased PSMD mediates the effect of increased age to contribute to poor AIS functional outcomes. PSMD could serve as a putative radiographic marker of brain age for stroke outcomes prognostication.

INTRODUCTION

In patients with acute ischemic stroke (AIS), cerebral small vessel disease (cSVD) is highly prevalent and a recognized risk factor for poor AIS outcomes.(1, 2) As one radiographic marker of cSVD, neuroimaging evidence of decreased white matter structural integrity predisposes to poor AIS outcomes in at least two processes: 1) by contributing to infarct growth; and 2) independent of the ischemic tissue outcome, ostensibly affecting stroke recovery.(1, 3, 4) Several radiographic modalities measuring chronic cSVD-mediated white matter injury, including white matter hyperintensities (WMH),(5) commonly seen on Fluid-attenuated inversion recovery (FLAIR) MRI sequences, and Diffusion Tensor Imaging (DTI)-based analysis of normal-appearing white matter (NAWM), are associated with poor AIS outcomes.(4, 6) While WMH volume and NAWM structural integrity are associated with AIS outcomes, they represent subpopulations of cerebral white matter. An open question, therefore, is whether a global assessment of white matter structural injury may better represent total cSVD burden and inform on AIS outcomes.

The peak width of skeletonized mean diffusivity (PSMD), a fully-automated DTI-based measure of global white matter microstructural injury,(7) represents one appealing cSVD marker for potential application in AIS populations. From the DTI sequences, PSMD captures a tract-based quantification of the heterogeneity of mean diffusivity (MD) in principal white matter tracts to inform on white matter microstructural integrity.(7) Importantly, PSMD has been shown to have high inter-scanner reproducibility and important associations with cognitive function in population-based studies and cSVD cohorts, outperforming other neuroimaging markers.(7-9) While preliminary data suggests the utility of PSMD as a cSVD marker in healthy aging and cSVD cohorts, it is unknown whether it can be applied to AIS populations and if it is a clinically relevant determinant of AIS outcomes.

AIMS

To test these questions, we measured PSMD in an AIS cohort with long-term functional outcomes. Our hypothesis was that increased PSMD would be an independent determinant of poor long-term functional outcomes. The aims of this study were: 1) to identify the clinical and radiographic variables in AIS associated with PSMD; 2) to compare the association of PSMD with long-term functional outcomes to other radiographic markers of white matter structural injury, like WMH

volume and NAWM MD; and 3) to determine how PSMD mediates the effect of age on long-term functional outcomes.

METHODS

Study design and participants

This study is a retrospective analysis of a single-center prospective study of acute ischemic stroke patients.

The details of study design and participants have been described previously (see Supplementary Materials).(4) In brief, all participants 18 years of age or older that presented to the Massachusetts General Hospital Emergency Department between 2003 and 2011 with signs and symptoms consistent with an acute ischemic stroke were eligible for enrollment in the prospective study. Additional inclusion criteria for this analysis included: (1) patients with an acute, unilateral, supratentorial infarct on MRI brain, defined as a DWI positive lesion compatible with the presenting symptoms; (2) within 48 hours of symptom onset; and (3) FLAIR and DTI sequences available for WMH quantification and DTI analysis.

Clinical assessments

Admission stroke severity and pre-stroke disability were assessed by a trained neurologist using the National Institutes of Health Stroke Scale score (NIHSS) and modified Rankin scale (mRS), respectively. Large-vessel occlusion (LVO) was defined as occlusion of the intracranial internal carotid artery, or middle cerebral artery M1 and proximal M2 segments. Functional outcomes were assessed between 3 and 6 months post-stroke at a median follow-up time of 154 days from index event (IQR 104-208.5 days).

MRI acquisition and processing

Briefly, a multimodal, whole-brain MRI protocol with axial FLAIR, DWI, and DTI sequences was acquired using a 1.5T MRI scanner (General Electric Signa scanner) within 48 hours of admission (see Supplementary Materials). DWI volume (DWIv) of the acute infarct was determined using a semi-automated approach and normalized for intracranial volume.(10)

WMH and NAWM segmentation were performed using MRIcro (www.mricro.com) as described previously.(4) WMH and chronic infarct masks were constructed on FLAIR images by a blinded expert. To create the probabilistic NAWM mask (90%) in the contralesional hemisphere, all images and masks were subsequently coregistered to the MNI 152 1 mm atlas.(11-13) WMHv was normalized to intracranial volume to adjust for differences in head size.(14) NAWM MD and FA were extracted as the median voxel values from the contralesional NAWM mask. PSMD was extracted from the contralesional hemisphere using a publicly available script (PSMD Marker Version 1.0; see Supplementary Materials for details).

Statistical analysis

All statistical analysis was performed in R Version 4.0.0. Pre-stroke disability was defined as an $mRS \geq 2$. Excellent functional outcome was dichotomized as $mRS < 2$. As appropriate, Student's t test, Wilcoxon rank sum, and Chi square test were used to evaluate for baseline differences in the group with excellent versus poor outcome. The details of our model building approaches are described in the supplement. In brief, we performed univariates analyses for determinants of PSMD and excellent outcomes and then developed multivariate models based on these results (see Supplementary Materials). Receiver operating characteristic (ROC) curves were constructed to compare model performance for prediction of excellent functional outcome. Mediation analysis was performed using the Lavaan package to estimate the direct and indirect causal mediation effects of age and PSMD on mRS score.(15) The weighted least squares mean and variance adjusted (WLSMV) method was used for model estimation given its non-assumption of normally distributed variables.(16)

RESULTS

The baseline demographics of the study population have been reported previously.(4, 10) In brief, of 481 initially enrolled participants, after excluding participants with the aforementioned exclusion criteria or with motion artifact precluding MRI processing and assessment, 300 participants were analyzed in this study (see Supplementary Figure 1), including 74 with chronic contralesional infarcts. Age at enrollment ranged from 18 to 101 years. Median admission NIHSS score was 3 (interquartile range, IQR 1-7) and follow up mRS was 1 (IQR 0-3). In comparison with the poor outcome group, AIS patients with excellent outcomes were younger, more likely to

be male, had lower rates of atrial fibrillation, pre-stroke disability, and LVO, lower NIHSS and DWI volume, and decreased PSMD (Table 1).

In univariate linear regression analysis for determinants of PSMD, increasing age, atrial fibrillation, coronary artery disease, hypertension, and pre-stroke disability were associated with increased PSMD (Table 2). Radiographic markers of increased white matter structural injury, WMHv, and NAWM MD were also associated with increased PSMD. In the multivariable linear regression model, pre-stroke disability and increased age, WMHv, and NAWM MD were independently associated with increased contralesional PSMD. Relative importance metrics analysis showed age and NAWM MD explained the largest proportion of variance (Supplementary Table 1 and 2).

Next, we pursued logistic regression analysis for determinants of excellent functional outcome. In univariable analysis, increasing age, female sex, atrial fibrillation, pre-morbid disability, alteplase treatment, admission NIHSS, DWIv, NAWM MD, and PSMD were associated with decreased likelihood of excellent functional outcome (Table 3). Using the significant variables in the univariable analysis, we constructed clinical and radiographic regression models for predictors of excellent functional outcome. In the clinical model, increasing age, admission NIHSS, and female sex were independent predictors of poor functional outcomes. In the radiographic model, increased DWIv and PSMD were independent predictors of poor functional outcomes (Table 3). Next, we performed backward stepwise logistic regression analysis to define the minimal regression model for excellent functional outcomes using the variables from the clinical and radiographic models. Given the strong effect of age on PSMD, separate multivariable regression analyses were performed in which we allowed either age or PSMD to enter the model. The final model with age included NIHSS, DWIv, and pre-stroke disability as independent determinants of poor outcome. In contrast, in the final model with PSMD, NIHSS, DWIv, and female sex were independent predictors of poor outcome (Table 4). ROC curve analysis showed that the final model with PSMD had the largest AUC for predicting excellent functional outcome (Supplementary Figure 1; AUC = 0.79) and that including PSMD in the model resulted in a small, but statistically significant improvement in model performance (Supplementary Figure 2 AUC = 0.79 vs. AUC = 0.76; P value <0.001).

Lastly, we pursued mediation analysis to evaluate the direct and indirect causal mediation effects of age and PSMD on functional outcomes (mRS). The total effect of age on functional outcome (mRS) was significant (β = 2.0; P<0.001). Additionally, both the direct effect of age on mRS (β = 1.08; P<0.012) and indirect effects of age on PSMD (β = 0.687; P<0.001) and PSMD on mRS (β = 1.37; P<0.001) were significant, suggesting that the effect of increasing age on poor functional outcomes after ischemic stroke is partially mediated by PSMD.

DISCUSSION

In this study of PSMD in AIS, we observed several important findings. First, increased age, pre-stroke disability, and markers of white matter structural injury (WMH volume and NAWM DTI measures) were associated with increased PSMD. Second, PSMD is an independent determinant of excellent long-term functional outcomes in regression models including WMH volume and NAWM DTI measures. Lastly, using mediation analysis, we demonstrate that PSMD partially mediates the effect of increasing age on poor post-stroke functional outcomes.

As a marker of global white matter microstructural integrity, we observed that increasing PSMD values were associated with increased age, pre-stroke disability, increased WMH and NAWM DTI measures. To our knowledge, this is the first report that PSMD is associated with increased age, pre-stroke disability, and white matter macrostructural injury in patients with AIS. These observations also extend prior observations in AIS patients showing that increasing age is strongly predictive of greater white matter micro- (NAWM) and macrostructural injury (WMH).(17) Our findings are also in agreement with similar observations of a relationship between PSMD and age in patients with sporadic and genetic forms of cSVD,(7) stroke-free individuals,(18) hemorrhagic variants of cSVD (i.e. cerebral amyloid angiopathy),(8, 19) and vascular cognitive impairment and dementia.(7) Collectively, the association between PSMD and age in multiple clinical cohorts suggest a broader potential clinical relevance for PSMD as a radiographic marker of the ageing process.

In the analysis of determinants of post-stroke functional outcomes, only PSMD and DWI volume were significant predictors of excellent functional outcomes when included in a multivariable model with WMH and NAWM DTI metrics. As a marker of global injury, PSMD probably reflects structural injury both in the form of WMH and microstructural injury, based on the strong association between these variables in our regression analysis. Both WMH volume and NAWM microstructural injury have previously been shown to be predictive of poor post-stroke functional outcomes.(1, 4, 20-22) In contrast to WMH volume and NAWM diffusivity anisotropy metrics, PSMD was the only variable representing white matter structural injury that remained significant in the final multivariable analysis for radiographic predictors of excellent functional outcomes. This observation supports the hypothesis that PSMD effectively integrates different forms of white matter injury that occur in the context of an adverse vascular risk profile and, as such, co-determines stroke outcomes. PSMD may therefore better reflect total prestroke white matter structural injury than WMHv or NAWM diffusivity measures, which is supported by our observation that pre-stroke disability is associated with PSMD.

To inform on the underlying etiology of how PSMD contributes to poor post-stroke functional outcomes and delineate the causal pathway, we pursued mediation analysis. We observed that part of the effect of increased age on poor post-stroke functional outcomes is mediated indirectly by PSMD. The direct effect of increased age on poor post-stroke functional outcomes is likely multifactorial with contributions from both clinical and social factors. One retrospective review of AIS patients showed that patients 80 years of age or older had higher admission stroke severity, decreased in-hospital improvement, more comorbidities, and were less likely to be discharged home.(23) Our results, however, suggest that PSMD is an important determinant of AIS functional outcomes, in part, by indirectly mediating the effect of age.

Our study has several important limitations. First, this was a retrospective, cross-sectional analysis of a prospective acute ischemic stroke study of patients with relatively mild stroke severity (admission NIHSS score 3). Supporting the hypothesis that white matter microstructural integrity similarly influences outcomes for more severe stroke syndromes, however, we observed the same associations in the subgroups with NIHSS > 6 and LVOs (see Supplementary Materials). Second, this analysis was restricted to unilateral, supratentorial AIS patients to allow quantification of DTI

measures in the contralesional hemisphere as an approach to offset any influence of the acute infarct on the DTI metrics, which could introduce selection bias. While 25% of the patient population had chronic infarcts contralesional to the acute infarct, future studies should include infratentorial strokes to broaden generalizability. Further, whether PSMD values in the ipsilesional hemisphere provide any meaningful information remains an open question. Differences in the DTI acquisition protocols between scanners could presumably be a source of error. Prior reports, however, have demonstrated that differences in diffusion gradient direction or excitations do not substantially alter the mean FA, MD or PSMD values.(8, 24) Baykara *et al.* also reported high inter-scanner reproducibility of PSMD with the highest intraclass correlation coefficient of the white matter structural injury radiographic markers, suggesting that these markers are, in general, stable across different protocols and can be suitable even for large multi-center trials.(7) Overall, we would maintain that this analysis of clinical MRI scans in acute ischemic stroke patients is a strength of this study as the observed relationship in this setting suggests a more widespread generalizability to other acute stroke patient populations.

In summary, in a cohort of AIS patients, we show that PSMD is a clinically feasible measure of global white matter microstructural injury that partially mediates of the effect of age on post-stroke functional outcomes. Future studies investigating the association of PSMD with other stroke outcome domains and comparing its utility to qualitative cSVD scores (25) are warranted.

CONFLICTS OF INTEREST/DISCLOSURES
The authors report no relevant conflicts of interest.

REFERENCES

1.   Rost NS, Cougo P, Lorenzano S, Li H, Cloonan L, Bouts MJ, et al. Diffuse microvascular dysfunction and loss of white matter integrity predict poor outcomes in patients with acute ischemic stroke. J Cereb Blood Flow Metab. 2018;38(1):75-86.

2.   Pantoni L. Cerebral small vessel disease: from pathogenesis and clinical characteristics to therapeutic challenges. Lancet Neurol. 2010;9(7):689-701.

3.   Rost NS, Fitzpatrick K, Biffi A, Kanakis A, Devan W, Anderson CD, et al. White matter hyperintensity burden and susceptibility to cerebral ischemia. Stroke. 2010;41(12):2807-11.

4.   Etherton MR, Wu O, Cougo P, Giese AK, Cloonan L, Fitzpatrick KM, et al. Integrity of normal-appearing white matter and functional outcomes after acute ischemic stroke. Neurology. 2017;88(18):1701-8.

5.   Wardlaw JM, Smith EE, Biessels GJ, Cordonnier C, Fazekas F, Frayne R, et al. Neuroimaging standards for research into small vessel disease and its contribution to ageing and neurodegeneration. Lancet Neurol. 2013;12(8):822-38.

6.   Sagnier S, Catheline G, Dilharreguy B, Linck PA, Coupe P, Munsch F, et al. Normal-Appearing White Matter Integrity Is a Predictor of Outcome After Ischemic Stroke. Stroke. 2020;51(2):449-56.

7.   Baykara E, Gesierich B, Adam R, Tuladhar AM, Biesbroek JM, Koek HL, et al. A Novel Imaging Marker for Small Vessel Disease Based on Skeletonization of White Matter Tracts and Diffusion Histograms. Ann Neurol. 2016;80(4):581-92.

8.   McCreary CR, Beaudin AE, Subotic A, Zwiers AM, Alvarez A, Charlton A, et al. Cross-sectional and longitudinal differences in peak skeletonized white matter mean diffusivity in cerebral amyloid angiopathy. Neuroimage Clin. 2020;27:102280.

9.   Deary IJ, Ritchie SJ, Munoz Maniega S, Cox SR, Valdes Hernandez MC, Luciano M, et al. Brain Peak Width of Skeletonized Mean Diffusivity (PSMD) and Cognitive Function in Later Life. Front Psychiatry. 2019;10:524.

10.   Etherton MR, Wu O, Cougo P, Giese AK, Cloonan L, Fitzpatrick KM, et al. Structural Integrity of Normal Appearing White Matter and Sex-Specific Outcomes After Acute Ischemic Stroke. Stroke. 2017;48(12):3387-9.

11.   Collins DL, Neelin P, Peters TM, Evans AC. Automatic 3D intersubject registration of MR volumetric data in standardized Talairach space. J Comput Assist Tomogr. 1994;18(2):192-205.

12.   Grabner G, Janke AL, Budge MM, Smith D, Pruessner J, Collins DL. Symmetric atlasing and model based segmentation: an application to the hippocampus in older adults. Med Image Comput Comput Assist Interv. 2006;9(Pt 2):58-66.

13.   Rex DE, Ma JQ, Toga AW. The LONI Pipeline Processing Environment. NeuroImage. 2003;19(3):1033-48.

14.   Ferguson KJ, Wardlaw JM, Edmond CL, Deary IJ, Maclullich AM. Intracranial area: a validated method for estimating intracranial volume. J Neuroimaging. 2005;15(1):76-8.

15.   Sarstedt M, Ringle CM. Structural Equation Models: From Paths to Networks (Westland 2019). Psychometrika. 2020;85(3):841-4.

16.   Proitsi P, Hamilton G, Tsolaki M, Lupton M, Daniilidou M, Hollingworth P, et al. A Multiple Indicators Multiple Causes (MIMIC) model of Behavioural and Psychological Symptoms in Dementia (BPSD). Neurobiol Aging. 2011;32(3):434-42.

17.   Etherton MR, Wu O, Giese AK, Rost NS. Normal-appearing white matter microstructural injury is associated with white matter hyperintensity burden in acute ischemic stroke. International journal of stroke : official journal of the International Stroke Society. 2019:1747493019895707.

18.   Beaudet G, Tsuchida A, Petit L, Tzourio C, Caspers S, Schreiber J, et al. Age-Related Changes of Peak Width Skeletonized Mean Diffusivity (PSMD) Across the Adult Lifespan: A Multi-Cohort Study. Front Psychiatry. 2020;11:342.

19.   Raposo N, Zanon Zotin MC, Schoemaker D, Xiong L, Fotiadis P, Charidimou A, et al. Peak Width of Skeletonized Mean Diffusivity as Neuroimaging Biomarker in Cerebral Amyloid Angiopathy. AJNR Am J Neuroradiol. 2021;42(5):875-81.

20.   Arsava EM, Rahman R, Rosand J, Lu J, Smith EE, Rost NS, et al. Severity of leukoaraiosis correlates with clinical outcome after ischemic stroke. Neurology. 2009;72(16):1403-10.

21.   Henninger N, Lin E, Baker SP, Wakhloo AK, Takhtani D, Moonis M. Leukoaraiosis predicts poor 90-day outcome after acute large cerebral artery occlusion. Cerebrovasc Dis. 2012;33(6):525-31.

22. Etherton MR, Wu O, Giese AK, Lauer A, Boulouis G, Mills B, et al. White Matter Integrity and Early Outcomes After Acute Ischemic Stroke. Transl Stroke Res. 2019;10(6):630-8.

23. Navis A, Garcia-Santibanez R, Skliut M. Epidemiology and Outcomes of Ischemic Stroke and Transient Ischemic Attack in the Adult and Geriatric Population. J Stroke Cerebrovasc Dis. 2019;28(1):84-9.

24. Ni H, Kavcic V, Zhu T, Ekholm S, Zhong J. Effects of number of diffusion gradient directions on derived diffusion tensor imaging indices in human brain. AJNR Am J Neuroradiol. 2006;27(8):1776-81.

25. Staals J, Booth T, Morris Z, Bastin ME, Gow AJ, Corley J, et al. Total MRI load of cerebral small vessel disease and cognitive ability in older people. Neurobiol Aging. 2015;36(10):2806-11.

Table 1. Baseline Demographics of 300 AIS patients with Excellent Functional Outcome (mRS < 2)

Variable	Poor Outcome (mRS ≥ 2), N = 110	Excellent Outcome (mRS < 2), N = 190	P value
Age, mean (SD), y	68.5 (15.8)	61.9 (15.5)	**< 0.001**
Male, n (%)	57 (51.8)	126 (66.3)	**0.008**
White race, n (%)	107 (97.2)	184 (96.8)	1
No pre-stroke disability (mRS < 2)	80 (77.7)	161 (91.4)	**0.002**
Medical history, n (%)			
Atrial fibrillation	27 (24.5)	21 (11.1)	**0.005**
Diabetes mellitus	20 (18.2)	25 (13.2)	0.37
Hyperlipidemia	44 (40.0)	76 (40.0)	0.93
Hypertension	71 (64.5)	104 (54.7)	0.22
Prior stroke/TIA	21 (19.1)	29 (15.3)	0.56
Admission data			
NIHSS score, median (IQR)	6.0 (3,13)	2.0 (0.3,4)	**< 0.001**
Small vessel occlusion stroke subtype (TOAST), n (%)	5 (4.5)	24 (12.6)	0.69
LVO, n (%)	46 (41.8)	22 (11.6)	**< 0.001**
WMH volume, median (IQR), cm^3	6.8 (4.1,12.6)	5.7 (2.8,12.5)	0.16
NAWM MD, median (IQR), 10^{-3} mm^2/s	0.81 (0.76, 0.86)	0.77 (0.72, 0.82)	**<0.001**
DWI volume, median (IQR), cm^3	12.7 (0.3,49.5)	2.0 (0.6,11.8)	**< 0.001**
PSMD, median (IQR), 10^{-3} mm^2/s	0.41 (0.34,0.58)	0.38 (0.3,0.44)	**< 0.001**
Intravenous alteplase, n (%)	29 (26.4)	28 (14.7)	**0.03**

Abbreviations: IQR – interquartile range; LVO – large-vessel occlusion; mRS – modified Rankin scale; NIHSS – National Institutes of Health Stroke Scale; PSMD – peak width of skeletonized mean diffusivity; SD – standard deviation; TIA – transient ischemic attack; TOAST – Trial of Org 10172 in Acute Stroke Treatment; WMH – white matter hyperintensity.

Table 2. Linear Regression for Clinical and Radiographic Determinants of PSMD in 300 AIS patients

Variable	Univariable Analysis			Multivariable Analysis		
	Estimate	Standard Error	P value	Estimate	Standard Error	P value
Age	6.8×10^{-3}	5.4×10^{-4}	**<0.001**	3.5×10^{-3}	6.1×10^{-4}	**<0.001**
Female sex	3.4×10^{-2}	2.2×10^{-2}	0.12			
Atrial fibrillation	1.5×10^{-1}	2.8×10^{-2}	**<0.001**	2.0×10^{-2}	2.1×10^{-2}	0.36
CAD	5.6×10^{-2}	2.7×10^{-2}	**0.04**	1.3×10^{-2}	2.0×10^{-2}	0.52
Diabetes	2.4×10^{-3}	3.0×10^{-2}	0.94			
Hypertension	8.9×10^{-2}	2.1×10^{-2}	**<0.001**			
Hyperlipidemia	4.2×10^{-2}	2.2×10^{-2}	0.05			
No pre-stroke disability	-2.1×10^{-1}	2.9×10^{-2}	**<0.001**	-1.06×10^{-1}	2.3×10^{-2}	**<0.001**
Alteplase treatment	-3.4×10^{-3}	2.7×10^{-2}	0.90			
Intra-arterial therapy	5.6×10^{-2}	6.3×10^{-2}	0.38			
Admission NIHSS	3.1×10^{-3}	1.6×10^{-3}	0.06			
WMHv	5.2×10^{-3}	6.9×10^{-4}	**<0.001**	1.1×10^{-3}	5.7×10^{-2}	0.05
DWIv	-2.7×10^{-4}	2.4×10^{-4}	0.26			
NAWM MD	1.1	7.6×10^{-2}	**<0.001**	7.4×10^{-1}	8.2×10^{-2}	**<0.001**
NAWM FA	-1.2	0.3	**<0.001**			

Abbreviations: CAD – coronary artery disease; DWIv – diffusion-weighted image lesion volume; FA – fractional anisotropy; MD – mean diffusivity; NAWM – normal-appearing white matter; NIHSS – National Institutes of Health Stroke Scale; WMHv – white matter hyperintensity volume.

Table 3. Univariable Logistic Regression for Determinants of Excellent Functional Outcome in 300 AIS patients

Variable	Estimate	Standard Error	Odds Ratio (95% CI)	P value
Age	-0.03	0.01	0.97 (0.96, 0.99)	**<0.001**
Female sex	-0.66	0.24	0.52 (0.32, 0.83)	**0.006**
Atrial fibrillation	-0.92	0.32	0.40 (0.21, 0.74)	**0.004**
CAD	0.09	0.31	1.09 (0.59, 2.02)	0.79
Diabetes	-0.35	0.33	0.71 (0.37, 1.34)	0.29
Hypertension	0.32	0.24	0.72 (0.45, 1.16)	0.18
Hyperlipidemia	0.05	0.24	1.05 (0.65, 1.69)	0.84
No pre-stroke disability	1.13	0.36	3.09 (1.53, 6.24)	**0.002**
Prior stroke/TIA	-0.23	0.31	0.79 (0.43, 1.47)	0.46
Alteplase treatment	-0.69	0.30	0.50 (0.28, 0.90)	**0.02**
Intra-arterial therapy	-0.76	0.68	0.47 (0.12, 1.77)	0.26
Admission NIHSS	-0.16	0.02	0.86 (0.82, 0.90)	**<0.001**
WMHv	0.01	0.01	1.00 (0.98, 1.02)	0.99
DWIv	-0.02	0.01	0.98 (0.97, 0.99)	**<0.001**
NAWM MD	-3.33	1.15	0.04 (0.01, 0.34)	**0.004**
NAWM FA	2.62	3.32	13.79 (0.02, 9287.90)	0.43
PSMD	-2.09	0.68	0.12 (0.03, 0.47)	**0.002**

Abbreviations: CAD – coronary artery disease; DWIv – diffusion-weighted image lesion volume; FA – fractional anisotropy; MD – mean diffusivity; NAWM – normal-appearing white matter; NIHSS – National Institutes of Health Stroke Scale; WMHv – white matter hyperintensity volume.

Table 4. Multivariable Logistic Regression for Determinants of Excellent Functional Outcome in 300 AIS patients

| Variables	Estimate	Standard Error	Odds Ratio (95% CI)	P value
Model 1 - Clinical				
Age	-0.02	0.01	0.98 (0.96, 0.99)	**0.04**
Female sex	-0.63	0.30	0.53 (0.30, 0.95)	**0.03**
Atrial fibrillation	-0.33	0.41	0.72 (0.32, 1.59)	0.42
No pre-stroke disability	0.84	0.43	2.33 (1.00, 5.42)	0.05
Alteplase treatment	0.13	0.41	1.13 (0.51, 2.51)	0.76
Admission NIHSS	-0.17	0.03	0.84 (0.79 (0.90)	**< 0.001**
Model 2 - Radiographic				
DWIv	-0.03	0.01	0.97 (0.96, 0.98)	**<0.001**
PSMD	-2.76	0.74	0.06 (0.01, 0.27)	**<0.001**
Model 3 - Final				
Female sex	-0.79	0.31	0.45 (0.25, 0.83)	**0.01**
Atrial fibrillation	-	-	-	-
No pre-stroke disability	0.84	0.45	2.32 (0.96, 5.63)	0.06
Alteplase treatment	-	-	-	-
Admission NIHSS	-0.12	0.03	0.89 (0.83, 0.94)	**<0.001**
DWIv	-0.02	0.01	0.98 (0.97, 0.99)	**0.002**
PSMD	-2.37	0.95	0.09 (0.01, 0.59)	**0.01**

Abbreviations: CAD – coronary artery disease; DWIv – diffusion-weighted image lesion volume; FA – fractional anisotropy; MD – mean diffusivity; NAWM – normal-appearing white matter; NIHSS – National Institutes of Health Stroke Scale; WMHv – white matter hyperintensity volume.

Figure 1: PSMD analysis in the hemisphere contralateral to the acute infarct.
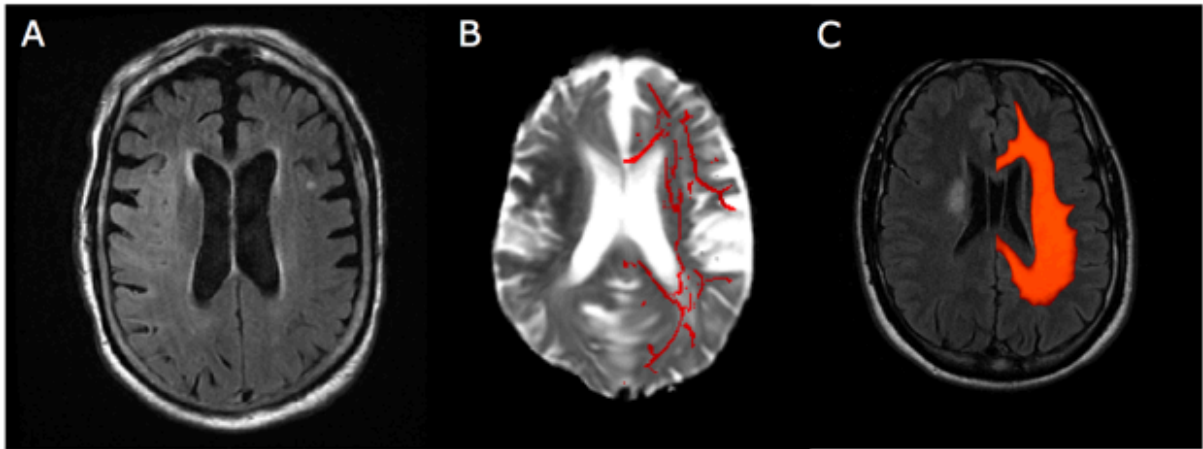
Representative A) FLAIR image; B) MD image with contralesional skeletonized FA mask shown for PSMD calculation (red); and C) FLAIR image with probabilistic NAWM mask in the contralesional hemisphere. D) Box plot of PSMD in AIS patients with excellent versus poor outcomes.

Figure 2: PSMD mediates the effect of age on 90-day modified Rankin Scale.
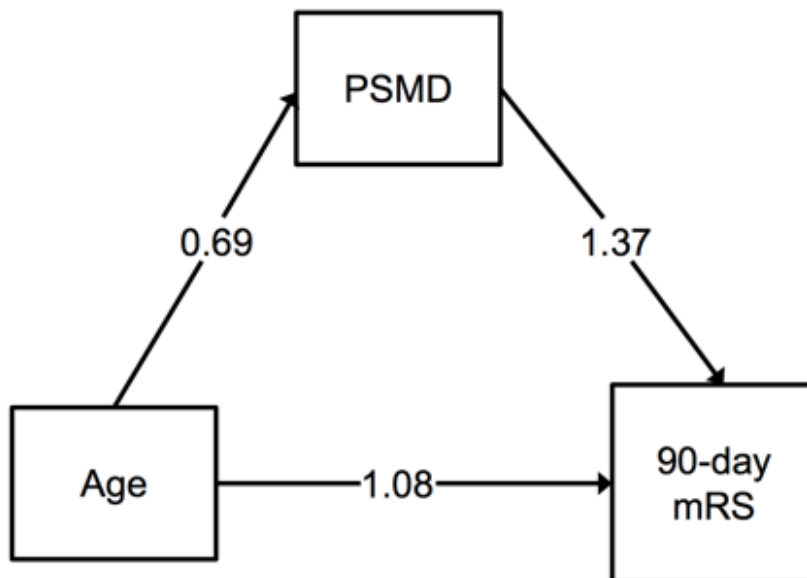
Mediation analysis for the model evaluating the effect of age and PSMD on 90-day modified Rankin Scale. Bold arrows indicate $P< 0.05$. Standardized path coefficients are used as effect estimate.

Appendix 4.5. "Contrast-agent-free state-of-the-art MRI on cerebral small vessel disease- part 1. ASL, IVIM, and CVR"

Reference: Paschoal AM, Secchinatto KF, Silva PHR, Zotin MCZ, Santos AC, Viswanathan A, et al. Contrast-agent-free state-of-the-art MRI on cerebral small vessel disease—part 1. ASL, IVIM, and CVR. Nmr Biomed. 2022;e4742.

Copyright/Source: John Wiley and Sons/NMR in Biomedicine®

Article reuse license

274

Licensed Content Issue	0
Licensed Content Pages	11
Type of use	Dissertation/Thesis
Requestor type	Author of this Wiley article
Format	Electronic
Portion	Full article
Will you be translating?	No
Title	PhD Thesis: Peak Width of Skeletonized Mean Diffusivity (PSMD) as Neuroimaging Biomarker for Vascular Cognitive Impairment in the Context of Cerebral Amyloid Angiopathy
Institution name	Faculdade de Medicina de Ribeirão Preto - Universidade de São Paulo
Expected presentation date	Aug 2022
Order reference number	0004
Requestor Location	Faculdade de Medicina de Ribeirão Preto - Universidade de São Paulo R. Ten. Catão Roxo, 3900 Monte Alegre Ribeirão Preto, SP 14015010 Brazil Attn: Faculdade de Medicina de Ribeirão Preto - Universidade de São Paulo

Publisher Tax ID	EU826007151

Total	0.00 USD

Terms and Conditions

Contrast-agent-free State-of-the-art Magnetic Resonance Imaging on Cerebral Small Vessel Disease – Part 1: ASL, IVIM, and CVR

André Monteiro Paschoal, Ph.D.[1,2]*; Kaio Felippe Secchinatto[1]*; Pedro Henrique Rodrigues da Silva, MSc[1]; Maria Clara Zanon Zotin, M.D.[2,3]; Antônio Carlos dos Santos M.D.[2]; Ph.D., Anand Viswanathan M.D., Ph.D.[3]; Octavio M. Pontes-Neto, Ph.D.[4]; Renata Ferranti Leoni, Ph.D.[1]

These authors have given the same contribution to the manuscript.

[1]Department of Physics, FFCLRP, University of São Paulo, Ribeirão Preto, SP, Brazil
[2]Department of Medical Imaging, Hematology and Clinical Oncology, Ribeirão Preto Medical School, University of São Paulo, Ribeirão Preto, SP, Brazil.
[3]J Philip Kistler Stroke Research Center, Department of Neurology, Massachusetts General Hospital, Harvard Medical School, Boston, MA, USA.
[4]Department of Neurosciences and Behavioral Science, Ribeirão Preto Medical School - University of Sao Paulo, Ribeirão Preto, SP, Brazil

Corresponding Author: Renata Ferranti Leoni
Department of Physics – FFCLRP – University of Sao Paulo
Av. Bandeirantes, 3900 – 14040-901 – Ribeirão Preto, São Paulo, Brazil
Phone: +55-16-3315 0083 / +55-16-99401 6368
leonirf@usp.br

Cover title: State-of-the-art MRI in cerebral small vessel disease

Total number of tables and figures: 3 figures, 1 table

Keywords: Arterial Spin Labeling; Blood oxygenation level-dependent contrast; Cerebral Small Vessel Disease; Cerebrovascular Reactivity; Intravoxel Incoherent Motion.

Word count: 3833

Abstract

Cerebral small vessel disease (cSVD), a common cause of stroke and dementia, is traditionally considered the small vessel equivalent of large artery occlusion or rupture that leads to cortical and subcortical brain damage. Microvessel endothelial dysfunction has also contributed to it. Brain imaging, including Magnetic Resonance Imaging (MRI), is useful to show the presence of a lesion of several types, although the association between conventional MRI measures and clinical features of cSVD are not always concordant. We assessed the additional contribution of contrast-agent-free, state-of-the-art MRI techniques, Arterial Spin Labeling (ASL), Diffusion Tensor Imaging (DTI), Functional Magnetic Resonance Imaging (fMRI), and Intravoxel Incoherent Motion (IVIM) applied to cSVD in the existing literature. We performed a review following the PICOS worksheet and Search Strategy, including original papers in English, published between 2000 and 2022. For each MRI method, we extracted information about their contributions, in addition to those established with traditional MRI methods and related information about the origins, pathology, markers, and clinical outcomes in cSVD. This paper presents the first part of the review, which includes 37 studies focusing on ASL, IVIM, and cerebrovascular reactivity (CVR) measures. In general, they have shown that, in addition to the white matter hyperintensities, alterations in other neuroimaging parameters such as blood flow and CVR also indicate the presence of cSVD. Such quantitative parameters were also related to cSVD risk factors. Therefore, they are promising, noninvasive tools to explore questions that have not yet been clarified about this clinical condition. However, protocol standardization is essential to increase their clinical use.

Introduction

Cerebral small vessel disease (cSVD) is a pathological condition that affects the human cerebrovascular system by deregulating the blood circulation through the arterioles, venules, and the correspondent perfusing brain tissue at the capillary bed. It results in damaged cortical and subcortical gray matter (GM) and white matter (WM) [1,2], is considered the most important cause of vascular cognitive impairment (VCI) [3] and is responsible for around 20% of all strokes worldwide [4]. Magnetic resonance imaging (MRI) has become crucial in evaluating brain changes and predicting cSVD-related cognitive decline in clinical and research settings [4,5].

However, reports on the association between conventional MRI measures and clinical features of cSVD are not always concordant [6]. Such MRI measures cannot delineate the heterogeneity of cSVD lesions with similar appearance and can only show part of the whole-brain damage related to cSVD [7]. Additionally, cSVD has been suggested as not a focal lesion disease, but it also affects remote brain areas, influencing the clinical outcome [7]. It also impairs structural and functional network connectivity, disrupting efficient communication in brain networks necessary for functional performance. Such facts have motivated the use of additional MRI acquisition and analysis models, which can disentangle differential assessment of cSVD-related brain damage, its effects on connections and cognition, and future clinical outcomes [8]. Moreover, contrast-agent-free state-of-the-art MRI techniques have shown subtle changes not observed with traditional imaging [9]. They have also allowed assessing pathophysiological processes underlying the cSVD development [10] and the extent of the overall brain damage that leads to a disconnection syndrome [7].

The administration of gadolinium-based contrast agents in MRI scans to enhance brain lesions for diagnosis is performed million times per year [11]. However, it has been criticized for rare but dangerous nephrogenic systemic fibrosis in patients with impaired renal function and its deposition in many organs, including the brain [11]. Then, the use and development of contrast-agent-free MRI techniques have been considered a safer alternative without loss of potential to diagnosis and prognosis.

In terms of pathophysiological processes, it is suggested that damage to functional units can cause cerebral blood flow (CBF) deregulation, affects cerebrovascular reactivity (CVR), and cause blood-brain barrier (BBB) leakage, among other effects, which together are responsible for the cSVD-related brain injuries [2]. Non-contrast MRI methods have been developed to assess such parameters. A powerful tool in assessing perfusion-related alterations in cSVD comes from MRI perfusion-weighted images. In that sense, arterial spin labeling (ASL), designed to explore the water molecules in the arterial blood as an endogenous tracer, allows a noninvasive approach to measure CBF and related parameters [12]. ASL has also been used to assess CVR when combined with a hypercapnia

challenge [13]. Because of its dependency on CBF, blood oxygenation level-dependent (BOLD) contrast is also a reliable and reproducible method to assess CVR at the tissue level [14]. Additionally, intravoxel incoherent movement (IVIM), a diffusion-weighted imaging technique, can quantitatively describe the perfusion and diffusion-related parameters of the brain microstructure without using an exogenous contrast agent [15].

Therefore, we performed a review focused on contrast-agent-free state-of-the-art MRI and its additional information compared to conventional MRI for the etiology, diagnosis, and prognosis of cSVD. We divided the review into two parts. The present paper presents the results regarding ASL, IVIM, and CVR measures. The second part of the review, published separately, focuses on diffusion tensor imaging (DTI) and functional magnetic resonance imaging (fMRI).

Methods

We followed the PRISMA-P (Preferred Reporting Items for Systematic Review and Meta-Analysis Protocols) 2015 checklist: recommended items to address in a systematic review protocol guidelines [16]. The review parameters were delineated using the PICOS worksheet and Search Strategy (Centre for reviews and dissemination. Systematic Reviews: CRD's Guidance for Undertaking Reviews in Health Care. York: University of York; 2006). The main question of our study was: What are the applications of contrast agent-free state-of-the-art MRI and its additional information compared to conventional MRI for the etiology, diagnosis, and prognosis of cSVD? Online searches in PubMed and Scopus were carried out considering the term "Cerebral Small Vessel Disease" combined with each one of the techniques: "Arterial Spin Labeling AND "Cerebral Small Vessel Disease," "Intravoxel Incoherent Motion" AND "Cerebral Small Vessel Disease," and "Cerebrovascular Reactivity" AND "Cerebral Small Vessel Disease." Inclusion criteria were original publications in English between 2000 and 2022 (last search on February 23rd, 2022), and with subjects of both sex, 18 years old or more.

For the identification, the authors independently researched the articles following the search strategy and inclusion criteria; then, they reached a consensus on which articles would be included in the final analysis. All the records and data selected had their title, authors' names, year of publication, MRI technique, and main findings (about pathophysiology, lesions, connections, and/or clinical outcomes) extracted using a standardized data extraction form shared among the authors.

Then, duplicates were removed, and records were screened, i.e., non-full-text articles such as reviews and editorials were removed. The remaining full-text articles were assessed for eligibility. In addition to the inclusion criteria mentioned, we considered the exclusion criteria: studies with animals, text

not available, methods development, no MRI technique used, another clinical group (instead of cSVD), trial presentation (description of future clinical trials), and drug use as cSVD prevention. The remaining full-text articles were included in the systematic review. The articles' details regarding Identification, Screening, Eligibility and Inclusion (PRISMA-P diagram flow) are described in Figure 1.

Results

We included 37 full-text articles that evaluated the contributions of ASL (N = 20), IVIM (N = 5), and CVR measures (N = 12) regarding the cSVD study. Table 1 shows a summary of the main findings.

Arterial Spin Labeling (ASL)

ASL is a perfusion-weighted MRI method designed to explore the water molecules in the arterial blood as an endogenous tracer, resulting in a noninvasive approach to measuring CBF and related parameters [17,18]. The arterial blood is used as a tracer by applying slab-selected radiofrequency pulses in a signal preparation step to be magnetically labeled. After a post-labeling delay (PLD), the labeled blood reaches the brain tissue, where the label image is acquired. A control image without any preparation pulse is also acquired. CBF is estimated by applying a physical model to subtract control and label images.

ASL: cSVD and CBF deregulation

Perfusion abnormalities are a common finding in cSVD, with evidence suggesting that CBF and cSVD severity are negatively associated [7,19]. Also, CBF changes have been associated with inflammation in gray matter and impaired cognitive function in different domains [20]. However, it remains unclear whether reduced CBF is consequential or contributing to the severity of white matter hyperintensities (WMH) observed in fluid-attenuated inversion recovery (FLAIR) or T2-weighted MRI, which emphasizes the need for longitudinal studies to address this issue further.

In 2014, a pseudocontinuous ASL (pCASL) study in Alzheimer's disease patients (AD) found that smaller normalized brain volume and higher WMH volume were both associated with lower CBF, suggesting that this perfusion metric might reflect the combined burden effects of both neurodegenerative and cSVD pathologies [21]. Moreover, a recent study reported CBF as a potential biomarker for cSVD progression in Cerebral Autosomal Dominant Arteriopathy with Subcortical Infarcts and Leukoencephalopathy (CADASIL) since it predicted progression of WMH [22]. In healthy elderly, CBF negatively predicted total WMH volume, even when brain iron is also

considered [23]. 3D-pCASL has also provided reliable measurements of CBF, which correlated with WMH volume in a cohort of elderly Latinx at risk of cSVD, showing a prognostic potential to early identification of dementia development [24].

A region of crucial attention in cSVD is the periventricular WM (PVWM), which is supplied exclusively by small vessels and is more susceptible to developing WMH lesions [25]. The development of novel ASL sequences has allowed more reliable CBF measurements in WM [26]. A large cohort using pCASL combined with background suppression and a 3D spiral readout reported the PVWM as the region with the lowest regional perfusion of the whole brain, coinciding with regions that most frequently showed WMH [27]. It suggests that periventricular CBF could be an early biomarker of cSVD. In another study, echocardiographic and deep regional CBF in arteriosclerotic cSVD showed association with total burden, suggesting a prognostic potential [28]. Also, a correlation was found between thalamic blood flow measured with ASL and gait in an elderly group with at least one vascular risk factor, suggesting that subcortical vascularity must be considered when studying the functional decline in the elderly population [29].

Finally, an ASL pulse sequence combined with diffusion gradients before the readout module (DP-pCASL, diffusion prepared pCASL) appears to be a promising approach to non-invasively map the water exchange across the BBB [30]. BBB dysfunction plays a significant role in the pathophysiology of cSVD, among other neurological diseases. The water exchange rate (k_w) measured through this new technique showed good reproducibility and correlated with WMH burden, vascular risk factors, and clinical endpoints, such as performance in cognitive tests, and may represent a promising biomarker of cSVD and VCI. Such a method was later compared to dynamic contrast-enhanced (DCE) measurements of BBB permeability in a group of risk for cSVD patients. While the k_w was shown to have a good test-retest reproducibility, the methods comparison revealed better spatial information for DCE-MRI over the DP-pCASL [31].

A study of patients with carotid stenosis recently reported that pre-operative WMH and lacunes were independently associated with postoperative cerebral hyperperfusion [32]. Therefore, cSVD may be a risk factor for hyperperfusion and hemorrhage after carotid endarterectomy.

ASL: cSVD and risk factors

Since arterial hypertension is considered a significant risk factor for cSVD, ASL has also been used to investigate the relationship between blood pressure (BP) and CBF in the elderly, yielding conflicting results [33,34]. While Clark et al. found mean arterial pressure (MAP) to be negatively associated with CBF in specific regions [33], data from a larger study did not show an association between BP measurements and CBF [34]. This issue was further addressed in the PRESERVE clinical

trial, in which 70 patients with severe cSVD were randomized to either standard (systolic BP < 130-140 mmHg) or intensive (systolic BP < 125 mmHg) BP targets [35]. Although pulsed ASL (PASL) to measure CBF, especially for WM quantification, represents a limitation, the results from this trial agreed with previous literature [34], showing no association between CBF and BP in both groups. An ongoing trial is applying ASL to investigate whether tadalafil, a pharmacological vasodilator, can increase CBF in cSVD patients, though results are not yet available [36].

Moreover, Wang et al. quantified CBF from patients in mild to moderate stages of hypertension using a pCASL labeling scheme with a fast spin-echo spiral readout to increase the signal-to-noise ratio (SNR) [37]. As expected, they found global GM-CBF reduction. However, more interestingly, 3D pCASL was capable of identifying subtle hemodynamic changes in regions of normal-appearing white matter (NAWM) even at an early stage of hypertension, suggesting it could potentially be useful as an early biomarker for cSVD (Figure 2).

Similarly, Shen et al. used a multi-PLD PASL approach combined with a 3D GRASE readout to investigate cerebral hemodynamic changes in patients with type-2 diabetes, another common risk factor for cSVD [38]. Although no CBF difference was observed in global GM between patients and controls, CBF values extracted from the WM were significantly lower in the diabetes group. Bolus arrival time and the number of WMHs were higher among diabetic patients, and, like reduced WM-CBF, they may reflect underlying cSVD.

Furthermore, ASL has also been applied to investigate whether human immunodeficiency virus (HIV) infection was associated with an increased cSVD burden [39]. Since neither CBF nor WMH volume was associated with the serologic condition, it was suggested that HIV status might not be related to the increased burden of cSVD [39].

Limitations and Future Directions

While CBF alterations in WM matter have been studied over the last years, it is essential to highlight that not all ASL sequences are reliable for WM CBF quantification. In that sense, optimized background suppression approaches, improving the labeling efficiency for single- and multi-PLD ASL, are required. Novel ASL sequences have been optimized to model vascular permeability, opening a new path to investigate BBB dysfunction, considered a hallmark pathological feature of cSVD [27,40,41]. Going to ultra-high field MRI (7T) is another exciting perspective for ASL measurements in WM. Although 7T ASL is still challenging, the gain in SNR due to the B0 field may contribute to answering important questions regarding pathways of cSVD, allowing more reliable measurements in WM and recently introducing novel measurements in the brain clearance mechanisms [42–44]. Finally, an exciting development in the field has been done with ASL

fingerprinting, which may make the ASL long acquisition duration smoother in the translation toward clinical use. Several studies have already shown dictionary matching approaches able to measure the hemodynamic parameters in agreement with traditional ASL measurements [45–49].

Intravoxel Incoherent Movement (IVIM)

IVIM is an MRI method weighted in different degrees of diffusion, aiming to distinguish the free diffusion of water molecules in the biological tissue from randomly moving with the flow [50,51]. The acquisition of multiple images under different diffusion weighting (or b-value) allows splitting the total signal decay into typically two main contributions: pure diffusion movement and pseudo-diffusion movement associated with blood perfusion.

IVIM applications in cSVD are mainly focused on investigating the integrity of WM lesions. In 2017, a study reported decreased pseudo-diffusion coefficient (D*), increased diffusion coefficient (D), and perfusion fraction (*f*) in both PVWM and deep WM when compared to the surrounding normal WM. Decreased D* suggests a reduction in CBF, while increased D and f are related to alterations in the tissue microstructure [52]. Interestingly, increased *f* was also independently associated with better cognitive performance, indicating it could represent a compensatory response to prevent further ischemic injury of the WM. Similar results were reported by Wong et al. [53], who showed an *f* increase in regions of NAWM, and by Zhang and colleagues [54], who demonstrated a reduction of microvascular perfusion in the NAWM and cortical GM associated with lower cognitive performance in cSVD patients. Alterations in *f* found in regions of NAWM could indicate that this measure might be capturing other underlying cSVD-related pathological changes, such as enlargement of perivascular spaces, BBB leakage, or increased vessel tortuosity.

A recent 2-year longitudinal study reported increased perilesional WM diffusivity measured with IVIM in patients with sporadic cSVD [55]. This increase was associated with BBB leakage at baseline, which must play a crucial role in WM degeneration.

An approach to IVIM spectral diffusion model was recently proposed, exploring the non-negative least-squares fitting method [56]. This method is particularly appealing because it does not require a fixed number of components to describe the IVIM signal, as was the case with the original methodology (parenchymal and microvascular components). This new methodology yields a diffusion spectrum, from which an intermediate diffusion component lying in between the traditional diffusion and pseudo-diffusion range could be identified within lesion-prone regions of cSVD patients. This intermediate component has been associated with WMH volume and enlarged perivascular spaces and could indicate increased interstitial fluid in degenerated tissue or perivascular

edema (Figure 3). The new component has also been identified in NAWM regions, where it might capture early tissue abnormalities, possibly linked to aging and glymphatic dysfunction [56].

Limitations and Future Directions

Although IVIM appeared as an exciting method to evaluate cerebrovascular diseases patients, it still lacks a quantitative model for perfusion information in physiological unities and standardization of acquisition protocol and analysis pipelines. The total number of b-values acquired, the low b-value ranges, and even the maximum b-value to be included directly influence the choice of the analysis model. Their non-standard use hampers the reproducibility of studies among different centers. As future perspectives for IVIM in cSVD, the ultra-high fields appear as an emerging application, while machine learning, artificial intelligence methods, including Bayesian models, are appealing computational tools that might improve the quality of IVIM maps.

Cerebrovascular Reactivity (CVR)

Several studies have reported that endothelial dysfunction may be a mechanism that alerts the development of cSVD [5,57,58]; therefore, CVR measures may be beneficial for cSVD assessment. Because of its dependency on CBF, BOLD contrast was shown as a reliable and reproducible method to assess cerebrovascular reactivity (CVR-BOLD) at the tissue level in response to changes in the flow speed caused by a vasoactive stimulus [14]. ASL has also been proposed for such application (CVR-ASL) since it provides CBF measures directly [59]. Hypercapnia is the most used stimulus to increase CBF. It can be induced in several ways, including inhalation of CO_2-enriched air [60–63], breath-holding test [64], and hyperventilation [65]. Acetazolamide injection, a carbonic anhydrase inhibitor that dilates cerebral microvasculature by increasing carbonic acid in arterial blood, is also often used to cause vasodilation in CVR studies [66,67].

Few studies have evaluated CVR in cSVD, and the characteristics of the patients varied between them. We included ten studies that used BOLD contrast to assess CVR. Atwi et al. found no difference in GM-CVR values between patients with moderate to severe WMH but showed increased WM-CVR values for patients compared to healthy subjects [60]. However, Stringer et al. reported lower CVR in WM and subcortical GM of patients with higher WMH volumes at both 1.5T and 3T [68]. After controlling for age, sex, and systolic blood pressure, Blair et al. also observed that lower WM-CVR was associated with higher WMH volume, periventricular WMH, Fazekas' score, and basal ganglia PVS score [69]. However, Thrippleton et al. showed that while lower CVR in most GM regions was found in patients with a history of vascular events than healthy controls, a significant difference in CVR was found in only one WM region when comparing these groups. Patients presented reduced

right frontal WM CVR values than healthy controls [63]. However, in two studies [60,63], the control group was much younger than the patient group, interfering with the result.

Besides, NAWM that evolved to WMH showed lower CVR than the NAWM that remains stable over the long term [62], and reduced CVR was associated with a higher total cSVD burden, including WMH, lacunes, and perivascular spaces [65]. On the other hand, two other studies reported no association between WMH and CVR [61,64], and one of them reported reducing CVR with the presence of microbleeds [64].

An ongoing longitudinal study in patients with a mild ischemic stroke, which assesses cSVD, clinical, and imaging outcomes, including CVR-BOLD, intends to open the understanding of cSVD and contribute to the detection of preclinical stages [70]. Moreover, Blair et al. reported that CVR-BOLD is feasible in clinical trials and that improvements in cerebrovascular function after specific medication can be measured with such an MRI method [71].

We also included two studies that used ASL to assess CVR. In patients with hypertensive cSVD, reduced CVR was observed in the basal ganglia and the temporal lobe after adjusting for age and sex. The reduction in the former region was significantly correlated with the total cSVD score [72]. However, a 2-year longitudinal study reported CBF, but not CVR, as a predictor of radiological progression of WMH in CADASIL patients [73].

Limitations and Future Directions

A possible explanation for the discordances between studies concerns the different vasodilatory stimuli used. Although there was a slight difference between breath-holding and CO_2 inhalation for CVR assessment, only ASL, not BOLD-MRI, was used [74]. Moreover, even with monitoring the end-tidal CO_2 (EtCO2), significant CVR variations are often observed across subjects and sessions [75]. Therefore, CVR status in cSVD is still an open question, and caution should be taken when interpreting such findings. An alternative for future studies is to evaluate CVR under resting state.

Discussion

The present review focused on the contributions of contrast-agent-free, state-of-the-art MRI techniques (ASL, IVIM, CVR-BOLD, and CVR-ASL) to understand cSVD underlying pathophysiology and relation with risk factors.

ASL can characterize the mechanisms underlying cSVD, useful for diagnosis, follow-up, and uncovering the disease's pathogenesis. Among the main findings, a global GM-CBF reduction and association with physiological parameters, such as the MAP, were observed. A systematic review in

2016 tried to understand better the cause-consequence relationship between CBF reduction and cSVD severity and concluded that WMH is more likely to drive CBF reduction, considering the adversities in measuring CBF in the WM [76]. While CBF alterations in WM matter have been studied over the last years, it is essential to highlight that not all ASL sequences are reliable for WM CBF quantification.

Furthermore, perfusion and diffusion assessment can be performed with IVIM. Although only a few studies have investigated IVIM performance in assessing cSVD, and it is crucial to evaluate the reproducibility of these results, exciting findings were already reported. Since IVIM is based on the water as an endogenous tracer and does not require any labeling, it is an excellent alternative to explore the white matter perfusion, especially in the NAWM, a possible early biomarker of dementia [52,53,56]. As a recent application, there is still an open field for the development of acquisition and analysis setups for the cSVD investigation, albeit to date, there is appealing evidence for considering IVIM as an essential tool for such application. Analysis models that do not require a previous definition regarding the number of components to the IVIM signal must be explored. In that sense, Bayesian methods and machine learning are potential strategies to be employed. On the other hand, exploring ultra-high field MRI could improve the measurements to investigate regions such as the NAWM.

Besides, MRI can investigate the cerebral hemodynamics of cSVD patients under the challenge of high metabolic demand through the CVR measurement. Although reduced cSVD-related CVR is reported in some studies, the available data do not point to a strong association between the worsening characteristics of cSVD and CVR. Future studies should clearly define the patient population's clinical characteristics, ensure the measurement of confounding variables, and use a standard CVR measurement method to compare studies better. Another point that must be discussed is considering the vasoactive stimulus used to minimize the patient's discomfort. Moreover, assessing CVR with ASL may be an alternative [14] since the BOLD signal depends on a complicated relationship between CBF, cerebral blood volume, and oxygen extraction. On the other hand, the ASL technique provides quantitative information about CBF and CVR with a single acquisition.

Conclusion

ASL, IVIM, and CVR measures are promising tools to assess the contribution of cSVD-related risk factors such as age, diabetes, and hypertension, in developing the disease. The effects of protective factors can also be considered with such methods. Once these conditions can lead to small vessel impairments, affecting CBF, vasoreactivity, and BBB permeability, ASL, IVIM, and CVR can

contribute mainly to the pathophysiology study. However, whether these imaging markers are independently associated with cSVD outcomes or have combined effects is still an open question.

Conflict(s)-of-Interest/Disclosure(s)

None.

References

[1]   L. Pantoni, Cerebral small vessel disease: from pathogenesis and clinical characteristics to therapeutic challenges, Lancet Neurol. 9 (2010) 689–701. https://doi.org/10.1016/S1474-4422(10)70104-6.

[2]   J.M. Wardlaw, C. Smith, M. Dichgans, Small vessel disease: mechanisms and clinical implications, Lancet Neurol. (2019). https://doi.org/10.1016/S1474-4422(19)30079-1.

[3]   M. Dichgans, D. Leys, Vascular Cognitive Impairment, Circ. Res. 120 (2017) 573–591. https://doi.org/10.1161/CIRCRESAHA.116.308426.

[4]   J.M. Wardlaw, E.E. Smith, G.J. Biessels, C. Cordonnier, F. Fazekas, R. Frayne, R.I. Lindley, J.T. O'Brien, F. Barkhof, O.R. Benavente, S.E. Black, C. Brayne, M. Breteler, H. Chabriat, C. DeCarli, F.-E. de Leeuw, F. Doubal, M. Duering, N.C. Fox, S. Greenberg, V. Hachinski, I. Kilimann, V. Mok, R. van Oostenbrugge, L. Pantoni, O. Speck, B.C.M. Stephan, S. Teipel, A. Viswanathan, D. Werring, C. Chen, C. Smith, M. van Buchem, B. Norrving, P.B. Gorelick, M. Dichgans, STandards for ReportIng Vascular changes on nEuroimaging (STRIVE v1), Neuroimaging standards for research into small vessel disease and its contribution to ageing and neurodegeneration, Lancet Neurol. 12 (2013) 822–838. https://doi.org/10.1016/S1474-4422(13)70124-8.

[5]   J.M. Wardlaw, C. Smith, M. Dichgans, Mechanisms of sporadic cerebral small vessel disease: Insights from neuroimaging, Lancet Neurol. (2013). https://doi.org/10.1016/S1474-4422(13)70060-7.

[6]   M. Pasi, I.W.M. Van Uden, A.M. Tuladhar, F.E. De Leeuw, L. Pantoni, White Matter Microstructural Damage on Diffusion Tensor Imaging in Cerebral Small Vessel Disease: Clinical Consequences, Stroke. (2016). https://doi.org/10.1161/STROKEAHA.115.012065.

[7]   A. Ter Telgte, E.M.C. Van Leijsen, K. Wiegertjes, C.J.M. Klijn, A.M. Tuladhar, F.E. De Leeuw, Cerebral small vessel disease: From a focal to a global perspective, Nat. Rev. Neurol. (2018). https://doi.org/10.1038/s41582-018-0014-y.

[8]   E.E. Smith, G.J. Biessels, F. De Guio, F.E. de Leeuw, S. Duchesne, M. Düring, R. Frayne, M.A. Ikram, E. Jouvent, B.J. MacIntosh, M.J. Thrippleton, M.W. Vernooij, H. Adams, W.H. Backes, L. Ballerini, S.E. Black, C. Chen, R. Corriveau, C. DeCarli, S.M. Greenberg, M.E. Gurol, M. Ingrisch, D. Job, B.Y.K. Lam, L.J. Launer, J. Linn, C.R. McCreary, V.C.T. Mok, L. Pantoni, G.B. Pike, J. Ramirez, Y.D. Reijmer, J.R. Romero, S. Ropele, N.S. Rost, P.S. Sachdev, C.J.M. Scott, S. Seshadri, M. Sharma, S. Sourbron, R.M.E. Steketee, R.H. Swartz, R. van Oostenbrugge, M. van Osch, S. van Rooden, A. Viswanathan, D. Werring, M. Dichgans, J.M. Wardlaw, Harmonizing brain magnetic resonance imaging methods for vascular contributions to neurodegeneration, Alzheimer's Dement. Diagnosis, Assess. Dis. Monit. 11 (2019) 191–204. https://doi.org/10.1016/j.dadm.2019.01.002.

[9]   M.C. Zanon Zotin, L. Sveikata, A. Viswanathan, P. Yilmaz, Cerebral small vessel disease and vascular cognitive impairment: from diagnosis to management, Curr. Opin. Neurol. 34 (2021) 246–257. https://doi.org/10.1097/WCO.0000000000000913.

[10]   G.W. Blair, M.V. Hernandez, M.J. Thrippleton, F.N. Doubal, J.M. Wardlaw, Advanced Neuroimaging of Cerebral Small Vessel Disease, Curr. Treat. Options Cardiovasc. Med. 19 (2017) 56. https://doi.org/10.1007/s11936-017-0555-1.

[11]   E.M. Gale, P. Caravan, Gadolinium-free contrast agents for magnetic resonance imaging of the central nervous system, ACS Chem. Neurosci. 9 (2018) 395. https://doi.org/10.1021/ACSCHEMNEURO.8B00044.

[12]   W.H.E. Wong, J.J. Maller, Arterial Spin Labeling Techniques 2009–2014, J. Med. Imaging Radiat. Sci. 47 (2016) 98–107. https://doi.org/10.1016/j.jmir.2015.08.002.

[13]   M.Y. Zhao, A.P. Fan, D.Y.-T. Chen, Y. Ishii, M.M. Khalighi, M. Moseley, G.K. Steinberg, G. Zaharchuk, Using arterial spin labeling to measure cerebrovascular reactivity in Moyamoya disease: Insights from simultaneous PET/MRI, J. Cereb. Blood Flow Metab. (2022) 0271678X2210834. https://doi.org/10.1177/0271678x221083471.

[14]   R.F. Leoni, I.A.F. Oliveira, O.M. Pontes-Neto, A.C. Santos, J.P. Leite, Cerebral blood flow and vasoreactivity in aging: An arterial spin labeling study, Brazilian J. Med. Biol. Res. (2017). https://doi.org/10.1590/1414-431X20175670.

[15]   A.M. Paschoal, R.F. Leoni, A.C. dos Santos, F.F. Paiva, Intravoxel incoherent motion MRI in neurological and cerebrovascular diseases, NeuroImage Clin. 20 (2018). https://doi.org/10.1016/j.nicl.2018.08.030.

[16]   L. Shamseer, D. Moher, M. Clarke, D. Ghersi, A. Liberati, M. Petticrew, P. Shekelle, L.A. Stewart, D.G. Altman, A. Booth, A.W. Chan, S. Chang, T. Clifford, K. Dickersin, M. Egger, P.C. Gøtzsche, J.M. Grimshaw, T. Groves, M. Helfand, J. Higgins, T. Lasserson, J. Lau, K. Lohr, J. McGowan, C. Mulrow, M. Norton, M. Page, M. Sampson, H. Schünemann, I. Simera, W. Summerskill, J. Tetzlaff, T.A. Trikalinos, D. Tovey, L. Turner, E. Whitlock, Preferred reporting items for systematic review and meta-analysis protocols (prisma-p) 2015: Elaboration and explanation, BMJ. (2015). https://doi.org/10.1136/bmj.g7647.

[17]   J.A. Detre, J.S. Leigh, D.S. Williams, A.P. Koretsky, Perfusion imaging, Magn Reson Med. 23 (1992) 37–45. http://www.ncbi.nlm.nih.gov/pubmed/1734182.

[18]   D.C. Alsop, J.A. Detre, X. Golay, M. Gunther, J. Hendrikse, L. Hernandez-Garcia, H. Lu, B.J. MacIntosh, L.M. Parkes, M. Smits, M.J. van Osch, D.J. Wang, E.C. Wong, G. Zaharchuk, Recommended implementation of arterial spin-labeled perfusion MRI for clinical applications: A consensus of the ISMRM perfusion study group and the European consortium for ASL in dementia, Magn Reson Med. 73 (2015) 102–116. https://doi.org/10.1002/mrm.25197.

[19]   C. Yu, W. Lu, J. Qiu, F. Wang, J. Li, L. Wang, Alterations of the Whole Cerebral Blood Flow in Patients With Different Total Cerebral Small Vessel Disease Burden, Front. Aging Neurosci. 12 (2020) 175. https://doi.org/10.3389/fnagi.2020.00175.

[20]   C.J. Huang, X. Zhou, X. Yuan, W. Zhang, M.X. Li, M.Z. You, X.Q. Zhu, Z.W. Sun, Contribution of Inflammation and Hypoperfusion to White Matter Hyperintensities-Related Cognitive Impairment, Front. Neurol. 12 (2022) 1–11. https://doi.org/10.3389/fneur.2021.786840.

[21]   M.R. Benedictus, M.A.A. Binnewijzend, J.P.A. Kuijer, M.D. Steenwijk, A. Versteeg, H. Vrenken, P. Scheltens, F. Barkhof, W.M. van der Flier, N.D. Prins, Brain volume and white matter hyperintensities as determinants of cerebral blood flow in Alzheimer's disease, Neurobiol. Aging. 35 (2014) 2665–2670. https://doi.org/10.1016/j.neurobiolaging.2014.06.001.

[22]   F.C. Moreton, B. Cullen, D.A. Dickie, R. Lopez Gonzalez, C. Santosh, C. Delles, K.W. Muir, Brain imaging factors associated with progression of subcortical hyperintensities in CADASIL over two year follow up, Eur. J. Neurol. (2020) ene.14534. https://doi.org/10.1111/ene.14534.

[23]   C.E. Bauer, V. Zachariou, E. Seago, B.T. Gold, White Matter Hyperintensity Volume and Location: Associations With WM Microstructure, Brain Iron, and Cerebral Perfusion, Front. Aging Neurosci. 13 (2021) 1–12. https://doi.org/10.3389/fnagi.2021.617947.

[24]   K. Jann, X. Shao, S.J. Ma, S.Y. Cen, L. D'Orazio, G. Barisano, L. Yan, M. Casey, J. Lamas, A.M. Staffaroni, J.H. Kramer, J.M. Ringman, D.J.J. Wang, Evaluation of Cerebral Blood Flow Measured by 3D PCASL as Biomarker of Vascular Cognitive Impairment and Dementia (VCID) in a Cohort of Elderly Latinx Subjects at Risk of Small Vessel Disease, Front. Neurosci. 15 (2021). https://doi.org/10.3389/fnins.2021.627627.

[25]   D.M. Moody, M.A. Bell, V.R. Challa, Features of the cerebral vascular pattern that predict vulnerability to perfusion or oxygenation deficiency: An anatomic study, Am. J. Neuroradiol. (1990).

[26]   L.R. Binnie, M.M.H. Pauls, P. Benjamin, M.P.K. Dhillon, S. Betteridge, B. Clarke, R. Ghatala, F.A.H. Hainsworth, F.A. Howe, U. Khan, C. Kruuse, J.B. Madigan, B. Moynihan, B. Patel, A.C. Pereira, E. Rostrup, A.B.Y. Shtaya, C.A. Spilling, S. Trippier, R. Williams, J.D. Isaacs, T.R. Barrick, A.H. Hainsworth, Test–retest reliability of arterial spin labelling for cerebral blood flow in older adults with small vessel disease, Transl. Stroke Res. (2022). https://doi.org/10.1007/s12975-021-00983-5.

[27]   S. Dolui, D. Tisdall, M. Vidorreta, D.R. Jacobs, I.M. Nasrallah, R.N. Bryan, D.A. Wolk, J.A. Detre, Characterizing a perfusion-based periventricular small vessel region of interest, NeuroImage Clin. 23 (2019) 101897. https://doi.org/10.1016/j.nicl.2019.101897.

[28]   X. Chen, D. Lu, N. Guo, Z. Kang, K. Zhang, J. Wang, X. Men, Z. Lu, W. Qiu, Left ventricular ejection fraction and right atrial diameter are associated with deep regional CBF in arteriosclerotic cerebral small vessel disease, BMC Neurol. 21 (2021). https://doi.org/10.1186/s12883-021-02096-w.

[29]   N.D. Koblinsky, S. Atwi, E. Cohen, N.D. Anderson, C.E. Greenwood, B.J. MacIntosh, A.D. Robertson, Lower Thalamic Blood Flow Is Associated With Slower Stride Velocity in Older Adults, Front. Aging Neurosci. 12 (2020) 571074. https://doi.org/10.3389/fnagi.2020.571074.

[30]   X. Shao, S.J. Ma, M. Casey, L. D'Orazio, J.M. Ringman, D.J.J. Wang, Mapping water exchange across the blood–brain barrier using 3D diffusion-prepared arterial spin labeled perfusion MRI, Magn. Reson. Med. 81 (2019) 3065–3079. https://doi.org/10.1002/mrm.27632.

[31]   X. Shao, K. Jann, S.J. Ma, L. Yan, A. Montagne, J.M. Ringman, B. V. Zlokovic, D.J.J. Wang, Comparison Between Blood-Brain Barrier Water Exchange Rate and Permeability to Gadolinium-Based Contrast Agent in an Elderly Cohort, Front. Neurosci. 14 (2020) 1–16. https://doi.org/10.3389/fnins.2020.571480.

[32]   X. Fan, Z. Lai, T. Lin, H. You, J. Wei, M. Li, C. Liu, F. Feng, Pre-operative Cerebral Small Vessel Disease on MR Imaging Is Associated With Cerebral Hyperperfusion After Carotid Endarterectomy, Front. Cardiovasc. Med. 8 (2021) 1–11. https://doi.org/10.3389/fcvm.2021.734392.

[33]   L.R. Clark, D.A. Nation, C.E. Wierenga, K.J. Bangen, S.I. Dev, D.D. Shin, L. Delano-Wood, T.T. Liu, R.A. Rissman, M.W. Bondi, Elevated cerebrovascular resistance index is associated with cognitive dysfunction in the very-old, Alzheimer's Res. Ther. 7 (2015) 1–9. https://doi.org/10.1186/s13195-014-0080-3.

[34]   J.C. Foster-Dingley, J.E.F. Moonen, A.J.M. De Craen, W. De Ruijter, R.C. Van Der Mast, J. Van Der Grond, Blood pressure is not associated with cerebral blood flow in older persons, Hypertension. 66 (2015) 954–960. https://doi.org/10.1161/HYPERTENSIONAHA.115.05799.

[35]   I.D. Croall, D.J. Tozer, B. Moynihan, U. Khan, J.T. O'Brien, R.G. Morris, V.C. Cambridge, T.R. Barrick, A.M. Blamire, G.A. Ford, H.S. Markus, Effect of Standard vs Intensive blood pressure control on cerebral blood flowin small vessel disease the preserve randomized clinical trial, JAMA Neurol. 75 (2018) 720–727. https://doi.org/10.1001/jamaneurol.2017.5153.

[36]   M.M.H. Pauls, N. Clarke, S. Trippier, S. Betteridge, F.A. Howe, U. Khan, C. Kruuse, J.B. Madigan, B. Moynihan, A.C. Pereira, D. Rolfe, E. Rostrup, C.E. Haig, T.R. Barrick, J.D. Isaacs, A.H. Hainsworth, Perfusion by Arterial Spin labelling following Single dose Tadalafil In Small vessel disease (PASTIS): Study protocol for a randomised controlled trial, Trials. 18 (2017) 1–8. https://doi.org/10.1186/s13063-017-1973-9.

[37]   T. Wang, Y. Li, X. Guo, D. Huang, L. Ma, D.J.J. Wang, X. Lou, Reduced perfusion in normal-appearing white matter in mild to moderate hypertension as revealed by 3D pseudocontinuous arterial spin labeling, J. Magn. Reson. Imaging. 43 (2016) 635–643. https://doi.org/10.1002/jmri.25023.

[38]   Y. Shen, B. Zhao, L. Yan, K. Jann, G. Wang, J. Wang, B. Wang, J. Pfeuffer, T. Qian, D.J.J. Wang, Cerebral hemodynamic and white matter changes of type 2 diabetes revealed by multi-TI arterial spin labeling and double inversion recovery sequence, Front. Neurol. 8 (2017) 1–9. https://doi.org/10.3389/fneur.2017.00717.

[39]   L.J. Haddow, C.H. Sudre, M. Sokolska, R.C. Gilson, I.G. Williams, X. Golay, S. Ourselin, A. Winston, C.A. Sabin, M.J. Cardoso, H.R. Jäger, Magnetic Resonance Imaging of Cerebral Small Vessel Disease in Men Living with HIV and HIV-Negative Men Aged 50 and above, AIDS Res. Hum. Retroviruses. 35 (2019) 453–460. https://doi.org/10.1089/aid.2018.0249.

[40]   L. Petitclerc, S. Schmid, W.M. Teeuwisse, M.J.P. Van Osch, Investigation into water transport mechanisms in the brain using a combination of T2 measurements and crusher gradients with ASL., Proc

18th Sci Meet Int Soc Magn Reson Med. 2018. (2018) 4–6.

[41]   Z. Lin, Y. Li, P. Su, D. Mao, Z. Wei, J.J. Pillai, A. Moghekar, M. van Osch, Y. Ge, H. Lu, Non-contrast MR imaging of blood-brain barrier permeability to water, Magn. Reson. Med. 80 (2018) 1507–1520. https://doi.org/10.1002/mrm.27141.

[42]   L. Petitclerc, L. Hirschler, J.A. Wells, D.L. Thomas, M.J.P. Van Osch, Blood-CSF Barrier Imaging in the Human Brain with Arterial Spin Labeling, Proc 21th Sci Meet Int Soc Magn Reson Med. 2021. (2021) 4–6.

[43]   P.G. Evans, M. Sokolska, A. Alves, I.F. Harrison, Y. Ohene, P. Nahavandi, O. Ismail, M.F. Lythgoe, D.L. Thomas, J.A. Wells, E. Miranda, Non-Invasive MRI of Blood-Cerebrospinal Fluid Barrier Function, Nat. Commun. (2020) 1–11. https://doi.org/10.1038/s41467-020-16002-4.

[44]   Y. Ohene, I.F. Harrison, P. Nahavandi, O. Ismail, E. V. Bird, O.P. Ottersen, E.A. Nagelhus, D.L. Thomas, M.F. Lythgoe, J.A. Wells, Non-invasive MRI of brain clearance pathways using multiple echo time arterial spin labelling: an aquaporin-4 study, Neuroimage. 188 (2019) 515–523. https://doi.org/10.1016/j.neuroimage.2018.12.026.

[45]   H. Fan, P. Su, J. Huang, P. Liu, H. Lu, Multi-band MR fingerprinting (MRF) ASL imaging using artificial-neural-network trained with high-fidelity experimental data, Magn. Reson. Med. 85 (2021) 1974–1985. https://doi.org/10.1002/mrm.28560.

[46]   Q. Zhang, P. Su, Z. Chen, Y. Liao, S. Chen, R. Guo, H. Qi, X. Li, X. Zhang, Z. Hu, H. Lu, H. Chen, Deep learning–based MR fingerprinting ASL ReconStruction (DeepMARS), Magn. Reson. Med. 84 (2020) 1024–1034. https://doi.org/10.1002/mrm.28166.

[47]   A. Lahiri, J.A. Fessler, L. Hernandez-Garcia, Optimizing MRF-ASL scan design for precise quantification of brain hemodynamics using neural network regression, Magn. Reson. Med. 83 (2020) 1979–1991. https://doi.org/10.1002/mrm.28051.

[48]   P. Su, D. Mao, P. Liu, Y. Li, M.C. Pinho, B.G. Welch, H. Lu, Multiparametric estimation of brain hemodynamics with MR fingerprinting ASL, Magn. Reson. Med. 78 (2017) 1812–1823. https://doi.org/10.1002/mrm.26587.

[49]   K.L. Wright, Y. Jiang, D. Ma, D.C. Noll, M.A. Griswold, V. Gulani, L. Hernandez-Garcia, Estimation of perfusion properties with MR Fingerprinting Arterial Spin Labeling, Magn. Reson. Imaging. 50 (2018) 68–77. https://doi.org/10.1016/j.mri.2018.03.011.

[50]   D. Le Bihan, E. Breton, D. Lallemand, P. Grenier, E. Cabanis, M. Laval-Jeantet, MR imaging of intravoxel incoherent motions: application to diffusion and perfusion in neurologic disorders, Radiology. 161 (1986) 401–407. https://doi.org/10.1148/radiology.161.2.3763909.

[51]   D. Le Bihan, E. Breton, D. Lallemand, M.L. Aubin, J. Vignaud, M. Laval-Jeantet, Separation of diffusion and perfusion in intravoxel incoherent motion MR imaging, Radiology. 168 (1988) 497–505. https://doi.org/10.1148/radiology.168.2.3393671.

[52]   J. Sun, X. Yu, Y. Jiaerken, R. Song, P. Huang, C. Wang, L. Yuan, Y. Mao, Y. Guo, H. Yu, M. Zhang, The relationship between microvasculature in white matter hyperintensities and cognitive function, Brain Imaging Behav. 11 (2017) 503–511. https://doi.org/10.1007/s11682-016-9531-8.

[53]   S.M. Wong, C.E. Zhang, F.C.G. van Bussel, J. Staals, C.R.L.P.N. Jeukens, P.A.M. Hofman, R.J. van Oostenbrugge, W.H. Backes, J.F.A. Jansen, Simultaneous investigation of microvasculature and parenchyma in cerebral small vessel disease using intravoxel incoherent motion imaging, Neuroimage-Clinical. 14 (2017) 216–221. https://doi.org/10.1016/j.nicl.2017.01.017.

[54]   C.E. Zhang, S.M. Wong, R. Uiterwijk, J. Staals, W.H. Backes, E.I. Hoff, T. Schreuder, C.R.L.P.N. Jeukens, J.F.A. Jansen, R.J. Van Oostenbrugge, Intravoxel Incoherent Motion Imaging in Small Vessel Disease: Microstructural Integrity and Microvascular Perfusion Related to Cognition, Stroke. 48 (2017) 658–663. https://doi.org/10.1161/STROKEAHA.116.015084.

[55]   D. Kerkhofs, S.M. Wong, E. Zhang, J. Staals, J.F.A. Jansen, R.J. van Oostenbrugge, W.H. Backes, Baseline Blood-Brain Barrier Leakage and Longitudinal Microstructural Tissue Damage in the Periphery of White Matter Hyperintensities, Neurology. 96 (2021) e2192–e2200. https://doi.org/10.1212/WNL.0000000000011783.

[56]   S.M. Wong, W.H. Backes, G.S. Drenthen, C.E. Zhang, P.H.M. Voorter, J. Staals, R.J. van Oostenbrugge, J.F.A. Jansen, Spectral Diffusion Analysis of Intravoxel Incoherent Motion MRI in Cerebral Small Vessel Disease, J. Magn. Reson. Imaging. (2019). https://doi.org/10.1002/jmri.26920.

[57]   A. Poggesi, M. Pasi, F. Pescini, L. Pantoni, D. Inzitari, Circulating biologic markers of endothelial dysfunction in cerebral small vessel disease: A review, J. Cereb. Blood Flow Metab. (2016). https://doi.org/10.1038/jcbfm.2015.116.

[58]   E.L. Bailey, C. Smith, C.L.M. Sudlow, J.M. Wardlaw, Pathology of lacunar ischemic stroke in humans - A systematic review, Brain Pathol. (2012). https://doi.org/10.1111/j.1750-3639.2012.00575.x.

[59]   P. Liu, J.B. De Vis, H. Lu, Cerebrovascular reactivity (CVR) MRI with CO2 challenge: A technical review, Neuroimage. 187 (2019) 104–115. https://doi.org/10.1016/j.neuroimage.2018.03.047.

[60]   S. Atwi, H. Shao, D.E. Crane, L. da Costa, R.I. Aviv, D.J. Mikulis, S.E. Black, B.J. MacIntosh, BOLD-based cerebrovascular reactivity vascular transfer function isolates amplitude and timing responses to better characterize cerebral small vessel disease, NMR Biomed. 32 (2019) 1–12. https://doi.org/10.1002/nbm.4064.

[61]   C.J. Gauthier, M. Lefort, S. Mekary, L. Desjardins-Crépeau, A. Skimminge, P. Iversen, C. Madjar, M. Desjardins, F. Lesage, E. Garde, F. Frouin, L. Bherer, R.D. Hoge, Hearts and minds: Linking vascular rigidity and aerobic fitness with cognitive aging, Neurobiol. Aging. 36 (2015) 304–314. https://doi.org/10.1016/j.neurobiolaging.2014.08.018.

[62]   K. Sam, J. Conklin, K.R. Holmes, O. Sobczyk, J. Poublanc, A.P. Crawley, D.M. Mandell, L. Venkatraghavan, J. Duffin, J.A. Fisher, S.E. Black, D.J. Mikulis, Impaired dynamic cerebrovascular response to hypercapnia predicts development of white matter hyperintensities, NeuroImage Clin. 11 (2016) 796–801. https://doi.org/10.1016/j.nicl.2016.05.008.

[63]   M.J. Thrippleton, Y. Shi, G. Blair, I. Hamilton, G. Waiter, C. Schwarzbauer, C. Pernet, P.J.D. Andrews, I. Marshall, F. Doubal, J.M. Wardlaw, Cerebrovascular reactivity measurement in cerebral small vessel disease: Rationale and reproducibility of a protocol for MRI acquisition and image processing, Int. J. Stroke. 13 (2018) 195–206. https://doi.org/10.1177/1747493017730740.

[64]   M.M.A. Conijn, J.M. Hoogduin, Y. van der Graaf, J. Hendrikse, P.R. Luijten, M.I. Geerlings, Microbleeds, lacunar infarcts, white matter lesions and cerebrovascular reactivity - A 7T study, Neuroimage. 59 (2012) 950–956. https://doi.org/10.1016/j.neuroimage.2011.08.059.

[65]   M. Hund-Georgiadis, S. Zysset, S. Naganawa, D.G. Norris, D.Y. Von Cramon, Determination of cerebrovascular reactivity by means of fMRI signal changes in cerebral microangiopathy: A correlation with morphological abnormalities, Cerebrovasc. Dis. 16 (2003) 158–165. https://doi.org/10.1159/000070596.

[66]   C. Federau, S. Christensen, Z. Zun, S.W. Park, W. Ni, M. Moseley, G. Zaharchuk, Cerebral blood flow, transit time, and apparent diffusion coefficient in moyamoya disease before and after acetazolamide, Neuroradiology. (2017). https://doi.org/10.1007/s00234-016-1766-y.

[67]   A.S. Vagal, J.L. Leach, M. Fernandez-Ulloa, M. Zuccarello, The acetazolamide challenge: Techniques and applications in the evaluation of chronic cerebral ischemia, Am. J. Neuroradiol. (2009). https://doi.org/10.3174/ajnr.A1538.

[68]   M.S. Stringer, G.W. Blair, Y. Shi, I. Hamilton, D.A. Dickie, F.N. Doubal, I.M. Marshall, M.J. Thrippleton, J.M. Wardlaw, A Comparison of CVR Magnitude and Delay Assessed at 1.5 and 3T in Patients With Cerebral Small Vessel Disease, Front. Physiol. 12 (2021). https://doi.org/10.3389/fphys.2021.644837.

[69]   G.W. Blair, M. Uk, M.J. Thrippleton, Y. Shi, I. Hamilton, Intracranial hemodynamic relationships in

patients with cerebral small vessel disease, 0 (2020). https://doi.org/10.1212/WNL.0000000000009483.

[70]   U. Clancy, D.J. Garcia, M.S. Stringer, M.J. Thrippleton, M.C. Valdés-Hernández, S. Wiseman, O.K. Hamilton, F.M. Chappell, R. Brown, G.W. Blair, W. Hewins, E. Sleight, L. Ballerini, M.E. Bastin, S.M. Maniega, T. MacGillivray, K. Hetherington, C. Hamid, C. Arteaga, A.G. Morgan, C. Manning, E. Backhouse, I. Hamilton, D. Job, I. Marshall, F.N. Doubal, J.M. Wardlaw, Rationale and design of a longitudinal study of cerebral small vessel diseases, clinical and imaging outcomes in patients presenting with mild ischaemic stroke: Mild Stroke Study 3, Eur. Stroke J. (2020) 239698732092961. https://doi.org/10.1177/2396987320929617.

[71]   G.W. Blair, E. Janssen, M.S. Stringer, M.J. Thrippleton, F. Chappell, Y. Shi, I. Hamilton, K. Flaherty, J.P. Appleton, F.N. Doubal, P.M. Bath, J.M. Wardlaw, Effects of Cilostazol and Isosorbide Mononitrate on Cerebral Hemodynamics in the LACI-1 Randomized Controlled Trial, Stroke. 53 (2022) 29–33. https://doi.org/10.1161/STROKEAHA.121.034866.

[72]   B.C. Lee, H.H. Tsai, A.P.H. Huang, Y.L. Lo, L.K. Tsai, Y.F. Chen, W.C. Wu, Arterial Spin Labeling Imaging Assessment of Cerebrovascular Reactivity in Hypertensive Small Vessel Disease, Front. Neurol. 12 (2021) 1–8. https://doi.org/10.3389/fneur.2021.640069.

[73]   F.C. Moreton, B. Cullen, D.A. Dickie, R. Lopez Gonzalez, C. Santosh, C. Delles, K.W. Muir, Brain imaging factors associated with progression of subcortical hyperintensities in CADASIL over 2-year follow-up, Eur. J. Neurol. 28 (2021) 220–228. https://doi.org/10.1111/ene.14534.

[74]   F.B. Tancredi, R.D. Hoge, Comparison of cerebral vascular reactivity measures obtained using breath-holding and CO 2 inhalation, J. Cereb. Blood Flow Metab. (2013). https://doi.org/10.1038/jcbfm.2013.48.

[75]   X. Hou, P. Liu, Y. Li, D. Jiang, J.B. De Vis, Z. Lin, S. Sur, Z. Baker, D. Mao, H. Ravi, K. Rodrigue, M. Albert, D.C. Park, H. Lu, The association between BOLD-based cerebrovascular reactivity (CVR) and end-tidal CO2 in healthy subjects, Neuroimage. 207 (2020) 116365. https://doi.org/10.1016/j.neuroimage.2019.116365.

[76]   Y. Shi, M.J. Thrippleton, S.D. Makin, I. Marshall, M.I. Geerlings, A.J.M. De Craen, M.A. Van Buchem, J.M. Wardlaw, Cerebral blood flow in small vessel disease: A systematic review and meta-analysis, J. Cereb. Blood Flow Metab. 36 (2016) 1653–1667. https://doi.org/10.1177/0271678X16662891.

Table 1: Summary of the reviewed MRI methods in cerebral small vessel disease, its applications, the main contributions, limitations, and open questions.

MRI technique	Characterization	Differential contribution to cSVD*	Main Applications	Limitations/Open questions
ASL	ASL is a perfusion-weighted MRI method designed to explore water molecules in arterial blood as an endogenous tracer, resulting in a noninvasive approach to measure cerebral blood flow (CBF) and related parameters.	PVWM CBF can be a valuable biomarker of microvascular disease. It is supplied exclusively by small vessels.	Study of the pathophysiology of cSVD evaluating BBB dysfunction. Investigate the effects of risk-factors	The vascular-related parameter changes are a consequence, or do they contribute to cSVD? How are they related to cognition?
IVIM	IVIM is an MRI method weighted in different degrees of diffusion, aiming to distinguish the free diffusion of water molecules in biological tissue from randomly moving with the flow.	An increase in IVIM perfusion fraction may represent an early biomarker for the deregulation of blood-brain barrier permeability, especially in regions of deep white matter.	Study of the pathophysiology of cSVD	What are the best b-values and fitting model to evaluate cSVD-related changes? How do the IVIM perfusion fraction changes relate to CBF changes in physiological unities?
CVR	It can be assessed using vasodilator stimuli and BOLD contrast.	Impaired CVR can be a valuable biomarker of microvascular disease progression and is associated with cardiovascular risk factors.	Study of the pathophysiology of cSVD evaluating endothelial dysfunction	More extensive studies using CVR need to be feasible, with more standardized vasoactive stimulus and CVR calculation methods.

*In comparison to conventional MRI markers. ASL: Arterial Spin Labeling. IVIM: Intravoxel Incoherent Movement. CVR: Cerebrovascular reactivity.

Figures

Figure 1: Flow diagram of the selection process.
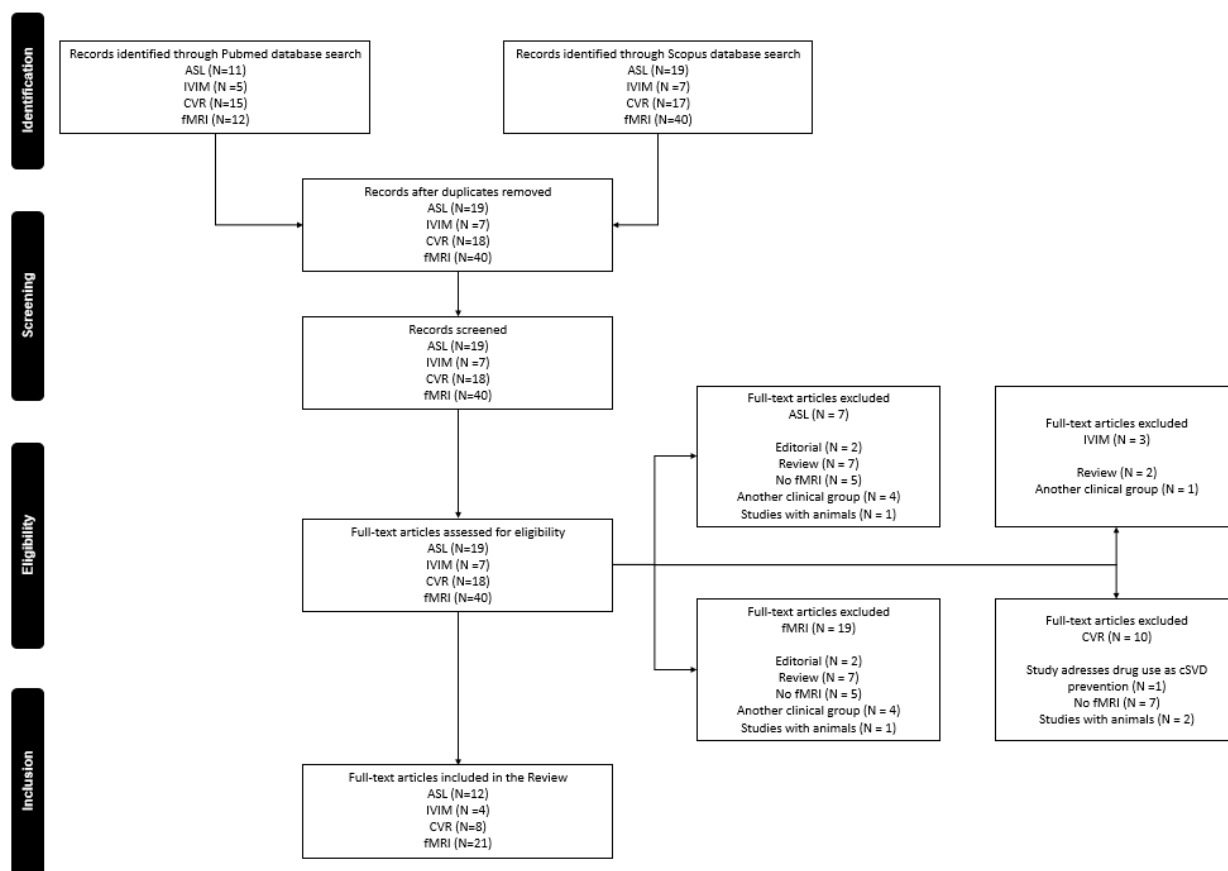
Figure 2: Eight regions of interest of NAWM placed symmetrically on tridimensional ASL raw images (a-c) and CBF maps (d-f). Subtle hemodynamic changes in regions of NAWM were observed [37].
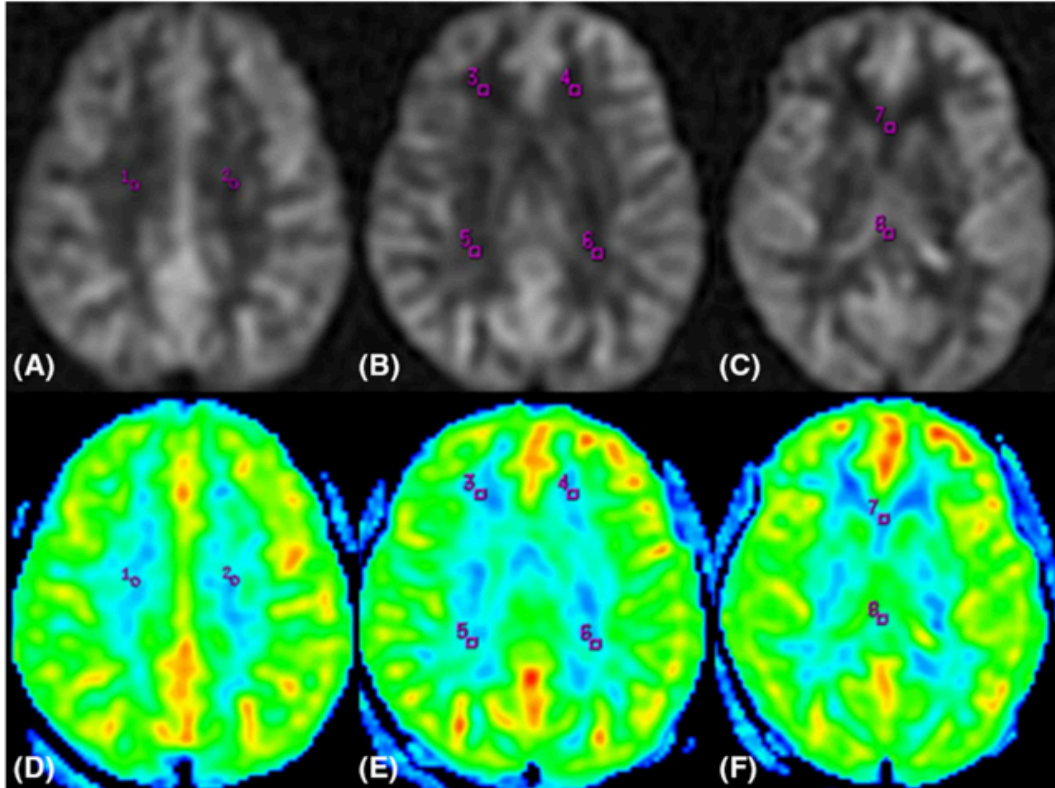
Figure 3: High values of intermediate diffusion volume fractions (color-coded map in b) strongly colocalize with WMH (FLAIR image in a). Images of a male, a 79-year-old patient with cerebral small vessel disease [56].
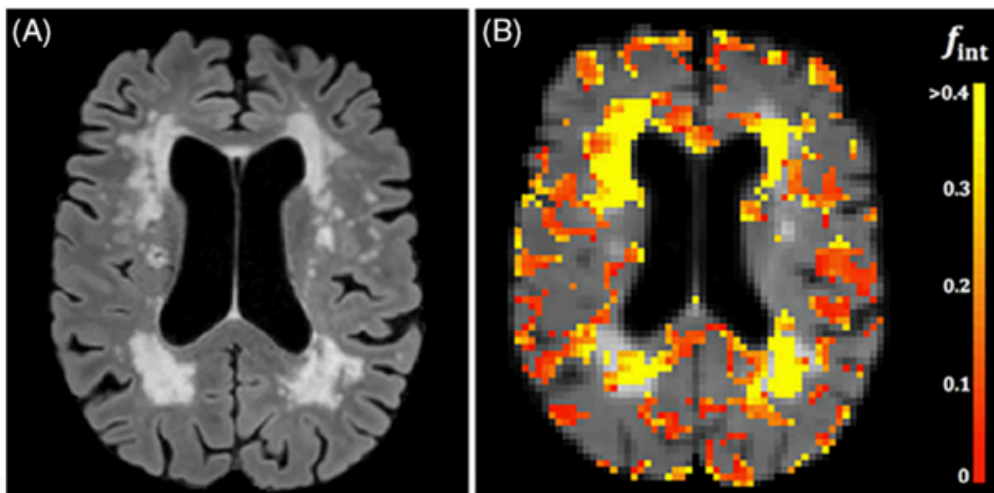
Appendix 4.6. "Contrast-agent-free state-of-the-art MRI on cerebral small vessel disease-part 2. Diffusion tensor imaging and functional magnetic resonance imaging"

Reference: Silva PHR, Paschoal AM, Secchinatto KF, Zotin MCZ, Santos AC, Viswanathan A, et al. Contrast agent-free state-of-the-art magnetic resonance imaging on cerebral small vessel disease – Part 2: Diffusion tensor imaging and functional magnetic resonance imaging. Nmr Biomed. 2022;e4743.

Copyright/Source: John Wiley and Sons/NMR in Biomedicine®

Article reuse license

298

Licensed Content Issue	0

| Licensed Content Pages | 17 |

| Type of use | Dissertation/Thesis |

| Requestor type | Author of this Wiley article |

| Format | Electronic |

| Portion | Full article |

| Will you be translating? | No |

| Title | PhD Thesis: Peak Width of Skeletonized Mean Diffusivity (PSMD) as Neuroimaging Biomarker for Vascular Cognitive Impairment in the Context of Cerebral Amyloid Angiopathy |

| Institution name | Faculdade de Medicina de Ribeirão Preto - Universidade de São Paulo |

| Expected presentation date | Aug 2022 |

| Order reference number | 0003 |

| Requestor Location | Maria Clara Zanon Zotin
Faculdade de Medicina de Ribeirão Preto
R. Ten. Catão Roxo, 3900
Monte Alegre
Ribeirão Preto, SP 14015010
Brazil
Attn: Faculdade de Medicina de Ribeirão Preto - Universidade de São Paulo |

Publisher   EU826007151
Tax ID

Total   0.00 USD

Terms and Conditions

Contrast-agent-free State-of-the-art Magnetic Resonance Imaging on Cerebral Small Vessel Disease – Part 2: DTI and fMRI

Pedro Henrique Rodrigues da Silva, MSc[1]; André Monteiro Paschoal, Ph.D.[1,2]; Kaio Felippe Secchinatto[1]; Maria Clara Zanon Zotin, M.D.[2,3]; Antônio Carlos dos Santos M.D.[2]; Ph.D., Anand Viswanathan M.D., Ph.D.[3]; Octavio M. Pontes-Neto, Ph.D.[4]; Renata Ferranti Leoni, Ph.D.[1]

[1]Department of Physics, FFCLRP, University of São Paulo, Ribeirão Preto, SP, Brazil
[2]Department of Medical Imaging, Hematology and Clinical Oncology, Ribeirão Preto Medical School, University of São Paulo, Ribeirão Preto, SP, Brazil.
[3]J Philip Kistler Stroke Research Center, Department of Neurology, Massachusetts General Hospital, Harvard Medical School, Boston, MA, USA.
[4]Department of Neurosciences and Behavioral Science, Ribeirão Preto Medical School - University of Sao Paulo, Ribeirão Preto, SP, Brazil

Corresponding Author: Renata Ferranti Leoni
Department of Physics – FFCLRP – University of Sao Paulo
Av. Bandeirantes, 3900 – 14040-901 – Ribeirão Preto, São Paulo, Brazil
Phone: +55-16-3315 0083 / +55-16-99401 6368
leonirf@usp.br

Cover title: State-of-the-art MRI in cerebral small vessel disease

Total number of tables and figures: 4 figures, 1 table

Word count: 5889

Abstract

Cerebral small vessel disease (cSVD) has been widely studied using conventional magnetic resonance imaging (MRI) methods, although the association between MRI findings and clinical features of cSVD is not always concordant. We assessed the additional contribution of contrast-agent-free, state-of-the-art MRI techniques, particularly Diffusion Tensor Imaging (DTI) and Functional Magnetic Resonance Imaging (fMRI), to understand brain damage and structural and functional connectivity impairment related to cSVD. We performed a review following the PICOS worksheet and Search Strategy, including 152 original papers in English, published between 2000 and 2022. For each MRI method, we extracted information about their contributions regarding the origins, pathology, markers, and clinical outcomes in cSVD. In general, DTI studies have shown that changes in mean, radial, and axial diffusivity measures are related to the presence of cSVD. In addition to the classical deficit in executive functions and processing speed, fMRI studies indicate connectivity dysfunctions in other domains, such as sensorimotor, memory, and attention. Neuroimaging metrics have been correlated with the diagnosis, prognosis, and rehabilitation of patients with cSVD. In short, the application of contrast-agent-free, state-of-the-art MRI techniques has provided a complete picture of cSVD markers and tools to explore questions that have not yet been clarified about this clinical condition. Longitudinal studies are desirable to look for causal relationships between image biomarkers and clinical outcomes.

Introduction

Cerebral small vessel disease (cSVD), a common cause of stroke and dementia, is traditionally considered the small vessel equivalent of large artery occlusion or rupture that leads to cortical and subcortical brain damage. However, microvessel endothelial dysfunction has also contributed to it [1]. Brain imaging, including Magnetic Resonance Imaging (MRI), is then useful to show the presence of a lesion of several types, such as white matter hyperintensities (WMH), cerebral microbleeds (CMB), lacunes, perivascular spaces (PVS), hemorrhage, and atrophy [2]. However, reports on the association between conventional MRI measures and clinical features of cSVD are not always concordant [3].

Contrast-agent-free state-of-the-art MRI techniques have added relevant information regarding the pathophysiological processes underlying the cSVD development, the cSVD burden effects on brain structural and functional networks, and how the disruptions contribute to the outcome [4].

In this context, the diffusion tensor image (DTI) has been used to evaluate cSVD due to its sensitivity to white matter damage [5], allowing quantifying the cSVD burden and assessing the integrity of the structural brain network. Different DTI methodologies have been applied to assess the white matter (WM) microstructure. Approaches include voxel-based analysis [6], tract-based spatial statistics (TBSS) [7], regions of interest (ROIs) analysis [8], and tractography [9]. Moreover, CSVD has been associated with motor and cognitive impairment. Functional MRI (fMRI) based on the blood oxygenation level-dependent (BOLD) contrast has been considered to study the functional brain networks in resting-state and task conditions [10,11].

Therefore, studies on the applications of contrast-agent-free state-of-the-art MRI to evaluate cSVD were systematically reviewed. The present paper focused on DTI and fMRI to understand their contributions to assess brain damage and structural and functional connectivity impairment related to cSVD. The first part of the review regarding arterial spin labeling (ASL), intravoxel incoherent motion (IVIM), and cerebrovascular reactivity (CVR) measures was published separately.

Methods

We followed the PRISMA-P (Preferred Reporting Items for Systematic Review and Meta-Analysis Protocols) 2015 checklist: recommended items to address in a systematic review protocol guidelines [12]. The review parameters were delineated using the PICOS worksheet and Search Strategy (Centre for reviews and dissemination. Systematic Reviews: CRD's Guidance for Undertaking Reviews in Health Care. York: University of York; 2006). The main question of our study was: "What are the applications of contrast agent-free state-of-the-art MRI and its additional information compared to

conventional MRI for the etiology, diagnosis, and prognosis of cSVD?" Online searches in PubMed and Scopus were carried out considering the term "Cerebral Small Vessel Disease" combined with each one of the techniques: "Diffusion Tensor Imaging" AND "Cerebral Small Vessel Disease," "Functional Magnetic Resonance Imaging" AND "Cerebral Small Vessel Disease." Inclusion criteria were original publications in English between 2000 and 2021 (last search on February 23rd, 2022), and with subjects of both sex, 18 years old or more.

For the identification, the authors independently researched the articles following the search strategy and inclusion criteria; then, they reached a consensus on which articles would be included in the final analysis. All the records and data selected had their title, authors' names, year of publication, MRI technique, and main findings (about pathophysiology, lesions, connections, and/or clinical outcomes) extracted using a standardized data extraction form shared among the authors.

Then, duplicates were removed, and records were screened, i.e., non-full-text articles such as reviews and editorials were removed. The remaining full-text articles were assessed for eligibility. In addition to the inclusion criteria mentioned, we considered the exclusion criteria: studies with animals, text not available, methods development, no MRI technique used, another clinical group (instead of cSVD), trial presentation (description of future clinical trials), and drug use as cSVD prevention. The remaining full-text articles were included in the systematic review. The articles' details regarding Identification, Screening, Eligibility and Inclusion (PRISMA-P diagram flow) are described in Figure 1.

Results

We included 124 full-text articles that evaluated the DTI additional contributions compared to conventional MRI, brain structural networks, DTI markers, and their relation with cSVD. We also included 28 studies on cSVD-related alterations in functional brain networks assessed by task-based and RS fMRI. Table 1 shows a summary of the main findings.

Diffusion Tensor Imaging (DTI)

Among several diffusion-weighted images (DWI) models, DTI is a proper quantitative method in assessing *in vivo* WM microstructure integrity. It measures water molecules' diffusion within WM tracts using magnetic diffusion gradients applied in at least six different directions. A diffusion tensor is then acquired, from which two quantitative measures, fractional anisotropy (FA) and mean diffusivity (MD), are obtained. High FA and low MD values usually reflect intact microstructural integrity [13,14].

A study protocol for the differential assessment of cSVD recommended quantitative DTI measurements of tissue integrity to assess WMH, less-intense and severe WMH, stroke lesions, normal-appearing WM (NAWM), deep gray matter (GM), and hippocampi [15]. In cSVD patients, DTI-derived parameters, such as FA and MD, have been altered in WMH and NAWM [16,17], were correlated with CMB [18,19] and predicted dementia, risk of mortality, and cSVD severity [20–22]. Moreover, DTI abnormalities have been associated with cSVD genetic [23] and risk factors, such as hypertension [24,25], increased salt intake [26], aortic stiffness [27], midlife systemic inflammation [28], renal function [29], and level of physical activity [30]. It raises whether management of modifiable risk factors could postpone microstructural changes [31,32].

DTI additional contributions in comparison to conventional MRI

A cross-sectional TBSS study on the NAWM of patients with mild cognitive impairment (MCI) reported that cSVD effects on WM go beyond the macrostructural damage visible through conventional MRI (Figure 2A) [33]. Tractography studies showed decreased FA and increased MD correlated with cognitive dysfunction [34–38] and a strong association between MD, Serum neurofilament Light chain (NfL), a blood marker to neuroaxonal damage, and information processing speed (IPS) scores in cSVD patients [39,40], which was also poorly correlated with conventional MRI markers.

Better performance of DTI in comparison to conventional MRI was also observed in longitudinal studies. Changes in MD and FA of cSVD patients were detectable over a 1-year follow-up [41]. Moreover, a 9-year longitudinal study showed that DTI could detect impaired WM microstructure preceding the conversion into WMH years before becoming visible on conventional neuroimaging [42].

Furthermore, while MD correlated significantly with executive function tests even after controlling for demographic variables and conventional MRI markers [43], radial diffusivity (RD) could better predict executive dysfunction in cSVD [34]. Such a strong association between executive function and DTI parameters was confirmed by a multimodal MRI model containing age, gender, brain volume, FA, and premorbid intelligence quotient, which explain 74% of the variance of executive function score [41]. Axial diffusivity (AxD) of the posterior frontal periventricular NAWM, right middle cingulum bundle, and mid-posterior corpus callosum also predicted cognitive impairment in cSVD patients [44]. Besides, MD of WM lesions (WML) and NAWM correlated with gait disturbances [45,46], linked to higher morbidity and mortality [47].

In longitudinal studies, FA changes in the thalamus correlated with WMH progression among cSVD patients [48]. Increased MD was also consistent with progressive degradation of WM integrity in

symptomatic cSVD [49], predicted cognitive decline [50], and was one of the best predictors of mortality [51]. Additionally, while the degree of baseline microstructural impairment explained clinical variability in patients with similar cSVD severity [42] and predicted incident dementia, risk of mortality, and cSVD severity [20–22], it did not correlate with CMB [35].

In contrast, other studies have questioned the advantages of using DTI over conventional MRI since the former requires sophisticated computational processing, is more time-consuming, and showed similar or worse results than conventional MRI in some cases [52–56]. However, despite the divergences, DTI has been widely used in cSVD. WMH was associated with two patterns of altered diffusion characteristics in the surrounding WM tracts. A penumbra pattern with improving diffusion characteristics was observed in lesion-free tracts distant from the WMH lesion. However, in the WMH tract, a Wallerian-type degeneration pattern was present [57]. Moreover, a study investigating hemispheric asymmetry in cSVD found that the right hemisphere is more susceptible to neurodegeneration, related to cognitive decline, and higher mortality [58]. Recently, cortical thinning was associated with WMH through structural connectivity mainly for periventricular WMH, even in the early stage of cSVD [59].

Radial diffusivity was a better predictor of WMH volume than brain iron concentration or cerebral blood flow [60]. Physiologic watershed (defined as CBF below the 10th percentile of mean WM CBF in a young, healthy group) overlapped spatially with regions of higher WMH load. Moreover, watershed oxygen extraction fraction, a signature of hypoxia-ischemia, was associated with WMH load and microstructural disruption, suggesting hypoxia-ischemia as a contributor to cSVD pathogenesis and WMH development [61].

Brain structural networks

The severity of structural disruption of brain networks in cSVD was correlated with total cSVD burden score (Figure 2C) [62–64] and cognitive impairment, mainly in executive functions, divided attention, IPS, psychomotor speed, episodic memory, and global cognition assessed by the Mini-Mental State Exam (MMSE) [65–68]. Such correlations were evident in highly connected network regions [69]. Cognitive impairment has been associated with functional and structural connectivity changes within brain networks, such as the default mode network (DMN), attributed to WMH progression [70]. The effect of WMH on dementia was reported to be mediated by global network efficiency and the peripheral connections' strength in the elderly with cSVD [71]. The brain network measurements may be regarded as a direct and independent surrogate marker of cognitive impairment in cSVD [72]. However, a recent study found WM integrity widely abnormal in nondemented cSVD patients, while structural connectivity was relatively preserved [73]. Microstructural changes

identified with DTI through graph-theory analysis and network-based statistical analysis can be found during the preclinical cognitive impairment and MCI stages [74], suggesting that early cognitive changes are related to a disruption pattern from peripheral to central connections [75]. Measures of network efficiency have been considered the best markers for cognitive performance and an essential contribution to the genesis of the cognitive decline in cSVD [76]. More recently, WMH volume, structural network local efficiency, and IPS performance were interrelated, with the structural connectivity partially mediating the effects of WMH on IPS [77].

Novel DTI-related markers of cSVD
DTI parameters, such as the peak-width skeletonized mean diffusivity (PSMD), free water (FW), and tissue compartment measures (FAt, MDt), have been recently proposed and used in the assessment of cSVD. PSMD was consistently associated with IPS in genetically defined, inherited, and sporadic cSVD cohorts and memory clinic patients, offering further advantages of a fast and fully automated marker. It also outperformed conventional MRI markers by explaining more cognitive variance in the IPS domain. In a longitudinal analysis, PSMD values changed significantly within 18 months and offered smaller sample size estimates than other imaging markers employed [78,79]. It was strongly associated with conventional cSVD markers and outperformed MD in cognition prediction [80]. PSMD was found altered and associated with processing speed performance in cerebral amyloid angiopathy patients [81]. Standardization of PSMD processing has been suggested due to the impact of processing choices in the results, mainly the choice of WM mask [82].

Recently, a more complex yet probably more realistic FW diffusion model has been applied in cSVD. Rather than alterations in the WM fiber organization, it was suggested that increased extracellular water is the main contributor to diffusion changes in CADASIL and sporadic cSVD patients [83]. Increased FW also correlated with an IL-18-centered inflammatory network [84], was found to mediate the association between deep medullary veins disruption and WM integrity in cSVD [16], was related to geriatric depressive symptoms [85] and presented a stronger association with cognitive deficits than conventional DTI method, showing to be a marker of cSVD-related degeneration [86]. Extracellular fluid quantified with FW-related parameters associated positively with microstructural degeneration and the presence of lacunes and CMB in CADASIL patients, suggesting a role for extracellular fluid in cSVD pathology [87].

An alternative diffusion tensor decomposition model has been developed to provide isotropic and anisotropic tensor components. Such parameters were significantly correlated with executive functions, IPS, and conversion to dementia in a 3-year longitudinal study [88,89]. Conventional DTI, multi-shell diffusion imaging, and advanced diffusion modeling were compared in cSVD patients.

The multi-shell scheme and the Diffusion Kurtosis Imaging provided metrics that correlated strongly with cognitive measures and better characterized WM damage related to cSVD than traditional DTI [90].

A non-invasive modified index for DTI analysis along the perivascular space was compared to classical detection of glymphatic clearance function using Glymphatic MRI after intrathecal administration of gadolinium in cSVD patients. It was found to represent glymphatic clearance function, which has been associated with cSVD pathology [91].

Complications and outcomes of cSVD associated with DTI-derived metrics

Low FA and high MD in several WM areas (mainly NAWM) were associated with decreased cognitive scores in cSVD in a cross-sectional TBSS study [92]. Recently, WM damage was restricted to specific segments in cSVD patients, disrupting some fibers related to many cognitive deficits [93]. No changes were found in FA and MD metrics in TBSS analysis with asymptomatic WMH patients [94]. Conversely, a 5-year prospective study showed no relationship between baseline WM and NAWM microstructural integrity, measured using mean FA and mean MD, and declined global cognitive performance after correcting multiple comparisons. Authors suggested that other factors, rather than solely WM integrity, might be related to cognitive impairment [95]. A two-year follow-up study reported that DTI measurements are the main predictor of clinical changes over time in CADASIL patients [96]. Compared to healthy controls, CADASIL patients showed decreased FA and increased diffusivity in several brain areas, with these microstructural integrity changes correlated with their cognitive performance [97]. However, in another study, compared to controls, CADASIL patients presented a reduced number of tracts in the bilateral hippocampal formation, while no associations were found with cognition [98].

In a multicenter study with symptomatic cSVD patients, DTI outputs and the number of lacunes were independently associated with global cognition and Montreal Cognitive Assessment (MoCA) scores. DTI markers were also independently associated with mental flexibility and verbal fluency [99]. Furthermore, working and long-term memory abilities were reduced in cSVD patients compared to controls and were partly explained by microstructural changes of the cingula and uncinated tracts, respectively (Figure 2B) [100]. Finally, in the elderly with cSVD, verbal memory performance was related to DTI-derived metrics extracted from the hippocampus and cingulum, even before macrostructural changes could be detected, suggesting that DTI metrics may detect early microstructural abnormalities [101,102].

MCI patients with cSVD showed microstructural abnormalities detected through DTI in the subcortical region, periventricular, and central semiovale WM [36] and the NAWM of the anterior

corpus callosum, internal and external capsule, and periventricular WM [33]. Moreover, disruption of structural connectivity has been detected even in cognitively normal cSVD patients, affecting mainly the prefrontal areas, whereas in MCI cSVD patients, networks from frontal and parietal regions were disrupted [103]. Interestingly, MD and FA were more strongly associated with MoCA than MMSE scores, suggesting that the former might be more useful as a cognitive screening tool for cSVD patients [92,104,105]. However, the T2 relaxation time of the NAWM in cSVD patients was associated with cognition, which the DTI metric of the NAWM failed to achieve [106].

Global FA, MD, PSMD, structural network measures, and ROI analysis were performed in a group of cSVD patients (from no cognitive impairment to MCI) and healthy controls to evaluate cognition. Significant differences in all cognitive domains were found among the groups, and DTI markers were sensitive to detect early-stage cSVD cognitive impairment and differences among the groups of cSVD regarding cognition [107]. DTI measures were a significant marker for cognitive impairment and future dementia in a study with six cohorts, while the conventional MRI markers relative contribution varied with the disease severity. Combining DTI measures with conventional MRI measures can be useful in evaluating severe cSVD patients [108].

Higher hippocampal MD correlated with an increased 5-year risk of dementia in the elderly with cSVD [109]. A preliminary study found mean FA within periventricular WMH associated with peripheral inflammatory markers in AD patients [110]. In a cross-sectional study with midlife participants, angiopoietin 2, a circulating growth factor involved in regulating vascular function, correlated with lower FA in WM tracts such as posterior thalamic radiation, middle cerebellar peduncle, and cingulum among APOE (apolipoprotein E)-ε4 midlife carriers [111]. In a multicenter study investigating six independent samples of memory clinic patients covering the entire spectrum of AD, mixed disease, and cSVD, DTI changes were more strongly associated with cSVD than with AD markers, suggesting that DTI might be particularly sensitive to cSVD-related pathology [112].

Besides cognitive decline, gait (lower extremities) abnormalities are also a clinical feature of cSVD and have been investigated using DTI. Recently, it was shown that cSVD patients with higher WMH burdens presented worse cognitive performance and balance issues affecting their daily lives [113]. One study reported that FA measured in the NAWM mediated the negative association between WMH and gait disturbances[114]. Although in a 5-year longitudinal study, baseline GM volume and DTI-derived cSVD markers did not correlate with gait impairment [115], progressive changes in WM volume, MD, AxD, and FA (extracted from a skeleton of the significant WM tracts) were associated with such gait decline in another study [116]. While CADASIL patients were found to have minor impairment in gait performance compared to controls, higher PSMD and MD (voxel-based) were associated with shorter single task stride length [117]. Mild parkinsonian signs, including gait and

balance disturbances, have been associated with the microstructural integrity of WMLs in the elderly with cSVD, measured through FA and MD, mainly in the frontal lobe [118]. Similarly, lower FA values have been found in bilateral frontal WM tracts of cSVD patients with vascular parkinsonism [119]. The association between structural network efficiency assessed with DTI measures and gait in cSVD patients is mediated by cognition [120]. Lower regional FA was related to worse manual dexterity (upper extremities) and increased serum ceramides in a group of asymptomatic cSVD [121]. In a longitudinal study, structural network disruption was related to gait impairment, independent of cognitive decline, in cSVD patients [122].

After intensive blood pressure lowering in severe cSVD patients, no difference in microstructural integrity evaluated with DTI was found, suggesting that blood pressure control is a protective factor for cSVD development and that DTI is a sensitive marker for evaluating such therapeutic strategy [123].

Finally, depression in the setting of cSVD has also been the subject of investigation. Depression in cSVD patients has been associated with reduced white matter integrity measured through FA [124]. Participants with cSVD and depressive symptoms showed damaged microstructural integrity, measured using FA and TBSS, mainly in fronto-subcortical WM tracts, potentially disrupting circuits involved in mood regulation [125,126]. Structural connectivity was also disrupted in cSVD patients with depression [126]. More specifically, depressive symptoms were shown to disrupt networks with reduced efficiency compared to cSVD patients without depressive symptoms [127]. In MCI patients with cSVD, decreased WM FA and increased WM MD were independently correlated with worse Geriatric Depression Scale (GDS) score [128].

Similarly, network connectivity is related to GDS in cognitively impaired patients and mediates the cSVD burden (WMH and lacunes) with GDS scores [129]. Apathy in cSVD patients was also correlated with microstructural disruption of WM tracts (strongest effect in limbic association tracts) using DTI metrics, which were not associated with depression [130]. Structural network disruption in premotor and cingulate regions underlies apathy, but not depression, in cSVD patients [131]. Moreover, reduced efficiency in the reward network was related to increased apathy in symptomatic cSVD subjects [132].

Limitations and Future Directions

Despite the additional contributions of DTI related-parameters to identify WM damage in cSVD patients and their association with cognition, more studies should explore changes in DTI measures mediating the effects of traditional cSVD markers in cognition. Additionally, it is still an open question the pathophysiology underlying WM abnormalities. While the interpretation that the

increased MD and reduced FA result from microstructural tissue damage is more prominent and that cSVD has a significant role in the loss of microstructural WM integrity, mechanisms other than cSVD must also be considered. WM microstructural abnormalities can be caused by ischemic damage due to cSVD and indirect effects of cSVD such as Wallerian degeneration. Future studies must be considered to address this issue. Finally, newer acquisitions and models such as Free Water Model have shown better correlations with WM damage and cognition when compared to the traditional DTI approach. Future studies should consider it to determine the best way to perform an association between WM damage and cognition in cSVD.

Functional Magnetic Resonance Imaging (fMRI)

BOLD-fMRI signal reflects differences in the magnetic susceptibility of intravascular hemoglobin, depending on whether it is bound to oxygen or not. Oxyhemoglobin is diamagnetic, while deoxyhemoglobin is paramagnetic. An increase in regional CBF surpassing an increase in oxygen consumption results in a reduction of deoxyhemoglobin concentration, increasing local signal intensity in T2*-weighted images. Task-based and resting-state (RS) fMRI have been performed to identify brain regions and their correspondent functions in the normal brain and provide insights into the effects of diseases and injuries in the functional organization [133].

CSVD has been associated with motor and cognitive impairment. Activation in the pre-supplementary motor area (SMA), related to complex motor tasks, has been correlated with frontal WMH load in the elderly with severe WMH but not cognitive dysfunction. It suggests that the WMH load can disturb the functional motor network at the early stage of the disease, even before cognitive impairment is present [134]. CSVD patients with gait impairment showed the reduced fractional amplitude of low-frequency fluctuation (fALFF) in the left SMA and increased fALFF in the right inferior frontal gyrus, the left caudate, and the left precuneus. They also presented lower RS functional connectivity in the left SMA and temporal lobe[135].

MCI patients with cSVD presented lower activation in the precuneus area for a working memory task than MCI patients without cSVD and controls. These activation differences between MCI patients with and without cSVD, which presented similar cognitive impairments, supports that cSVD can affect MCI patients cognitively (Figure 3A) [136]. Furthermore, MCI patients with cSVD who underwent a cognitive rehabilitation program presented increased activation in brain circuits involved in attention and working memory [137].

In an attention-demanding test evaluated with multi-echo BOLD-fMRI, subjects with WMH showed lower activation in frontoparietal regions and temporal-parietal junctions than healthy elderly. They also presented higher activation in the precuneus and posterior cingulate gyrus in an executive

function contrast. These results suggest that WMH may disrupt functional brain networks that underlie salience and cognitively mediated attention [138].

CSVD patients at the initial stages of the disease presented lower resting-state functional connectivity (rs-FC) in frontoparietal networks and higher in cerebellar regions than healthy controls. Such changes correlated with WMH and cognitive impairments widely associated with the cSVD condition [139]. More recently, decreased gray matter volume and functional connectivity of the cerebellum were associated with cognitive impairment in cSVD patients [140].

In patients with severe WMH load, impaired functional and structural connectivity between the posterior cingulate cortex (PCC) and thalamus were independent risk factors for slower IPS. In contrast, PCC-middle frontal gyrus functional connectivity and PCC-hippocampus structural connectivity were related to memory decline [70]. Resting-state whole-brain regional homogeneity of MCI patients with cSVD correlated significantly with MoCA and Stroop scores, distinctive in this clinical group (Figure 3B) [141].

Both cSVD patients with and without cognitive impairment showed decreased connectivity within the DMN network and weak negative connectivity between the DMN with dorsal attention network (DAN) and frontoparietal control network (FPCN) networks. The cSVD with cognitive impairment group showed within- and between-network alterations of the FPCN correlated with its cognitive function, while the connectivity of the FPCN and the DMN correlated with deep WMH volume in cSVD subjects. These findings suggest that cognitive alterations of cSVD subjects may be mediated by the FPCN connectivity impaired by the deep WMH burden [142].

WMHs in basal ganglia (BG) have been significantly associated with vascular cognitive impairment. Patients with subcortical vascular MCI (SVMCI) presented higher WMHs, mainly in caudate regions, than patients with amnestic mild cognitive impairment (aMCI) and healthy control subjects. In SVMCI patients, BG WMHs in both dorsal and ventral caudate correlated with functional connectivity and verbal episodic memory performance, while such correlations did not happen in aMCI patients. These findings suggest a relationship between structural changes due to cSVD, the functional integrity of BG circuits, and episodic memory performance in SVMCI [143]. In a study with 269 elderly subjects with cSVD, the BG resting-state functional connectivity was related to gait speed, independently of locomotor risk factors such as WMH [144].

Moreover, the graph theory approach showed that MCI patients with cSVD presented changes in Executive Control Network (ECN) and DMN compared to MCI patients without cSVD. More specifically, the connectivity of the right inferior frontal gyrus of the ECN mediated the relationship between periventricular WMH and visuospatial processing in MCI patients with cSVD [145]. Recently, lower global efficiency of the DMN in CADASIL patients with higher cSVD burden was

reported [146]. cSVD patients with lacunes on the thalamus presented subtle changes in their functional connectome when compared to those without thalamus lacunes and correlated with mild cognitive impairment in episodic memory and IPS, suggesting that lacunes on the thalamus played a vital role in mediating the functional neural changes of cSVD patients (Figure 3C) [147]. When comparing ALFF, fALFF, and regional homogeneity (ReHo) between cSVD with CMB and healthy, the patients showed functional alterations in the DMN, sensorimotor network, and frontoparietal network, suggesting that alterations in spontaneous brain activity are also related to cSVD [148]. In contrast, in a study comparing functional and structural networks as markers of symptomatic cSVD severity, only structural networks supported evidence to detect clinical and control differences [22]. Recently, the underlying mechanism behind WMH effects on cognition was explored. The degree centrality in the functional network of the WMH group compared to the control group was significantly different in portions of the frontal and parietal lobes. The patients' WMH level differences were found in the frontal, temporal and parietal lobes [149]. In a very early-stage WMH asymptomatic adult group, anomalies in functional connectivity strength and fALFF were found in the cerebellum and left superior frontal gyrus, respectively. Additionally, the mild-WMH group presented increased fALFF in the right cerebellum lobule V. Nodal changes in the DMN were found in the CADASIL group compared to controls and associated with cognitive impairment [98]. Degree centrality and fALFF changes in DMN of vascular mild cognitive impairment patients were associated with cognitive scores, suggesting a role for the spontaneous activity of the DMN in cognitive impairment of cSVD patients [150].

Recent studies also used fMRI to investigate risk factors, genetic factors, and outcomes of cSVD. In middle-aged adults with type 1 diabetes mellitus, brain activation changes seem to mediate the disease with slower IPS, although it did not associate with the presence of cSVD[151]. In an event-related Go/No-go task, CADASIL patients showed lower activation in the alerting network and areas involved in executive functions, probably related to the presence of cSVD [152].

In a voxel-based morphometry analysis, both the MCI with and without depressive symptoms presented decreased GM density in the left parahippocampal, right hippocampus, and right middle cingulate cortex (rMCC) when compared to normal controls. The increased GM density in the rMCC correlated with rs-FC with right parahippocampal in the MCI with depressive symptoms compared to the MCI without depressive symptoms[153].

In Alzheimer's disease, the emergence of amyloid plaques is followed by forming tau-containing neurofibrillary tangles correlated with neurodegeneration and dementia symptoms. In an rs-fMRI study, functional connectivity correlated with tau-PET uptake independently of dementia symptoms, amyloid deposition assessed by amyloid-PET, or cSVD, supporting the view that prion-like tau

spreading is facilitated by neural activity [154]. Additionally, the effect of cSVD on Alzheimer's disease onset and progression was evaluated, with cSVD patients showing more static and dynamic FC changes associated with cognitive impairment [155].

Finally, the BOLD-fMRI physiological noise within WM measured as raw physiological noise and cardiac pulsatility showed that graded increases in cardiac pulsations in NAWM are related to both age and the presence of cSVD, independently. These measures are suggested as a complementary dynamic measure of WM integrity to the static fluid-attenuated inversion recovery images [156]. A correlation between ultrasound and fMRI measures of cerebrovascular pulsatility was also shown. This association provided insight into the transmission of pulsatile energy from large basal arteries at the Circle of Willis to downstream cerebrovascular beds and has implications for the utility of cardiac-related pulsatility as a potential marker for cSVD [157].

Limitations and Future Directions

Concerning fMRI additional contribution to cSVD research, the non-identification on whether the changes are associated with the impaired flow or impaired metabolism is a limitation. Evaluation of traditional MRI markers such as WMH, lacunes, PVS, CMB, and risk and protective factors of cSVD with fMRI findings should be performed along with the possible mediating effects of fMRI metrics on cSVD lesions and cognition. The relationship between structural and functional networks and their effects on the clinical outcome in cSVD patients must be explored in future studies. Finally, longitudinal studies must be performed to look for causal relationships between functional network disruption and cSVD.

Discussion

The present review focused on the contributions of contrast-agent-free, state-of-the-art MRI techniques (DTI and BOLD-fMRI) to the understanding of cSVD related lesions, underlying pathophysiology, effects on connections and cognition, and influences on clinical outcomes.

DWI and, more specifically, DTI is the most used technique for the diffusion assessment in cSVD. The first DTI studies showed whether DTI-derived metrics such as MD and FA could be sensitive to WM damage and correlate better with cognitive function than conventional MRI imaging. Such tissue damage identified by DTI metrics in asymptomatic and symptomatic cSVD was associated with metabolic changes that reflect axonal loss/dysfunction [158,159]. MD and FA were already considered sensitive to measure WM damage and better markers for cognitive impairment in cSVD compared to traditional MRI measures [160,161]. Issues such as the role in the clinical management

of microbleeds present in a significant proportion of cSVD patients arose [160]. Additionally, the full impact of tractography techniques on cSVD has not been performed [161].

DTI-derived markers have been correlated with cardiovascular risk factors, other MRI markers, and clinical features, including cognitive impairment. Additionally, longitudinal findings support the hypothesis that conventional MRI markers of cSVD (e.g., WMH, lacunes, and CMB) cause cognitive decline and dementia via disruption of structural brain networks [22,63]. Therefore, DTI has provided new insights into understanding the mechanisms of the main clinical consequences of cSVD, particularly by evaluating the structural integrity of the cerebral WM architecture. Moreover, DTI may furnish reliable surrogate markers to be applied in future clinical trials, investigating potential therapeutic interventions.

However, the pathophysiology underlying WM abnormalities remains incompletely understood. While the interpretation that the increased MD and reduced FA result from microstructural tissue damage is notable and cSVD has a significant role in losses of microstructural WM integrity [162], mechanisms other than cSVD must also be considered. WM microstructural abnormalities can be caused by ischemic damage due to cSVD and indirect effects of cSVD, such as Wallerian degeneration. Future studies must be considered to address this issue.

fMRI can also be a valuable tool for investigating cSVD, providing insights into the functional networks disruption related to cSVD and cognitive decline, dementia, and mortality. Findings reported task-based activation changes in motor [134], working memory [136,137], and attentional [138] brain functions in cSVD patients. RS-FC studies [139,143,145] indicated the DAN, ECN, FPCN, and DMN functional connectivity as essential markers of cSVD functional changes. Joint analysis with structural findings [153], tau-PET intake [154], and novel approaches [156,157] with BOLD-fMRI also showed brain changes associated with the occurrence of cSVD. However, only structural networks supported evidence to detect clinical and control differences [22]. Future studies must also include testing the associations among fMRI metrics and WMH, lacunes, microbleeds, and other conventional markers and risk factors of cSVD. Finally, longitudinal studies are desirable to look for causal relationships between functional network disruption and cSVD.

In addition to the individual contribution of each technique, it is possible to see how they could be used together for an integrated cSVD assessment. Figure 4 also includes the contributions of ASL, IVIM, and CVR measures discussed in the first part of the review published separately. The contribution of risk factors in developing the disease and the effects of protective factors can be studied through ASL, CVR, IVIM, and DTI. Since small vessel impairment affects CBF, CVR, and blood-brain barrier permeability, ASL, BOLD-MRI, and IVIM can contribute mainly to

understanding the cSVD pathophysiology. In contrast, DTI can contribute to the understanding of lesions.

Regarding mediation effects, brain structural connectivity disruption has been suggested to mediate WMH and cognition in cSVD patients. More specifically, it has been suggested that structural network local efficiency partially mediates the effects of WMH volume on IPS [77]. Global network efficiency and the peripheral connections' strength in the elderly with cSVD mediates the effect of WMH on dementia [71]. Additionally, it has been shown that WMH areas present altered CVR but not CBF [163], proposing more longitudinal studies to explain the cSVD development and the relationship between these metrics and the underlying mechanisms of the cSVD.

Although the literature has not demonstrated the definitive way to assess the effects of the disease on brain structure, focal lesions in the network of structural and functional connections seem to contribute to the patient's clinical outcome. However, some questions remain regarding the vascular-related changes being consequences or contributing to cSVD and their relation with cognition; whether the DTI changes mediate the effects of traditional cSVD markers in cognition; and if the functional changes are due to impaired flow or impaired metabolism, and their implications.

Recently, two initiatives have provided resources, such as harmonized acquisition protocols and software databases, to reduce variability in MRI studies of cerebral small vessel disease [164,165]. In brief, it typically takes about 5-7 minutes to acquire images from each technique. They are acquired under resting state, so no specific requirement is necessary on the patient other than stay quietly avoiding movement. ASL is adequate for microvascular perfusion evaluation if the consensual acquisition is performed [166]. For the assessment of microstructural and functional changes in cSVD patients related to risk factors and cognitive decline, DTI and fMRI are suitable. However, a standardization for IVIM image acquisition and analysis is needed, and a careful reproducibility evaluation is recommended.

Conclusion

Although cSVD is still a challenging research topic with many open questions, contrast-free MRI methods have been a valuable tool for addressing some of the main questions. Such MRI methods and their related quantitative parameters are promising tools for evaluating risk factors and applying prevention strategies, especially modifiable ones. It has also been applied to study pathophysiological mechanisms underlying WM damage and promote markers for evaluating therapies. Finally, it has been used to assess damage to structural and functional brain connectivity, the first being suggested as a mediator of the effects of structural damage on cognition. New developments and ongoing studies

are essential to delineate more accurate MRI measures for the diagnosis, prognosis, and prediction of cSVD.

Conflict(s)-of-Interest/Disclosure(s)

None.

References

[1]   J.M. Wardlaw, H. Benveniste, A. Williams, Cerebral Vascular Dysfunctions Detected in Human Small Vessel Disease and Implications for Preclinical Studies., Annu. Rev. Physiol. 84 (2022) 409–434. https://doi.org/10.1146/annurev-physiol-060821-014521.

[2]   J.M. Wardlaw, E.E. Smith, G.J. Biessels, C. Cordonnier, F. Fazekas, R. Frayne, R.I. Lindley, J.T. O'Brien, F. Barkhof, O.R. Benavente, S.E. Black, C. Brayne, M. Breteler, H. Chabriat, C. DeCarli, F.E. de Leeuw, F. Doubal, M. Duering, N.C. Fox, S. Greenberg, V. Hachinski, I. Kilimann, V. Mok, R. van Oostenbrugge, L. Pantoni, O. Speck, B.C.M. Stephan, S. Teipel, A. Viswanathan, D. Werring, C. Chen, C. Smith, M. van Buchem, B. Norrving, P.B. Gorelick, M. Dichgans, Neuroimaging standards for research into small vessel disease and its contribution to ageing and neurodegeneration, Lancet Neurol. (2013). https://doi.org/10.1016/S1474-4422(13)70124-8.

[3]   M. Pasi, I.W.M. Van Uden, A.M. Tuladhar, F.E. De Leeuw, L. Pantoni, White Matter Microstructural Damage on Diffusion Tensor Imaging in Cerebral Small Vessel Disease: Clinical Consequences, Stroke. (2016). https://doi.org/10.1161/STROKEAHA.115.012065.

[4]   G.W. Blair, M.V. Hernandez, M.J. Thrippleton, F.N. Doubal, J.M. Wardlaw, Advanced Neuroimaging of Cerebral Small Vessel Disease, Curr. Treat. Options Cardiovasc. Med. 19 (2017) 56. https://doi.org/10.1007/s11936-017-0555-1.

[5]   M. Pasi, I.W.M. Van Uden, A.M. Tuladhar, F.E. De Leeuw, L. Pantoni, White Matter Microstructural Damage on Diffusion Tensor Imaging in Cerebral Small Vessel Disease: Clinical Consequences, Stroke. 47 (2016) 1679–1684. https://doi.org/10.1161/STROKEAHA.115.012065.

[6]   W. Van Hecke, A. Leemans, L. Emsell, DTI analysis methods: Voxel-based analysis, in: Diffus. Tensor Imaging A Pract. Handb., 2016. https://doi.org/10.1007/978-1-4939-3118-7_10.

[7]   S.M. Smith, M. Jenkinson, H. Johansen-Berg, D. Rueckert, T.E. Nichols, C.E. Mackay, K.E. Watkins, O. Ciccarelli, M.Z. Cader, P.M. Matthews, T.E.J. Behrens, Tract-based spatial statistics: Voxelwise analysis of multi-subject diffusion data, Neuroimage. (2006). https://doi.org/10.1016/j.neuroimage.2006.02.024.

[8]   M. Froeling, P. Pullens, A. Leemans, DTI analysis methods: Region of interest analysis, in: Diffus. Tensor Imaging A Pract. Handb., 2016. https://doi.org/10.1007/978-1-4939-3118-7_9.

[9]   P.J. Basser, S. Pajevic, C. Pierpaoli, J. Duda, A. Aldroubi, In vivo fiber tractography using DT-MRI data, Magn. Reson. Med. (2000). https://doi.org/10.1002/1522-2594(200010)44:4<625::AID-MRM17>3.0.CO;2-O.

[10]   N.K. Logothetis, J. Pauls, M. Augath, T. Trinath, A. Oeltermann, Neurophysiological investigation of the basis of the fMRI signal, Nature. 412 (2001) 150–157. https://doi.org/10.1038/35084005.

[11]   S. Ogawa, T.M. Lee, A.R. Kay, D.W. Tank, Brain magnetic resonance imaging with contrast dependent on blood oxygenation., Proc. Natl. Acad. Sci. U. S. A. 87 (1990) 9868–72. https://doi.org/10.1073/pnas.87.24.9868.

[12]   L. Shamseer, D. Moher, M. Clarke, D. Ghersi, A. Liberati, M. Petticrew, P. Shekelle, L.A. Stewart, D.G. Altman, A. Booth, A.W. Chan, S. Chang, T. Clifford, K. Dickersin, M. Egger, P.C. Gøtzsche, J.M. Grimshaw, T. Groves, M. Helfand, J. Higgins, T. Lasserson, J. Lau, K. Lohr, J. McGowan, C. Mulrow, M. Norton, M. Page, M. Sampson, H. Schünemann, I. Simera, W. Summerskill, J. Tetzlaff, T.A. Trikalinos, D. Tovey, L. Turner, E. Whitlock, Preferred reporting items for systematic review and meta-analysis protocols (prisma-p) 2015: Elaboration and explanation, BMJ. (2015). https://doi.org/10.1136/bmj.g7647.

[13]   A. Salami, J. Eriksson, L.G. Nilsson, L. Nyberg, Age-related white matter microstructural differences partly mediate age-related decline in processing speed but not cognition, Biochim. Biophys. Acta - Mol. Basis Dis. (2012). https://doi.org/10.1016/j.bbadis.2011.09.001.

[14]   A.L. Alexander, J.E. Lee, M. Lazar, A.S. Field, Diffusion Tensor Imaging of the Brain, Neurotherapeutics. (2007). https://doi.org/10.1016/j.nurt.2007.05.011.

[15]   M. del C. Valdés Hernández, P.A. Armitage, M.J. Thrippleton, F. Chappell, E. Sandeman, S. Muñoz Maniega, K. Shuler, J.M. Wardlaw, Rationale, design and methodology of the image analysis protocol for studies of patients with cerebral small vessel disease and mild stroke, Brain Behav. (2015). https://doi.org/10.1002/brb3.415.

[16]   R. Zhang, P. Huang, Y. Jiaerken, S. Wang, H. Hong, X. Luo, X. Xu, X. Yu, K. Li, Q. Zeng, X. Wu, M. Lou, M. Zhang, Venous disruption affects white matter integrity through increased interstitial fluid in cerebral small vessel disease, J. Cereb. Blood Flow Metab. (2020). https://doi.org/10.1177/0271678X20904840.

[17]   Y. Zhou, Q. Li, R. Zhang, W. Zhang, S. Yan, J. Xu, S. Wang, M. Zhang, M. Lou, Role of deep medullary veins in pathogenesis of lacunes: Longitudinal observations from the CIRCLE study, J. Cereb. Blood Flow Metab. (2019). https://doi.org/10.1177/0271678X19882918.

[18]   S. Akoudad, M. De Groot, P.J. Koudstaal, A. Van Der Lugt, W.J. Niessen, A. Hofman, M.A. Ikram, M.W. Vernooij, Cerebral microbleeds are related to loss of white matter structural integrity, Neurology. (2013). https://doi.org/10.1212/01.wnl.0000436609.20587.65.

[19]   J.Y. Liu, Y.J. Zhou, F.F. Zhai, F. Han, L.X. Zhou, J. Ni, M. Yao, S. Zhang, Z. Jin, L. Cui, Y.C. Zhu, Cerebral microbleeds are associated with loss of white matter integrity, Am. J. Neuroradiol. (2020). https://doi.org/10.3174/ajnr.A6622.

[20]   A.M. Tuladhar, I.W.M. Van Uden, L.C.A. Rutten-Jacobs, A. Lawrence, H. Van Der Holst, A. Van Norden, K. De Laat, E. Van Dijk, J.A.H.R. Claassen, R.P.C. Kessels, H.S. Markus, D.G. Norris, F.E. De Leeuw, Structural network efficiency predicts conversion to dementia, Neurology. (2016). https://doi.org/10.1212/WNL.0000000000002502.

[21]   A.M. Tuladhar, J. Tay, E. van Leijsen, A.J. Lawrence, I.W.M. van Uden, M. Bergkamp, E. van der Holst, R.P.C. Kessels, D. Norris, H.S. Markus, F.-E. De Leeuw, Structural network changes in cerebral small vessel disease, J. Neurol. Neurosurg. Psychiatry. 91 (2020) 196–203. https://doi.org/10.1136/jnnp-2019-321767.

[22]   A.J. Lawrence, D.J. Tozer, E.A. Stamatakis, H.S. Markus, A comparison of functional and tractography based networks in cerebral small vessel disease, NeuroImage Clin. (2018). https://doi.org/10.1016/j.nicl.2018.02.013.

[23]   L.C.A. Rutten-Jacobs, D.J. Tozer, M. Duering, R. Malik, M. Dichgans, H.S. Markus, M. Traylor, Genetic study of white matter integrity in UK Biobank (N=8448) and the overlap with stroke, depression, and dementia, Stroke. (2018). https://doi.org/10.1161/STROKEAHA.118.020811.

[24]   R.A.R. Gons, K.F. De Laat, A.G.W. Van Norden, L.J.B. Van Oudheusden, I.W.M. Van Uden, D.G. Norris, M.P. Zwiers, F.E. De Leeuw, Hypertension and cerebral diffusion tensor imaging in small vessel disease, Stroke. (2010). https://doi.org/10.1161/STROKEAHA.110.597237.

[25]   J.C. Foster-Dingley, J.E.F. Moonen, A.A. van den Berg-Huijsmans, A.J.M. de Craen, W. de Ruijter, J. van der Grond, R.C. van der Mast, Lower Blood Pressure and Gray Matter Integrity Loss in Older Persons, J. Clin. Hypertens. (2015). https://doi.org/10.1111/jch.12550.

[26]   A.K. Heye, M.J. Thrippleton, F.M. Chappell, M.D.C. Valdés Hernández, P.A. Armitage, S.D. Makin, S. Muñoz Maniega, E. Sakka, P.W. Flatman, M.S. Dennis, J.M. Wardlaw, Blood pressure and sodium: Association with MRI markers in cerebral small vessel disease, J. Cereb. Blood Flow Metab. (2016). https://doi.org/10.1038/jcbfm.2015.64.

[27]   J. Wei, P. Palta, M.L. Meyer, A. Kucharska-Newton, B.W. Pence, A.E. Aiello, M.C. Power, K.A. Walker, A.R. Sharrett, H. Tanaka, C.R. Jack, T.H. Mosley, R.I. Reid, D.A. Reyes, G. Heiss, Aortic Stiffness and White Matter Microstructural Integrity Assessed by Diffusion Tensor Imaging: The ARIC-NCS, J. Am. Heart Assoc. (2020). https://doi.org/10.1161/JAHA.119.014868.

[28]   K.A. Walker, M.C. Power, R.C. Hoogeveen, A.R. Folsom, C.M. Ballantyne, D.S. Knopman, B.G. Windham, E. Selvin, C.R. Jack, R.F. Gottesman, Midlife systemic inflammation, late-life white matter

integrity, and cerebral small vessel disease the atherosclerosis risk in communities study, Stroke. (2017). https://doi.org/10.1161/STROKEAHA.117.018675.

[29]   E. Auriel, E. Kliper, S. Shenhar-Tsarfaty, J. Molad, S. Berliner, I. Shapira, D. Ben-Bashat, L. Shopin, O. Tene, G.A. Rosenberg, N.M. Bornstein, E. Ben Assayag, Impaired renal function is associated with brain atrophy and poststroke cognitive decline, Neurology. (2016). https://doi.org/10.1212/WNL.0000000000002699.

[30]   R.A.R. Gons, A.M. Tuladhar, K.F. De Laat, A.G.W. Van Norden, E.J. Van Dijk, D.G. Norris, M.P. Zwiers, F.E. De Leeuw, Physical activity is related to the structural integrity of cerebral white matter, Neurology. (2013). https://doi.org/10.1212/WNL.0b013e3182a43e33.

[31]   R.A.R. Gons, L.J.B. Van Oudheusden, K.F. De Laat, A.G.W. Van Norden, I.W.M. Van Uden, D.G. Norris, M.P. Zwiers, E. Van Dijk, F.E. De Leeuw, Hypertension is related to the microstructure of the corpus callosum: The RUN DMC study, J. Alzheimer's Dis. (2012). https://doi.org/10.3233/JAD-2012-121006.

[32]   C.M.N.C.M. Nassir, M.M. Ghazali, A.A. Safri, U. Jaffer, W.Z. Abdullah, N.S. Idris, M. Muzaimi, Elevated circulating microparticle subpopulations in incidental cerebral white matter hyperintensities: A multimodal study, Brain Sci. 11 (2021). https://doi.org/10.3390/brainsci11020133.

[33]   J.M. Papma, M. de Groot, I. de Koning, F.U. Mattace-Raso, A. van der Lugt, M.W. Vernooij, W.J. Niessen, J.C. van Swieten, P.J. Koudstaal, N.D. Prins, M. Smits, Cerebral small vessel disease affects white matter microstructure in mild cognitive impairment, Hum. Brain Mapp. (2014). https://doi.org/10.1002/hbm.22370.

[34]   A.J. Lawrence, B. Patel, R.G. Morris, A.D. MacKinnon, P.M. Rich, T.R. Barrick, H.S. Markus, Mechanisms of Cognitive Impairment in Cerebral Small Vessel Disease: Multimodal MRI Results from the St George's Cognition and Neuroimaging in Stroke (SCANS) Study, PLoS One. (2013). https://doi.org/10.1371/journal.pone.0061014.

[35]   H. Zhou, Y. Tang, Y. Liu, W. Wang, Atypical cortical thickness and subcortical volumes in cerebral microbleed patients: A combined freesurfer and diffusion tensor imaging study, J. Med. Imaging Heal. Informatics. (2015). https://doi.org/10.1166/jmihi.2015.1635.

[36]   W.W. Cao, Y. Wang, Q. Dong, X. Chen, Y.S. Li, Y. Zhou, L. Gao, Y. Deng, Q. Xu, Deep microbleeds and periventricular white matter disintegrity are independent predictors of attention/executive dysfunction in non-dementia patients with small vessel disease, Int. Psychogeriatrics. (2017). https://doi.org/10.1017/S1041610216002118.

[37]   S.M. Heringa, Y.D. Reijmer, A. Leemans, H.L. Koek, L.J. Kappelle, G.J. Biessels, Multiple microbleeds are related to cerebral network disruptions in patients with early Alzheimer's disease, J. Alzheimer's Dis. (2014). https://doi.org/10.3233/JAD-130542.

[38]   J. Tang, L. Shi, Q. Zhao, M. Zhang, D. Ding, B. Yu, J. Fu, Coexisting cortical atrophy plays a crucial role in cognitive impairment in moderate to severe cerebral small vessel disease patients, Discov. Med. (2017).

[39]   M.M. D'Souza, S.P. Gorthi, K. Vadwala, R. Trivedi, C. Vijayakumar, P. Kaur, S. Khushu, Diffusion tensor tractography in cerebral small vessel disease: correlation with cognitive function, Neuroradiol. J. (2018). https://doi.org/10.1177/1971400916682753.

[40]   M. Duering, M.J. Konieczny, S. Tiedt, E. Baykara, A.M. Tuladhar, E. van Leijsen, P. Lyrer, S.T. Engelter, B. Gesierich, M. Achmüller, C. Barro, R. Adam, M. Ewers, M. Dichgans, J. Kuhle, F.E. de Leeuw, N. Peters, Serum neurofilament light chain levels are related to small vessel disease burden, J. Stroke. (2018). https://doi.org/10.5853/jos.2017.02565.

[41]   A. Nitkunan, T.R. Barrick, R.A. Charlton, C.A. Clark, H.S. Markus, Multimodal MRI in Cerebral Small Vessel Disease, Stroke. (2008). https://doi.org/10.1161/strokeaha.107.507475.

[42]   E.M.C. Van Leijsen, M.I. Bergkamp, I.W.M. Van Uden, M. Ghafoorian, H.M. Van Der Holst, D.G.

Norris, B. Platel, A.M. Tuladhar, F.E. De Leeuw, Progression of white matter hyperintensities preceded by heterogeneous decline of microstructural integrity, Stroke. (2018). https://doi.org/10.1161/STROKEAHA.118.020980.

[43] M. O'Sullivan, R.G. Morris, B. Huckstep, D.K. Jones, S.C.R. Williams, H.S. Markus, Diffusion tensor MRI correlates with executive dysfunction in patients with ischaemic leukoaraiosis, J. Neurol. Neurosurg. Psychiatry. (2004). https://doi.org/10.1136/jnnp.2003.014910.

[44] L.A. Dobrynina, Z.S. Gadzhieva, K. V. Shamtieva, E.I. Kremneva, B.M. Akhmetzyanov, L.A. Kalashnikova, M. V. Krotenkova, Microstructural Predictors of Cognitive Impairment in Cerebral Small Vessel Disease and the Conditions of Their Formation, Diagnostics. (2020). https://doi.org/10.3390/diagnostics10090720.

[45] K.F. De Laat, A.M. Tuladhar, A.G.W. Van Norden, D.G. Norris, M.P. Zwiers, F.E. De Leeuw, Loss of white matter integrity is associated with gait disorders in cerebral small vessel disease, Brain. (2011). https://doi.org/10.1093/brain/awq343.

[46] K.F. De Laat, A.G.W. Van Norden, R.A.R. Gons, L.J.B. Van Oudheusden, I.W.M. Van Uden, D.G. Norris, M.P. Zwiers, F.E. De Leeuw, Diffusion tensor imaging and gait in elderly persons with cerebral small vessel disease, Stroke. (2011). https://doi.org/10.1161/STROKEAHA.110.596502.

[47] J. Verghese, A. LeValley, C.B. Hall, M.J. Katz, A.F. Ambrose, R.B. Lipton, Epidemiology of gait disorders in community-residing older adults, J. Am. Geriatr. Soc. (2006). https://doi.org/10.1111/j.1532-5415.2005.00580.x.

[48] M. Cavallari, N. Moscufo, D. Meier, P. Skudlarski, G.D. Pearlson, W.B. White, L. Wolfson, C.R.G. Guttmann, Thalamic fractional anisotropy predicts accrual of cerebral white matter damage in older subjects with small-vessel disease, J. Cereb. Blood Flow Metab. (2014). https://doi.org/10.1038/jcbfm.2014.86.

[49] E.A. Zeestraten, P. Benjamin, C. Lambert, A.J. Lawrence, O.A. Williams, R.G. Morris, T.R. Barrick, H.S. Markus, Application of diffusion tensor imaging parameters to detect change in longitudinal studies in cerebral small vessel disease, PLoS One. (2016). https://doi.org/10.1371/journal.pone.0147836.

[50] E.A. Zeestraten, A.J. Lawrence, C. Lambert, P. Benjamin, R.L. Brookes, A.D. Mackinnon, R.G. Morris, T.R. Barrick, H.S. Markus, Change in multimodal MRI markers predicts dementia risk in cerebral small vessel disease, Neurology. (2017). https://doi.org/10.1212/WNL.0000000000004594.

[51] H.M. Van Der Holst, I.W.M. Van Uden, A.M. Tuladhar, K.F. De Laat, A.G.W. Van Norden, D.G. Norris, E.J. Van Dijk, L.C. Rutten-Jacobs, F.E. De Leeuw, Factors associated with 8-year mortality in older patients with cerebral small vessel disease the Radboud University Nijmegen Diffusion Tensor and Magnetic Resonance Cohort (RUN DMC) study, JAMA Neurol. (2016). https://doi.org/10.1001/jamaneurol.2015.4560.

[52] B. Gunda, R. Porcher, M. Duering, J.P. Guichard, J. Mawet, E. Jouvent, M. Dichgans, H. Chabriat, ADC histograms from routine DWI for longitudinal studies in cerebral small vessel disease: A field study in CADASIL, PLoS One. (2014). https://doi.org/10.1371/journal.pone.0097173.

[53] A.G.W. Van Norden, K.F. De Laat, E.J. Van Dijk, I.W.M. Van Uden, L.J.B. Van Oudheusden, R.A.R. Gons, D.G. Norris, M.P. Zwiers, F.E. De Leeuw, Diffusion tensor imaging and cognition in cerebral small vessel disease. The RUN DMC study., Biochim. Biophys. Acta - Mol. Basis Dis. (2012). https://doi.org/10.1016/j.bbadis.2011.04.008.

[54] A.G.W. Van Norden, K.F. De Laat, E.J. Van Dijk, F.E. De Leeuw, Cognitive function in small vessel disease: The additional value of diffusion tensor imaging to conventional magnetic resonance imaging: The RUN DMC study, J. Alzheimer's Dis. (2012). https://doi.org/10.3233/JAD-2012-120784.

[55] P. Benjamin, E. Zeestraten, C. Lambert, I. Chis Ster, O.A. Williams, A.J. Lawrence, B. Patel, A.D. Mackinnon, T.R. Barrick, H.S. Markus, Progression of MRI markers in cerebral small vessel disease: Sample size considerations for clinical trials, J. Cereb. Blood Flow Metab. (2016). https://doi.org/10.1038/jcbfm.2015.113.

[56]   I.W.M. Van Uden, H.M. Van Der Holst, A.M. Tuladhar, A.G.W. Van Norden, K.F. De Laat, L.C.A. Rutten-Jacobs, D.G. Norris, J.A.H.R. Claassen, E.J. Van Dijk, R.P.C. Kessels, F.E. De Leeuw, White matter and hippocampal volume predict the risk of dementia in patients with cerebral small vessel disease: The RUN DMC study, J. Alzheimer's Dis. (2015). https://doi.org/10.3233/JAD-150573.

[57]   W. Reginold, K. Sam, J. Poublanc, J. Fisher, A. Crawley, D.J. Mikulis, Impact of white matter hyperintensities on surrounding white matter tracts, Neuroradiology. (2018). https://doi.org/10.1007/s00234-018-2053-x.

[58]   H. Zhou, Y. Tang, Z. Yuan, White matter asymmetries in patients with cerebral small vessel disease, J. Integr. Neurosci. (2018). https://doi.org/10.3233/JIN-170037.

[59]   C. Mayer, B.M. Frey, E. Schlemm, M. Petersen, K. Engelke, U. Hanning, A. Jagodzinski, K. Borof, J. Fiehler, C. Gerloff, G. Thomalla, B. Cheng, Linking cortical atrophy to white matter hyperintensities of presumed vascular origin., J. Cereb. Blood Flow Metab. Off. J. Int. Soc. Cereb. Blood Flow Metab. 41 (2021) 1682–1691. https://doi.org/10.1177/0271678X20974170.

[60]   C.E. Bauer, V. Zachariou, E. Seago, B.T. Gold, White Matter Hyperintensity Volume and Location: Associations With WM Microstructure, Brain Iron, and Cerebral Perfusion, Front. Aging Neurosci. 13 (2021). https://doi.org/10.3389/fnagi.2021.617947.

[61]   P. Kang, C. Ying, Y. Chen, A.L. Ford, H. An, J.-M. Lee, Oxygen Metabolic Stress and White Matter Injury in Patients With Cerebral Small Vessel Disease., Stroke. (2021) STROKEAHA121035674. https://doi.org/10.1161/STROKEAHA.121.035674.

[62]   X. Xu, K.K. Lau, Y.K. Wong, H.K.F. Mak, E.S. Hui, The effect of the total small vessel disease burden on the structural brain network., Sci. Rep. 8 (2018) 7442. https://doi.org/10.1038/s41598-018-25917-4.

[63]   Y.D. Reijmer, P. Fotiadis, G.A. Riley, L. Xiong, A. Charidimou, G. Boulouis, A.M. Ayres, K. Schwab, J. Rosand, M.E. Gurol, A. Viswanathan, S.M. Greenberg, Progression of Brain Network Alterations in Cerebral Amyloid Angiopathy, Stroke. (2016). https://doi.org/10.1161/STROKEAHA.116.014337.

[64]   Y.D. Reijmer, P. Fotiadis, A. Charidimou, S.J. Van Veluw, L. Xiong, G.A. Riley, S. Martinez-Ramirez, K. Schwab, A. Viswanathan, M.E. Gurol, S.M. Greenberg, Relationship between white matter connectivity loss and cortical thinning in cerebral amyloid angiopathy, Hum. Brain Mapp. (2017). https://doi.org/10.1002/hbm.23629.

[65]   S. Ciulli, L. Citi, E. Salvadori, R. Valenti, A. Poggesi, D. Inzitari, M. Mascalchi, N. Toschi, L. Pantoni, S. Diciotti, Prediction of Impaired Performance in Trail Making Test in MCI Patients with Small Vessel Disease Using DTI Data, IEEE J. Biomed. Heal. Informatics. (2016). https://doi.org/10.1109/JBHI.2016.2537808.

[66]   A.J. Lawrence, A.W. Chung, R.G. Morris, H.S. Markus, T.R. Barrick, Structural network efficiency is associated with cognitive impairment in small-vessel disease, Neurology. (2014). https://doi.org/10.1212/WNL.0000000000000612.

[67]   A.M. Tuladhar, E. van Dijk, M.P. Zwiers, A.G.W. van Norden, K.F. de Laat, E. Shumskaya, D.G. Norris, F.E. de Leeuw, Structural network connectivity and cognition in cerebral small vessel disease, Hum. Brain Mapp. (2016). https://doi.org/10.1002/hbm.23032.

[68]   H.F. Chen, L.L. Huang, H.Y. Li, Y. Qian, D. Yang, Z. Qing, C.M. Luo, M.C. Li, B. Zhang, Y. Xu, Microstructural disruption of the right inferior fronto-occipital and inferior longitudinal fasciculus contributes to WMH-related cognitive impairment, CNS Neurosci. Ther. (2020). https://doi.org/10.1111/cns.13283.

[69]   A.M. Tuladhar, A. Lawrence, D.G. Norris, T.R. Barrick, H.S. Markus, F.E. de Leeuw, Disruption of rich club organisation in cerebral small vessel disease, Hum. Brain Mapp. (2017). https://doi.org/10.1002/hbm.23479.

[70] X. Chen, L. Huang, Q. Ye, D. Yang, R. Qin, C. Luo, M. Li, B. Zhang, Y. Xu, Disrupted functional and structural connectivity within default mode network contribute to WMH-related cognitive impairment, NeuroImage Clin. (2019). https://doi.org/10.1016/j.nicl.2019.102088.

[71] E.M.C. van Leijsen, I.W.M. van Uden, M.I. Bergkamp, H.M. van der Holst, D.G. Norris, J.A.H.R. Claassen, R.P.C. Kessels, F.E. de Leeuw, A.M. Tuladhar, Longitudinal changes in rich club organization and cognition in cerebral small vessel disease, NeuroImage Clin. (2019). https://doi.org/10.1016/j.nicl.2019.102048.

[72] J. Du, Y. Wang, N. Zhi, J. Geng, W. Cao, L. Yu, J. Mi, Y. Zhou, Q. Xu, W. Wen, P. Sachdev, Structural brain network measures are superior to vascular burden scores in predicting early cognitive impairment in post stroke patients with small vessel disease, NeuroImage Clin. (2019). https://doi.org/10.1016/j.nicl.2019.101712.

[73] C. Liu, L. Zou, X. Tang, W. Zhu, G. Zhang, Y. Qin, W. Zhu, Changes of white matter integrity and structural network connectivity in nondemented cerebral small-vessel disease, J. Magn. Reson. Imaging. (2020). https://doi.org/10.1002/jmri.26906.

[74] H.J. Kim, J.J. Yang, H. Kwon, C. Kim, J.M. Lee, P. Chun, Y.J. Kim, N.Y. Jung, J. Chin, S. Kim, S.Y. Woo, Y.S. Choe, K.H. Lee, S.T. Kim, J.S. Kim, J.H. Lee, M.W. Weiner, D.L. Na, S.W. Seo, Relative impact of amyloid-β, lacunes, and downstream imaging markers on cognitive trajectories, Brain. (2016). https://doi.org/10.1093/brain/aww148.

[75] J. Du, H. Zhu, J. Zhou, P. Lu, Y. Qiu, L. Yu, W. Cao, J. Yang, Q. Xu, J. Sun, Y. Zhou, Structural Brain Network Disruption at Preclinical Stage of Cognitive Impairment Due to Cerebral Small Vessel Disease, Neuroscience. (2020). https://doi.org/10.1016/j.neuroscience.2020.08.037.

[76] E.M. Boot, E. MC van Leijsen, M.I. Bergkamp, R.P.C. Kessels, D.G. Norris, F.E. de Leeuw, A.M. Tuladhar, Structural network efficiency predicts cognitive decline in cerebral small vessel disease, NeuroImage Clin. (2020). https://doi.org/10.1016/j.nicl.2020.102325.

[77] L.W.M. Vergoossen, J.F.A. Jansen, T.T. Van Sloten, C.D.A. Stehouwer, N.C. Schaper, A. Wesselius, P.C. Dagnelie, S. Köhler, M.P.J. Van Boxtel, A.A. Kroon, J.J.A. De Jong, M.T. Schram, W.H. Backes, Interplay of White Matter Hyperintensities, Cerebral Networks, and Cognitive Function in an Adult Population: Diffusion-Tensor Imaging in the Maastricht Study, Radiology. 298 (2021). https://doi.org/10.1148/RADIOL.2021202634.

[78] E. Baykara, B. Gesierich, R. Adam, A.M. Tuladhar, J.M. Biesbroek, H.L. Koek, S. Ropele, E. Jouvent, H. Chabriat, B. Ertl-Wagner, M. Ewers, R. Schmidt, F.E. de Leeuw, G.J. Biessels, M. Dichgans, M. Duering, A Novel Imaging Marker for Small Vessel Disease Based on Skeletonization of White Matter Tracts and Diffusion Histograms, Ann. Neurol. (2016). https://doi.org/10.1002/ana.24758.

[79] N. Wei, Y. Deng, L. Yao, W. Jia, J. Wang, Q. Shi, H. Chen, Y. Pan, H. Yan, Y. Zhang, Y. Wang, A neuroimaging marker based on diffusion tensor imaging and cognitive impairment due to cerebral white matter lesions, Front. Neurol. (2019). https://doi.org/10.3389/fneur.2019.00081.

[80] A. Low, E. Mak, J.D. Stefaniak, M. Malpetti, N. Nicastro, G. Savulich, L. Chouliaras, H.S. Markus, J.B. Rowe, J.T. O'Brien, Peak Width of Skeletonized Mean Diffusivity as a Marker of Diffuse Cerebrovascular Damage, Front. Neurosci. 14 (2020). https://doi.org/10.3389/fnins.2020.00238.

[81] N. Raposo, M.C. Zanon Zotin, D. Schoemaker, L. Xiong, P. Fotiadis, A. Charidimou, M. Pasi, G. Boulouis, K. Schwab, M.D. Schirmer, M.R. Etherton, M.E. Gurol, S.M. Greenberg, M. Duering, A. Viswanathan, Peak Width of Skeletonized Mean Diffusivity as Neuroimaging Biomarker in Cerebral Amyloid Angiopathy., AJNR. Am. J. Neuroradiol. 42 (2021) 875–881. https://doi.org/10.3174/ajnr.A7042.

[82] A.R. Fouto, R.G. Nunes, J. Pinto, L. Alves, S. Calado, C. Gonçalves, M. Rebolo, M. Viana-Baptista, P. Vilela, P. Figueiredo, Impact of white-matter mask selection on DTI histogram-based metrics as potential biomarkers in cerebral small vessel disease., MAGMA. (2022). https://doi.org/10.1007/s10334-021-00991-4.

[83] M. Duering, S. Finsterwalder, E. Baykara, A.M. Tuladhar, B. Gesierich, M.J. Konieczny, R. Malik, N.

Franzmeier, M. Ewers, E. Jouvent, G.J. Biessels, R. Schmidt, F.E. de Leeuw, O. Pasternak, M. Dichgans, Free water determines diffusion alterations and clinical status in cerebral small vessel disease, Alzheimer's Dement. (2018). https://doi.org/10.1016/j.jalz.2017.12.007.

[84] M. Altendahl, P. Maillard, D. Harvey, D. Cotter, S. Walters, A. Wolf, B. Singh, V. Kakarla, I. Azizkhanian, S.A. Sheth, G. Xiao, E. Fox, M. You, M. Leng, D. Elashoff, J.H. Kramer, C. Decarli, F. Elahi, J.D. Hinman, An IL-18-centered inflammatory network as a biomarker for cerebral white matter injury, PLoS One. (2020). https://doi.org/10.1371/journal.pone.0227835.

[85] R. Zhang, W. Yu, X. Wu, Y. Jiaerken, S. Wang, H. Hong, K. Li, Q. Zeng, X. Luo, X. Yu, X. Xu, M. Zhang, P. Huang, Disentangling the pathologies linking white matter hyperintensity and geriatric depressive symptoms in subjects with different degrees of vascular impairment, J. Affect. Disord. 282 (2021). https://doi.org/10.1016/j.jad.2020.12.171.

[86] P. Huang, R. Zhang, Y. Jiaerken, S. Wang, H. Hong, W. Yu, C. Lian, K. Li, Q. Zeng, X. Luo, X. Yu, X. Wu, X. Xu, M. Zhang, White Matter Free Water is a Composite Marker of Cerebral Small Vessel Degeneration, Transl. Stroke Res. (2021). https://doi.org/10.1007/s12975-021-00899-0.

[87] X. Yu, X. Yin, H. Hong, S. Wang, Y. Jiaerken, F. Zhang, O. Pasternak, R. Zhang, L. Yang, M. Lou, M. Zhang, P. Huang, Increased extracellular fluid is associated with white matter fiber degeneration in CADASIL: in vivo evidence from diffusion magnetic resonance imaging., Fluids Barriers CNS. 18 (2021) 29. https://doi.org/10.1186/s12987-021-00264-1.

[88] O.A. Williams, E.A. Zeestraten, P. Benjamin, C. Lambert, A.J. Lawrence, A.D. Mackinnon, R.G. Morris, H.S. Markus, R.A. Charlton, T.R. Barrick, Diffusion tensor image segmentation of the cerebrum provides a single measure of cerebral small vessel disease severity related to cognitive change, NeuroImage Clin. (2017). https://doi.org/10.1016/j.nicl.2017.08.016.

[89] O.A. Williams, E.A. Zeestraten, P. Benjamin, C. Lambert, A.J. Lawrence, A.D. Mackinnon, R.G. Morris, H.S. Markus, T.R. Barrick, R.A. Charlton, Predicting dementia in cerebral small vessel disease using an automatic diffusion tensor image segmentation technique, Stroke. (2019). https://doi.org/10.1161/STROKEAHA.119.025843.

[90] M.J. Konieczny, A. Dewenter, A. Ter Telgte, B. Gesierich, K. Wiegertjes, S. Finsterwalder, A. Kopczak, M. Hübner, R. Malik, A.M. Tuladhar, J.P. Marques, D.G. Norris, A. Koch, O. Dietrich, M. Ewers, R. Schmidt, F.E. de Leeuw, M. Duering, Multi-shell Diffusion MRI Models for White Matter Characterization in Cerebral Small Vessel Disease, Neurology. 96 (2021). https://doi.org/10.1212/WNL.0000000000011213.

[91] W. Zhang, Y. Zhou, J. Wang, X. Gong, Z. Chen, X. Zhang, J. Cai, S. Chen, L. Fang, J. Sun, M. Lou, Glymphatic clearance function in patients with cerebral small vessel disease., Neuroimage. 238 (2021) 118257. https://doi.org/10.1016/j.neuroimage.2021.118257.

[92] A.M. Tuladhar, A.G.W. Van Norden, K.F. De Laat, M.P. Zwiers, E.J. Van Dijk, D.G. Norris, F.E. De Leeuw, White matter integrity in small vessel disease is related to cognition, NeuroImage Clin. (2015). https://doi.org/10.1016/j.nicl.2015.02.003.

[93] L. Huang, X. Chen, W. Sun, H. Chen, Q. Ye, D. Yang, M. Li, C. Luo, J. Ma, P. Shao, H. Xu, B. Zhang, X. Zhu, Y. Xu, Early Segmental White Matter Fascicle Microstructural Damage Predicts the Corresponding Cognitive Domain Impairment in Cerebral Small Vessel Disease Patients by Automated Fiber Quantification, Front. Aging Neurosci. 12 (2021). https://doi.org/10.3389/fnagi.2020.598242.

[94] S. Guan, X. Kong, S. Duan, Q. Ren, Z. Huang, Y. Li, W. Wang, G. Gong, X. Meng, X. Ma, Neuroimaging Anomalies in Community-Dwelling Asymptomatic Adults With Very Early-Stage White Matter Hyperintensity., Front. Aging Neurosci. 13 (2021) 715434. https://doi.org/10.3389/fnagi.2021.715434.

[95] I.W.M. van Uden, H.M. van der Holst, P. Schaapsmeerders, A.M. Tuladhar, A.G.W. van Norden, K.F. de Laat, D.G. Norris, J.A.H.R. Claassen, E.J. van Dijk, E. Richard, R.P.C. Kessels, F.E. de Leeuw, Baseline

white matter microstructural integrity is not related to cognitive decline after 5years: The RUN DMC study, BBA Clin. (2015). https://doi.org/10.1016/j.bbacli.2015.10.001.

[96] M. Holtmannspötter, N. Peters, C. Opherk, D. Martin, J. Herzog, H. Brückmann, P. Sämann, A. Gschwendtner, M. Dichgans, Diffusion magnetic resonance histograms as a surrogate marker and predictor of disease progression in CADASIL a two-year follow-up study, Stroke. (2005). https://doi.org/10.1161/01.STR.0000189696.70989.a4.

[97] S. Ban, H. Wang, M. Wang, S. Xu, Z. Qin, J. Su, X. Du, J.R. Liu, Diffuse Tract Damage in CADASIL Is Correlated with Global Cognitive Impairment, Eur. Neurol. (2019). https://doi.org/10.1159/000501612.

[98] P. Li, Q. Huang, S. Ban, Y. Qiao, J. Wu, Y. Zhai, X. Du, F. Hua, J. Su, Altered Default Mode Network Is Associated With Cognitive Impairment in CADASIL as Revealed by Multimodal Neuroimaging., Front. Neurol. 12 (2021) 735033. https://doi.org/10.3389/fneur.2021.735033.

[99] I.D. Croall, V. Lohner, B. Moynihan, U. Khan, A. Hassan, J.T. O'Brien, R.G. Morris, D.J. Tozer, V.C. Cambridge, K. Harkness, D.J. Werring, A.M. Blamire, G.A. Ford, T.R. Barrick, H.S. Markus, Using DTI to assess white matter microstructure in cerebral small vessel disease (SVD) in multicentre studies, Clin. Sci. (2017). https://doi.org/10.1042/CS20170146.

[100] A. Metoki, R.L. Brookes, E. Zeestraten, A.J. Lawrence, R.G. Morris, T.R. Barrick, H.S. Markus, R.A. Charlton, Mnemonic function in small vessel disease and associations with white matter tract microstructure, Neuropsychologia. (2017). https://doi.org/10.1016/j.neuropsychologia.2017.07.027.

[101] A.G.W. van Norden, K.F. de Laat, I. Fick, I.W.M. van Uden, L.J.B. van Oudheusden, R.A.R. Gons, D.G. Norris, M.P. Zwiers, R.P.C. Kessels, F.E. de Leeuw, Diffusion tensor imaging of the hippocampus and verbal memory performance: The RUN DMC Study, Hum. Brain Mapp. (2012). https://doi.org/10.1002/hbm.21231.

[102] H.M. van der Holst, A.M. Tuladhar, A.G.W. van Norden, K.F. de Laat, I.W.M. van Uden, L.J.B. van Oudheusden, M.P. Zwiers, D.G. Norris, R.P.C. Kessels, F.E. de Leeuw, Microstructural integrity of the cingulum is related to verbal memory performance in elderly with cerebral small vessel disease. The RUN DMC study., Neuroimage. (2013). https://doi.org/10.1016/j.neuroimage.2012.09.060.

[103] C. Liu, L. Shi, W. Zhu, S. Yang, P. Sun, Y. Qin, X. Tang, S. Zhang, Y. Yao, Z. Wang, W. Zhu, D. Wang, Fiber Connectivity Density in Cerebral Small-Vessel Disease Patients With Mild Cognitive Impairment and Cerebral Small-Vessel Disease Patients With Normal Cognition, Front. Neurosci. (2020). https://doi.org/10.3389/fnins.2020.00083.

[104] M. Pasi, E. Salvadori, A. Poggesi, L. Ciolli, A. Del Bene, S. Marini, S. Nannucci, F. Pescini, R. Valenti, A. Ginestroni, N. Toschi, S. Diciotti, M. Mascalchi, D. Inzitari, L. Pantoni, White matter microstructural damage in small vessel disease is associated with montreal cognitive assessment but not with mini mental state examination performances: Vascular mild cognitive impairment tuscany study, Stroke. (2015). https://doi.org/10.1161/STROKEAHA.114.007553.

[105] Z. Liao, C. Dang, M. Li, Y. Bu, R. Han, W. Jiang, Microstructural damage of normal-appearing white matter in subcortical ischemic vascular dementia is associated with Montreal Cognitive Assessment scores, J. Int. Med. Res. (2019). https://doi.org/10.1177/0300060519863520.

[106] A. Brandhofe, C. Stratmann, J.R. Schüre, U. Pilatus, E. Hattingen, R. Deichmann, U. Nöth, M. Wagner, R.M. Gracien, A. Seiler, T2 relaxation time of the normal-appearing white matter is related to the cognitive status in cerebral small vessel disease, J. Cereb. Blood Flow Metab. (2020). https://doi.org/10.1177/0271678X20972511.

[107] J. Du, H. Zhu, L. Yu, P. Lu, Y. Qiu, Y. Zhou, W. Cao, D. Lu, W. Zhao, J. Yang, J. Sun, Q. Xu, Multi-Dimensional Diffusion Tensor Imaging Biomarkers for Cognitive Decline From the Preclinical Stage: A Study of Post-stroke Small Vessel Disease., Front. Neurol. 12 (2021) 687959. https://doi.org/10.3389/fneur.2021.687959.

[108] M. Egle, S. Hilal, A.M. Tuladhar, L. Pirpamer, E. Hofer, M. Duering, J. Wason, R.G. Morris, M.

Dichgans, R. Schmidt, D. Tozer, C. Chen, F.-E. de Leeuw, H.S. Markus, Prediction of dementia using diffusion tensor MRI measures: the OPTIMAL collaboration., J. Neurol. Neurosurg. Psychiatry. 93 (2022) 14–23. https://doi.org/10.1136/jnnp-2021-326571.

[109] I.W.M. van Uden, A.M. Tuladhar, H.M. van der Holst, E.M.C. van Leijsen, A.G.W. van Norden, K.F. de Laat, L.C.A. Rutten-Jacobs, D.G. Norris, J.A.H.R. Claassen, E.J. van Dijk, R.P.C. Kessels, F.E. de Leeuw, Diffusion tensor imaging of the hippocampus predicts the risk of dementia; the RUN DMC study, Hum. Brain Mapp. (2016). https://doi.org/10.1002/hbm.23029.

[110] W. Swardfager, D. Yu, J. Ramirez, H. Cogo-Moreira, G. Szilagyi, M.F. Holmes, C.J.M. Scott, G. Scola, P.C. Chan, J. Chen, P. Chan, D.J. Sahlas, N. Herrmann, K.L. Lanctôt, A.C. Andreazza, J.A. Pettersen, S.E. Black, Peripheral inflammatory markers indicate microstructural damage within periventricular white matter hyperintensities in Alzheimer's disease: A preliminary report, Alzheimer's Dement. Diagnosis, Assess. Dis. Monit. (2017). https://doi.org/10.1016/j.dadm.2016.12.011.

[111] M.R. Raman, J.J. Himali, S.C. Conner, C. DeCarli, R.S. Vasan, A.S. Beiser, S. Seshadri, P. Maillard, C.L. Satizabal, Circulating vascular growth factors and magnetic resonance imaging markers of small vessel disease and atrophy in middle-aged adults, Stroke. (2018). https://doi.org/10.1161/STROKEAHA.118.022613.

[112] S. Finsterwalder, N. Vlegels, B. Gesierich, M. Araque Caballero, N.A. Weaver, N. Franzmeier, M.K. Georgakis, M.J. Konieczny, H.L. Koek, C.M. Karch, N.R. Graff-Radford, S. Salloway, H. Oh, R.F. Allegri, J.P. Chhatwal, F. Jessen, E. Düzel, L. Dobisch, C. Metzger, O. Peters, E.I. Incesoy, J. Priller, E.J. Spruth, A. Schneider, K. Fließbach, K. Buerger, D. Janowitz, S.J. Teipel, I. Kilimann, C. Laske, M. Buchmann, M.T. Heneka, F. Brosseron, A. Spottke, N. Roy, B. Ertl-Wagner, K. Scheffler, S.W. Seo, Y. Kim, D.L. Na, H.J. Kim, H. Jang, M. Ewers, J. Levin, R. Schmidt, O. Pasternak, M. Dichgans, G.J. Biessels, M. Duering, Small vessel disease more than Alzheimer's disease determines diffusion MRI alterations in memory clinic patients, Alzheimer's Dement. (2020). https://doi.org/10.1002/alz.12150.

[113] A.E.S.A.M.T. Eldin, W.S. Bahnasy, N.L. Dabees, H.A.E.R. Fayed, Cognitive and balance impairments in people with incidental white matter hyperintensities, Egypt. J. Neurol. Psychiatry Neurosurg. 56 (2020). https://doi.org/10.1186/s41983-020-00228-6.

[114] B.L. Rosario, A.L. Rosso, H.J. Aizenstein, T. Harris, A.B. Newman, S. Satterfield, S.A. Studenski, K. Yaffe, C. Rosano, Cerebral white matter and slow gait: Contribution of hyperintensities and normal-appearing parenchyma, Journals Gerontol. - Ser. A Biol. Sci. Med. Sci. (2016). https://doi.org/10.1093/gerona/glv224.

[115] H.M. van der Holst, I.W.M. van Uden, K.F. de Laat, E.M.C. van Leijsen, A.G.W. van Norden, D.G. Norris, E.J. van Dijk, A.M. Tuladhar, F.E. de Leeuw, Baseline Cerebral Small Vessel Disease Is Not Associated with Gait Decline After Five Years, Mov. Disord. Clin. Pract. (2017). https://doi.org/10.1002/mdc3.12435.

[116] H.M. van der Holst, A.M. Tuladhar, V. Zerbi, I.W.M. van Uden, K.F. de Laat, E.M.C. van Leijsen, M. Ghafoorian, B. Platel, M.I. Bergkamp, A.G.W. van Norden, D.G. Norris, E.J. van Dijk, A.J. Kiliaan, F.E. de Leeuw, White matter changes and gait decline in cerebral small vessel disease, NeuroImage Clin. (2018). https://doi.org/10.1016/j.nicl.2017.12.007.

[117] S. Finsterwalder, M. Wuehr, B. Gesierich, A. Dietze, M.J. Konieczny, R. Schmidt, R. Schniepp, M. Duering, Minor gait impairment despite white matter damage in pure small vessel disease, Ann. Clin. Transl. Neurol. (2019). https://doi.org/10.1002/acn3.50891.

[118] K.F. de Laat, A.G.W. van Norden, L.J.B. van Oudheusden, I.W.M. van Uden, D.G. Norris, M.P. Zwiers, F.E. de Leeuw, Diffusion tensor imaging and mild parkinsonian signs in cerebral small vessel disease, Neurobiol. Aging. (2012). https://doi.org/10.1016/j.neurobiolaging.2011.09.001.

[119] H.M. Van Der Holst, I.W.M. Van Uden, A.M. Tuladhar, K.F. De Laat, A.G.W. Van Norden, D.G. Norris, E.J. Van Dijk, R.A.J. Esselink, B. Platel, F.E. De Leeuw, Cerebral small vessel disease and incident parkinsonism, Neurology. (2015). https://doi.org/10.1212/WNL.0000000000002082.

[120] M. Cai, M.A. Jacob, D.G. Norris, M. Duering, F.E. de Leeuw, A.M. Tuladhar, Cognition mediates the relation between structural network efficiency and gait in small vessel disease, NeuroImage Clin. 30 (2021). https://doi.org/10.1016/j.nicl.2021.102667.

[121] Y. Hannawi, L.R. Yanek, B.G. Kral, L.C. Becker, D. Vaidya, N.J. Haughey, D.M. Becker, P.A. Nyquist, White Matter Injury Is Associated with Reduced Manual Dexterity and Elevated Serum Ceramides in Subjects with Cerebral Small Vessel Disease, Cerebrovasc. Dis. 50 (2021). https://doi.org/10.1159/000511937.

[122] M. Cai, M.A. Jacob, D.G. Norris, F.-E. de Leeuw, A.M. Tuladhar, Longitudinal Relation Between Structural Network Efficiency, Cognition, and Gait in Cerebral Small Vessel Disease., J. Gerontol. A. Biol. Sci. Med. Sci. 77 (2022) 554–560. https://doi.org/10.1093/gerona/glab247.

[123] H.S. Markus, M. Egle, I.D. Croall, H. Sari, U. Khan, A. Hassan, K. Harkness, A. MacKinnon, J.T. O'Brien, R.G. Morris, T.R. Barrick, A.M. Blamire, D.J. Tozer, G.A. Ford, PRESERVE: Randomized Trial of Intensive Versus Standard Blood Pressure Control in Small Vessel Disease., Stroke. 52 (2021) 2484–2493. https://doi.org/10.1161/STROKEAHA.120.032054.

[124] R.L. Brookes, V. Herbert, A.J. Lawrence, R.G. Morris, H.S. Markus, Depression in small-vessel disease relates to white matter ultrastructural damage, not disability, Neurology. (2014). https://doi.org/10.1212/WNL.0000000000000882.

[125] I.W.M. Van Uden, A.M. Tuladhar, K.F. De Laat, A.G.W. Van Norden, D.G. Norris, E.J. Van Dijk, I. Tendolkar, F.E. De Leeuw, White matter integrity and depressive symptoms in cerebral small vessel disease: The RUN DMC study, Am. J. Geriatr. Psychiatry. (2015). https://doi.org/10.1016/j.jagp.2014.07.002.

[126] X. Xie, Y. Shi, J. Zhang, Structural network connectivity impairment and depressive symptoms in cerebral small vessel disease, J. Affect. Disord. (2017). https://doi.org/10.1016/j.jad.2017.05.039.

[127] Y. Lu, Y. Li, Q. Feng, R. Shen, H. Zhu, H. Zhou, Z. Zhao, Rich-Club Analysis of the Structural Brain Network in Cases with Cerebral Small Vessel Disease and Depression Symptoms., Cerebrovasc. Dis. 51 (2022) 92–101. https://doi.org/10.1159/000517243.

[128] M. Pasi, A. Poggesi, E. Salvadori, S. Diciotti, L. Ciolli, A. Del Bene, S. Marini, S. Nannucci, F. Pescini, R. Valenti, A. Ginestroni, N. Toschi, M. Mascalchi, D. Inzitari, L. Pantoni, White matter microstructural damage and depressive symptoms in patients with mild cognitive impairment and cerebral small vessel disease: The VMCI-Tuscany Study, Int. J. Geriatr. Psychiatry. (2016). https://doi.org/10.1002/gps.4368.

[129] Y. Kim, H. Jang, S.J. Kim, S.H. Cho, S.E. Kim, S.T. Kim, H.J. Kim, S.H. Moon, M. Ewers, K. Im, H. Kwon, D.L. Na, S.W. Seo, Vascular Effects on Depressive Symptoms in Cognitive Impairment, J. Alzheimers. Dis. (2018). https://doi.org/10.3233/JAD-180394.

[130] M.J. Hollocks, A.J. Lawrence, R.L. Brookes, T.R. Barrick, R.G. Morris, M. Husain, H.S. Markus, Differential relationships between apathy and depression with white matter microstructural changes and functional outcomes, Brain. (2015). https://doi.org/10.1093/brain/awv304.

[131] J. Tay, A.M. Tuladhar, M.J. Hollocks, R.L. Brookes, D.J. Tozer, T.R. Barrick, M. Husain, F.E. De Leeuw, H.S. Markus, Apathy is associated with large-scale white matter network disruption in small vessel disease, Neurology. (2019). https://doi.org/10.1212/WNL.0000000000007095.

[132] D.M. Lisiecka-Ford., D.J. Tozer, R.G. Morris, A.J. Lawrence, T.R. Barrick, H.S. Markus, Involvement of the reward network is associated with apathy in cerebral small vessel disease, J. Affect. Disord. (2018). https://doi.org/10.1016/j.jad.2018.02.006.

[133] L. Raimondo, Ícaro A.F. Oliveira, J. Heij, N. Priovoulos, P. Kundu, R.F. Leoni, W. van der Zwaag, Advances in resting state fMRI acquisitions for functional connectomics, Neuroimage. 243 (2021) 118503. https://doi.org/10.1016/J.NEUROIMAGE.2021.118503.

[134] P. Linortner, F. Fazekas, R. Schmidt, S. Ropele, B. Pendl, K. Petrovic, M. Loitfelder, C. Neuper, C.

Enzinger, White matter hyperintensities alter functional organization of the motor system, Neurobiol. Aging. (2012). https://doi.org/10.1016/j.neurobiolaging.2010.06.005.

[135] X. Zhou, C. Zhang, L. Li, Y. Zhang, W. Zhang, W. Yin, X. Yu, X. Zhu, Y. Qian, Z. Sun, Altered Brain Function in Cerebral Small Vessel Disease Patients With Gait Disorders: A Resting-State Functional MRI Study, Front. Aging Neurosci. (2020). https://doi.org/10.3389/fnagi.2020.00234.

[136] J.M. Papma, T. Den Heijer, I. De Koning, F.U. Mattace-Raso, A. Van Der Lugt, F. Van Der Lijn, J.C. Van Swieten, P.J. Koudstaal, M. Smits, N.D. Prins, The influence of cerebral small vessel disease on default mode network deactivation in mild cognitive impairment, NeuroImage Clin. (2013). https://doi.org/10.1016/j.nicl.2012.11.005.

[137] L. Pantoni, A. Poggesi, S. Diciotti, R. Valenti, S. Orsolini, E. Della Rocca, D. Inzitari, M. Mascalchi, E. Salvadori, Effect of Attention Training in Mild Cognitive Impairment Patients with Subcortical Vascular Changes: The RehAtt Study, J. Alzheimer's Dis. (2017). https://doi.org/10.3233/JAD-170428.

[138] S. Atwi, A.W.S. Metcalfe, A.D. Robertson, J. Rezmovitz, N.D. Anderson, B.J. MacIntosh, Attention-related brain activation is altered in older adults with white matter hyperintensities using multi-echo fMRI, Front. Neurosci. (2018). https://doi.org/10.3389/fnins.2018.00748.

[139] A. Schaefer, E.M. Quinque, J.A. Kipping, K. Arélin, E. Roggenhofer, S. Frisch, A. Villringer, K. Mueller, M.L. Schroeter, Early small vessel disease affects frontoparietal and cerebellar hubs in close correlation with clinical symptoms -a resting-state fMRI study, J. Cereb. Blood Flow Metab. 34 (2014) 1091–1095. https://doi.org/10.1038/jcbfm.2014.70.

[140] S. Cao, J. Nie, J. Zhang, C. Chen, X. Wang, Y. Liu, Y. Mo, B. Du, Y. Hu, Y. Tian, Q. Wei, K. Wang, The Cerebellum Is Related to Cognitive Dysfunction in White Matter Hyperintensities., Front. Aging Neurosci. 13 (2021) 670463. https://doi.org/10.3389/fnagi.2021.670463.

[141] S. Diciotti, S. Orsolini, E. Salvadori, A. Giorgio, N. Toschi, S. Ciulli, A. Ginestroni, A. Poggesi, N. De Stefano, L. Pantoni, D. Inzitari, M. Mascalchi, Resting state fMRI regional homogeneity correlates with cognition measures in subcortical vascular cognitive impairment, J. Neurol. Sci. (2017). https://doi.org/10.1016/j.jns.2016.12.003.

[142] R. Liu, W. Wu, Q. Ye, Y. Gu, J. Zou, X. Chen, Y. Jiang, F. Bai, Y. Xu, C. Wang, Distinctive and pervasive alterations of functional brain networks in cerebral small vessel disease with and without cognitive impairment, Dement. Geriatr. Cogn. Disord. (2019). https://doi.org/10.1159/000496455.

[143] A. Acharya, X. Liang, W. Tian, C. Jiang, Y. Han, L. Yi, White Matter Hyperintensities Relate to Basal Ganglia Functional Connectivity and Memory Performance in aMCI and SVMCI, Front. Neurosci. (2019). https://doi.org/10.3389/fnins.2019.01204.

[144] H.T. Karim, A. Rosso, H.J. Aizenstein, N.I. Bohnen, S. Studenski, C. Rosano, Resting state connectivity within the basal ganglia and gait speed in older adults with cerebral small vessel disease and locomotor risk factors, NeuroImage Clin. (2020). https://doi.org/10.1016/j.nicl.2020.102401.

[145] R. Liu, H. Chen, R. Qin, Y. Gu, X. Chen, J. Zou, Y.C. Jiang, W. Li, F. Bai, B. Zhang, X. Wang, Y. Xu, The altered reconfiguration pattern of brain modular architecture regulates cognitive function in cerebral small vessel disease, Front. Neurol. (2019). https://doi.org/10.3389/fneur.2019.00324.

[146] B. Gesierich, A.M. Tuladhar, A. ter Telgte, K. Wiegertjes, M.J. Konieczny, S. Finsterwalder, M. Hübner, L. Pirpamer, M. Koini, A. Abdulkadir, N. Franzmeier, D.G. Norris, J.P. Marques, P. zu Eulenburg, M. Ewers, R. Schmidt, F.E. de Leeuw, M. Duering, Alterations and test–retest reliability of functional connectivity network measures in cerebral small vessel disease, Hum. Brain Mapp. (2020). https://doi.org/10.1002/hbm.24967.

[147] Y. Qin, W. Zhu, C. Liu, Z. Wang, W. Zhu, Functional brain connectome and its relation to mild cognitive impairment in cerebral small vessel disease patients with thalamus lacunes: A cross-sectional study, Med. (United States). (2019). https://doi.org/10.1097/MD.0000000000017127.

[148] M. Feng, H. Wen, H. Xin, N. Zhang, C. Liang, L. Guo, Altered Spontaneous Brain Activity Related to Neurologic Dysfunction in Patients With Cerebral Small Vessel Disease., Front. Aging Neurosci. 13 (2021) 731585. https://doi.org/10.3389/fnagi.2021.731585.

[149] B. Du, S. Cao, Y. Liu, Q. Wei, J. Zhang, C. Chen, X. Wang, Y. Mo, J. Nie, B. Qiu, P. Hu, K. Wang, Abnormal Degree Centrality in White Matter Hyperintensities: A Resting-State Functional Magnetic Resonance Imaging Study., Front. Psychiatry. 12 (2021) 684553. https://doi.org/10.3389/fpsyt.2021.684553.

[150] H. Li, X. Jia, Y. Li, X. Jia, Q. Yang, Aberrant Amplitude of Low-Frequency Fluctuation and Degree Centrality within the Default Mode Network in Patients with Vascular Mild Cognitive Impairment., Brain Sci. 11 (2021). https://doi.org/10.3390/brainsci11111534.

[151] M. Hwang, D.L. Tudorascu, K. Nunley, H. Karim, H.J. Aizenstein, T.J. Orchard, C. Rosano, Brain Activation and Psychomotor Speed in Middle-Aged Patients with Type 1 Diabetes: Relationships with Hyperglycemia and Brain Small Vessel Disease, J. Diabetes Res. (2016). https://doi.org/10.1155/2016/9571464.

[152] G. Gavazzi, S. Orsolini, E. Salvadori, A. Bianchi, A. Rossi, I. Donnini, V. Rinnoci, F. Pescini, S. Diciotti, M.P. Viggiano, M. Mascalchi, L. Pantoni, Functional magnetic resonance imaging of inhibitory control reveals decreased blood oxygen level dependent effect in cerebral autosomal dominant arteriopathy with subcortical infarcts and leukoencephalopathy, Stroke. (2019). https://doi.org/10.1161/STROKEAHA.118.022923.

[153] H. Lyu, J. Wang, J. Xu, H. Zheng, X. Yang, S. Lin, J. Chen, L. Zhou, Y. Hu, Z. Guo, Structural and Functional Disruptions in Subcortical Vascular Mild Cognitive Impairment With and Without Depressive Symptoms, Front. Aging Neurosci. (2019). https://doi.org/10.3389/fnagi.2019.00241.

[154] N. Franzmeier, A. Rubinski, J. Neitzel, Y. Kim, A. Damm, D.L. Na, H.J. Kim, C.H. Lyoo, H. Cho, S. Finsterwalder, M. Duering, S.W. Seo, M. Ewers, Functional connectivity associated with tau levels in ageing, Alzheimer's, and small vessel disease, Brain. (2019). https://doi.org/10.1093/brain/awz026.

[155] K. Li, Z. Fu, X. Luo, Q. Zeng, P. Huang, M. Zhang, C.D. Vince, The Influence of Cerebral Small Vessel Disease on Static and Dynamic Functional Network Connectivity in Subjects Along Alzheimer's Disease Continuum., Brain Connect. 11 (2021) 189–200. https://doi.org/10.1089/brain.2020.0819.

[156] I. Makedonov, S.E. Black, B.J. MacIntosh, BOLD fMRI in the White Matter as a Marker of Aging and Small Vessel Disease, PLoS One. (2013). https://doi.org/10.1371/journal.pone.0067652.

[157] S. Atwi, A.D. Robertson, A.E. Theyers, J. Ramirez, R.H. Swartz, S. Marzolini, B.J. MacIntosh, Cardiac-Related Pulsatility in the Insula Is Directly Associated With Middle Cerebral Artery Pulsatility Index, J. Magn. Reson. Imaging. (2019). https://doi.org/10.1002/jmri.26950.

[158] A. Nitkunan, D.J.O. McIntyre, T.R. Barrick, M. O'Sullivan, Y. Shen, C.A. Clark, F.A. Howe, H.S. Markus, Correlations between MRS and DTI in cerebral small vessel disease, NMR Biomed. (2006). https://doi.org/10.1002/nbm.1052.

[159] A. Nitkunan, R.A. Charlton, D.J.O. McIntyre, T.R. Barrick, F.A. Howe, H.S. Markus, Diffusion tensor imaging and MR spectroscopy in hypertension and presumed cerebral small vessel disease, Magn. Reson. Med. (2008). https://doi.org/10.1002/mrm.21461.

[160] D. Nyenhuis, G.T. Stebbins, Nonconventional MR techniques for imaging cerebral small vessel disease, in: Cereb. Small Vessel Dis., 2011. https://doi.org/10.1017/CBO9781139382694.015.

[161] B. Patel, H.S. Markus, Magnetic resonance imaging in cerebral small vessel disease and its use as a surrogate disease marker, Int. J. Stroke. (2011). https://doi.org/10.1111/j.1747-4949.2010.00552.x.

[162] A.A. Gouw, A. Seewann, W.M. Van Der Flier, F. Barkhof, A.M. Rozemuller, P. Scheltens, J.J.G. Geurts, Heterogeneity of small vessel disease: A systematic review of MRI and histopathology correlations, J. Neurol. Neurosurg. Psychiatry. (2011). https://doi.org/10.1136/jnnp.2009.204685.

[163] G.W. Blair, M.J. Thrippleton, Y. Shi, I. Hamilton, M. Stringer, F. Chappell, D.A. Dickie, P. Andrews, I. Marshall, F.N. Doubal, J.M. Wardlaw, Intracranial hemodynamic relationships in patients with cerebral small vessel disease, Neurology. 94 (2020) e2258–e2269. https://doi.org/10.1212/WNL.0000000000009483.

[164] E.E. Smith, G.J. Biessels, F. De Guio, F.E. de Leeuw, S. Duchesne, M. Düring, R. Frayne, M.A. Ikram, E. Jouvent, B.J. MacIntosh, M.J. Thrippleton, M.W. Vernooij, H. Adams, W.H. Backes, L. Ballerini, S.E. Black, C. Chen, R. Corriveau, C. DeCarli, S.M. Greenberg, M.E. Gurol, M. Ingrisch, D. Job, B.Y.K. Lam, L.J. Launer, J. Linn, C.R. McCreary, V.C.T. Mok, L. Pantoni, G.B. Pike, J. Ramirez, Y.D. Reijmer, J.R. Romero, S. Ropele, N.S. Rost, P.S. Sachdev, C.J.M. Scott, S. Seshadri, M. Sharma, S. Sourbron, R.M.E. Steketee, R.H. Swartz, R. van Oostenbrugge, M. van Osch, S. van Rooden, A. Viswanathan, D. Werring, M. Dichgans, J.M. Wardlaw, Harmonizing brain magnetic resonance imaging methods for vascular contributions to neurodegeneration, Alzheimer's Dement. Diagnosis, Assess. Dis. Monit. 11 (2019) 191–204. https://doi.org/10.1016/j.dadm.2019.01.002.

[165] H. Lu, A.H. Kashani, K. Arfanakis, A. Caprihan, C. DeCarli, B.T. Gold, Y. Li, P. Maillard, C.L. Satizabal, L. Stables, D.J.J. Wang, R.A. Corriveau, H. Singh, E.E. Smith, B. Fischl, A. van der Kouwe, K. Schwab, K.G. Helmer, S.M. Greenberg, MarkVCID cerebral small vessel consortium: II. Neuroimaging protocols, Alzheimers. Dement. 17 (2021) 716–725. https://doi.org/10.1002/ALZ.12216.

[166] D.C. Alsop, J.A. Detre, X. Golay, M. Günther, J. Hendrikse, L. Hernandez-Garcia, H. Lu, B.J. Macintosh, L.M. Parkes, M. Smits, M.J.P. Van Osch, D.J.J. Wang, E.C. Wong, G. Zaharchuk, Recommended implementation of arterial spin-labeled Perfusion mri for clinical applications: A consensus of the ISMRM Perfusion Study group and the European consortium for ASL in dementia, Magn. Reson. Med. 73 (2015) 102–116. https://doi.org/10.1002/mrm.25197.

Table 1: Summary of the reviewed MRI methods in cerebral small vessel disease, its applications, the main contributions, limitations, and open questions.

MRI technique	Characterization	Differential contribution to cSVD*	Main Applications	Limitations/Open questions
DTI	It measures water molecules' diffusion within WM tracts using magnetic diffusion gradients applied in at least six different directions. A diffusion tensor is then acquired, from which two quantitative measures, fractional anisotropy (FA) and mean diffusivity (MD), are obtained.	DTI-derived markers have been correlated with cardiovascular risk factors, with several other MRI markers, with clinical features, including cognitive impairment. Additionally, longitudinal findings support the hypothesis that conventional MRI markers of cSVD (WMH, lacunes, and microbleeds) cause cognitive decline and dementia via disruption of structural brain networks.	Study the pathophysiology of cSVD using two-compartment models. Investigate effects of risk-factors. Evaluate the relationship between MRI markers of cSVD and cognitive decline. Associations with outcomes	DTI related-parameters changes mediating the effects of traditional cSVD markers in cognition. The pathophysiology of cSVD is still incompletely understood. Newer acquisitions and models have shown better correlations with WM damage and cognition when compared to the traditional DTI approach.
fMRI	fMRI is based on the blood oxygen level-dependent (BOLD) effect. It is an indirect measurement of brain activity.	Brain functional activity and connectivity were found in cSVD patients. It provides insights into functional network disruption related to cSVD and cognitive decline, dementia, and mortality.	Investigate the functional changes and recovery mechanisms related to cSVD	What is the relationship with focal lesions? Are the changes due to impaired flow or impaired metabolism?

*In comparison to conventional MRI markers. DTI: Diffusion Tensor Imaging. fMRI: functional Magnetic Resonance Imaging.

Figures

Figure 1: Flow diagram of the selection process.
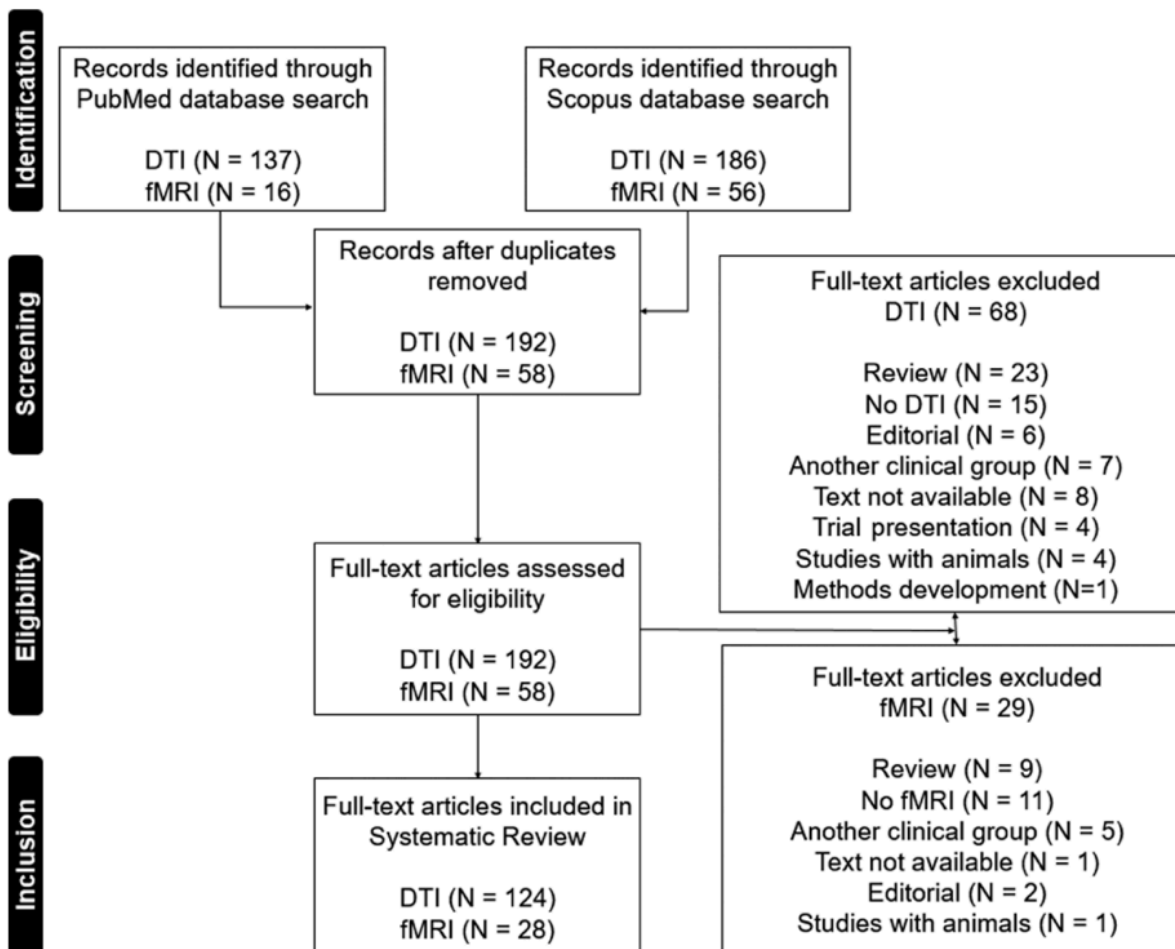
Figure 2: Three DTI methods applied to cSVD. (A) TBSS skeleton projections on the WMH map are superimposed on the mean FA image [33]. (B) Tractography representation of the cingula tract whose integrity loss explained memory performance [100]. (C) Group structural brain network of patients with first TIA or ischemic stroke. In red, regions with significantly lower nodal efficiency due to the presence of cSVD. The node size and edge width are weighted by nodal efficiency and the number of connections [62].
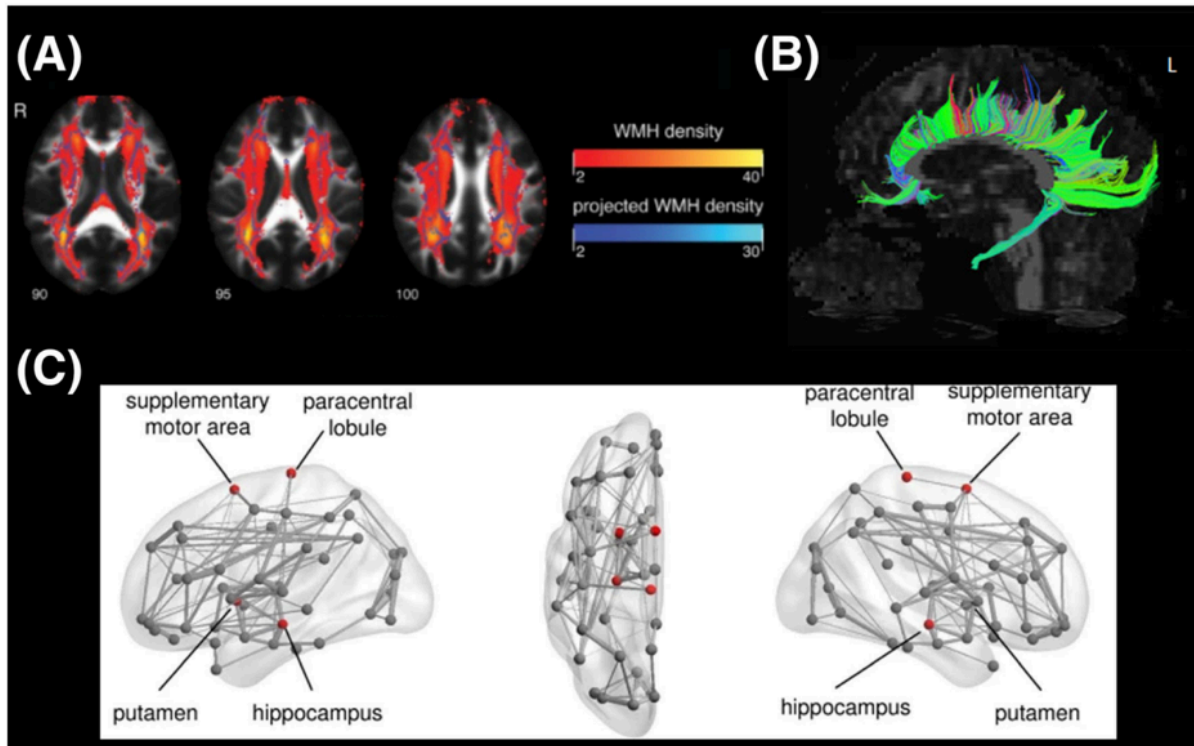
Figure 3: Three fMRI studies applied to cSVD. (A) Group activation for different levels of working memory load (0-back versus rest; 1-back versus rest, 2-back versus rest) (p-FWE < 0.05) [136]. (B) Significant associations between regional homogeneity (ReHo) and cognitive performance ($p < 0.05$, corrected for multiple comparisons). On the left, a negative association between ReHo and MoCA score in the left posterior cerebellum. On the right, positive association between ReHo and Stroop score in the bilateral middle cingulate cortex [141]. (C) Significantly decreased brain functional connectome nodal centralities in cSVD patients with thalamus lacunes compared to healthy controls ($p < 0.05$, network-based statistics). Different-color nodes represent different brain regions. DCG.L: left middle cingulum, DCG.R: right middle cingulum, OLF.R: right olfactory, PAL.L: left pallidum, REC.L: left rectus, REC.R: right rectus [147].
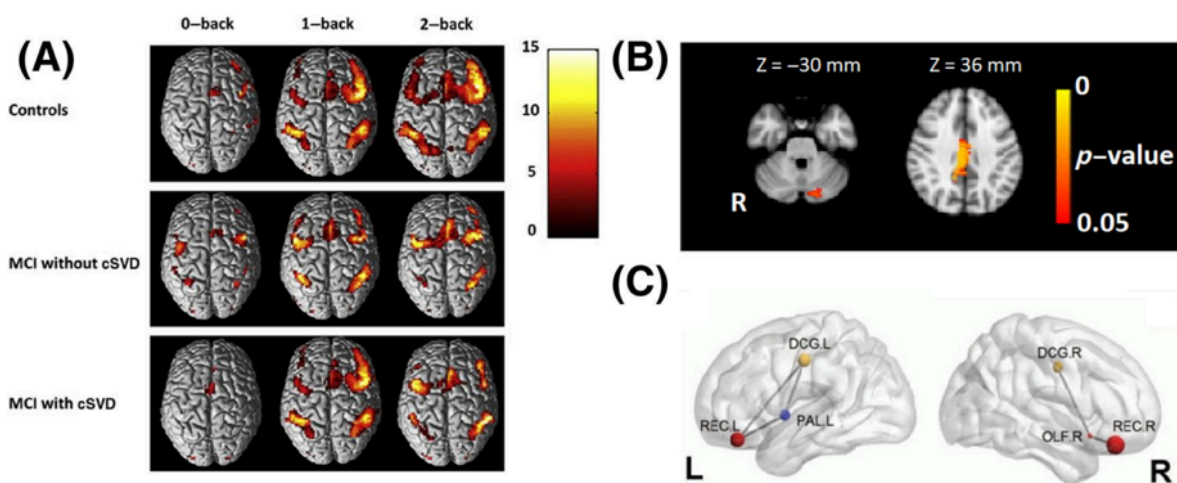
Figure 4: Application of contrast agent-free MRI methods in cerebral small vessel disease (cSVD). Left box: description of research topics in cSVD. From top to bottom: risk and protective factors that may, respectively, contribute to the onset of the disease or to protect against it, followed by possible pathophysiological mechanisms not yet fully elucidated, including small vessel, neurodegenerative and mixed pathology, which translate into damage to the brain tissue, the most famous being WMH. The damage is said to have "distant" effects, impacting brain networks, making the disease a disconnect syndrome, which would help to understand the heterogeneity in terms of cognitive deficits presented by patients. Right box: description of contrast agent-free MRI techniques applied for each research topic mentioned in the left box. Each colored octagon represents an MRI technique previously applied and revised in the present paper, and the items represent which variables the technique may assess regarding the disease. ASL: arterial spin labeling. BBB: blood-brain barrier. BOLD: blood oxygen level-dependent. CBF: cerebral blood flow. CVR: cerebrovascular reactivity. DTI: diffusion tensor imaging. fMRI: functional magnetic resonance imaging. IVIM: intravoxel incoherent motion. MRI: magnetic resonance imaging. WMH: white matter hyperintensity. Figure created in the Mind the Graph platform (www.mindthegraph.com).
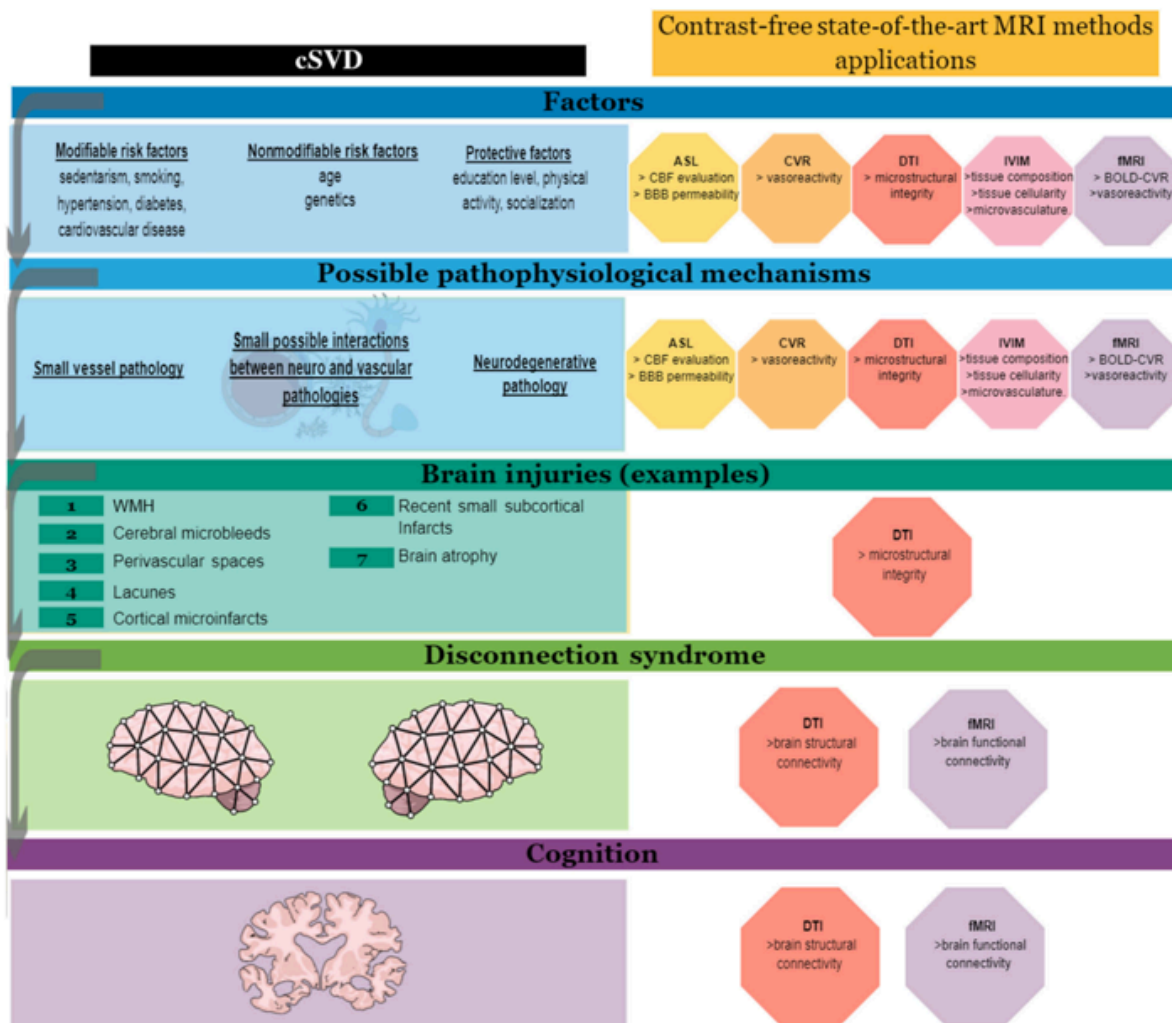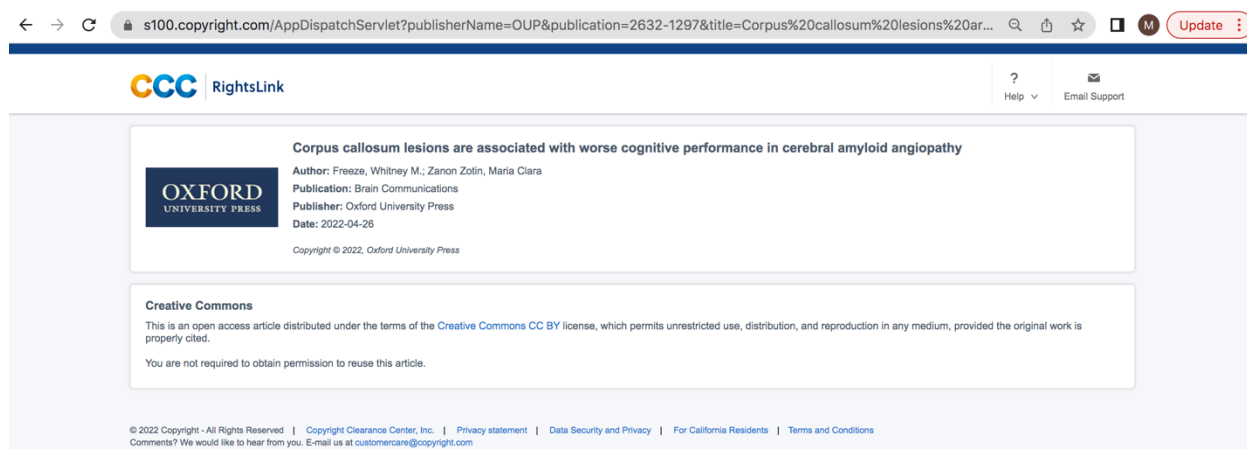
Appendix 4.7. "Corpus callosum lesions are associated with worse cognitive performance in cerebral amyloid angiopathy"

Reference: Freeze WM, Zotin MCZ, Scherlek AA, Perosa V, Auger CA, Warren AD, et al. Corpus callosum lesions are associated with worse cognitive performance in cerebral amyloid angiopathy. Brain Commun. 2022;4(3):fcac105-.

Copyright/Source: 2022, Oxford University Press /Brain Communications®

Article reuse license

Corpus callosum lesions are associated with worse cognitive performance in cerebral amyloid angiopathy

Whitney M. Freeze[1,2]; Maria Clara Zanon Zotin[3,4]; Ashley A. Scherlek[5]; Valentina Perosa[3]; Corinne A. Auger[5]; Andrew D. Warren[3]; Louise van der Weerd[1]; Dorothee Schoemaker[6]; Mitchell J. Horn[3]; M. Edip Gurol[3]; Elif Gokcal[3]; Brian J. Bacskai[5]; Anand Viswanathan[3]; Steven M. Greenberg[3]; Yael D. Reijmer[7]; and Susanne J. van Veluw[1,3,5]

Abstract

Background and Objective: The impact of vascular lesions on cognition is location-dependent. Here, we assessed the contribution of small vessel disease lesions in the corpus callosum (CC) to vascular cognitive impairment in cerebral amyloid angiopathy, as a model for cerebral small vessel disease.

Methods: 65 patients with probable cerebral amyloid angiopathy underwent 3T MRI, including a diffusion tensor imaging scan, and neuropsychological testing. Microstructural white matter integrity was quantified by fractional anisotropy and mean diffusivity. Z-scores on individual neuropsychological tests were averaged into five cognitive domains: information processing speed, executive functioning, memory, language, and visuospatial ability. Corpus callosum lesions were defined as hemorrhagic (microbleeds or larger bleeds) or ischemic (microinfarcts, larger infarcts, diffuse fluid-attenuated inversion recovery hyperintensities). Associations between corpus callosum lesion presence, microstructural white matter integrity, and cognitive performance were examined with multiple regression models. The prevalence of corpus callosum lesions was confirmed in an independent cohort of memory clinic patients with and without cerebral amyloid angiopathy (n=82). In parallel, we assessed corpus callosum lesions on ex vivo MRI in cerebral amyloid angiopathy patients (n=19) and controls (n=5) and determined associated tissue abnormalities with histopathology.

Results: A total number of 21 corpus callosum lesions was found in 19/65 (29%) cerebral amyloid angiopathy patients. Corpus callosum lesion presence was associated with reduced microstructural white matter integrity within the corpus callosum and in the whole brain white matter. Patients with corpus callosum lesions performed significantly worse on all cognitive domains except language, compared to those without corpus callosum lesions after correcting for age, sex, education, and time between MRI and neuropsychological assessment. This association was independent of presence of intracerebral hemorrhage, whole brain fractional anisotropy and mean diffusivity, and white matter hyperintensity volume and brain volume for

the domains of information processing speed and executive functioning. In the memory clinic patient cohort, corpus callosum lesions were present in 14/54 (26%) patients with probable and 2/8 (25%) patients with possible cerebral amyloid angiopathy, and in 3/20 (15%) patients without cerebral amyloid angiopathy. In the ex vivo cohort, corpus callosum lesions were present in 10/19 (53%) patients and 2/5 (40%) controls. On histopathology, ischemic corpus callosum lesions were associated with tissue loss and demyelination, which extended beyond the lesion core.

Discussion: Together, these data suggest that corpus callosum lesions are a frequent finding in cerebral amyloid angiopathy, and that they independently contribute to cognitive impairment through strategic microstructural disruption of white matter tracts.

Author affiliations:

[1] Department of Radiology, Leiden University Medical Center, Leiden, the Netherlands

[2] Department of Neuropsychology and Psychiatry, Maastricht University, Maastricht, the Netherlands

[3] Department of Neurology, J. Philip Kistler Stroke Research Center, MGH, Boston, MA, USA

[4] Department of Medical Imaging, Hematology and Clinical Oncology, Ribeirão Preto Medical School,USP, SP, Brazil.

[5] MassGeneral Institute for Neurodegenerative Disease, MGH, Charlestown, MA, USA

[6] Department of Psychiatry, MGH, Boston, MA, USA

[7] Department of Neurology, Brain Center Rudolf Magnus, University Medical Center Utrecht, Utrecht, the Netherlands

Introduction

Cerebral small vessel disease (cSVD) is a major contributor to vascular cognitive impairment. The impact of vascular lesions on cognition strongly depends on the lesion location, with lesions located in strategic brain regions being more relevant in explaining cognitive impairment than global lesion volume [1,2].

Cerebral amyloid angiopathy (CAA) is a common type of cSVD and is pathologically characterized by the deposition of amyloid-β within the small cortical and leptomeningeal arteries in the brain [3]. On magnetic resonance imaging (MRI), CAA manifests as both hemorrhagic (i.e. lobar cerebral microbleeds, cortical superficial siderosis) and ischemic (i.e. cerebral microinfarcts, white matter hyperintensities (WMH), lobar lacunar infarcts) tissue injury [4,5]. In addition to these overt MRI lesions, CAA has been associated with white matter atrophy [6] and microstructural tissue injury in the white matter, which can be detected with diffusion tensor imaging (DTI)[7]. These microstructural abnormalities are characterized by changes in fractional anisotropy (FA) and mean diffusivity (MD) DTI measures, which quantify the directional dependency and degree of water diffusion within each voxel. A post-mortem MRI study in CAA patients has demonstrated that DTI changes correspond to tissue rarefaction, in particular axonal loss and myelin loss [8]. Although the exact mechanisms underlying CAA-related DTI changes have not been specified, multiple small white matter lesions have been suggested to cumulatively contribute to this type of covert tissue injury [5,9], possibly by inducing widespread secondary damage beyond the lesion core [10-13]. Because white matter diffusion abnormalities are independently associated with cognitive functioning in CAA [7], in particular information processing speed and executive functioning, small strategic white matter lesions may be of high clinical significance.

Previous work in CAA suggests that the white matter microstructure is not homogeneously disrupted throughout the brain, but that temporal and posterior brain regions are affected at a greater extent and/or earlier than frontal regions [14,15]. Because of the predilection of CAA pathology for posterior brain regions, previous studies have dedicated attention to microstructural changes within posterior white matter tracts [7,15]. In contrast, the strategically located corpus callosum (CC) has received relatively little attention in CAA, despite its importance as the main fiber tract that connects both cerebral hemispheres. Overt lesions in the CC have been associated with neurological deficits in a number of neurologic diseases [16,17] and reductions in CC white matter integrity are associated with lower cognitive performance [18,19]. To the best of our knowledge, the occurrence of CC lesions in patients with CAA has not

been assessed before and it remains unknown whether they independently contribute to cognitive impairment. We addressed these outstanding questions in a cohort of patients with probable CAA, recruited through our stroke clinic. In addition, we assessed the prevalence of CC lesions in an independent cohort of memory clinic patients with and without probable CAA to check whether the prevalence of CC lesions is comparable in CAA patients recruited from a different source and in non-CAA patients with cognitive problems. Finally, we assessed ex vivo MRI scans of intact hemispheres in a third cohort of patients with pathologically-confirmed CAA and controls to determine the histopathological nature of CC lesions, to check for the presence of CAA in their immediate vicinity, and to explore the severity of peri-lesional damage. Studying the CC in CAA, as a model for cSVD in general, will clarify the contribution of CC lesions to vascular cognitive impairment.

Materials and methods

Participants stroke clinic cohort

Patients were included through an ongoing single-center longitudinal cohort study at Massachusetts General Hospital (MGH). Details on patient selection and inclusion have been described previously [15]. In short, nondemented patients with probable CAA defined by the modified Boston criteria [20, 21] were prospectively recruited through the stroke clinic. Participants with a diagnosis of neurological disease other than CAA or MRI contraindications were excluded from the study. We included all patients with available 3 tesla (T) magnetic resonance imaging (MRI) research scans and a diagnosis of probable CAA according to the modified Boston criteria based on clinical scans at enrollment [21]. Because the high-resolution research scans revealed additional deep cerebral microbleeds (CMBs) in a few patients, which were not detected on the clinical scans, we decided the following: Patients with >2 deep CMBs and/or deep intracerebral hemorrhage (ICH) on research scans (n=3) were excluded because it was unclear whether CAA was the predominant type of cSVD in these participants. We decided to keep participants with ≤2 deep CMBs on research scans who otherwise fulfilled the criteria of probable CAA (n=7) as CAA pathology in these patients appeared to be predominant and excluding these patients would lead to a loss of generalizability, and statistical power. It should be noted that these patients fulfilled the criteria for probable CAA based on the clinical scans. However, since a diagnosis of mixed-type cSVD would have been more appropriate based on the research scans, we decided to perform post-hoc sensitivity analyses by excluding these individuals from the analyses. We used cross-sectional data from the most recent study visit.

The study was approved by the MGH Institutional Review Board and informed consent was obtained from all patients or their surrogates.

In vivo MR imaging protocol

MR images were acquired on a 3T MR imaging system with a 32-channel head coil (Siemens, Magnetom Prisma-Fit). The protocol included a 3D T1-weighted multi-echo scan (repetition time (TR), 2510ms; echo time (TE), 1.69, 3.55, 5.41, 7.27 ms; voxel size, $1.0mm^3$ isotropic), a 3D T2-weighted Fluid-attenuated inversion recovery (FLAIR) scan (TR, 5000ms; TE, 356ms; inversion time, 1800ms; voxel size, $0.90mm^3$ isotropic) a susceptibility-weighted imaging scan (SWI; TR, 30ms; TE, 20ms; voxel size, $0.90x0.90x1.4mm^3$), a T2*-weighted gradient echo scan (GRE; TR, 500ms; voxel size, $2.0mm^3$ isotropic), and a diffusion-weighted scan (TR, 8000ms; TE, 82ms; voxel size, $2.0mm^3$ isotropic; 64 gradient directions with a b-value of 700 s/mm^2 and one b=0 s/mm^2 image).

Diffusion tensor imaging processing

Diffusion-weighted imaging scans were analyzed and processed in ExploreDTI (www.exploredti.com). Corrections for subject motion and eddy current induced geometric distortions were applied [22]. Affine transformation was used for registration of a normalized white matter atlas to each individual DTI scan [23]. The average fractional anisotropy (FA) and mean diffusivity (MD) of the CC (not excluding any lesions) and the rest of the white matter (excluding the CC and corticospinal tract because the brainstem was not included in the field of view for all participants) were computed for each participant[23]. In patients with unilateral ICH (n=31), we excluded the diffusion metrics in the affected hemisphere to account for the possible effects of ICH on the microstructural white matter integrity.

Neuroimaging markers

Conventional CAA-related imaging markers were scored by two experienced raters (M.C.Z.Z. and E.G.) who were blinded to clinical and neuropsychological data. Presence or absence of ICH and number of CMBs (excluding CMBs close to ICH), presence or absence of cortical superficial siderosis and the number of cerebral microinfarcts were scored based on established criteria [13, 24, 25].

WMH volume was calculated using an automated method similar to the one previously described [26, 27]. In short, T1-weighted images were volumetrically segmented with FreeSurfer (http://surfer.nmr.mgh.harvard.edu/). Subsequently, each patient's FLAIR image was skull-

stripped and registered to the reconstructed T1-weighted images. The registered FLAIR was then masked and binarized using the tissue segmentation maps to exclude all non-white matter contributions. Abnormal white matter was identified through a threshold of voxel intensity of mean white matter + 1.3 standard deviation (SD), which was the optimal threshold for this dataset. Only clusters of a minimum of 30 contiguous voxels exhibiting hyperintensity beyond the threshold were included in the final calculation. In patients with unilateral ICH (n=31), we excluded the WMH volume in the affected hemisphere, and multiplied the WMH volume in the unaffected hemisphere by two to account for the possible effects of ICH on WMH volume. Normalized WMH was expressed as the percentage of estimated intracranial volume (ICV) from the FreeSurfer parcellation. To calculate normalized brain volume, the BrainSegNotVent variable from the FreeSurfer parcellation was used, and expressed as a percentage of ICV.

CC lesions were scored by two experienced raters (W.M.F. and S.J.v.V.), who were blinded to clinical and neuropsychological data, on T1, FLAIR, and blood-sensitive sequences (SWI and/or GRE). CC lesions were classified as ischemic or hemorrhagic. Presumed ischemic CC lesions included microinfarcts (focal demarcated lesions typically <5mm in size)[13], larger infarcts (including lacunar infarcts characterized by cavitation with a hyperintense rim on FLAIR images) [25], and diffuse FLAIR hyperintensities, which typically had a bilateral symmetrical shape in the CC. Hemorrhagic CC lesions included CMBs [25] and ICH extension into the CC. The location of each lesion was noted (genu, body, and/or splenium). Inter-rater reliability for the presence of CC lesions was substantial (κ (95% confidence interval (CI)) = 0.76 (0.58-0.94)). Few discrepancies were resolved during a consensus meeting.

Clinical evaluation

Demographic variables and medical history were recorded. A brief cognitive screening test (Mini-Mental State Examination) and standardized neuropsychological test battery were administered to assess cognitive performance. Composite scores were computed for the following cognitive domains based on neuropsychological theory[28]: executive functioning (Controlled Oral Word Association test – FAS; Trail Making Test B; Digit Span Backward), processing speed and attention (Trail Making Test A; WAIS-III Digit-Symbol Coding; Digit Span Forward), memory (Hopkins Verbal Learning Test, delayed recall; Free and Cued Selective Reminding Test, free recall), language (Boston Naming Test (15 items); Semantic Fluency (animals)), and visuospatial processing (Benton Facial Recognition test (short form); Benton Judgment of Line Orientation (30 items)). Z-scores for each test were calculated based

on the mean and SD of the whole study sample and averaged across tests to obtain a single average z-score per cognitive domain.

Participants memory clinic cohort

The presence of CC lesions was assessed in an independent cohort of memory clinic patients, which included both patients with and without probable CAA (supplementary Table 1). The study was designed to include around 50% of patients with CAA and 50% of patients with (mild) cognitive impairment without CAA. They underwent the same MR imaging protocol as described for the stroke clinic cohort above. Further details on this cohort have been described elsewhere [29]. The study was approved by the MGH Institutional Review Board and informed consent was obtained from all patients or their surrogates. For practical reasons, CC lesions in this cohort were assessed by a third experienced rater (M.C.Z.Z.) after establishing substantial inter-rater agreement on a subset of images from the stroke clinic cohort (κ (95% CI) = 0.74 (0.4-1)).

Ex vivo cohort

Intact human brain hemispheres from 19 patients with definite CAA [20] and 5 non-CAA control cases were included from an ongoing post-mortem MRI study at MGH. Details on the inclusion process, scanning procedures, and tissue block sampling have been described previously [8, 30]. In short, the hemispheres were fixed in 10% formalin for several weeks after autopsy. Prior to ex vivo 3T MRI the hemispheres were placed in a plastic bag filled with periodate-lysine-paraformaldehyde and vacuum sealed. The samples were scanned overnight on a 3T MR system (Siemens, Magnetom trioTim syngo) using a 32-channel head coil. The protocol included a T2-weighted turbo-spin echo (TSE) sequence (TR, 1800ms; TE, 61ms; voxel size, 500μm^3 isotropic) and a gradient-echo fast low angle shot (FLASH) sequence (TR, 20ms; voxel size, 500μm^3 isotropic). Presumed ischemic and hemorrhagic CC lesions were identified by the same raters (W.M.F. and S.J.v.V.) who were blinded to CAA severity or other histopathologic findings. Inter-rater reliability for the presence of CC lesions was substantial (κ (95% CI) = 0.75 (0.48-1)).

Histopathology

After scanning, the hemispheres were cut in 10-mm thick coronal brain slabs. Next, four small tissue blocks were systematically sampled from the frontal, temporal, parietal, and occipital

lobe and embedded in paraffin, after which 6μm-thick sections were cut on a microtome. Brightfield immunohistochemistry against amyloid-β (Aβ) (mouse, clone 6F/3D; Agilent Technologies, Santa Clara, CA; 1:200) was performed as previously described[8]. Cortical and leptomeningeal CAA severity was evaluated by two independent raters (S.J.v.V. and V.P.) on all Aβ-stained sections using a four-point scale (absent, 0; scant Aβ deposition, 1; some circumferential Aβ, 2; widespread circumferential Aβ, 3) [31], followed by a consensus rating to obtain a final score [32]. Scores from the four cortical areas were added to form a single cumulative CAA burden score (0-12) for the cortical and leptomeningeal vessels. Similarly, parenchymal Aβ plaque severity was assessed for each tissue block using a four-point scale (absent, 0; mild, 1; moderate, 2; severe, 3) by the same raters (S.J.v.V., V.P.), followed by a consensus rating to obtain a final score. Scores from the four cortical areas were added to form a single cumulative Aβ plaque burden score (0-12). On H&E-stained sections, arteriolosclerosis severity was assessed in the white matter for each tissue block using a four-point scale (grade 0 to 3) by two raters (V.P., C.A.A.)[33], followed by a consensus rating to obtain a final score. Scores from the four areas were added to form a single cumulative arteriolosclerosis burden score (0-12). In addition, MRI-guided selection of tissue blocks with representative CC lesions was performed on three patients and 6μm-thick serial sections were cut on a microtome using anatomical landmarks. Sections were stained with standard Luxol Fast Blue and/or Hematoxylin and Eosin to characterize the MRI-visible lesions microscopically. Also, a Perls Prussian blue stain was performed to assess the presence of iron in hemorrhagic lesions, and immunohistochemistry against Aβ was performed to assess whether CAA was present within the CC.

The post-mortem study was approved by the MGH Institutional Review board and informed consent was obtained from the next of kin prior to autopsy.

Statistical analyses

Group differences between patients with and without CC lesions were assessed with independent samples T-tests for continuous variables that followed a normal data distribution, and Mann-Whitney U tests for continuous variables that followed a non-normal data distribution. Pearson chi-square or Fisher's exact tests were applied for categorical variables. We set out to investigate the relationship between CC lesion presence and microstructural white matter integrity (FA and MD within the CC, and whole brain white matter FA and MD (excluding CC)) with multiple regression models, controlling for age, sex, and normalized

WMH volume. Normalized WMH volume was log transformed to correct for heteroscedasticity of the residuals. In addition, we assessed associations between CC lesion presence as independent variable and performance on each cognitive domain as dependent variable using multiple linear regression analyses, controlling for age, sex, years of education, and time between MRI acquisition and neuropsychological assessment. Subsequently, we tested whether the observed associations were independent of potential confounding variables, including presence of ICH, whole brain white matter FA and MD (excluding the CC), normalized WMH volume, and normalized brain volume, by first adding each of these variables separately and subsequently adding them all together in the regression model. We repeated the analyses after excluding patients with bilateral ICH (n=17), or patients with deep CMBs (n=7), to assess whether this changed the results. Finally, to estimate the relative importance of CC lesions for cognitive performance, we ran regression models including all markers of white matter integrity and brain volume (normalized WMH volume, normalized brain volume, whole brain white matter FA and MD (excluding CC), and CC lesion presence) as dependent variables, and applied a model decomposition method proposed by Lindeman et al. [34] as implemented in the R package 'relaimpo' (version 2.2-3) [35]. False discovery rate corrections were applied to control for multiple comparisons of five cognitive domains [36]. Inter-rater reliability for determining the presence of CC lesions was computed with Cohen's Kappa. Mann-Whitney U tests were used to assess differences in the prevalence of CC lesions in memory clinic patients with and without probable CAA in the independent cohort. A threshold of $\alpha<0.05$ was used to determine statistical significance and all p-values are two-tailed. Analyses were conducted using R statistical software (version 3.6.1.) [37].

Data availability

Data can be made available by the corresponding author upon reasonable request.

Results

Stroke clinic cohort

Data from 65 patients with probable CAA were included in this study (see Supplemental Figure 1 for a flow chart). One patient was excluded from the DTI analyses due to insufficient scan quality. A total number of 21 CC lesions was found in nineteen patients (29%); seventeen patients had one CC lesion and two patients had two CC lesions. Most CC lesions (17/21, 81%) were of ischemic nature, compared to only a few hemorrhagic lesions (4/21, 19%). The most frequent subtypes were diffuse FLAIR hyperintensities (10/21, 48%), followed by

microinfarcts (5/21, 24%), and ICH extension into the CC (3/21, 14%). The remaining 3 lesions were two larger infarcts and a microbleed. Lesions were most frequently located in the splenium (10/21, 48%), followed by the genu (7/21, 33%), and the body of the CC (2/21, 10%). Two patients had diffuse FLAIR hyperintensities that covered multiple CC regions. Representative examples of each type of CC lesion are shown in figure 1. Baseline characteristics of patients with and without CC lesions are described in table 1. No differences were found for age, sex, years of education, any of the neuroimaging markers, or presence of vascular risk factors between patients with and without CC lesions.

CC lesions and microstructural white matter integrity

After correcting for age, sex, and normalized WMH, CC lesion presence was significantly associated with decreased microstructural white matter integrity within the CC (standardized beta coefficient [95% CI] FA = -0.467 [-0.685, -0.248], p <0.001; MD = 0.343 [0.115, 0.572], p = 0.005) and in the whole brain white matter (excluding the CC) (standardized beta coefficient [95% CI] FA = -0.414 [-0.634, -0.194], p < 0.001); MD = 0.337 [0.111, 0.562], p = 0.005). The results did not change when patients with bilateral ICH or patients with deep CMBs were excluded from the analyses.

CC lesions and cognition

After correcting for age, sex, years of education, and time between MRI and neuropsychological assessment, CC lesion presence was significantly associated with decreased performance on the domains of executive functioning, processing speed, memory, and visuospatial functioning (table 2). After correction for additional confounding variables, including presence of ICH, microstructural white matter integrity (FA and MD in the whole brain white matter), and normalized WMH and brain volume, CC lesion presence was significantly associated with executive functioning and processing speed, but no longer with memory and visuospatial functioning. The results did not change when patients with bilateral ICH or deep CMBs were excluded from the analyses (table 2). In regression models including CC lesion presence, normalized WMH volume, normalized brain volume and whole brain FA and MD as independent variables, and executive functioning and processing speed as dependent variables, the total explained variance (R^2) was 27.6% and 40.2% (figure 2). CC lesion presence explained around 55% (executive functioning) and 33% (information processing speed) of this total explained variance in cognitive performance, so around 15% and 13% of the total explained variance (figure 2).

Memory clinic patient cohort

A total number of 82 memory clinic patients were included in this study, of which 54 fulfilled criteria for probable CAA, 8 possible CAA, and 20 were considered non-CAA control patients (this group included both patients with ($n=8$) and without ($n=12$) MRI markers of cSVD). CC lesions were present in 14/54 (26%) probable CAA patients, 2/8 (25%) possible CAA patients, and in 3/20 (15%) memory clinic patients without CAA. We did not find group differences for the presence of CC lesions (Fisher exact test p-value =.608).

Ex vivo cohort

Details of the ex vivo cohort are described in Table 3. CC lesions were present in 10/19 CAA patients (53%) and 2/5 non-CAA controls (40%, Fisher's Exact Test p-value = 1). Like the in vivo stroke clinic cohort, most CC lesions in the CAA patients (7/10, 70%) were of ischemic appearance, whereas fewer hemorrhagic lesions were observed (3/10, 30%). Similarly, the most common subtype was diffuse T2 hyperintensities (4/10, 40%), followed by microinfarcts (2/10, 20%) and extension of ICH into the CC (2/10, 20%). Only one lacunar infarct (1/10, 10%) and one microbleed (1/10, 10%) were observed. Lesions were located in the splenium (3/10, 30%), genu (3/10, 30%), or body of the CC (1/10, 10%). Three CAA patients had diffuse T2 hyperintensities or ICH extension into the CC that covered multiple CC regions. The CC lesions in the control cases were a diffuse T2 hyperintensity and a lacunar infarct, both located in the genu. There were no statistically significant differences in arteriolosclerosis score, Aβ plaque burden and cortical or leptomeningeal CAA scores between CAA patients with and without CC lesions (all $p > 0.05$). Examples of representative CC lesions on ex vivo MRI and corresponding histological findings are shown in figure 3-5. White matter rarefaction, axonal damage, and demyelination were observed beyond the core of ischemic lesions (T2 hyperintensity and lacunar infarct) (figure 3 and 5), but not the microbleed (figure 4). Although CAA was prominent in adjacent cortical areas, the walls of blood vessels within the CC were negative for Aβ immunoreactivity.

Discussion

In the current study, we reported the prevalence, characteristics, and neuroradiological and clinical correlates of CC lesions in patients with CAA. Our main findings can be summarized as follows: (1) CC lesions were prevalent in patients with probable (in vivo stroke clinic cohort, 29%; in vivo memory clinic patient cohort, 26%) and definite (ex vivo cohort, 53%) CAA, and

were mostly of ischemic nature, (2) CAA patients with CC lesions had reduced white matter integrity within the CC and in the rest of the white matter compared to those without CC lesions, (3) CC lesions were associated with reduced cognitive performance in the domains of information processing speed, executive functioning, memory, and visuospatial processing, and (4) in the domains of information processing speed and executive functioning, this association was independent of other conventional neuroimaging markers of CAA, including ICH presence, WMH volume, brain volume, and whole brain microstructural white matter integrity. Furthermore, we confirmed the ischemic and hemorrhagic nature of CC lesions with ex vivo MRI and histology, and observed damage to the myelinated white matter within and surrounding ischemic CC lesions. As expected, CAA pathology was not present within the CC white matter in CAA patients.

While lesions in the CC are typically associated with neurological diseases such as multiple sclerosis (hyperintense T2 lesions have been reported in up to 90% of MS patients) [38, 39] or primary brain tumors[40, 41], their presence has been previously reported in patients with genetic or rare forms of cSVD. These include cerebral autosomal dominant arteriopathy with subcortical infarcts and leukoencephalopathy (CADASIL) (with white matter hyperintensities as the typical CC lesion type), Binswanger's disease, and Susac syndrome (with small infarcts as the typical lesion type), although the prevalence of CC lesions in these cSVD patient groups remains unclear [16, 41, 42]. To our knowledge, the presence of CC lesions has never been assessed before in patients with CAA. This study demonstrates that CC lesions are common MRI findings in CAA and that they are mostly of ischemic nature (~70-80%). The prevalence of CC lesions in probable CAA was comparable in both in vivo cohorts (29% vs. 26%). The higher prevalence in our ex vivo cohort (53%) can potentially be attributed to increased disease severity or longer disease duration in patients that came to autopsy, or the higher resolution of the ex vivo imaging protocol.

The exact mechanisms underlying the formation of CC lesions in CAA remain unknown. While approximately half of the CC lesions were located in the splenium, which matches the typical posterior predilection for CAA pathology, no CAA-positive blood vessels were found locally in the CC on histology. In a previous study on rare focal CC infarcts, the majority of lesions were also located within the splenium of the CC [43], suggesting that the splenium may in general be more vulnerable to ischemic lesions compared with the genu and midbody. The CC receives blood supply from three arterial systems. The anterior communicating artery branches into the

subcallosal and medial callosal arteries which provide the main supply for the anterior part of the CC. The pericallosal branch of the anterior cerebral artery supplies the body of the CC, and the posterior pericallosal artery, a branch from the posterior cerebral artery, supplies the splenium [44]. Because the CC receives such rich blood supply, large CC infarcts are uncommon [45], which was in line with our findings. In contrast, our results suggest that the CC is not equally resilient to focal lesions in the form of small infarcts and hemorrhages. Arteriolosclerosis could be a potential mechanism underlying the formation of small CC lesions, although this study did not reveal an association between hypertension and CC lesion presence.

The presence of CC lesions was associated with reduced microstructural white matter integrity, not only within the CC itself but also within the rest of the white matter. This association was independent of age and WMH volume. Surprisingly, we did not observe significant associations between CC lesion presence and vascular risk factors or conventional neuroimaging markers of CAA, including the presence of ICH, the presence of cortical superficial siderosis, WMH volume, or the number of cortical microinfarcts or lobar microbleeds. Furthermore, we did not observe a significant association between CC lesion presence and cortical or leptomeningeal CAA severity in our ex vivo cohort. Together, these findings suggest that CC lesions are not a specific marker for CAA, but rather that 1) CC lesions may independently affect the remote white matter microstructure, and/or 2) that CC lesions arise as a consequence of remote and invisible or strategically located neurodegenerative and/or vascular brain damage (i.e., as a secondary mechanism). The first hypothesis is supported by many previous studies that have shown the potential damaging remote effects of focal lesions located in the white matter [10-12, 46, 47], and may apply to focal small infarcts and/or microbleeds within the CC. The second hypothesis may apply to more diffuse FLAIR hyperintense CC lesions and is supported by recent work in animals, showing that Wallerian degeneration following distal strategic cerebral infarction can affect the non-ischemic CC [48]. Interestingly, another recent animal study has demonstrated that even a single cortical microinfarct can induce remote damage extending into the contralateral CC [49]. Moreover, previous work in patients with Alzheimer's disease and mild cognitive impairment has shown that CC FLAIR hyperintensities are more frequently observed in patients with cognitive impairment compared to cognitively normal controls [50], which suggests that neurodegenerative processes (i.e., cortical atrophy) could potentially contribute to the formation of WMH abnormalities within the CC through Wallerian degeneration. Since CAA typically has a posterior predilection, the

relatively high prevalence of CC lesions in the splenium could be a secondary consequence of CAA-related hemorrhagic and neurodegenerative posterior cortical damage. Future work could explore these hypotheses further by performing tract-based DTI of the CC and connected cortical brain regions [8, 9]. Such studies should also consider the impact of ischemic vs. hemorrhagic lesion types on the integrity of white matter fiber bundles, since our ex vivo findings suggest that the white matter integrity is more severely affected around ischemic compared to hemorrhagic lesions. Furthermore, the prevalence of CC lesions should be explored in cohorts with other types of cSVD and non-cSVD cognitively normal older controls.

The clinical relevance of CC lesions is underlined by their strong association with cognitive performance in multiple cognitive domains. Patients with CC lesions performed on average between 0.5 and 0.9 SDs lower in each cognitive domain compared to patients without CC lesions. The association between CC lesion presence and performance on the domains of memory and visuospatial processing dissipated after correcting for normalized brain volume, which might be explained by the impact of AD- or CAA-related neurodegeneration on these cognitive domains. However, the association between CC lesions and information processing speed and executive functioning was independent of all other neuroimaging markers that were considered relevant in our model. After controlling for the impact of other neuroimaging markers of white matter integrity and brain volume, the total amount of unique explained variance by CC lesion presence was around 13% for processing speed and around 15% for executive functioning (based on figure 2). CC lesions may directly impact cognition by strategically disrupting white matter connectivity, thereby hampering communication between interhemispheric brain regions. The important association between CC microstructural white matter integrity and cognitive performance has been previously established in many studies, for example in patients with cSVD [51], Parkinson's disease [19], or traumatic brain injury [52]. Furthermore, the CC was identified as an important strategic region for global post-stroke cognitive impairment in a lesion-symptom mapping study [1]. Our findings now contribute to the existing literature by underlining the clinical relevance of underexplored non-lobar brain damage distal to CAA-affected vessel segments in CAA [5, 8], which may serve as a model for other sporadic cSVDs. The strong association with processing speed and executive functioning confirms the important role of interhemispheric communication in these cognitive domains [53,

350

Strengths of this study include the well-characterized cohort of stroke clinic patients with probable CAA, the inclusion of an independent cohort for the assessment of CC lesion prevalence in memory clinic patients with and without probable CAA, and the ex vivo validation of CC lesion presence in patients with pathologically confirmed (i.e. definite) CAA. Our results show that CC lesions are a frequent finding in CAA. A limitation is the lack of an age-matched control group to determine whether CC lesions are more frequently observed in CAA patients compared to healthy individuals. Of note, CC lesions were also observed in 3/20 (15%) of the non-CAA memory clinic patients, and 2/5 (40%) of the autopsy non-CAA control cases, which suggests that damage to the CC is likely not specific for CAA, which is in line with previous studies [16, 39]. Please note that we did not hypothesize that CC lesions are specific to CAA, but we aimed to assess their clinical relevance in the context of vascular cognitive impairment. Our findings warrant replication in other CAA and non-CAA cSVD cohorts, recruited from different sources. It would also be interesting to assess whether similar associations with cognitive performance can be found in other neurologic conditions in which CC lesions are prevalent, such as demyelinating lesions in MS. Furthermore, we did not have enough statistical power to explore the impact of different lesion types (i.e. hemorrhagic vs. ischemic or focal vs. diffuse) on microstructural white matter integrity and cognition, and for the same reason we were not able to assess the impact of lesion size or to explore the preferential localization of each lesion type within the CC. Although we controlled for the presence of ICH, and we replicated our findings while excluding cases with bilateral ICH, we did not explore differences in the precise location and volume of the ICH or other distal lesions between cases with and without CC lesions, a topic for future studies. The cause of death in the ex vivo cohort, which could have influenced the presence of CC lesions in non-CAA controls, was not known for all individuals. The cross-sectional nature of the present study hampers our ability to draw causative conclusions. Future studies are needed to elucidate the mechanisms underlying CC lesion formation in CAA. Because of their apparent clinical significance, CC lesions deserve more attention in both clinical and research settings.

Funding

References

1.   Zhao L, Biesbroek JM, Shi L, et al. Strategic infarct location for post-stroke cognitive impairment: A multivariate lesion-symptom mapping study. *J Cereb Blood Flow Metab*. Aug 2018;38(8):1299-1311. doi:10.1177/0271678x17728162

2.   Biesbroek JM, Weaver NA, Biessels GJ. Lesion location and cognitive impact of cerebral small vessel disease. *Clinical science (London, England : 1979)*. Apr 25 2017;131(8):715-728. doi:10.1042/cs20160452

3.   Vinters HV. Cerebral amyloid angiopathy. A critical review. *Stroke*. Mar-Apr 1987;18(2):311-24.

4.   Charidimou A, Martinez-Ramirez S, Reijmer YD, et al. Total Magnetic Resonance Imaging Burden of Small Vessel Disease in Cerebral Amyloid Angiopathy: An Imaging-Pathologic Study of Concept Validation. *JAMA neurology*. Aug 1 2016;73(8):994-1001. doi:10.1001/jamaneurol.2016.0832

5.   Reijmer YD, van Veluw SJ, Greenberg SM. Ischemic brain injury in cerebral amyloid angiopathy. *J Cereb Blood Flow Metab*. Jan 2016;36(1):40-54. doi:10.1038/jcbfm.2015.88

6.   Fotiadis P, Reijmer YD, Van Veluw SJ, et al. White matter atrophy in cerebral amyloid angiopathy. *Neurology*. Aug 4 2020;95(5):e554-e562. doi:10.1212/wnl.0000000000010017

7.   Reijmer YD, Fotiadis P, Martinez-Ramirez S, et al. Structural network alterations and neurological dysfunction in cerebral amyloid angiopathy. *Brain : a journal of neurology*. Jan 2015;138(Pt 1):179-88. doi:10.1093/brain/awu316

8.   van Veluw SJ, Reijmer YD, van der Kouwe AJ, et al. Histopathology of diffusion imaging abnormalities in cerebral amyloid angiopathy. *Neurology*. Feb 26 2019;92(9):e933-e943. doi:10.1212/wnl.0000000000007005

9.   Auriel E, Edlow BL, Reijmer YD, et al. Microinfarct disruption of white matter structure: a longitudinal diffusion tensor analysis. *Neurology*. Jul 8 2014;83(2):182-8. doi:10.1212/wnl.0000000000000579

10.   Reijmer YD, Freeze WM, Leemans A, Biessels GJ. The effect of lacunar infarcts on white matter tract integrity. *Stroke*. Jul 2013;44(7):2019-21. doi:10.1161/strokeaha.113.001321

11.   Kuchcinski G, Munsch F, Lopes R, et al. Thalamic alterations remote to infarct appear as focal iron accumulation and impact clinical outcome. *Brain : a journal of neurology*. Jul 1 2017;140(7):1932-1946. doi:10.1093/brain/awx114

12.	Duering M, Righart R, Wollenweber FA, Zietemann V, Gesierich B, Dichgans M. Acute infarcts cause focal thinning in remote cortex via degeneration of connecting fiber tracts. *Neurology*. Apr 21 2015;84(16):1685-92. doi:10.1212/wnl.0000000000001502

13.	van Veluw SJ, Shih AY, Smith EE, et al. Detection, risk factors, and functional consequences of cerebral microinfarcts. *The Lancet Neurology*. Sep 2017;16(9):730-740. doi:10.1016/s1474-4422(17)30196-5

14.	Salat DH, Smith EE, Tuch DS, et al. White matter alterations in cerebral amyloid angiopathy measured by diffusion tensor imaging. *Stroke*. Jul 2006;37(7):1759-64. doi:10.1161/01.STR.0000227328.86353.a7

15.	Reijmer YD, Fotiadis P, Riley GA, et al. Progression of Brain Network Alterations in Cerebral Amyloid Angiopathy. *Stroke*. Oct 2016;47(10):2470-5. doi:10.1161/strokeaha.116.014337

16.	Renard D, Castelnovo G, Campello C, et al. An MRI review of acquired corpus callosum lesions. *Journal of neurology, neurosurgery, and psychiatry*. Sep 2014;85(9):1041-8. doi:10.1136/jnnp-2013-307072

17.	Marco EJ, Harrell KM, Brown WS, et al. Processing speed delays contribute to executive function deficits in individuals with agenesis of the corpus callosum. *Journal of the International Neuropsychological Society : JINS*. May 2012;18(3):521-9. doi:10.1017/s1355617712000045

18.	Voineskos AN, Rajji TK, Lobaugh NJ, et al. Age-related decline in white matter tract integrity and cognitive performance: a DTI tractography and structural equation modeling study. *Neurobiology of aging*. Jan 2012;33(1):21-34. doi:10.1016/j.neurobiolaging.2010.02.009

19.	Bledsoe IO, Stebbins GT, Merkitch D, Goldman JG. White matter abnormalities in the corpus callosum with cognitive impairment in Parkinson disease. *Neurology*. Dec 11 2018;91(24):e2244-e2255. doi:10.1212/wnl.0000000000006646

20.	Knudsen KA, Rosand J, Karluk D, Greenberg SM. Clinical diagnosis of cerebral amyloid angiopathy: validation of the Boston criteria. *Neurology*. Feb 27 2001;56(4):537-9.

21.	Linn J, Halpin A, Demaerel P, et al. Prevalence of superficial siderosis in patients with cerebral amyloid angiopathy. *Neurology*. Apr 27 2010;74(17):1346-50. doi:10.1212/WNL.0b013e3181dad605

22.	Leemans A, Jones DK. The B-matrix must be rotated when correcting for subject motion in DTI data. *Magnetic resonance in medicine*. Jun 2009;61(6):1336-49. doi:10.1002/mrm.21890

23. Mori S, Oishi K, Jiang H, et al. Stereotaxic white matter atlas based on diffusion tensor imaging in an ICBM template. *Neuroimage*. Apr 1 2008;40(2):570-582. doi:10.1016/j.neuroimage.2007.12.035

24. Greenberg SM, Vernooij MW, Cordonnier C, et al. Cerebral microbleeds: a guide to detection and interpretation. *The Lancet Neurology*. Feb 2009;8(2):165-74. doi:10.1016/s1474-4422(09)70013-4

25. Wardlaw JM, Smith EE, Biessels GJ, et al. Neuroimaging standards for research into small vessel disease and its contribution to ageing and neurodegeneration. *The Lancet Neurology*. Aug 2013;12(8):822-38. doi:10.1016/s1474-4422(13)70124-8

26. Reijmer YD, Fotiadis P, Piantoni G, et al. Small vessel disease and cognitive impairment: The relevance of central network connections. *Human brain mapping*. Jul 2016;37(7):2446-54. doi:10.1002/hbm.23186

27. Hedden T, Van Dijk KR, Shire EH, Sperling RA, Johnson KA, Buckner RL. Failure to modulate attentional control in advanced aging linked to white matter pathology. *Cerebral cortex (New York, NY : 1991)*. May 2012;22(5):1038-51. doi:10.1093/cercor/bhr172

28. Lezak MD HD, Loring DW. Neuropsychological assessment. *New York, NY: Oxford University Press*. 2004;4th ed.

29. Xiong L, Boulouis G, Charidimou A, et al. Dementia incidence and predictors in cerebral amyloid angiopathy patients without intracerebral hemorrhage. *J Cereb Blood Flow Metab*. Feb 2018;38(2):241-249. doi:10.1177/0271678x17700435

30. van Veluw SJ, Scherlek AA, Freeze WM, et al. Different microvascular alterations underlie microbleeds and microinfarcts. *Annals of neurology*. Aug 2019;86(2):279-292. doi:10.1002/ana.25512

31. Love S, Chalmers K, Ince P, et al. Development, appraisal, validation and implementation of a consensus protocol for the assessment of cerebral amyloid angiopathy in post-mortem brain tissue. *American journal of neurodegenerative disease*. 2014;3(1):19-32.

32. Charidimou A, Perosa V, Frosch MP, Scherlek AA, Greenberg SM, van Veluw SJ. Neuropathological correlates of cortical superficial siderosis in cerebral amyloid angiopathy. *Brain : a journal of neurology*. Dec 5 2020;143(11):3343-3351. doi:10.1093/brain/awaa266

33. Blevins BL, Vinters HV, Love S, et al. Brain arteriolosclerosis. *Acta Neuropathol*. Jan 2021;141(1):1-24. doi:10.1007/s00401-020-02235-6

34. Lindeman RH, Merenda PF, Gold RZ. *Introduction to Bivariate and Multivariate Analysis*. Scott Foresman and Company; 1980.

35.   Groemping U. Relative Importance for Linear Regression in R: The Package relaimpo. *2006*. 2006-09-01 2006;17(1):27. doi:10.18637/jss.v017.i01

36.   Benjamini Y, Hochberg Y. Controlling the False Discovery Rate: A Practical and Powerful Approach to Multiple Testing. *Journal of the Royal Statistical Society Series B (Methodological)*. 1995;57(1):289-300.

37.   *R: A language and Environment for Statistical Computing*. 2016.

38.   Simon JH, Holtås SL, Schiffer RB, et al. Corpus callosum and subcallosal-periventricular lesions in multiple sclerosis: detection with MR. *Radiology*. Aug 1986;160(2):363-7. doi:10.1148/radiology.160.2.3726114

39.   Cocozza S, Olivo G, Riccio E, et al. Corpus callosum involvement: a useful clue for differentiating Fabry Disease from Multiple Sclerosis. *Neuroradiology*. Jun 2017;59(6):563-570. doi:10.1007/s00234-017-1829-8

40.   Dayani F, Young JS, Bonte A, et al. Safety and outcomes of resection of butterfly glioblastoma. *Neurosurg Focus*. Jun 2018;44(6):E4. doi:10.3171/2018.3.Focus1857

41.   Ho ML, Moonis G, Ginat DT, Eisenberg RL. Lesions of the corpus callosum. *AJR Am J Roentgenol*. Jan 2013;200(1):W1-16. doi:10.2214/ajr.11.8080

42.   Engelhardt E, Moreira DM, Alves GO, et al. The corpus callosum in Binswanger's disease: A quantitative fractional anisotropy analysis. *Dement Neuropsychol*. Oct-Dec 2008;2(4):278-283. doi:10.1590/s1980-57642009dn20400008

43.   Chrysikopoulos H, Andreou J, Roussakis A, Pappas J. Infarction of the corpus callosum: computed tomography and magnetic resonance imaging. *Eur J Radiol*. Jul 1997;25(1):2-8. doi:10.1016/s0720-048x(96)01155-2

44.   Türe U, Yaşargil MG, Krisht AF. The arteries of the corpus callosum: a microsurgical anatomic study. *Neurosurgery*. Dec 1996;39(6):1075-84; discussion 1084-5. doi:10.1097/00006123-199612000-00001

45.   Yang L-L, Huang Y-N, Cui Z-T. Clinical features of acute corpus callosum infarction patients. *International journal of clinical and experimental pathology*. 2014;7(8):5160-5164.

46.   Chen Y, Wang A, Tang J, et al. Association of white matter integrity and cognitive functions in patients with subcortical silent lacunar infarcts. *Stroke*. Apr 2015;46(4):1123-6. doi:10.1161/strokeaha.115.008998

47.   Duering M, Schmidt R. Remote changes after ischaemic infarcts: a distant target for therapy? *Brain : a journal of neurology*. Jul 1 2017;140(7):1818-1820. doi:10.1093/brain/awx135

48.   Zuo M, Guo H, Wan T, et al. Wallerian degeneration in experimental focal cortical ischemia. *Brain Res Bull*. Jul 2019;149:194-202. doi:10.1016/j.brainresbull.2019.04.023

49.   Lubart A, Benbenishty A, Har-Gil H, et al. Single Cortical Microinfarcts Lead to Widespread Microglia/Macrophage Migration Along the White Matter. *Cerebral cortex (New York, NY : 1991)*. Sep 21 2020;doi:10.1093/cercor/bhaa223

50.   Yoshita M, Fletcher E, Harvey D, et al. Extent and distribution of white matter hyperintensities in normal aging, MCI, and AD. *Neurology*. Dec 26 2006;67(12):2192-8. doi:10.1212/01.wnl.0000249119.95747.1f

51.   Tuladhar AM, van Norden AGW, de Laat KF, et al. White matter integrity in small vessel disease is related to cognition. *NeuroImage: Clinical*. 2015/01/01/ 2015;7:518-524. doi:https://doi.org/10.1016/j.nicl.2015.02.003

52.   Arenth PM, Russell KC, Scanlon JM, Kessler LJ, Ricker JH. Corpus callosum integrity and neuropsychological performance after traumatic brain injury: a diffusion tensor imaging study. *The Journal of head trauma rehabilitation*. Mar-Apr 2014;29(2):E1-e10. doi:10.1097/HTR.0b013e318289ede5

53.   Zhao J, Manza P, Wiers C, et al. Age-Related Decreases in Interhemispheric Resting-State Functional Connectivity and Their Relationship With Executive Function. Original Research. *Frontiers in aging neuroscience*. 2020-February-26 2020;12(20)doi:10.3389/fnagi.2020.00020

54.   Roland JL, Snyder AZ, Hacker CD, et al. On the role of the corpus callosum in interhemispheric functional connectivity in humans. *Proceedings of the National Academy of Sciences*. 2017;114(50):13278. doi:10.1073/pnas.1707050114

Tables

Table 1: Characteristics of CAA cases with and without CC lesions

	CC lesion absent (n=46)	CC lesion(s) present (n=19)	p-value
Demographics			
Age (y) (sd)	69.0 (8.0)	71.2 (4.0)	.154
Female, n (%)	18 (39)	9 (47)	.737
Education (y) (sd)#	16.5 (2.6)	17.0 (4.5)	.672
Neuroimaging markers			
Brain volume (%ICV) (sd)	66.2 (3.8)	63.4 (4.7)	**0.027**
ICH present, n (%)	34 (74)	14 (74)	1
Lobar CMB (median) [range]	31.5 [0-495]	32 [3-740]	.644
Normalized WMH (median) [range]	0.36 [0.00-1.63]	0.30 [0.01-3.20]	.470
Cortical CMI present, n (%)	22 (48)	8 (42)	.883
≤2 deep CMB present, n (%)	13 (6)	5 (1)	.631
cSS present, n (%)	33 (72)	17 (89)	.223
Vascular risk factors			
Hypertension, n (%)#	18 (42)	10 (53)	.611
Hypercholesterolemia, n (%)#	16 (37)	8 (42)	.935
Type II diabetes mellitus, n (%)#	3 (7)	1 (5)	1
Cardiac disease, n (%)#	4 (9)	3 (16)	.665
Current tobacco use, n (%)#	0 (0)	1 (5)	.307
Current alcohol use, n (%)#	21 (49)	11 (58)	.702
Microstructural white matter integrity			
CC FA (sd)#	0.48 (0.05)	0.42 (0.05)	**<.001**
CC MD (sd)#	1.09×10^{-3} (9.2×10^{-4})	1.18×10^{-3} (1.0×10^{-3})	**.004**
Total WM FA (sd)#	0.38 (0.03)	0.34 (0.04)	**.002**
Total WM MD (sd)#	1.06×10^{-3} (7.0×10^{-4})	1.14×10^{-3} (1.1×10^{-3})	**.01**
Cognition			
MMSE, median [range]#	28 [21-30]	28 [21-30]	.08
Executive functioning (sd)#	0.21 (0.68)	-0.56 (0.72)	**<.001**
Processing speed (sd)#	0.20 (0.50)	-0.53 (1.0)	**.008**
Memory (sd) #	0.17 (0.93)	-0.39 (0.90)	**0.032**
Language (sd)#	0.10 (0.87)	-0.34 (1.1)	0.130
Visuospatial processing (sd)#	0.15 (0.72)	-0.40 (0.99)	**0.047**

Values represent mean (standard deviation) unless otherwise specified. Group comparisons were performed using Mann-Whitney U tests, Chi-square tests or Fishers exact test when applicable. Significant differences (p<0.05) are depicted in bold.

Abbreviations: CC, corpus callosum; ICH, intracerebral hemorrhage; CMB, cerebral microbleeds; CMI, cerebral microinfarcts; WMH, white matter hyperintensities; FA, fractional anisotropy; MD, mean diffusivity.

Data were missing: education, n=2; hypertension, n=3; hypercholesterolemia, n=3; type II diabetes mellitus, n=3; cardiac disease, n=3; current tobacco use, n=3; current alcohol use, n=3; CC FA, n=1; CC MD, n=1; total WM FA, n=1; total WM MD, n=1; MMSE, n=1; executive functioning, n=1; information processing speed, n=1; memory, n=2; language, n=1; visuospatial processing, n=3.

Table 2: Associations between CC lesions and cognition

Standard covariates	Additional covariate (potential confounders)					All covariates together
Age, sex, education, time between NPA and MRI	ICH presence	Whole brain FA (except CC)	Whole brain MD (except CC)	Normalized WMH	Normalized brain volume	
Executive functioning						
-0.726 [-1.118, -0.334], p<0.001	**-0.722 [-1.110, -0.335], p<.001**	**-0.680 [-1.122, -0.238], p=.003**	**-0.714 [-1.139, -0.290], p=.001**	**-0.645 [-1.028, -0.262], p=.001**	**-0.452 [-1.174, -0.345], p=0.001**	**-0.427 [-1.168, -0.255], p=.003**
Information processing speed						
-0.709 [-1.108, -0.309], p<0.001	**-0.707 [-1.108, -0.306], p<.001**	**-0.728 [-1.182, -0.274], p=.002**	**-0.750 [-1.185, -0.315], p=.001**	**-0.602 [-0.980, -0.225], p=.002**	**-0.322 [-0.940, -0.144], p=0.009**	**-0.312 [-0.980, -0.122], p=.013**
Memory						
-0.593 [-1.098, -0.087], p=0.022	**-0.590 [-1.098, -0.082], p=.024**	**-0.670 [-1.126, -0.144], p=.015**	**-0.653 [-1.189, -0.118], p=.018**	-0.512 [-1.017, 0.006], p=.047	-0.232 [-0.994, 0.059], p=0.081	-0.294 [-1.152; -0.013], p=0.045
Language						
-0.345 [-0.853, 0.114], p=0.180	-0.342 [-0.851, 0.167], p=.184	-0.369 [-0.939, 0.202], p=.201	-0.404 [-0.9248, 0.140], p=.143	-0.225 [-0.716, 0.265], p=.361	-0.161 [-0.874, 0.205], p=0.219	-0.138 [-0.849, 0.281], p=.318
Visuospatial processing						
-0.552 [-0.980, -0.124], p=0.013	**-0.555 [-0.986, -.123], p=0.013**	**-0.590 [-1.073, -0.109], p=.017**	**-0.638 [-1.096, -0.180], p=.007**	**-0.544 [-0.978, -0.109], p=.015**	-0.244 [-0.881; -0.013], p=0.044	-0.261 [-0.970, 0.012], p=.056

Values represent beta coefficients [95% confidence interval] of CC lesion presence. Significant associations after false discovery rate correction are depicted in bold.

Key: CC, corpus callosum; FA, fractional anisotropy; MD, mean diffusivity.

Table 3: case characteristics ex vivo cohort

Case No.	Path diagnosis	Age at death (years)	Sex	Post-mortem interval (hours)	Cortical CAA burden score	Leptomeningeal CAA burden score	Amyloid-beta plaque score	Arteriolosclerosis	CC lesion type	CC lesion location
1	CAA	80	M	N/A	5	6	9	8	WMH	Splenium
2	CAA	70	M	16	9	5	9	12	WMH	Multiple
3	CAA	76	M	27	7	8	10	9	Lacune	Genu
4	CAA	65	M	14	7	7	3	7	ICH	Midbody
5	CAA	81	M	N/A	5	7	12	8	WMH	Multiple
6	CAA	70	F	N/A	6	11	9	5	None	
7	CAA	67	M	N/A	10	8	12	11	None	
8	CAA	69	M	36	10	11	7	10	CMB	Splenium
9	CAA	64	F	30	8	11	11	6	WMH	Splenium
10	CAA	79	F	37	8	11	11	8	CMI	Genu
11	CAA	67	M	24	5	12	12	9	None	
12	CAA	88	F	11	8	9	7	5	None	
13	CAA	67	F	16	10	11	12	9	None	
14	CAA	84	F	32	8	9	11	10	None	
15	CAA	67	M	N/A	12	12	8	8	ICH	Multiple
16	CAA	76	M	20	11	12	9	8	None	
17	CAA	78	F	24	7	11	11	8	None	
18	CAA	86	M	20	10	12	10	9	CMI	Genu
19	CAA	85	M	N/A	12	12	11	6	None	
1	CTRL	90	M	6	0	1	9	4	None	
2	CTRL	95	F	4	0	2	1	6	WMH	Genu
3	CTRL	88	F	9	0	1	1	0	None	
4[a]	CTRL	85	M	38	1	4	10	8	CMI	Genu
5	CTRL	82	F	N/A	1	2	2	3	None	

[a] Note that this case had multiple lobar microbleeds during life, but at autopsy only mild CAA was observed in the leptomeningeal vessels and as such considered a CTRL in this study.

Figure legends

Figure 1: Representative examples of CC lesions in patients with CAA.
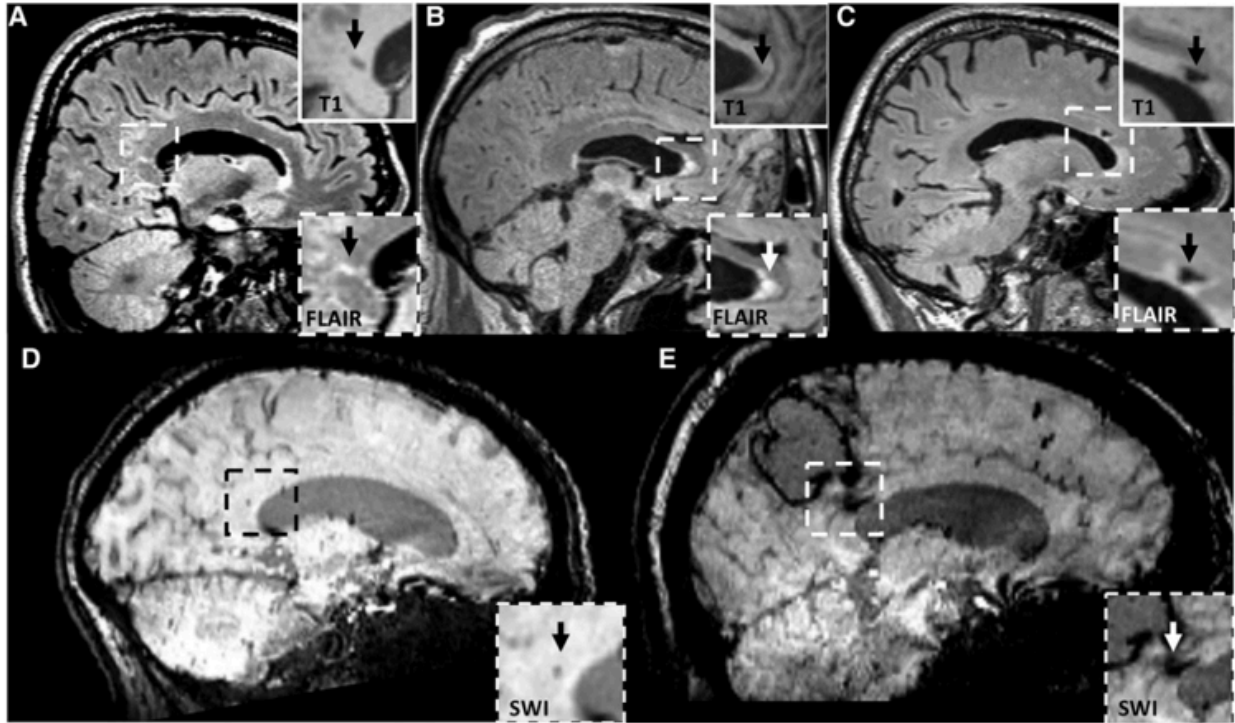
(A) Cerebral microinfarct located in the splenium of the corpus callosum. **(B)** Diffuse FLAIR hyperintensity located in the genu of the corpus callosum. **(C)** Lacunar infarct located in the genu of the corpus callosum. **(D)** Cerebral microbleed located in the splenium of the corpus callosum. **(E)** Extension of intracerebral hemorrhage into the splenium of the corpus callosum.

Figure 2: Association between imaging markers of white matter integrity and cognitive performance.
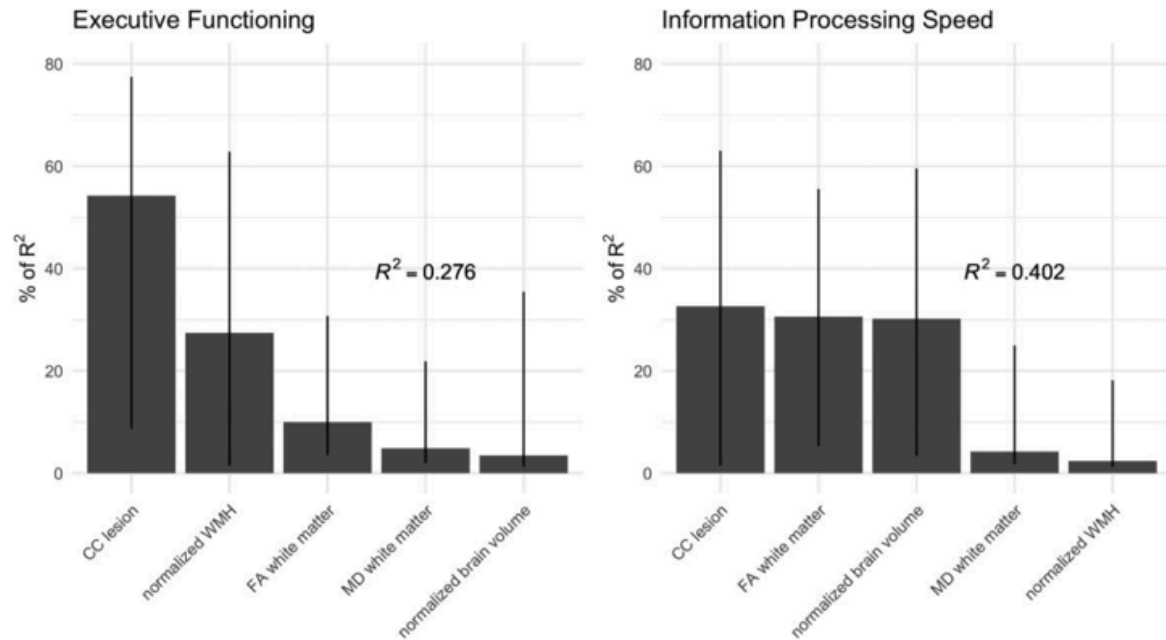
The contribution of each imaging marker (corpus callosum (CC) lesion presence, normalized white matter hyperintensity (WMH) volume, normalized brain volume, fractional anisotropy (FA) in the whole white matter (except CC), and mean diffusivity (MD) in the whole white matter (except CC) to the total explained variance in multiple regression models with information processing speed (n=63) and executive functioning (n=63) as outcome variable as estimated by the Lindeman et al. method [34]. Lines represent 95% confidence intervals after bootstrapping.

Figure 3: Diffuse T2 hyperintense lesion in the splenium of the corpus callosum.
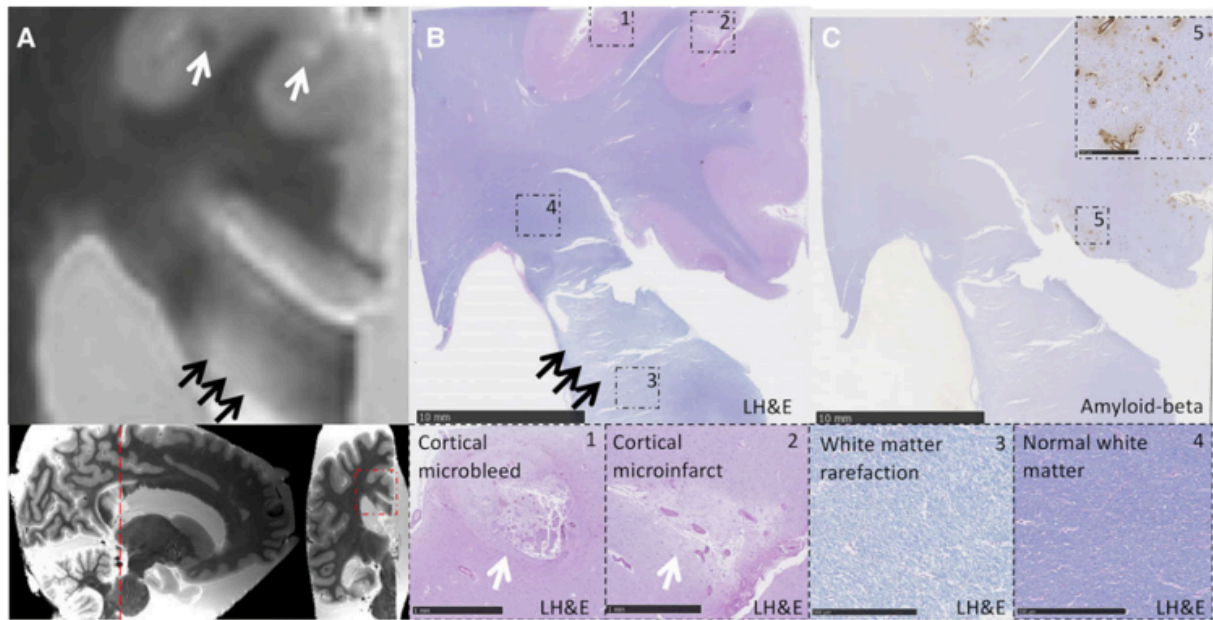
(A) A diffuse T2 hyperintense lesion can be observed on coronal T2-weighted ex vivo MRI (black arrows) in a patient with pathologically confirmed CAA (case 2). A cortical microbleed (left), and cortical microinfarct (right) can be observed in the adjacent cortex (white arrows). (B) The corresponding Luxol Fast Blue and Hematoxylin and Eosin (LH&E) stained section is shown. Inset 1 and 2 show the location of the cortical microbleed (inset 1) and cortical microinfarct (inset 2) that were observed on MRI. Inset 3 shows white matter rarefaction at the location corresponding to the T2 hyperintense corpus callosum lesion on MRI. Distal from the lesion, the white matter appears normal (inset 4). (C) The presence of CAA pathology was confirmed within the cortex on the adjacent Aβ-stained section (inset 5). No CAA was observed within the corpus callosum.

Figure 4: Cerebral microbleed located in the splenium of the corpus callosum.
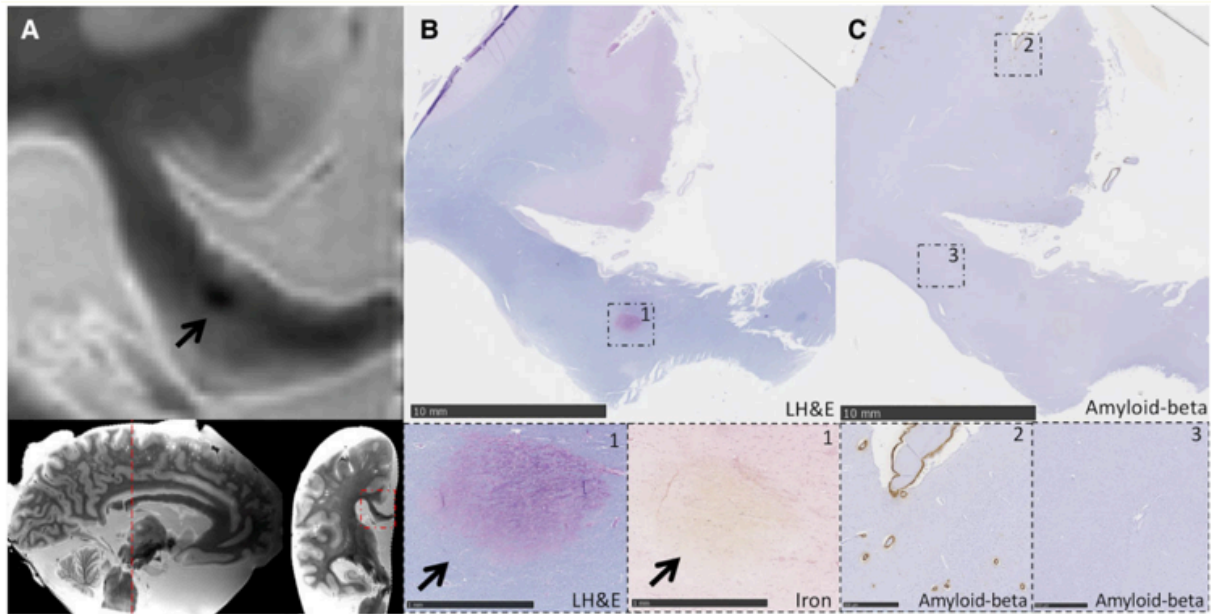

(A) A cerebral microbleed located in the splenium of the CC can be observed on coronal T2-weighted ex vivo MRI (black arrow) in a patient with pathologically confirmed CAA (case 8). Note that this patient also had participated in the in vivo stroke clinic cohort during life. No lesions were observed on the in vivo scans that were performed in the same individual approximately 6 months before death (not shown). (B) The corresponding Luxol Fast Blue and Hematoxylin and Eosin (LH&E) stained section is shown. The inset shows the presence of lysed red blood cells, indicative of a (sub)acute microbleed (bottom left image, arrow). The relatively acute stage of the microbleed is confirmed by the absence of iron positivity in the adjacent Perls Prussian blue stained section (bottom right image, arrow). (C) The adjacent section stained for Aβ revealed the presence of CAA in the cortex (inset 2), while vascular Aβ is absent within the corpus callosum (inset 3).

Figure 5: Lacunar infarct located in the genu of the corpus callosum.
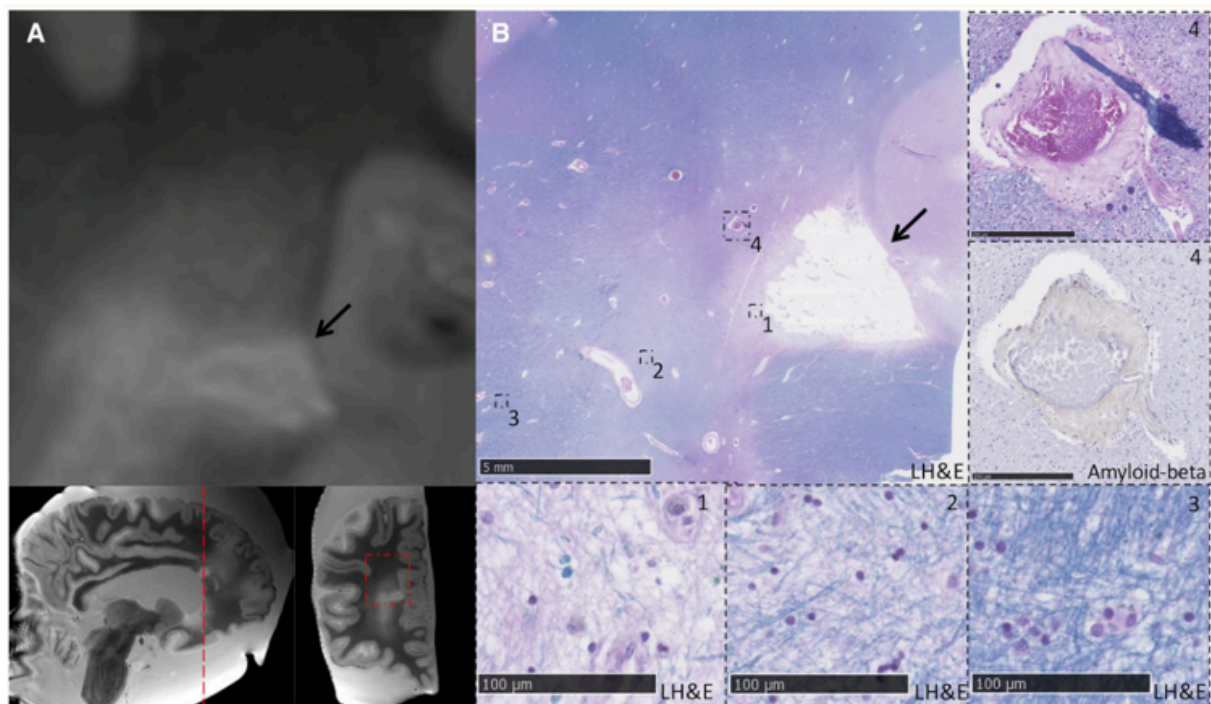
A) A lacunar infarct can be observed in the genu of the CC on T2-weighted ex vivo MRI (black arrow) in a patient with pathologically confirmed CAA (case 3). **B)** The corresponding LH&E stained section is shown. The cavitated lacunar infarct is indicated by the black arrow. The insets (1-3) reveal damage to the myelinated fibers in the immediate area surrounding the infarct (inset 1), as well as in the vicinity of the lesion (inset 2). At a larger distance, the white matter appears normal (inset 3). Inset 4 shows an abnormal blood vessel in the vicinity of the lacune. The lipohyalinotic and thickened appearance of the vessel wall, which is negative for Aβ, is suggestive of arteriolosclerosis.

7. References

1. Zotin MCZ, Sveikata L, Viswanathan A, Yilmaz P. Cerebral small vessel disease and vascular cognitive impairment: from diagnosis to management. Curr Opin Neurol. 2021;34(2):246–57.

2. Filley CM, Fields RD. White matter and cognition: making the connection. J Neurophysiol. 2016;116(5):2093–104.

3. Sarbu N, Shih RY, Jones RV, Horkayne-Szakaly I, Oleaga L, Smirniotopoulos JG. White Matter Diseases with Radiologic-Pathologic Correlation. Radiographics. 2016;36(5):1426–47.

4. Wardlaw JM, Smith C, Dichgans M. Small vessel disease: mechanisms and clinical implications. Lancet Neurology. 2019;18(7):684–96.

5. Cannistraro RJ, Badi M, Eidelman BH, Dickson DW, Middlebrooks EH, Meschia JF. CNS small vessel disease: A clinical review. Neurology. 2019;92(24):1146–56.

6. Onteddu SR, Goddeau RP, Minaeian A, Henninger N. Clinical impact of leukoaraiosis burden and chronological age on neurological deficit recovery and 90-day outcome after minor ischemic stroke. J Neurol Sci. 2015;359(1–2):418–23.

7. Sagnier S, Catheline G, Munsch F, Bigourdan A, Poli M, Debruxelles S, et al. Severity of Small Vessel Disease Biomarkers Reduces the Magnitude of Cognitive Recovery after Ischemic Stroke. Cerebrovasc Dis. 2021;50(4):456–63.

8. Bordes C, Sargurupremraj M, Mishra A, Debette S. Genetics of common cerebral small vessel disease. Nat Rev Neurol. 2022;18(2):84–101.

9. Marini S, Anderson CD, Rosand J. Genetics of Cerebral Small Vessel Disease. Stroke. 2020;51(1):12–20.

10. Rutten-Jacobs LCA, Rost NS. Emerging insights from the genetics of cerebral small-vessel disease. Ann Ny Acad Sci. 2020;1471(1):5–17.

11. Blevins BL, Vinters HV, Love S, Wilcock DM, Grinberg LT, Schneider JA, et al. Brain arteriolosclerosis. Acta Neuropathol. 2021;141(1):1–24.

12. Charidimou A, Boulouis G, Gurol ME, Ayata C, Bacskai BJ, Frosch MP, et al. Emerging concepts in sporadic cerebral amyloid angiopathy. Brain. 2017;140(7):1829–50.

13. Greenberg SM, Bacskai BJ, Hernandez-Guillamon M, Pruzin J, Sperling R, Veluw SJ van. Cerebral amyloid angiopathy and Alzheimer disease — one peptide, two pathways. Nat Rev Neurol. 2020;16(1):30–42.

14. Biffi A, Greenberg SM. Cerebral Amyloid Angiopathy: A Systematic Review. J Clin Neurol. 2011;7(1):1.

15. PANTELAKIS S. [A particular type of senile angiopathy of the central nervous system: congophilic angiopathy, topography and frequency]. Mon Psychiatr Neurol. 1954;128(4):219–56.

16. Vinters HV. Cerebral amyloid angiopathy. A critical review. Stroke. 1987;18(2):311–324.

17. Arvanitakis Z, Leurgans SE, Wang Z, Wilson RS, Bennett DA, Schneider JA. Cerebral amyloid angiopathy pathology and cognitive domains in older persons. Ann Neurol. 2011;69(2):320–7.

18. Keage HA, Carare RO, Friedland RP, Ince PG, Love S, Nicoll JA, et al. Population studies of sporadic cerebral amyloid angiopathy and dementia: a systematic review. Bmc Neurol. 2009;9(1):3.

19. Jäkel L, Kort AMD, Klijn CJM, Schreuder FHBM, Verbeek MM. Prevalence of cerebral amyloid angiopathy: A systematic review and meta-analysis. Alzheimer's Dementia. 2021;18(1):10–28.

20. Jellinger KA. Alzheimer disease and cerebrovascular pathology: an update. J Neural Transm. 2002;109(5):813–36.

21. Viswanathan A, Greenberg SM. Cerebral amyloid angiopathy in the elderly. Ann Neurol. 2011;70(6):871–80.

22. Iadecola C. The Pathobiology of Vascular Dementia. Neuron. 2013;80(4):844–66.

23. Veluw SJ van, Hou SS, Calvo-Rodriguez M, Arbel-Ornath M, Snyder AC, Frosch MP, et al. Vasomotion as a Driving Force for Paravascular Clearance in the Awake Mouse Brain. Neuron. 2020;105(3):549-561.e5.

24. Mestre H, Mori Y, Nedergaard M. The Brain's Glymphatic System: Current Controversies. Trends Neurosci. 2020;43(7):458–66.

25. Zago W, Schroeter S, Guido T, Khan K, Seubert P, Yednock T, et al. Vascular alterations in PDAPP mice after anti-Aβ immunotherapy: Implications for amyloid-related imaging abnormalities. Alzheimer's Dementia. 2013;9(5):S105–15.

26. Perosa V, Oltmer J, Munting LP, Freeze WM, Auger CA, Scherlek AA, et al. Perivascular space dilation is associated with vascular amyloid-β accumulation in the overlying cortex. Acta Neuropathol. 2021;143(3):331–48.

27. Carare RO, Aldea R, Bulters D, Alzetani A, Birch AA, Richardson G, et al. Vasomotion Drives Periarterial Drainage of Aβ from the Brain. Neuron. 2020;105(3):400–1.

28. Fultz NE, Bonmassar G, Setsompop K, Stickgold RA, Rosen BR, Polimeni JR, et al. Coupled electrophysiological, hemodynamic, and cerebrospinal fluid oscillations in human sleep. Science. 2019;366(6465):628–31.

29. Sveikata L, Charidimou A, Viswanathan A. Vessels Sing Their ARIAs: The Role of Vascular Amyloid in the Age of Aducanumab. Stroke. 2022;53(1):298–302.

30. Sperling RA, Jack CR, Black SE, Frosch MP, Greenberg SM, Hyman BT, et al. Amyloid-related imaging abnormalities in amyloid-modifying therapeutic trials: Recommendations from the Alzheimer's Association Research Roundtable Workgroup. Alzheimer's Dementia. 2011;7(4):367–85.

31. Veluw SJ van, Arfanakis K, Schneider JA. Neuropathology of Vascular Brain Health: Insights From Ex Vivo Magnetic Resonance Imaging–Histopathology Studies in Cerebral Small Vessel Disease. Stroke. 2022;53(2):404–15.

32. Greenberg SM, Rebeck GW, Vonsattel JPG, Gomez-Isla T, Hyman BT. Apolipoprotein E ϵ4 and cerebral hemorrhage associated with amyloid angiopathy. Ann Neurol. 1995;38(2):254–9.

33. Greenberg SM, Edgar MA. Case records of the Massachusetts general hospital, case 22–1996. The New England journal of medicine. 1996 Jul 18;335:189–196.

34. Linn J, Halpin A, Demaerel P, Ruhland J, Giese AD, Dichgans M, et al. Prevalence of superficial siderosis in patients with cerebral amyloid angiopathy. Neurology. 2010;74(17):1346–50.

35. Charidimou A, Frosch MP, Salman RAS, Baron JC, Cordonnier C, Hernandez-Guillamon M, et al. Advancing diagnostic criteria for sporadic cerebral amyloid angiopathy: Study protocol for a multicenter MRI-pathology validation of Boston criteria v2.0. Int J Stroke. 2019;14(9):956–71.

36. Greenberg SM, Charidimou A. Diagnosis of Cerebral Amyloid Angiopathy. Stroke. 2018;49(2):491–7.

37. Martinez-Ramirez S, Romero J, Shoamanesh A, McKee AC, Etten EV, Pontes-Neto O, et al. Diagnostic value of lobar microbleeds in individuals without intracerebral hemorrhage. Alzheimer's Dementia. 2015;11(12):1480–8.

38. Rodrigues MA, Samarasekera N, Lerpiniere C, Humphreys C, McCarron MO, White PM, et al. The Edinburgh CT and genetic diagnostic criteria for lobar intracerebral haemorrhage associated with cerebral amyloid angiopathy: model development and diagnostic test accuracy study. Lancet Neurology. 2018;17(3):232–40.

39. Feigin VL, Krishnamurthi RV, Parmar P, Norrving B, Mensah GA, Bennett DA, et al. Update on the Global Burden of Ischemic and Hemorrhagic Stroke in 1990-2013: The GBD 2013 Study. Neuroepidemiology. 2015;45(3):161–76.

40. Rizzi L, Aventurato ÍK, Balthazar MLF. Neuroimaging Research on Dementia in Brazil in the Last Decade: Scientometric Analysis, Challenges, and Peculiarities. Front Neurol. 2021;12:640525.

41. Silva NCBS, Bracko O, Nelson AR, Oliveira FF de, Robison LS, Shaaban CE, et al. Vascular cognitive impairment and dementia: An early career researcher perspective. Alzheimer's Dementia Diagnosis Assess Dis Monit. 2022;14(1):e12310.

42. Malhotra K, Zompola C, Theodorou A, Katsanos AH, Shoamanesh A, Gupta H, et al. Prevalence, Characteristics, and Outcomes of Undetermined Intracerebral Hemorrhage: A Systematic Review and Meta-Analysis. Stroke. 2021;52(11):3602–12.

43. Malhotra K, Theodorou A, Katsanos AH, Zompola C, Shoamanesh A, Boviatsis E, et al. Prevalence of Clinical and Neuroimaging Markers in Cerebral Amyloid Angiopathy: A Systematic Review and Meta-Analysis. Stroke. 2022;53(6):1944–53.

44. Pasi M, Charidimou A, Boulouis G, Auriel E, Ayres A, Schwab KM, et al. Mixed-location cerebral hemorrhage/microbleeds. Neurology. 2018;90(2):e119–26.

45. Dichgans M, Leys D. Vascular Cognitive Impairment. Circ Res. 2017;120(3):573–91.

46. Iadecola C, Duering M, Hachinski V, Joutel A, Pendlebury ST, Schneider JA, et al. Vascular Cognitive Impairment and Dementia. J Am Coll Cardiol. 2019;73(25):3326–44.

47. Telgte A ter, Leijsen EMC van, Wiegertjes K, Klijn CJM, Tuladhar AM, Leeuw FE de. Cerebral small vessel disease: from a focal to a global perspective. Nat Rev Neurol. 2018;14(7):387–98.

48. Kuohn LR, Witsch J, Steiner T, Sheth KN, Kamel H, Navi BB, et al. Early Deterioration, Hematoma Expansion, and Outcomes in Deep Versus Lobar Intracerebral Hemorrhage: The FAST Trial. Stroke. 2022;101161STROKEAHA121037974.

49. Smith EE, Charidimou A, Ayata C, Werring DJ, Greenberg SM. Cerebral Amyloid Angiopathy–Related Transient Focal Neurologic Episodes. Neurology. 2021;97(5):231–8.

50. Charidimou A, Peeters A, Fox Z, Gregoire SM, Vandermeeren Y, Laloux P, et al. Spectrum of transient focal neurological episodes in cerebral amyloid angiopathy: multicentre magnetic resonance imaging cohort study and meta-analysis. Stroke. 2012;43(9):2324–30.

51. Xiong L, Davidsdottir S, Reijmer YD, Shoamanesh A, Roongpiboonsopit D, Thanprasertsuk S, et al. Cognitive Profile and its Association with Neuroimaging Markers of Non-Demented Cerebral Amyloid Angiopathy Patients in a Stroke Unit. J Alzheimer's Dis. 2016;52(1):171–8.

52. Case NF, Charlton A, Zwiers A, Batool S, McCreary CR, Hogan DB, et al. Cerebral Amyloid Angiopathy Is Associated With Executive Dysfunction and Mild Cognitive Impairment. Stroke. 2016;47(8):2010–6.

53. Xiong L, Boulouis G, Charidimou A, Roongpiboonsopit D, Jessel MJ, Pasi M, et al. Dementia incidence and predictors in cerebral amyloid angiopathy patients without intracerebral hemorrhage. J Cereb Blood Flow Metabolism. 2017;38(2):241–9.

54. Sachdev P, Kalaria R, O'Brien J, Skoog I, Alladi S, Black SE, et al. Diagnostic Criteria for Vascular Cognitive Disorders: A VASCOG Statement. Alz Dis Assoc Dis. 2014;28(3):206–18.

55. Hachinski V, Iadecola C, Petersen RC, Breteler MM, Nyenhuis DL, Black SE, et al. National Institute of Neurological Disorders and Stroke–Canadian Stroke Network Vascular Cognitive Impairment Harmonization Standards. Stroke. 2006;37(9):2220–41.

56. Watson N, Bonsack F, Sukumari-Ramesh S. Intracerebral Hemorrhage: The Effects of Aging on Brain Injury. Front Aging Neurosci. 2022;14:859067.

57. Almandoz JED, Schaefer PW, Goldstein JN, Rosand J, Lev MH, González RG, et al. Practical Scoring System for the Identification of Patients with Intracerebral Hemorrhage at Highest Risk of Harboring an Underlying Vascular Etiology: The Secondary Intracerebral Hemorrhage Score. Am J Neuroradiol. 2010;31(9):1653–60.

58. Boulouis G, Morotti A, Brouwers HB, Charidimou A, Jessel MJ, Auriel E, et al. Association Between Hypodensities Detected by Computed Tomography and Hematoma Expansion in Patients With Intracerebral Hemorrhage. Jama Neurol. 2016;73(8):961–8.

59. Potter GM, Chappell FM, Morris Z, Wardlaw JM. Cerebral Perivascular Spaces Visible on Magnetic Resonance Imaging: Development of a Qualitative Rating Scale and its Observer Reliability. Cerebrovasc Dis. 2015;39(3–4):224–31.

60. Charidimou A, Boulouis G, Haley K, Auriel E, Etten ES van, Fotiadis P, et al. White matter hyperintensity patterns in cerebral amyloid angiopathy and hypertensive arteriopathy. Neurology. 2016;86(6):505–11.

61. Biffi A, Bailey D, Anderson CD, Ayres AM, Gurol EM, Greenberg SM, et al. Risk Factors Associated With Early vs Delayed Dementia After Intracerebral Hemorrhage. Jama Neurol. 2016;73(8):969.

62. Potter T, Lioutas VA, Tano M, Pan A, Meeks J, Woo D, et al. Cognitive Impairment After Intracerebral Hemorrhage: A Systematic Review of Current Evidence and Knowledge Gaps. Front Neurol. 2021;12:716632.

63. Moulin S, Labreuche J, Bombois S, Rossi C, Boulouis G, Hénon H, et al. Dementia risk after spontaneous intracerebral haemorrhage: a prospective cohort study. Lancet Neurology. 2016;15(8):820–9.

64. Pasi M, Sugita L, Xiong L, Charidimou A, Boulouis G, Pongpitakmetha T, et al. Association of Cerebral Small Vessel Disease and Cognitive Decline After Intracerebral Hemorrhage. Neurology. 2020;96(2):e182–92.

65. Puy L, Pasi M, Rodrigues M, Veluw SJ van, Tsivgoulis G, Shoamanesh A, et al. Cerebral microbleeds: from depiction to interpretation. J Neurology Neurosurg Psychiatry. 2021;92(6):598–607.

66. Greenberg SM, Vernooij MW, Cordonnier C, Viswanathan A, Salman RAS, Warach S, et al. Cerebral microbleeds: a guide to detection and interpretation. Lancet Neurology. 2009;8(2):165–74.

67. Veluw SJ van, Biessels GJ, Klijn CJM, Rozemuller AJM. Heterogeneous histopathology of cortical microbleeds in cerebral amyloid angiopathy. Neurology. 2016;86(9):867–71.

68. Veluw SJ van, Charidimou A, Kouwe AJ van der, Lauer A, Reijmer YD, Costantino I, et al. Microbleed and microinfarct detection in amyloid angiopathy: a high-resolution MRI-histopathology study. Brain. 2016;139(12):3151–62.

69. Veluw SJ, Scherlek AA, Freeze WM, Telgte A, Kouwe AJ, Bacskai BJ, et al. Different microvascular alterations underlie microbleeds and microinfarcts. Ann Neurol. 2019;86(2):279–92.

70. Charidimou A, Shams S, Romero JR, Ding J, Veltkamp R, Horstmann S, et al. Clinical significance of cerebral microbleeds on MRI: A comprehensive meta-analysis of risk of intracerebral hemorrhage, ischemic stroke, mortality, and dementia in cohort studies (v1). Int J Stroke. 2017;13(5):454–68.

71. Reijmer YD, Veluw SJ van, Greenberg SM. Ischemic brain injury in cerebral amyloid angiopathy. J Cereb Blood Flow Metabolism. 2015;36(1):40–54.

72. Debette S, Schilling S, Duperron MG, Larsson SC, Markus HS. Clinical Significance of Magnetic Resonance Imaging Markers of Vascular Brain Injury: A Systematic Review and Meta-analysis. Jama Neurol. 2018;76(1):81–94.

73. Ding J, Sigurðsson S, Jónsson PV, Eiriksdottir G, Meirelles O, Kjartansson O, et al. Space and location of cerebral microbleeds, cognitive decline, and dementia in the community. Neurology. 2017;88(22):2089–97.

74. Cipriano L, Saracino D, Oliva M, Campana V, Puoti G, Conforti R, et al. Systematic Review on the Role of Lobar Cerebral Microbleeds in Cognition. J Alzheimer's Dis. 2022;86(3):1025–35.

75. Charidimou A, Perosa V, Frosch MP, Scherlek AA, Greenberg SM, Veluw SJ van. Neuropathological correlates of cortical superficial siderosis in cerebral amyloid angiopathy. Brain. 2020;143(11):3343–51.

76. Charidimou A, Boulouis G, Xiong L, Pasi M, Roongpiboonsopit D, Ayres A, et al. Cortical Superficial Siderosis Evolution: A Biomarker of Cerebral Amyloid Angiopathy and Intracerebral Hemorrhage Risk. Stroke. 2019;50(4):954–62.

77. Wollenweber FA, Opherk C, Zedde M, Catak C, Malik R, Duering M, et al. Prognostic relevance of cortical superficial siderosis in cerebral amyloid angiopathy. Neurology. 2018;92(8):e792–801.

78. Charidimou A, Boulouis G, Greenberg SM, Viswanathan A. Cortical superficial siderosis and bleeding risk in cerebral amyloid angiopathy: A meta-analysis. Neurology. 2019;93(24):e2192–202.

79. Li Q, Zotin MCZ, Warren AD, Ma Y, Gurol E, Goldstein JN, et al. CT-visible convexity subarachnoid hemorrhage is associated with cortical superficial siderosis and predicts recurrent ICH. Neurology. 2020;96(7):10.1212/WNL.0000000000011052.

80. Raposo N, Charidimou A, Roongpiboonsopit D, Onyekaba M, Gurol ME, Rosand J, et al. Convexity subarachnoid hemorrhage in lobar intracerebral hemorrhage: A prognostic marker. Neurology. 2019;94(9):e968–77.

81. Wardlaw JM, Smith EE, Biessels GJ, Cordonnier C, Fazekas F, Frayne R, et al. Neuroimaging standards for research into small vessel disease and its contribution to ageing and neurodegeneration. Lancet Neurol. 2013;12(8):822–38.

82. Joutel A, Chabriat H. Pathogenesis of white matter changes in cerebral small vessel diseases: beyond vessel-intrinsic mechanisms. Clin Sci. 2017;131(8):635–51.

83. Haglund M, Englund E. Cerebral Amyloid Angiopathy, White Matter Lesions and Alzheimer Encephalopathy – A Histopathological Assessment. Dement Geriatr Cogn. 2002;14(3):161–6.

84. Ly JV, Donnan GA, Villemagne VL, Zavala JA, Ma H, O'Keefe G, et al. 11C-PIB binding is increased in patients with cerebral amyloid angiopathy–related hemorrhage(Podcast). Neurology. 2010;74(6):487–93.

85. Keith J, Gao F qiang, Noor R, Kiss A, Balasubramaniam G, Au K, et al. Collagenosis of the Deep Medullary Veins: An Underrecognized Pathologic Correlate of White Matter Hyperintensities and Periventricular Infarction? J Neuropathology Exp Neurology. 2017;76(4):299–312.

86. McAleese KE, Walker L, Graham S, Moya ELJ, Johnson M, Erskine D, et al. Parietal white matter lesions in Alzheimer's disease are associated with cortical neurodegenerative pathology, but not with small vessel disease. Acta Neuropathol. 2017;134(3):459–73.

87. Gouw AA, Seewann A, Flier WM van der, Barkhof F, Rozemuller AM, Scheltens P, et al. Heterogeneity of small vessel disease: a systematic review of MRI and histopathology correlations. J Neurology Neurosurg Psychiatry. 2011;82(2):126.

88. Rosand J, Muzikansky A, Kumar A, Wisco JJ, Smith EE, Betensky RA, et al. Spatial clustering of hemorrhages in probable cerebral amyloid angiopathy. Ann Neurol. 2005;58(3):459–62.

89. Smith EE, Gurol ME, Eng JA, Engel CR, Nguyen TN, Rosand J, et al. White matter lesions, cognition, and recurrent hemorrhage in lobar intracerebral hemorrhage. Neurology. 2004;63(9):1606–12.

90. Thanprasertsuk S, Martinez-Ramirez S, Pontes-Neto OM, Ni J, Ayres A, Reed A, et al. Posterior white matter disease distribution as a predictor of amyloid angiopathy. Neurology. 2014;83(9):794–800.

91. Zhu YC, Chabriat H, Godin O, Dufouil C, Rosand J, Greenberg SM, et al. Distribution of white matter hyperintensity in cerebral hemorrhage and healthy aging. J Neurol. 2012;259(3):530–6.

92. Alber J, Alladi S, Bae HJ, Barton DA, Beckett LA, Bell JM, et al. White matter hyperintensities in vascular contributions to cognitive impairment and dementia (VCID):

Knowledge gaps and opportunities. Alzheimer's Dementia Transl Res Clin Interventions. 2019;5(1):107–17.

93. Durrani R, Wang M, Cox E, Irving E, Saad F, McCreary CR, et al. Mediators of cognitive impairment in cerebral amyloid angiopathy. Int J Stroke. 2022;174749302210993.

94. Pasi M, Boulouis G, Fotiadis P, Auriel E, Charidimou A, Haley K, et al. Distribution of lacunes in cerebral amyloid angiopathy and hypertensive small vessel disease. Neurology. 2017;88(23):2162–8.

95. Ling Y, Chabriat H. Incident cerebral lacunes: A review. J Cereb Blood Flow Metabolism. 2020;40(5):909–21.

96. Cheng Z, Zhang W, Zhan Z, Xia L, Han Z. Cerebral small vessel disease and prognosis in intracerebral haemorrhage: A systematic review and meta-analysis of cohort studies. Eur J Neurol. 2022;

97. Veluw SJ van, Shih AY, Smith EE, Chen C, Schneider JA, Wardlaw JM, et al. Detection, risk factors, and functional consequences of cerebral microinfarcts. Lancet Neurology. 2017;16(9):730–40.

98. Xiong L, Veluw SJ van, Bounemia N, Charidimou A, Pasi M, Boulouis G, et al. Cerebral Cortical Microinfarcts on Magnetic Resonance Imaging and Their Association With Cognition in Cerebral Amyloid Angiopathy. Stroke. 2018;49(10):2330–6.

99. Gregoire SM, Charidimou A, Gadapa N, Dolan E, Antoun N, Peeters A, et al. Acute ischaemic brain lesions in intracerebral haemorrhage: multicentre cross-sectional magnetic resonance imaging study. Brain. 2011;134(8):2376–86.

100. Wardlaw JM, Benveniste H, Nedergaard M, Zlokovic BV, Mestre H, Lee H, et al. Perivascular spaces in the brain: anatomy, physiology and pathology. Nat Rev Neurol. 2020;16(3):137–53.

101. Brown R, Benveniste H, Black SE, Charpak S, Dichgans M, Joutel A, et al. Understanding the role of the perivascular space in cerebral small vessel disease. Cardiovasc Res. 2018;114(11):1462–73.

102. Charidimou A, Boulouis G, Pasi M, Auriel E, Etten ES van, Haley K, et al. MRI-visible perivascular spaces in cerebral amyloid angiopathy and hypertensive arteriopathy. Neurology. 2017;88(12):1157–64.

103. Boulouis G, Charidimou A, Pasi M, Roongpiboonsopit D, Xiong L, Auriel E, et al. Hemorrhage recurrence risk factors in cerebral amyloid angiopathy: Comparative analysis of the overall small vessel disease severity score versus individual neuroimaging markers. J Neurol Sci. 2017;380:64–7.

104. Pinho J, Araújo JM, Costa AS, Silva F, Francisco A, Quintas-Neves M, et al. Intracerebral Hemorrhage Recurrence in Patients with and without Cerebral Amyloid Angiopathy. Cerebrovasc Dis Extra. 2021;11(1):15–21.

105. Raposo N, Zotin MCZ, Schoemaker D, Xiong L, Fotiadis P, Charidimou A, et al. Peak Width of Skeletonized Mean Diffusivity as Neuroimaging Biomarker in Cerebral Amyloid Angiopathy. Am J Neuroradiol. 2021;

106. Das AS, Regenhardt RW, Vernooij MW, Blacker D, Charidimou A, Viswanathan A. Asymptomatic Cerebral Small Vessel Disease: Insights from Population-Based Studies. J Stroke. 2019;21(2):121–38.

107. Smith EE, Biessels GJ, Guio FD, Leeuw FE, Duchesne S, Düring M, et al. Harmonizing brain magnetic resonance imaging methods for vascular contributions to neurodegeneration. Alzheimer's Dementia Diagnosis Assess Dis Monit. 2019;11(1):191–204.

108. Nitkunan A, Lanfranconi S, Charlton RA, Barrick TR, Markus HS. Brain Atrophy and Cerebral Small Vessel Disease: A Prospective Follow-Up Study. Stroke. 2011;42(1):133–8.

109. Guio FD, Duering M, Fazekas F, Leeuw FED, Greenberg SM, Pantoni L, et al. Brain atrophy in cerebral small vessel diseases: Extent, consequences, technical limitations and perspectives: The HARNESS initiative. J Cereb Blood Flow Metabolism. 2019;40(2):231–45.

110. Heinen R, Groeneveld ON, Barkhof F, Bresser J, Exalto LG, Kuijf HJ, et al. Small vessel disease lesion type and brain atrophy: The role of co-occurring amyloid. Alzheimer's Dementia Diagnosis Assess Dis Monit. 2020;12(1):e12060.

111. Fotiadis P, Rooden S van, Grond J van der, Schultz A, Martinez-Ramirez S, Auriel E, et al. Cortical atrophy in patients with cerebral amyloid angiopathy: a case-control study. Lancet Neurology. 2016;15(8):811–9.

112. Fotiadis P, Reijmer YD, Veluw SJV, Martinez-Ramirez S, Karahanoglu FI, Gokcal E, et al. White Matter Atrophy in Cerebral Amyloid Angiopathy. Neurology. 2020;10.1212/WNL.0000000000010017.

113. Staals J, Makin SDJ, Doubal FN, Dennis MS, Wardlaw JM. Stroke subtype, vascular risk factors, and total MRI brain small-vessel disease burden. Neurology. 2014;83(14):1228–34.

114. Klarenbeek P, Oostenbrugge RJ van, Rouhl RPW, Knottnerus ILH, Staals J. Ambulatory blood pressure in patients with lacunar stroke: association with total MRI burden of cerebral small vessel disease. Stroke J Cereb Circulation. 2013;44(11):2995–9.

115. Fazekas F, Chawluk J, Alavi A, Hurtig H, Zimmerman R. MR signal abnormalities at 1.5 T in Alzheimer's dementia and normal aging. Am J Roentgenol. 1987;149(2):351–6.

116. Brutto VJD, Mera R, Recalde BY, Rumbea DA, Costa AF, Brutto OHD. Total cerebral small vessel disease score and all-cause mortality in older adults of Amerindian ancestry: The Atahualpa Project. European Stroke J. 2021;6(4):412–9.

117. Du H, Wu S, Lei H, Ambler G, Werring DJ, Li H, et al. Total Cerebral Small Vessel Disease Score and Cerebral Bleeding Risk in Patients With Acute Stroke Treated With Intravenous Thrombolysis. Front Aging Neurosci. 2022;14:790262.

118. Seiffge DJ, Wilson D, Ambler G, Banerjee G, Hostettler IC, Houlden H, et al. Small vessel disease burden and intracerebral haemorrhage in patients taking oral anticoagulants. J Neurology Neurosurg Psychiatry. 2021;92(8):805–14.

119. Ryu WS, Jeong SW, Kim DE. Total small vessel disease burden and functional outcome in patients with ischemic stroke. Plos One. 2020;15(11):e0242319.

120. Lioutas VA, Wu B, Norton C, Helenius J, Modak J, Selim M. Cerebral small vessel disease burden and functional and radiographic outcomes in intracerebral hemorrhage. J Neurol. 2018;265(12):2803–14.

121. Li X, Yuan J, Qin W, Yang L, Yang S, Li Y, et al. Higher Total Cerebral Small Vessel Disease Burden Was Associated With Mild Cognitive Impairment and Overall Cognitive Dysfunction: A Propensity Score-Matched Case–Control Study. Front Aging Neurosci. 2021;13:695732.

122. Charidimou A, Martinez-Ramirez S, Reijmer YD, Oliveira-Filho J, Lauer A, Roongpiboonsopit D, et al. Total Magnetic Resonance Imaging Burden of Small Vessel Disease in Cerebral Amyloid Angiopathy: An Imaging-Pathologic Study of Concept Validation. Jama Neurol. 2016;73(8):994.

123. Yilmaz P, Ikram MA, Ikram MK, Niessen WJ, Viswanathan A, Charidimou A, et al. Application of an Imaging-Based Sum Score for Cerebral Amyloid Angiopathy to the General Population: Risk of Major Neurological Diseases and Mortality. Front Neurol. 2019;10:1276.

124. Paschoal AM, Secchinatto KF, Silva PHR, Zotin MCZ, Santos AC, Viswanathan A, et al. Contrast-agent-free state-of-the-art MRI on cerebral small vessel disease—part 1. ASL, IVIM, and CVR. Nmr Biomed. 2022;e4742.

125. Silva PHR, Paschoal AM, Secchinatto KF, Zotin MCZ, Santos AC, Viswanathan A, et al. Contrast agent-free state-of-the-art magnetic resonance imaging on cerebral small vessel disease – Part 2: Diffusion tensor imaging and functional magnetic resonance imaging. Nmr Biomed. 2022;e4743.

126. Martins-Filho RK, Zotin MC, Rodrigues G, Pontes-Neto O. Biomarkers Related to Endothelial Dysfunction and Vascular Cognitive Impairment: A Systematic Review. Dement Geriatr Cogn. 2020;49(4):365–74.

127. Thrippleton MJ, Backes WH, Sourbron S, Ingrisch M, Osch MJP van, Dichgans M, et al. Quantifying blood-brain barrier leakage in small vessel disease: Review and consensus recommendations. Alzheimer's Dementia. 2019;15(6):840–58.

128. Huisa BN, Caprihan A, Thompson J, Prestopnik J, Qualls CR, Rosenberg GA. Long-Term Blood–Brain Barrier Permeability Changes in Binswanger Disease. Stroke. 2018;46(9):2413–8.

129. Zhang CE, Wong SM, Haar HJ van de, Staals J, Jansen JFA, Jeukens CRLPN, et al. Blood–brain barrier leakage is more widespread in patients with cerebral small vessel disease. Neurology. 2017;88(5):426–32.

130. Li Y, Li M, Zhang X, Shi Q, Yang S, Fan H, et al. Higher blood–brain barrier permeability is associated with higher white matter hyperintensities burden. J Neurol. 2017;264(7):1474–81.

131. Li Y, Li M, Zuo L, Shi Q, Qin W, Yang L, et al. Compromised Blood–Brain Barrier Integrity Is Associated With Total Magnetic Resonance Imaging Burden of Cerebral Small Vessel Disease. Front Neurol. 2018;9:221.

132. Wardlaw JM, Doubal FN, Valdes-Hernandez M, Wang X, Chappell FM, Shuler K, et al. Blood–Brain Barrier Permeability and Long-Term Clinical and Imaging Outcomes in Cerebral Small Vessel Disease. Stroke. 2013;44(2):525–7.

133. Raja R, Rosenberg GA, Caprihan A. MRI measurements of Blood-Brain Barrier function in dementia: A review of recent studies. Neuropharmacology. 2018;134(Pt B):259–71.

134. Shi Y, Thrippleton MJ, Makin SD, Marshall I, Geerlings MI, Craen AJ de, et al. Cerebral blood flow in small vessel disease: A systematic review and meta-analysis. J Cereb Blood Flow Metabolism. 2016;36(10):1653–67.

135. Onkenhout L, Appelmans N, Kappelle LJ, Koek D, Exalto L, Bresser J de, et al. Cerebral Perfusion and the Burden of Small Vessel Disease in Patients Referred to a Memory Clinic. Cerebrovasc Dis. 2020;49(5):481–6.

136. Yu C, Lu W, Qiu J, Wang F, Li J, Wang L. Alterations of the Whole Cerebral Blood Flow in Patients With Different Total Cerebral Small Vessel Disease Burden. Front Aging Neurosci. 2020;12:175.

137. Shi Y, Thrippleton MJ, Blair GW, Dickie DA, Marshall I, Hamilton I, et al. Small vessel disease is associated with altered cerebrovascular pulsatility but not resting cerebral blood flow. J Cereb Blood Flow Metabolism. 2018;40(1):85–99.

138. Promjunyakul N on, Lahna DL, Kaye JA, Dodge HH, Erten-Lyons D, Rooney WD, et al. Comparison of cerebral blood flow and structural penumbras in relation to white matter hyperintensities: A multi-modal magnetic resonance imaging study. J Cereb Blood Flow Metabolism. 2016;36(9):1528–36.

139. Zonneveld HI, Loehrer EA, Hofman A, Niessen WJ, Lugt A van der, Krestin GP, et al. The Bidirectional Association between Reduced Cerebral Blood Flow and Brain Atrophy in the General Population. J Cereb Blood Flow Metabolism. 2015;35(11):1882–7.

140. Wolters FJ, Zonneveld HI, Hofman A, Lugt A van der, Koudstaal PJ, Vernooij MW, et al. Cerebral Perfusion and the Risk of Dementia: A Population-Based Study. Circulation. 2017;136(8):719–28.

141. Thrippleton MJ, Shi Y, Blair G, Hamilton I, Waiter G, Schwarzbauer C, et al. Cerebrovascular reactivity measurement in cerebral small vessel disease: Rationale and reproducibility of a protocol for MRI acquisition and image processing. Int J Stroke. 2017;13(2):195–206.

142. Alsop DC, Detre JA, Golay X, Günther M, Hendrikse J, Hernandez-Garcia L, et al. Recommended implementation of arterial spin-labeled perfusion MRI for clinical applications: A consensus of the ISMRM perfusion study group and the European consortium for ASL in dementia. Magnet Reson Med. 2015;73(1):102–16.

143. Blair GW, Doubal FN, Thrippleton MJ, Marshall I, Wardlaw JM. Magnetic resonance imaging for assessment of cerebrovascular reactivity in cerebral small vessel disease: A systematic review. J Cereb Blood Flow Metabolism. 2016;36(5):833–41.

144. Blair GW, Thrippleton MJ, Shi Y, Hamilton I, Stringer M, Chappell F, et al. Intracranial hemodynamic relationships in patients with cerebral small vessel disease. Neurology. 2020;94(21):e2258–69.

145. Sam K, Peltenburg B, Conklin J, Sobczyk O, Poublanc J, Crawley AP, et al. Cerebrovascular reactivity and white matter integrity. Neurology. 2016;87(22):2333–9.

146. Sam K, Crawley AP, Conklin J, Poublanc J, Sobczyk O, Mandell DM, et al. Development of White Matter Hyperintensity Is Preceded by Reduced Cerebrovascular Reactivity. Ann Neurol. 2016;80(2):277–85.

147. Ni L, Zhang B, Yang D, Qin R, Xu H, Ma J, et al. Lower Cerebrovascular Reactivity Contributed to White Matter Hyperintensity-Related Cognitive Impairment: A Resting-State Functional MRI Study. J Magn Reson Imaging. 2021;53(3):703–11.

148. Dumas A, Dierksen GA, Gurol ME, Halpin A, Martinez-Ramirez S, Schwab K, et al. Functional magnetic resonance imaging detection of vascular reactivity in cerebral amyloid angiopathy. Ann Neurol. 2012;72(1):76–81.

149. Switzer AR, McCreary C, Batool S, Stafford RB, Frayne R, Goodyear BG, et al. Longitudinal decrease in blood oxygenation level dependent response in cerebral amyloid angiopathy. Neuroimage Clin. 2016;11:461–7.

150. Leurent C, Goodman JA, Zhang Y, He P, Polimeni JR, Gurol ME, et al. Immunotherapy with ponezumab for probable cerebral amyloid angiopathy. Ann Clin Transl Neur. 2019;6(4):795–806.

151. Lawrence AJ, Tozer DJ, Stamatakis EA, Markus HS. A comparison of functional and tractography based networks in cerebral small vessel disease. Neuroimage Clin. 2018;18:425–32.

152. Wang R, Liu N, Tao YY, Gong XQ, Zheng J, Yang C, et al. The Application of rs-fMRI in Vascular Cognitive Impairment. Front Neurol. 2020;11:951.

153. Skrobot OA, Black SE, Chen C, DeCarli C, Erkinjuntti T, Ford GA, et al. Progress toward standardized diagnosis of vascular cognitive impairment: Guidelines from the Vascular Impairment of Cognition Classification Consensus Study. Alzheimer's Dementia. 2018;14(3):280–92.

154. Wortmann M. Dementia: a global health priority - highlights from an ADI and World Health Organization report. Alzheimer's Res Ther. 2012;4(5):40.

155. Corriveau RA, Bosetti F, Emr M, Gladman JT, Koenig JI, Moy CS, et al. The Science of Vascular Contributions to Cognitive Impairment and Dementia (VCID): A Framework for Advancing Research Priorities in the Cerebrovascular Biology of Cognitive Decline. Cell Mol Neurobiol. 2016;36(2):281–8.

156. Gorelick PB, Scuteri A, Black SE, Decarli C, Greenberg SM, Iadecola C, et al. Vascular contributions to cognitive impairment and dementia: a statement for healthcare professionals from the american heart association/american stroke association. Stroke. 2011;42(9):2672–713.

157. Boyle PA, Yu L, Wilson RS, Leurgans SE, Schneider JA, Bennett DA. Person-specific contribution of neuropathologies to cognitive loss in old age. Ann Neurol. 2018;83(1):74–83.

158. Du J, Xu Q. Neuroimaging studies on cognitive impairment due to cerebral small vessel disease. Stroke Vasc Neurology. 2019;4(2):svn-2018-000209.

159. Roman GC, Tatemichi TK, Erkinjuntti T, Cummings JL, Masdeu JC, Garcia JH, et al. Vascular dementia: Diagnostic criteria for research studies: Report of the NINDS-AIREN International Workshop. Neurology. 1993;43(2):250–250.

160. Erkinjuntti T, Inzitari D, Pantoni L, Wallin A, Scheltens P, Rockwood K, et al. Research criteria for subcortical vascular dementia in clinical trials. J Neural Transm Suppl. 2000;59:23–30.

161. Lu H, Kashani AH, Arfanakis K, Caprihan A, DeCarli C, Gold BT, et al. MarkVCID cerebral small vessel consortium: II. Neuroimaging protocols. Alzheimer's Dementia. 2021;17(4):716–25.

162. Freeze WM, Zotin MCZ, Scherlek AA, Perosa V, Auger CA, Warren AD, et al. Corpus callosum lesions are associated with worse cognitive performance in cerebral amyloid angiopathy. Brain Commun. 2022;4(3):fcac105-.

163. Zhao L, Biesbroek JM, Shi L, Liu W, Kuijf HJ, Chu WW, et al. Strategic infarct location for post-stroke cognitive impairment: A multivariate lesion-symptom mapping study. J Cereb Blood Flow Metabolism. 2017;38(8):1299–311.

164. Veluw SJ van, Reijmer YD, Kouwe AJ van der, Charidimou A, Riley GA, Leemans A, et al. Histopathology of diffusion imaging abnormalities in cerebral amyloid angiopathy. Neurology. 2019;92(9):e933–43.

165. Finsterwalder S, Vlegels N, Gesierich B, Caballero MÁA, Weaver NA, Franzmeier N, et al. Small vessel disease more than Alzheimer's disease determines diffusion MRI alterations in memory clinic patients. Alzheimer's Dementia. 2020;16(11):1504–14.

166. Caballero MÁA, Suárez-Calvet M, Duering M, Franzmeier N, Benzinger T, Fagan AM, et al. White matter diffusion alterations precede symptom onset in autosomal dominant Alzheimer's disease. Brain. 2018;141(10):3065–80.

167. Williams OA, Zeestraten EA, Benjamin P, Lambert C, Lawrence AJ, Mackinnon AD, et al. Diffusion tensor image segmentation of the cerebrum provides a single measure of cerebral small vessel disease severity related to cognitive change. Neuroimage Clin. 2017;16:330–42.

168. Boot EM, Leijsen EM van, Bergkamp MI, Kessels RPC, Norris DG, Leeuw FE de, et al. Structural network efficiency predicts cognitive decline in cerebral small vessel disease. Neuroimage Clin. 2020;27:102325.

169. Baykara E, Gesierich B, Adam R, Tuladhar AM, Biesbroek JM, Koek HL, et al. A Novel Imaging Marker for Small Vessel Disease Based on Skeletonization of White Matter Tracts and Diffusion Histograms. Ann Neurol. 2016;80(4):581–92.

170. Duering M, Finsterwalder S, Baykara E, Tuladhar AM, Gesierich B, Konieczny MJ, et al. Free water determines diffusion alterations and clinical status in cerebral small vessel disease. Alzheimer's Dementia. 2018;14(6):764–74.

171. Lawrence AJ, Zeestraten EA, Benjamin P, Lambert CP, Morris RG, Barrick TR, et al. Longitudinal decline in structural networks predicts dementia in cerebral small vessel disease. Neurology. 2018;90(21):e1898–910.

172. Reijmer YD, Fotiadis P, Martinez-Ramirez S, Salat DH, Schultz A, Shoamanesh A, et al. Structural network alterations and neurological dysfunction in cerebral amyloid angiopathy. Brain. 2015;138(1):179–88.

173. Tuladhar AM, Uden IWM van, Rutten-Jacobs LCA, Lawrence A, Holst H van der, Norden A van, et al. Structural network efficiency predicts conversion to dementia. Neurology. 2016;86(12):1112–9.

174. Tuladhar AM, Tay J, Leijsen E van, Lawrence AJ, Uden IWM van, Bergkamp M, et al. Structural network changes in cerebral small vessel disease. J Neurology Neurosurg Psychiatry. 2020;91(2):196.

175. Xu X, Lau KK, Wong YK, Mak HKF, Hui ES. The effect of the total small vessel disease burden on the structural brain network. Sci Rep-uk. 2018;8(1):7442.

176. Tuladhar AM, Dijk E van, Zwiers MP, Norden AGW van, Laat KF de, Shumskaya E, et al. Structural network connectivity and cognition in cerebral small vessel disease. Hum Brain Mapp. 2016;37(1):300–10.

177. Kim HJ, Im K, Kwon H, Lee JM, Kim C, Kim YJ, et al. Clinical effect of white matter network disruption related to amyloid and small vessel disease. Neurology. 2015;85(1):63–70.

178. Salat DH, Smith EE, Tuch DS, Benner T, Pappu V, Schwab KM, et al. White Matter Alterations in Cerebral Amyloid Angiopathy Measured by Diffusion Tensor Imaging. Stroke. 2006;37(7):1759–64.

179. Viswanathan A, Patel P, Rahman R, Nandigam RNK, Kinnecom C, Bracoud L, et al. Tissue Microstructural Changes Are Independently Associated With Cognitive Impairment in Cerebral Amyloid Angiopathy. Stroke. 2008;39(7):1988–92.

180. Reijmer YD, Fotiadis P, Riley GA, Xiong L, Charidimou A, Boulouis G, et al. Progression of Brain Network Alterations in Cerebral Amyloid Angiopathy. Stroke. 2016;47(10):2470–5.

181. Reijmer YD, Fotiadis P, Charidimou A, Veluw SJ van, Xiong L, Riley GA, et al. Relationship between white matter connectivity loss and cortical thinning in cerebral amyloid angiopathy. Hum Brain Mapp. 2017;38(7):3723–31.

182. Williams OA, Zeestraten EA, Benjamin P, Lambert C, Lawrence AJ, Mackinnon AD, et al. Predicting Dementia in Cerebral Small Vessel Disease Using an Automatic Diffusion Tensor Image Segmentation Technique. Stroke. 2019;50(10):2775–82.

183. McCreary CR, Beaudin AE, Subotic A, Zwiers AM, Alvarez A, Charlton A, et al. Cross-sectional and Longitudinal Differences in Peak Skeletonized White Matter Mean Diffusivity in Cerebral Amyloid Angiopathy. Neuroimage Clin. 2020;27:102280.

184. Lam BYK, Leung KT, Yiu B, Zhao L, Biesbroek JM, Au L, et al. Peak width of skeletonized mean diffusivity and its association with age-related cognitive alterations and vascular risk factors. Alzheimer's Dementia Diagnosis Assess Dis Monit. 2019;11(1):721–9.

185. Bastiani M, Cottaar M, Fitzgibbon SP, Suri S, Alfaro-Almagro F, Sotiropoulos SN, et al. Automated quality control for within and between studies diffusion MRI data using a non-parametric framework for movement and distortion correction. Neuroimage. 2019;184:801–12.

186. Yendiki A, Koldewyn K, Kakunoori S, Kanwisher N, Fischl B. Spurious group differences due to head motion in a diffusion MRI study. Neuroimage. 2014;88:79–90.

187. Roalf DR, Quarmley M, Elliott MA, Satterthwaite TD, Vandekar SN, Ruparel K, et al. The impact of quality assurance assessment on diffusion tensor imaging outcomes in a large-scale population-based cohort. Neuroimage. 2016;125:903–19.

188. Sullivan G, Galdi P, Cabez MB, Borbye-Lorenzen N, Stoye DQ, Lamb GJ, et al. Interleukin-8 dysregulation is implicated in brain dysmaturation following preterm birth. Brain Behav Immun. 2020;90:311–8.

189. Blesa M, Galdi P, Sullivan G, Wheater EN, Stoye DQ, Lamb GJ, et al. Peak Width of Skeletonized Water Diffusion MRI in the Neonatal Brain. Front Neurol. 2020;11:235.

190. Graham MS, Drobnjak I, Zhang H. Realistic simulation of artefacts in diffusion MRI for validating post-processing correction techniques. Neuroimage. 2016;125:1079–94.

191. Andersson JLR, Sotiropoulos SN. An integrated approach to correction for off-resonance effects and subject movement in diffusion MR imaging. Neuroimage. 2016;125:1063–78.

192. Smith SM. Fast robust automated brain extraction. Hum Brain Mapp. 2002;17(3):143–55.

193. Jenkinson M, Beckmann CF, Behrens TEJ, Woolrich MW, Smith SM. FSL. Neuroimage. 2012;62(2):782–90.

194. Basser PJ, Mattiello J, Lebihan D. Estimation of the Effective Self-Diffusion Tensor from the NMR Spin Echo. J Magnetic Reson Ser B. 1994;103(3):247–54.

195. Andersson JLR, Graham MS, Zsoldos E, Sotiropoulos SN. Incorporating outlier detection and replacement into a non-parametric framework for movement and distortion correction of diffusion MR images. Neuroimage. 2016;141:556–72.

196. Andersson JLR, Graham MS, Drobnjak I, Zhang H, Filippini N, Bastiani M. Towards a comprehensive framework for movement and distortion correction of diffusion MR images: Within volume movement. Neuroimage. 2017;152:450–66.

197. Andersson JLR, Graham MS, Drobnjak I, Zhang H, Campbell J. Susceptibility-induced distortion that varies due to motion: Correction in diffusion MR without acquiring additional data. Neuroimage. 2018;171:277–95.

198. Vos SB, Jones DK, Viergever MA, Leemans A. Partial volume effect as a hidden covariate in DTI analyses. Neuroimage. 2011;55(4):1566–76.

199. Alexander AL, Hasan KM, Lazar M, Tsuruda JS, Parker DL. Analysis of partial volume effects in diffusion-tensor MRI. Magnet Reson Med. 2001;45(5):770–80.

200. Metzler-Baddeley C, O'Sullivan MJ, Bells S, Pasternak O, Jones DK. How and how not to correct for CSF-contamination in diffusion MRI. Neuroimage. 2012;59(2):1394–403.

201. Soares JM, Marques P, Alves V, Sousa N. A hitchhiker's guide to diffusion tensor imaging. Front Neurosci-switz. 2013;7:31.

202. Smith SM, Jenkinson M, Johansen-Berg H, Rueckert D, Nichols TE, Mackay CE, et al. Tract-based spatial statistics: Voxelwise analysis of multi-subject diffusion data. Neuroimage. 2006;31(4):1487–505.

203. Beaudet G, Tsuchida A, Petit L, Tzourio C, Caspers S, Schreiber J, et al. Age-Related Changes of Peak Width Skeletonized Mean Diffusivity (PSMD) Across the Adult Lifespan: A Multi-Cohort Study. Frontiers Psychiatry. 2020;11:342.

204. Bozzali M, Cherubini A. Diffusion tensor MRI to investigate dementias: a brief review. Magn Reson Imaging. 2007;25(6):969–77.

205. Tofts PS, Davies GR, Dehmeshki J. Quantitative MRI of the Brain: Measuring Changes Caused by Disease. 2004;581–610.

206. Zeestraten EA, Benjamin P, Lambert C, Lawrence AJ, Williams OA, Morris RG, et al. Application of Diffusion Tensor Imaging Parameters to Detect Change in Longitudinal Studies in Cerebral Small Vessel Disease. Plos One. 2016;11(1):e0147836.

207. Croall ID, Lohner V, Moynihan B, Khan U, Hassan A, O'Brien JT, et al. Using DTI to assess white matter microstructure in cerebral small vessel disease (SVD) in multicentre studies. Clin Sci. 2017;131(12):1361–73.

208. Brun L, Pron A, Sein J, Deruelle C, Coulon O. Diffusion MRI: Assessment of the Impact of Acquisition and Preprocessing Methods Using the BrainVISA-Diffuse Toolbox. Front Neurosci-switz. 2019;13:536.

209. Low A, Mak E, Stefaniak JD, Malpetti M, Nicastro N, Savulich G, et al. Peak Width of Skeletonized Mean Diffusivity as a Marker of Diffuse Cerebrovascular Damage. Front Neurosci-switz. 2020;14:238.

210. Frey BM, Petersen M, Mayer C, Schulz M, Cheng B, Thomalla G. Characterization of White Matter Hyperintensities in Large-Scale MRI-Studies. Front Neurol. 2019;10:238.

211. Etherton MR, Wu O, Cougo P, Giese AK, Cloonan L, Fitzpatrick KM, et al. Integrity of normal-appearing white matter and functional outcomes after acute ischemic stroke. Neurology. 2017;88(18):1701–8.

212. Maniega SM, Hernández MCV, Clayden JD, Royle NA, Murray C, Morris Z, et al. White matter hyperintensities and normal-appearing white matter integrity in the aging brain. Neurobiol Aging. 2015;36(2):909–18.

213. Raja R, Rosenberg G, Caprihan A. Review of Diffusion MRI Studies in Chronic White Matter Diseases. Neurosci Lett. 2018;694:198–207.

214. McGrath S, Zhao X, Steele R, Thombs BD, Benedetti A, Levis B, et al. Estimating the sample mean and standard deviation from commonly reported quantiles in meta-analysis. Stat Methods Med Res. 2020;29(9):2520–37.

215. Petersen M, Frey BM, Schlemm E, Mayer C, Hanning U, Engelke K, et al. Network Localisation of White Matter Damage in Cerebral Small Vessel Disease. Sci Rep-uk. 2020;10(1):9210.

216. Frey BM, Petersen M, Schlemm E, Mayer C, Hanning U, Engelke K, et al. White matter integrity and structural brain network topology in cerebral small vessel disease: The Hamburg city health study. Hum Brain Mapp. 2020;

217. Liu Y, Chan DKY, Thalamuthu A, Wen W, Jiang J, Paradise M, et al. Plasma lipidomic biomarker analysis reveals distinct lipid changes in vascular dementia. Comput Struct Biotechnology J. 2020;18:1613–24.

218. Vinciguerra C, Giorgio A, Zhang J, Nardone V, Brocci RT, Pastò L, et al. Peak width of skeletonized mean diffusivity (PSMD) and cognitive functions in relapsing-remitting multiple sclerosis. Brain Imaging Behav. 2020;1–6.

219. Vinciguerra C, Giorgio A, Zhang J, Donato ID, Stromillo ML, Brocci RT, et al. Peak width of skeletonized mean diffusivity (PSMD) as marker of widespread white matter tissue damage in multiple sclerosis. Mult Scler Relat Dis. 2018;27:294–7.

220. Wickham H. ggplot2, Elegant Graphics for Data Analysis [Internet]. 2016th ed. Springer-Verlag New York; 2016. Available from: https://ggplot2.tidyverse.org

221. Herzog R, Álvarez-Pasquin MJ, Díaz C, Barrio JLD, Estrada JM, Gil Á. Are healthcare workers' intentions to vaccinate related to their knowledge, beliefs and attitudes? a systematic review. Bmc Public Health. 2013;13(1):154.

222. Yuan T, Fitzpatrick T, Ko NY, Cai Y, Chen Y, Zhao J, et al. Circumcision to prevent HIV and other sexually transmitted infections in men who have sex with men: a systematic review and meta-analysis of global data. Lancet Global Heal. 2019;7(4):e436–47.

223. Ranganathan P, Aggarwal R. Study designs: Part 1 - An overview and classification. Perspectives Clin Res. 2018;9(4):184–6.

224. Maillard P, Lu H, Arfanakis K, Gold BT, Bauer CE, Zachariou V, et al. Instrumental Validation of Free Water, Peak-Width of Skeletonized Mean Diffusivity and White Matter Hyperintensities: MarkVCID Neuroimaging kits. Alzheimer's & Dementia: Diagnosis, Assessment & Disease Monitoring. 2022;

225. Oberlin LE, Respino M, Victoria L, Abreu L, Hoptman MJ, Alexopoulos GS, et al. Late-life depression accentuates cognitive weaknesses in older adults with small vessel disease. Neuropsychopharmacol. 2021;1–8.

226. Schouten TM, Vos F de, Rooden S van, Bouts MJRJ, Opstal AM van, Feis RA, et al. Multiple Approaches to Diffusion Magnetic Resonance Imaging in Hereditary Cerebral Amyloid Angiopathy Mutation Carriers. J Am Heart Assoc. 2019;8(3):e011288.

227. Wei N, Deng Y, Yao L, Jia W, Wang J, Shi Q, et al. A Neuroimaging Marker Based on Diffusion Tensor Imaging and Cognitive Impairment Due to Cerebral White Matter Lesions. Front Neurol. 2019;10:81.

228. Deary IJ, Ritchie SJ, Maniega SM, Cox SR, Hernández MCV, Luciano M, et al. Brain Peak Width of Skeletonized Mean Diffusivity (PSMD) and Cognitive Function in Later Life. Frontiers Psychiatry. 2019;10:524.

229. Ni H, Kavcic V, Zhu T, Ekholm S, Zhong J. Effects of number of diffusion gradient directions on derived diffusion tensor imaging indices in human brain. Ajnr Am J Neuroradiol. 2006;27(8):1776–81.

230. Zhou X, Sakaie KE, Debbins JP, Narayanan S, Fox RJ, Lowe MJ. Scan-rescan repeatability and cross-scanner comparability of DTI metrics in healthy subjects in the SPRINT-MS multicenter trial. Magn Reson Imaging. 2018;53:105–11.

231. Konieczny MJ, Dewenter A, Telgte A ter, Gesierich B, Wiegertjes K, Finsterwalder S, et al. Multi-shell diffusion MRI models for white matter characterization in cerebral small vessel disease. Neurology. 2020;96(5):10.1212/WNL.0000000000011213.

232. Grech-Sollars M, Hales PW, Miyazaki K, Raschke F, Rodriguez D, Wilson M, et al. Multi-centre reproducibility of diffusion MRI parameters for clinical sequences in the brain. Nmr Biomed. 2015;28(4):468–85.

233. Prohl AK, Scherrer B, Tomas-Fernandez X, Filip-Dhima R, Kapur K, Velasco-Annis C, et al. Reproducibility of Structural and Diffusion Tensor Imaging in the TACERN Multi-Center Study. Frontiers Integr Neurosci. 2019;13:24.

234. Lebel C, Gee M, Camicioli R, Wieler M, Martin W, Beaulieu C. Diffusion tensor imaging of white matter tract evolution over the lifespan. Neuroimage. 2012;60(1):340–52.

235. Hasan KM, Sankar A, Halphen C, Kramer LA, Brandt ME, Juranek J, et al. Development and organization of the human brain tissue compartments across the lifespan using diffusion tensor imaging. Neuroreport. 2007;18(16):1735–9.

236. Cox SR, Ritchie SJ, Tucker-Drob EM, Liewald DC, Hagenaars SP, Davies G, et al. Ageing and brain white matter structure in 3,513 UK Biobank participants. Nat Commun. 2016;7(1):13629.

237. Moll NM, Rietsch AM, Thomas S, Ransohoff AJ, Lee J, Fox R, et al. Multiple sclerosis normal-appearing white matter: Pathology–imaging correlations. Ann Neurol. 2011;70(5):764–73.

238. Charidimou A, Gang Q, Werring DJ. Sporadic cerebral amyloid angiopathy revisited: recent insights into pathophysiology and clinical spectrum. J Neurology Neurosurg Psychiatry. 2012;83(2):124.

239. Planton M, Saint-Aubert L, Raposo N, Branchu L, Lyoubi A, Bonneville F, et al. High prevalence of cognitive impairment after intracerebral hemorrhage. Plos One. 2017;12(6):e0178886.

240. Boyle PA, Yu L, Nag S, Leurgans S, Wilson RS, Bennett DA, et al. Cerebral amyloid angiopathy and cognitive outcomes in community-based older persons. Neurology. 2015;85(22):1930–6.

241. Heinen R, Vlegels N, Bresser J de, Leemans A, Biessels GJ, Reijmer YD, et al. The cumulative effect of small vessel disease lesions is reflected in structural brain networks of memory clinic patients. Neuroimage Clin. 2018;19:963–9.

242. O'Sullivan M, Jones DK, Summers PE, Morris RG, Williams SCR, Markus HS. Evidence for cortical "disconnection" as a mechanism of age-related cognitive decline. Neurology. 2001;57(4):632–8.

243. Martinez-Ramirez S, Greenberg SM, Viswanathan A. Cerebral microbleeds: overview and implications in cognitive impairment. Alzheimer's Res Ther. 2014;6(3):33.

244. Charidimou A, Ni J, Martinez-Ramirez S, Vashkevich A, Ayres A, Rosand J, et al. Cortical Superficial Siderosis in Memory Clinic Patients: Further Evidence for Underlying Cerebral Amyloid Angiopathy. Cerebrovasc Dis. 2016;41(3–4):156–62.

245. Petersen RC. Mild cognitive impairment as a diagnostic entity. J Intern Med. 2004;256(3):183–94.

246. Crum RM, Anthony JC, Bassett SS, Folstein MF. Population-Based Norms for the Mini-Mental State Examination by Age and Educational Level. Jama. 1993;269(18):2386–91.

247. Weintraub S, Salmon D, Mercaldo N, Ferris S, Graff-Radford NR, Chui H, et al. The Alzheimer's Disease Centers' Uniform Data Set (UDS). Alz Dis Assoc Dis. 2009;23(2):91–101.

248. Corrigan JD, Hinkeldey NS. Relationships between parts A and B of the Trail Making Test. J Clin Psychol. 1987;43(4):402–9.

249. Joy S, Kaplan E, Fein D. Speed and memory in the WAIS-III Digit Symbol—Coding subtest across the adult lifespan. Arch Clin Neuropsych. 2004;19(6):759–67.

250. Sánchez-Cubillo I, Periáñez JA, Adrover-Roig D, Rodríguez-Sánchez JM, Ríos-Lago M, Tirapu J, et al. Construct validity of the Trail Making Test: role of task-switching, working memory, inhibition/interference control, and visuomotor abilities. J Int Neuropsychological Soc Jins. 2009;15(3):438–50.

251. Brandt J. The hopkins verbal learning test: Development of a new memory test with six equivalent forms. Clin Neuropsychol. 1991;5(2):125–42.

252. D W. Wechsler Memory Scale-Revised Manual. San Antonio: The Psychological Corporation; 1987.

253. Mack WJ, Freed DM, Williams BW, Henderson VW. Boston Naming Test: Shortened Versions for Use in Alzheimer's Disease. J Gerontology. 1992;47(3):P154–8.

254. Tombaugh TN, Kozak J, Rees L. Normative Data Stratified by Age and Education for Two Measures of Verbal Fluency FAS and Animal Naming. Arch Clin Neuropsych. 1999;14(2):167–77.

255. Fastenau PS, Denburg NL, Mauer BA. Parallel Short Forms for the Boston Naming Test: Psychometric Properties and Norms for Older Adults. J Clin Exp Neuropsyc. 1998;20(6):828–34.

256. Tombaugh TN. Trail Making Test A and B: Normative data stratified by age and education. Arch Clin Neuropsych. 2004;19(2):203–14.

257. Charidimou A, Linn J, Vernooij MW, Opherk C, Akoudad S, Baron JC, et al. Cortical superficial siderosis: detection and clinical significance in cerebral amyloid angiopathy and related conditions. Brain. 2015;138(8):2126–39.

258. Charidimou A, Martinez-Ramirez S, Shoamanesh A, Oliveira-Filho J, Frosch M, Vashkevich A, et al. Cerebral amyloid angiopathy with and without hemorrhage. Neurology. 2015;84(12):1206–12.

259. Smith EE, Beaudin AE. New insights into cerebral small vessel disease and vascular cognitive impairment from MRI. Curr Opin Neurol. 2018;31(1):36–43.

260. Andersson JLR, Sotiropoulos SN. Non-parametric representation and prediction of single- and multi-shell diffusion-weighted MRI data using Gaussian processes. Neuroimage. 2015;122:166–76.

261. Dale AM, Fischl B, Sereno MI. Cortical Surface-Based Analysis I. Segmentation and Surface Reconstruction. Neuroimage. 1999;9(2):179–94.

262. Schmidt P. Bayesian inference for structured additive regression models for large-scale problems with applications to medical imaging. 2017.

263. Lindeman RH, F. P, Gold RZ. Introduction to Bivariate and Multivariate Analysis. Scott, Foresman; 1980. 444 p.

264. Grömping U. Relative Importance for Linear Regression in R : The Package relaimpo. J Stat Softw. 2006;17(1).

265. Vinters HV, Gilbert JJ. Cerebral amyloid angiopathy: incidence and complications in the aging brain. II. The distribution of amyloid vascular changes. Stroke. 1983;14(6):924–8.

266. Auriel E, Edlow BL, Reijmer YD, Fotiadis P, Ramirez-Martinez S, Ni J, et al. Microinfarct disruption of white matter structure. Neurology. 2014;83(2):182–8.

267. Dalen JW van, Scuric EEM, Veluw SJ van, Caan MWA, Nederveen AJ, Biessels GJ, et al. Cortical Microinfarcts Detected In Vivo on 3 Tesla MRI. Stroke. 2015;46(1):255–7.

268. Chen YW, Lee MJ, Smith EE. Cerebral Amyloid Angiopathy in East and West. Int J Stroke. 2010;5(5):403–11.

269. Morris JC, Schindler SE, McCue LM, Moulder KL, Benzinger TLS, Cruchaga C, et al. Assessment of Racial Disparities in Biomarkers for Alzheimer Disease. Jama Neurol. 2019;76(3):264–73.

270. Moon H, Badana ANS, Hwang SY, Sears JS, Haley WE. Dementia Prevalence in Older Adults: Variation by Race/Ethnicity and Immigrant Status. Am J Geriatric Psychiatry. 2019;27(3):241–50.

271. Chen C, Zissimopoulos JM. Racial and ethnic differences in trends in dementia prevalence and risk factors in the United States. Alzheimer's Dementia Transl Res Clin Interventions. 2018;4(1):510–20.

272. Turney IC, Lao PJ, Rentería MA, Laing KK, Beato JM, Chesebro AG, et al. Association between race/ethnicity and neuroimaging biomarkers in middle- and older-aged adults. Alzheimer's Dementia. 2020;16(S4).

273. Castello JP, Pasi M, Abramson JR, Rodriguez-Torres A, Marini S, Demel S, et al. Contribution of Racial and Ethnic Differences in Cerebral Small Vessel Disease Subtype and Burden to Risk of Cerebral Hemorrhage Recurrence. Neurology. 2021;96(20):e2469–80.

274. Gannon OJ, Robison LS, Custozzo AJ, Zuloaga KL. Sex differences in risk factors for vascular contributions to cognitive impairment & dementia. Neurochem Int. 2019;127:38–55.

275. Ganguli M, Lee CW, Hughes T, Snitz BE, Jakubcak J, Duara R, et al. Who wants a free brain scan? Assessing and correcting for recruitment biases in a population-based sMRI pilot study. Brain Imaging Behav. 2015;9(2):204–12.

276. Farina N, Ibnidris A, Alladi S, Comas-Herrera A, Albanese E, Docrat S, et al. A systematic review and meta-analysis of dementia prevalence in seven developing countries: A STRiDE project. Glob Public Health. 2020;15(12):1–16.

277. Lotufo PA, Goulart AC, Passos VM de A, Satake FM, Souza M de FM de, França EB, et al. Cerebrovascular disease in Brazil from 1990 to 2015: Global Burden of Disease 2015. Revista Brasileira De Epidemiologia Braz J Epidemiology. 2017;20Suppl 01(Suppl 01):129–41.

278. Grinberg LT, Nitrini R, Suemoto CK, Ferretti-Rebustini RE de L, Leite REP, Farfel JM, et al. Prevalence of dementia subtypes in a developing country: a clinicopathological study. Clinics. 2013;68(8):1140–5.

279. Berman JI, Lanza MR, Blaskey L, Edgar JC, Roberts TPL. High Angular Resolution Diffusion Imaging Probabilistic Tractography of the Auditory Radiation. Am J Neuroradiol. 2013;34(8):1573–8.

280. Etherton MR, Schirmer MD, Zotin MCZ, Rist PM, Boulouis G, Lauer A, et al. Global white matter structural integrity mediates the effect of age on ischemic stroke outcomes. Int J Stroke. 2021;174749302110559.

281. Wilcock D, Jicha G, Blacker D, Albert MS, D'Orazio LM, Elahi FM, et al. MarkVCID cerebral small vessel consortium: I. Enrollment, clinical, fluid protocols. Alzheimer's Dementia J Alzheimer's Assoc. 2021;17(4):704–15.

282. Robalo BM de B, Biessels GJ, Chen C, Dewenter A, Duering M, Hilal S, et al. Diffusion MRI harmonization enables joint-analysis of multicentre data of patients with cerebral small vessel disease. Neuroimage Clin. 2021;32:102886.